NUREG/CR-4567
EPRI NP-4572
BAW-1905

Once-Through Integral System (OTIS): Final Report

Babcock & Wilcox

Prepared for
U.S. Nuclear Regulatory Commission

and
Babcock & Wilcox Owners Group

and
Electric Power Research Institute

DISCLAIMER

NUREG/CR-4567
EPRI NP-4572
BAW-1905
R2

Once-Through Integral System (OTIS): Final Report

Manuscript Completed: February 1986
Date Published: September 1986

NUREG/CR--4567

TI87 900169

J. R. Gloudemans
Principle Author

Principle Contributors:

ARC		NPD
D. P. Birmingham	R. P. Ferron	G. O. Geissler
H. R. Carter	G. C. Rush	K. W. Turner
M. T. Childerson		

Prepared by

Babcock & Wilcox
Nuclear Power Division
P. O. Box 10935
Lynchburg, VA 24506-0935

Babcock & Wilcox
Alliance Research Center
1562 Beeson Street
Alliance, OH 44601

Prepared for

Division of Reactor System Safety
Office of Nuclear Regulatory Research
U. S. Nuclear Regulatory Commission
Washington, DC 20555
NRC FIN B8909

Babcock & Wilcox Owners Group
P. O. Box 10935
Lynchburg, VA 24506-0935

Electric Power Research Institute
P. O. Box 10412
Palo Alto, CA 94303

Legal Notice

This report was prepared by the Babcock & Wilcox Company as an account of work sponsored by the Nuclear Regulatory Commission, the Electric Power Research Institute, the Babcock & Wilcox Company, and the B&W Owners Group. No person acting on behalf of the NRC, the Institute, members of the Institute, the Babcock & Wilcox Company, or the B&W Owners Group:

1. makes any warranty, express or implied, with respect to the use of any information, apparatus, method, or process disclosed in this report or that such use may not infringe privately owned rights; or

2. assumes any liabilities with respect to the use of, or for damages resulting from the use of any information, apparatus, method, or process disclosed in this report.

Babcock & Wilcox
Nuclear Power Division
Lynchburg, Virginia

January 1986

OTIS Final Report

J. R. Gloudemans

Key Words: IST, OTIS, SBLOCA

ABSTRACT

A scaled experimental facility, designated the once-through integral system (OTIS), was used to acquire post-small break loss-of-coolant accident (SBLOCA) data for benchmarking system codes. OTIS was also used to investigate the application of the Abnormal Transient Operating Guidelines (ATOG) used in the Babcock & Wilcox (B&W) designed nulcear steam supply system (NSSS) during the course of an SBLOCA. OTIS was a single-loop facility with a plant to model power scale factor of 1686. OTIS maintained the key elevations, approximate component volumes, and loop flow resistances, and simulated the major component phenomena of a B&W raised-loop nuclear plant.

A test matrix consisting of 15 tests divided into four categories was performed. The largest group contained 10 tests and was defined to parametrically obtain an extensive set of plant-typical experimental data for code benchmarking. Parameters such as leak size, leak location, and high-pressure injection (HPI) shut-off head were individually varied. The remaining categories were specified to study the impact of the ATOGs (2 tests), to note the effect of guard heater operation on observed phenomena (2 tests), and to provide a data set for comparison with previous test experience (1 test).

A summary of the test results and a detailed discussion of Test 220100 is presented. Test 220100 was the nominal or reference test for the parametric studies. This test was performed with a scaled 10-cm^2 leak located in the cold leg suction piping.

The OTIS test results provide a challenging SBLOCA data set, based on plant-typical boundary system variations, for system code benchmarking. The OTIS results also illustrate the effectiveness of ATOGs for rapid system recovery from an SBLOCA.

CONTENTS

CONTENTS (Cont'd)

CONTENTS (Cont'd)

CONTENTS (Cont'd)

CONTENTS (Cont'd)

The OTIS data plots are on microfiche inside the back cover.

List of Tables

List of Tables

List of Tables (Cont'd)

List of Tables (Cont'd)

List of Figures

List of Figures (Cont'd)

List of Figures (Cont'd)

List of Figures (Cont'd)

List of Figures (Cont'd)

List of Figures (Cont'd)

List of Figures (Cont'd)

List of Figures (Cont'd)

List of Figures (Cont'd)

NOMENCLATURE

Auxiliary Feedwater .....AFW
Abnormal Transient Operator Guidelines.....ATOG
Boiler-Condensor Mode .....BCM
Cold Leg.....CL
CL suction, discharge.....CLS,CLD
Downcomer.....DC
Differential Pressure.....DP
Temperature Difference.....DT
Hot Leg, HL U-Bend.....HL,HLUB
HL piping beyond the HLUB.....HL Stub
High-Pressure Injection.....HPI
HL High Point Vent.....HLHVP,HPV
Inside Diameter.....ID
Lower Tube Sheet Upper Face (reference elevation).....LTSUF
Once-Through Steam Generator.....OTSG
Once-Through Integral System (test facility).....OTIS
Power-Operated Relief Valve.....PORV
Pressurizer.....PZR
Reactor Coolant Pump.....RCP
Resistance Temperature Detector.....RTD
Reactor Vessel.....RV
RV Upper Head Vent.....RVUHV
RV (internals) Vent Valve.....RVVV
Steam Generator LTSUF.....SGLTSUF
Thermocouple.....TC,T/C
Upper Downcomer.....UDC

EXECUTIVE SUMMARY

INTRODUCTION

OTIS (once-through integral system) testing was sponsored by the Nuclear Regulatory Commission (NRC), the Babcock & Wilcox Owners Group, Babcock & Wilcox (B&W),and the Electric Power Research Institute (EPRI). OTIS was a one-loop representation of raised-loop reactor systems of the B&W design.[1] OTIS generated post-small break loss-of-coolant accident (SBLOCA) integral system data with which to verify predictive computer codes.

FACILITY

Facility scaling considered full elevation, major two-phase phenomena, power-to-volume ratio, and irrecoverable pressure drop. Prototypical elevations were maintained throughout the system. The diameter of the model hot leg (2.63 in.) was chosen primarily to obtain plant-similar two-phase performance. This hot leg diameter did obtain a hot leg volume in excess of power-to-volume scaling, however. The power scaling factor, set by the pre-existing model steam generator, was 1686. The model steam generator contained full-length tubes of prototypical material, dimensions, and arrangement, thus providing a full-elevation subsection of the plant generator. The model core, of half prototypical length, also represented a subsection of the plant core.

OTIS simulated the key plant boundary systems: high-pressure injection, the pressurizer power-operated relief valve, primary system vents, and steam generator secondary steam and feed controls. The major characteristics of these boundary systems were automated. Controlled leak sites, as well as noncondensible gas injection sites, were provided at several locations of interest. OTIS relied on standard measurements (temperature, pressure, and differential pressure for level and flow rate) to record system performance. Turbinemeters, supplemented by discharge weigh tanks, provided primary boundary stream mass flow rates with which to determine the primary system mass and energy balances.

The integral of the composite primary boundary flow rates obtained current primary system fluid mass. This was compared with the indicated fluid mass

obtained from component liquid level measurements and local fluid conditions. A similar check was performed on primary system total fluid energy. These closure calculations confirmed the exceptional leak integrity of OTIS. Comparisons of injected and recovered non-condensible gas volumes gave similar confirmation. Special attention was given to system sealing during OTIS design and construction. Model heat losses were also given careful consideration. Extraneous penetrations were minimized, loop structural supports were insulated, and active guard heaters were used on the hot leg, pressurizer, surge line, and upper reactor vessel. Guard heating not only countered model heat loss, but also simplified the computer code modelling of the loop -- guard-heated components could be modelled with an adiabatic boundary condition.

TEST MATRIX

The original OTIS test matrix consisted of 13 tests in the following 3 categories: (1) a benchmark test, (2) 10 single-variable tests, and (3) 2 composite tests conducted by an operator versed in plant procedures. The 10 single-variable tests consisted of 7 SBLOCA transients, an HPI-PORV (feed-and-bleed) cooldown, and 2 natural circulation cooldowns. Each of the 7 SBLOCA transients varied a single major boundary condition from the conditions of the nominal test.

Two additional tests were added to the original matrix. These tests, 2202AA and 2202BB, were based on the larger (scaled 15-cm^2) leak, Test 220201, and investigated guard heater effects. Test 2202AA repeated the 15-cm^2 leak conditions, but with the pressurizer isolated at test initiation. Test -BB then repeated the conditions of -AA, but with the guard heaters de-energized at test initiation.

SBLOCA SEQUENCE (NOMINAL TEST 220100)

The nominal and "single-variable" tests examined the effects of one major boundary condition on the post-SBLOCA transient. This transient commonly consisted of the following five phases: (1) primary depressurization and saturation of the loop fluid, (2) intermittent circulation with periods of primary repressurization, (3) condensation of primary vapor in the SG, the so-called "boiler-condenser mode", (4) refill, and (5) post-refill natural circulation and cooldown. The nominal Test 220100 encountered each of these phases, as described below.

During the first phase, the primary system depressurization following leak actuation was relatively rapid; it was augmented when the pressurizer drained, but abruptly halted when the loop (and/or reactor vessel) fluid reached saturation. The hot leg U-bend defined the highest-elevation loop fluid between the core and the steam generator. When the fluid in this region saturated and then separated, the absence of liquid at the spillover abruptly interrupted loop flow. The continuing core energy deposition caused heating of the core-region fluid and primary repressurization. Loop flow restarted sporadically, attenuating these repressurizations. These reinitiations of loop flow were generally attributable to two different types of interactions. The earlier flow restarts were triggered by the heating and expansion of the core-region and lower hot leg fluid, as well as by voiding in the upper reactor vessel which displaced liquid into the hot leg. The later resurgence of loop flow, on the other hand, coincided with the decrease of the reactor vessel collapsed liquid level to the elevation of the hot leg nozzle, and was thus caused by vapor flow through the hot leg.

The continuing depletion of primary liquid inventory ultimately precluded further spillover circulation. During this period, core power was generally offset by HPI-leak cooling, which was enabled by reactor vessel vent valve (RVVV or internals vent valve) actuation. The RVVV discharged core-heated fluid to the downcomer where it mixed with HPI-cooled fluid. The condensed and cooled fluid continued down the downcomer to the core inlet, completing the inner flow loop.

The primary-to-secondary decoupling usually persisted until the SG began to condense primary vapor, the BCM (Boiler-Condenser Mode) phase. If auxiliary feedwater (AFW) was active when primary vapor was adjacent to the AFW injection elevation, the AFW BCM would occur. Should the primary level decrease to the elevation of the SG secondary pool or lower, primary vapor would condense in this region (as well as near the AFW injection site) and the "pool BCM" would be activated. Either type of BCM readily depressurized the primary.

The falling primary pressure diminished the leak flow and allowed increased high pressure injection flow, usually reversing the primary fluid mass depletion. This was the fourth (refill) phase of the post-SBLOCA transient.

Refill rapidly raised the primary level above the steam generator secondary pool, preventing pool BCM and later, AFW BCM. The steam generator was thus again decoupled. The primary conditions then approached equilibrium, prolonging the completion of refill. Natural circulation began shortly after refill. The primary then cooled with the secondary for the remainder of the transient.

Single-Variable Tests (Tests 220201 through 220756)

Six single-variable tests each varied one boundary condition setting from the nominal setting. These were Test 220201, leak size of 15 rather than 10 cm^2; Test 220304, half of nominal high pressure injection capacity; Test 220402, 10- rather than a 38-foot steam generator level; Test 220503, cold leg discharge rather than suction leak location; Test 220604, altered high pressure injection head-flow characteristics; and Test 220756, leak isolation. These variations from nominal were tested singly to accentuate their separate impact and, hence, to facilitate the interpretation and code modelling of the governing conditions. These six tests provided a broad range of loop responses. At one extreme, leak isolation caused early systems repressurization (but short of the relief setting), refill, and post-refill natural circulation and cooldown. The tests with increased leak size (Test 220201) and reduced high pressure injection capacity (Test 220304), on the other hand, had early and accentuated primary depressurizations. Indeed, the primary was not refilled in the half-capacity high pressure injection test, even with PORV actuation and a reduction of core power beyond the decay simulation. Core heat transfer was maintained throughout each of the tests. The inter-test variations also generated a spectrum of BCM (Boiler-Condenser Mode) responses. AFW BCM only, Pool BCM only, and both types of BCM heat transfer were observed during these single-variable tests, thus heightening their usefulness for code benchmarking.

Cooldown Tests (Tests 220899 through 221099)

Three tests examined cooldown interactions. Test 220899 enacted the HPI-PORV ("feed-and-bleed") mode of core cooling. Three phases of HPI-PORV cooling were observed: (1) relatively rapid depressurization while the pressurizer filled following PORV actuations for the initial ten minutes of the test transient, (2) continued primary depressurization but at a reduced

rate, as the PORV intermittently discharged liquid or vapor, for approximately one hour, and (3) slow primary depressurization as the upper-elevation hot leg fluid approached saturation. The rate of cooldown of the core-region fluid remained almost constant at 60F/h throughout these phases. System conditions become increasingly oscillatory as the test progressed. Actuation of the hot leg high-point vent apparently would have facilitated primary depressurization by cooling the uppermost loop fluid.

Cooldown Tests 220999 and 221099 employed steam generator cooling in natural circulation, using the reactor vessel head vent to fill and cool the head in Test 221099. Head vent actuation did permit the head to fill and cool, but natural circulation and system cooldown continued uninterrupted, while adhering to the pressure-temperature envelope, in both tests.

Two composite tests (Tests 230199 and 230299) introduced operator guidelines. An operator trained in plant procedures controlled the test evolutions. The initialization and initiation conditions paralleled those of the single-variable tests except that auxiliary feedwater was not available until one hour after test initiation. Also, the 10-cm^2 cold leg suction leak was isolated after 30 minutes of testing. Both tests simulated full high pressure injection (HPI) capacity. Test 230199 simulated high-head HPI characteristics, while low-head HPI was simulated in Test 230299. The operator controlled system conditions similarly in the two tests. With feedwater unavailable, the operator used intermittent PORV actuations to control primary pressure. When auxiliary feedwater became available, the operator used throttled feedwater to depressurize the primary through the BCM. Refill, post-refill circulation, and cooldown were rapidly achieved. The operator felt that model interactions were realistic and would provide valuable experience for plant operators.

Guard Heater Tests 2202AA and -BB

Guard heater Tests 2202AA and 2202BB were added to the OTIS test matrix to explore the effects of guard heating. Both were based on the "single-variable" Test 220201 which used a scaled 15-cm^2 (cold leg discharge) leak. This test was chosen for reference because the increased leak size obtained lower-than-usual primary pressures and, hence, an increased difference between the loop saturation temperature and the temperature at which the

guard heaters had been adjusted. Guard heater Test 2202AA replicated the conditions of Test 220201 except that the pressurizer (and hence the effects of pressurizer guard heating) was isolated. In Test 2202BB the pressurizer was isolated and all the guard heaters were de-energized upon test initiation.

These tests indicated that OTIS guard heating had little impact on the depressurization phases of the transient -- even without guard heating, the metal stored heat was sufficient to superheat the (upper elevation) hot leg vapor. Guard heating did delay refill by increasing both the amount of primary repressurization during refill and the excess (upper-elevation) metal temperatures that needed to be quenched upon refill. These guard heater tests also indicated the effect of RVVV control during refill. As the hot leg liquid level was elevated to the spillover elevation, the intermittent flow perturbed the differential pressure across the RVVV. The valve may have closed had its control been in automatic (it was generally in manual-open at this stage in the transient to prevent valve cycling and hence, to avoid valve failure). If the valve had closed during the latter stages of the refill phase, the resulting flow diversion may have sustained primary-to-secondary heat transfer, reducing primary pressure and completing the system refill.

SUMMARY

OTIS was a 1 x 1 full-elevation model of a domestic, raised-loop B&W plant. Testing was performed to obtain integral system data for code benchmarking. The following post-SBLOCA events were encountered in OTIS: depressurization to loop saturation, intermittent circulation with repressurization, the BCM (Boiler-Condenser Mode), refill with HPI-leak cooling, and post-refill circulation, cooldown, and depressurization.

The BCM was an effective means of primary depressurization and heat removal. The following two types of BCM were observed:

- AFW BCM, in which primary steam was condensed by the introduction of cold AFW while the primary level in the steam generator was above that of the secondary.
- Pool BCM, where the steam generator primary level dropped below the secondary level.

System refill was generally prolonged. HPI-leak cooling kept the core-region fluid cool, but the primary often approached mass and energy equilibrium. Actuation of the hot leg high-point vent hastened refill in several tests.

The single-variable tests generated a wide range of system interactions. Various depressurization mechanisms and trends, combinations of BCMs, as well as refill responses were observed. The guard heater tests examined their impact on system interactions.

The composite tests indicated the usefulness of operator actions, as well as the ability of the model to provide operator experience. OTIS obtained a wealth of code-challenging data.

1. INTRODUCTION

The Nuclear Regulatory Commission, the B&W Owners Group, Babcock & WIlcox (B&W), and the Electric Power Research Institute sponsored a scaled, experimental facility, designated the Once-Through Integral System (OTIS), to acquire post-small break loss-of-coolant accident (SBLOCA) data for benchmarking system codes. OTIS was also used to investigate the application of the Abnormal Transient Operating Guidelines (ATOG) used in the B&W-designed nuclear steam supply system during the course of an SBLOCA. OTIS was a single-loop facility with a plant to model power scale factor of 1686. OTIS maintained the key elevations, approximate component volumes, and loop flow resistances, and simulated the major component phenomena, of a B&W raised-loop nuclear plant.

A test matrix consisting of 15 tests divided into four categories was performed. The largest group contained ten tests and was defined to parametrically obtain an extensive set of plant-typical experimental data for code benchmarking. Parameters such as leak size, leak location, and high-pressure injection shut-off head were individually varied. The remaining categories were specified to study the impact of ATOG (two tests), to note the effect of guard heater operation on observed phenomena (two tests), and to provide a data set for comparison with previous test experience (one test)[1].

The OTIS test results provide a challenging SBLOCA data set, based on plant-typical boundary system variations, for system code benchmarking. The OTIS results also illustrate the effectiveness of ATOG for rapid system recovery from an SBLOCA in OTIS.

OTIS is described in section 2 and the OTIS test specifications are summarized in section 3. Sections 4 through 10 address the individual test categories. Specifically, subsections 6.2 through 6.7 describe the six single-variable tests and subsection 6.8 provides a comparison among them. Results are summarized in section 11, while the final section provides recommendations for future testing. The development and organization of the appended OTIS data plots are provided in Appendix A, the OTIS documentation is described in Appendix B, and the equilibrium plot is explained in Appendix C.

2. SYSTEM DESCRIPTION

OTIS was an experimental test facility at the B&W Alliance Research Center[1,2]. It was designed to evaluate the thermal-hydraulic conditions in the reactor coolant system and steam generator during the natural circulation phases of an SBLOCA of a raised-loop B&W reactor. The test facility was a scaled 1x1 (one hot leg, one cold leg) electrically heated loop simulating the important features of the plant. Separate-effect and integral system tests were performed at scaled power levels of 1 to 5% of full power.

The loop consisted of one 19-tube once-through steam generator (OTSG), a simulated reactor, a pressurizer, a single hot leg, and a single cold leg. Reactor decay heat following a scram was simulated by electrical heaters in the reactor vessel. No pump was included in the basic system, but a multipurpose pump in an isolatable cold leg bypass line could be used to provide forced primary flow. The test loop, approximately 95 feet high, retained the full raised-loop plant elevations, and was shortened to approximately 6 feet in the horizontal plane to maintain approximate volumetric scaling.

Other primary loop components included a reactor vessel vent valve (RVVV), pressurizer power-operated relief valve (PORV), and hot leg and reactor vessel high point vents. Auxiliary systems were available for scaled high-pressure injection, controlled primary leaks in both the two-phase and single-phase regions, auxiliary feedwater to the steam generator, steam generator steam pressure control, gas addition, and gas sampling.

2.1 Scaling

OTIS scaling is documented in the OTIS Design Requirements[1] which supplement the GERDA* Design Requirements (B&W Document No. 12-1123163-01).

---

* "GERDA" is an acronym for the Geradrohr Dampferzeuger Anlage, German for "straight-tube steam generator facility." GERDA was designed, constructed, and tested as a joint effort by Brown Boveri Reaktor and B&W. GERDA testing preceded OTIS; both test programs used the same basic test facility at the Alliance Research Center.

The configuration of the test loop was dictated by scaling considerations. The four scaling criteria used to configure OTIS, in order of priority were as follows:

1. Elevations
2. Post-SBLOCA flow phenomena
3. Volumes
4. Irrecoverable pressure losses

OTIS power and volume scaling originated with the size of the model steam generator. The model steam generator contained 19 full-length and plant-typical tubes, which represented the 16,013 tubes in each of the two steam generators used in the 205-fuel assembly plants. Therefore, the dominant power and volume scaling in the loop was

$$\text{Scaling Factor} = \frac{2 \times 16013}{19} = 1686. \qquad (2\text{-}1)$$

The distance between secondary faces of the lower and upper tubesheets in the 19-tube steam generator was full length. Auxiliary feedwater nozzles were located at two elevations in the model steam generator. The tubesheet thicknesses in the model steam generator were not plant-typical, and the model inlet and outlet plenums were reducers. Therefore, the hot leg-to-steam generator inlet and steam generator-to-cold leg lengths were atypical. Piping extensions beyond the steam generator inlet and exit plenums were used to retain plant-typical elevations.

The hot leg inside diameter was scaled to preserve Froude number, and thus, the ratio of fluid inertial-to-buoyant forces. This criterion was invoked to approximately preserve two-phase flow regimes and reflooding phenomenon according to certain correlations. Scaling with Froude number resulted in a hot leg diameter twice that indicated by ideal volumetric scaling. Although this added approximately 20% to the ideal system (total loop) volume, this choice of hot leg inside diameter was considered most likely to avoid the whole-pipe slugging behavior which had been observed in other scaled SBLOCA test facilities.

The spillover elevation of the plant hot leg U-bend was retained in OTIS by matching the elevations of the bottom (inside) of the plant and model hot

leg U-bend pipes. The radius of the U-bend obtained exact volumetric scaling of this component.

The pressurizer in OTIS was volume and elevation scaled. The elevation of the bottom of the pressurizer was plant typical, as was the spillunder elevation of the pressurizer surge line. The centerline elevation of the hot leg-to-pressurizer surge connection matched that of the plant.

An electrically heated reactor vessel provided heat input to the primary fluid to simulate reactor decay heat levels up to 8% of scaled full power. Based on a plant power rating of 3600 MWt, 1% of scaled full power in OTIS was 21.4 kW. The model core heat input capacity was 180 kW. OTIS primary system flow scaling obtained 1% of scaled full flow = 0.259 lbm/s; on the secondary side, 1% of scaled full secondary flow = 0.0265 lbm/s. These conversion factors are discussed in more detail in the OTIS Test Specification[3], and are listed in Table 2.1.

The annular downcomer of the plant reactor vessel was simulated by a single external downcomer in OTIS. The spillunder elevation in the horizontal run at the bottom of the model downcomer corresponded to the elevation of the uppermost flow hole in the plant lower plenum cylinder. The OTIS reactor vessel consisted of three regions: a lower plenum, a heated section, and an upper and top plenum. The center of the heated length of the model core corresponded to the center of the active fuel length in the plant core. (The model heated length was half of full scale). The core region of the model reactor vessel contained excess volume due to construction constraints; therefore, to maintain the total reactor vessel scaled volume, the reactor vessel was shorter than plant-typical. Non-flow lengths were sacrificed to maintain the reactor vessel scaled volume.

The center of the cold leg-to-downcomer connection in OTIS matched the cold leg-to-reactor vessel nozzle centerline in the plant. Similarly, the center of the hot leg-to-upper plenum connection in OTIS corresponded to the reactor vessel-to-hot leg nozzle centerline in the plant. The model cold leg did not contain an in-loop pump, since OTIS was designed to simulate the natural circulation phases of an SBLOCA. Upstream of the reactor coolant pump spillover point, a flange was provided in the cold leg piping to admit a flow restrictor which simulated the irrecoverable pressure loss characteristic of a stalled reactor coolant pump rotor. The model

cold leg originated at the lower plenum of the 19-tube OTSG and extended downward to match the spillunder elevation of the plant cold leg. The highest point in the cold leg (the spillover into the sloping cold leg discharge line) matched the reactor coolant pump spillover elevation in the plant. Because horizontal distances were shortened in OTIS, the slope of the cold leg discharge line was atypically large.

OTIS atypicalities are summarized as follows:

- OTIS was predominantly a one-dimensional, vertical system, due to the shortened horizontal distances and small cross sections of the various components, such as the piping, steam generator, and reactor vessel.
- Because of the small size of the piping used in the model, the ratio of loop piping wall surface area-to-fluid volume was approximately 20 times that of the plant. Therefore, the fluid and wall-surface temperatures were much more closely coupled than those of a plant.
- In high-pressure models, the ratio of metal volume-to-fluid volume increases as the model piping is made smaller. The ratio of model metal volume-to-fluid volume in OTIS was approximately twice that of the plant.

The pipe surface-to-fluid volume ratio atypicality results in higher heat losses in the scaled facilities than in the plants. The effect was minimized by using both guard heaters and passive insulation on the model piping. Guard heating was used for the OTIS hot leg, pressurizer, surgeline, and reactor vessel upper head.

The OTIS secondary system provided the steam generator secondary inventory and those fluid boundary conditions which affect SBLOCA phenomena. These included the steam generator level, auxiliary feedwater flow rate, and steam pressure control systems.

The OTIS instrumentation included: pressure and differential-pressure measurements; thermocouple and resistance temperature detector measurements of fluid, metal, and insulation temperatures; level and phase indications by optical-ports and conductivity probes, as well as by differential pressures; and Pitot tubes and flowmeters for measurements of flow rates in the loop. In addition to these measurements, the following loop boundary flow

rates were metered: high pressure injection, venting (hot leg and reactor vessel), (controlled) leak, PORV, and secondary steam and feed. Noncondensible gas (NCG) injections were controlled and metered; NCG discharges with the two-phase primary effluent streams were measured; and the aggregate primary effluent was cooled and collected for integrated metering. OTIS instrumentation consisted of approximately 250 channels of data which were processed by a high-speed data acquisition system. The data acquisition rate could be either event-actuated, or adjusted by the loop operator to acquire and store a full set of data as often as every five seconds.

2.2 Features

OTIS consisted of a closed primary loop, closed secondary loop, and several auxiliary systems. A general arrangement showing the relationship of the key components of these systems is shown in Figure 2.1. The key features are as follows:

- Multiple leak locations
- Guard heating
- Scaled high pressure injection
- Simulated reactor vessel vent valve
- Steam generator level control
- Automatic cooldown
- High- and low-elevation auxiliary feedwater addition

Controlled leaks were located at the bottom of the lower plenum of the reactor vessel, in the cold leg upstream of the simulated reactor coolant pump (RCP) spillover, in the cold leg downstream of the RCP spillover, at the high-point vents (at the top of the hot leg U-bend and in the reactor vessel upper head), and at the simulated PORV at the top of the pressurizer. Leak flow rate was controlled by an orifice located just downstream of the leak site. The leak flow control orifice was located in a 5/8-inch diameter tube, as shown in Figure 2.2. The details of the orifice design are illustrated in Figure 2.3. Scaled leaks of 10 cm^2 and 15 cm^2 were tested in the single-phase regions (cold leg leaks), while 10-cm^2 leaks were tested at the PORV. The actual diameter of the scaled leak was obtained using the ideal volume scaling factor of 1686. Thus, a scaled 10-cm^2 leak had a

diameter of 0.034 inches in OTIS. Throughout this report, the model leak flow area sizes are referred to in terms of their unscaled area.

To preclude leakage from the loop, sealed-stem valves were used where possible. Additionally, all instrument fittings in the reactor coolant system above the top of the core heaters were seal welded. A helium leak check was performed to ensure that the loop was leak tight.

As a result of the large surface area-to-fluid volume ratio, heat loss in the loop was proportionally greater than that in a plant. To minimize this effect, guard heaters were used along the hot leg piping, pressurizer, surge line, and reactor vessel upper head. The objective of the guard heating system was to provide heat to the components in an amount equal to the heat loss of that component to ambient. The concept used for guard heating is illustrated in Figure 2.4. A layer of control insulation, approximately 1/2-inch thick, enclosed by a thin shell of stainless steel lagging, was placed over the pipe sections to be guard heated. The heater tapes were spirally wrapped over the lagging material, covering nearly all of the pipe section. Two layers of passive insulation covered the guard heaters. The heaters were controlled based on the thermocouples on the pipe outside diameter and at a point midway into the control insulation. Tests were performed to evaluate the heat loss from the loop and to characterize the operation of the guard heaters.

Two high pressure injection (HPI) locations were provided -- one at the cold leg low point, upstream of the simulated RCP spillover, the other in the downward sloping cold leg, downstream of the RCP spillover. A scaled HPI flow rate was provided by a positive displacement pump. The flow into the loop was controlled to simulate the scaled head-flow curves of the plant pumps. In OTIS, HPI flow was directed exclusively to the cold leg discharge piping.

The reactor vessel vent valve (RVVV) was simulated by a single pipe extending from the upper plenum of the reactor vessel to the external downcomer. The pipe elevation matched the spillover elevation of the plant RVVV. A pneumatically operated, automatically controlled valve was located in the pipe. This valve was controlled to open and close when the

differential pressure between the reactor vessel and downcomer reached preset values. A vertically-oriented slit orifice in the pipe, downstream of the valve, established the resistance of the simulated vent valve.

The secondary loop consisted of the 19-tube steam generator, steam piping, a water-cooled condenser, hot well, feedwater pump, feedwater heater, and feedwater piping. The secondary side simulation of the plant was limited to the steam generator and the elevation of the auxiliary feedwater inlets. Additionally, the following functions were used to simulate plant performance:

1. Continuous level (inventory) control
2. Band level control
3. Steam pressure control
4. Automatic cooldown

Two modes of steam generator level control were available -- continuous level control and band level control. With continuous level control, the operator set the desired steam generator level from 0 to 100% full. The controller maintained the collapsed water level at this setpoint by adjusting the feedwater flow rate. In the band mode of steam generator level control, the operator set the desired upper and lower steam generator secondary levels. The controller then actuated when the level descended to the lower setpoint, causing feedwater to be injected at full capacity (using the simulated head-flow characteristics). When the steam generator level had been increased to the upper setpoint, the band controller caused feed to be interrupted. The signal for the collapsed level, for both modes of level control, was based on a differential pressure. Refer to the Functional Specification[2] for additional details.

The secondary loop could operate at steam pressures of approximately 200 to 1200 psia. Steam pressure was automatically controlled by a steam control valve, based on a signal from the steam pressure transmitter. In addition to automatic steam pressure control, the steam pressure could be controlled to decrease at a pre-programmed rate. This feature allowed the simulation of a controlled cooldown. The desired cooldown rate was keyed into the controller as a series of linear segments of pressure versus time. When activated, the steam pressure control valve modulated to obtain the stipulated depressurization rate.

Auxiliary feedwater (AFW) could be injected at either of two locations in the steam generator -- at a high elevation, typical of the domestic B&W plants, or at a low elevation. The AFW nozzle at either elevation could be configured for maximum wetting or for minimum wetting of the steam generator tubes. The two configurations allowed the comparison of the effects of the spray pattern on heat transfer (typical of the outer rows of tubes near the AFW nozzles in the plant) with the effects of pool heat transfer (typical of the large majority of tubes that are away from the AFW nozzles in the plant).

The OTIS arrangement and instrumentation are further illustrated in Figures 2.5 through 2.12.

The instrument indications are tabulated in the final pages of Appendix A. This tabulation is arranged by component, instrument type, and elevation.

2.3 Boundary System Simulations

Boundary system simulations are defined in the OTIS Test Specification[3]. Their incorporation into OTIS is described in detail in the OTIS Loop Functional Specification.[2] Their application during testing is prescribed in the tests procedures.[4,5]

2.3.1 Post-Trip Power

Post-trip power is the sum of post-trip fissions and the decay of radioactive nuclides. The post-trip fission contribution has been calculated using a point neutron kinetics code with thermal-hydraulic feedback assuming a reactivity insertion which is the smallest expected for the 177-FA (fuel assembly) lowered-loop plants. The reactivity data was gathered from the 177-FA plants, rather than from the 205-FA plants, to take advantage of the operating history and multiple fuel reloads of the 177-FA plants; the post-trip power levels of the two types of plants (expressed as a fraction of their respective full power levels) are expected to be similar. The decay contribution has been calculated using the methods of ANS 5.1 for a plant tripped from ten years of operation at full power. The calculations are described in References 6, 7, and 8. The results of these calculations (with power expressed as percentage of full power versus time after reactor trip) were used in OTIS. These results are repeated in Table 2.1 and

Figure 2.13 herein. Recall that 1% of scaled full power in OTIS is approximately 21.4 kW. Also note that test facility conduction heat losses to ambient ($\sim$1/2% of scaled full power) must be added to these power-versus-time values for the simulation of power decay.

2.3.2 High-Pressure Injection (HPI)

Two sets of HPI head-flow characteristics were to be simulated in OTIS: high-head and full-capacity HPI and low-head, full-capacity HPI.* The high- and low-head characteristics were taken from those of the TVA Bellefonte plant (a domestic, raised-loop, 205-FA plant) and the Davis-Besse plant (a domestic, raised-loop 177-FA plant), Figure 2.14. These plant HPI flow rates were applied to the OTIS HPI simulation by dividing the Bellefonte and Davis-Besse capacities by 1686 and 1300, respectively. The results are given in Figure 2.15.

The OTIS (full-head, high-capacity) HPI head-flow response is compared to leak flow rate in Figure 2.16. The leak size is 10 cm^2 in the liquid region; the leak is assumed to discharge saturated liquid. The equilibrium pressure (the pressure at which the HPI mass flow rate equals leak discharge) is between approximately 1200 and 2200 psia. As the leak-source fluid subcools (such as by drawing HPI fluid to the leak site without significant heating), the leak flow rate increases and the equilibrium pressure drops. Equilibrium may then be obtained at $\sim$1000 psia, at which pressure the HPI flow rate is approximately 80% of the maximum HPI flow rate. The uncertainties attendant to these leak-HPI equilibrium estimates plus the limited capacity of the HPI suggests that the low-pressure injection (LPI) contribution be considered. LPI need not be specifically modelled, rather the HPI head-flow characteristics can be modified to approximate the LPI effects; this modification serves to more realistically limit the lowest leak-HPI/LPI mass flow rate equilibrium pressure. The resulting LPI-supplemented HPI head-flow characteristics to be used in OTIS are shown in Figure 2.17 and Table 2.2.

---

*The half-capacity test is to use one-half of the high-head, full capacity HPI flow rate.

2.3.3 Auxiliary Feedwater (AFW) Characteristics

AFW characteristics, typical for a 205-FA plant, are shown in Figure 2.18. Figure 2.19 shows the OTIS-scaled AFW head-flow curve using the 1686 scale factor (curve "TVA & OTIS"). Also shown is the Davis-Besse AFW characteristic curve[9] scaled by 1300 (curve "DB").

2.3.4 Pressure-Temperature Limitations

The plant Technical Specifications require the operator to maintain the plant conditions within the bounds defined by a p-T envelope. These p-T bounds are set by the limits defined in the key of Figure 2.20. Plant p-T (pressure-temperature) limitations were invoked for the natural circulation cooldown and composite tests. Figure 2.20 gives the p-T envelope for Davis-Besse.[10]

Table 2.1 OTIS Conversion Factors

OTIS power levels and flowrates are generally expressed as percents of scaled full power and full flow. This usage was adopted to facilitate the conversion between model and plant values, and also to facilitate data interpretation among users having different customary systems of units. The OTIS scaling factor is 1686, refer to Appendix A for additional discussion.

Quantity	Units: Normalized	English	SI
Power Level	1% (of scaled full power)	20.3 Btu/s	21.4 kw
Primary Flowrate	1% (of scaled full primary flowrate)	0.259 lbm/s	0.117 kg/s
Secondary Flowrate	1% (of scaled full secondary flowrate)	0.0265 lbm/s	0.0120 kg/s

Table 2.2 POST TRIP POWER.[6,7,8]

Time After Reactor Trip	Power, % Full Power		
	Fission	Decay	Total
0.5 min	2.51	3.64	6.15
1	1.27	3.26	4.53
1.5	0.63	3.03	3.66
2	0.33	2.87	3.20
2.5	0.18	2.76	2.94
3	0.11	2.67	2.78
4	0.04	2.53	2.57
4.5	0.03	2.48	2.51
5	0.02	2.43	2.45
6	0.01	2.34	2.35
10	0	2.12	2.12
20		(decay only)	1.80
40 min			1.47
1 h			1.28
2			1.02
4			0.85
8			0.73
12 h			0.67

Table 2.3 OTIS LPI-Supplemented HPI Characteristics.

Points from Figure 2.17. Lowest-pressure points (*) reflect LPI.

Pressure, psia	OTIS Flow Rate (lb_m/s)	
	Low-head, Full Capacity**	High-head, Full Capacity
182	0.47*	---
186	0.186	---
200	0.184	---
230	---	0.37*
240	---	0.123
400	0.172	0.119
800	0.144	0.109
1200	0.108	0.098
1600	0.036	0.086
1630	0	---
2000	---	0.072
2400	---	0.049

**Full capacity denotes the simulation of two plant HPI pumps plus the simulation of two plant LPI pumps when applicable.

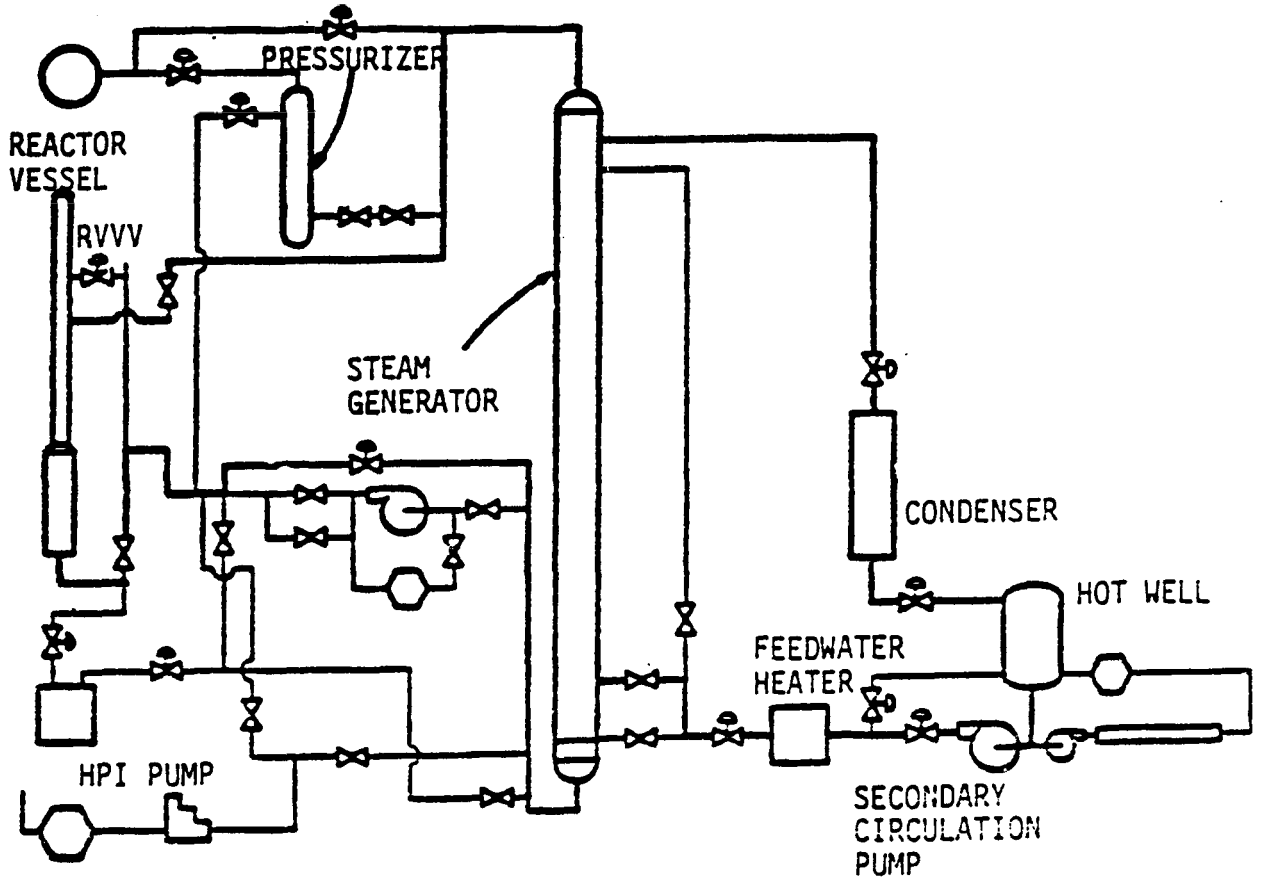

Figure 2.1 OTIS General Arrangement

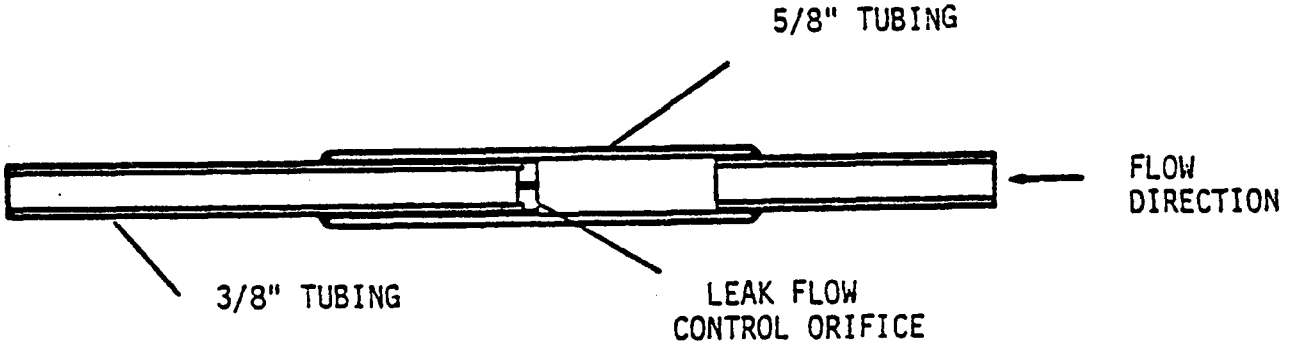

Figure 2.2 Leak Flow Control Orifice Assembly

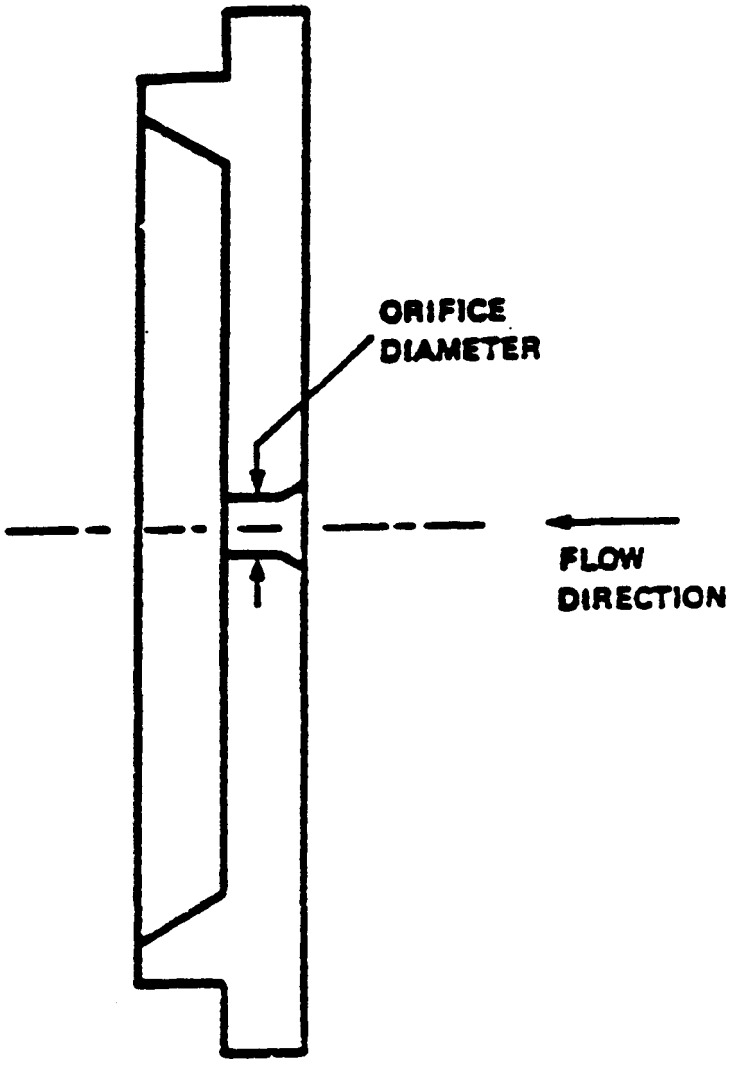

Figure 2.3 Leak Flow Control Orifice

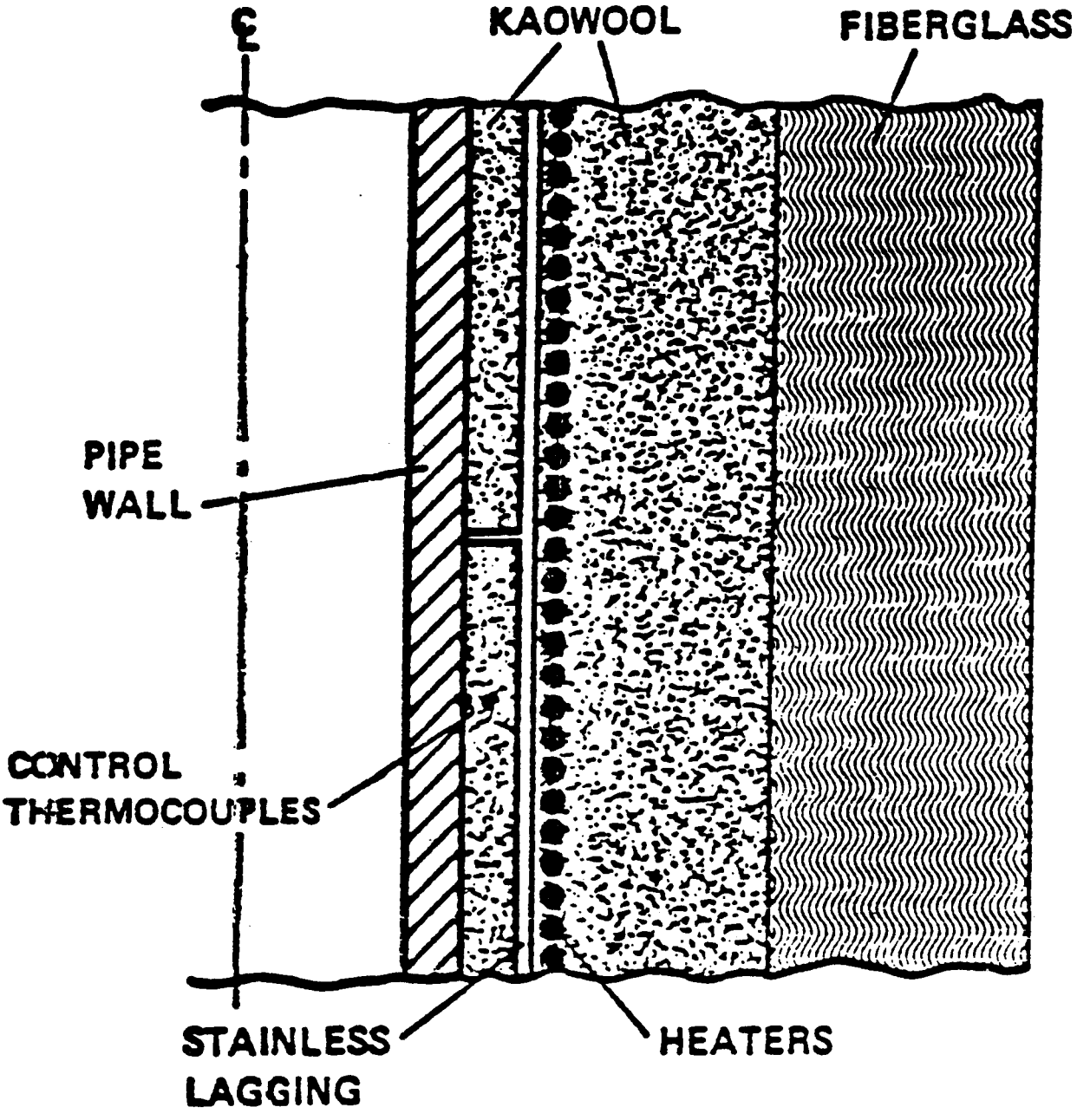

Figure 2.4 Guard Heater Concept

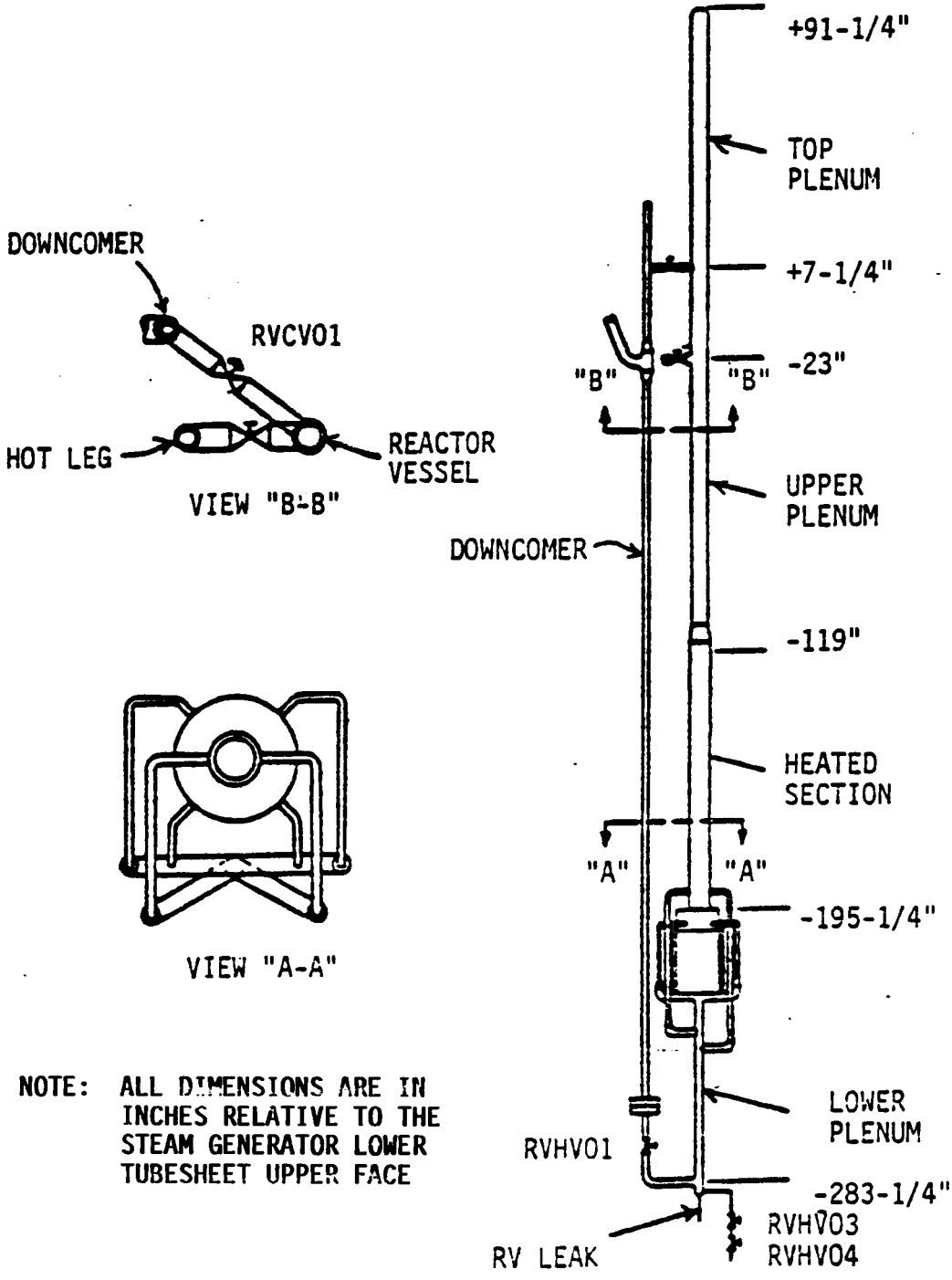

Figure 2.5 Reactor Vessel and Downcomer General Arrangement

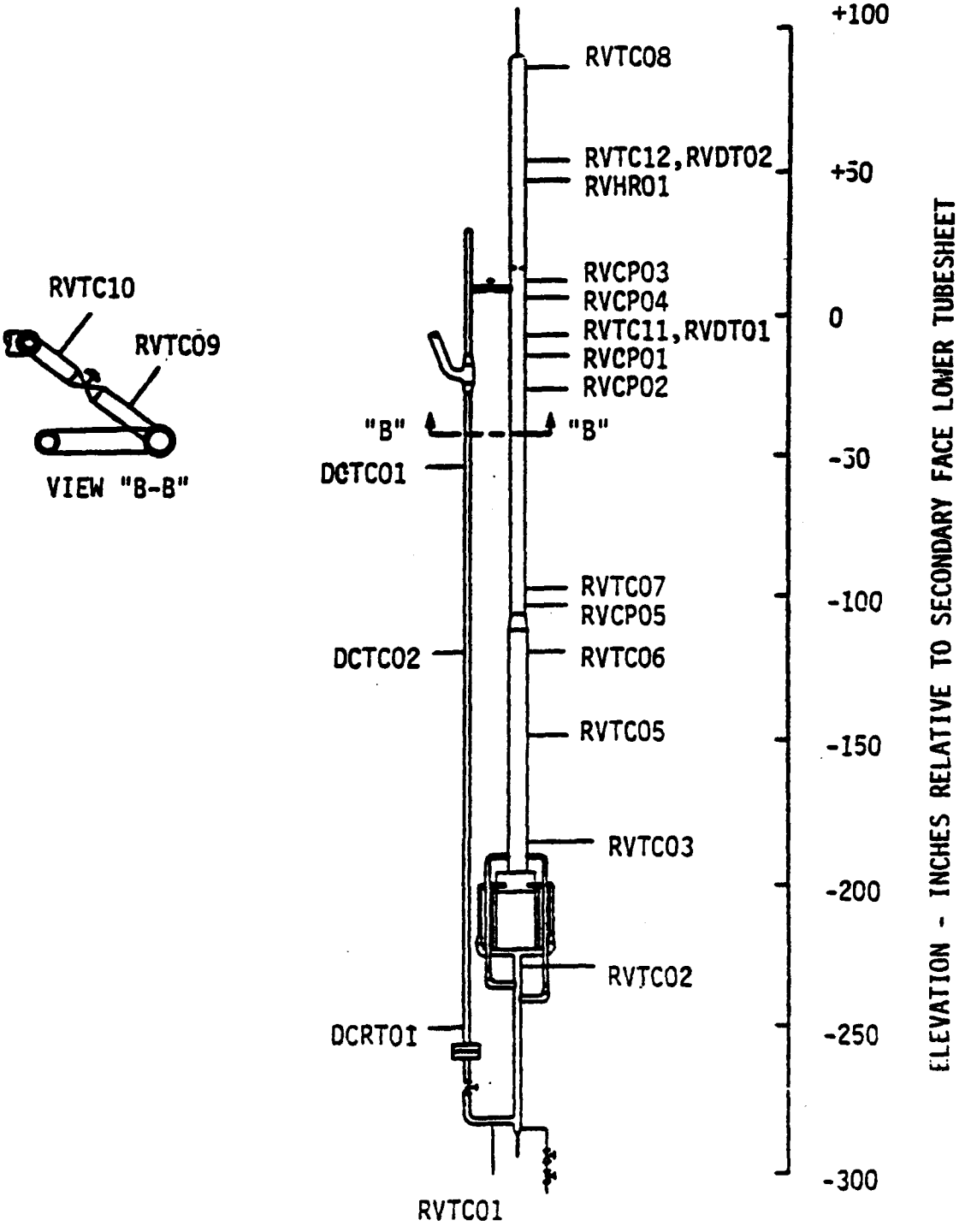

Figure 2.6 Reactor Vessel and Downcomer Instrumentation -- Thermocouples.

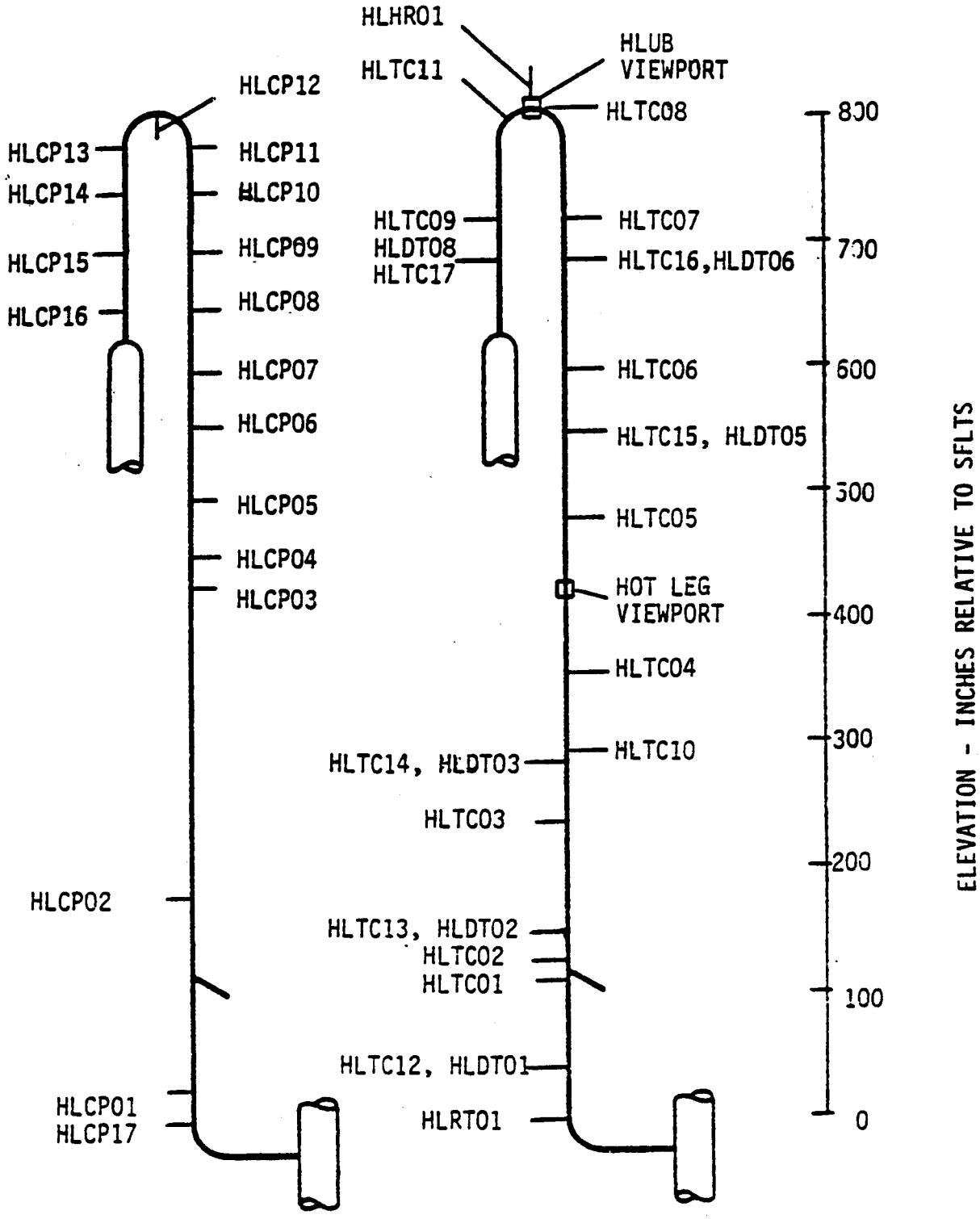

Figure 2.7 Hot Leg Instrumentation -- Thermocouples, RTDs, Conductivity Probes, and Viewports

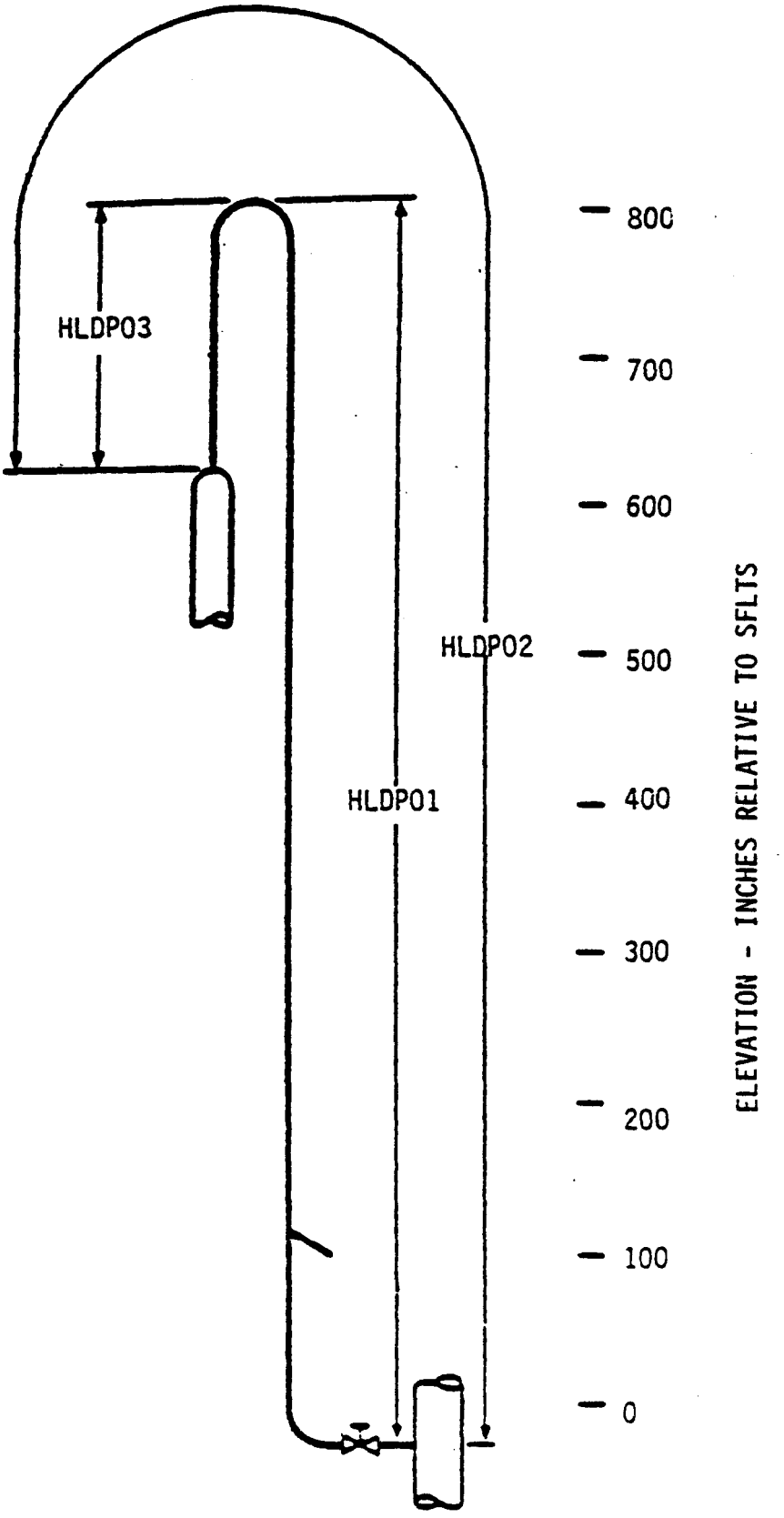

Figure 2.8 Hot Leg Instrumentation -- Differential Pressure Measurements

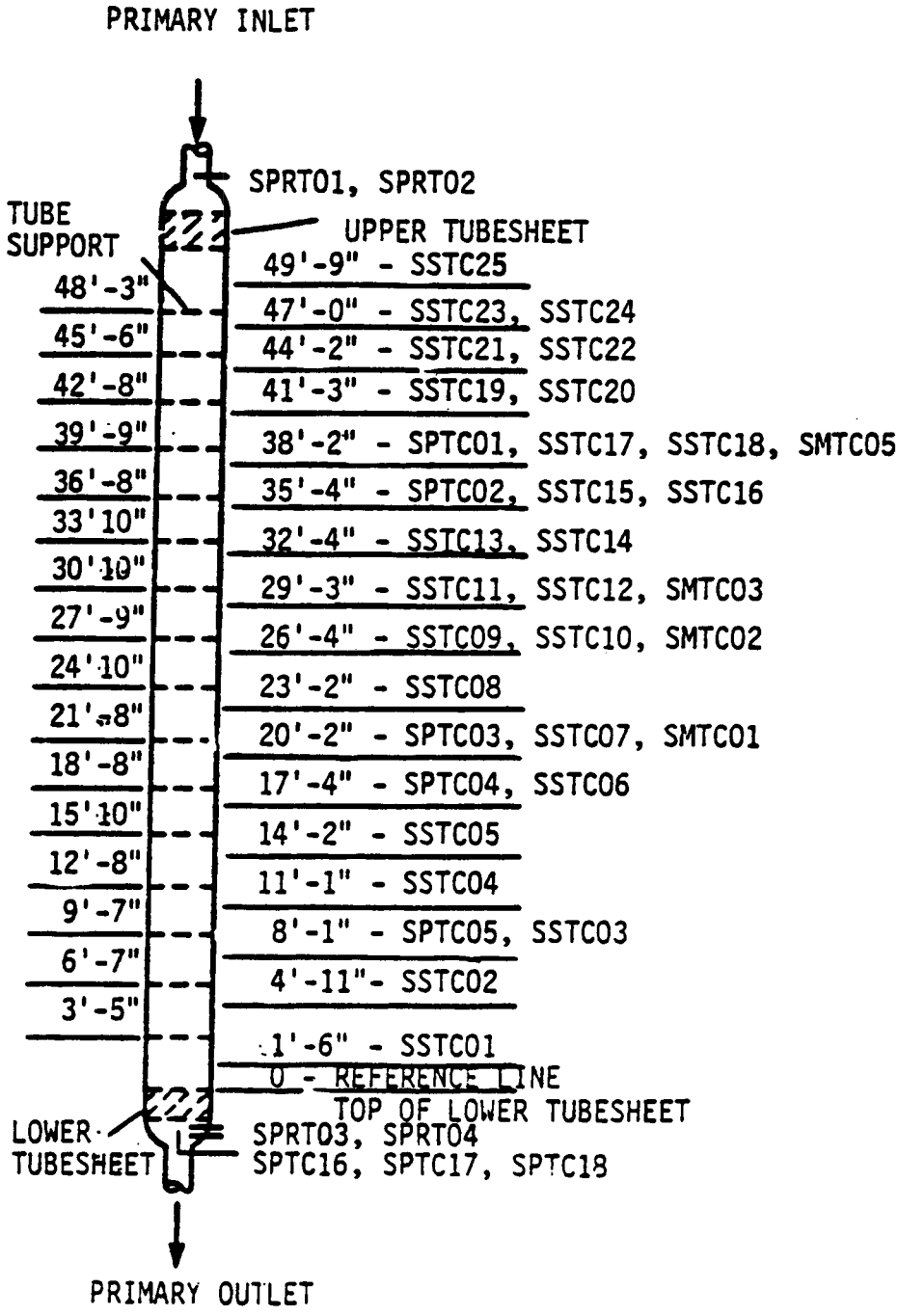

Figure 2.9 OTSG Temperature Measurements and Tube Support Plate Elevations

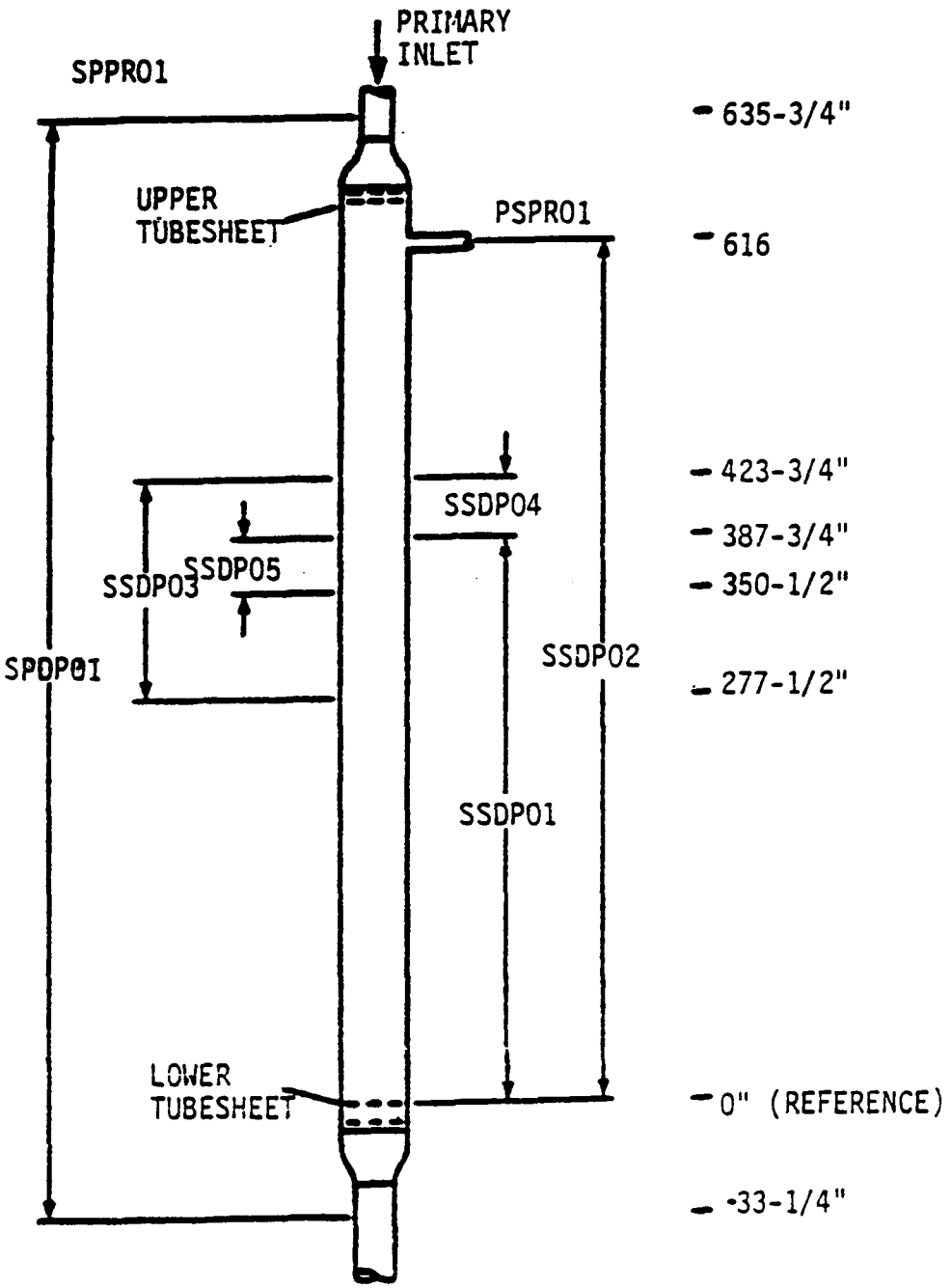

Figure 2.10 OTSG Pressure and Differential Pressure Measurements

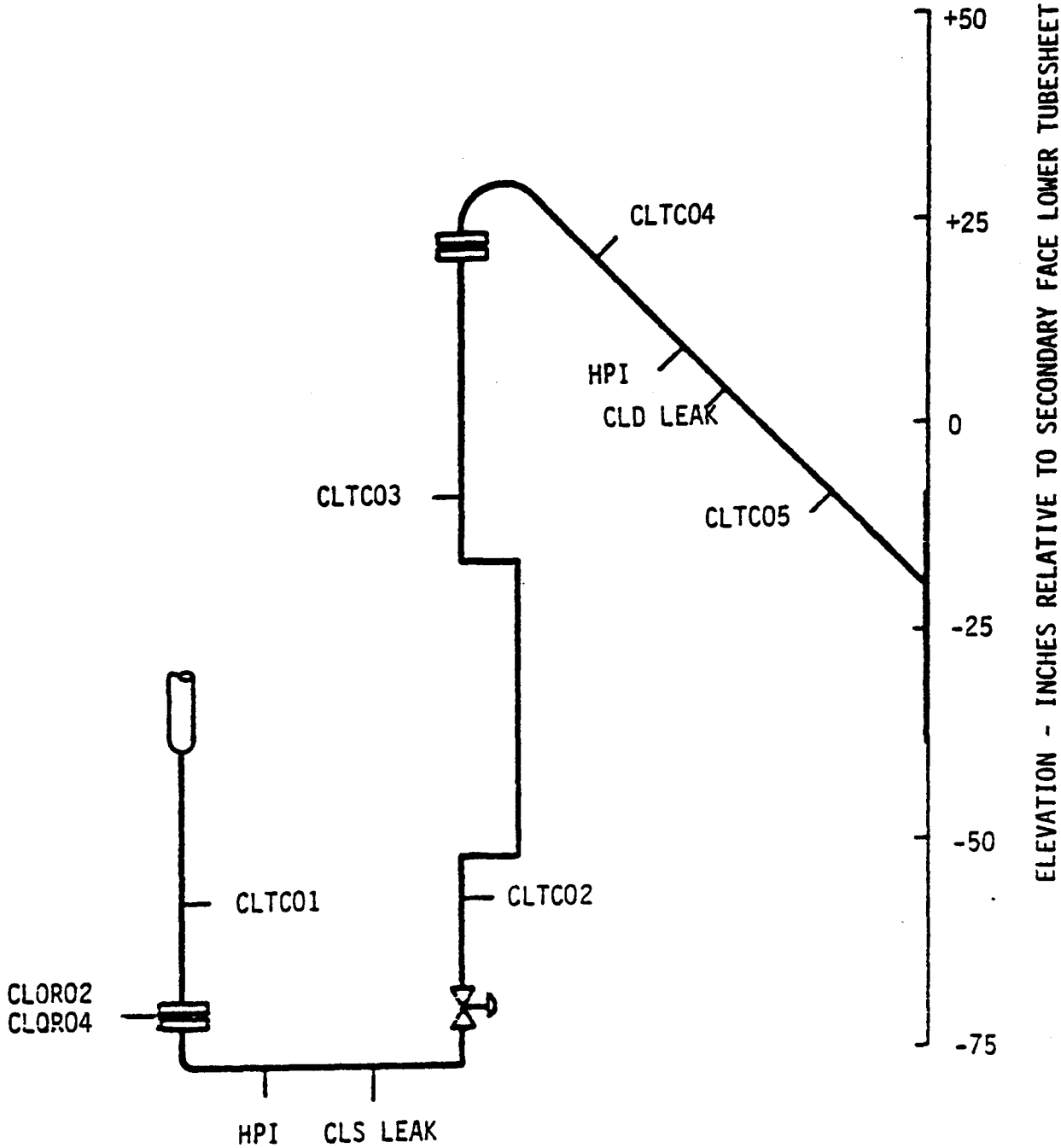

Figure 2.11 Cold Leg Piping -- Temperature and Flow Measurements, Location of HPI and Cold Leg Leaks

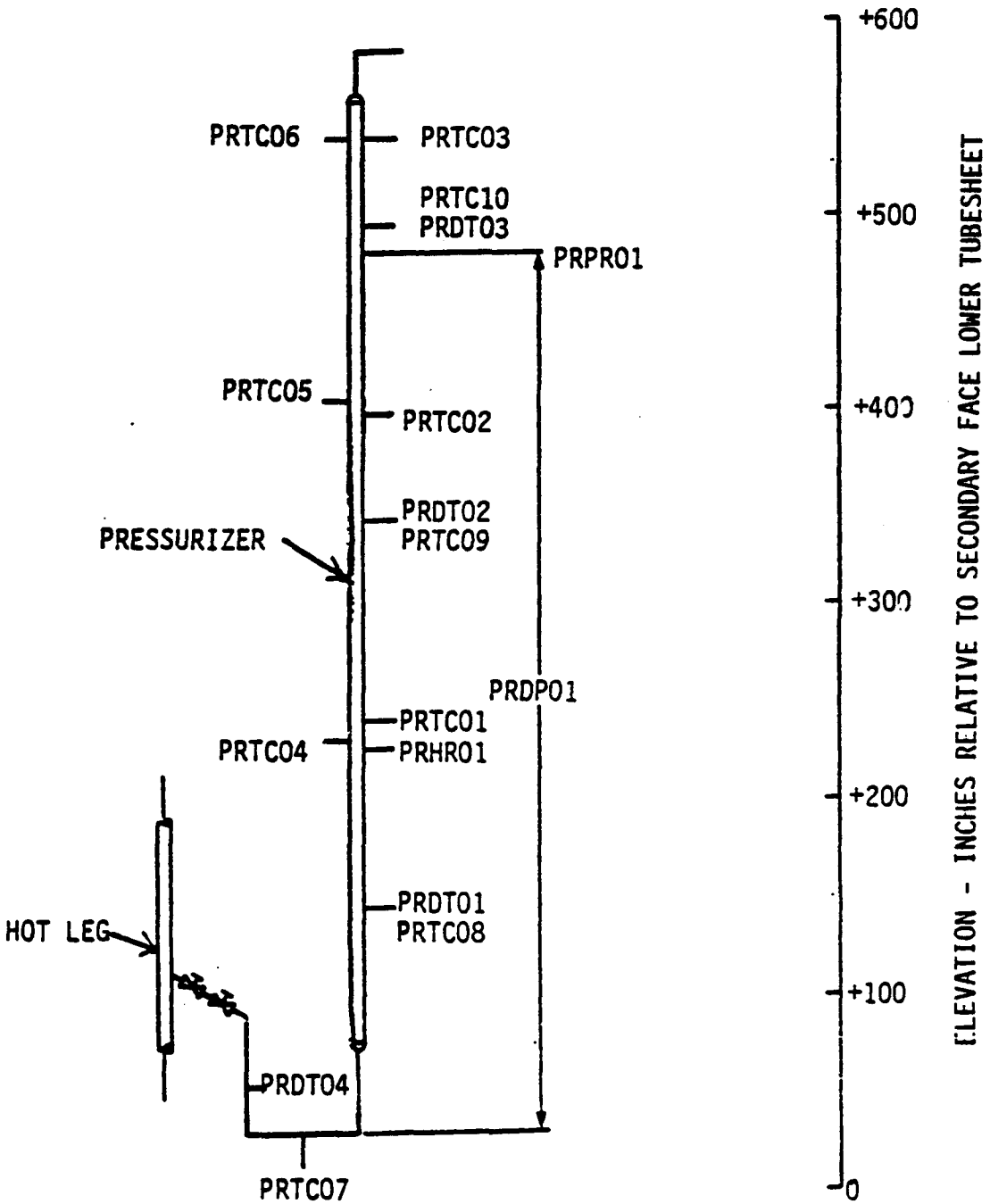

Figure 2.12 Pressurizer Instrumentation

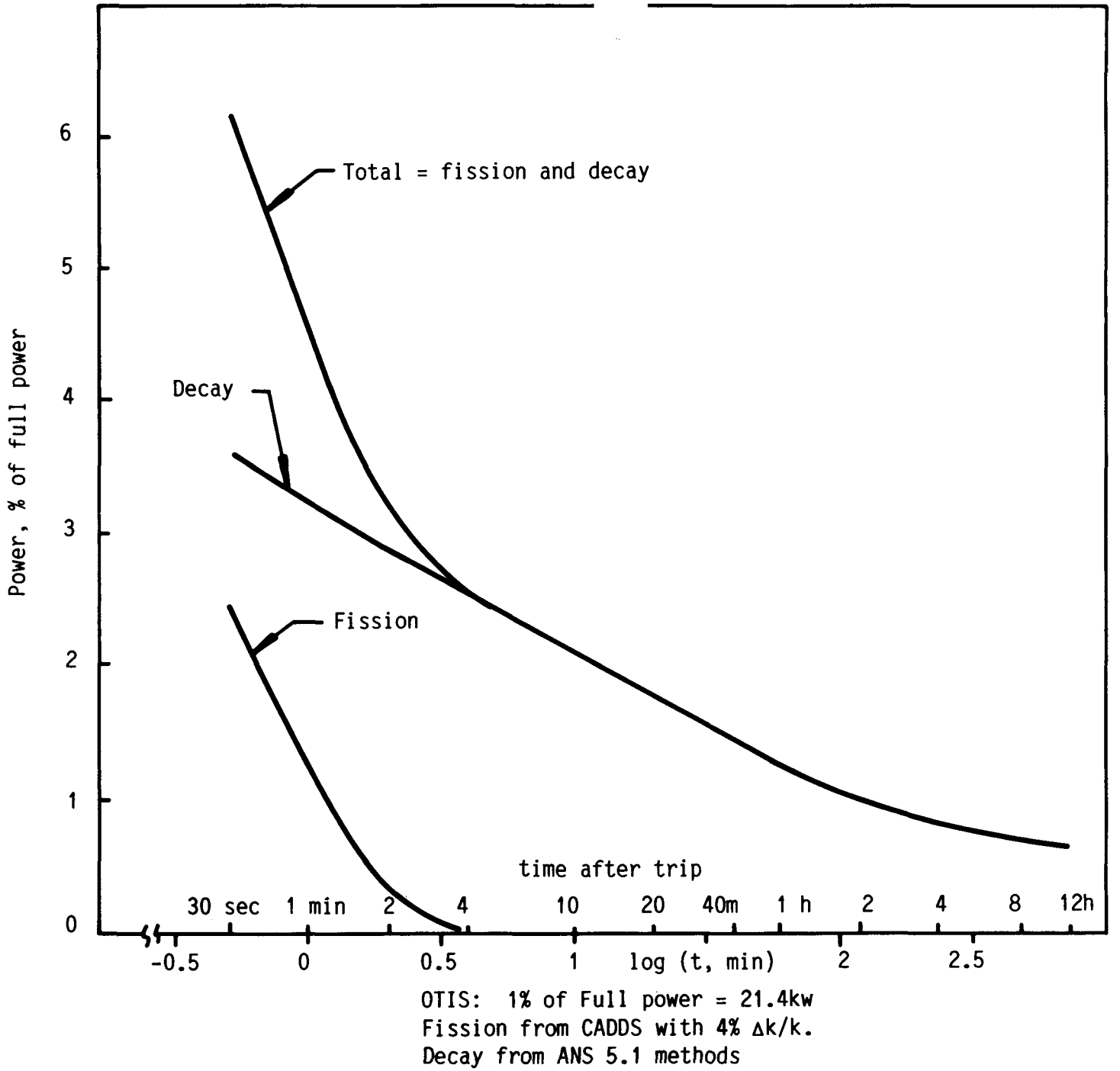

Figure 2.13 Post-Trip Core Power

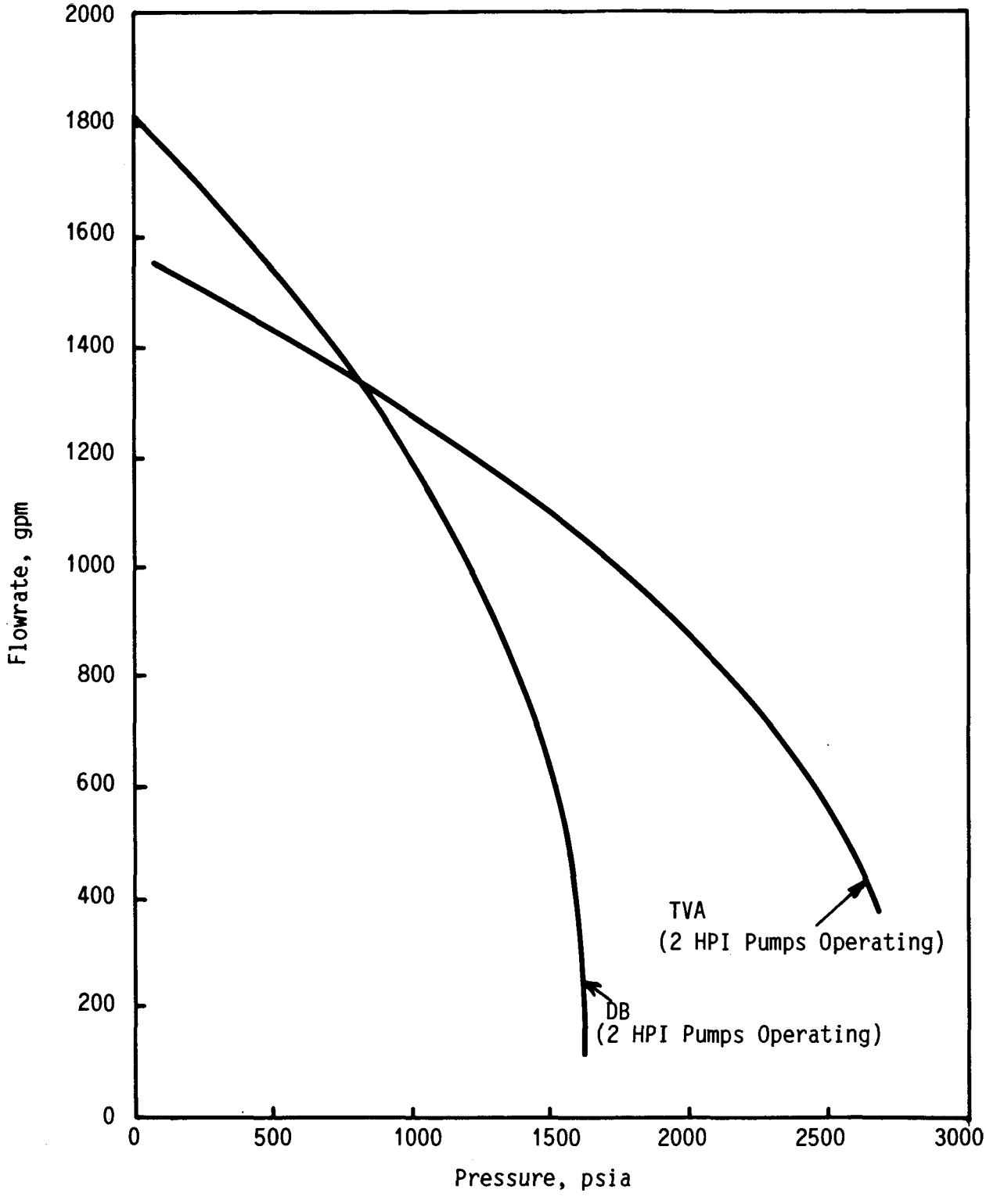

Source: Davis Besse: 74-1125531-00
TVA: ATOG, 74-1135402-00

Figure 2.14 Plant HPI Flowrates

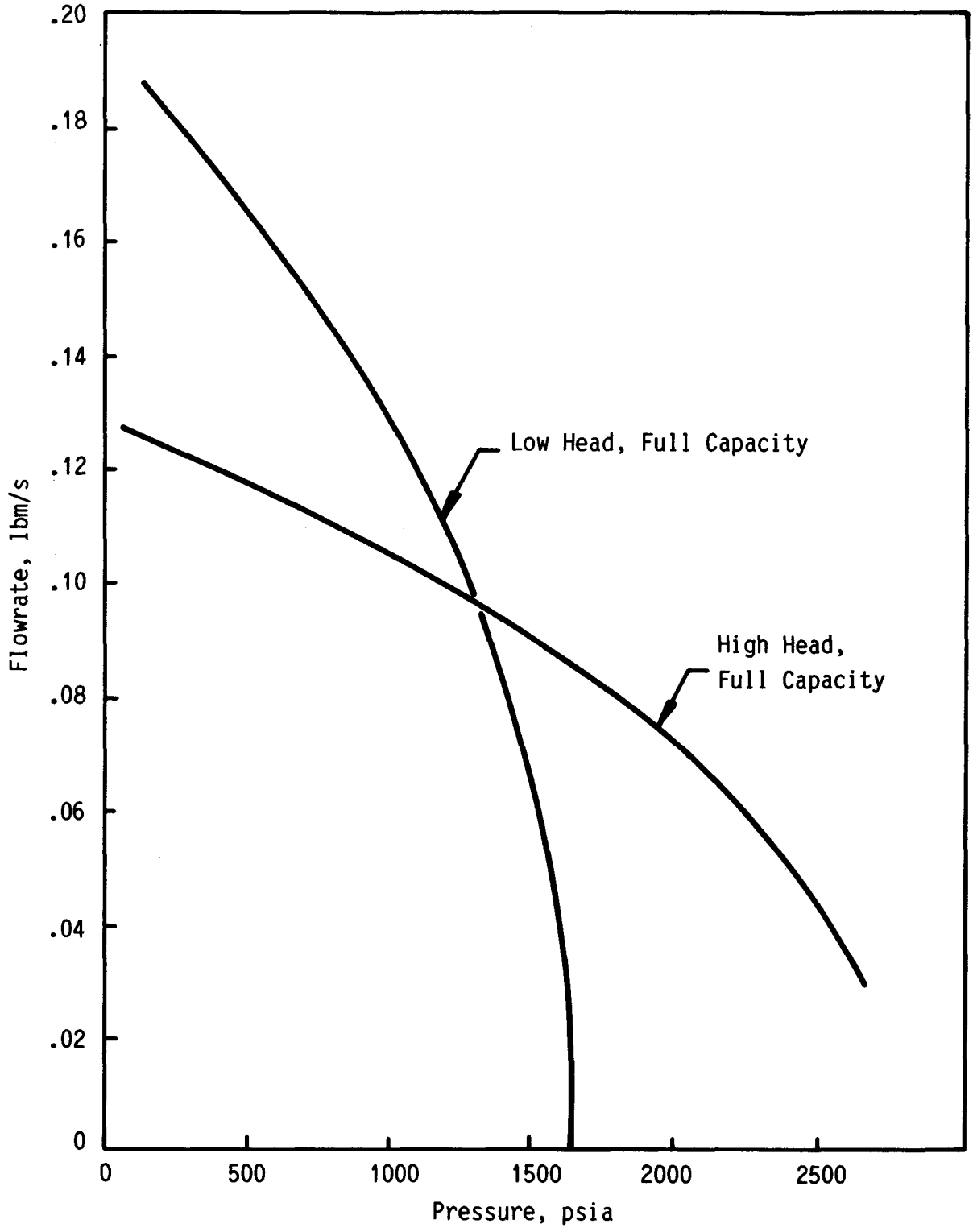

"High Head Full Capacity": TVA/1686
"Low Head, Full Capacity": DB/1300

Full Capacity Denotes the Simulation of Two Plant HPI Pumps

Figure 2.15 OTIS HPI Characteristics

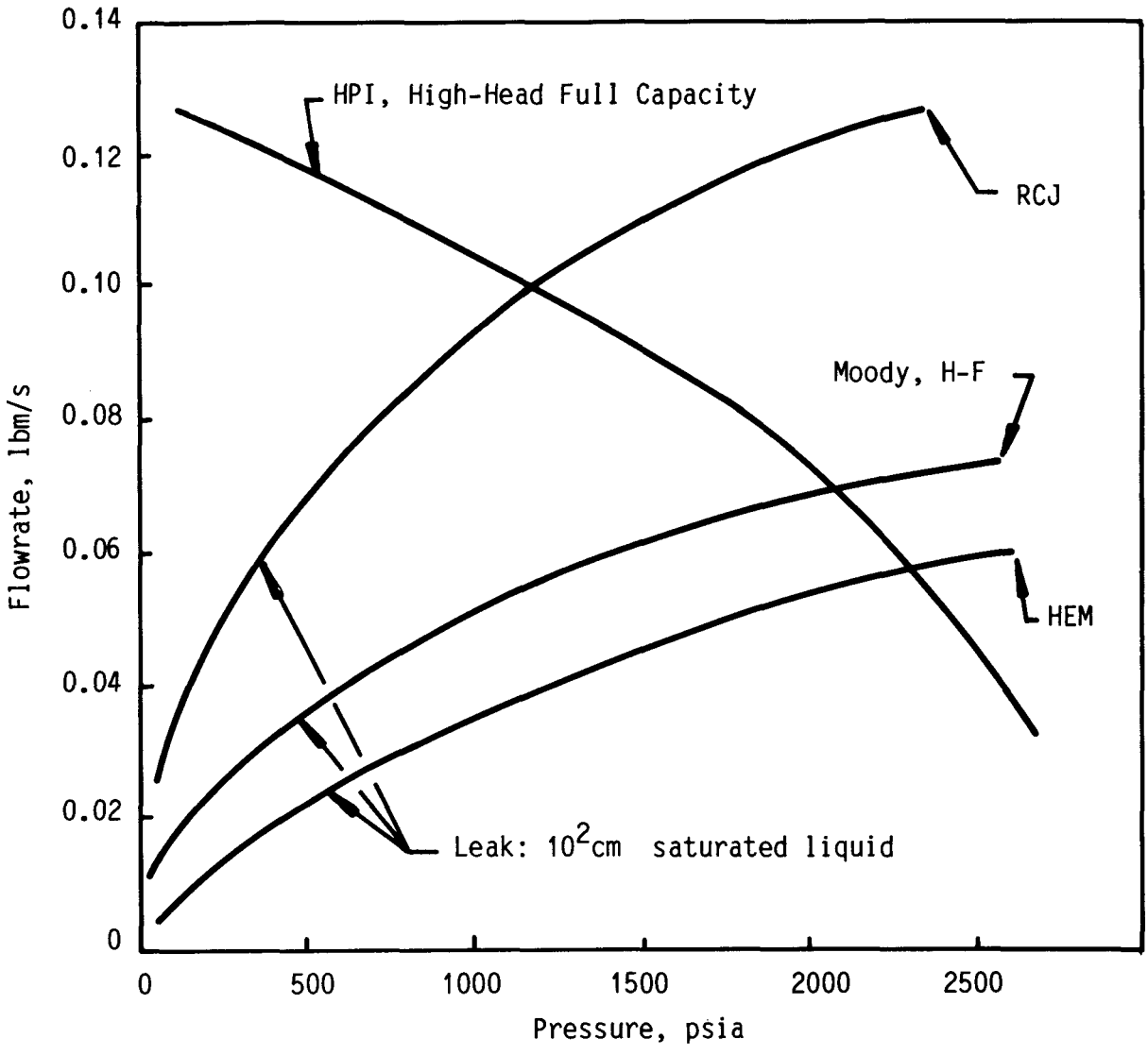

HPI: High Head, Full Capacity, cf. Figure 2.15

Leak: 10 cm^2 (S = 1686), Saturated Liquid.
"Moody," "H-F" (Henry Fauske), "HEM" (Homogeneous Equilibrium Model) Critical Flow From ANCR-NUREG-1335 pp 145ff (Sept 76).

"RCJ" - Orifice Equation With C_D = 0.7.

Full capacity denotes the simulation of two plant HPI pumps.

Figure 2.16 Leak-HPI Equilibrium

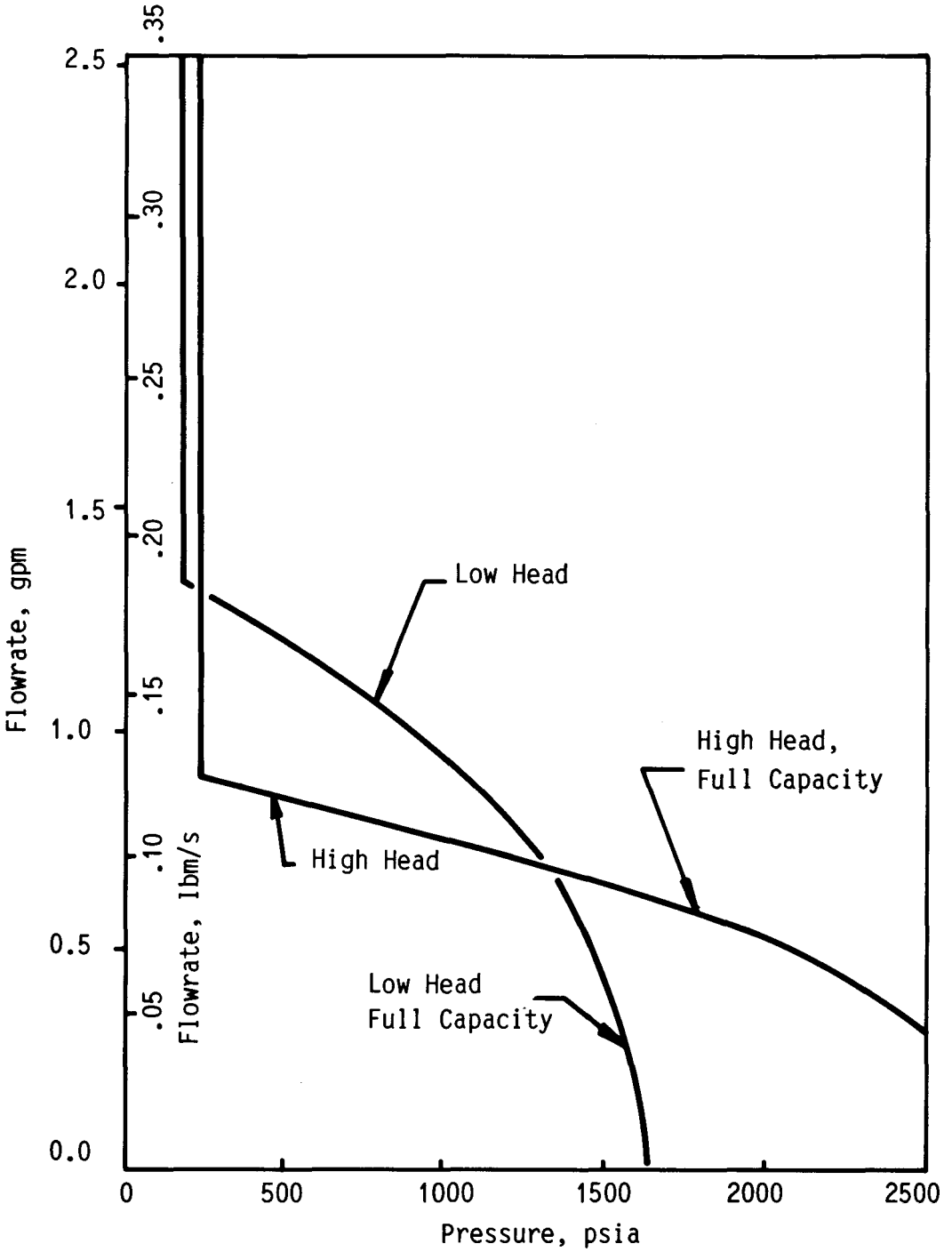

HPI Characteristics from Figure 2.15
LPI Characteristics from FSAR's:
DB - FSAR Figures 6-9 and 6-9a
TVA - FSAR Figure 6.3.1-5

Full Capacity Denotes the Simulation of Two Plant HPI Pumps Plus the Simulation of Two Plant LPI Pumps When Applicable.

Figure 2.17 OTIS LPI-Supplemented HPI Characteristics

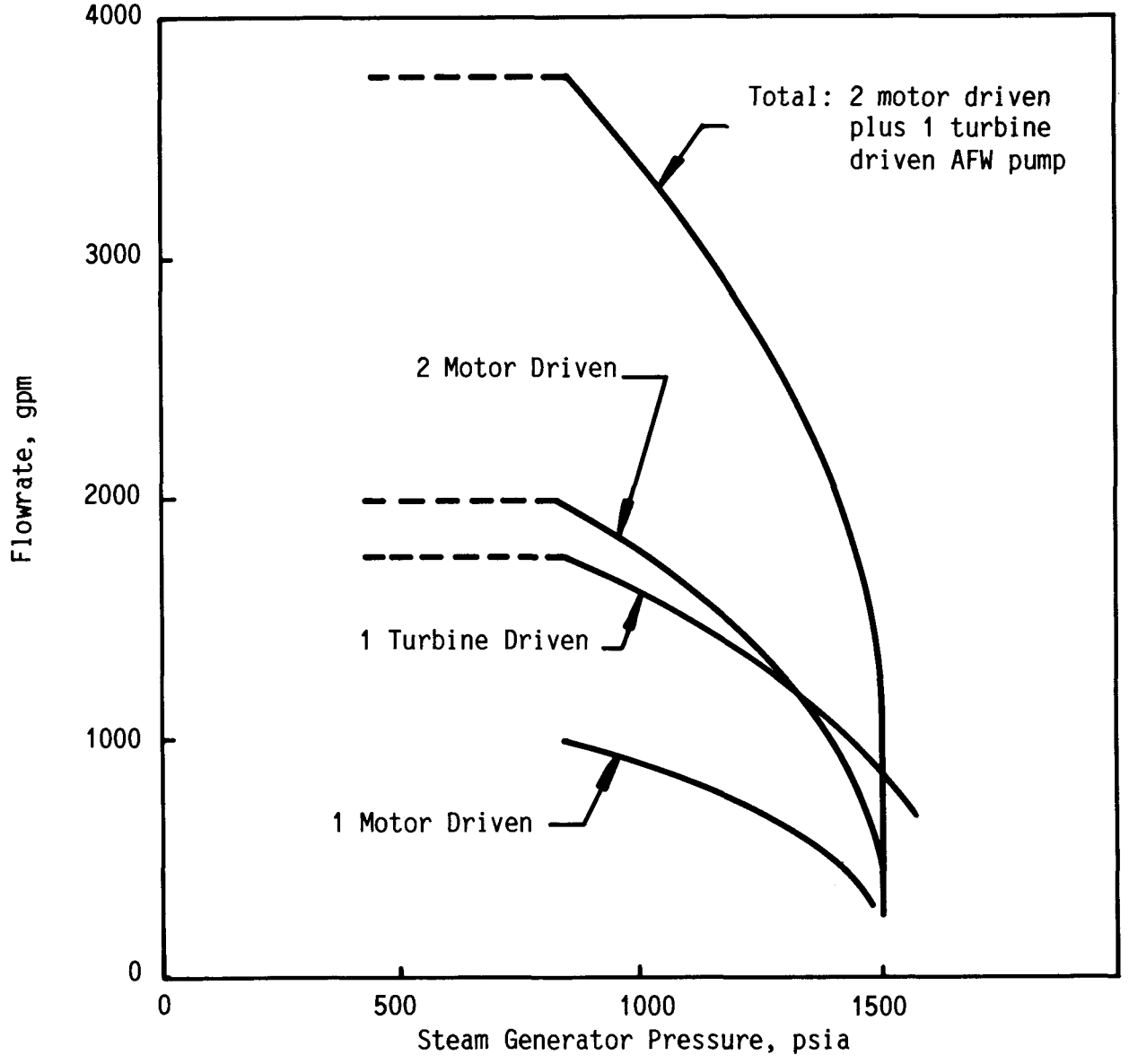

AFW Head-Flow Typical of a 205 FA Plant.

Characteristics for Various AFW Pump Combinations,
Total is Shown Without Further Allowance For Feed Header losses.

Figure 2.18 Plant AFW Characteristics

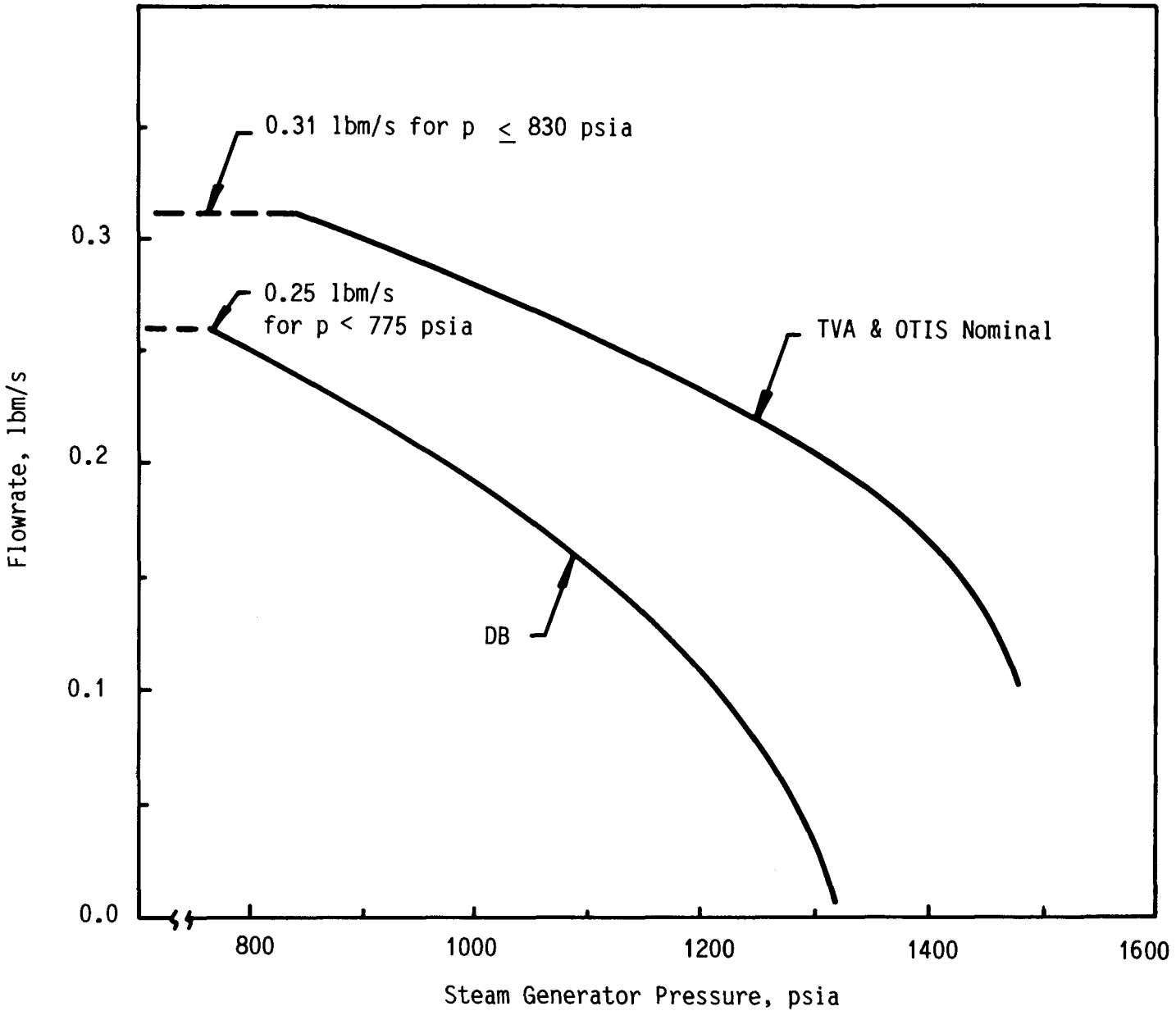

"TVA" from Figure A.6a, "Total"/1686
"DB" from Davis-Besse AFW/1300, Source 51-1134814-01,
for Two AFW Pumps

Figure 2.19 OTIS AFW Characteristics

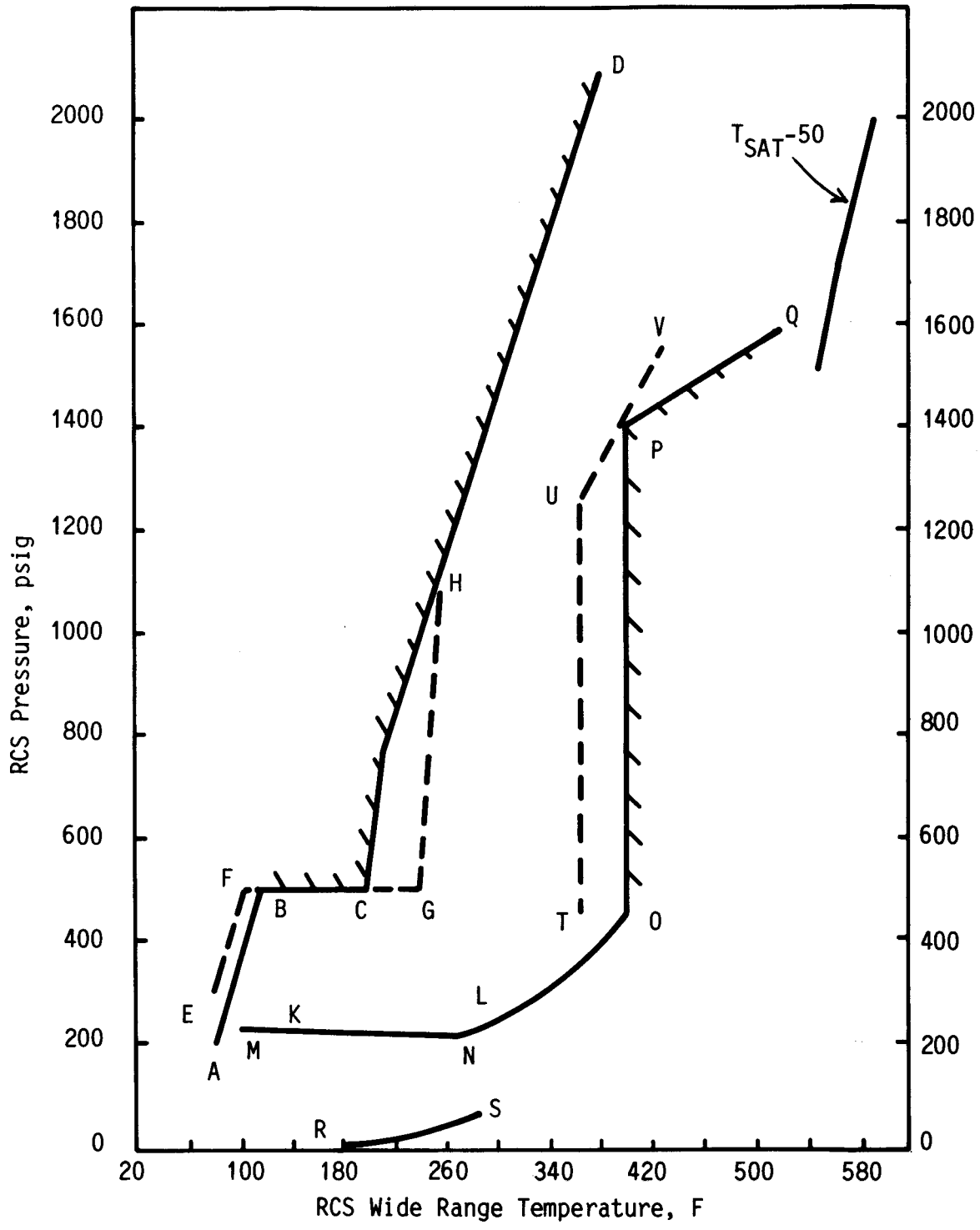

Pressure-Temperature Limits For Cooldown,
Source: Ref. 10. Key on page following.

Figure 2.20 P-T Limits

Figure 2.20 Key

Key to p-T limits, From Ref. 10

LINE	SOURCE
ABCD	Maximum RCS Pressure/Temperature during cooldown based on DTT-175°F.
EFGHD	Maximum RCS Pressure/Temperature during hydrostatic testing with cooldown.
KL	Maximum RCS Pressure/Temperature during simultaneous operation of decay heat pumps and any combination of RCP's.
MN	Minimum Pressure/Temperature to provide proper RCP seal pressure staging.
NO	Minimum Pressure/Temperature to provide RCP NPSH.
OPQ	Minimum Pressure/Temperature to maintain fuel in compression.
RS	Minimum Pressure/Temperature to prevent boiling in the top of the hot leg.
TUV	Minimum Pressure/Temperature to maintain fuel in compression during a cooldown by natural circulation.

3. THE OTIS TEST MATRIX

The OTIS tests, in conjunction with the GERDA data, were intended to supply post-SBLOCA integral system information for code verification. The planned test matrix is given in Table 3.1. There were three categories of OTIS tests:

I. OTIS-GERDA benchmark (1 test)
II. Single-variable (10 tests)
III. Composite (2 tests)

Guard heater tests were added, as discussed in section 3.2.5.11.

The OTIS-GERDA benchmark test reproduced a GERDA boiler-condenser mode test, supplying a direct evaluation of the effects of the interfacility modifications (outlined in the OTIS Design Requirements[1]). This benchmark test also provided information regarding the differences between the system responses using high-elevation versus low-elevation auxiliary feedwater (AFW) injection with a partially voided primary system.

The ten single-variable tests were designed to highlight the effects of major system variables such as leak configuration, high pressure injection characteristics, and AFW characteristics. Throughout these tests, simulations of operator actions were simplified as much as possible to facilitate test control, analysis, and interpretation.

The two composite tests investigated the transitions among cooling modes and used simulated plant operator actions.

The test specifications[3] for all the tests are summarized in the following paragraphs. It should be noted that these specifications were developed before testing and thus may include event-triggered actions which were not encountered during the actual test transient. For example, the natural circulation cooldown test specifications (given in subsections 3.2.5.9 and 3.2.5.10) contain detailed procedures regarding flow interruptions, but such interruptions did not occur.

3.1 Category I: OTIS-GERDA Benchmark, Test 210100

The OTIS-GERDA benchmark test was conducted to provide a direct evaluation of the inter-facility changes. This test also gave insight into the impact

of high-elevation versus low-elevation auxiliary fedwater (AFW) introduction with a voided primary system. (The differences between OTIS and GERDA are given in the OTIS Design Requirements.[1]) The basis for comparison was a boiler-condenser mode (BCM) test.

This test included three phases: draining, BCM with low-elevation AFW injection, and BCM with high-elevation AFW. The first phase was typical of the GERDA BCM test initiation evolutions and provided several checks of measurement consistency. The second phase, BCM with low-elevation AFW injection, duplicated the conditions and trends of GERDA BCM Test 0900AA. The first two test phases provided an assessment of the facility modifications made for the OTIS test program. The third phase gave insight into the influence of high-elevation AFW introduction with a partially voided primary. The steps for test conduct during the various phases were as follows.

3.1.1 Initialization

The test was to be initialized with a full and subcooled primary on pressurizer pressure control. The initial primary system pressure is not significant because it will be controlled by the primary-to-secondary temperature difference when the boiler-condenser mode (BCM) is established; an initial primary pressure of approximately 1000 psia is convenient. Core power was replacing losses to ambient ($\sim$0.6% of full power, 1% = 21.4 kW). All OTIS guard heaters were to be functioning in automatic.

The secondary was to be at a constant level of 29 feet and constant steam pressure of 710 psia. AFW at $\sim$100F was to be injected using the minimum wetting and low-elevation AFW nozzles.

3.1.2 Drain

The reactor vessel vent valve (RVVV) was to be set to automatic actuation on differential pressure with open/close settings of 0 $\pm$ 0.005 psia (as in GERDA Test 0900AA). The data acquisition system (DAS) was to be activated to acquire measurements at 1-minute intervals. (Data requirements are described in section 3.6.) The 10-cm^2 cold leg suction (CLS) leak was to be opened and the primary system drained to obtain a 5-foot condensing length, i.e., a primary level downstream of the hot leg U-bend of 24 feet. (Elevations herein are referenced to the steam generator lower tubesheet upper face, SGLTSUF.)

3.1.3 BCM With Lower-Elevation AFW

As soon as the primary drain had been completed, core power was to be increased to 2.6% of full power in excess of ambient losses (corresponding to 2.5% of full power in GERDA wherein 1% of full power = 22.3 kW). An approximate steady state was to be obtained for at least 30 minutes, observing the rate of change of the steam generator (SG) primary outlet fluid temperature and obtaining a long-term variation of less than 20F/hour. When (cyclic) steady state had been obtained, the DAS was to be adjusted to record data at 5-second intervals, and run to record for 5 minutes.

Maintaining the 5-second DAS scans, RVVV control was to be transferred from automatic to manual-open and 5 minutes of data recorded with this setting. The DAS was then to be set to take data at 1-minute intervals. The next actions specified were to take manual control of the AFW flow control valve and maintain a constant valve position to obtain an approximately constant SG secondary level through the cyclic conditions variations, if any.

After this transition to manually-controlled AFW flow had been completed, data was to be taken for 5 minutes at 5-second intervals.

3.1.4 BCM With High-Elevation AFW

The 5-second DAS scans were to be continued and the AFW transferred from low-elevation to high-elevation injection in automatic control to maintain a constant secondary level (at the current SG secondary level, approximately 29 feet). Data was to be taken for 5 minutes, then switched to 1-minute data scans.

After 30 minutes (and after any major noncyclic primary condition transients had subsided) 5-second data scans were to be used for 5 minutes.

RVVV control was to be switched from manual-open to automatic actuation on differential pressure (at 0 ± 0.005 psi) and 5 minutes of data recorded with this setting. Latching the RVVV open and adjusting the RVVV open/ close settings to approximately 0.25 psi to open and 0.125 psi to close, RVVV control was to be transferred to automatic for 5 additional minutes of data. Then, this test was to be terminated.

3.2 Category II: Single-Variable Tests

Ten tests examined the effects of changing only one major control variable. Simulations of operator actions were minimized and/or simplified to retain test clarity while approximating the plant boundary conditions. Intertest comparison and, therefore code assessment were augmented by concentrating on a nominal test, attempting to alter only the variable of interest for subsequent (single-off-nominal) tests. Consistent with this technique, the initialization and conduct of most of these tests were identical.

3.2.1 Initialization

The initialization of each of the first eight single-variable (Category II) tests was to be identical. It was directed to the achievement of realistic model conditions after test initiation. Because OTIS simulated neither forced primary flow nor flow coastdown, this time of the start of plant transient simulation in the model was limited to conditions after reactor coolant pump trip and coastdown.

Reactor coolant pump operation following an SBLOCA differs among plants and event sequences. In most plants, the operator trips the pumps on a low-pressure engineered safety features actuation system (ESFAS) signal and/or on a loss of (primary fluid) subcooling margin; on one plant the pump trip is automatic. The system events accompanying an SBLOCA may precipitate a simultaneous loss of power to the pumps. If the pumps are kept in operation for perhaps a minute after reactor scram, the post-coastdown coolant temperatures are approximately equal and are close to the secondary steam temperature, ∿550F. On the other hand, if the reactor and pump trips occur nearly simultaneously, post-coastdown power is higher, as are both the primary loop temperature difference and the hot leg (fluid and metal) temperatures. Because the latter scenario produces more challenging system conditions, it was selected for simulation in OTIS.

Test initialization and initiation were thus defined to simulate plant conditions at approximately 1-1/2 minutes after reactor trip, after pump coastdown, and with the boundary systems (HPI and AFW) activated. OTIS was to be initialized in steady state under the following conditions:

- Core power = 3.7 ± 0.1% of full power (1% full power = 21.4 kW) plus losses to ambient.
- Natural circulation.

- Primary pressure = 2200 ± 50 psia.
- Pressurizer liquid height = 10 ± 2 feet (16.6 ± 2 ft above the SGLTSUF).
- Pressurizer main and guard heaters adjusted for an approximately adiabatic pressurizer.
- Reactor vessel upper head vent (RVUHV) and hot leg high-point vent (HLHPV) closed.
- RVVV in automatic (differential-pressure) control with open/close setpoints of 0.25 and 0.125 psi.
- AFW at ∿100F injected at the upper elevation using the minimum-wetting nozzle.
- SG secondary (collapsed) liquid level = 5 ± 1 feet with constant level control.
- SG secondary pressure (∿1000 psia) adjusted to obtain a primary hot leg fluid temperature of 610 ± 2F. (Use the model hot leg fluid temperature indication at 60 feet, HLTC07.)
- HPI and leak systems not in use. Primary noncondensible gas additions were not to be tested.

Initialization was to be continued until the following system steady state was obtained:

- Pressurizer metal temperatures at saturation (650F) ± 10F,
- The RVVV not cycling, and
- The steam generator fluid temperatures varying less than 10F/h (exception: cyclic secondary fluid temperature variations associated with high AFW injection, and with internal circulation within the secondary liquid pool, were acceptable).

3.2.2 Initiation

Initiation involved two steps, both designed to obtain plant-similar conditions at the time of (model and plant) loop fluid saturation. The initial step was simply to open the designated leak (starting the pressurizer drain and the relatively slow primary system depressurization).

The second step occurred at the depletion of the pressurizer liquid inventory. When the pressurizer liquid height reached 2 feet (collapsed liquid level = 8.6 feet relative to the SG lower tubesheet), the following three steps were to be performed in rapid succession:

1. Actuate HPI to the cold leg discharge piping.
2. Begin the core power ramp (simulating post-trip power decay from 1-1/2 minutes after reactor trip).
3. Adjust the AFW control to obtain the specified secondary level and feed characteristics.

3.2.3 Conduct

After test initiation, most of these single-variable tests required only one operator control interaction. When the SG level had been increased to the post-initiation setpoint, the operator was to actuate the SG secondary depressurization from 1000 psia to obtain a 50F/h secondary cooldown. Requirements of individual tests are addressed in section 3.2.5. When the SG secondary pressure reached the facility minimum (set by low-pressure control limits, $\sim$100 psia), it was to be maintained at that value. Data requirements are given in section 3.2.6. After the loop piping had been refilled, the HPI flow rate was to be throttled to maintain the pressurizer level roughly at mid-height.

3.2.4 Termination

Each single-variable test was to be continued through loop refill and one hour of continuous cooldown. "Loop refill" denotes that liquid remains above the HLUB spillover elevation; the reactor vessel upper head and pressurizer may be voided. Each test was to be conducted for at least two hours. In addition, the "nominal" test (220100) was to be extended to demonstrate long-term cooling as described subsequently. The termination of the natural circulation cooldown tests (220999 and 221099) is described in section 3.2.5.9.

If any single-variable test extended beyond five hours without refilling the hot leg to the U-bend spillover elevation, the hot leg level change was to be examined. If the rate of change of the hot leg level (upstream of the U-bend) was less than 5 feet/hour, the HLHPV was to be opened and testing continued for an additional two hours with the HLHPV open.

If the HLUB had not refilled after this additional testing, and if the PORV was not already open, the PORV was to be opened. Testing was to be continued for an additional hour with the HLHPV and PORV open.

If the HLUB had not refilled after this additional two or three hours of testing, core power was to have been reduced smoothly, to transfer from current power to sustaining power (replacing conduction heat losses to ambient) in approximately one-half hour. Testing was to be terminated after a final additional hour with sustaining power and with the PORV and HLHPV open.

3.2.5 Tests

Each of the single-variable tests are addressed separately. Data requirements are given in section 3.2.6.

3.2.5.1 Nominal Test 220100

Test 220100 embodied the nominal single-variable conditions and served as a comparison test for the subsequent off-nominal tests. Test conditions included:

- (Scaled) 10-cm^2 (0.010 ft^2) CLS leak, no leak isolation.
- Nominal HPI (full capacity and high head with low pressure injection supplementation, cf. Figure 2.17), to the cold leg discharge piping.
- Upon test initiation, the SG secondary level was fed up to 38 feet as limited by AFW head-flow characteristics at half AFW capacity (simulating the 3 ft/min level rate control). At 38 feet, a constant SG level was to be maintained and the SG secondary depressurization was to be actuated to obtain a 50F/h secondary cooldown.
- Neither high point vent (RVUHV nor HLHPV) is used (except as noted in section 3.2.4).
- The leak is maintained unisolated.
- The PORV is in the automatic (overpressure control) mode.

Test initialization and initiation are as given in sections 3.2.1 and 3.2.2 above. As mentioned in section 3.2.4, this nominal test was to be extended to demonstrate long-term cooldown. Testing was to be continued beyond refill and through cooldown until all primary fluid temperatures, observed over at least a 15-minute period, were varying less than 10F/h. If this maximum temperature change rate could not be met, the test was to be terminated after ten hours.

This nominal test was expected to experience each of the major post-SBLOCA events: loop saturation, flow interruption and repressurization, boiler-condenser mode, refill, and cooldown. The onset of the boiler-condensor mode may occur when the primary liquid-vapor interface reaches the elevation of high-elevation AFW injection, rather than the elevation of the secondary liquid pool, provided AFW is being introduced at this time. Leak-HPI equilibrium pressure was expected to be approximately 1000 psia. Refill was expected to occur roughly 2 hours into the transient. Post-refill cooling may not engender whole-loop natural circulation (the initiation of

natural circulation will likely be linked to the re-initiation of high-elevation AFW injection upon feed demand, i.e., upon secondary steaming or SG level contraction).

3.2.5.2 Test 220201, Leak Size

The cold leg suction leak size was modified from 10 to 15 cm^2 in Test 220201. Test details were to be otherwise identical to those of the nominal test, cf. sections 3.1 through 3.5.1. The abbreviated test termination was to be used (terminating after one hour of post-refill cooldown, cf. section 3.4). Leak-HPI flow rate equilibrium was expected to occur at approximately 500 psia with this 15-cm^2 CLS leak, that is at a lower primary pressure and higher leak and HPI flow rates. At this higher leak rate, refill may also be prolonged beyond that with the 10-cm^2 leak.

3.2.5.3 Test 220304, HPI Characteristics (Half Capacity, High Head)

Test 220304 varied only high-pressure injection (HPI) capacity from the conditions of the nominal test. Test performance is otherwise identical, cf. sections 3.2.1 through 3.2.5.1. In this test, HPI capacity was to be one-half of nominal, see Figure 2.15. For example, at 1000 psia primary pressure, the HPI flow rate was to be approximately 1/2 x 0.106 or 0.053 lbm/s. With this halved HPI capacity, the HPI-leak mass flow rate equilibrium pressure will approximate the pressure of LPI augmentation (cf. Figures 2.16 and 2.17). Refill will be greatly prolonged.

3.2.5.4 Test 220402, SG Secondary Characteristics (10-Foot Level)

Test 220402 varied steam generator (SG) secondary level control from that of the nominal test. Upon test initiation, secondary level was to be increased from 5 to 10-1/2 feet at the full AFW head-flow capacity. The SG level was to be maintained at 10 ± 1/2 feet using band control. The level is raised to 10-1/2 feet using full AFW capacity (limited only by head versus scaled flow, cf. Figure 2.19, curve "DB"); at 10-1/2 feet, feed is stopped and the level is allowed to steam down to 9-1/2 feet; at 9-1/2 feet, AFW is again introduced at full capacity to return the level to 10-1/2 feet; this sequence is repeated for 15 minutes. After 15 minutes, SG secondary level control was to be transferred from the previously

described band control to constant level control at a 10-foot secondary level. Test performance was to be otherwise identical to that of the nominal test, cf. sections 3.1 through 3.5.1. The test was to be terminated after one hour of post-refill cooldown.

Test 220402, with a lower-than-nominal secondary level, was thought likely to delay the onset of the BCM and subsequent events. Also the SG heat removal zone (without AFW introduction) was to be lower such that the re-initiation of primary natural circulation was delayed.

3.2.5.5 Test 220503, Leak Location (CLD)

Test 220503 used a 10-cm^2 leak at the cold leg discharge (CLD) site. It was otherwise identical to the nominal test, cf. sections 3.2.1 through 3.2.5.1 but with test termination after one hour of post-refill cooldown.

The reorientation of the leak site toward the downcomer, compared with the nominal test, was thought likely to increase leak fluid temperature and therefore to decrease leak flow rate. Leak-HPI flow rate equilibrium pressure would thus be higher than in the nominal test, and the post-SBLOCA sequence of events is likely to occur somewhat sooner. (This variation of leak fluid temperature with cold leg leak location was perceived to be atypically enhanced by the single cold leg of the model loop).

3.2.5.6 Test 220604, HPI Capacity

Test 220604 varied high pressure injection (HPI) head-flow characteristics from those of the Nominal Test, test performance was to be otherwise identical (see sections 3.2.1 through 3.2.5.1). The revised HPI characteristics of this test simulated a low-head system and the full (scaled) installed HPI flow capacity (cf. Figure 2.17). The test was to be terminated after one hour of stable cooldown. The revised HPI characteristics of this test were to lower the equilibrium pressure at which the leak and HPI flow rates are equal, and thus prolong the post-SBLOCA sequence of events, compared to that of the Nominal Test.

3.2.5.7 Test 220756, Leak Isolation

Test 220756 investigated the effects of leak isolation. This test was initialized and initiated in exactly the same fashion as the Nominal Test, cf. sections 3.2.1 and 3.2.2. (Note: Control secondary pressure to stay

within the design limit on the maximum primary-to-secondary pressure difference.)* The (10-cm^2 cold leg suction) leak was to be isolated at the most inopportune time, i.e., when there was no means of removing heat from the primary system. This time was to be based on the results of Test 220100. The leak was to be isolated (and kept isolated) approximately at the middle of the period of probable decoupling of primary-to-secondary heat transfer. The end of this period was to be marked (using Test 220100) by the primary liquid level downstream of the HLUB decreasing to the elevation of the SG upper tubesheet. (Primary-to-secondary heat transfer would occur beyond this time, upon actuation of high-elevation AFW). The beginning of this period of probable decoupling was to be at the end of the last preceding occurrence of primary loop flow and/or primary-to-secondary heat transfer.

The time to isolate was to be 10 to 20 minutes after test initiation. Immediately upon isolation, primary fluid mass inventory was expected to increase and the primary system to repressurize. The model PORV simulation (relief valve on the pressurizer) was to actuate on overpressure at 2300 psia. When the PORV actuated, the PORV control mode was to be switched from automatic (overpressure control) to manually open. The PORV was to be left open for the duration of the test. The primary was to be cooled by HPI-PORV flow, the so-called "feed-and-bleed" cooling.

This cooling mode (and SG secondary depressurization to obtain 50F/h secondary cooldown) was to be continued through primary system refill plus one hour of cooldown.

3.2.5.8 Test 220899, HPI Cooldown

Test 220899 examined an HPI-PORV cooldown with auxiliary feedwater (AFW) unavailable. Test initialization was that of the nominal test (cf. section 3.2.1), but test initiation was different and test conduct most closely resembled that of the preceding leak isolation test.

No leak was to be simulated in this test, therefore the customary leak-initiation step preceding test initiation was not applicable. This test was to be initiated by three simultaneous actions:

---

*It was suggested that the secondary depressurization ramp be interrupted at 800 psia, if necessary, until either of two criteria is met: (1) The PORV had actuated, or (2) the HLUB piping had been refilled, and primary and secondary pressures were coupled.

1. Actuate HPI (full capacity, full head).
2. Stop AFW.
3. Begin the usual core power decay ramp.

The SG secondary was to be kept isolated through the test, except as required to assure model generator integrity (it may be necessary to periodically reestablish a liquid inventory in the SG secondary to maintain secondary pressure within the maximum primary-to-secondary pressure limits; steam bleeding may also be necessary to preclude lifting the SG code safety).

Primary inventory and pressure were expected to increase at test initiation. The PORV was to actuate at 2300 psia on overpressure. Upon automatic actuation, the PORV control mode was to be transferred from automatic (on overpressure) to manual-open. The PORV was to be maintained open for the duration of the test. The primary was then to be cooled by HPI-PORV flow as in the previous test. Testing was to continue through primary refill plus one hour of cooling. (Note: The minimum test duration was 2 hours.)

3.2.5.9 Test 220999, Natural Circulation Cooldown

Test 220999 and the Test 221099 investigated the influence of the reactor vessel upper head vent (RVUHV) on a natural circulation cooldown. Testing was thus to be quite different from the previous single-variable tests, and necessarily involved increased operator action.

Compared with the previous single-variable tests, this natural circulation cooldown test was to be initialized to simulate conditions later after reactor trip. Initialization and testing were to be performed at a constant 1% of scaled core power (plus facility conduction heat losses to ambient). The primary was to be subcooled in natural circulation, and primary pressure was to be 2200 psia. The pressurizer level was to be 15 feet.* Secondary pressure was to be 1100 psia** and the secondary liquid level was to be held constant at 12 feet using 100F AFW injected at the upper elevation with the minimum wetting nozzle. No leak was to be used in this test, nor was HPI to be employed in the usual fashion. Test initiation consisted of two actions:

---

* This 15-foot pressurizer liquid level is ∿22 feet relative to the SG lower tube-sheet.

** Secondary pressure of 1100 psia (versus 1000 psia of the previous tests) was to be used to elevate the initial primary fluid temperatures.

1. Begin the SG secondary depressurization to obtain a 50F/h secondary cooldown.
2. Actuate and throttle HPI to maintain pressurizer level. Attempt to use a continuous and smoothly varying injection flow rate (simulating controlled plant makeup to offset shrinkage of the primary fluid). Do not adjust the HPI flow rate during the PORV lifts described below.

Primary Pressure Control

Primary pressure was to be maintained within the pressure-temperature limits for cooldown shown in Figure 2.20. Primary depressurization was to be accomplished using the PORV. The PORV was to be actuated to obtain a primary pressure decrease of approximately 200 psi per actuation (this will require about one minute of actuation). At least 15 minutes were to be allowed between actuations. (The waiting period between PORV actuations must be increased as the primary cooldown rate is decreased to stay within the specified pressure-temperature limits of Figure 2.20). The resulting pressure-time variation was to be a series of step functions, but with pressure varying about the center of the allowable pressure-temperature envelope.

As primary pressure is decreased, the RVUH will void. This void volume may continue to expand until the liquid-vapor interface reaches the hot leg nozzle. Vapor may periodically vent into the hot leg. This vapor may collect at the HLUB, interrupting primary loop flow and primary-to-secondary heat transfer. Such an occurrence would be evidenced by the following conditions:

- Vapor only (stagnant) at the HLUB viewport.
- Loop flow rate indications decrease rapidly, from $\sim$3% of full flow toward zero.
- SG secondary steam and feed flow rates decrease abruptly.
- Primary-to-secondary temperature differences across the generator (at each elevation) decrease abruptly toward zero.
- Indicated primary liquid levels on both sides of the HLUB (including level uncertainty) drop below the elevation of the HLUB spillover.
- Primary pressure begins to increase independent of operator control.
- Core-region fluid temperatures abruptly begin to increase.

If two or more of these indications of interruption were observed and if the HLUB viewport indicated (stagnant) vapor only, it was to be assumed that interruption had occurred, and the following actions were to be taken:

- Interrupt the secondary depressurization ramp, and adjust the SG secondary steam valve control to maintain current secondary pressure.
- Actuate the pressurizer heaters to repressurize the primary system to the maximum pressure allowed by the pressure-temperature envelope.
- If the previous pressure increase does not refill the HLUB, actuate the HLHPV using throttled HPI to maintain pressurizer level.

When the HLUB had been refilled and/or primary loop natural circulation had been restored, the following steps were specified:

- Close the HLHPV.
- Re-initiate primary depressurization.
- Re-initiate the secondary depressurization from the current secondary pressure.

Had this interruption-refill event occured twice at 50F/h, the secondary side depressurization rate was to be reduced to obtain a 20F/h cooldown (maintaining the SG secondary pressure constant while changing the programmed depressurization rate.) If this rate also obtained two interruptions, the ramp was to be further reduced, to 10F/h. This ramp reduction scheme was to be continued as required (i.e., 2 ramps each of 50, 20, 10, 5, 2, and 1F/h); if the 1F/h cooldown interrupted, this test was to be terminated.

Testing was to be continued for an additional 30 minutes after the ramped secondary depressurization reaches the facility low-pressure limit. In the event of depressurization ramp reductions, testing was to be terminated after 10 hours of cooldown (i.e., 10 hours plus the times required to restore the primary liquid level to the HLUB).

3.2.5.10 Test 221099, RVUHV Effects (On Natural Circulation Cooldown)

Test 221099 was to be identical to the previous test except that the reactor vessel upper head vent (RVUHV) was to be used to suppress reactor vessel upper head voiding. The cooldown was to be started with the RVUHV closed. As the primary system depressurized (using the PORV), a voided region would form in the reactor vessel upper head and would expand downward with continued depressurization. When this voided region extended down approximately to the elevation of the OTIS reactor vessel upper plenum orifice plate, the RVUHV was to be actuated. Venting was to be continued until the upper head vapor region had been displaced. After the RV had

been refilled with liquid, the RVUHV was to be closed for four minutes, then opened and vented for one minute. This schedule (closed four minutes, open one minute) was to be continued for the duration of the test. (This cyclic RVUHV operation simulates 205-FA plant venting of at least 3000 gallons per 5OF of cooldown. Pressurizer level will vary through the vent/no-vent cycles, therefore maintain a roughly constant time-averaged pressurizer level). Otherwise, the test was to be initiated, performed, and terminated exactly as Test 220999.

3.2.5.11 Additional Testing

Upon completion of the originally planned OTIS tests, the Program Management Group approved two additional tests. The intent of these tests was to determine the effect of the guard heaters (hot leg, reactor vessel upper head and pressurizer) on the transient response of the system. These tests are of the Category II single-variable test type. They are described in the following sections.

Test 2202AA, Pressurizer Guard Heater Effects

Test 2202AA is identical to Test 220201 except that the pressurizer was to be isolated from the primary system during the initiation of the test. All previous single-variable tests involved actions which were keyed to the depletion of the pressurizer liquid inventory. This test required an additional action which was also keyed to the depletion of the pressurizer liquid inventory.

The second step of the initiation for this test occurs when the pressurizer liquid height reaches 2 feet (collapsed liquid level = 8.6 feet relative to the SG lower tubesheet). The following four steps were to be performed in rapid succession:

1. Actuate HPI to the cold leg discharge piping.
2. Begin the core power ramp (simulating post-trip power decay from 1-1/2 minutes after reactor trip).
3. Alter AFW control to obtain the specified secondary level and feed characteristics.
4. Isolate the pressurizer from the primary loop and make the necessary adjustments to the pressurizer guard heaters.

The conduct for this test was also to be identical to Test 220201 except that after the loop piping had been refilled, an attempt was to be made to maintain approximately 50F subcooling in the HL by varying the HPI flow rate. It should be noted that the potential for a liquid-solid loop and, therefore, an HPI-induced pressure excursion existed.

Test termination was to be identical to Test 220201 except that if the HLUB had not refilled in two hours after the HLHPV was opened, testing was to be continued for an additional hour with the HLHPV open (total elapsed time with the HLHPV open was therefore to be three hours). Since the pressurizer was to be isolated, the PORV was not to be used for this test.

This test was intended to identify the impact of the pressurizer guard heaters on the transient response of the system.

Test 2202BB, Hot Leg, Reactor Vessel Upper Head and Pressurizer Guard Heater Effects

Test 2202BB was to be identical to Test 2202AA except that the hot leg and the reactor vessel upper head guard heaters were to be turned off during the initiation of the test.

The second step of the initiation for this test was to occur when the pressurizer liquid height reached 2 feet (collapsed liquid level = 8.6 feet relative to the SG lower tubesheet). The following 5 steps were to be performed in rapid succession:

1. Actuate HPI to the cold leg discharge piping.
2. Begin the core power ramp (simulating post-trip power decay from 1-1/2 minutes after reactor trip).
3. Alter AFW control to obtain the specified secondary level and feed characteristics.
4. Isolate the pressurizer from the primary loop and make the necessary adjustments to the pressurizer guard heaters.
5. De-energize all hot leg and RV upper head guard heaters.

The test conduct and termination criteria for this test were to be identical to that of Test 2202AA.

This test was intended to identify the combined impact of all the guard heaters on the transient response of the system.

3.2.6 Data Requirements

Each of the OTIS tests (in all three categories) required a complete set of system condition measurements. Minimum measurements included:

- Each primary system component (reactor vessel, hot leg, steam generator primary, cold leg, pressurizer) and steam generator secondary:
  - Pressure
  - Fluid temperatures
  - Pressure differences (for collapsed liquid levels)
- Each boundary system (secondary steam and feed, HPI, and active primary discharge streams):
  - Control valve limit switch indication
  - Flow rate
  - Temperature
- Core power
- reactor vessel vent valve:
  - Limit switch indication
  - Actuating pressure difference
- Primary loop flow rate
- Conductivity probe output from selected probes

Table 3.2 identifies the required instruments.

Each of the transient tests encountered similar data frequency requirements. These tests were estimated to last from several hours up to a half day, therefore dense data scans had to be used judiciously. Dense data (scans at five-second intervals) were to be taken:

- From the end of steady-state test initialization through the initial loop flow interruptions.
- As the primary level dropped into the elevation of the steam generator and AFW actuation initiates the boiler-condenser mode.
- At leak isolation.
- At PORV actuation.
- At the transitions among cooling modes.
- At (HLUB) spillover circulation during hot leg refill.
- At vent actuation.
- At the other similar threshold events.

Data taking was to be reduced to one-minute intervals during the intervening, relatively quiescent periods. During extended periods of sparse data, 2 minutes of dense data were to be taken approximately every 30 minutes. The viewport indications were to be continuously recorded on videotape.

If higher-frequency condition perturbations were suggested by the dense data, or by on-site observations of analog signals or viewports, separate records of a few minutes of continuous (analog) signals from several instruments were specified to give insight into the oscillation source; e.g., fluid temperatures bracketing the leak site and leak flow rate are germane to leak flow rate oscillations; upper downcomer and cold leg fluid temperatures plus RVVV pressure difference may highlight condensation oscillations, etc.

3.3 Category III: Composite Tests

Two composite tests introduced a wide range of operator actions into post-SBLOCA loop control. Whereas the ten single-variable tests (Category II) minimized operator interaction to highlight the effects of the off-nominal variable, these two composite tests maximized operator-system interactions to examine their effects. An engineer versed in plant operator guidelines was to be onsite during these two tests. He was to be furnished model loop conditions and was to direct the test loop operator throughout the evolutions needed to control the system transient using plant operating procedures.

The model indications to simulate those available in the plant included:

- Pressure-temperature display: Saturation temperature, (T_{sat} - 50F), and current T_{hot}, T_{core}, and T_{cold}, all versus primary pressure.
- Collapsed liquid levels: reactor vessel head, hot leg, and pressurizer.
- Flow rate: HPI and AFW.
- Secondary pressure, fluid temperature, and level.
- Primary system pressure.
- Reactor vessel upper head fluid and/or metal temperature.

Model measurements appropriate for these indications were as follows:

Primary pressure - PRPR20, pressurizer pressure at 40.5 feet.

T_{HOT} - HLTC07, hot leg fluid temperature at 60 feet.

T_{COLD} - CLTC03, cold leg suction fluid temperature at -0.1 foot.

T_{CORE} - RVTC07, core outlet fluid temperature at -8.3 feet.
Reactor vessel upper head (fluid) temperature - RVTC08 at +6.8 feet.

The two composite tests, 230199 and 230299, were to be similar. Both involved the following three sequential testing phases:

(1) Break initiation, (2) break isolation, and (3) reactivation of AFW.

The break was to be isolated one-half hour after test initiation. AFW, initially unavailable, was to be reactivated later in the test as described below. The loop was to be cooled within the prescribed pressure-temperature envelope and within the limit of maximum SG tube-to-shell temperature difference. The transitions between modes of primary cooling were of particular interest. Any model boundary system simulating that of a plant, (viz., throttled HPI, PORV actuation, hot leg vent or RVUHV, pressurizer heaters, secondary steam and feed control, etc.) could have been used at the discretion of the loop operator. (Data requirements have been given in section 3.2.6.)

Initialization of these composite tests was to exactly replicate the initialization of the nominal single-variable test, cf. section 3.1. Initiation of the composite tests was also to parallel that of the nominal test (section 3.2) except as follows:

- AFW was to be terminated at test initiation.
- In the second composite test, 230299, HPI characteristics were to be modified to simulate low-head and full-capacity HPI with LPI assist (the "piggyback" mode of HPI). This simulation is approximated by increasing the HPI head-flow pressures by the low-pressure injection (LPI) shutoff head, 186 psia. For example, referring to Figure 2.17, the low-head and full-capacity HPI characteristics obtain approximately 0.129 lbm/s at 1000 psia (primary system pressure). The piggyback simulation for Test 230299 should have obtained 0.129 lbm/s at 1000 + 186 or 1186 psia primary pressure. The shutoff head for the low-head HPI characteristics is 1630 psia. With the piggyback simulation of Test 230299, the shutoff head was increased to 1630 + 186 = 1816 psia. The LPI supplementation (the abrupt increase in flow rate for pressures at and below 186 psia, cf. Figure 2.17) was left unchanged for the piggyback simulation. Also in Test 230299, the SG secondary refill level was 10 feet using full AFW, curve "DB" of Figure 2.19.

AFW Reactivation

AFW was to be re-introduced with a relatively low primary inventory. This obtains a hot leg level criterion for AFW reactivation. To preclude premature test termination by automatic core heater trip, AFW reactivation criteria were also specified based on the reactor vessel collapsed liquid level and on outlet fluid temperature. A default AFW reactivation criterion based on test duration was also specified, to be used if the primary did not void sufficiently to trigger the preceding criteria. The several AFW reactivation criteria, each of which are separately sufficient to trigger the reactivation of AFW during both the composite tests, were as follows:

- Hot leg collapsed liquid level less than 20 feet.
- With an reactor vessel collapsed liquid level less than -1 foot, core outlet fluid temperature (indicated by RVTC07 at -8.3 feet) greater than 625F.
- Reactor vessel collapsed liquid level less than -6 feet.
- Test duration (after leak initiation) greater than one hour.

Both composite tests were to be conducted for at least four hours, and until it was perceived that a stable cooldown had been achieved.

Table 3.1 OTIS Test Matrix

				VARIABLES:		1	2	3	4	5	6	7	Test Termination Criteria		
						Leak Size	SG Sec'y. Level/Rate	Leak Location	HPI Capacity/max-p	Leak Isolation	PORV Operation	RVHPV Operation			
				UNITS/NOTES:		cm^2	Note 1	Note 2	Note 3	Note 4	Note 5	-			
				Settings:	1	10	38/3	CLS	full/>2500	none	Automatic	None	Refill and 1 hour cooldown.		
					2	15	38/full	CLD	full/1630	at stagnation	Open @ 2300	Periodic	Refill and long-term cooldown.		
					3	None	10/full	-	throttle	at 30 min.	Manual	-	Cooldown completed.		
					4	-	No AFW	-	half/>2500	-	-	-	Steady-state		
	TESTS				Contract Test Number										
NUMBER	DESCRIPTION														
210100	Category I, OTIS-GERDA Benchmark				1	[Repeat GERDA Boiler-Condensor Mode Test 0900AA.]					4		4		
	Category II, Single-Variable Tests														
220100	Nominal				3(1)	1	1	1	1	1	1	1	2		
220201	Leak Size				3(2)	2	1	1	1	1	1	1	1		
220304	HPI Characteristics: Half Capacity					1	1	1	4	1	1	1	1		
220402	SG Characteristics: 10%', Full AFW				4	1	3	1	1	1	1	1	1		
220503	Leak Location: Cold Leg Discharge				8	1	1	2	1	1	1	1	1		
220604	HPI Characteristics: Low Head				5	1	1	1	2	1	1	1	1		
220756	Isolated Leak				3(3)	1	1	1	1	2	2	1	1		
220899	HPI Cooldown				6	3	4	na	1	na	2	1	1		
220999	Natural Circulation Cooldown				-	3	(Note 6)	na	3	na	1	1	3		
221099	Natural Circulation Cooldown w/RVHPV				2	3	(Note 6)	na	3	na	1	2	3		
	Category III, Composite Tests														
230199	Nominal HPI				7	1	1	1	1	3	3	1	2		
230299	Low-Head HPI				9	1	1	1	2	3	3	1	2		

NOTES: Table 3.1 OTIS Test Matrix

1. Steam generator (SG) Secondary Characteristics:

   "38/3" - Refill the SG secondary to 38 feet using half-capacity AFW (simulating 3 ft/min level rate control).

   "38/full" - Refill the SG secondary to 38 feet using "OTIS-nominal" AFW head-flow characteristics (cf. Figure 2.19). (This setting is not currently being tested).

   "10/full" - Refill the SG secondary to 10-1/2 feet using "DB" AFW head-flow characteristics (cf. Figure 2.19). At 10-1/2 feet, stop feed and begin band level control, steaming without feed to 9-1/2 feet, then feeding to 10-1/2 feet. After 15 minutes, revert to constant level control at 10 feet. For Composite Test 230299, band level control is not to be used; therefore, when feed is reactivated, refill the SG secondary to 10 feet and use constant level control.

2. Leak Location:

   "CLS" = cold leg suction piping
   "CLD" = cold leg discharge piping.
   (Leak size is given in unscaled cm^2. Also, 929 cm^2 = 1 ft^2 i.e., 10 $cm^2 \tilde{=} 0.01$ ft^2.)

3. HPI (high-pressure injection) Capacity/Max-p:

   "Full/>2500" refers to the full-capacity and high shutoff head HPI characteristics supplemented by LPI (low-pressure injection).

   "Full/1630" refers to the low shutoff head HPI characteristics supplemented by LPI. Both are shown in Figure 2.17. HPI and LPI are to be piggybacked for Composite Test 230299, cf. test text.

   "Half/>2500" refers to high shutoff head HPI with half the nominal capacity (with LPI supplementation).

NOTES: Table 3.1 OTIS Test Matrix (Cont'd)

4. Leak Isolation

   "None" = Leak left open.

   "At stagnation" = Leak isolated at a time likely to experience interruption of primary loop flow and primary-to-secondary heat transfer, cf. Test 220756 text.

5. PORV Operation:

   "Automatic" = opens/reseats at 2300/2250 psia.

   "Open @ 2300" = Opens automatically at 2300 psia, at which time the PORV control is to be transferred to manually open.

   "Manual" = manually opened and closed.

6. Tests 220999 and 221099, Natural Circulation Cooldown (with and without RVHPV), use a constant 12-foot SG secondary level and a constant core power level of 1% of scaled full power plus heat loss, cf. test text.

7. Guard heater tests 2202AA and 2202BB were added to the test matrix, cf. section 3.2.5.11.

Table 3.2 Required Instruments

The OTIS measurements listed herein were the minimum required for each of the 13 OTIS tests. (Instrument requirements could have been relaxed slightly for the GERDA-OTIS benchmark tests, but it was more convenient to maintain and adhere to a single set of requirements for all tests.) The listed instruments were a minimum; every effort short of test delay was to be made to check and record every installed instrument, i.e., to go beyond these minimum requirements. The required instruments listed herein were to be operable throughout each of the OTIS tests.

Table 3.2 Required Instruments

Measurement	Instruments	Number
Power		
Core Power	RVWM01	1
Guard Heater Control ΔT		
Reactor Vessel	All RV DT	2
Hot Leg	All HL DT	8
Pressurizer	All Pzr DT	3
Pressure		
Primary	RV or SP or PRPR20	1*
Secondary	PSPR20	1
Level (Collapsed Liquid Level)		
Primary	Overall level in each component	6*
Secondary	Overall level	1*
Flow Rate		
Primary Loop (CL+DC)	CLOR20 and DCOR20	2*
Primary Boundary	Each active stream (including HPI, HLHPV, PORV, and planned discharge)	4
Secondary Boundary (Feed and Steam)	SFOR20 and PSOR20	2*
RVVV ΔP	RVDP03	1
Fluid Temperature		
RV	RVTC01,2,7,8,9, and 10	6
HL	> 75% X 10	8
SG Primary	> 75% X 29	22
CL	All CLTCs	5
DC	DCTC01 and DCRT01	2
Pzr	PRTC01 and 03	2
SG Secondary	> 75% X 24	18
Primary Boundary Systems	HPI, planned liquid-region discharge	2
AFW	SFRF01	1
Limit Switches		
RVVV	RVLS20	1
Primary Boundary	HLHPV, PORV, RVUHV, planned discharge (4)	7
Secondary Boundary (Feed and Steam)	SF and PSLS01 and 02	4
Instrument Reference Measurements	MSTC01-03, MSRF01	4

*Denotes auctioneered and composite indications requiring that the multiple ingredient measurements be operational.

4. BENCHMARK TEST (TEST 210100)

4.1 Introduction

The OTIS-GERDA benchmark test provided a direct evaluation of the inter-facility changes. This test also gave insight into the impact of high-elevation versus low-elevation auxiliary feedwater (AFW) introduction with a voided primary system. (The differences between OTIS and GERDA are given in the OTIS Design Requirements.[1]) The basis for comparison was a boiler-condenser mode (BCM) test.

This test was composed of the following three phases: draining, BCM with low-elevation AFW injection, and BCM with high-elevation AFW. The first phase was typical of the GERDA BCM test initiation evolutions and provided several checks of measurement consistency. The second phase, BCM with low-elevation AFW injection, duplicated the conditions and trends of GERDA BCM Test 0900AA. The first two test phases thus provided an assessment of the facility modifications made for the OTIS test program. The third phase gave insight into the influence of high-elevation AFW introduction with a partially voided primary.

4.2 Performance

Test initialization, conduct, and measurements are compared to their specifications.

4.2.1 Initialization

Test initial conditions are summarized in Table 4.1. Actual initial conditions correspond to those specified in each detail.

4.2.2 Conduct

Test conduct is summarized in Table 4.2, Operator's Comments. Additional information is available in the operator's log (not included herein) and by reviewing the accompanying data plots. The following operator actions were performed as specified:

Draining Phase

- Placed the reactor vessel vent valve (RVVV) in automatic actuation on a differential pressure of 0±0.005 psi.

- Actuated a 10-cm^2 (scaled) cold leg suction leak.
- Established a 5-foot condensing length.

BCM With Low-Elevation AFW

- Increased core power from sustaining to 2.6% of full power above sustaining.
- Obtained (time-averaged) steady-state BCM.
- Transferred RVVV control from automatic to manual-open.
- Transferred AFW control from automatic-constant level to manual, manually adjusted feed flow to maintain a (cyclically) constant steam generator level.

BCM With High-Elevation AFW

- Transferred AFW injection elevation from low to high (with constant-level AFW control).
- Obtained approximately steady-state BCM with high-elevation AFW injection.
- Transferred RVVV control from manual-open to automatic actuation at 0±0.005 psi pressure difference.
- Adjusted RVVV actuation setpoints from 0±0.005 psi to 0.25 psi to open and 0.125 psi to close.

The single difference between test specification and conduct occurred in the draining phase. A second liquid-region leak site, the cold leg discharge, was actuated to hasten draining. This affected the calculation of the energy discharge rate and hence system energy closure, but had no impact on the system mass balance or on the BCM behavior being examined in this test.

4.2.3 Measurements

Measurements unavailable in this test are listed in Table 4.3. The majority of these instruments were not critical to testing, e.g., RV and hot leg conductivity probes (cf. section 3 for the identification of critical instruments). Several inactive measurements were not in the data base, namely, HPI and two-phase discharge flow rates. The string thermocouple (TC) SG primary fluid temperature measurements which were unavailable do reduce the SG primary instrumentation below the minimum level; this string TC failure was caused by a steam leak through the string sheath (and was the subject of a separate communication with the PMG). This entire string was ultimately severed and sealed to prevent leakage from the primary system.

4.3 Observations

Test observations are conveniently grouped according to the three testing phases: 1. Drain, 2. BCM with low-elevation AFW injection, and 3. BCM with high-elevation AFW injection.

The major evolutions during these phases are listed in Table 4.4. These phases are also indicated in Figure 4.1. This figure is plot type 1 from the appended data plots and traces primary and secondary system pressures versus time. The origins of this plot as well as the others are discussed at some length in Appendix A herein. A few plot features are worth noting here:

- Plot ordinates are chosen to fit the maximum point ordinates to be plotted, unless indicated otherwise in the ordinate label.
- Time-based plots are generally referenced to test initiation. For this benchmark test, zero time corresponds to the time at which the data acquisition system (DAS) was activated, approximately 1059 on 7 March 1984.
- Point density on the first curve (symbol "+") of each time-based plot gives the data density; point symbols are omitted from successive curves for plot clarity.
- Measured and directly derived variables are supplied a 6-character instrument identifier under "VTAB"; other calculated variables are labelled "CALCD."
- 100-series plots are numbered by component: 1 = reactor vessel (RV), 2 = hot leg (HL) to the HLUB spillover, 3 = steam generator primary, 4 = cold leg, 5 = downcomer, 6 = pressurizer, 7 = RVVV, and 9 = SG secondary. Thus, plot 111 shows RV fluid temperatures, 121 shows HL fluid temperatures, etc.

4.3.1 Drain Phase, 0 to 127 Minutes

The drain phase from 0 to 127 minutes after DAS activation included the primary drain, a low-power stabilization period, and, finally, a power increase preceding the next phase. The most significant inference from the draining phase is its impact on primary fluid mass, Figure 4.2. This is Plot 18 of the appended plots and shows calculated and indicated primary system fluid mass. Calculated fluid mass is set equal to indicated fluid mass at time zero, then advanced by integrating net primary system boundary mass flow rate (cf. Plot 17). Indicated fluid mass is obtained from the sum of fluid mass for each primary component, obtained in turn from fluid density, indicated collapsed liquid levels, and component fluid volume

versus elevation. (Appendix A gives more information regarding plot origins.) The primary drain is apparent, Figure 4.2. The pre-drain mass was 448 lbm, the total mass after the drain was 225 lbm, calculated, and 237 lbm, indicated. The drained mass of 223 lbm calculated, or 211 lbm indicated, approximately equals the weigh tank reading recorded by the operator, 210 lbm. (Indicated and calculated total primary fluid mass remained constant for the remainder of the test (5 hours), except that the indicated mass abruptly increased at 335 minutes when the pressurizer collapsed liquid level exceeded the elevation of its upper level tap.)

An interesting point regarding liquid levels can be found in Figure 4.3. This is Plot 4 showing collapsed liquid levels versus time; each level is referenced to the common elevation datum, the steam generator lower tubesheet upper face (SGLTSUF). Note the crossover of the hot leg (HL) and steam generator primary (SGP) levels at 65 minutes. By this time, the liquid had been drained well down from the HLUB (at 67 feet), the HL and steam generator primary formed two legs of a balanced manometer. Because the HL fluid density was less than that of the colder SGP fluid, its level would be higher than that of the SGP to balance the forces (density x elevation) between the legs. But beyond 65 minutes, the HL level was below that of the SGP. The explanation of this apparent imbalance relates to voiding at the lower elevations. Note the depleted levels in the reactor vessel (RV) and in the downcomer. The RV and DC collapsed liquid levels were approximately equal. The equivalent vapor length in the RV extended up to the HL nozzle at -1.9 feet, but that in the DC extended up to the cold leg (CL) spillover elevation at +2.5 feet. The excess voided elevation on the CL side of approximately four feet and the effects of the CL loop seal required that the SGP collapsed liquid level be greater than that in the HL to balance the whole-loop manometer. Thus the aforementioned crossover of the upper-elevation levels is attributable to unequal voided lengths at the lower elevations.

4.3.2 BCM With Low-Elevation AFW Injection, 127 to 253 Minutes

From 127 to 253 minutes after DAS activation, BCM with low-elevation AFW injection was observed. This phase of the test was comparable to the GERDA BCM Test 0900AA. After observing BCM from 127 minutes to 208 minutes at conditions comparable to those of GERDA, two boundary condition changes

were introduced. At 208, the RVVV (internals vent valve simulation) control was changed from automatic to manual-open. Because the valve had been fully open, no change was produced. At 213 minutes, AFW control was changed from automatic (to maintain a constant SG level) to manual. The valve position was then manually adjusted to obtain a constant time-averaged SG secondary level with a constant valve setting. Following this manual adjustment, which was completed at 239 minutes, BCM with constant AFW flow control was observed until 251 minutes, then with automatic AFW flow control, until 253 minutes.

The major questions addressed by this BCM testing phase were the ability of this mode to remove primary system energy and the similarity of BCM between OTIS and GERDA. Heat transfer effectiveness may be inferred directly from the primary-to-secondary pressure difference displayed on Figure 4.1. Approximately 2-1/2% of scaled full power is transferred within the SG with a pressure difference of less than 100 psi. This pressure difference corresponds to a primary-to-secondary temperature difference of less than 2OF, thus demonstrating the efficiency of heat transfer in the BCM.

This observation regarding heat transfer, as well as the cyclic behavior of the system, parallel the observations made in GERDA testing. It should be emphasized that the periodic system behavior is directly related to the absence of both HPI and a leak in this BCM benchmark test. With HPI, lower-elevation condensation would be relatively continuous and the system conditions changes seen in this BCM benchmark test would be experienced infrequently and non-cyclically. These assertions regarding BCM with HPI active are based on observations made in later tests such as the single-variable series. But examination of this cyclic BCM behavior aids in understanding system interactions. For this reason, the system conditions changes observed in this phase of the BCM benchmark test are examined at some length in the following paragraphs.

This BCM phase of the benchmark test was characterized by repetitive primary pressure variations, cf. Figure 4.1. Pressure perturbed approximately 50 psi at 3- to 5-minute intervals. This behavior may be understood by examining primary levels and cold leg temperatures, Figures 4.4 and 4.5. These figures present the usual time-based information, but time has been expanded to show more detail; selected points between 242 and 253 minutes are plotted.

Referring to Figure 4.4, the cold leg (CL) suction level increased to the CL spillover elevation, 2.5 feet, at 246 min. and again at 250 min. These CL level increases were accompanied by abrupt increases in downcomer (DC) level and by abrupt decreases in steam generator primary (SGP) level; the DC level increases and the SGP level decreases were equal in magnitude. Referring to Figure 4.5, the CL fluid temperatures upstream of the CL spillover elevation, TCs CLTC01 through CLTC03, were customarily near 200F; those beyond the spillover elevation, CLTC04 and CLTC05, were customarily at the saturation temperature, ∿510F. But when the CL liquid level approached the CL spillover elevation, the CL fluid temperature just beyond the spillover (CLTC04) abruptly subcooled; then it returned toward saturation temperature and the fluid upstream of the spillover (CLTC03) saturated.

During the period of increasing CL level, the uppermost CL liquid was apparently at saturation, insulating the lower, subcooled CL liquid from the saturated steam beyond the CL spillover and in the upper DC. When the CL refilled to the spillover elevation, the overlaying saturated liquid drained to the cold leg discharge (CLD) piping, exposing subcooled CL liquid to saturated steam. The continued throughput of condensate from the steam generator and, to a greater extent, the condensation event in the cold leg discharge piping, transported steam generator primary and cold leg liquid into the downcomer. The momentary excess of downcomer level over core-region (RV) level drove liquid from the downcomer (DC) into the core, and steam from the core into the upper DC through the reactor vessel vent valve (RVVV). The increased steam condensation reduced the primary pressure toward that of the secondary. The downcomer liquid level exceeded the elevation of the cold leg nozzle during the condensation event, and the cold leg suction liquid level receded from the elevation of the cold leg spillover. Both these occurrences suppressed further condensation. The continuing production of steam in the core region, and the transport of this vapor to the downcomer through the reactor vessel vent valve, reheated and revoided the upper downcomer and cold leg discharge fluid volumes. The fluid conditions were thus returned to their states preceding the condensation event, giving rise to the repetitive nature of these conditions variations.

4.3.3 BCM With High-Elevation AFW Injection, 253 to 366 Minutes

The AFW injection elevation was changed from low to high at 253 minutes, thus initiating the third and final testing phase. Toward the end of this phase, at 351 minutes, the RVVV differential pressure actuation setpoints were adjusted from 0±0.005 psi, to 0.25 psi to open and 0.125 psi to reclose. The BCM with high-elevation AFW injection continued to be an effective method of primary system heat removal. Approximately 2-1/2% of scaled full power was transferred within the steam generator with a primary-to-secondary pressure difference of 40 psi and a temperature difference of 6F.

An abrupt reduction of the time-averaged primary-to-secondary pressure difference of roughly 10 psi occurred at the onset of high-elevation AFW introduction, cf. Figure 4.1. More striking was the cessation of the periodic primary behavior with continued high-elevation AFW, cf. Figure 4.1. This stabilization relates to the preceding discussion of cyclic behavior and is described below.

Figures 4.6 and 4.7 present SG secondary fluid temperatures (at the lower elevations) and cold leg fluid temperatures versus time. Referring to Figure 4.6, the SG fluid temperatures abruptly began to rise toward saturation as AFW injection was transferred to the high elevation at 253 minutes. The SG primary fluid temperatures responded accordingly, as did the cold leg fluid temperatures (Figure 4.7). By approximately 300 minutes, the coldest CL fluid temperatures (CLTC02 and 03, lagging the reheat of CLTC01) exceeded 350F. Even with the continuing spillover of CL fluid, its subcooling was insufficient to trigger the previously observed lower-elevation condensation, and the system conditions perturbations ceased.

Throughout the test, the pressurizer had been gaining liquid inventory, cf. Figure 4.3. This gradual insurge may have been caused by the repetitive insurge/outsurge cycles observed during BCM with low-elevation AFW, and may also have involved guard heater control. The effect of this insurge was to lower the hot leg and steam generator primary liquid levels. The resulting increase of the steam generator condensing length (SG secondary level less SG primary level) reduced the primary-to-secondary temperature difference

required for heat transfer. If the steam generator primary level had been reduced below approximately 6 feet, the relatively short axial length of primary-to-secondary liquid-to-liquid heat transfer would have impeded SG primary outlet fluid subcooling. This would also have led to stable BCM, but the secondary pool heatup with high-elevation AFW is perceived to be the major stabilization mechanism.

4.4 Results

Test performance including initialization, conduct, and measurements was generally as specified. The single exception, the actuation of two leaks versus one leak during draining, had no effect on the BCM phases of the test.

The BCM was observed to be an effective means of primary system heat removal, both with low-elevation AFW injection and with high-elevation injection. System conditions perturbations caused by lower-elevation condensation events in the primary system were observed with low-elevation AFW injection, but they eventually stopped after the AFW injection was elevated. This stabilization of the BCM resulted from a gradual heatup of the SG secondary liquid pool. The BCM observations of this test parallel those of GERDA Test 0900AA. OTIS Test 210100 was thus satisfactory in its execution and in the results it provided.

Table 4.1 Initial Conditions[a] (Benchmark Test 210100).

Condition	Specified	Actual
Primary Pressure, psia	1000	935
Core Power, % of scaled full power (1% = 21.4 kw)	0.6	0.7
Guard Heater Control	Auto	Auto
SG Secondary Level, ft	29	30
SG Steam Pressure, psia	710	695
AFW Temperature, F	100 (approx.)	90 to 110
AFW Injection Elevation	Low	Low

[a]Unlike the other OTIS tests, this benchmark Test 210100 was composed of a series of nearly steady states with transitions between then. "Initial Conditions" are therefore less meaningful for this test than for the others.

Table 4.2 Operator Comments, Benchmark Test 210100.

Operator Comments

Operator comments are extracted from the operator's log.
Times are referenced to data acquisition system (DAS) activation.

Time	Comment
0	Activated DAS @ 1058, March 7, 1984.
2	Transferred reactor vessel vent valve (RVVV) control from manual-closed to automatic (valve opened).
5	Opened CLS (cold leg suction) 10-cm^2 leak.
9-10	RVVV cycling, pressurizer draining. Pressurizer (PZR) main heaters are off, adjusted the bias on the Pzr guard heaters.
30	Opened the CLD (cold leg discharge) 10-cm^2 leak.
43	Closed CLD leak.
45	Closed CLS leak, final drained weight is 210 lb_m.
107	Increasing core power from 14.5 kW (0.7% of scaled full power) to 70 kW (3.3%).
127	Core power at 70 kW, waiting for primary fluid temperatures to stabilize.
168	Recording video displays; a water level is visible in the hot leg viewport at 35 feet.
205	Steam generator primary inlet fluid temperature has cyclically stabilized (the time-averaged value is almost constant). The AFW flow control valve setting is varying between 10 and 40% open with a period of approximately 4 minutes.
208	Transferred RVVV control to manual-open, valve position did not change.
213	Transferred AFW flow control from automatic (constant level) to manual. Adjusting valve position to maintain a constant time-averaged SG level with a fixed valve setting.
239	Achieved a roughly constant time-averaged SG secondary level.
247-251	Preparing for AFW injection elevation change.
253	Changed AFW injection elevation from low to high.

Table 4.2 (Cont'd)

Time	Comment
314	The RV level oscillations have stopped (observation from a strip chart trace of RV level).
335	The Pzr is nearly liquid full, Pzr level oscillations have stopped (observation from strip chart).
336	Transferred RVVV control from manual-open to automatic, valve remained open.
341	Returned RVVV control to manual-open, adjusting automatic control setpoints to 0.25 psi to open and 0.125 psi to reclose.
351	Transferred RVVV control from manual-open to automatic with the revised setpoints. RVVV is cycling near closed, RV level is oscillating.
366	Completed data recording.

Table 4.3 Unavailable Measurements, Benchmark Test 210100.

SUMMARY OF VARIABLES DISCARDED ON INPUT, TEST 210100

NO.	VTAB	SYSTEM	INST.	ELEVATION	D E S C R I P T I O N
1	254RVCP02	1RV	16 CP	-2.40	CORE VESL. CONDCTVTY (WET/DRY)
2	253RVCP01	1RV	16 CP	-1.40	CORE VESL. CONDCTVTY (WET/DRY)
3	256RVCP04	1RV	16 CP	.60	CORE VESL. CONDCTVTY (WET/DRY)
4	255RVCP03	1RV	16 CP	.70	CORE VESL. CONDCTVTY (WET/DRY)
5	257RVCP05	1RV	23RCP	-8.90	CORE VESL. REF. C.P.
6	155HLTC06	2HL	2FTC	50.00	HOT LEG FLUID TEMP (F)
7	258HLCP01	2HL	16 CP	1.00	HOT LEG CONDCTVTY (WET/DRY)
8	259HLCP02	2HL	16 CP	15.00	HOT LEG CONDCTVTY (WET/DRY)
9	260HLCP03	2HL	16 CP	35.00	HOT LEG CONDCTVTY (WET/DRY)
10	261HLCP04	2HL	16 CP	37.00	HOT LEG CONDCTVTY (WET/DRY)
11	262HLCP05	2HL	16 CP	41.00	HOT LEG CONDCTVTY (WET/DRY)
12	263HLCP06	2HL	16 CP	45.00	HOT LEG CONDCTVTY (WET/DRY)
13	264HLCP07	2HL	16 CP	49.00	HOT LEG CONDCTVTY (WET/DRY)
14	265HLCP08	2HL	16 CP	53.00	HOT LEG CONDCTVTY (WET/DRY)
15	266HLCP09	2HL	16 CP	57.00	HOT LEG CONDCTVTY (WET/DRY)
16	267HLCP10	2HL	16 CP	61.00	HOT LEG CONDCTVTY (WET/DRY)
17	268HLCP11	2HL	16 CP	65.00	HOT LEG CONDCTVTY (WET/DRY)
18	269HLCP12	2HL	16 CP	67.20	HOT LEG CONDCTVTY (WET/DRY)
19	274HLCP17	2HL	23RCP	.50	HOT LEG REF. C.P.
[illegible]	273HLCP16	3SGP	16 CP	53.10	SG PRIMRY. CONDCTVTY (WET/DRY)
[illegible]	272HLCP15	3SGP	16 CP	56.90	SG PRIMRY. CONDCTVTY (WET/DRY)
[illegible]	271HLCP14	3SGP	16 CP	60.90	SG PRIMRY. CONDCTVTY (WET/DRY)
23	270HLCP13	3SGP	16 CP	64.90	SG PRIMRY. CONDCTVTY (WET/DRY)
24	222HPTM01	10HPI	13TMF	-999.00	HP INJECT. TURB.FLOW (LBM/SEC)
25	223HPTM02	10HPI	13TMF	-999.00	HP INJECT. TURB.FLOW (LBM/SEC)
26	224HPTM03	10HPI	13TMF	-999.00	HP INJECT. TURB.FLOW (LBM/SEC)
27	218HPAC01	10HPI	19ACC	-999.00	HP INJECT. ACCD.FLOW (LBM)
28	220V2AC01	12V2	19ACC	-999.00	2-PH VENT. ACCD.FLOW (LBM)
29	221V2AC02	12V2	19ACC	-999.00	2-PH VENT. ACCD.FLOW (LBM)
30	318V2RF20	12V2	38FLO	-999.00	2-PH VENT. CALD.FLOW (LBM/SEC)
31	79SMTC02	22SGS	25MTC	26.30	SG SECOND. METAL TC (F)
32	76SMTC06	22SGS	25MTC	44.20	SG SECOND. METAL TC (F)
33	289SSCP20	22SGS	32KCP	0.00	SG SECOND. UP.WET.CP (REF. FT)
34	344V1TC03	34CLD	2FTC	-999.00	CLD LEAK FLUID TEMP (F)

Table 4.4 Test Phases, Benchmark Test 210100.

"Time" is elapsed time after DAS activation and is the timing base for the data plots.

Time, min.	Evolution
0-127	Drain
0	Activated DAS @ 1058, March 7, 1984.
3	RVVV (internals vent valve simulation) to automatic actuation (at 0±0.005 psi DP).
5	Actuated 10-cm^2 (CLS) leak.
30	Actuated 10-cm^2 (CLD) leak.
43	Closed CLD leak.
45	Closed CLS leak.
107	Increasing core power to 70.1 kW (3.3% of scale full power).
127	Completed power escalation.
127-253	BCM With Low-Elevation AFW Injection
208	Transferred RVVV control form automatic to manual-open (valve remained open).
213	Transferred AFW flow control from constant SG level to manual. Adjusting AFW flow control valve manually for constant time-averaged SG level.
239	Completed AFW flow control valve adjustments.
251	Returned AFW flow control to automatic to maintain constant (29-foot) SG level.
253-366	BCM With High-Elevation AFW Injection
253	Transferred AFW injection elevation from low to high.
336	Transferred RVVV control from manual-open to automatic actuation on 0±0.005 psi differential pressure (valve remained open).
341	Returned RVVV control to manual-open (for setpoint adjustments).
351	Transferred RVVV control from manual-open to automatic actuation on differential pressure with 0.25 psi to open and 0.125 psi to reclose (valve began cycling).
366	Completed data acquisition.

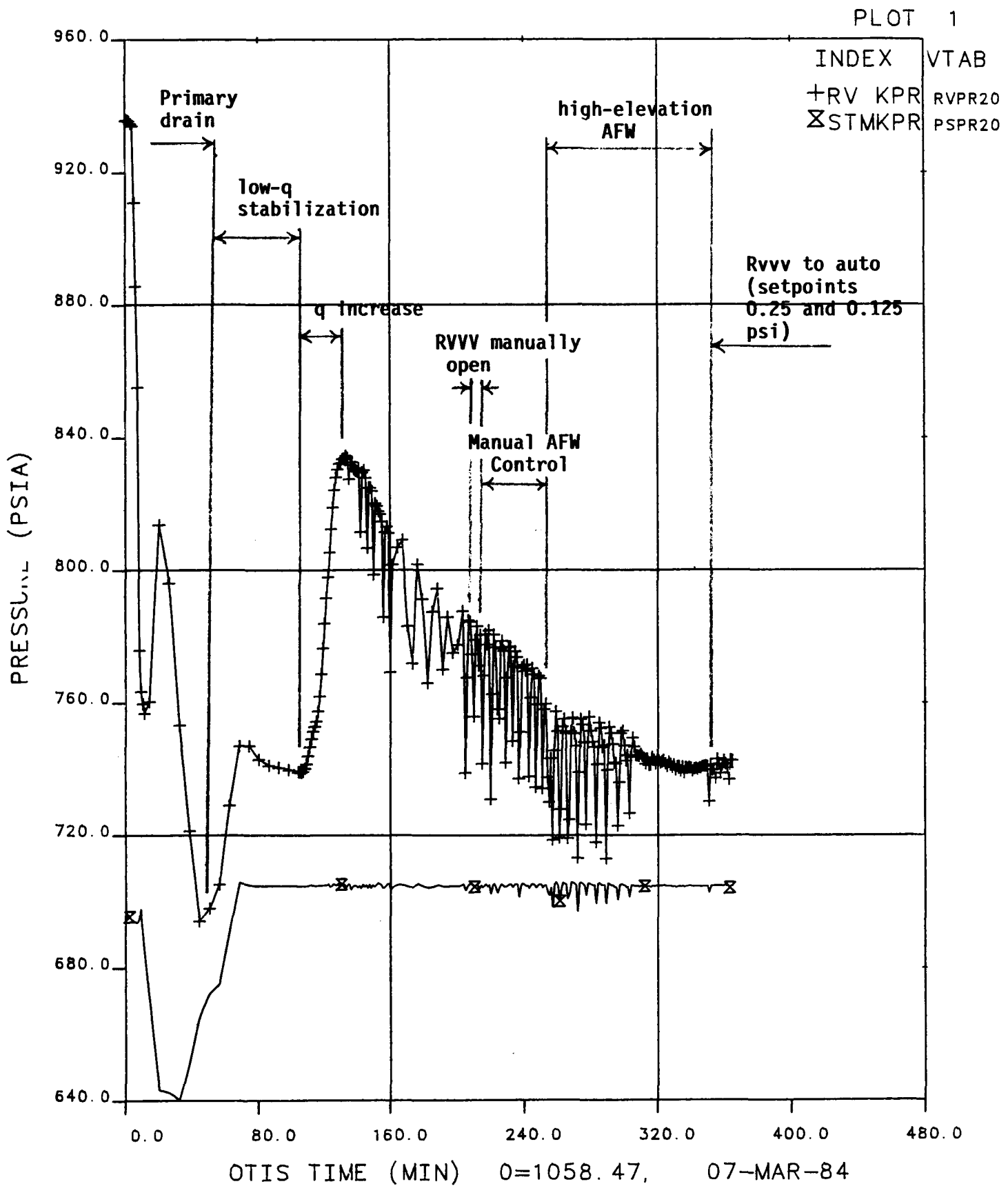

Figure 4.1 Test Evolutions: Pressure Vs. Time

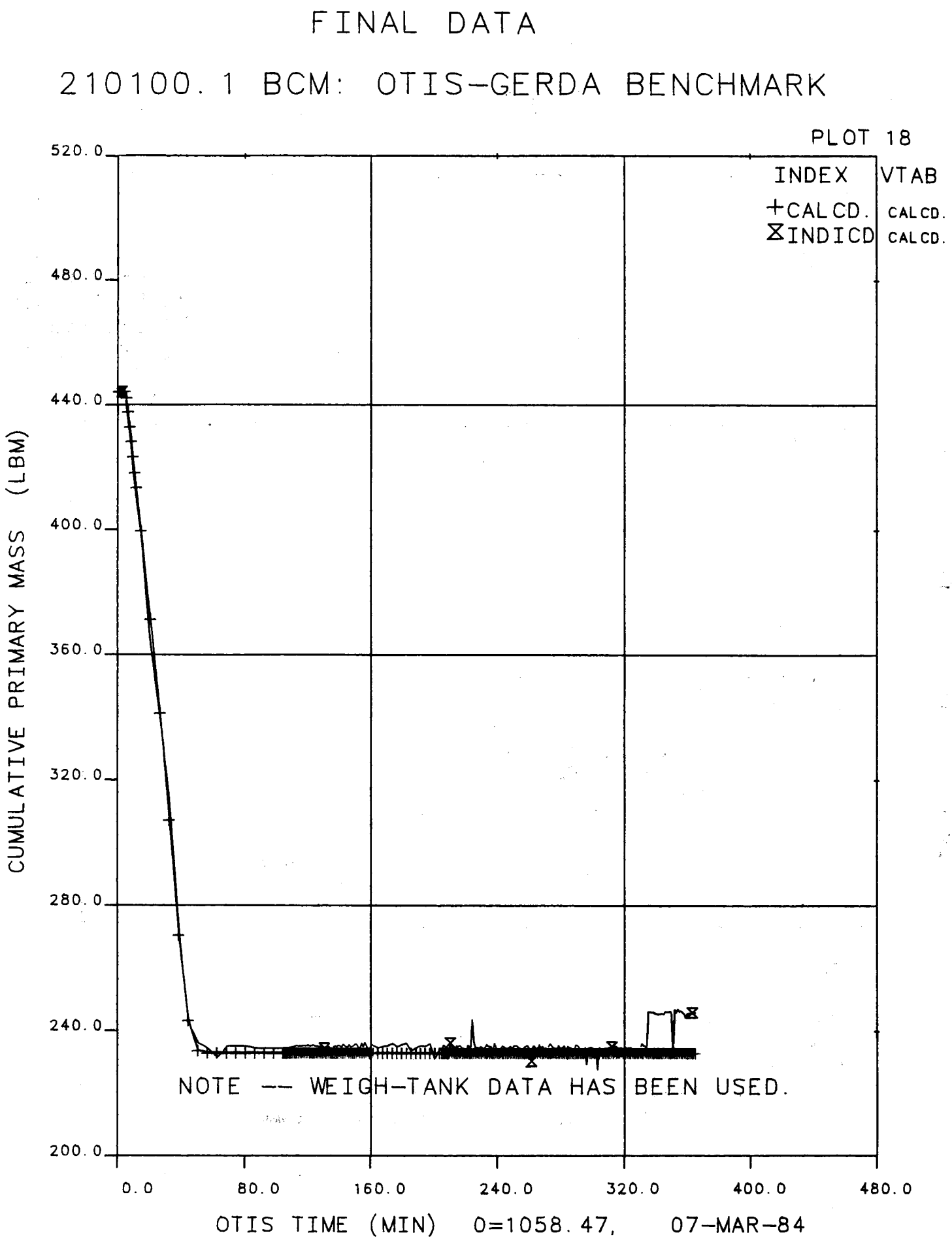

Figure 4.2 Cumulative Primary Fluid Mass

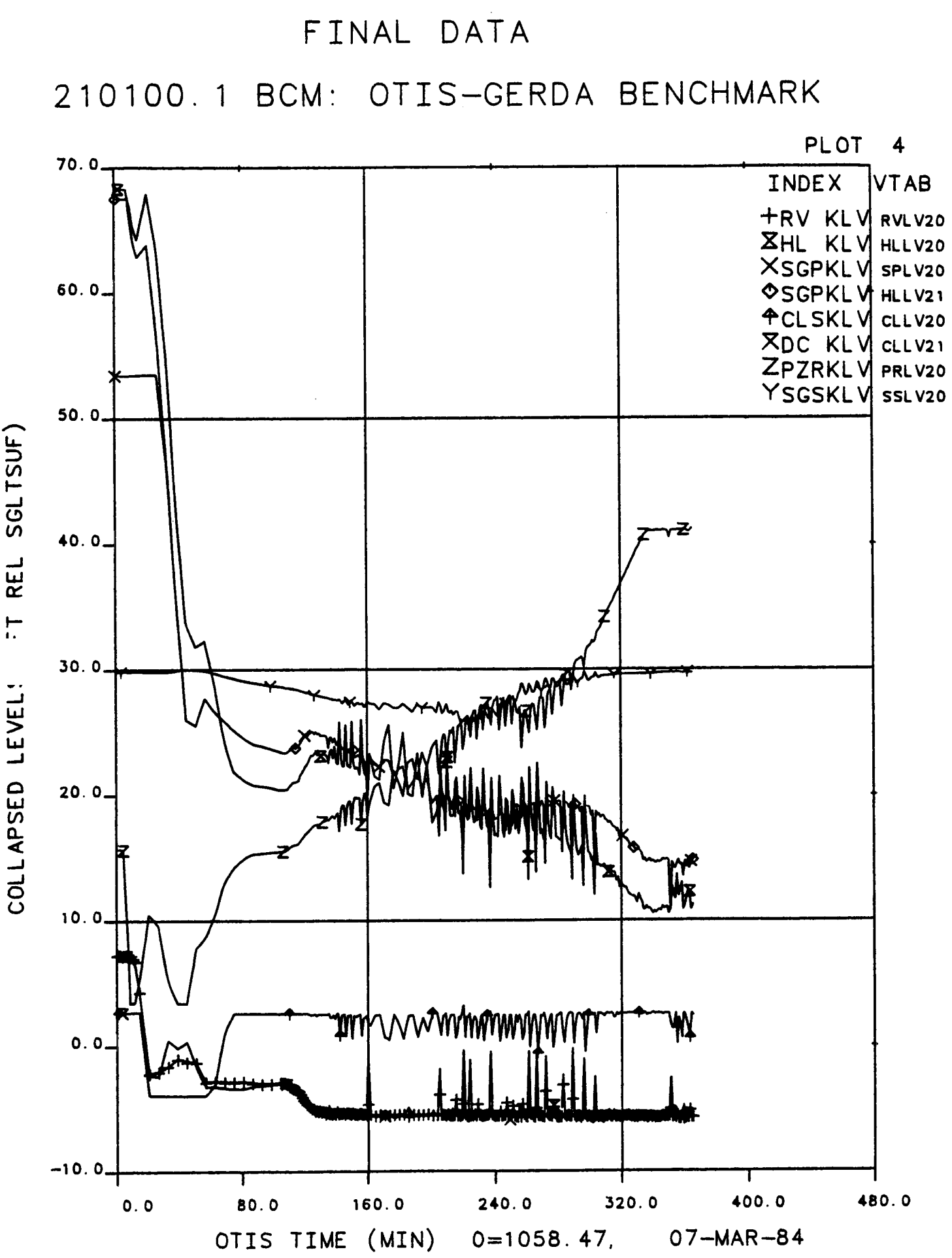

Figure 4.3 Collapsed Liquid Levels

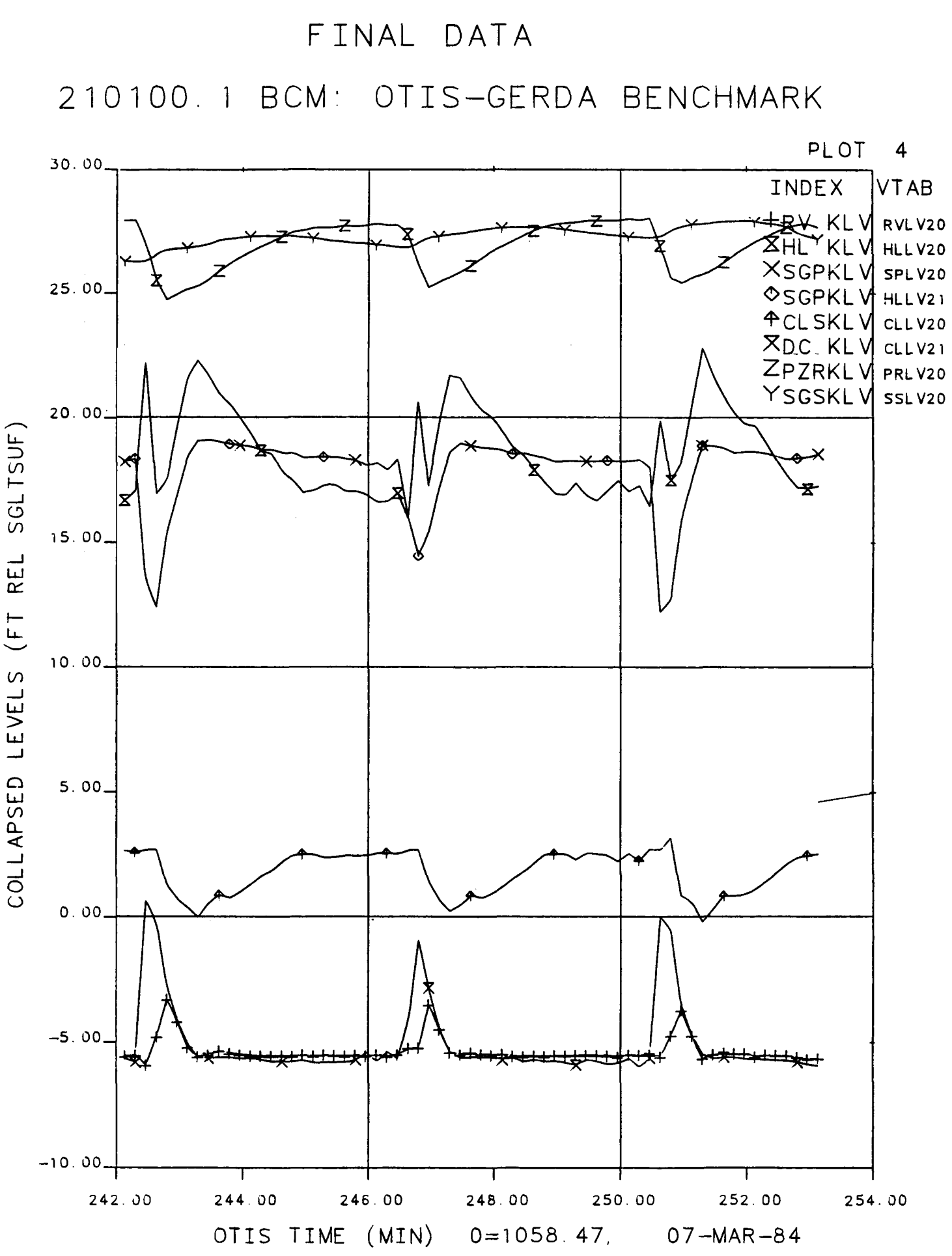

Figure 4.4 BCM: Collapsed Levels, 242 to 253 Min.

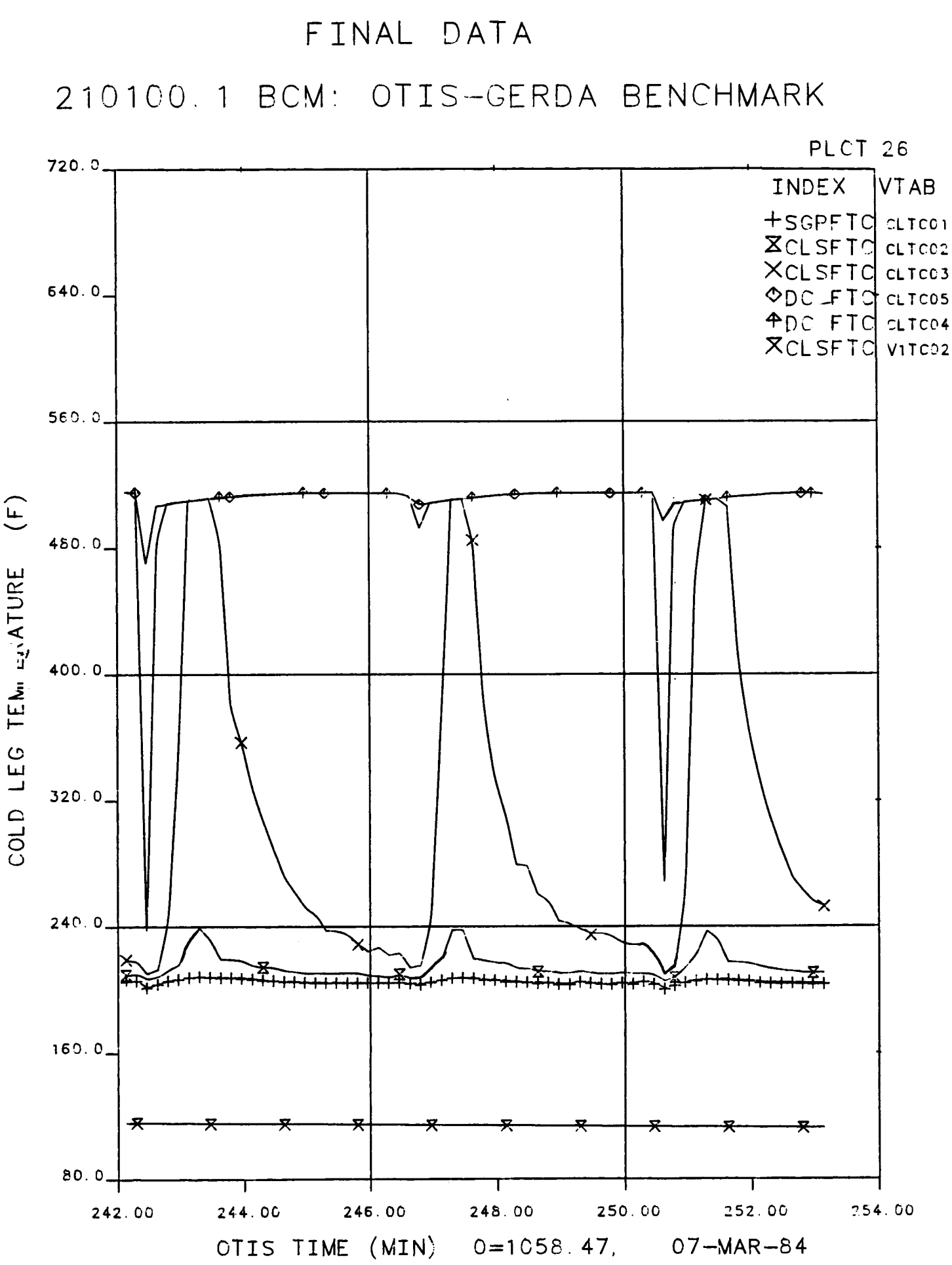

Figure 4.5 BCM: Cold Leg Temperatures, 242 to 253 Min.

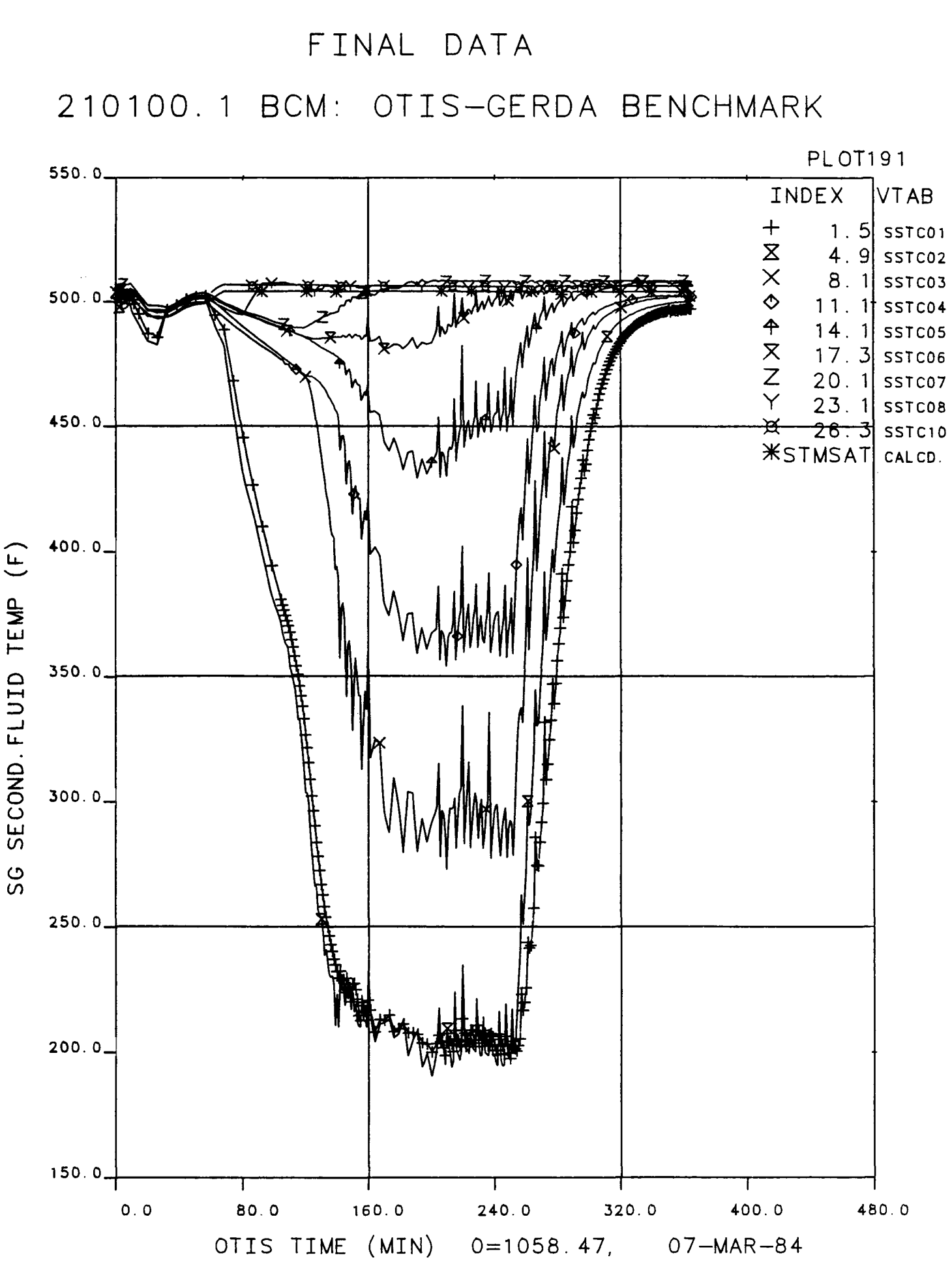

Figure 4.6 SG Secondary Fluid Temperatures Vs. Time

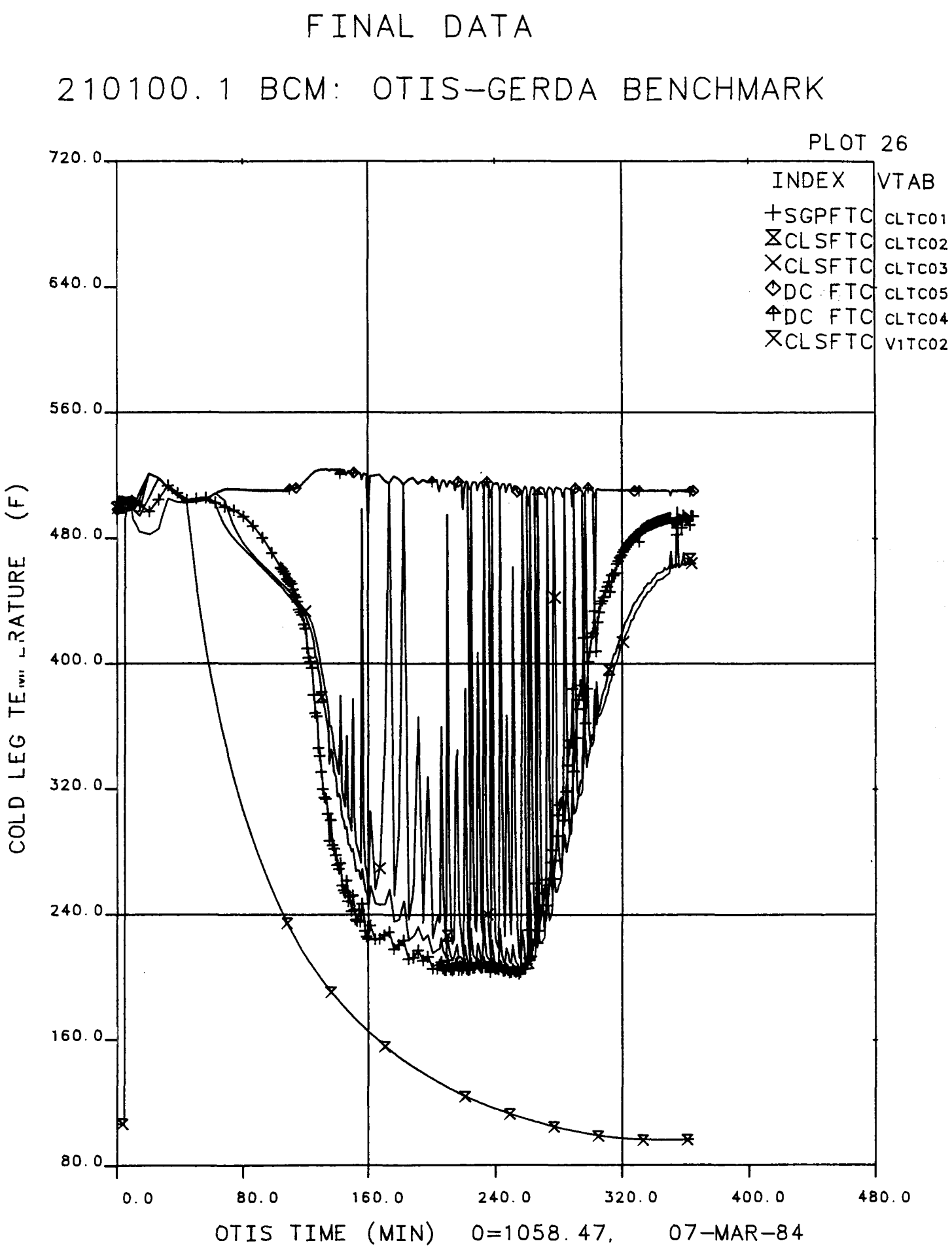

Figure 4.7. Cold Leg Fluid Temperatures Vs. Time

5.0 NOMINAL TEST (Test 220100)

Nominal Test 220100 was the reference test for the ten single-variation OTIS tests.

5.1 Introduction

The following Test 220100 conditions were designated as nominal for this test series:

- o 10-cm^2 (unisolated) cold leg suction leak.
- o Full high-pressure injection (HPI) capacity with high-head pumps.
- o 38-foot steam generator (SG) secondary level, obtained with a secondary refill rate of 3 feet of level per minute.
- o Automatic PORV actuation.
- o No reactor vessel upper head vent actuation.

Subsequent OTIS tests altered only the boundary conditions of interest but otherwise retained the conditions of this Nominal Test to facilitate inter-test comparisons and, therefore, code assessment. Test specifications are given in section 3 herein, and in references 3 and 4.

5.2 Performance

5.2.1 Initialization

Planned and actual initial conditions are compared in Table 5.1. Core power, primary pressure, steam generator secondary level, hot leg fluid temperature, and system controls were as planned. The pressurizer level was 21 feet versus 15 to 19 feet planned, and pressurizer metal temperatures ranged from 655 to 690F, compared to 640 to 660F planned. These differences are perceived to have had no impact on test behavior (pressurizer metal temperature effects were the object of an additional test).

5.2.2 Conduct

The following test control actions were performed as planned:

- o Opened the (scaled) 10-cm^2 cold leg suction (CLS) leak;

As the pressurizer collapsed liquid level dropped below 2 feet in the pressurizer (9 feet relative to the common elevation datum, the SG lower tubesheet upper face) the following events occurred:

- Actuated HPI.
- Initiated the core power ramp.
- Began the SG secondary level increase.
- De-energized the pressurizer main heaters.

- As the SG secondary level attained 38 feet, initiated the secondary depressurization ramp (to obtain 50F/h from 1000 psia).
- Opened the hot leg high-point vent five hours after leak initiation.
- Extended testing beyond refill, observed 2-1/2 hours of continuous cooldown.

The SG secondary level rate of increase (following test initiation) approximated 3 ft/min as planned. The subsequent SG secondary depressurization rate obtained 50F/h secondary cooldown as planned. Core power was decreased to approximate the specified decay characteristics (given in section 2 herein).

Test conduct as recorded by the loop operator is summarized in Table 5.2. Specific areas of test performance are discussed in the subsequent paragraphs; these discussions are generic to several of the OTIS single-variable tests. Areas addressed include: AFW control, RVVV control, HPI, primary discharge measurements, and guard heating.

Auxilary Feedwater (AFW)

AFW control was to maintain a 38-foot level in the steam generator (SG) secondary after secondary refill. Several times during the test, the operator took manual control of the AFW control valve to increase its response speed and to keep it closed. This usually occurred at the end of a period of relatively high feed demand (such as after primary-to-secondary heat transfer coupling), at which time the operator manually closed the valve as the SG secondary level exceeded the 38-foot setpoint. Because the valve was kept closed until ensuing secondary steaming had reduced the secondary liquid inventory back to the control level, the effect of this type of AFW operation was to weaken some primary-to-secondary heat transfer coupling events. The behavior of primary pressure during refill without venting was qualitatively similar among the single-variable tests; on this basis, the impact of these feed control adjustments on loop performance was apparently minor.

The constant secondary level mode of AFW control (after secondary refill) is expected to be adequate for code prediction purposes. When manual AFW control affects loop performance, such AFW control changes should be included in the code prediction boundary conditions; these occurrences are highlighted in the "Observations" sections herein.

Reactor Vessel Vent Valve (RVVV)

The RVVV (internals vent valve simulation) was controlled automatically to open at reactor vessel upper plenum-to-downcomer differential pressures greater than 0.25 psi, and to reclose at differential pressures less than 0.125 psi. The RVVV was initially closed during natural circulation. After loop flow interrupted early in the transient, the RVVV pressure difference increased and the valve customarily opened. As the test progressed and the reactor vessel upper head (RVUH) voided, the downcomer-to-reactor vessel manometer that governs the RVVV differential pressure (DP) became increasingly imbalanced. The RVVV opened and heated the upper downcomer fluid. Continued core steam production and HPI condensation of vapor in the cold leg discharge piping and/or the upper downcomer created a continuing positive RVVV differential pressure. The long-term steam production and condensation rates, however, were far too low to maintain the RVVV fully open. The model RVVV stayed fully open until the DP was reduced to 0.125 psi, then it drove fully closed. With the RVVV fully closed, the continuing steam production regenerated a differential pressure sufficient to reopen the RVVV. This cyclic RVVV operation persisted during the several-hour period of core steam production. The valve position was commonly observed to alternate between closed and only slightly open. (The plant valve would have remained slightly open, and its increased resistance at partially open would have compensated for the relatively small steam flow rate to balance the actuating differential pressure, but the model RVVV did not accommodate continuous partially open operation.)

The model RVVV would not tolerate prolonged operation with rapid cycling. Therefore, the operator transferred the RVVV control to manual-open after a period of rapid cycling was observed. Then the RVVV DP no longer varied between 0.25 and 0.125 psi; the downcomer level adjusted downward, and/or the reactor vessel level adjusted upward, both by less than six inches, reflecting the near-zero RVVV DP with continuing steam flow.

As refill occurred, the operator was to transfer RVVV control back to automatic actuation on DP. Any delay in retransferring RVVV control only retarded outer-loop natural circulation by maintaining the inner-loop flowpath (core-RVVV-downcomer) and may have retarded spillovers and refill. Such a delay may be simulated readily in a system code.

In summary, the model RVVV was opened manually to preserve the valve while simulating the partially open plant RVVV. The impact of this RVVV control change is thought to be small. (It is addressed in some detail in the discussion of the guard heater tests, in section 10 herein.) This control change is readily introduced into a code model.

High-Pressure Injection (HPI)

After loop refill, the operator was to manually throttle (i.e., reduce) HPI to maintain a mid-height pressurizer level. In several tests, the operator took manual control of HPI, increased its output, and exceeded the HPI head-flow characteristics being simulated (to raise the pressurizer level to mid-height). Such was the case in Test 220100. This post-refill operation had no impact on the preceding test events.

Primary Boundary Flow Rates

The OTIS primary boundary discharges were metered using accumulating flowmeters. These flowmeters gave detailed traces of discharged mass versus time, but they sometimes registered spurious signals. Such occurrences were apparent in the comparison of primary system fluid mass obtained by independent measurements. This comparison is given in (appended) Plot 18, "Indicated" and "Calculated" cumulative primary fluid mass. The indicated value was obtained using component fluid mass summed over the primary components; the fluid mass of each component was obtained from component liquid level, fluid volume versus elevation, and local fluid specific volume. The calculated value, on the other hand, was obtained by integrating the "net" primary boundary mass flow rate (Plot 17). Net flow rate is the signed difference between HPI and the aggregate primary discharges.

Backup information was available with which to supplement the accumulating flowmeter information. These were the discharge weigh-tank readings periodically recorded by the operator. This weigh-tank information has been

introduced as noted on Plots 17 and 18. The weigh tank data was used to calculate the offset between accumulated mass and weigh-tank mass at each time of weigh-tank observation. These offsets were then linearly interpolated to the intermediate times of data acquisition and used to modify each accumulated mass entry. This technique retained the flow rate detail of the accumulating flowmeters while obtaining the total mass closure available using the weigh tanks.

Guard Heating

OTIS used guard heaters over the hot leg, upper reactor vessel, and pressurizer (including the surgeline) to obtain approximately adiabatic fluid system boundary conditions. As described in section 2, guard heater power was controlled using pipe wall-to-insulation temperature differences. These temperature differences were biased from zero to counteract increased local heat losses such as occur at flanges and instrument penetrations. This bias was set at a specific primary fluid condition. As primary conditions changed from this setpoint, the active guard heating became correspondingly non-adiabatic. Test 220100 was not particularly responsive in this regard, but some reheating of the upper reactor vessel metal can be seen (see Plot 114 of the appended plots, from 60 to 130 minutes). The guard heater impact was more pronounced in tests that experienced a relatively long period of low primary pressure such as Test 220201, during which the primary fluid temperatures remained below the temperature at which the guard heater bias had been set. These observations have led to supplementary Tests 2202AA and -BB, which pursue pressurizer and guard heater effects. These tests are described in section 10 herein.

5.3 Observations

Five major phases were observed:

(1) draining, saturation, and intermittent circulation, 0 to 43 minutes.
(2) BCM, 43 to 105 minutes,
(3) refill without venting, <105 to 305 minutes,
(4) refill with high point venting, 305 to 433 minutes, and
(5) post-refill cooldown beyond 433 minutes.

These phases are indicated on the display of primary and secondary pressure versus time, Figure 5.1. Events comprising these phases are listed chronologically in Table 5.4. Observations are discussed by phase in the following paragraphs.

5.3.1 Draining, Saturation, and Intermittent Circulation (0 to 43 Minutes)

The data acquisition system (DAS) was activated at 0932 on 15 March 1984. Steady-state data at the test initial conditions were taken for 46.8 minutes. These initial conditions were: primary subcooled in natural circulation, 4.17% core power (3.7% plus losses to ambient, 1% of scaled full power = 21.4 kW), 609F hot leg fluid temperature, and 5.5-foot steam generator secondary collapsed liquid level. The scaled 10-cm^2 cold leg suction leak was opened 47 minutes after the DAS was activated (this defined time zero based on leak initiation, which is a common prediction-code reference time).

Primary pressure immediately began to decrease with draining (Figure 5.2), and the pressurizer level decreased from 20 feet initially to 2 feet (within the pressurizer) by 2 minutes (Figure 5.3). This triggered the second group of test initiation actions. The operator actuated high-pressure injection (HPI) and the core power ramp (simulating decay from 1-1/2 minutes after reactor trip), and initiated auxiliary feedwater (AFW) to refill the steam generator secondary from 5 to 38 feet at approximately 3 ft/min. As these initiation steps were completed at $\sim$3 minutes, the pressurizer drained completely, causing the primary depressurization rate to increase from 100 to 350 psi/min. Concurrent with this primary pressure decrease, the hot leg fluid was heated by the outsurge of pressurizer fluid (Figure 5.4). By 3 minutes the primary system pressure had descended to the saturation pressure of the upper-elevation hot leg fluid, 1700 psia. The ongoing depletion of the primary system fluid inventory then caused the hot leg U-bend (HLUB) region to void. The difference in fluid densities between the vertical piping runs upstream and downstream of the HLUB caused the downstream leg to void more extensively than the upstream leg. But the voided volume upstream of the HLUB spillover was sufficiently large to impede flow, and the primary loop flow rate abruptly decreased (Figure 5.5).

As flow diminished and the downcomer fluid temperatures began to decrease, the differential pressure across the RVVV increased, causing the valve to actuate at 4 minutes. The valve discharged slightly-subcooled fluid to the upper downcomer, immediately heating the fluid downstream of the valve from 583 to 602F (Figure 5.6). The downcomer flowrate increased in response to RVVV actuation, although the cold leg loop flow rate continued to decrease. The core exit fluid saturated at $\sim$5 minutes (Plot 5.7); the reactor vessel (RV) began to gradually lose liquid inventory. (The RV collapsed liquid level finally decreased to the RVVV elevation at 15 min, the RVVV-bracketing conductivity probes began to indicate voiding at 15.9 min.)

The period between loop fluid saturation (3 min after leak actuation) and about 16 min was interspersed with brief periods of intermittent loop flow. The loop flow activation events at times 7, 9, and 12 minutes were of lesser magnitude than the event at 16 min (Figure 5.5). The earlier events were preceded by mild primary repressurizations that are traceable to continued core void production with the reactor vessel level still well above the hot leg nozzle and RVVV elevations. Liquid spilled over the HLUB; this relatively hot primary fluid entered the top of the steam generator wherein AFW was active. (AFW was being used to refill the secondary side to 38 feet.) As a result, the cold HPI fluid was directed into the downcomer, ultimately cooling the core inlet fluid and retarding the rate of core steam production. Although this sequence of events is evidenced on many plots, the time trace of cold leg (CL) fluid temperatures is especially revealing (Figure 5.8). With interrupted loop flow, the cold HPI moved upstream (toward the break) within the CL; thus, the upstream fluid temperature (CLTC04) decreased rapidly. Upon the reactivation of primary loop flow at each spillover event, steam generator outlet fluid was swept into the CL, and HPI fluid was directed downstream toward the downcomer. The CL fluid temperature immediately upstream of the HPI point (CLTC04) abruptly increased to the upstream CL fluid temperature, and the CL fluid temperature downstream of the HPI point (CLTC05) abruptly responded to HPI cooling. Thus, the CL fluid temperature trends quite clearly annotate loop events.

The behavior of the steam generator wetted-tube primary fluid during this phase of intermittent circulation is of special significance (Figure 5.9). With positive primary loop flow, the primary fluid temperatures down the AFW-wetted tube decreased regularly with elevation. When primary flow interrupted with the AFW remaining active, the contained primary fluid cooled rapidly. Using the high elevation injection of AFW, all the wetted-tube temperature indications were affected except the highest (SPTC15), which was just above the AFW injection elevation. Twice in this period, at 8.7 and 13.0 minutes, the contained primary fluid was cooled to less than the secondary saturation temperature. Clearly, this cooling was caused by the relatively cold AFW. This is confirmed by the cooling distribution; the temperature indication immediately below the AFW injection elevation became the coldest. The significance of this AFW cooling lies in the heat transfer coupling that it implies. Highly subcooled AFW was able to wet and to cool the primary tube so that primary-to-tube heat transfer obtained the primary fluid cooling just described. These wetting and AFW sensible heat transfer phenomena indicate the role of AFW cooling in the BCM.

At 16 minutes, the reactor vessel collapsed liquid level approached the elevation of the hot leg (HL) nozzle; vapor was apparently discharged to the HL causing its level to rise (the HLUB conductivity probe rewetted) and triggering a spillover and a relatively major primary-to-secondary heat transfer event. AFW had stopped at 12.7 minutes (Figure 5.10) as the SG secondary was refilled. This recoupling raised secondary steam pressure (to the current control presssure), activating both SG steam flow and AFW. The primary depressurized from 1670 to 1540 psia during this approximately one-minute event (Figure 5.2).

Beyond this spillover at 16 minutes, loop conditions were relatively continuous until 38 minutes. Leak flow continued to exceed HPI flow (Figure 5.11), thus system fluid mass and loop liquid levels decreased. The reactor vessel level hovered near the HL nozzle elevation; thus core-region steam vented to the HL without significant primary repressurization. At 30 minutes the HL level downstream of the HLUB (the "HL Stub" level) decreased to an elevation below that of the SG upper tubesheet. The operator returned AFW control to automatic at 35 min, and at 38 min AFW activated

(Figure 5.12) to maintain the SG secondary level. This AFW-caused BCM augmented the primary depressurization rate. The secondary pressure, however, was initially below its control value (Figure 5.13), and the SG did not begin to steam; thus this boiler-condenser mode was not self-sustaining. The leak rate continued to exceed the HPI flow rate, and the SG primary collapsed liquid level approached that of the secondary by 43 min (Figure 5.14).

5.3.2 Boiler-Condenser Mode (BCM), 43 to 105 Minutes

At 43 minutes the steam generator (SG) primary collapsed liquid level was within 2 feet of the SG secondary level (Figure 5.14). Primary vapor condensed near the level interface, the upper secondary fluid superheated, the SG began to steam, AFW actuated, and the primary depressurized at 33 psi/min (Figure 5.13) due to the reduction of both primary steam volume and primary fluid energy. As the leak fluid temperature reheated (with forward loop flow), and as primary pressure decreased, the leak flow rate decreased. The HPI flow rate concurrently rose with decreasing primary pressure such that the leak and HPI flow rates intersected at 54 minutes (Figure 5.11) and the system fluid inventory began to increase. The BCM persisted, however. The primary and secondary levels remained adjacent until 61 min. By this time the primary had depressurized to 800 psia (versus 700 psia in the secondary); thus the primary-to-secondary saturation temperature difference had diminished to only 15F during the preceding BCM. The SG secondary steaming rate decreased, as did the rate of AFW injection, so that the primary and secondary pressures began to diverge. When AFW first deactivated at 65 minutes, the primary and secondary pressures were 770 and 690 psia (giving a saturation temperature difference of 10F). AFW triggered intermittently while the SG primary level remained below the elevation of the tubesheet. At 106 minutes, AFW was finally stopped by the operator to restore SG secondary level (from 39 feet). Primary pressure achieved a minimum at this time, 680 psia, but secondary pressure was now 500 psia.

During the BCM just described, the cold leg (CL) underwent a level perturbation (Figure 5.14). As the leak and HPI flow rates became approximately equal at 54 minutes, the CL fluid between the cold leg suction (CLS) leak site and the HPI injection point at the cold leg

discharge (CLD) was relatively stagnant. Examining the CL fluid temperatures (Figure 5.15), it is apparent that some heating of this CL fluid by RVVV-discharged fluid must have occurred. This effect was most pronounced just as the downcomer (and CLD) began to void. The combination of increasing CL fluid temperature and decreasing primary saturation temperature progressively flashed the CL fluid. By 56 minutes, the CL level had decreased to its lowest DP (level) tap and the CLS leak fluid temperature approached saturation (the leak mass flow rate trace indicates that the leak fluid remained single-phase liquid). The excess of HPI over leak flow and the dwindling loop flow caused CL refill and subcooling at 63 min.

5.3.3 Refill Without Venting, (before) 105 Minutes to 305 Minutes

The system began to gain fluid mass at 54 minutes, as previously noted. The HL and SG primary levels increased after 70 minutes. After the SG primary level rose above the elevation of the tubesheet at approximately 113 min (Figure 5.16), the major remaining mechanism of primary energy removal was by the heating of the HPI-to-leak fluid. As refill progressed, HPI increasingly cooled the CL fluid near the leak (Figure 5.17), and leak-HPI heat removal decreased. The model HL (stub) flow area was larger than that of the SG primary; therefore, the diversion of HPI toward the leak site became more pronounced as the primary level increased above the elevation of the SG primary. Also, the guard-heated HL stub metal was relatively hot compared to that of the SG. As a result of these heat transfer changes, the primary system gained energy, causing a weak primary repressurization with refill. Primary pressure peaked at 790 psia at approximately 233 minutes (Figure 5.18). This repressurization increased the leak flow and suppressed HPI so that both primary system total fluid energy and mass were nearly constant beyond approximately 230 minutes (Figure 5.19). Beyond $\sim$ 233 minutes, the pressurizer began to gain inventory at an increasing rate, and the HL stub level again decreased to an elevation below that of the SG upper tubesheet (Figure 5.16). The resulting increased SG heat removal from the primary very gradually decreased primary pressure (Figure 5.18). (This increasing pressuzizer level with a constant or decreasing primary pressure appears to be inconsistent and was apparently caused by non-uniform pressurizer guard heating.)

5.3.4 Refill With Venting, 305 to 433 Minutes

At 305 minutes the operator opened the HL HPV (High Point Vent) as specified. The primary depressurization rate immediately increased (Figure 5.20) due to the augmented steam volume removal. This depressurization led to an excess of HPI over leak flow (Figure 5.21). The pressurizer level remained constant at 16 feet but the HL and HL stub levels began to increase at roughly 5 ft/hour (Figure 5.22). These increasing HL levels caused increased primary-to-secondary coupling through spillovers and thus enhanced the primary system depressurization.

At 368 minutes the reactor vessel level increased toward the RVVV elevation, then fell back to the HL nozzle plane. The ensuing HL swell, spillover, and primary heat removal sequence was relatively strong. By 413 minutes the HL (upstream) level resided near the HLUB spillover. Thereafter spillover flows and primary-to-secondary heat transfer events occurred at a relatively high frequency and the core-region fluid subcooled (Figure 5.23).

5.3.5 Post-Refill Cooldown, 433 Minutes and Beyond

Both the upstream and downstream HL levels indicated full by 433 minutes (Figure 5.22), and the HL HPV began to discharge single-phase liquid (as signalled by its flow rate increase, cf. Figure 5.21). The SG secondary liquid voided, steam pressure increased, and the primary depressurized (to 440 psia by 441 minutes). The operator returned RVVV control to automatic actuation on differential pressure, the valve closed, and the CL and downcomer flow rates equalized at $\sim$2% of full flow (Figure 5.24). The primary flow rate remained quite stable for the duration of the test. The primary loop fluid temperatures decreased regularly and tracked secondary saturation temperature.

At 516 minutes, the operator took manual control of HPI to obtain a pressurizer level (a 25-foot pressurizer level was realized at 583 minutes); the HPI flow rate during this evolution somewhat exceeded the HPI head-flow characteristics to be simulated (Figure 5.21) but is perceived to have had no adverse impact on the continuing cooldown.

The test was completed at 600 minutes, having observed 167 minutes of post-refill cooldown. At the test termination, the primary loop was full, subcooled, and in natural circulation. The RV level was just above the RVVV elevation; the uppermost RV fluid temperature remained ∿50F superheated (Figure 5.23). Primary and secondary pressures were 570 and 60 psia; the corresponding saturation temperatures were 480 and 293F. Primary fluid temperatures from the core outlet to the cold leg and all steam generator secondary temperatures were at the secondary saturation temperature. The CL exit, downcomer, and core inlet fluid temperatures were 245F (reflecting HPI cooling).

5.4 Results

This Nominal OTIS Test 220100 was the reference test for the succeeding single-variable tests. Nominal conditions included a scaled 10-cm^2 cold leg suction leak, full-capacity and high-head HPI, and a 38-foot steam generator secondary level after secondary refill. The test was initialized largely as planned, and steady initial conditions were recorded for 47 minutes preceding leak opening. Test conduct was largely as planned. The items discussed in the text (AFW control, RVVV control, HPI, primary discharge measurements, and guard heating) should not preclude code prediction of the transient.

This Nominal Test experienced each of the post-SBLOCA events: draining, saturation, intermittent circulation with primary repressurization, the boiler-condenser mode (BCM), refill equilibrium without venting, refill, and post-refill circulation and cooldown. In addition to these major integral-system responses, this test has displayed several additional interactions of interest. Among these are auxiliary feedwater (AFW) cooling and cold leg fluid heating. With interrupted primary flow and AFW active, the primary fluid within the tube wetted by AFW was cooled below the secondary saturation temperature. The attendant wetting and heat transfer affected the ability of high-elevation AFW (alone) to trigger the boiler-condenser mode. Midway into the BCM, the CL fluid briefly saturated and voided. This was caused by CL fluid heating and the concurrent primary system depressurization (with BCM). But the observed CL fluid temperatures

indicated that its heat source was core-region fluid, i.e., vapor discharged through the RVVV. Considering the relative locations of the HPI point (at the CL discharge just upstream of the CL-downcomer junction) and the RVVV (discharging into the top of the downcomer), the core region vapor generation rate (produced by core heating and by flashing with system depressurization) apparently exceeded the cooilng capability of the HPI.

Table 5.1 Initial Conditions, Nominal Test 220100.

	Specified	Actual
o Core power (% of full power, 1% full power = 24.1 kW), includes 0.5% to replace losses to ambient.	4.2±0.1	4.17
o Natural circulation.	X	X
o Primary pressure, psia.	2200±50	2197
o Pressurizer liquid height, ft from SGLTSUF.	16.6±2	20.6
o Pressurizer main and guard heaters adjusted for an approximately adiabatic pressurizer.	X	X
o RVUHV and HLHPV closed.	X	X
o RVVV in automatic (differential-pressure) control with open/close setpoints of 0.25 and 0.125 psi.	X	X
o AFW at 100F injected at the upper elevation using the minimum-wetting nozzle.	X	(115F)
o SG secondary (collapsed) liquid level (with constant level control).	5 ± 1	5.5
o Hot leg fluid temperature, F.	610 ± 2	609
o HPI and leak systems are not yet in use. Primary noncondensible gas additions are not to be tested.	X	X
Initialization is continued until a suitable system steady state is obtained:		
o Pressurizer metal temperatures, F.	650±10	655-690
o The RVVV is not cycling.	X	X
o The steam generator fluid temperatures are varying less than 10F/h (exception: cyclic secondary fluid temperature variations associated with high AFW injection, and with internal circulation within the secondary liquid pool, are acceptable).	X	X
Other initial conditions: T_{cold} = 571F, primary flow rate = 5.5%, SG pressure = 1201 psia, feed and steam flow rate = 2.2%.		

Table 5.2 Operator Comments, Nominal Test 220100.

Operator comments are extracted from the operator's log. Times are referenced to leak actuation.

Clock Time	(Leak) Time, min	Comment
0932	-46.8	Activated the data acquisition system @ 0932, 15 March 1984. Started steady-state data recording.
1017	-2	Adjusted pressurizer guard heater bias.
1018	0	Opened a scaled 10-cm^2 cold leg suction leak.
1020	1	Activated HPI.
1021	2	Deactivated pressurizer main heaters; HPI flow was being indicated; began core power ramp and SG secondary level increase.
1022	3	RVVV opened.
1030	11	Spillover observed (the usual indication is obtained from the HLUB viewport).
1031	12	The SG secondary has been refilled to the control level; transferred AFW control to constant level and initiated the secondary depressurization ramp.
1035	16	RVVV is cycling between open and closed.
1037	18	RVVV is closed, but with brief cycles toward open and then back closed (again observed at 24 min).
1038	19	Took manual control of AFW and shut the valve to return SG secondary level to the control point; returned AFW control to automatic on constant level at 35 min. Subsequent periods of manual AFW control (times in min) = 106-116, 155-174, 190-199, 288-368, 386-391, and >498.
1050	31	Transferred RVVV control from automatic to manual-open. The reactor vessel collapsed liquid level increased ∿1/2 foot and its level oscillations decreased from approximately 1/2 foot to 2 inches (operator observations from strip chart recordings).

Table 5.2. (Cont'd)

Clock Time	Time, min	Comment
1123	64	The RVVV control relay is starting to cycle (the valve remains manually open, relay actuation indicates that differential pressure is crossing the opening or closing setpoint; audible observation).
1534	305	Opened the HLHPV.
1540	321	Adjusted the HPI system valve setting to stabilize HPI flow rate.
1629	370	Spillover observed (spillover observations are made using the HLUB viewport and/or the automatic opening of the SG secondary steam pressure control valve). Subsequent spillover observation times (m): 375, 382, 388, 415 (slight), 418 (small), 422-427 (SG secondary steam flow), and 430.
1630	371	Leak effluent was not collected in the weigh tank, for 18 min.
1734	435	Large spillover, HL filled, and pressurizer emptied; transferred RVVV control to automatic actuation on differential pressure and the valve closed.
1743	444	Natural circulation has restarted at ∿2000 lbm/h (∿2% of scaled full flow).
1856	517	Pressurizer level is fairly stable at 15 feet (relative to the common datum, the SG lower tubesheet upper face). Taking manual control of HPI to establish a pressurizer level of 23 feet.
2018	600	Completed testing, de-activated the data analysis system at 2018, March 15, 1984. Test duration was 10h47m, or 10 hours from leak opening.

Table 5.3 Unavailable Measurements, Nominal Test 220100.

SUMMARY OF VARIABLES DISCARDED ON INPUT, TEST 220100

NO.	VTAB	SYSTEM	INST.	ELEVATION	DESCRIPTION
1	155HLTC06	2HL	2FTC	50.00	HOT LEG FLUID TEMP (F)
2	262HLCP05	2HL	16 CP	41.00	HOT LEG CONDCTVTY (WET/DRY)
3	263HLCP06	2HL	16 CP	45.00	HOT LEG CONDCTVTY (WET/DRY)
4	264HLCP07	2HL	16 CP	49.00	HOT LEG CONDCTVTY (WET/DRY)
5	265HLCP08	2HL	16 CP	53.00	HOT LEG CONDCTVTY (WET/DRY)
6	266HLCP09	2HL	16 CP	57.00	HOT LEG CONDCTVTY (WET/DRY)
7	274HLCP17	2HL	23RCP	.50	HOT LEG REF. C.P.
8	273HLCP16	3SGP	16 CP	53.10	SG PRIMRY. CONDCTVTY (WET/DRY)
9	272HLCP15	3SGP	16 CP	56.90	SG PRIMRY. CONDCTVTY (WET/DRY)
10	223HPTM02	10HPI	13TMF	-999.00	HP INJECT. TURB.FLOW (LBM/SEC)
11	221V2AC02	12V2	19ACC	-999.00	2-PH VENT. ACCD.FLOW (LBM)
12	79SMTC02	24SGS	25MTC	26.30	SG SECOND. METAL TC (F)
13	76SMTC06	22SGS	25MTC	44.20	SG SECOND. METAL TC (F)
14	344V1TC03	34CLD	2FTC	-999.00	CLD LEAK FLUID TEMP (F)

Table 5.4 Test Events, Nominal Test 22010.

DAS Time, min	Leak Time, min	Events
0	--	The DAS was activated at 0932 on March 15, 1984; recording pre-test steady state initial conditions.
Draining, Saturation, Intermittent Circulation; 46 to 90 Min.		
46.8	0	The scaled 10-cm^2 CLS leak was opened. The primary system began to depressurize, the Pzr began to lose inventory.
∿50	∿3	The operator actuated HPI, the core power decay ramp, and SG refill at ∿3 ft/min. The Pzr drained, the primary depressurization rate increased from 100 to 350 psi/min (at ∿3m, current pressure is 1900 psia).
50.0	3.2	The HLUB fluid saturated, primary pressure stabilized at 1700 psia. The HL stub (downstream of the HLUB) began to lose inventory, primary loop flow rate abruptly decreased.
51	5	The RVVV (internals vent valve simulation) differential pressure exceeded 0.25 psi; the valve actuated; the temperature of the fluid downstream of the valve rapidly increased to the temperature of the fluid upstream of the valve and DC flow increased independently of CL primary loop flow.
53	6	The RV fluid above the core saturated.
54	7	A brief and minor spillover occurred. After this event, the continuing AFW cooled the upper primary fluid in the wetted tube to below the secondary saturation temperature (to 510F versus 551F secondary saturation temperature). The primary system repressurized weakly during this event.
56	9	The RV outlet and top plenums began to void, HPI-cooled fluid flowed toward the SG in the CL.
56	∿10	A brief spillover occurred, halting the primary pressure increase and draining the pressurizer.

Table 5.4 (Cont'd)

DAS Time, min	Leak Time, min	Events
60	13	The SG secondary refill to 38 feet was completed, the operator activated the secondary depressurization from 1000 psia to obtain 50F/h secondary cooldown. The RV liquid level began to decrease more rapidly, the HL stub level had dropped below 60 feet, the HL upstream level was higher but was also voided. The primary began to repressurize from 1560 psia, a pressurizer insurge began.
62	16	The RV liquid level decreased past the RVVV elevation. The RV fluid above the core exit was at saturation temperature.
∿64	∿17	RV liquid level dropped to the elevation of the HL nozzle. A relatively large HLUB spillover occured: The primary depressurized from 1670 to 1540 psia, secondary pressure increased to the control pressure, SG feed and steam flow rates increased from 0 to 5% of full secondary flow, and the pressurizer drained.
65-90	18-43	Primary levels (HL and stub) decreased at 1 ft/min. The RV level remained in the vicinity of the HL nozzle, primary pressure stayed roughly constant. At 29 min, the SG primary liquid level entered the SG. At 32 min, the operator transfered RVVV control from automatic (on differential pressure) to manual-open; the downcomer flow rate began to increase regularly. At 38 min, AFW actuated to maintain SG level and the primary and secondary were briefly coupled.
BCM, 90 to 150 Minutes		
90+	44+	At 43 min, the SG primary liquid level approached the SG secondary liquid level (to within 2 feet). SG steam flow and AFW actuated, the primary and secondary coupled (BCM), and the primary system depressurizes at 33 psi/min. The CL fluid flashed at 53 min. Its level decreases to -4 feet by 56 min.
∿ 100	54	The increasing HPI flow rate and decreasing leak mass flow rate crossed. The HL and steam generator primary levels began to gradually increase at approximately 70 minutes after leak opening.

Table 5.4 (Cont'd)

DAS Time, min	Leak Time, min	Events
108	61	The SGP liquid level began to increase, the BCM weakened. The SG heat removal rate was decreasing, the leak-HPI energy removal was also decreasing due to the decreasing leak flow rate and leak fluid temperature; hence, the net primary system energy change became positive.
110	63	The CL refilled, the HL level dropped abruptly.
Refill Without Venting, <150 to 352 Minutes		
∿ 152	∿ 105	The SG primary liquid level increased above the SG upper tubesheet. Primary pressure began to increase from a minimum of 680 psia (SG secondary pressure was 490 psia and decreasing).
∿ 175	∿ 128	The increasing leak mass flow rate approached the HPI flow rate. The SG primary level briefly dropped to 50 feet, primary loop flow briefly re-activated.
258-260	211-213	The reactor vessel level momentarily increased above the HL nozzle elevation, then the HL level peaked at the HLUB spillover elevation. Primary loop flow reactivated temporarily, the primary system pressure increase was interrupted.
280	233	Primary pressure attained a broad maximum of 790 psia. The primary fluid mass inventory was roughly constant. The HL level was roughly constant; the HL stub level was decreasing and the pressurizer level was increasing.
300	253	The HL stub level decreased below 52 feet causing mild primary-to-secondary heat transfer.
352	305	The operator opened the HL high point vent (HPV) as specified. The primary system depressurization began to strengthen.
415	368	The reactor vessel level increased well above the HL nozzle elevation, then decreased. The HL level increased to the spillover elevation. Primary-to-secondary heat transfer ensued, enhancing the primary system depressurization

Table 5.4 (Cont'd)

DAS Time, min	Leak Time, min	Events
		and primary loop flow. The RV inlet fluid subcooled, the core- region void fraction decreased toward zero in an oscillatory fashion. The excess of HPI over leak flow increased.
460-480	413-433	The HL level approached the HLUB spillover elevation. Loop flow oscillated at a relatively high frequency. CL fluid temperatures varied between 150 and 300F. The HL fluid temperatures decreased from 480 to 320F, starting with the lowest-elevation HL fluid.
Post-Refill Cooldown, >480 Minutes		
480	433	The HLUB refilled, loop flow rate stabilized at ∿2% flow. SG secondary pressure increased, the SG secondary liquid voided. The operator returned the RVVV control to automatic, the valve closed.
563	516	The operator took manual control of HPI to obtain a mid-height pressurizer level (the pressurizer level reached ∿25 feet at 583 min.).
647	600	The test was completed. Final conditions: The primary loop was full and subcooled, pressurizer level was 25 feet, RV level was ∿0.5 feet (near the RVVV elevation). Primary pressure was 570 psia (480F saturation), SG secondary pressure was 60 psia (293F saturation). Primary fluid temperatures were decreasing at ∿ 12F/h. Primary loop flow rate remained at ∿2% flow. The RV top plenum void fraction was ∿ 70%, the uppermost RV fluid temperature remained ∿50F superheated.

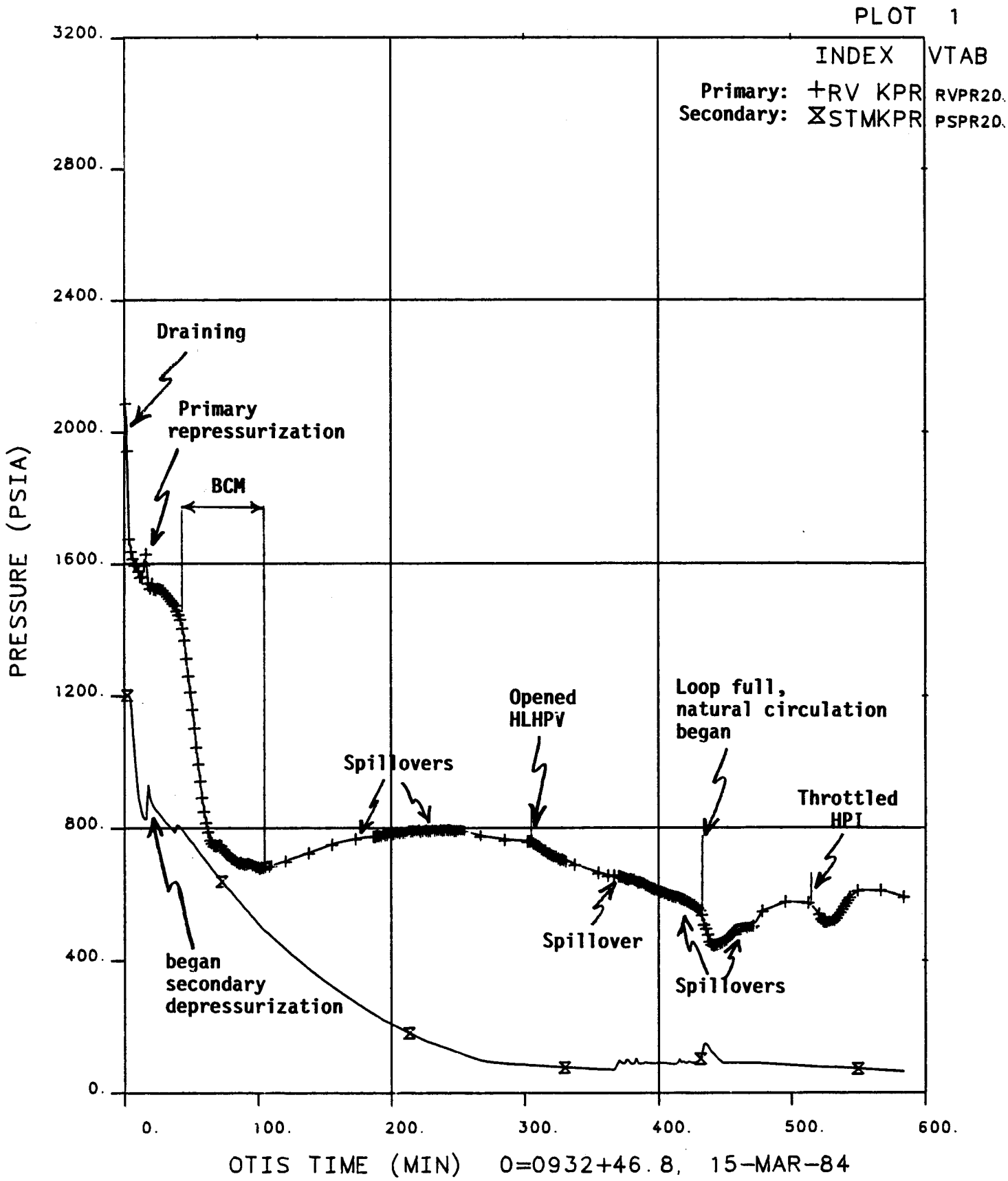

Figure 5.1 Pressures and Test Phases

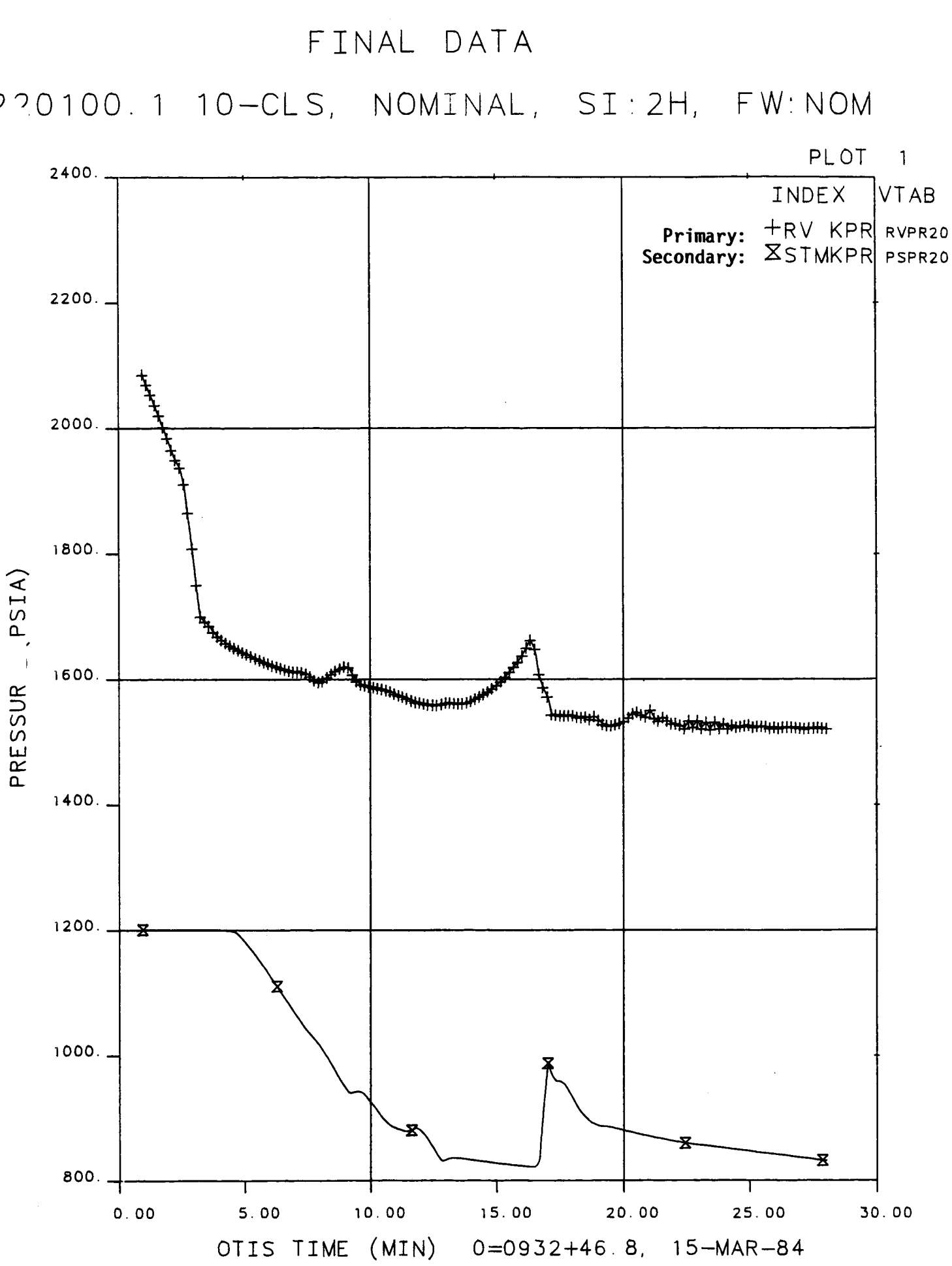

Figure 5.2 Primary and Secondary Pressures

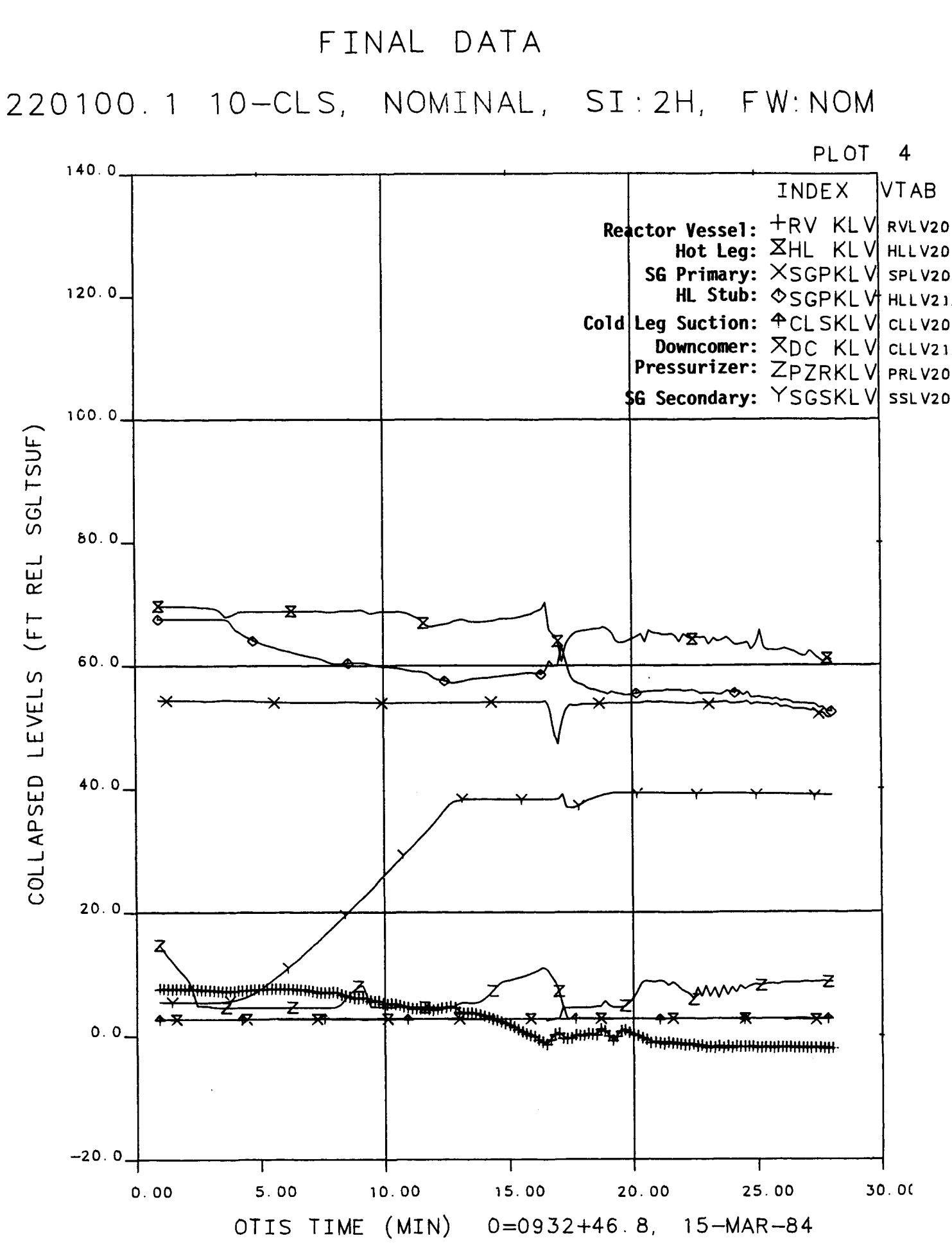

Figure 5.3 Collapsed Liquid Levels

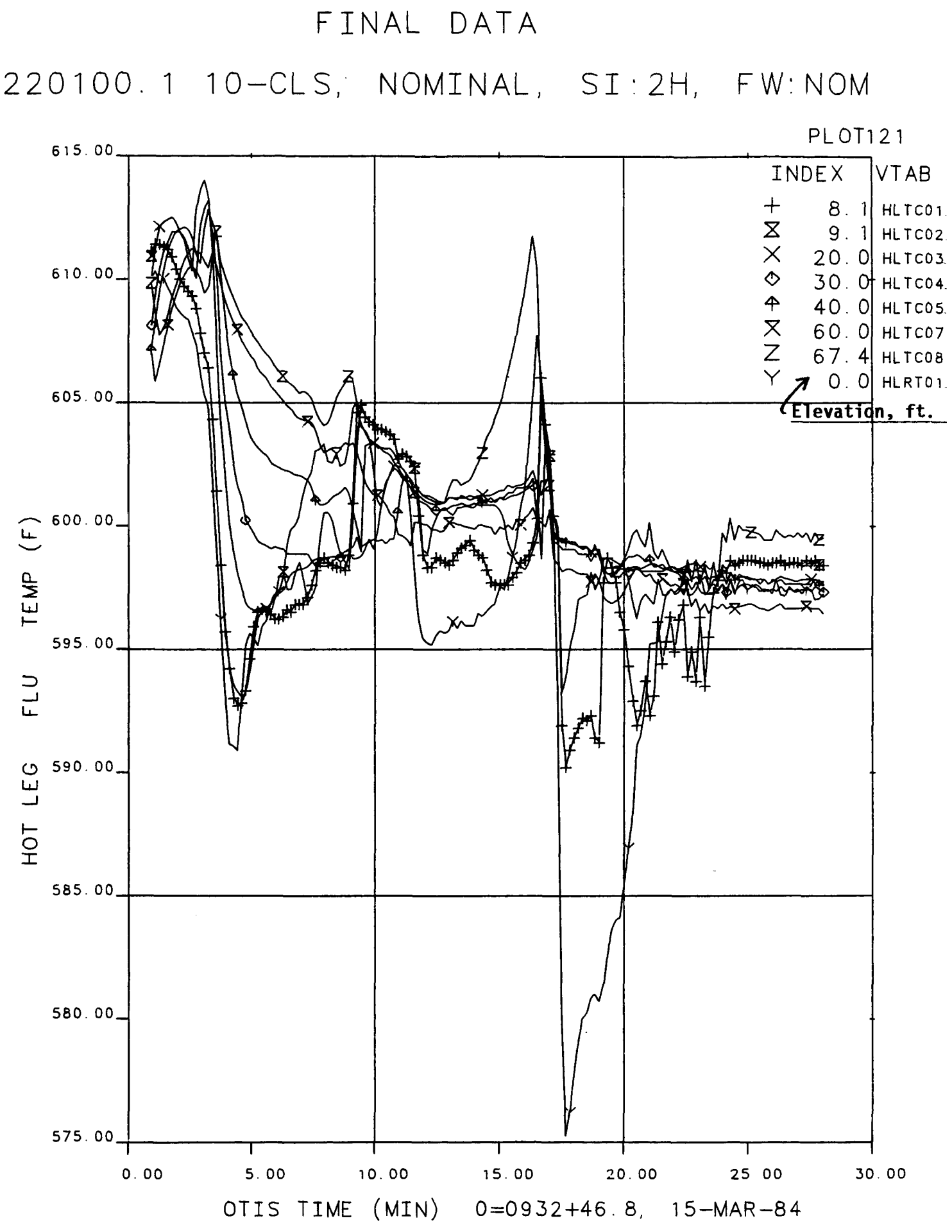

Figure 5.4 Hot Leg Fluid Temperatures

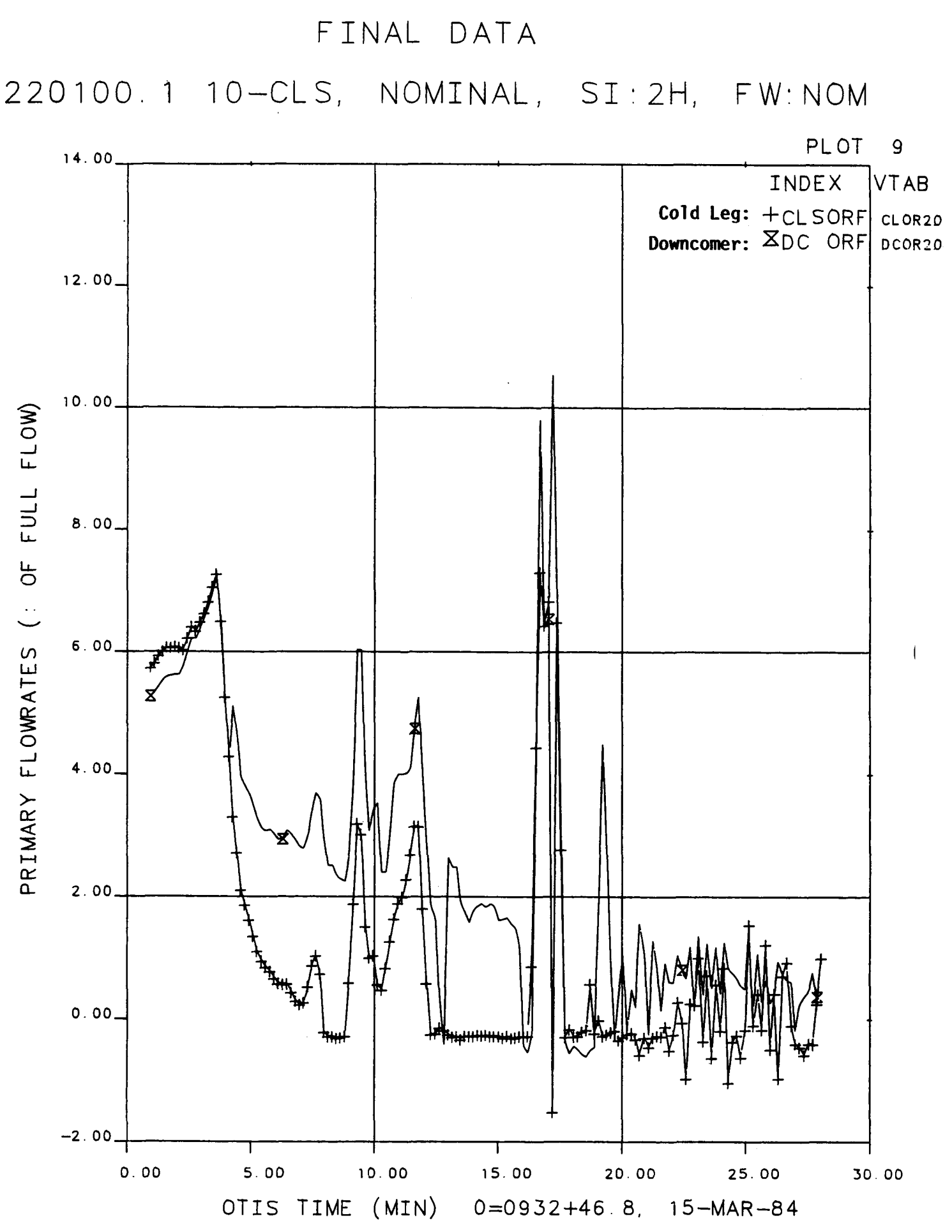

Figure 5.5 Primary Flowrates

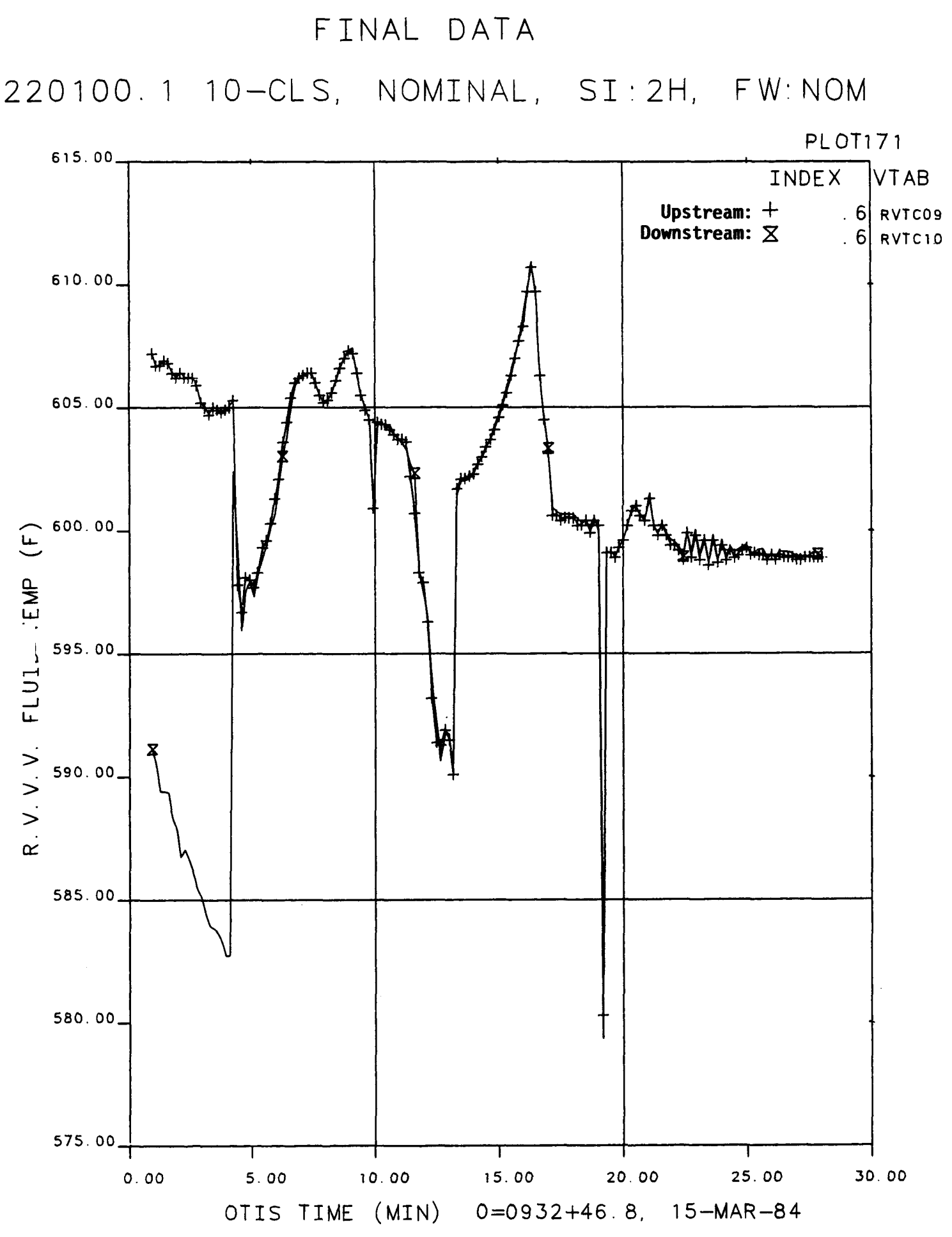

Figure 5.6 RVVV Fluid Temperatures

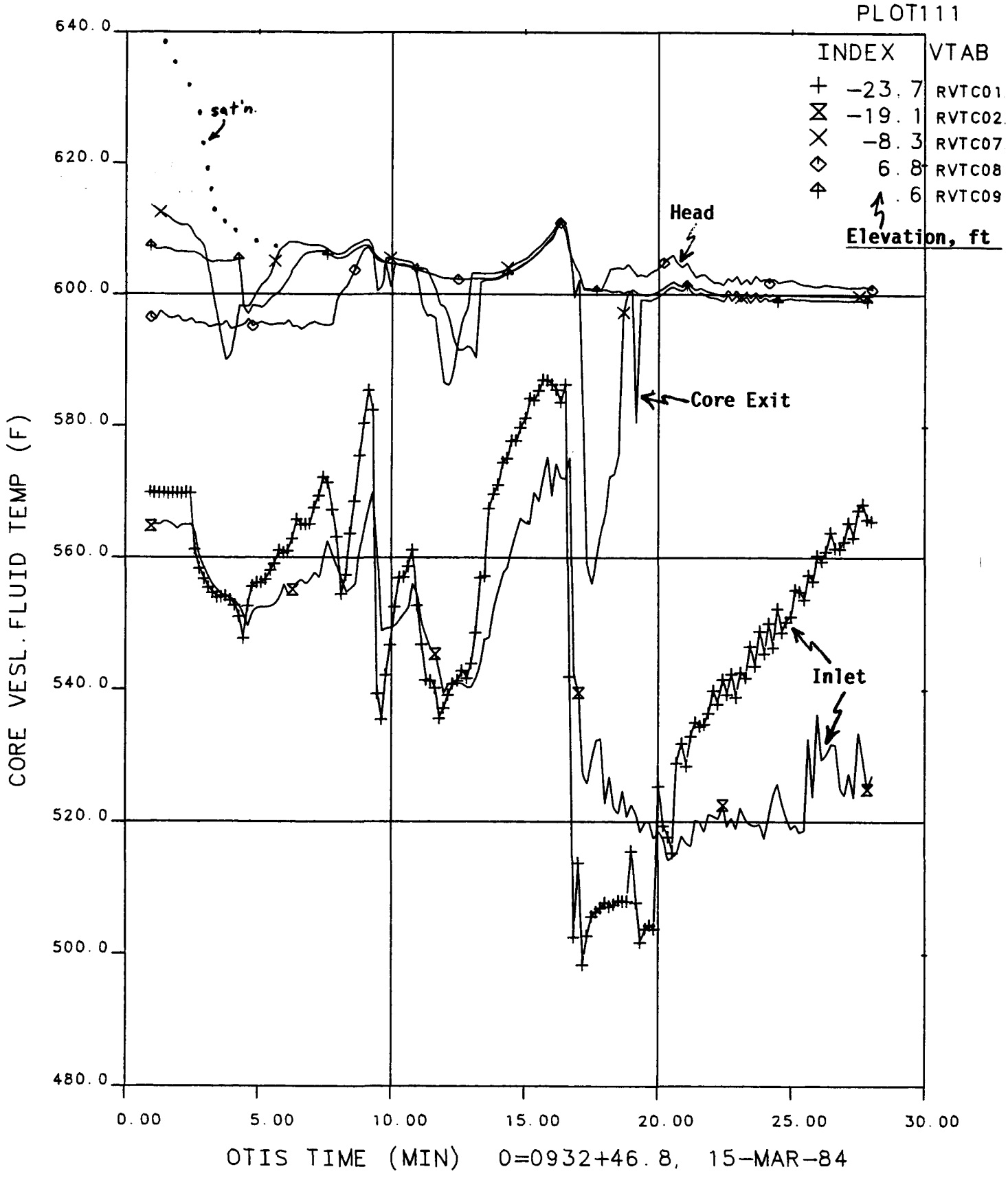

Figure 5.7 Core Vessel Fluid Temperatures

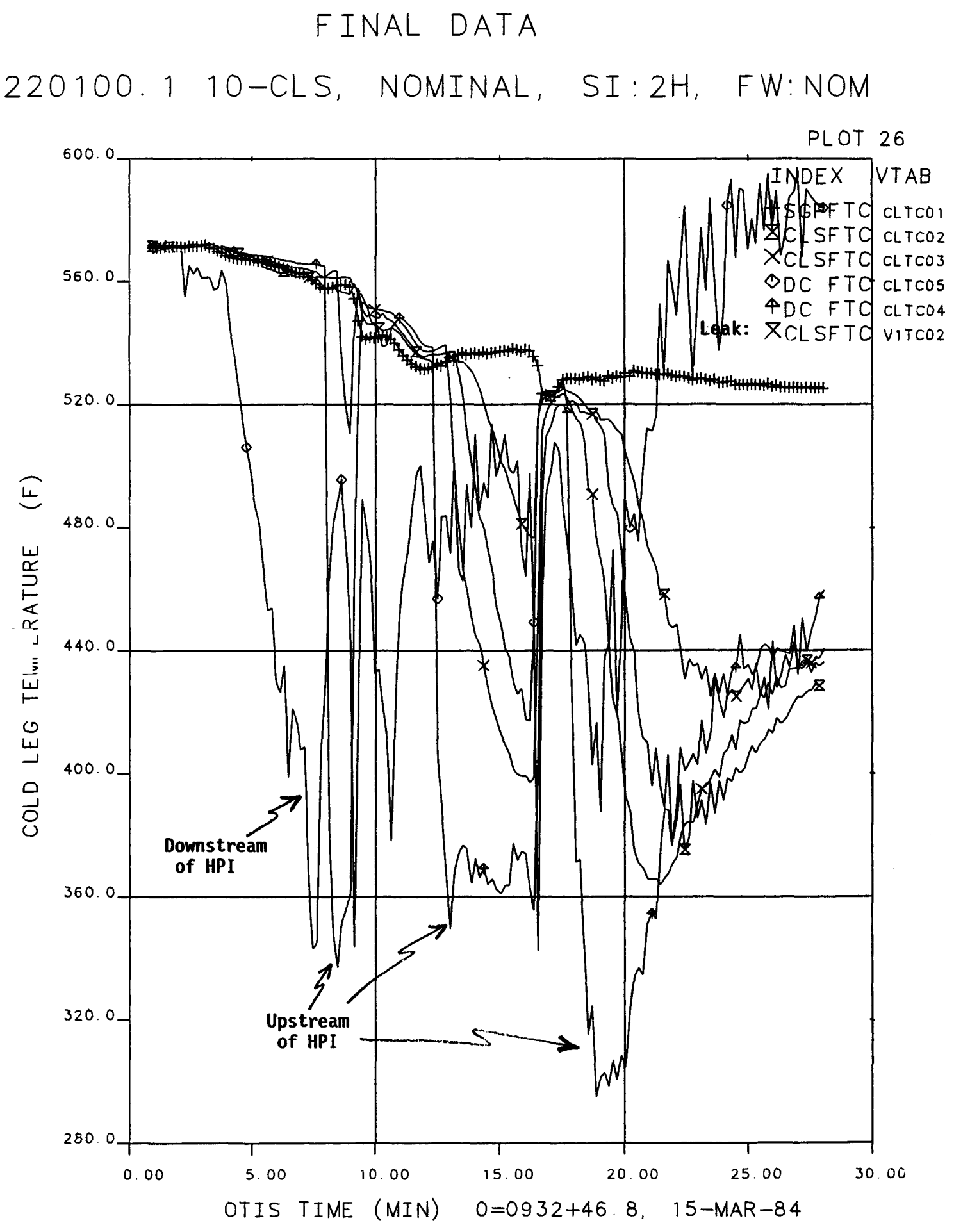

Figure 5.8 Cold Leg Fluid Temperatures

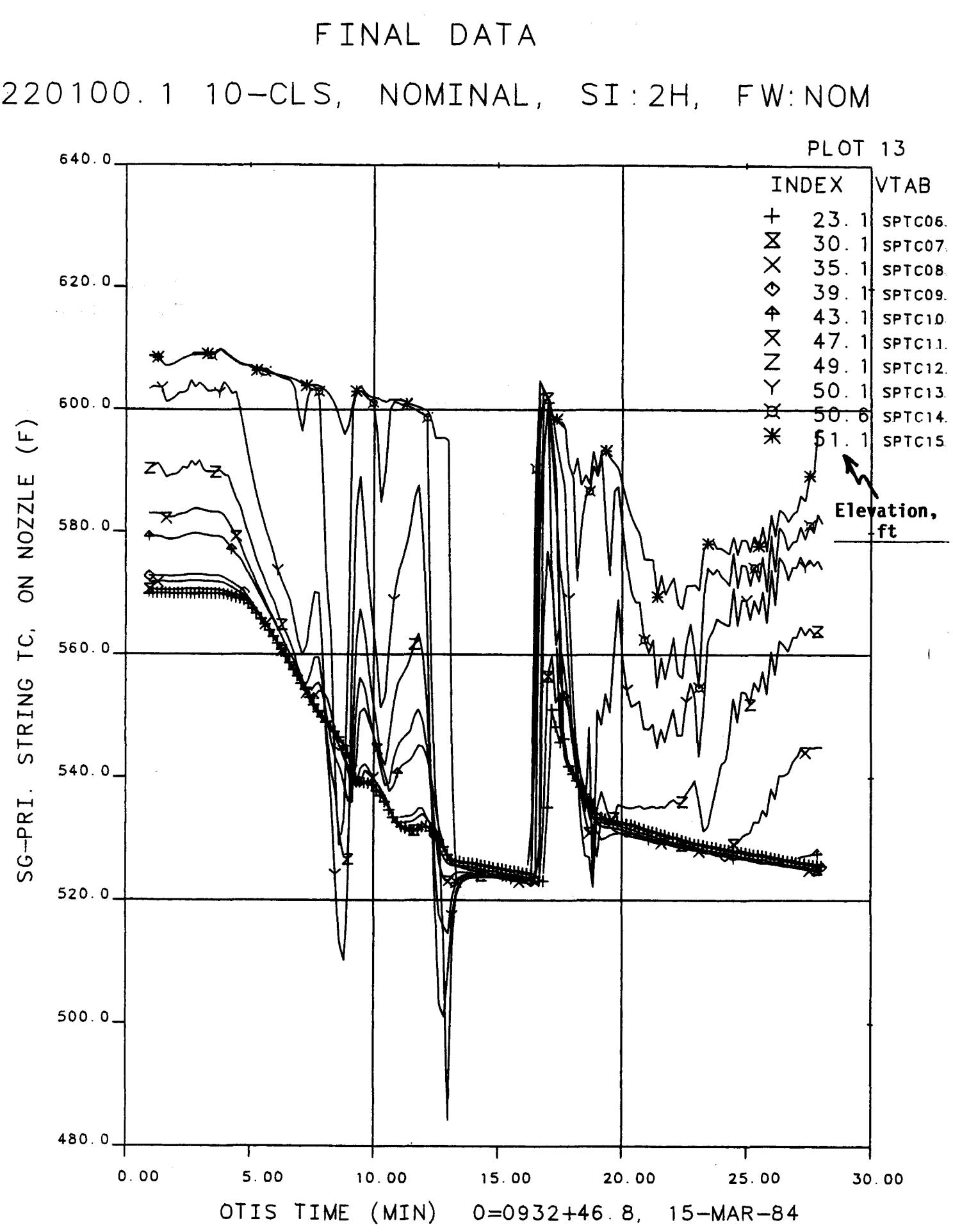

Figure 5.9 Wetted-Tube SG Primary Fluid Temperatures

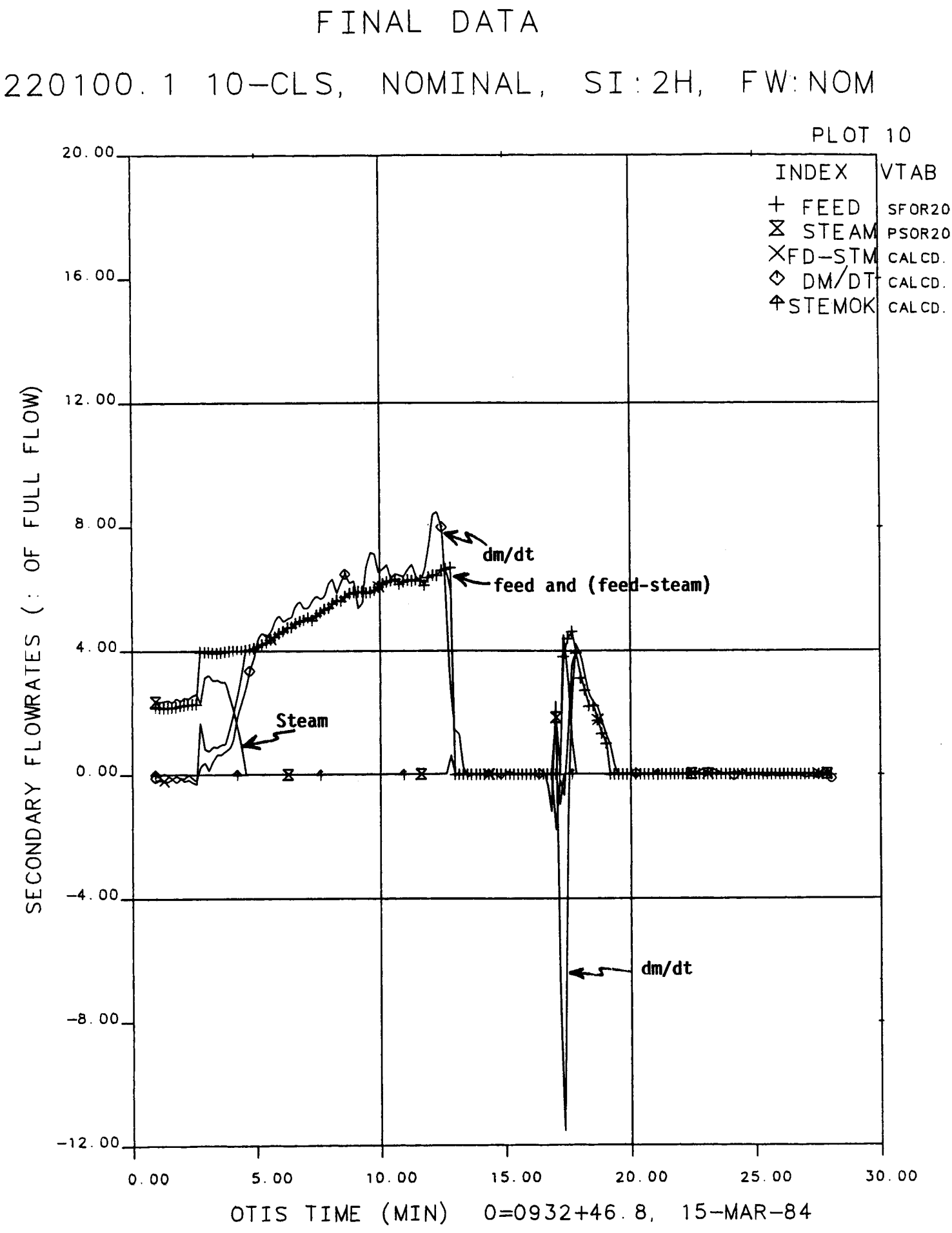

Figure 5.10 Secondary FLowrates

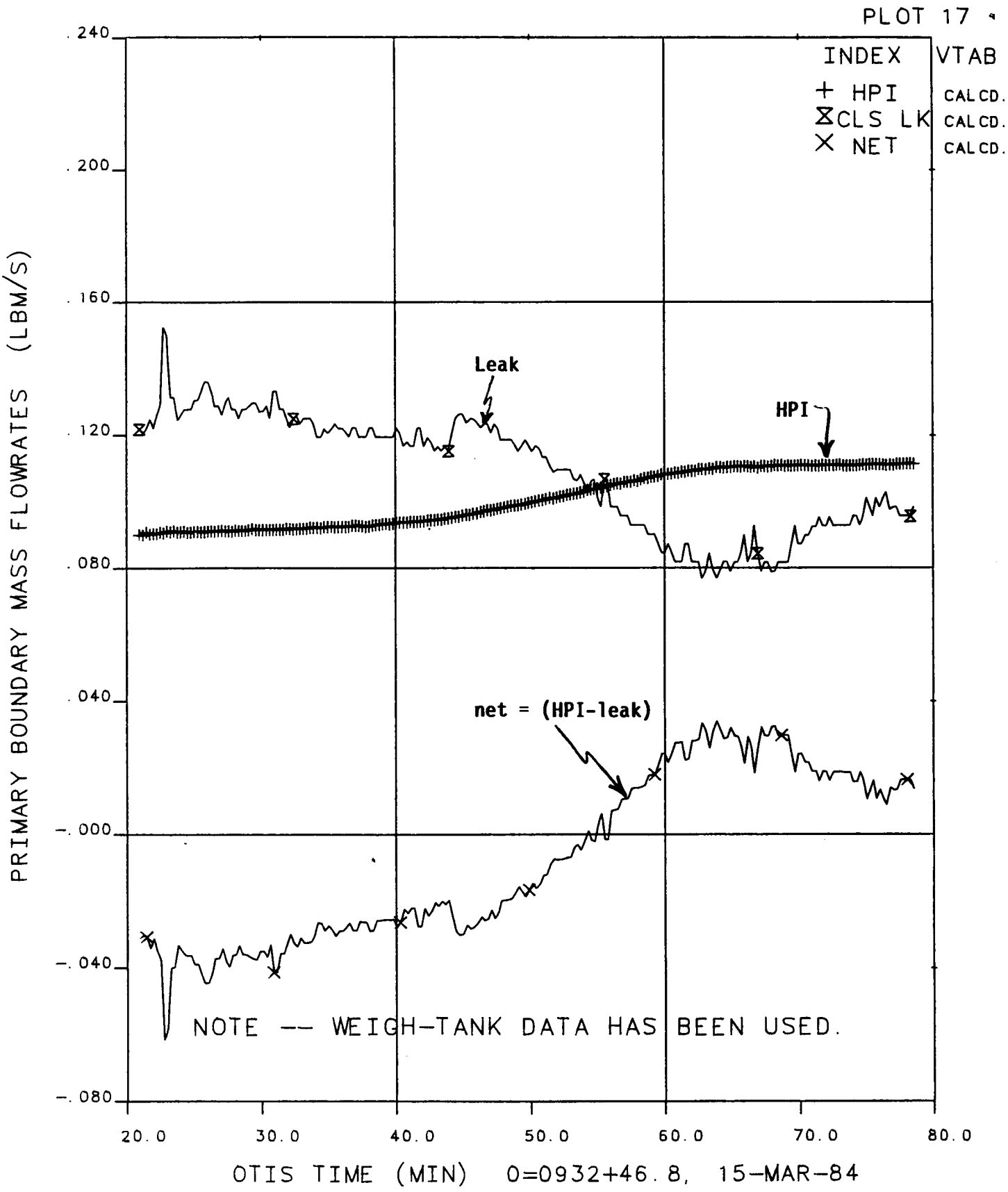

Figure 5.11 Primary Boundary Mass Flowrates

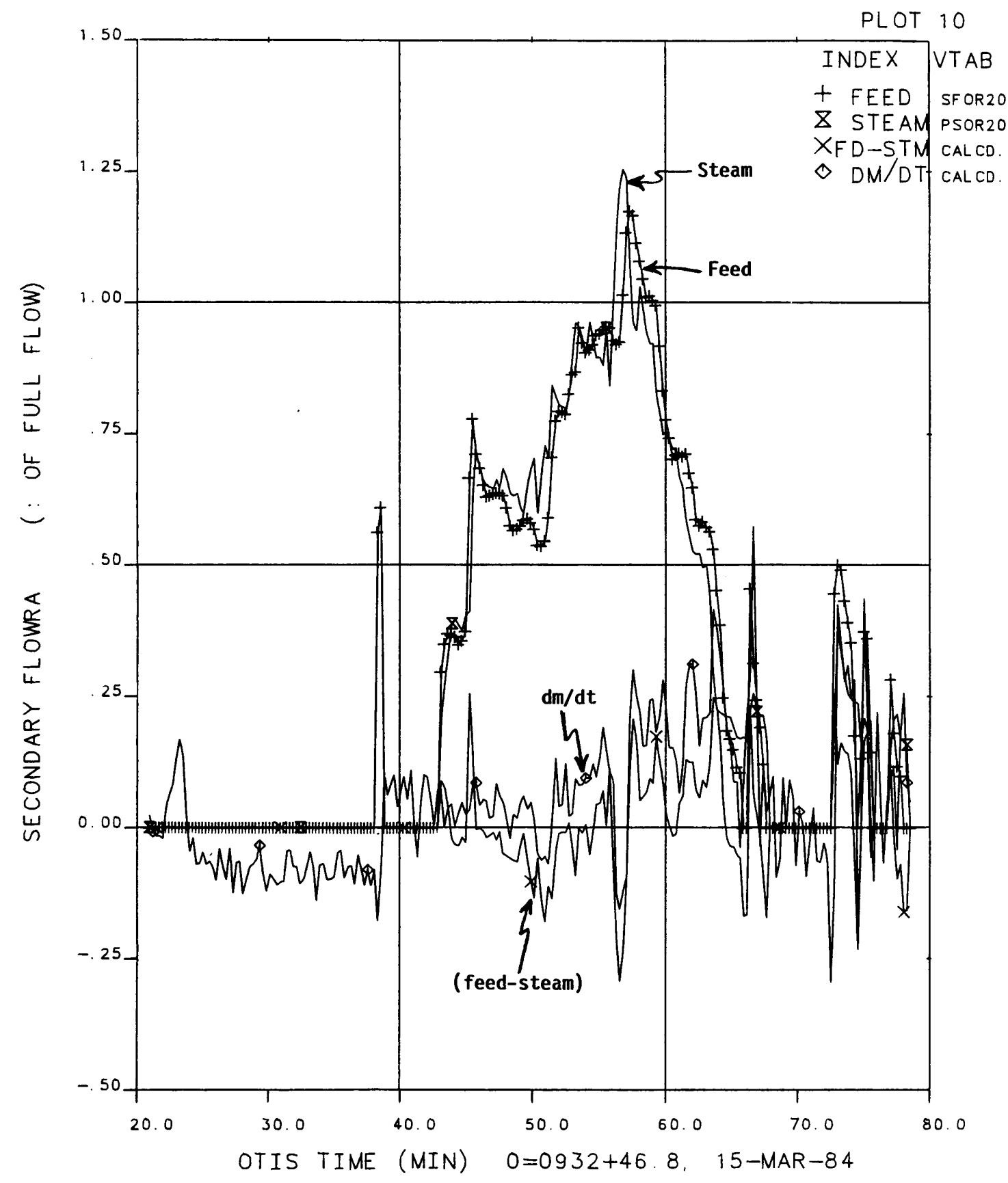

Figure 5.12 Secondary Flowrates

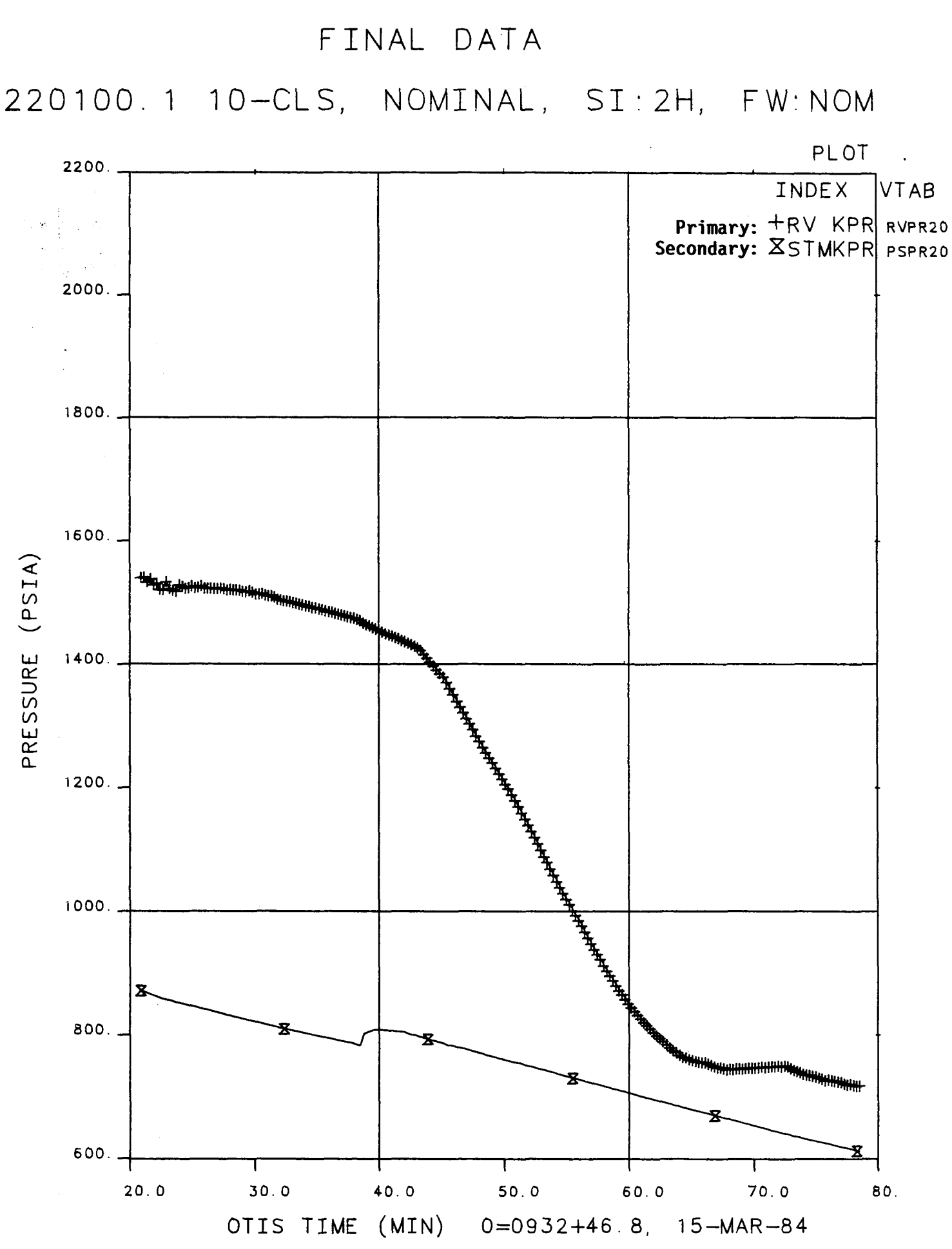

Figure 5.13 Primary and Secondary Pressures

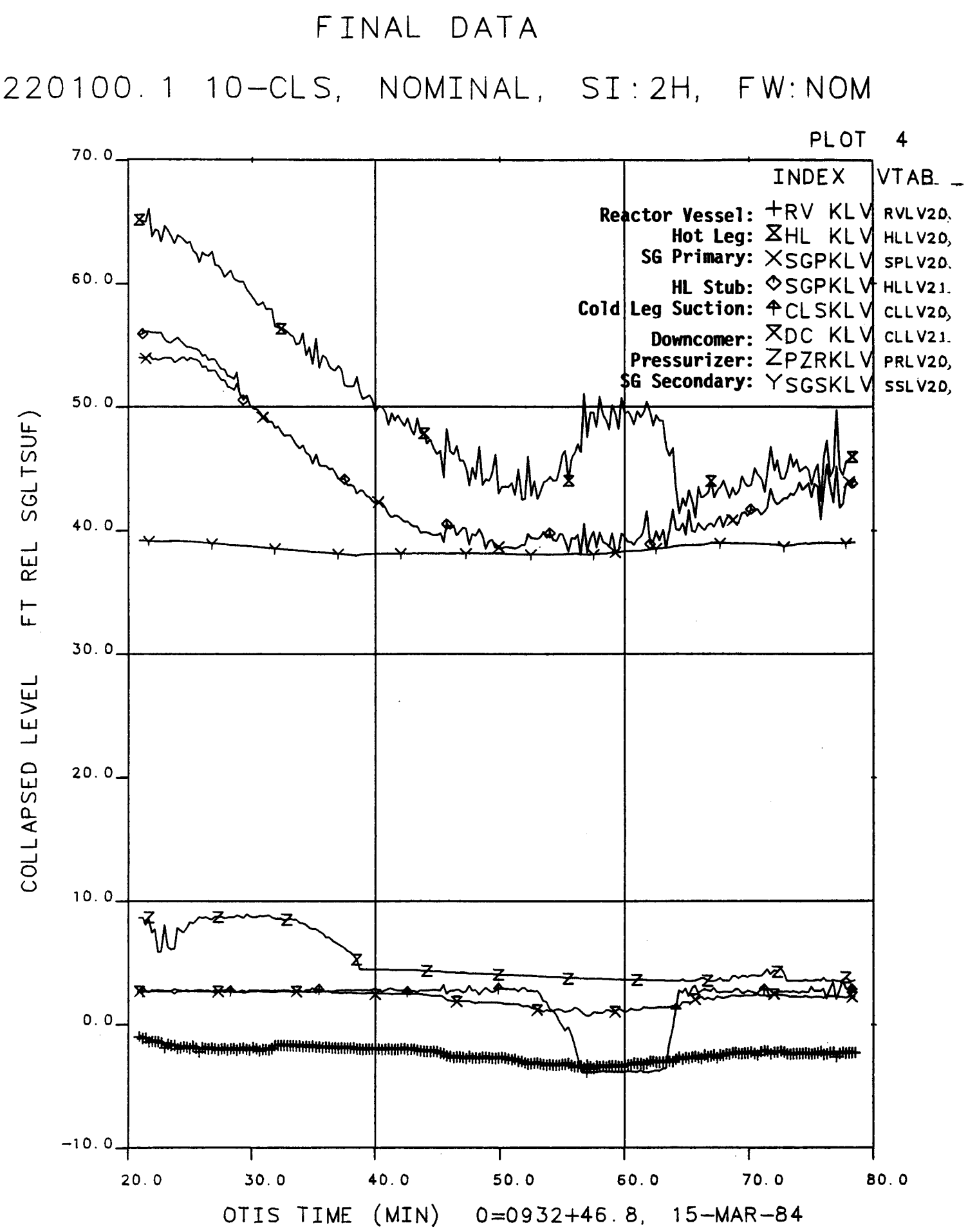

Figure 5.14 Collapsed Liquid Levels

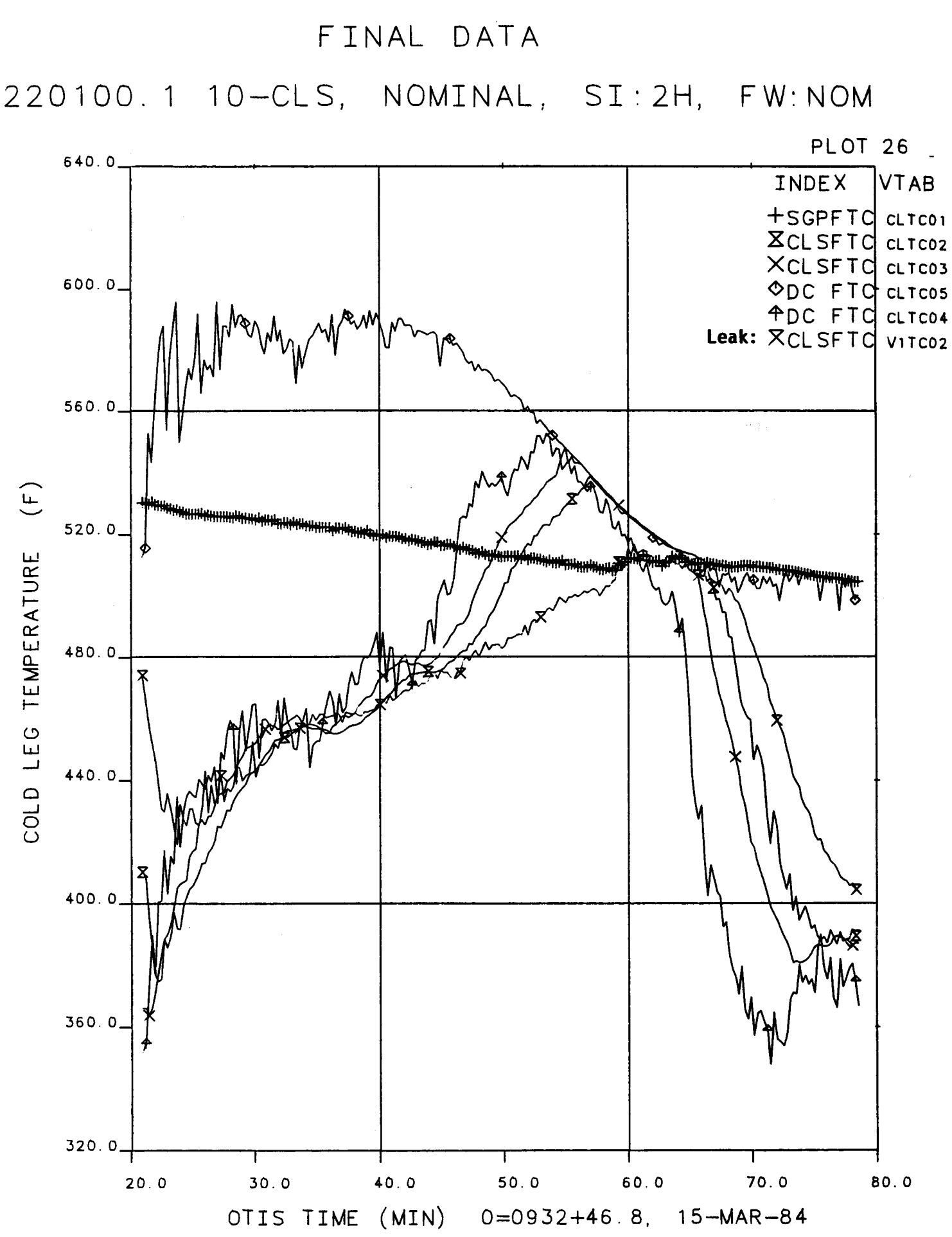

Figure 5.15 Cold Leg Fluid Temperatures

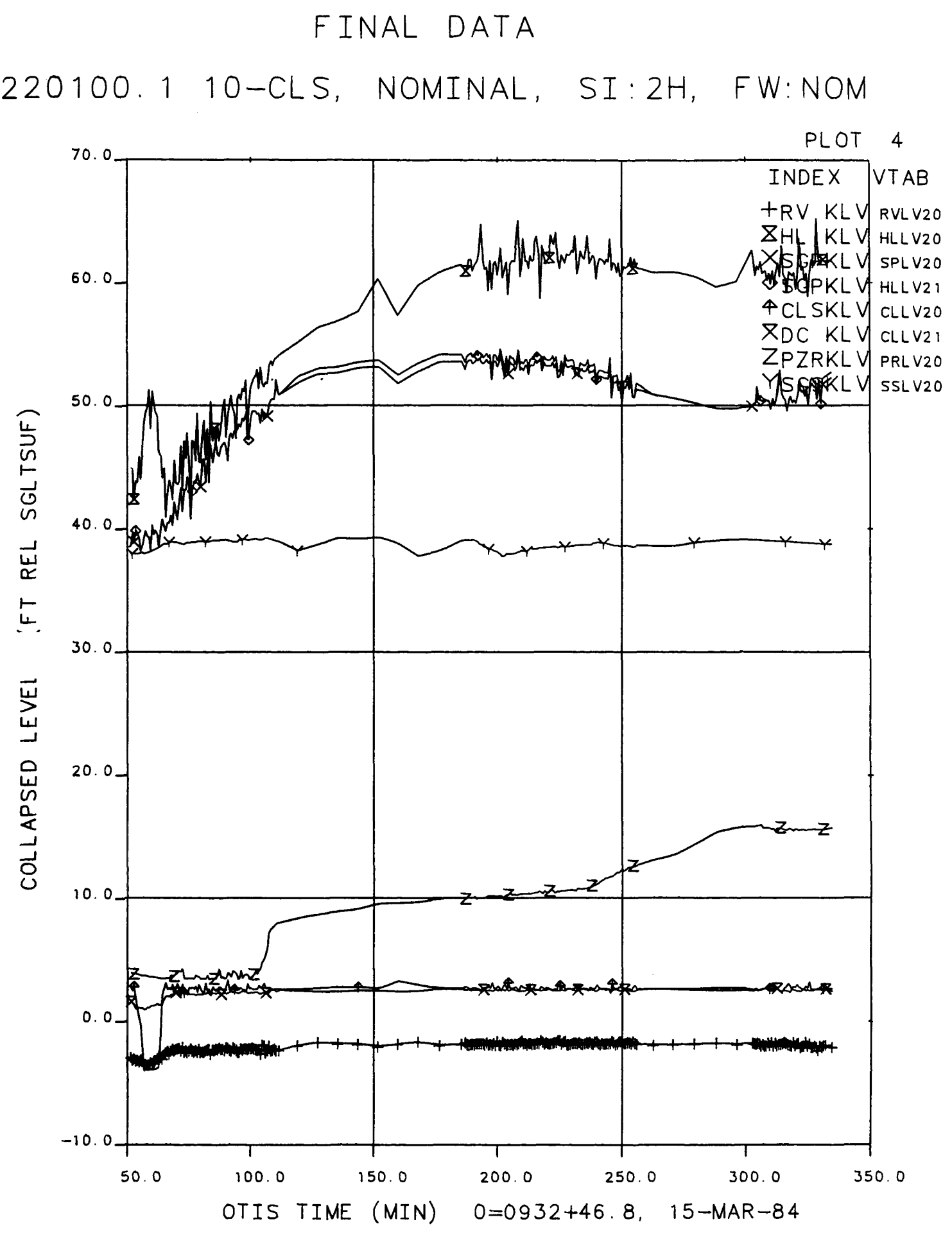

Figure 5.16 Collapsed Liquid Levels

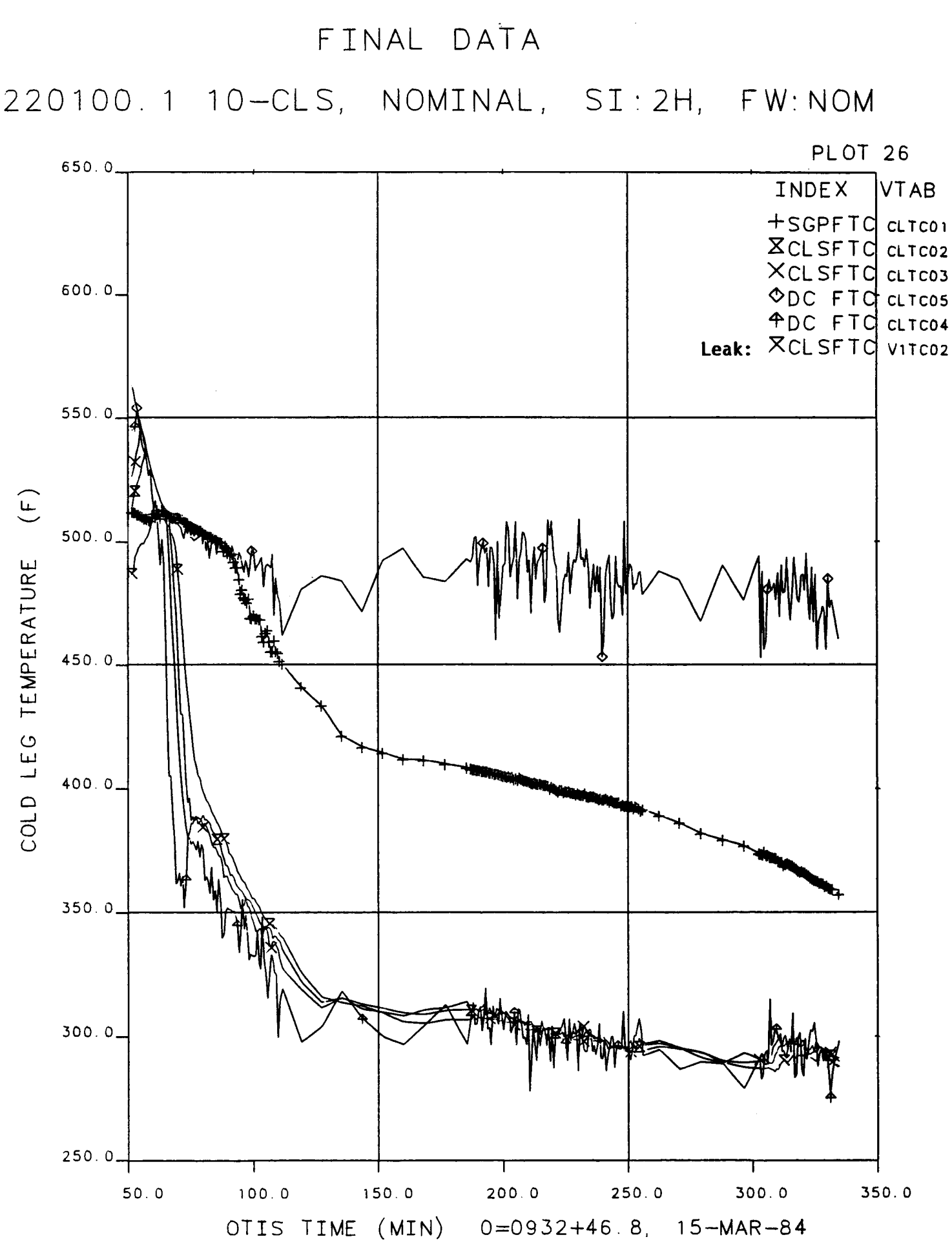

Figure 5.17 Cold Leg Fluid Temperatures

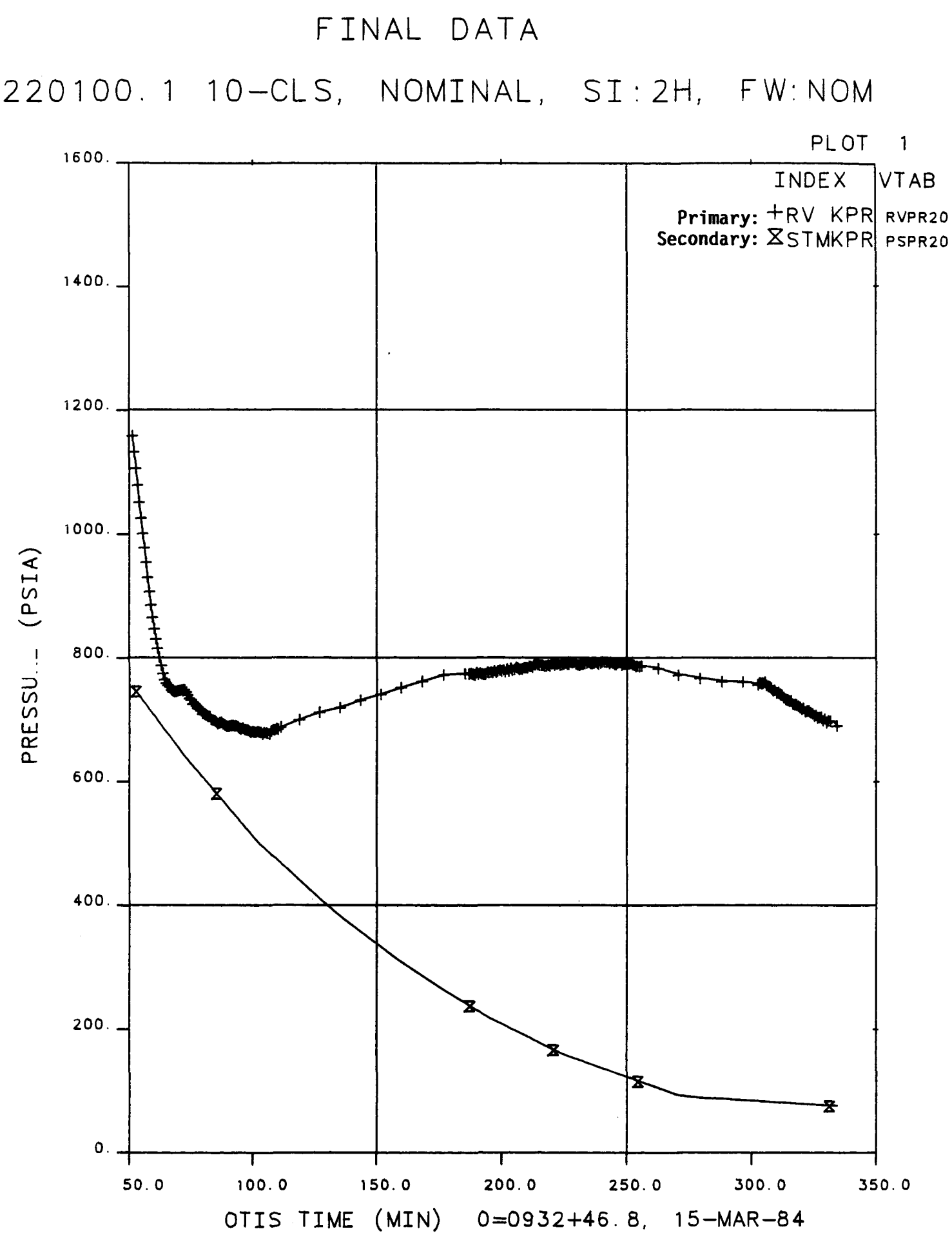

Figure 5.18 Primary and Secondary Pressures

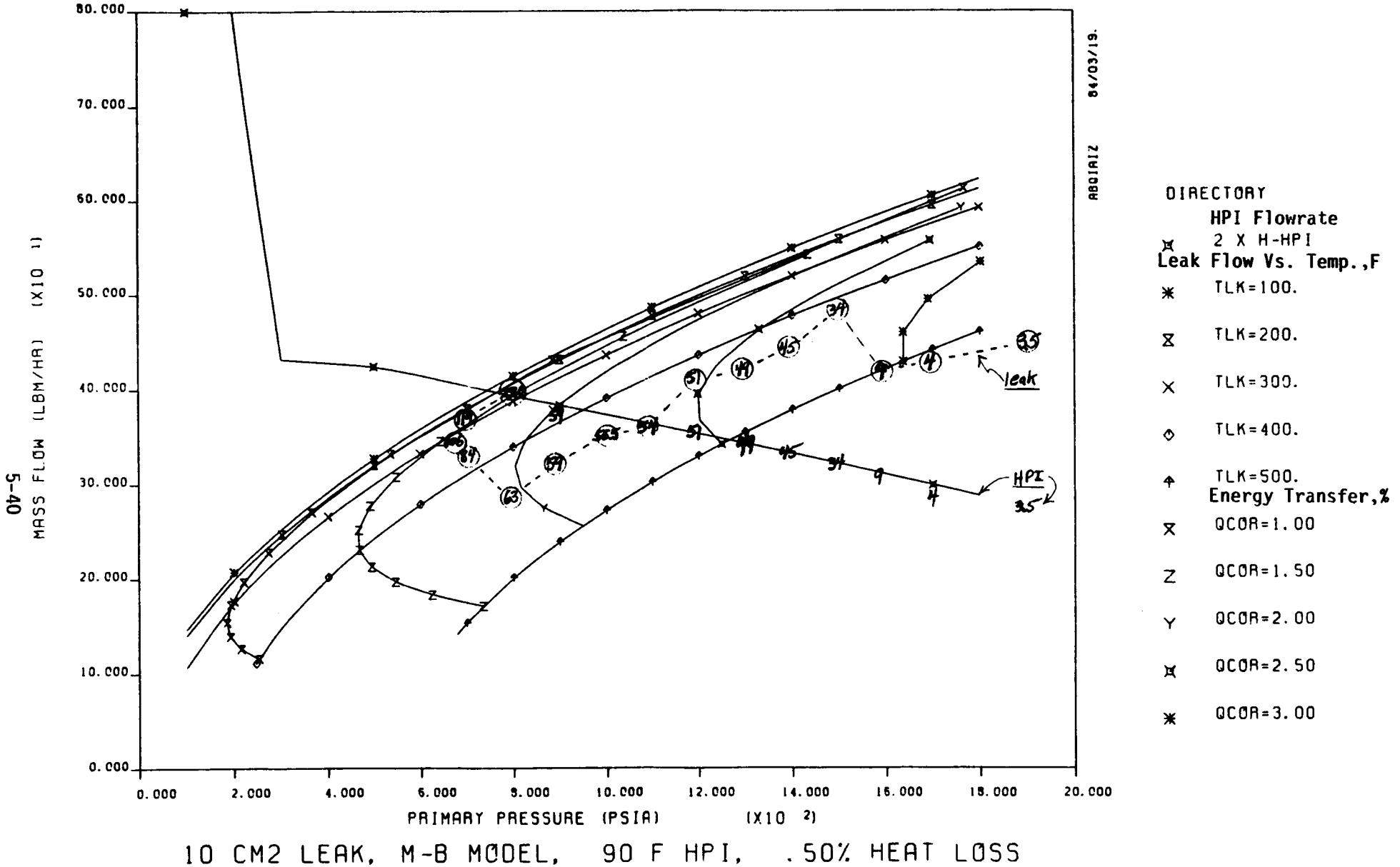

Figure 5.19 Refill Equilibrium

Actual leak mass flow rate versus pressure is shown by circled numbers (giving minutes after leak actuation), critical leak flow at temperature is from 0.84X Modified Burnell. HPI mass flow rate versus pressure is from the test specs, selected actual HPI flow rates are also shown. Refer to Appendix C for a detailed explanation of this equilibrium plot.

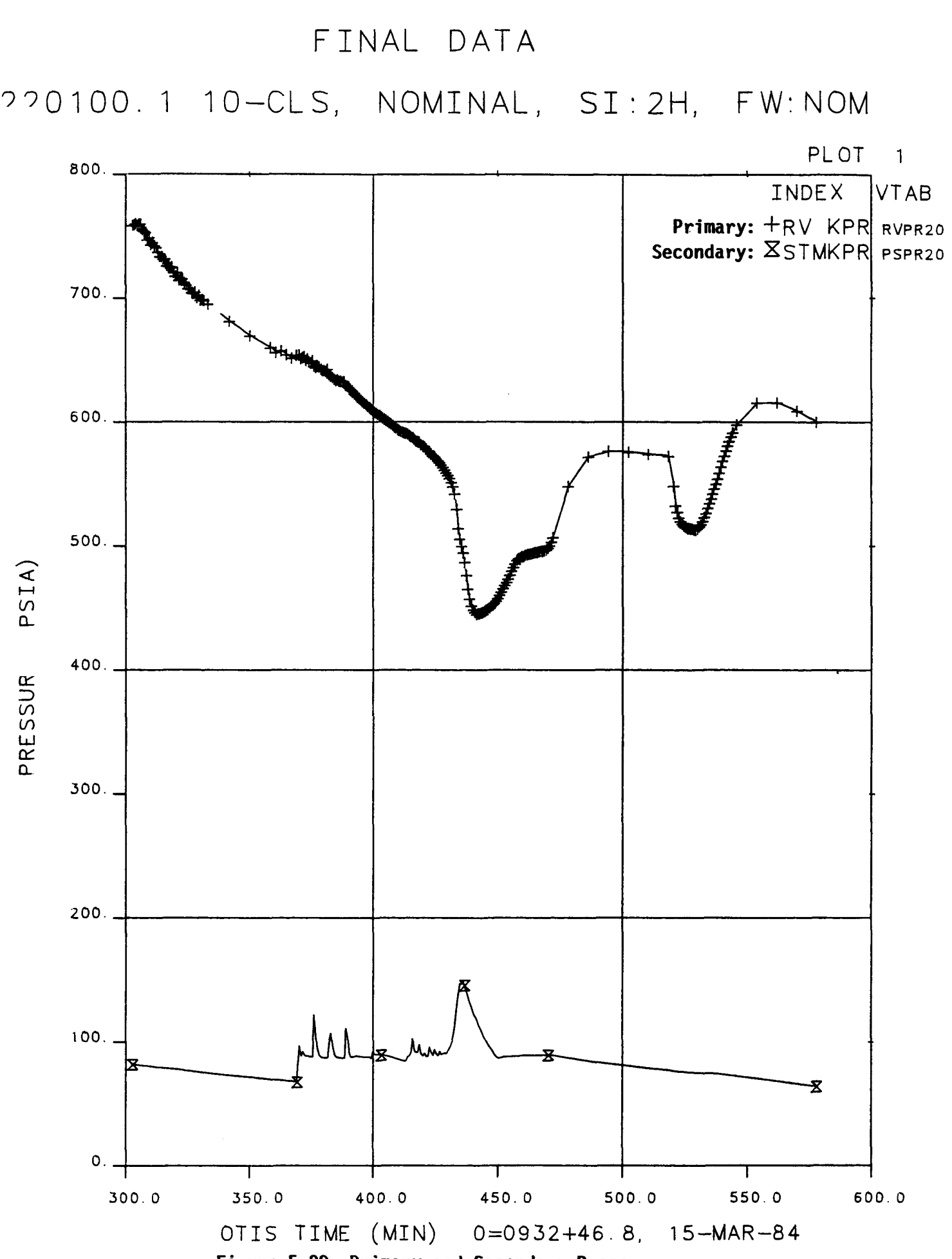

Figure 5.20 Primary and Secondary Pressures

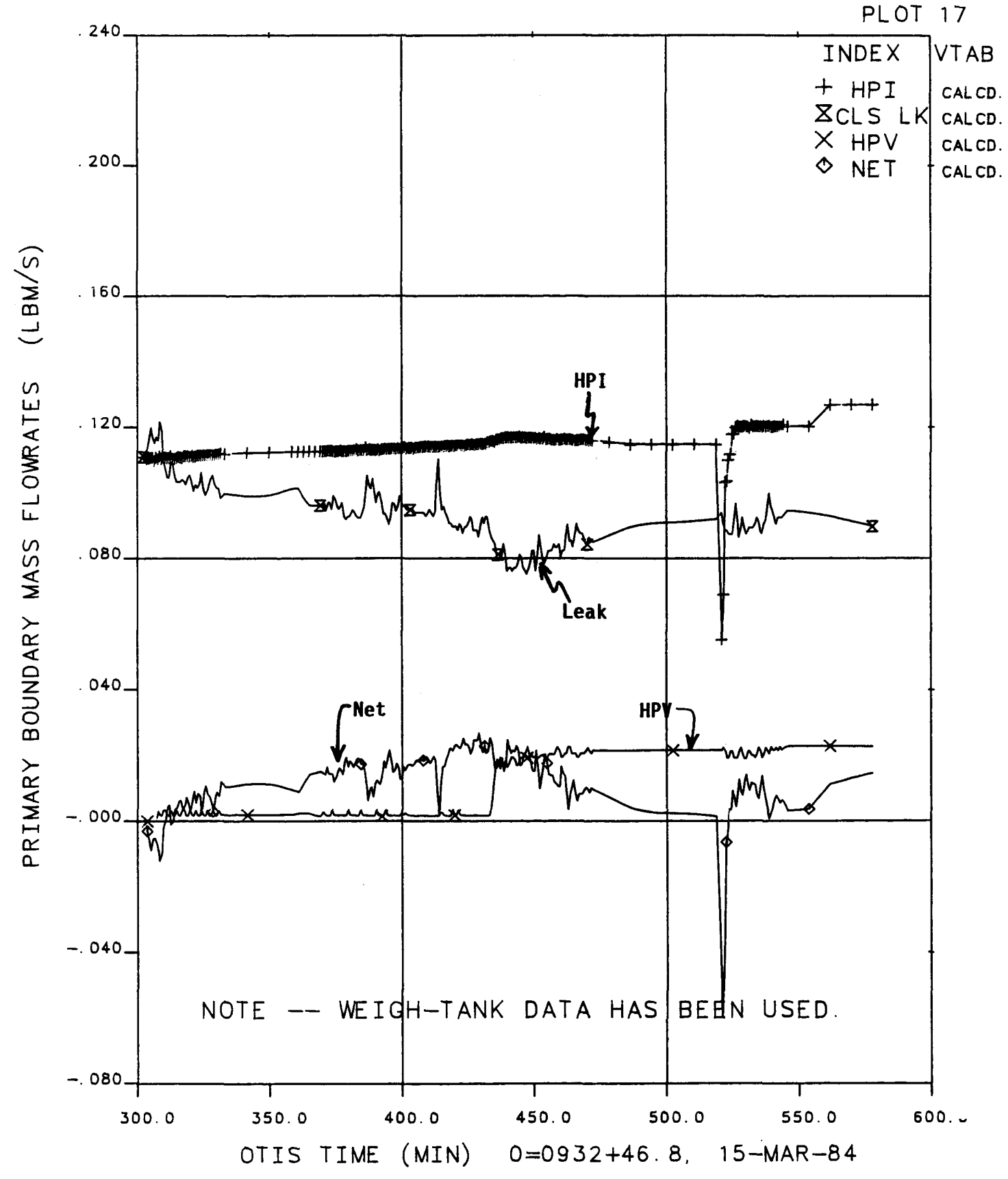

Figure 5.21 Primary Boundary Flowrates

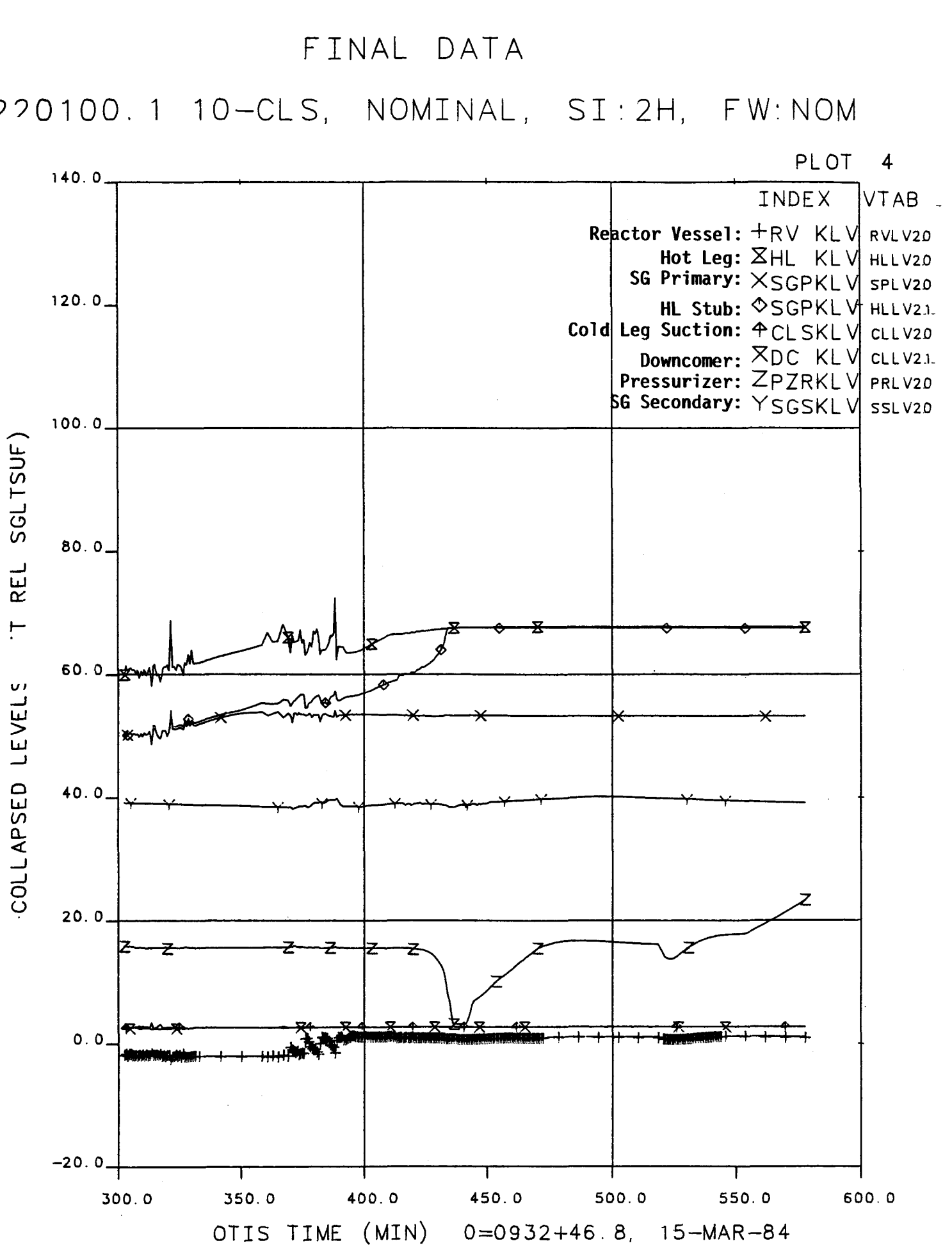

Figure 5.22 Collapsed Liquid Levels

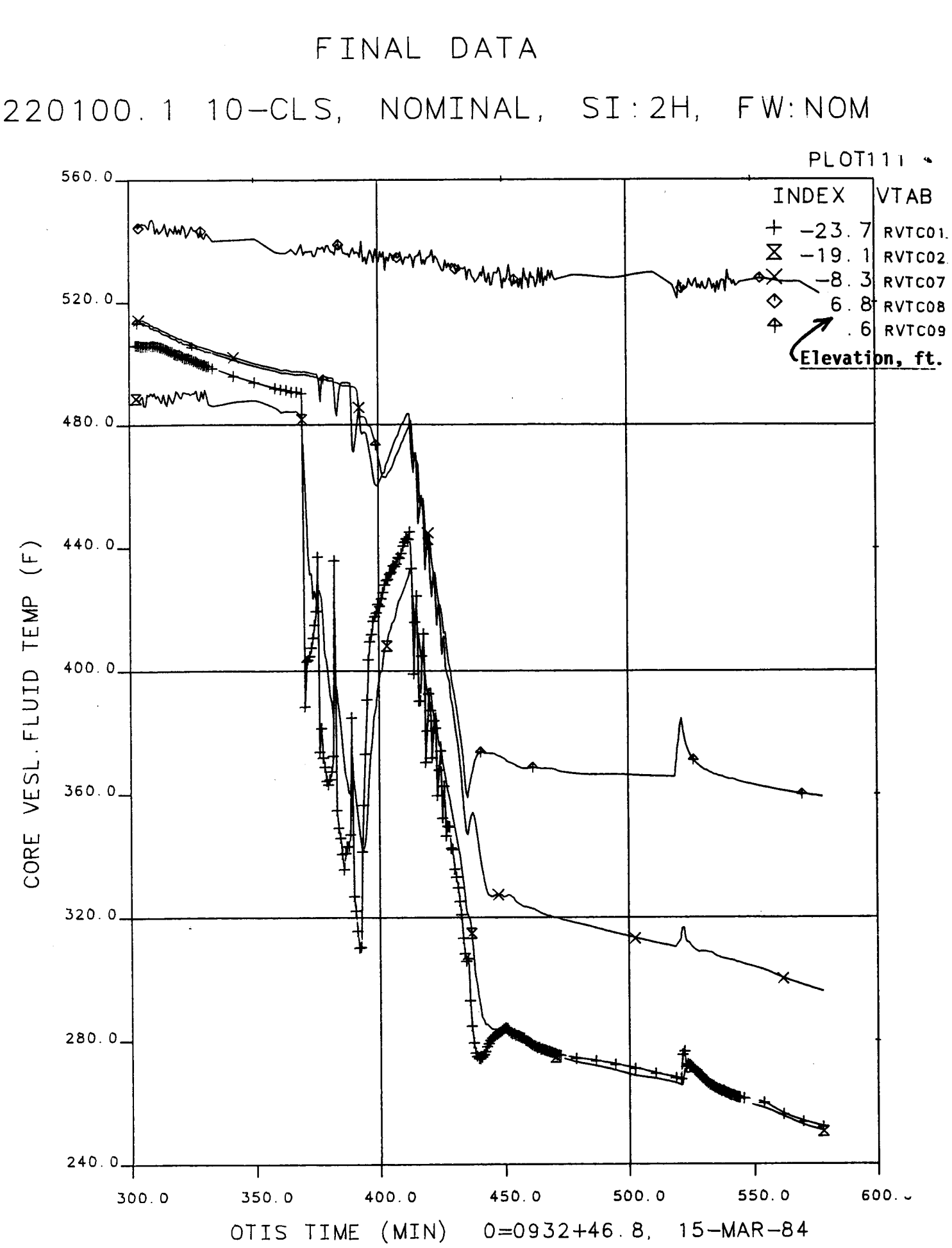

Figure 5.23 Core Vessel Fluid Temperatures

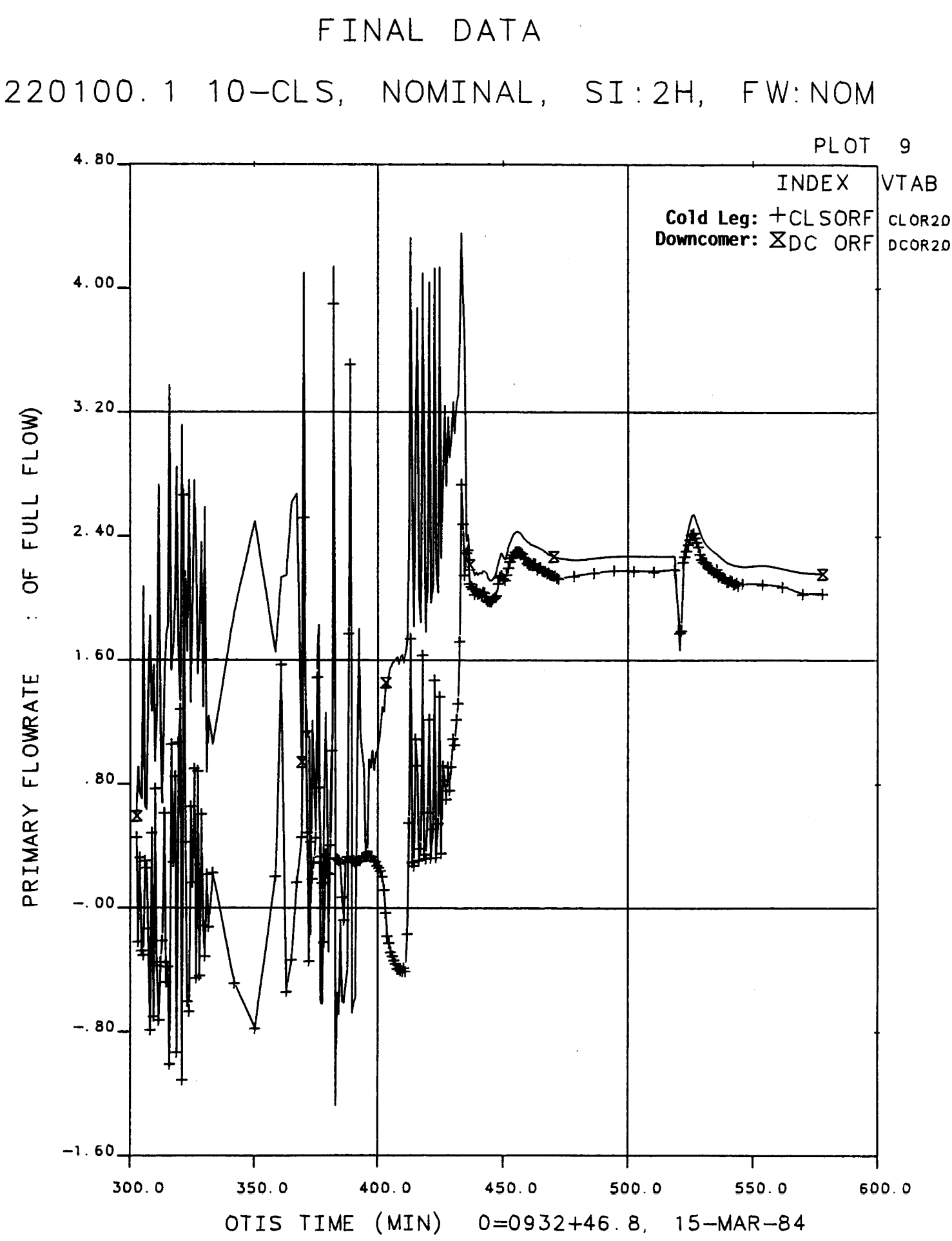

Figure 5.24 Primary FLowrates

6. SINGLE-VARIABLE TESTS

Six single-variable tests paralleled the Nominal Test but each altered a single boundary condition. These tests are addressed separately in sections 6.2 through 6.7, then intercompared and summarized in section 6.8. (The Nominal Test 220100 was described in section 5.)

6.1 Introduction

The six single-variable test specifications have been described in section 3 and are listed in Table 6.1. The base conditions are those of the Nominal Test 220100. Test 220202 used an increased leak size, 15 versus 10 cm^2 (scaled by 1686 in leak flow area). Test 220304 used half of the nominal HPI capacity. The SG level (after SG secondary refill) was reduced from 38 to 10 feet in Test 220402. Leak location was varied in Test 220503; the cold leg discharge rather than the cold leg suction leak site was used (both were at the bottom of the pipe). Test 220604 used low-head HPI characteristics, see section 6.6 for a comparison of these characteristics to the nominal set. Finally, Test 220756 simulated leak isolation; i.e., the Nominal Test conditions were repeated until the time of the primary flow interruption preceding the descent of the primary level to the elevation of the SG. At this time the controlled leak was closed. Each single-variable test is described separately in sections 6.2 through 6.7. Section 6.8 summarizes test performance and observations, and provides comparisons of the trends observed in these tests. Several transients are traced on so-called "equilibrium plots"; the generation of these plots is described in Appendix C.

6.2 Test 220201 (15 cm^2 Leak)

OTIS Test 220201 varied leak size. A scaled 15-cm^2 CLS leak was used versus 10-cm^2 in the Nominal Test (Test 220100, described in section 5 herein). Test boundary conditions were otherwise those of the Nominal Test.

6.2.1 Performance

Initialization

The OTIS leak size test, 220201, was conducted on March 22, 1984. The test was performed in accordance with the OTIS Test Specification.[3] Table 6.2 summarizes the specified initial conditions and compares them with those achieved; all the prescribed conditions except the pressurizer metal temperature were satisfied. Two pressurizer metal temperatures were observed to be out of specification, with readings of 675 and 697F (PRTC06 and PRTC10 on appended Plot 163). This condition is not perceived to have had a singificant influence on test behavior.

Conduct

The actions performed by the OTIS loop operator are indicated in Table 6.3. Scheduled actions such as the opening of the HLHPV occurred at 315 minutes, or approximately five hours after leak initiation, as specified by the Test Procedures.[4] Unspecified actions such as automatic to manual AFW control occurred infrequently. These actions are discussed in detail in the description of the Nominal Test. Automatic controls, i.e., core power, secondary pressure, and HPI pump head-flow, were achieved as specified in the test procedures.

This test, having a leak size that is larger than that of the nominal case, experienced a prolonged period of relatively low primary pressure. This low-pressure operation exacerbated the effects of the loop guard heaters, which had been adjusted for adiabatic control at 500F primary fluid temperature. These effects were apparent in the pressurizer, reactor vessel upper head, and HL metal temperatures, cf. Plots 163, 114, and 124 of the appended plots. These observations led to subsequent guard heater tests, cf. section 10.

At the end of Test 220201, the loop operator transferred HPI control from automatic to manual (as allowed by the test procedure) to maintain pressurizer level. However, the resulting HPI flow rate exceeded the pump head-flow curve. This action did not affect the bulk of the test.

Measurements

Measurements unavailable in this test are listed in Table 6.4. The majority of these instruments were not critical to testing. As with Test 220100, the HL conductivity probes (HLCP05-17) and steam generator string thermocouples (SPTC20-28) dominate the list. The reasons for discarding the string TCs are discussed in section 5. Appended plot 18, "Indicated Versus Calculated Cumulative Primary Fluid Mass," shows a mass difference of 45 lbm after nearly 9 hours of testing. Expressed as a fraction of the customary HPI flow rate, this mass difference over the testing period is equivalent to less than 1% of the HPI flow.

6.2.2 Observations

Test observations are grouped according to the following test phases:

1. Draining, intermittent circulation, and interruption.
2. Boiler-condenser mode (BCM).
3. Refill without venting.
4. Refill with venting.
5. Natural circulation cooldown.

The key events for the test are summarized in Table 6.5 and are also indicated on Figure 6.1. Data plots are included in Figures 6.1 through 6.6 and additional data plots are appended. These plots are described in Appendix A.

Draining, Saturation, Intermittent Circulation, and Interruption, 0-24 Minutes

The transient began at 12.8 minutes after DAS activation, following a period of steady-state loop operation. In quick succession, the following events occurred: The leak was opened, HPI and AFW were actuated, and the core power ramp was initiated. Immediately, the primary pressure decreased

sharply, Figure 6.1, from 2209 to 1856 psia by ∿1 minute, at which time the pressurizer emptied and the HL began to saturate. The rate of change in primary pressure leveled off at 2.3 minutes (Figure 6.1). The HL spillover temperature (HLTC07, Plot 121) was 612F at 2.1 minutes, indicating that voiding was occurring. This was further reflected by the HL level decrease shown in Figure 6.2. HL voiding continued until 3.5 minutes when the HLUB totally voided, interrupting flow to the steam generator. The resulting decoupling of the primary and secondary systems caused primary pressure to increase momentarily at 6.1 minutes. Almost immediately, a spillover occurred; this is observable on Figure 6.2 as an increase in SG primary level, from 60 to 61 feet. Steam pressure, Figure 6.1, also began to increase as primary and secondary heat transfer momentarily recoupled. Primary flow interrupted again at ∿8 minutes and primary pressure began to increase. Additional spillovers were precluded by the continued decrease of the HL and SG primary levels, well below the U-bend region. At 12 minutes into the test, the secondary side level reached the control setpoint of 38 feet, terminating AFW injection. The steam generator primary level reached the AFW injection site (approximately 51 feet) at 13 minutes. However, since AFW injection was inactive, no boiler-condenser effects were observed. Both the HL and SG primary levels continued to decrease until 24 minutes.

Boiler-Condenser Mode (BCM), 24-200 Minutes

At 24 minutes the SG primary level reached the secondary pool elevation, uncovering a primary-side condensing surface. As a result, primary-to-secondary heat transfer was enhanced, causing an increased rate of primary depressurization. Pressure decreased from 1350 to 850 psia at 37 minutes; the primary pressure was then within 25 psi of the secondary pressure, cf. Figure 6.1. For the next 163 minutes, the primary and secondary systems remained coupled, as indicated on Figure 6.1. The primary system depressurization caused by BCM heat transfer resulted in a steady increase in HPI flow (Figure 6.3). At 104 minutes, leak flow was approximately 410 lbm/h and decreasing, whereas HPI flow was also 410 lbm/h but increasing. As a result, refill began as indicated on Figure 6.2. Refill and further depressurization continued at the secondary depressurization rate corresponding to 50F/h until ∿200 minutes.

Refill Without Venting, 200-302 Minutes

At ∿200 minutes into the test, the refill of the primary system caused the SG primary level to exceed the secondary level, ending BCM heat transfer and partially decoupling the primary from the secondary. Primary pressure began to rise (Figure 6.1). The loop flow rate decreased, causing an increased amount of HPI to migrate toward the leak site. As a result, the leak temperature decreased, reaching approximately 237F at 230 minutes (Figure 6.4). The decrease in leak temperature and increase in primary pressure caused an increase in leak flow, significantly lowering the refill rate. The rate of primary level increase diminished but still remained positive until approximately 237 minutes (Figure 6.2). At 237 minutes the HPI and leak flow were momentarily equal (Figure 6.3). However, beyond this time, there were brief periods of primary-to-secondary heat transfer coupling (confirmed by AFW flow rate, cf. appended Plot 12). The resulting forward loop flow reheated the leak fluid temperature, thereby suppressing the leak flow rate and allowing refill to continue.

Refill With Venting, 302 to 459 Minutes

At five hours into the test, the loop operator opened the HL high point vent (HLHPV). Primary pressure decreased slowly as a result. The HL and SG primary levels maintained their rate of increase (Figure 6.2). At 342 minutes, the first HL spillover was observed and reported by the operator. Spillovers caused increased SG coupling at 358 minutes, cf. appended Plot 13. Continued SG coupling and loop depressurization resulted in more frequent spillovers and ultimately in loop refill at 459 minutes. Figure 6.3 (HPV flow) shows a step change in flow rate as the HPV discharge became liquid.

Natural Circulation and Cooldown, 459 Minutes to Test Termination.

Loop refill at 459 minutes promoted primary-to-secondary heat transfer. The primary began to depressurize at a faster rate (Figure 6.1). HL temperatures, Figure 6.5, show an abrupt decrease. The CL fluid temperatures increased (Figure 6.4) as primary loop flow (Figure 6.6) predominated leak flow. Enhanced loop flow and SG coupling resulted in total loop cooldown, cf. appended Plot 2. All primary fluid temperatures indicated subcooling except those of the pressurizer and the reactor vessel upper head (RVTC08,

Plot 111), cf. appended Plots 111, 121, 131, 141, 151, 161, and 171. At 467 minutes, the operator assumed manual control of the HPI pump for pressurizer level control. The resulting HPI injection rate (Figure 6.3) exceeded the HPI head-flow curve. The primary pressure increased dramatically as a result, Figure 6.1. The presssurizer level increased quickly from 7 to 18 feet by 511 minutes. The test was terminated after having observed more than a half-hour of post-refill cooldown.

6.2.3 Results

Test 220201 progressed in a manner similar to that of OTIS Nominal Test 220100. The progression of the test is shown on Figure 6.7; the development of the "equilibrium plot" of Figure 6.7 is explained in Appendix C. At 19 minutes the loop was draining rapidly as indicated by the leak flow of 600 lbm/h versus the HPI flow of 325 lbm/h. However, the SG primary level was approaching that of the secondary and the loop was at the onset of the Boiler-Condenser Mode (BCM) at 23 minutes. The rapid depressurization caused by the BCM is illustrated by the decreased primary pressure at 56 minutes. The continued depressurization and decrease in the saturation temperature during BCM operation caused the leak temperature to also decrease (to 430F at 56 minutes), causing the leak flow to remain greater than the HPI flow (460 versus 400 lbm/h). As a result, loop inventory continued to decrease until approximately 104 minutes at which time both the leak and HPI flow were 410 lbm/h. From 104 to 200 minutes, BCM operation and refill continued as HPI flow exceeded leak flow. At 200 minutes, the SG primary level rose above the secondary level, ending BCM heat transfer. From 202 to 302 minutes, the loop repressurized and the leak temperature decreased, resulting in a convergence of leak and HPI flow and a correspondingly decreased refill rate. At 302 minutes, the HL high point vent (HLHPV) was opened without a major effect on the system conditions. It appears that refill would have occurred without the HPV for this test, as indicated in Plot 4 (Figure 6.2) by the increasing hot leg and steam generator primary levels before the vent actuation at 302 minutes.

Comparing Test 220201 with the Nominal Test 220100, the larger leak size of 15 cm^2 versus 10 cm^2 resulted in more rapid loop draining and in an earlier BCM (24 versus 43 minutes). The mismatch in leak and HPI flow from the

onset of BCM to 104 minutes also led to a longer period of BCM operation (176 versus 62 minutes) and a greater depressurization of the primary system. The end of the BCM led to a significant decrease in the refill rate in both tests. However, the decrease in Test 220201 did not preclude the ultimate refill of the loop. The opening of the HLHPV had little effect on the refill rate and, at 459 minutes, the loop began to cool in natural circulation. The primary system pressure in Test 220201 was 400 psia at test termination versus 500 psia in Test 220100, with similar loop temperatures.

Test 220201 exhibited many similarities to the Nominal Test 220100. In each test, the anticipated modes were observed, namely draining, intermittent circulation, interruption, boiler-condenser, refill (without and with high-point venting), and natural circulation cooldown.

6.3 Test 220304 (Half-Capacity HPI)

OTIS Test 220304 was another of the single-variable series. In this test, the nominal conditions were altered by reducing the HPI flow rate at pressure by one half.

6.3.1 Performance

Initialization

OTIS Test 220304 was conducted on April 7, 1984. The planned and actual conditions are compared in Table 6.6. Core power, primary pressure, SG secondary level, hot leg fluid temperature, pressurizer metal temperatures, and system controls were as planned. The pressurizer level was 19.6 feet versus the 14.6 to 18.6 feet planned. This difference is perceived to have had a negligible impact on test behavior.

Conduct

The following test control actions were performed as planned:

- Opened the (scaled) 10-cm^2 cold leg suction leak.
- As the pressurizer collapsed liquid level dropped below 2 feet in the pressurizer (8 feet relative to the common elevation datum, the SG lower tubesheet upper face):
  - Actuated HPI.
  - Initiated the core power ramp.
  - Began the SG secondary level increase.
  - De-energized the pressurizer main heaters.
- As SG secondary level attained 38 feet, initiated the secondary depressurization ramp (to obtain 50F/h from 1000 psia).
- Opened the HLHPV 5 hours after leak initiation.
- Opened the pressurizer relief valve 7 hours after leak initiation.
- Reduced core power to sustaining power 8 hours after leak initiation.
- Terminated the test after 9-1/2 hours (without refilling).

The SG secondary level rate of increase (following test initiation) approximated 3 ft/min as planned. The subsequent SG secondary depressurization rate obtained 50F/h secondary cooldown, also as planned. Core power was decreased to approximate the specified decay characteristics.

Test conduct as recorded by the loop operator is summarized in Table 6.7. Operator actions involving the AFW control system and the reactor vessel vent valve are discussed in detail in the description of the OTIS Nominal Test, cf. section 5.

High-Pressure Injection (HPI)

The HPI flow control system (described in the OTIS Loop Function Specification[2]) utilized a positive displacement pump and bypass flow control valve to obtain the specified head-flow characteristics. Operator action was sometimes necessary to change the pump speed to achieve the continued rangeability of the bypass control valve. In this test, this action was delayed, resulting in the eventual loss of the desired characteristics when the control valve fully opened. An atypical HPI head-flow characteristic resulted, beginning at 126 minutes and ending at 235 minutes when the pump speed was reduced from 30 to 10% (see Table 6.7). The specified HPI head-flow characteristics are compared to those achieved, in Figure 6.8. A significant increase in HPI flow is apparent. The extent of the atypicality is well documented and can be simulated in a code model. Plot 18 of the appended plots reflects the excellent agreement between the measured and calculated total primary system fluid mass.

Low-Pressure Injection (LPI)

The LPI system flow was simulated by modifying the HPI system. Table 6.8 compares the specified head versus flow with that observed during the tests. The comparison indicates that the actual flow rate (from 534 to 587 minutes) was approximately 20% less than that specified. In prior tests, the LPI flow had been either totally absent (Nominal Test 220100) or of brief duration; however, in this test it was activated for more than 50 minutes. An inspection of Figure 6.8 shows the head-flow curve for the loop conditions during this time to be nearly vertical. As a result, a small error in the control pressure has a large effect on the LPI flowrate. The impact of this characteristic of the LPI head-flow curve should be noted for code prediction purposes.

6.3.2 Observations

Five major phases were observed: (1) draining, saturation and intermittent circulation, 0 to 17 minutes, (2) BCM, 17 to 195 minutes, (3) refill without venting, 130 to 304 minutes, (4) equilibrium with venting and reduced power, 304 to 534 minutes, and (5) refill with LPI, 534 to 587 minutes (test termination). These phases are indicated on Figure 6.9. The events composing these phases are listed chronologically in Table 6.9.

Draining, Saturation, and Intermittent Circulation, 0 to 17 Minutes

The data acquisition system was activated for Test 220304 at 1009 on 7 April 1984. Steady-state data at the initial conditions were taken for 14 minutes. The initial conditions for this test are summarized in Table 6.6. The scaled 10-cm^2 cold leg suction leak was then opened, defining time zero. Primary pressure immediately began to decrease with draining (Figure 6.9), and the pressurizer level decreased from 19.6 to approximately 2 feet by 2 minutes (Figure 6.10). At this time, as specified by test procedure, the operator actuated the HPI and AFW systems and initiated the core power (decay heat) ramp. The SG secondary began to fill toward the control level of 38 feet, at a rate of approximately 3 feet per minute. As the boundary systems were being actuated, the pressurizer drained completely at 2.3 minutes, causing an increased primary depressurization rate until the HL began to saturate. Primary pressure reached 1700 psia by 3 minutes (Figure 6.9). As the HLUB voided at 3 minutes, the primary flow decreased abruptly. With the interruption of flow, the SG primary began to drain, as indicated in Figure 6.10 at 3 minutes. The reactor vessel level began a steady decline starting shortly thereafter at 7 minutes. Also, at 7 minutes, fluid from the partially drained HL spilled over into the SG. The loop flow rate increased sharply (Figure 6.11). The sudden surge of flow caused an increase in primary-to-secondary heat transfer, and secondary pressure increased momentarily (Figure 6.9). A mild depressurization of the primary also occurred. Following the spillover, flow again stalled and the primary pressure increased again at 11 minutes (Figure 6.9). During this time, the RV level continued to steadily decrease until it reached the HL nozzle at 11 minutes and stabilized (Figure 6.10). The DC and CL saturated (Figures 6.12 and 6.13) and their levels began to decrease

(Figures 6.10, 6.14, and 6.15). At 13 minutes the secondary level approached the control setpoint (38 feet) and the AFW was terminated. The secondary depressurization ramp was then initiated, obtaining a 50F/h cooldown rate. At 15 minutes, as the DC level reached the CL nozzle, the RVVV pressure differential decreased, causing the valve to close.

When the RVVV closed, the DC level decreased at a faster rate and the DC flow rate decreased, both as a result of the loss of recirculated steam from the core. These effects tended to re-establish the RVVV pressure differential, which increased to 0.25 psi at 16 minutes, opening the valve. Reopening the RVVV re-established steam flow to the CL causing it to re-void at 16.2 minutes. However, the venting of steam from the core through the RVVV to the CL and the continued venting of steam into the HL (nozzle still uncovered) resulted in the loss of RVVV differential pressure again at 17 minutes and closed the valve. With valve closure, the HPI collapsed the CL void. A significant spillover occurred this time, however, and the CL and DC refilled instantly. The collapse of the CL and DC voids resulted in a slight primary pressure decrease (Figure 6.16) and a rapid decrease in HL and SG levels (Figure 6.14) to approximately 50 feet at 17 minutes. The decrease in pressure caused flashing to occur in the HL, resulting in a spillover of HL fluid into the SG. With spillover, primary-to-secondary heat transfer was established and steam pressure increased at 17 minutes. The loss of level in the secondary resulted in the initiation of AFW (Figure 6.17). With the (50-foot) SG primary level below the AFW injection site (51 feet), a primary condensing surface was exposed to the cold AFW, and high-elevation BCM occurred.

Boiler-Condenser Mode (BCM), 17 to 195 Minutes

At 17 minutes, primary vapor condensed near the AFW injection point. The upper secondary fluid superheated, the SG continued to steam, and the primary system depressurized at a rapid rate, reaching approximately 1125 psia by 19.5 minutes (Figure 6.16). As the primary depressurized, the leak flow rate decreased while the HPI flow increased (Figure 6.18); however, the leak flow dominated and the loop continued to lose inventory. At 19.5 minutes, the spillover flow ended and primary-to-secondary heat transfer decreased. The decreased steaming of the secondary resulted in a level increase in the SG secondary and reduction of AFW at 20 minutes. As a

result, the BCM heat transfer was greatly reduced. The depressurization of the secondary maintained enough steam flow and primary-to-secondary heat transfer to maintain the AFW injection and, at 26 minutes, an intermittent BCM occurred (Figure 6.9). At approximately 87 minutes, the SG primary level decreased to the secondary pool level, firmly establishing continuous Pool BCM coupling. Figure 6.9 indicates the strong coupling of primary and secondary pressures at this time; this continued until 195 minutes.

Refill Without Venting, 130 to 304 Minutes

At 126 minutes, with the primary pressure at approximately 400 psia, an anomaly in the HPI flow control system resulted in an increase in HPI flow (Figure 6.18). As a result, the HPI flow exceeded the leak flow at 130 minutes, and the primary system began refilling (Figure 6.10). The SG primary level increased from a low point of 28 feet, reaching a level of 53 feet by 235 minutes. The HL level increased during the same time. At 176 minutes, as the HPI flow reached 0.08 lbm/s and exceeded the leak flow (0.06 lbm/s), Figure 6.18, the CL refilled. This refill resulted in a new manometric balance between the HL and SG levels as displayed on Figure 6.10. The HL level fell approximately 3 feet while the SG primary level increased approximately 9 feet. The net increase (of SG primary minus HL level) of 6 feet is roughly equivalent to the CL level change. The increase in SG primary level precipitated the end of pool BCM. At 235 minutes, the loop operators decreased the HPI pump speed and corrected the control dysfunction. HPI flow (Figure 6.18) quickly resumed its proper value. The new flow rate was less than the leak flow and the CL re-voided, reestablishing the former HL-to-SG manometric balance and ending loop refill.

From 235 to 304 minutes, the primary system conditions changed very little. Secondary pressure reached its minimum value of approximately 100 psia at 276 minutes, the steaming rate was insufficient to couple the primary to the secondary. The leak and HPI flow rates were in equilibrium at 0.06 lbm/s. The primary system pressure was a constant 370 psia (Figure 6.9).

Venting, PORV Opening and Core Power Reduction, 304 to 534 Minutes

At 304 minutes the operator opened the HL high point vent (HLHPV). A very mild primary depressurization began. An almost imperceptible refill

resulted but the HL and SG primary levels remained nearly constant (Figure 6.10). At 381 minutes, AFW injection occurred, raising the secondary level to 44 feet by 391 minutes (Figure 6.10). By 430 minutes, the primary pressure had decreased to 350 psia (Figure 6.9). The operator opened the pressurizer power-operated relief valve (PORV) as had been specified. Immediately, the pressurizer began to fill. However, the effect on primary pressure was small, and the HPI flow rate remained almost constant (Figure 6.18). As a result, the inventory gain of the pressurizer due to the venting of the steam space caused a decrease in both the HL and SG primary levels (Figure 6.10). The pressurizer level rose from 9 feet at 429 minutes to 30 feet at 493 minutes. The net effect of the PORV discharge during this period was to shift inventory from the loop to the pressurizer. At 496 minutes, the operator began a core power reduction from 1.21 to 0.5% of scaled full power over a 30-minute period, also as had been specified. As power was reduced, pressure began to decline slowly (Figure 6.9) and loop temperatures began to decrease. The decrease in steam produced in the core allowed the HPI flow to fill the cold leg at 506 minutes (Figure 6.10). The CL refill caused the HL level to drop correspondingly. Primary pressure decreased to 240 psia by 534 minutes.

Refill With Low-Pressure Injection (LPI), 534 to 587 Minutes

With the primary pressure at 240 psia, the LPI system shutoff pressure was reached and the further pressure decrease resulted in an abrupt increase in injection system flow. Figure 6.18 shows HPI flow increasing from 0.06 to 0.12 lbm/s at 544 minutes, simulating the LPI system influence. The increased flow resulted in a rapid increase in HL and SG primary levels, Figure 6.10. The CL discharge fluid temperatures (Figure 6.12) experienced a sharp decrease. Figure 6.19 shows the core inlet subcooling at 534 minutes. At 587 minutes into the test (and before system refill), the test was terminated. Although the system was nearly full, natural circulation flow was not yet established, and the core exit and HL temperatures were still saturated. The pressurizer level, indicating approximately 40 feet, was almost full (Figure 6.10).

6.3.3 Results

Test 220304 with reduced HPI capacity exhibited many of the same phenomena displayed in the OTIS Nominal Test 220100. All phases of the test were

affected by the half-capacity HPI flow. The first phase of the test (draining, saturation, and intermittent circulation) lasted only 17 minutes following leak initiation, compared with ∿38 minutes in the Nominal Test. That is, the duration of the draindown period appeared to be proportional to the HPI capacity. The reduced HPI capacity led to the voiding of the CL in this test, whereas it generally remained full in the Nominal Test. Both tests exhibited spillover or intermittent circulation. However, the CL voiding in this test caused pronounced changes in the HL and SG levels. The BCM was encountered earlier (17 minutes post-leak) and rather abruptly. In the Nominal Test, the BCM occurred at 38 minutes after leak opening and in a less dramatic manner. Once in BCM, both tests exhibited high-elevation and pool-level condensation of the primary steam. Each test demonstrated enhanced depressurization characteristics as a result of BCM. Refill of the loop occurred in the Nominal Test as the HPI flow exceeded leak flow. In Test 220304, refill began prematurely as a result of its atypical HPI system response. Once corrected, refill ceased; however, the SG primary level was above the AFW injection site, inhibiting further BCM condensation. The Nominal Test refilled on HPI alone and was further augmented by the opening of the HL vent (HLHPV). In Test 220304, the HLHPV and the PORV had little effect on system refill. Detectable level increases were not realized until core power was reduced and LPI system flow was achieved. The test lasted over ten hours and was terminated before total loop refill, whereas the Nominal Test refilled 433 minutes after leak initiation.

6.4 Test 220402 (10-Foot SG Level)

OTIS Test 220402 used a 10-foot SG secondary level versus the nominal 38-foot level. Boundary conditions were otherwise those of the Nominal Test.

6.4.1 Performance

Initialization

Test initial conditions are summarized in Table 6.11. Actual initial conditions corresponded to those specified with the exception of the pressurizer level and the pressurizer metal temperature. These conditions are not perceived to have had a significant influence on test behavior.

Conduct

Test conduct is summarized in Table 6.12. The following operator actions were performed as specified:

- Actuated the 10-cm^2 cold leg suction leak.
- Actuated two high-head HPI pumps.
- Actuated the core power ramp.
- Increased the AFW flow rate.
- Actuated the SG depressurization ramp.
- Actuated the HL high point vent.

Guard heater operation, SG secondary level control, HPI flow rate and reactor vessel vent valve control mode differences from those specified are addressed in the following paragraphs.

Guard Heater Operation

The HL metal temperature response near the U-bend and the stub (the HL pipe leading to the SG) indicated increases of 2 to 10F during the later phase of the BCM and refill (cf. appended Plot 124). Correspondingly higher fluid temperatures were also observed. This indicates that the guard heaters in these regions were potentially adding heat to the system in excess of the amount required to maintain an adiabatic condition. This observation, and similar observations in other tests, led to the supplementary guard heater effects Tests 2202AA and 2202BB, cf. section 10 herein.

SG Secondary Level Control

SG secondary level control was adversely affected by a sluggish control system, by relatively slight leakage across the AFW control valve, and by differences between the level used to drive the AFW control system and the "actual" level (the collapsed liquid level corrected for local fluid density which is determined using local fluid pressures and temperatures). These difficulties caused level overshoots and undershoots and repeatedly prompted the operator to take manual control of feed (the operator usually closed the valve manually). These instances of manual feed control are listed in Table 6.13 and indicated on Figure 6.20.

High-Pressure Injection (HPI) Flow Rate

The turbine meter used to control HPI flow rate to simulate the HPI head-flow characteristics, HPTM01, tended to read low for this test. This degraded HPI turbine flowmeter, discovered subsequent to the completion of this test (and confirmed by post-test fluid inventory checks and the redundant turbine meter HPTM03), resulted in HPI flow rates that exceeded those specified. The overall excess HPI flow rate was approximately 6% of the intended flow rate, but brief periods of from 9 to 24% excess HPI flow rate were encountered. The indicated and specified HPI flow rates are compared in Figure 6.21. (Random times during the first 304 minutes of the transient were chosen to provide this comparison.)

Reactor Vessel Vent Valve (RVVV) Control

The RVVV was manually opened during prolonged two-phase conditions to preserve the valve. In this test, the return of valve control to automatic was delayed until approximately three minutes after refill.

HPI Flow Rate in Excess of the Simulated Heat-Flow Curve

The HPI flow rate was manually increased beyond the specified head-flow curve near the end of the test in an attempt to obtain a 23-ft level in the pressurizer. This increase in HPI flow rate did not affect the preceding phenomena of interest (draining phase, BCM, and refill).

The impact of guard heater operation is addressed in section 10. The intricacies of the SG secondary level control are shown in Table 6.13 and Figure 6.20. System interactions likely to have been affected by the

existant SG secondary level control are identified as they are encountered. The deviations of HPI flow rate from that specified were usually less than 10%, but the actual flow rate should be used in code predictions. The RVVV control mode changes are readily introduced into a code model.

Those differences associated with the SG secondary level and the manual AFW control valve actions, although departures from the test specification, are potentially prototypical plant occurrences.

Measurements

Measurements unavailable in this test are listed in Table 6.14. The majority of these instruments were not critical to testing, e.g., reactor vessel and hot leg conductivity probes. The loss of the string thermocouple SG primary fluid temperature measurements did reduce the SG primary instrumentation below the minimum level. This string TC failure was caused by a steam leak through the string sheath and was the subject of a separate communication with the PMG. This entire string was subsequently severed and sealed to prevent leakage from the primary system.

The calculated leak flow rate employed weigh-tank measurements, as has been discussed in section 5. The turbine meter used to control the HPI flow rate (HPTM01) sometimes gave inaccurate indications, necessitating the use of the redundant meter, HPTM03. This affected the HPI flow rate simulation, as was addressed in the previous section.

6.4.2 Observations

Test observations are grouped according to the following observed test phases:

1. Draining, saturation, intermittent circulation and flow interruption.
2. Boiler-Condenser Mode (BCM).
3. Refill without venting.
4. Refill with venting.
5. Natural circulation cooldown.

The key events of the test are summarized in Table 6.15 and are also indicated on Figure 6.22. Key data plots are included as Figures 6.20 through 6.24, additional data plots are appended to this report.

Draining, Saturation, Intermittent Circulation and Interruption, 0-67 Minutes

Following a period of steady-state loop operation, the transient was initiated after 11 minutes of data acquisition. The scaled 10-cm^2 cold leg suction leak was opened and, when the pressurizer had drained to approximately 8.6 feet above the upper face of the SG lower tubesheet, the HPI was actuated, the core power ramp was initiated, and AFW was increased to raise the SG secondary level from approximately 6 feet to 10.5 feet. The primary pressure (Figure 6.22) immediately decreased from 2198 to 1947 psia (by 2 minutes) when the pressurizer emptied. The HLUB began voiding at 3 minutes and the primary pressure stabilized at approximately 1680 psia (Figure 6.22). The HLUB temperatures (HLTC07 and 08 of appended Plot 121) were saturated at approximately 611F, and the HL levels began to decrease (Figure 6.20). The SG secondary level reached the band control setpoint (10-1/2 feet) at 5 minutes, and the AFW control system terminated the AFW. For the next 15 minutes, the SG secondary level was controlled between approximately 8 and 11.8 feet. The HL continued to void and intermittent circulation was observed. This is indicated on Figure 6.22 by the momentary primary pressure increases occurring when the primary and secondary system decoupled, and by the subsequent primary pressure decrease when a spillover occurred, causing the primary and secondary to momentarily recouple (two occurrences were observable, at times 11 and 18 minutes). This is also observable on Figure 6.20 as an increase in the SG primary level at approximately 11 minutes. This level change, however, was not apparent at 18 minutes.

Subsequent to the last spillover, primary flow was interrupted and the core outlet and the HL fluid temperatures were governed by the depressurization of the primary side (caused by a continuous primary-to-secondary coupling as the SG was depressurized). At approximately 20 minutes, the SG secondary level control was placed into constant level control. The SG secondary level at this time was approximately 11.5 feet, or 1.5 feet above the control setpoint. In an attempt to achieve the specified SG secondary level of 10 ft, the operator manually closed the AFW control valve at approximately 37 minutes (with the level at approximately 12 feet). The secondary level diminished through the steaming of the SG in response to the SG depressurization ramp. During this period, primary-to-secondary

heat transfer occurred as indicated by the primary pressure response, cf. Figure 6.22. As the SG secondary level approached the control setpoint, the loop operator placed the SG secondary level control back into constant level control at approximately 56 minutes, with the level at approximately 11 feet. The HL and the SG primary levels continued to decrease until approximately 67 minutes into the test (Figure 6.20). The excess SG secondary inventory prevented the activation of AFW and precluded the boiler-condenser heat transfer mode until 67 minutes.

Boiler-Condenser Mode (BCM), 67 to 97 Minutes

At approximately 67 minutes, AFW was actuated (the secondary level was about 10.4 feet). The SG primary level was approximately 28 feet at this time, thus the secondary pool level was 18 feet below this level. When the AFW flow began, the increased primary-to-secondary heat transfer enhanced the depressurization of the primary loop. This increased heat transfer caused the initial 25 psi increase in SG secondary steam pressure, approximately 1 minute after the onset of AFW flow (Figure 6.22); AFW and steam flow continued for approximately 20 minutes (appended Plot 10). The primary system pressure decreased from 1297 psia at 67 minutes, to 582 psia at 90 minutes, at which time the primary pressure was 47 psi greater than the secondary pressure, cf. Figure 6.22. The significance of this observation is that it confirms the occurrence of boiler-condenser heat transfer with high-elevation AFW injection only, i.e., a pool condensing surface was unavailable.

The depressurization caused by (high-elevation) AFW BCM heat transfer resulted in an increase in HPI flow (Figure 6.23) and a decrease in the leak flow. At approximately 74 minutes, the HPI flow began to exceed the leak flow (Figure 6.23) and refill began (Figure 6.20). Near the end of the BCM, the metal temperatures in the U-bend region and the upper portions of the HL increased (HLTC11 and HLTC15, appended Plot 124), indicating potential anomalies of the guard heaters.

Cyclical behavior of the reactor vessel vent valve (RVVV) was observed. Therefore, at approximately 88 minutes, the loop operator manually opened the valve. Following this manual opening of the RVVV, at approximately 89 minutes, a significant increase in the DC flow rate was observed (appended Plot 9). Examination of the pressure difference across the vent valve

subsequent to this manual action (appended Plot 172) indicates that the vent valve would also have opened had the valve remained in the automatic mode of operation.

Refill Without High-Point Vent Actuation, 97 to 306 Minutes

As the primary loop was depressurized through the BCM, the primary-to-secondary pressure and temperature differences decreased and, hence, the heat transfer rates were diminished. The dwindling SG steaming rate reduced the feed demand. At approximately 97 minutes, the AFW injection was terminated, the BCM ceased, and the primary and secondary systems decoupled. When this occurred, the energy dissipated by the leak discharge was insufficient to offset the core energy (appended Plot 20); therefore the primary pressure began to rise (Figure 6.22). Refill resulted in a portion of the HPI flow being directed towards the SG, i.e., reverse flow in the CL. As a result, the leak temperature decreased continuously to approximately 273F at 134 minutes (Figure 6.24). The decreasing leak temperature and the increasing primary pressure caused a continuously decreasing refill rate. At approximately 183 minutes, the HPI flow was only slightly greater than the leak flow (Figure 6.23) and the refill rate was correspondingly reduced (Figure 6.20).

During the refill process, there were brief periods of primary-to-secondary heat transfer and slight HLUB spillovers, as indicated by the AFW and steam flow rates (appended Plot 12). However, these occurrences did not appear to have resulted in (high-elevation) AFW BCM. The SG primary level was apparently above the SG tubesheet, therefore a condensing surface did not exist.

The HL level continued to rise slowly until approximately 300 minutes, resulting in a spillover. The attendant primary-to-secondary heat transfer caused several changes: a corresponding decrease in primary pressure and increase in steam pressure (Figure 6.22), an increase in the loop flow rate (appended Plot 9), an increase in the SG primary temperatures (appended Plot 13), an increase in the leak temperature (Figure 6.24), a decrease in the DC temperature (appended Plot 151), and an increase in steam flow (appended Plot 10). During this spillover the AFW control valve was manually closed because the SG secondary level had been above the control

setpoint. Therefore, there was no demand for AFW. The steam flow control valve choked. The SG secondary level momentarily increased (perhaps due to the altered conditions of the SG secondary fluid) and then gradually decreased. AFW initiation during this spillover may have refilled the primary loop much earlier than observed. The increasing HL levels and the spillover which occurred before opening the HL high point vent imply that primary loop refill was imminent and may have occurred without venting.

Refill With Venting, 306 to 424 Minutes

At approximately five hours into the test (306 min after leak opening), the loop operator opened the HL high point vent (HLHPV) as specified. This caused a slow decrease of primary pressure. The loop operator noted a spillover at approximately 330 minutes (this spillover is also confirmed by the plots). Three subsequent spillovers resulted in primary-to-secondary coupling and loop depressurization. These spillovers occurred as a result of void formation in the reactor vessel. During the first three spillovers, the AFW control valve had been manually closed. The SG level, however, would indicate a demand for AFW during the second and third spillover. The loop operator placed the AFW control valve into automatic (constant level) control at approximately 350 minutes. When the fourth spillover occurred (at about 352 minutes) AFW flow was initiated and continued until approximately 365 minutes. This AFW activity caused a general reduction of the SG primary fluid temperatures (appended Plot 13) and an enhanced rate of primary loop depressurization (Figure 6.22). The primary loop continued to cool and to refill. At approximately 379 minutes another spillover occurred, momentarily coupling the primary and secondary systems. The SG secondary level was above the control setpoint, thus no AFW flow was obtained during this spillover.

The two spillovers at approximately 347 and 355 minutes lowered the core inlet temperature sufficiently to momentarily subcool the core outlet fluid (appended Plot 111). During these spillovers, the RVVV control was in the manual-open position; this may have affected the ability of the loop to sustain circulation. Between approximately 399 and 417 minutes, a number of spillovers occurred and the primary and secondary were coupled. At approximately 403 minutes, the SG secondary level decreased, reaching a level of approximately 7 feet by 420 minutes (Figure 6.20). AFW did not actuate

during this period. The loop operator, noticing the reduced SG secondary level, transferred the AFW control to manual-open and back to automatic. This actuated AFW causing a more pronounced coupling of the primary and secondary, Figure 6.22. At 424 minutes the HL U-bend filled (Figure 6.20) and the HL vent flow rate abruptly increased as it began to discharge liquid (Figure 6.23).

Natural Circulation and Cooldown, 424 Minutes to Test Termination (484 Minutes)

The loop refill at 424 minutes increased the primary-to-secondary heat transfer. The primary depressurized at a faster rate (Figure 6.22), and continuous primary loop flow was established (appended Plot 9). This primary loop flow was confirmed by the abrupt decrease of the core outlet and HL fluid temperatures (appended Plots 111 and 121), the decrease in SG primary fluid temperatures (appended Plots 13 and 131), the increase in the cold leg fluid temperatures (Figure 6.24), and the decrease in the downcomer fluid temperatures (appended Plot 151), which reflected forward flow. Enhanced loop flow and primary-to-secondary coupling obtained a general loop cooldown (appended Plot 2). All the primary fluid temperatures became subcooled except those in the pressurizer and the reactor vessel upper head (RVTC08, appended Plot 111, cf. appended Plots 111, 121, 131, 141, 151, 161, and 171).

At approximately 427 minutes, the reactor vessel vent valve (RVVV) control was placed in the automatic position, i.e., open at 0.25 psi and closed at 0.125 psi. The RVVV initially closed due to the low pressure drop across the valve (as a result of the previously initiated loop flow); it then cycled open and closed several times. After approximately 433 minutes it remained closed as sustained natural circulation was established (appended Plot 9).

At approximately 432 minutes, the loop operator took manual control of the HPI pump to increase the pressurizer level. The resulting HPI flow rate (Figure 6.23) exceeded the HPI head-flow curve and caused a gradual repressurization of the primary (Figure 6.22), as well as a gradual increase in the pressurizer level (Figure 6.20). As the primary pressure increased, the HPI flow decreased and the leak flow increased (Figure 6.23). Thus, the pressurizer refill rate diminished (Figure 6.20) and the loop operator

continued to increase HPI flow manually until the pressurizer level reached 25 feet at about 484 minutes. At 484 minutes, the test was terminated after having observed one hour of post-refill cooldown.

6.4.3 Results

Test 220402 exhibited phenomena similar to those of OTIS Nominal Test 220100. The major observation of this test was the effectiveness of high-elevation "AFW BCM" (auxilary feedwater boiler-condenser mode). The existance of this mode of heat transfer was proven by the absence of a condensing surface at the SG secondary level (i.e., the absence of pool BCM).

The progression of this test is shown on Figure 6.21 as loci of leak and HPI conditions. At 4 minutes, the loop was draining rapidly as indicated by the leak flow of 445 lbm/h versus the HPI flow of 323 lbm/h. From 4 to 66 minutes, a reduced depressurization rate, corresponding to the boiling-off of excess SG inventory, was observed. At 66 minutes, the leak flow was 459 lbm/h and the HPI flow was 358 lbm/h. Between 66 minutes and 86 minutes, the impact of the AFW-induced BCM was observed. The rapid depressurization caused by the BCM is illustrated by the decreased primary pressure at 86 minutes. During the BCM, refill was initiated between 74 and 86 minutes when the HPI flow exceeded the leak flow. At 86 minutes, the HPI flow was 454 lbm/h and the leak flow was 271 lbm/h. By approximately 100 minutes, BCM heat transfer had ceased. From 100 to 173 minutes, the primary loop repressurized and the leak temperature decreased, resulting in a convergence of the leak and HPI flow rates and a correspondingly decreased refill rate. From 173 minutes until the HL high point vent (HLHPV) was opened (306 minutes), the HPI flow was greater than the leak flow. The collapsed liquid levels (Figure 6.20) indicate that refill was progressing before opening the HLHPV; this was substantiated by the observed spillover before opening the vent. Therefore, it appears that refill may have occurred without venting.

Although the overall HPI flow rate was approximately 6% greater than specified (Figure 6.21), it should be noted that there was a discernible time dependence of this offset. During the depressurization (76 to 89 minutes), the HPI flow rate was approximately 10% greater than the

specified value, while during the repressurization (97 to 173 minutes), this offset was decreasing.

Comparing Test 220402 with the Nominal Test 220100, the lower SG level of Test 220402 resulted in a longer loop drain and a later BCM (67 versus 43 minutes after the leak was opened). However, SG secondary level control had an impact on the availability of AFW during this phase of the transient. Had AFW been available, it is anticipated that the BCM may have occurred earlier (at approximately 28 minutes, when the SG primary level dropped below the SG tubesheet). The HL levels for Test 220402 decreased to approximately 30 ft, whereas those in Test 220100 decreased to approximately 40 ft at the end of the BCM. This is representative of the gradual depressurization between approximately 19 and 67 minutes, and the resulting mismatch between leak and HPI flow observed in Test 220402. The refill phases of the two tests were similar. The opening of the high point vent had little effect on the refill of the loop. At approximately 428 minutes, a natural circulation cooldown was established. Loop pressure in Test 220402 was 750 psia at test termination versus 500 psia in Test 220100, with similar loop temperatures.

6.5 Test 220503 (Cold Leg Discharge Leak)

OTIS Test 220503 used a cold leg discharge leak rather than a cold leg suction leak. The boundary conditions were otherwise those of the OTIS Nominal Test, Test 220100.

6.5.1 Performance

Test conduct paralleled the test specifications. Initial conditions, given in Table 6.16, were similar to those specified. The pressurizer level was 1 foot higher than specified, the maximum pressurizer metal temperature was 24F higher, and the SG secondary liquid level was 0.1 foot higher than specified. None of these differences are perceived to have adversely affected the test transient. Several operator actions were performed as specified, cf. Table 6.17. As occurred in the Nominal Test, the simulated reactor vessel vent valve (RVVV) control was changed from automatic to manual-open after approximately one hour of testing. In this test, vent valve control was returned to automatic (and the valve closed) after approximately seven hours, when the loop refilled and natural circulation began. (The rationale for these RVVV control changes has been discussed in the description of the Nominal Test, cf. section 5). Near the end of the test, the operator increased the HPI flow rate to obtain a pressurizer level rather than throttling HPI to maintain level.

The unavailable measurements are listed in Table 6.18. This list is similar to those of previous tests and is predominated by the HL conductivity probes and the off-nozzle string thermocouples; the unavailable measurements did not significantly impair transient analysis. The appended plots highlight two additional areas of measurement and control difficulties: SG level and leak flow rate. SG secondary level is displayed on appended Plot 8. Although it remained within a few feet of the specified control level after secondary refill, the level was somewhat variable and should be used in conjunction with the auxiliary feedwater flow rates (labelled "AFW") of appended Plot 10. (The secondary level control is discussed in section 5.) The periods of manual AFW control are listed in Table 6.19.

The indicated leak flow rates displayed aphysical flow spikes, cf. appended Plot 17, for example at 40 min. This prompted the incorporation of the

weigh-tank data shown on Plot 17, and obtained the total fluid mass agreement of appended Plot 18. Plot 17 with weigh-tank correction demonstrates the impact of this correction: The flow spikes persist after adjustment, but their magnitude is reduced so that the integrated flow rate matches that of the weigh-tank. The adjusted flow rate becomes more appropriate as the frequency of weigh-tank readings is increased. Leak flow rate measurements have also been discussed in section 5.

6.5.2 Observations

Major transient events (and operator actions) are listed in Table 6.17. Key events are also indicated on Figure 6.25. Figures 6.26 through 6.32 are expanded-time plots of test initialization, initiation, saturation, and intermittent circulation; they augment the discussion of these phases of the transient. The appended plots supplement the descriptions of the BCM, and post-BCM refill and cooldown. Leak flow rate is plotted against system conditions in Figure 6.33; the basis for this "equilibrium plot" is given in Appendix C.

Initiation, Saturation, and Intermittent Circulation

The data acquisition system was activated at 0948, 20 March 1984. The steady-state initial conditions are given in Table 6.16. After 10.6 minutes of steady-state data acquisition, the scaled 10-cm^2 cold leg discharge (CLD) leak was opened. Approximately two minutes after leak opening, the pressurizer level approached 2 feet, and the operator performed the second set of initiating actions: HPI was actuated, AFW was augmented to obtain a 3 ft/min SG secondary refill rate, the core power ramp (simulating decay from 1-1/2 minutes) was begun, and the pressurizer heater controls were adjusted. The leak fluid temperature rapidly cooled, cf. Figures 6.26 and 6.33. It became colder than any of the CL fluid temperatures, unlike its intermediate temperatures observed with a leak in the cold leg suction piping. [The CLD leak site is just downstream of the HPI location, both are located at the bottom of the cold leg (sloping) pipe.] Refer to Figures 6.26 through 6.32 to supplement the remainder of this discussion.

The pressurizer drained and the primary rapidly depressurized toward the saturation pressure corresponding to the hottest loop fluid. Approximately

three minutes after leak actuation the HLUB fluid saturated with a primary pressure of 1690 psia. The primary loop flow diminished and primary pressure stabilized. The uppermost RV fluid saturated just after the HLUB fluid. The RV upper plenum void fraction grew rapidly, at approximately 9 minutes after leak actuation. The fluid displaced from the reactor vessel provoked a spillover, which is most evident by the brief increase of primary loop flow and the resurgence of secondary pressure.

After primary flow reinterrupted, the AFW flow rate continued (completing the refill of the SG secondary to the specified control level). The near-stagnant primary fluid in the AFW-wetted SG tubes was abruptly cooled, attaining temperatures as low as 485F (50F less than the current SG secondary saturation temperature).

At 13 minutes the secondary level approached its control point and the AFW injection was terminated. The primary system pressure gradually increased, reaching 1650 psia at 15 minutes. The reactor vessel level fell to the elevation of the HL nozzle at this time. The resulting augmented vapor flow to the HL apparently promoted a relatively strong resurgence of primary flow and primary-to-secondary coupling.

Boiler-Condenser Mode (BCM)

Beyond the spillover at about 15 minutes, the primary loop flow remained nearly stagnant and primary pressure was approximately constant at 1550 psia (refer to the appended plots). At 27 minutes the declining primary liquid level (beyond the HL U-bend) reached the elevation of the SG upper tubesheet. Primary pressure began to decrease slowly. At approximately 41 minutes, AFW was actuated and the "AFW BCM" began (this is the condensation of primary vapor near the AFW injection elevation, with the primary level in the SG above the secondary level). The indicated primary and secondary levels in the SG remained offset by approximately 4 feet. Primary pressure fell rapidly toward that of the SG secondary. By 60 minutes, the primary depressurization had progressed sufficiently to cause the HPI flow rate to exceed the leak flow rate such that refill began.

Post-BCM Refill and Cooldown

At two hours, the increasing primary level returned to the top of the SG, primary-to-secondary heat transfer was thereby impaired, and the primary

system slowly repressurized (refer to the appended plots). The cold leg discharge leak fluid temperature stabilized near 300F, the primary repressurized to almost 900 psia, and the primary approached (total fluid mass and energy) equilibrium.

At five hours, the HL high point vent was opened as specified. The upper-elevation HL metal was cooled, primary pressure was gradually lowered, intermittent spillovers were observed, and the loop refilled at seven hours. At this time, control of the reactor vessel vent valve was returned to automatic and the valve closed. Natural circulation restarted almost concurrently. At 7-1/2 hours, the operator increased the HPI flow rate to obtain a pressurizer level, and at eight hours testing was terminated. The loop fluid temperatures at termination were approximately 300F, although the reactor vessel upper head remained voided and superheated. HPI-leak cooling predominated. Referring to appended Plot 302, the entire primary loop was approximately isothermal except for a 50F temperature reduction at the HPI site and a corresponding increase across the core.

6.5.3 Results

OTIS Test 220503 exhibited the expected post-SBLOCA interactions. The (scaled 10-cm^2) leak was located in the cold leg discharge piping, just downstream of the HPI location, rather than in the cold leg suction piping as in the Nominal Test. The leak fluid evidenced a more rapid response to HPI cooling than was seen in the Nominal Test, but the long-term HPI-leak cooling was similar between the two tests. This similarity was underscored by the agreement in timing and events of these two tests. The most noticeable difference (other than the timing of the leak fluid temperature response) involved the Boiler-Condenser Mode (BCM): The Nominal Test had approximately equal primary and secondary levels indicating Pool BCM; Test 220503 maintained an approximately 4-foot excess of primary level over secondary level, indicating AFW BCM. However, the BCM depressurization rates were similiar between the tests. AFW control variations between the two tests may have influenced these differences in BCM behavior.

6.6 Test 220604 (Low-Head HPI)

Single-variable Test 220604 used low discharge-head HPI characteristics, versus the nominal high-head characteristics. These HPI characteristics have been given in section 2 herein, and are repeated in Figure 6.34. The remaining boundary conditions were those of the Nominal Test.

6.6.1 Performance

Initialization

The HPI Characteristics Test 220604 was conducted on 19 March 1984. The test was performed as specified. Table 6.20 summarizes the initial conditions and compares them with those specified. All prescribed conditions except the pressurizer metal temperature and pressurizer level specification were achieved. Two pressurizer metal thermocouples (PRTC06 and PRTC10, appended Plot 163) were observed to be more than 10F above the saturation temperature (650F). This condition is not perceived to have had a deleterious effect on test behavior.

Conduct

The actions of the loop operator are indicated on Table 6.21. Scheduled actions such as opening the HL vent occurred as specified at 313 minutes, approximately 5 hours after leak initiation. Manipulations of the AFW control valve (SFCV03) occurred frequently (cf. Table 6.22). The majority of these manipulations were of short duration and were performed to expedite valve closure in order to prevent the overfilling of the secondary system; the secondary level was generally maintained within the specified range (cf. appended Plot 8). The AFW system was sometimes inactive when spillovers of HL fluid were observed. The impact of these situations is perceived to be minor but would tend to delay primary-to-secondary coupling and, thus, loop refill. These and other actions are discussed further in section 5. The automatic controls i.e., core power, secondary pressure, and HPI pump head-flow, performed as specified.

Measurements

Measurements unavailable in this test are listed in Table 6.23. The majority of these instruments were not critical to testing (cf. section 3 for the identification of critical measurements). The HL conductivity probes (HLCP05 through HLCP09 and HLCP17) and the SG string thermocouples (SPTC19 through 28) predominate the list.

6.6.2 Observations

The test observations are grouped according to the following test phases:

1. Draining, intermittent circulation, and flow interruption.
2. Boiler-Condenser Mode (BCM).
3. Refill without venting.
4. Refill with venting.
5. Natural circulation cooldown.

The key test events are summarized in Table 6.24 and the test phases are shown on Figure 6.35. Selected data plots are included in this section, Figures 6.35 through 6.39, and additional data plots are appended to this report.

Draining, Saturation, Intermittent Circulation, 0 to 12 Minutes

The transient began at 10.7 minutes after data acquisition system activation following a period of steady-state operation. At time zero the cold leg suction scaled 10-cm^2 leak was opened. At 2.7 minutes, the HPI system was activated, the core power ramp was initiated, and the AFW flow rate was increased. With the opening of the leak, primary pressure decreased rapidly (cf. Figure 6.35), from 2200 to 1950 psia by $\sim$2 minutes, at which time the pressurizer emptied and the HL began to saturate. The rate of change of the primary pressure diminished (Figure 6.35) at 2.5 minutes as the HLUB fluid temperature attained 610F at 1672 psia, indicating that saturation and voiding occurred. This was further reflected in the HL level decrease shown in Figure 6.36 at the same time. At 4.9 and 6.7 minutes, small perturbations of primary pressure and HL level indicated spillovers and intermittent flow to the SG. The effect of

the intermittent flow rate is further evident on Figure 6.35 at 7 minutes as secondary pressure rose from 1100 to nearly 1200 psia. At 7 minutes, a relatively long flow interruption began and primary pressure increased from 1624 to 1729 psia by 12 minutes. As a result, the pressurizer level increased to about 10 feet. During the same period, the reactor vessel level dropped below the RVVV elevation, and the downcomer and cold leg levels began to decrease (Figure 6.36). The CL fluid temperatures (Figure 6.37) indicated saturated conditions and voiding at this time. At $\sim$9 minutes, the reactor vessel level descended below the HL nozzle, sending steam into the HL. As a result, a large spillover occurred, ending the primary repressurization (Figure 6.35). The spillover recoupled the primary and secondary systems and raised the liquid levels in the downcomer and reactor vessel.

Boiler-Condenser Mode (BCM), 13 to 89 Minutes

The increase of the downcomer and reactor vessel liquid inventories resulted in a precipitous drop of the SG primary level (Figure 6.36) to approximately 45 feet, exposing a primary condensing surface near the high-elevation AFW site. As a result, the primary system pressure (Figure 6.35) decreased from 1641 to 1149 psia between 12.9 and 16.9 minutes. However, the impact of the AFW BCM was diminished by the termination of AFW at 13.6 minutes when the secondary level control setpoint was attained. As pressure dropped below 1600 psia at 13.4 min., the HPI flow began (Figure 6.38). The advent of HPI ensured the subcooling of the CL discharge region fluid. AFW injection began again at 14.3 minutes and continued sporadically throughout the remainder of the test. With the ongoing BCM, the primary pressure gradually decreased (Figure 6.35). The decreasing primary pressure obtained increased amounts of HPI flow. However, this increase was partially offset by the increasing leak flow, which was attributable to the decreasing leak temperature. Although the HPI flow rate briefly exceeded the leak flow rate at 15 minutes (following the BCM depressurization), sustained refill was delayed until approximately 56 minutes.

Refill Without Venting, 89 to 313 Minutes

By 89 minutes of testing, the BCM coupling had diminished such that the primary and secondary pressures began to diverge. By 100 minutes the SG primary level reached 52.8 feet, covering the SG upper tubesheet and thus

precluding the AFW BCM. The primary pressure continued to diverge from that of the secondary (Figure 6.35). The SG primary level remained nearly constant from 90 to 313 minutes, whereas the HL level increased, although at a diminished rate (Figure 6.36). A decrease in SG primary and HL level began at approximately 149 minutes, whereas the pressurizer level increased. At 296 minutes, a small spillover was observed by the operator. With the primary pressure nearly constant, the reactor vessel and HL fluid temperatures remained nearly constant at the saturated fluid conditions.

Refill With Venting, 313 to 389 Minutes

At five hours, the loop operator opened the HL high point vent (V2LS01, appended Plot 16) and primary pressure began to decrease (Figure 6.35). Numerous spillovers were observed by the operator; these occurred at 338, 343, 359, 363, and 365 minutes, and are reflected on appended Plots 4, 13, and 26. The spillovers caused increased SG coupling as can be observed on Plot 13. Continued SG coupling and loop depressurization resulted in loop refill at 389 minutes. Figure 6.38 shows the step increase in HPV flow rate as the discharge changed from vapor to liquid.

Loop refill at 389 minutes established primary-to-secondary heat transfer. The primary began to depressurize at an accelerated rate (Figure 6.35). The HL temperatures, Figure 6.39, showed a rapid decrease. The CL fluid temperatures, Figure 6.37, likewise indicated an abrupt increase as primary flow predominated leak flow. Enchanced loop flow and SG coupling caused a general loop cooldown (cf. appended Plot 2). The RVVV closed at 395 minutes when its control was returned to automatic. All primary fluid temperatures indicated subcooled conditions except those in the pressurizer and reactor vessel upper head (RVTC08, appended Plot 111, cf. appended Plots 111, 121, 131, 141, 151, 161, and 171). At 495 minutes, the test was terminated, following more than an hour of post-refill cooldown.

6.6.3 Results

Test 220604 progressed in a manner similar to that of OTIS Nominal Test 220100. The early phases of the test displayed the greatest differences as a result of the low-head HPI characteristics used for this test (cf. Figure 6.34). Because the HPI shut-off head was approximately 1600 psia, no HPI

was available until approximately 13 minutes after leak initiation. The loop thus lost inventory at a faster rate than it did in the nominal transient. Furthermore, the collapsed level in the reactor vessel quickly decreased sufficiently to uncover the HL and CL nozzles and, thus, caused extensive voiding of the CL discharge volume. However, the rapid loss of inventory led to the earlier uncovery of a condensation surface in the SG primary, with low-head HPI. This promoted an early BCM and primary system depressurization. Test 220604 was further distinguishable from the Nominal Test in that the BCM occurred exclusively at the AFW site. The effects of the BCM were diminshed by its early occurrence. That is, the secondary pressure was relatively high, resulting in a reduced primary-to-secondary temperature difference and decreased heat transfer. The BCM ended after approximately 89 minutes when the primary level recovered the SG upper tubesheet. The Nominal Test with pool-level condensation (Pool BCM) exhibited a shorter BCM, but depressurized to 725 psia versus 925 psia in this test. The extended duration of BCM with low-head HPI was due to the faster loss of inventory early in this test and, more importantly, to the on-off nature of the AFW system. Although BCM heat transfer was highly efficient, the AFW injection rate generally exceeded the steaming rate and led to the termination of AFW whenever the secondary level reached its control setpoint. Another major difference between low-head and high-head HPI involves the rate of refill. Figure 6.34 shows the HPI head versus flow curves used in the Nominal Test (high head) and Test 220604 (low head). At pressures below approximately 1325 psia, the low-head characteristics have the greater capacity. The BCM reduced primary pressure well below this crossover pressure. Test 220604 thus exhibited a greater HPI-leak flow differential during the early stages of refill. This contributed to a relatively early HL spillover, before the opening of the HLHPV. The enhanced loop inventory at the time of vent opening allowed system refill and natural circulation to begin only 394 minutes after leak opening, as opposed to 435 minutes in the Nominal Test.

Figure 6.40 illustrates the BCM and refill-without-venting phases using an equilibrium plot. Referring to Figure 6.40, the loop was rapidly depressurizing to 1200 psia by 7 minutes. The primary further depressurized when, at approximately 13 minutes, the BCM began. At 89 minutes, the BCM ended with the primary depressurized to 925 psia. From 89 to 300 minutes,

refill continued as HPI flow exceeded leak flow, and the primary pressur hovered around 1000 psia.

Test 220604 exhibited the same SBLOCA phases as the Nominal Test 220100. The anticipated modes were observed in both tests, i.e., draining, intermittent circulation, interruption, boiler-condenser, refill (with and without high-point venting), and natural circulation cooldown. The low-head HPI characteristics resulted in a faster draindown, an earlier onset of the BCM, BCM at the AFW site, and a longer BCM. Continuing refill and a HL spillover were observed, before vent actuation, indicating that high-point venting may not have been required to establish a natural circulation cooldown.

6.7 Test 220756 (Isolated Leak)

Single-variable Test 220756 repeated the boundary conditions of the Nominal Test 220100, except that the leak was isolated during the period of probable decoupling of primary-to-secondary heat transfer. This timing was determined using the observations of the Nominal Test transient, cf. section 5.

6.7.1 Performance

OTIS Test 220756 was conducted on 27 March, 1984. Test performance was as specified. The conditions designated for the test were as follows:

1. 10-cm^2 cold leg suction leak. Leak isolation was to occur midway between the time of interruption of natural circulation flow and the time of system draindown to the SG upper tubesheet elevation as observed in the Nominal Test 220100. This time was determined to be $\sim$21 minutes after leak opening (in Test 220100, the last interruption occurred at 16 min and the time of the upper tubesheet uncovery was 29 min).
2. Full HPI capacity with high-head pumps.
3. 38-foot SG secondary level, obtained with a refill rate of 3 ft/min.
4. Automatic PORV actuation.
5. No reactor vessel upper head vent actuation.
6. Cooldown by depressurization of the SG secondary at 50F/h.
7. Test termination at one hour after primary system refill.

The initial conditions observed versus those specified are compared in Table 6.25. Other initial conditions were as follows: (1) primary flow 5.5% of scaled full flow, (2) CL temperature 571F, (3) secondary flow 2.3% of full flow, and (4) AFW temperature 118F. All observed conditions were as specified except the pressurizer metal temperatures. However, this discrepancy is not perceived to have affected the test results.

The test was initiated following a 13-minute period of steady-state operation, by opening the 10-cm^2 cold leg suction leak. Two minutes later, as the pressurizer level decreased to two feet, the core power decay ramp, the HPI system, and the AFW injection systems were actuated according to procedure. These and other key operator actions are shown in Table 6.26. Instruments discarded from the data base are listed in Table 6.27. The HL conductivity probes and the off-nozzle string thermocouples on the SG primary side dominated the list of unavailable instruments.

6.7.2 Observations

Test 220756 encountered several transient phases including intermittent primary system circulation, refill, and post-refill natural circulation. Refill occurred approximately 33 minutes following leak initiation and 12 minutes after leak isolation. The major test phases are briefly described below. Figures 6.41 through 6.47 support these discussions.

Draining, Saturation and Intermittent Circulation, 0 to 21 Minutes

The 10-cm^2 cold leg suction leak was opened 12.8 minutes after data acquisition was begun. The operator completed the initiating actions by activating the HPI system, activating the core power decay ramp, and increasing the AFW flow rate. Within 3 minutes, the upper HL fluid saturated. A brief repressurization at 7 minutes resulted from an interruption of primary flow. The primary pressure increase ended at 9 minutes with a spillover at the HL U-bend that caused an abrupt increase in secondary pressure. This was further confirmed by the downstream U-bend level increase at this time. Flow interruption occurred again at 13 minutes, and the primary again began to repressurize. The leak mass flow rate continued to exceed the HPI flow rate, and the SG primary level decreased to 59 feet at 13 minutes. However, further level decrease was delayed by an additional spillover at about 15 minutes. By 13 minutes, the SG secondary level had approached the 38-foot control level, terminating AFW injection; the secondary depressurization ramp was then actuated.

Leak Isolation and Refill, 21 to 34 Minutes

At 21 minutes after leak opening, the operator isolated the leak. Refill began immediately, as evidenced by the increasing HL and SG primary levels. As the HL level reached the U-bend at 24 minutes, a spillover occurred and was reflected in the primary pressure decrease, secondary pressure increase, and the increase in SG primary level. The introduction of HL fluid into the SG primary system reactivated the AFW system, obtaining a feed cycle at 24 minutes. From 24 to 32 minutes, both the SG primary and reactor vessel levels increased, refilling the primary system as HPI flow continued at a rate of approximately 0.09 lbm/s. The maximum primary pressure achieved during refill was 1975 psia. At 32 minutes, both the HL and SG

primary levels reached the U-bend, and a minor spillover occurred as the primary and secondary pressures responded to the flow. By 34 minutes, the loop was refilled and primary-to-secondary coupling was re-established, as reflected in the increased primary and secondary flow rates.

Natural Circulation Cooldown, From 34 Minutes to Test Termination (117 Minutes)

Although primary-to-secondary coupling was established at 33 minutes and the primary system began to cool, the HPI rate exceeded the fluid contraction rate causing the primary system to repressurize. Primary pressure rose from 1540 psia at 34 minutes to 1975 psia at 45 minutes as the pressurizer level increased from 9 to 26 feet, compressing the steam space. At 45 minutes, the operator manually throttled the HPI flow rate to control the primary pressure and pressurizer level, according to the test procedure. Primary pressure began to decrease. For the remainder of this test, the loop continued to cool at a characteristic 50F/h rate in response to the secondary depressurization. This was reflected in the fluid and metal temperature trends. At 117 minutes, the test was terminated with the primary pressure at 1630 psia, primary flow equal to 4% of full flow, secondary pressure at 430 psia, and a secondary flow rate of 1.3% of full flow. All primary fluid temperatures indicated subcooling except the pressurizer and the reactor vessel upper head (RVTCO, appended Plot 111).

6.7.3 Results

OTIS Test 220756 was conducted as planned. The measurements appeared consistent and sufficient for test analysis. The test exhibited intermittent flow, refill, and natural circulation cooldown phenomena similar to the prior OTIS tests. The test was initialized and begun in a manner similar to that of the Nominal Test. Its results were analogous until 21 minutes following leak opening, at which time the leak was isolated. The primary system quickly refilled (34 minutes post-leak), and a natural circulation cooldown was established.

6.8 Comparison.

The performance of the single-variable tests (test initialization, initiation, conduct, and measurements) is addressed in section 6.8.1. Section 6.8.2 compares the test transients including timing, the effects of varied boundary conditions, and long-term trends. Results are summarized in section 6.8.3.

6.8.1 Performance

Initialization

The initialization of the six single-variable tests was largely as specified. Each of the specified initial values was met except pressurizer level and pressurizer metal temperature, neither of which are perceived to have significantly affected the test transients. The actual initial conditions have been compared with those specified in the separate description of each single-variable test, in sections 6.2 through 6.7.

The more significant initial conditions of the single-variable tests are presented for inter-test comparison in Table 6.28. Also shown are the initial conditions for the Nominal Test 220100. This tabulation confirms the consistency of the initial conditions among the tests. The initial conditions of each of the single-variable tests is well-approximated by the following single set:

PRIMARY

Core power, %	4.17	(1% = 21.4 kW)
Pressure, psia	2200	
T_{hot}, F	609	
T_{cold}, F	571	
Flow rate, %	5.5	(1% = 0.259 lbm/s)
PZR level, ft	19	

SECONDARY

Pressure, psia	1200	
Level, ft	5.8	
Feed and steam flow rates, %	2.25	(1% = 0.0265 lbm/s)
(Saturation temperature at 1200 psia, F	567)	
Max. steam temperature, F	585	
AFW temperature, F	115	

These conditions are readily evaluated for consistency.*

The losses to ambient are estimated to be 0.275% of full power from the SG secondary and 0.38% from the primary. The total SG secondary heat removal rate is then the steaming rate plus its losses to ambient, i.e., q_{SG} = 3.30 + 0.28 = 3.58%, and the primary loop heat transfer rate is $q_{primary}$ = 3.68 + 0.38 = 4.06%. (Most of the primary heat losses occur outside the T_{hot}-to-T_{cold} region, i.e., in the CL beyond the T_{cold} fluid temperature measurement, in the DC, and in the RV.)

The total heat rate out of the SG secondary, 3.58% of scaled full power, is comparable to the energy transferred from the primary to the SG, 3.68%. And the total energy transferred from the primary loop, 4.06%, is comparable to the core power, 4.17%. The apparent discrepancies are 0.1% across the SG

---

*The primary loop heat transfer rate is $q = \dot{m}\Delta h$

where

$$\Delta h = h(2200 \text{ psia}, 609F) - h(2200, 571F)$$
$$= 626.6 - 574.2 = 52.4 \text{ B/lbm}$$

$$\text{thus, } q = \dot{m}\Delta h$$
$$= 5.5\% \times \left[\frac{0.259 \frac{\text{lbm}}{\text{s}}}{\%}\right] \left[52.4 \frac{\text{B}}{\text{lbm}} \times \frac{3600}{3412} \frac{\text{kWs}}{\text{B}} \times \frac{\%}{21.4 \text{ KW}}\right]$$
$$= 3.68\%;$$

on the secondary side, h(1200 psia, 585F) = 1207.2, h(1200, 115F) = 86.1, Δh = 1121.1 B/lbm,

$$\text{thus, } q = \left[2.25\% \times \frac{0.0265 \frac{\text{lbm}}{\text{s}}}{\%}\right] \left[1121.1 \frac{\text{B}}{\text{lbm}} \frac{3600}{3412} \frac{\text{KWS}}{\text{B}} \times \frac{\%}{21.4 \text{ KW}}\right] = 3.30\%$$

and another 0.1% across the core. This total disagreement of 0.2% of scaled full power is 5% of the initial power level. It becomes more significant as core power is reduced to simulate decay; at 1% power, this total power discrepancy becomes 20% of the current power level. The (code-calculated) primary energy balances confirm this difference, cf. appended Plots 19 and 20 during steady-state initialization. The "net" calculated primary system (fluid) energy charge is +0.2% of full power (Plot 19), but the indicated primary system fluid total energy is virtually constant (Plot 20). Based on the constancy of the indicated total energy, the calculated energy discrepancy is fictitious and all the core energy deposition is being transferred from the system. Based on the similar discrepancy in both the primary system and SG secondary energy balances (approximately 0.1% each), a likely source of error is the estimated losses to ambient. (To achieve overall consistency, they should be approximately 0.38% of full power from the SG secondary, and 0.47% of full power from the primary loop.) Flow metering inaccuracy, especially in the SG secondary, is another likely source of energy balance differences.

Initiation

The initiating operator actions were to be similar among the single-variable tests, cf. section 3. Following leak initiation, the second set of operator actions (activate HPI, increase the AFW flow rate, and begin the core power ramp) were to occur as the pressurizer emptied. This timing was specified to obtain plant-similar conditions as the loop fluid approached saturation.

Actual initiation event timing is presented in Table 6.29. Initiation proceeded exactly as planned for each of the single-variable tests, i.e., the boundary systems were active as the loop approached saturation. The entries of Table 6.29 reflect observed boundary system effects resulting from their activation, rather than times of control manipulation. Thus, the low-head HPI of Test 220604 was not observed (no fluid was injected) until 13.4 minutes after leak initiation, although the system was activated with the others at approximately 3 minutes after leak initiation. This simply reflects the delay until primary system pressure fell below the shutoff head of the simulated low-head HPI pumps, and is as planned.

The entries of Table 6.29 are keyed to leak initiation times, rather than data acquisition system (DAS) activation times, as are the entries in the subsequent tables. The first line of Table 6.29 and the last lines of Table 6.28 list the time lag in minutes between DAS activation and leak initiation. Plots have been keyed to the time of leak actuation. Leak time frequently defines time zero for computer code predictions of transients and is more amenable to inter-test comparison.

Conduct

The major boundary system characteristics were automated for the single-variable tests to facilitate transient analysis and inter-test comparison. Automated systems included HPI head-flow, RVVV actuation, core power decay ramp, SG secondary level control, and SG secondary depressurization. The operator was to transfer SG secondary AFW control from the refill mode to the constant-level mode when the SG secondary level reached its specified control level; the SG secondary depressurization to obtain a 50F/h cooldown was also to be initiated. Few other operator actions were specified. The HL high point vent was to be opened after five hours of testing if refill was not imminent. The operator was also to throttle HPI to maintain a pressurizer level during pressurizer refill late in the transient. PORV actuation and the reduction of the core power to the sustaining level were specified for the longest tests. The specifics of the operator actions and their criteria have been given herein as part of the test specifications in section 3. Several of the boundary system controls and operator actions that varied from test to test are addressed in the following paragraphs.

The following test control actions were performed as planned:

- Opened the specified leak, nominally the (scaled) 10-cm^2 cold leg suction leak.

As the pressurizer collapsed liquid level dropped below approximately 2 ft in the pressurizer ($\sim$8 ft relative to the common elevation datum which is the SGLTSUF, the upper or secondary face of the SG lower tubesheet):

- Actuated HPI.
- Initiated the core power ramp.
- Began the SG secondary level increase.
- De-energized the pressurizer main heaters.

- As the SG secondary level attained the specified control level, nominally 38 ft, initiated the secondary depressurization ramp (to obtain 50F/h from 1000 psia).
- Opened the HL high-point vent approximately five hours after leak initiation.
- Extended testing beyond refill, observed 2-1/2 hours of continuous cooldown in the Nominal Test and approximately one hour in the single-variable tests.

The rate of SG secondary level increase (following test initiation) approximated 3 ft/min as planned. The subsequent SG secondary depressurization rate obtained 50F/h secondary cooldown as planned. Core power was decreased to approximate the specified decay characteristics (given in section 2 herein).

Auxiliary Feedwater (AFW)

AFW control was to maintain a specified level, nominally 38 ft, in the SG secondary after secondary refill. Several times during these tests, the operator took manual control of the AFW control valves to increase its response speed and to keep it closed. This action usually occurred at the end of a period of relatively high feed demand (such as after primary-to-secondary heat transfer coupling), at which time the operator manually closed the valve as the SG secondary level exceeded the 38-foot setpoint. Because the valve was kept closed until ensuing secondary steaming had reduced the secondary liquid inventory back to the control level, the effect of this type of AFW operation was to weaken certain primary-to-secondary heat transfer coupling events.

When manual AFW control affected loop performance, such AFW control changes should be included in a code prediction model; these instances have been highlighted in the "Observations" sections herein. The effects of imprecise AFW control were particularly apparent in Test 220402 which used a 10-foot SG secondary level (rather than the nominal 38 ft). In this test, the AFW BCM was not initiated until 67 minutes after leak initiation, although the primary level had descended to the elevation of the SG at 29 minutes. This delay was caused by an initial overfill of the SG secondary and subsequent manual control of AFW.

The general behavior of primary pressure during primary refill was qualitatively similar among the single-variable tests. On this basis, the impact of these feed control adjustments on overall loop performance was apparently minor, even though specific events were affected.

Reactor Vessel Vent Valve (RVVV)

The RVVV (internals vent valve simulation) was controlled automatically to open at reactor vessel upper plenum-to-downcomer differential pressures greater than 0.25 psi, and to reclose at differential pressures less than 0.125 psi. The RVVV was initially closed during natural circulation. After loop flow interrupted early in the transient, the RVVV pressure difference increased and the valve customarily opened. As the test progresssed and the RVVV differential pressure (DP) became increasingly imbalanced, the RVVV opened and its discharge heated the upper downcomer fluid. Continued core steam production and HPI condensation of vapor in the cold leg discharge piping and in the upper downcomer created a continuing positive RVVV DP. But the long term steam production and condensation rates were far too low to maintain the RVVV fully open. The model RVVV stayed fully open until the DP was reduced to 0.125 psi, then it was driven fully closed. With the RVVV fully closed, the continuing steam production regenerated a DP sufficient to reopen the RVVV. This cyclic RVVV operation persisted during the several hours of core steam production. The valve position was commonly observed to alternate between closed and only slightly open. (The plant valve would have remained slightly open, its increased hydraulic resistance at the partially-open position would have compensated for the relatively small steam flow rate and balanced the actuating DP; but the model RVVV did not accommodate partially-open operation.)

The model RVVV would not tolerate prolonged operation with rapid cycling. Therefore, the operator transferred the RVVV control to manual-open after a period of rapid valve cycling. The RVVV DP no longer varied between 0.25 and 0.125 psi; the downcomer level adjusted downward and the reactor level adjusted upward, both by less than six inches, reflecting the near-zero RVVV DP with the ongoing steam flow.

As refill occurred, the operator was to transfer RVVV control back to automatic actuation on DP. Any delay in transferring RVVV control only retarded outer-loop natural circulation by maintaining the inner-loop flowpath

(core-RVVV-downcomer) and may have retarded spillovers and refill. Such a delay may readily be simulated in a system code.

In summary, the model RVVV was opened manually to preserve the valve while simulating the partially open plant RVVV. The impact of this RVVV control change is addressed further in section 10 herein.

Guard Heating

OTIS used guard heaters over the HL, upper reactor vessel, and pressurizer (including the surgeline) to obtain approximately adiabatic fluid containment boundary conditions. As described in section 2 herein, guard heater power was controlled using pipe wall-to-insulation temperature differences. These temperature differences were biased from zero to counteract heat losses from regions of increased heat loss, such as flanges and instrument penetrations. This bias was set at a specific primary fluid condition. As primary conditions changed from the setpoint, the guard heating became correspondingly non-adiabatic. Test 220100 was not particularly responsive in this regard, but some reheating of the upper reactor vessel metal can be seen (cf. Plot 114 of the appended plots at approximately 100 minutes). Guard heater impact was more pronounced in tests that experienced a relatively long period of low primary pressure such as Test 220201 (larger break), during which time the primary fluid temperatures remained below the temperature at which the guard heater bias had been set. These observations led to supplementary Tests 2202AA and -BB which pursue pressurizer and guard heater effects. These guard heater tests are described in section 10 herein.

High-Pressure Injection

After loop refill, the operator was to manually throttle (i.e., reduce) high-pressure injection (HPI) to maintain a mid-height pressurizer level. In several tests, the operator took manual control of HPI, increased its output, and exceeded the HPI head-flow characteristics being simulated (to raise the pressurizer level to mid-height). Such was the case in Test 220100. This post-refill operation had no impact on the preceding test events.

Two redundant HPI flowmeters were used. The comparison of these two flow measurements sometimes indicated differences attributable to malfunctioning of the meter which was being used to signal HPI output to the HPI head-flow simulation controller. The resulting deviation of the HPI flow rate from the desired flow rate-at-pressure was generally on the order of 5% of the specified output; this affected Tests 220201, 220402, 220503, and 220604, after which the subject turbine meter was replaced. The redundant (downstream) HPI turbine meter was apparently measuring accurately. Its output has been used in the pertinent plots (e.g., appended Plots 17 and 181). HPI head-flow differences from those specified were especially apparent in Test 220402.

The OTIS HPI simulation used a positive-displacement pump with a controlled bypass valve. As primary pressure varied during a transient, the operator had to adjust pump speed periodically to maintain the pump output within the range of the bypass flow circuit. In Test 220304 (half HPI capacity) the operator inadvertently delayed this pump speed adjustment. The obtained HPI flow rate was as much as 25% greater than specified; the period of excess flow continued for nearly two hours. This HPI anomaly caused an early start of system refill. These events are described in detail in section 6.3 herein.

Measurements

The required OTIS instruments are listed in the test specifications, section 3 herein. Each of the specified instruments was generally available. As indicated in the previous section, the flow-controlling HPI turbine meter was sometimes inaccurate (and was replaced), but a redundant measurement was available and has been used to provide the actual HPI flow rate.

Several conductivity probes (CPs) are listed as being unavailable. This situation reflects the decision to record analog signals from individual CPs, rather than an autioneered signal obtained by combining several CPs. The individual signals supply much more information than the combined signal. However, there were insufficient data acquisition system channels to individually record every CP, hence the deletion of selected CP signals.

The off-nozzle thermocouple (TC) string began to leak steam early in the OTIS testing program. In light of the available options, and with review by the project participants, it was decided to sever and seal the leaking string. This deletion of the nine primary-fluid string TCs lowered the number of available SG primary fluid temperature indications below the specified minimum number which was 22. Only sparse indication of the off-nozzle SG primary fluid temperatures remained.

Primary Boundary Flow Rates

The OTIS primary boundary discharges were metered using accumulating flowmeters. These flowmeters gave detailed traces of discharged mass versus time, but they sometimes registered spurious signals. Such occurrences were apparent in the comparison of primary system fluid mass obtained by independent measurements. This comparison is given in (appended) Plot 18. The indicated value was obtained using component fluid mass summed over the primary. Component mass was obtained from component liquid level, fluid volume versus elevation, and local fluid specific volume. The calculated value was obtained by integrating the net primary boundary mass flow rate ("Net" Plot 17). Net flow rate is the (signed) difference between HPI and aggregate primary discharges.

Backup information was available to supplement the accumulating flowmeter information. Discharge weigh-tank readings were periodically recorded by the operator. This weigh-tank data was used to calculate an offset between accumulated mass and weigh-tank mass at each time of weigh-tank observation. These offsets were then linearly interpolated to the intermediate times of data acquisition and used to modify each accumulated mass entry. This technique retained the flow rate detail of the accumulating flowmeters while obtaining the total mass closure available using the weigh tanks.

The weigh-tank data was applied for all the tests. This application has been signaled by the message "NOTE - WEIGH-TANK DATA HAS BEEN USED" printed on (appended) Plots 17 and 18. The calculated versus indicated mass comparison of Plot 18 generally improves with the application of weight-tank data.

6.8.2 Observations

The single-variable test transients are described and compared in the paragraphs following. These discussions draw on the detailed test transient descriptions of sections 6.2 through 6.7. The single-variable tests are referenced to the Nominal Test which has been discussed in Section 5 herein.

The boundary conditions of the single-variable tests have been outlined in the test matrix, section 3, and are summarized in Table 6.1. The timing and major conditions of these tests are listed in Table 6.28, 6.29, 6.30, and 6.31. Four figures are used to summarize these events: Figures 6.48, 6.49, 6.50, and 6.51. This comparison of the single-variable tests is facilitated by using abbreviated test numbers, e.g. "Test 1" for Test 220100 Nominal, "Test 2" for Test 220201 leak size, and so on. These abbreviated test numbers are also listed in Table 6.1.

Early Events

The early transient events included depressurization, saturation, and intermittent primary flow. The HLUB fluid saturated from 2.3 to 3.2 minutes after leak initiation, cf. Table 6.29. There is little discernable correlation of the time to saturate to the imposed (single-variable) boundary conditions except that the larger-break test (15 versus 10 cm^2, Test 2) and the low-head HPI test (Test 6) saturated slightly earlier than the rest. The saturation pressure closely corresponded to the initial hot leg metal and fluid temperature and thus was similar among each of the tests.

Note the occurrence of saturation in Test 7. This test replicated the Nominal Test until leak isolation, and the HLUB saturated at 3.0 minutes after leak actuation rather than 3.2 minutes in the Nominal Test. This 12-second difference gives an indication of the reproducibility of these early events.

The core exit fluid saturated soon after the HLUB fluid saturated, from 3.6 to 6.5 minutes after leak initiation. Again, the larger break occurrence preceded the rest, and the dependence of event timing on the imposed test

boundary condition variations became more apparent. The reactor vessel upper head fluid saturated at roughly the same time as the primary flow first interrupted, from about 5 to 10 minutes after leak initiation. Transient timing has now become clearly dependent on the inter-test boundary condition variations, cf. Figure 6.48. Tests 4, 5, and 7 are tracking approximately with the Nominal Test. On the other hand Tests 2, 3, and 6 are proceeding together and more rapidly than the Nominal Test. The faster tests first interrupt flow at 3.5 to 6 minutes after leak initiation, versus about 8 minutes in the Nominal Test transient. Based on leak size only, the initial events such as pressurizer draining would be expected to occur 15/10 or 1.5 times faster with a 15- versus 10-cm^2 leak size. If the difference in initial pressurizer levels (listed in Table 6.28) is taken into account, the ratio of expected drain times becomes roughly two. This is close agreeement with the observed ratio of times.

The time to flow interruption for Test 5 may be somewhat misleading; primary flow decreased precipitously from $\sim$4 minutes after leak initiation, approaching but not reaching zero flow at $\sim$6 minutes, then it increased briefly before a complete interruption. This earlier near-interruption in Test 5 apparently corresponded to the complete flow interruption in the Nominal Test. Test 5 had a CLD rather than a CLS leak location. The tendancy to retain circulation in Test 5 may be related to its leak location. With the leak just downstream of the point at which HPI is introduced, and with forward loop flow, HPI cooling is reduced as evidenced by the lower leak fluid temperatures early in Test 5. HPI thus cools and condenses less RVVV-discharged fluid, vapor flow up the HL is increased, and therefore (two-phase) circulation is prolonged in Test 5. Internals vent valve (RVVV) actuation occurred 3 to 4 minutes after leak actuation in all the single-variable tests. This followed HLUB saturation by approximately 1 minute, and may be a more reliable indication of primary flow interruptions.

Two types of spillovers were generally observed early in the transients. The initial HLUB spillover was closely tied to the occurrence of reactor vessel upper head saturation, cf. Table 6.29. As the upper head voided, the displaced liquid caused the HL inventory to increase, promoting spillover. Should the declining reactor vessel level reach the elevation of the HL nozzle, the attendant increase in vapor flow up the HL provided a second mechanism for spillover. This (spillover) transport of liquid

over the HL U-bend recoupled the primary and secondary systems, caused heat transfer, and depressurized the primary system. This spillover coupling was brief. Several of these spillover events often preceded the final interruption of primary flow.

Figures 6.48 and 6.49 show transient timing for each of the single-variable tests, versus that of the Nominal Test. The abcissa is event timing in the Nominal Test (on a log scale). The ordinate is the ratio of event timing in a single-variable test to event timing in the Nominal Test. For example, the pressurizer drained at 2.5 minutes (after leak opening) in the Nominal Test, obtaining an abscissa entry; in Test 3 the pressurizer drained at 2.3 minutes, or just slightly faster than in the Nominal Test; this obtained the "3" point at 0.92. An ordinate of 1.0 indicates simultaneous event occurrence. For this event, Test 2 had the earliest occurrence, 1.2 minutes, or 1.2/2.5 = 0.48 times the Nominal Test timing.

Scanning the event timing trends of Figure 6.48, most of the off-nominal test events occurred at or before those in the Nominal Test (i.e., ratios $\lesssim 1$). The exception is Test 4 (10-foot SG level). Events after 5 minutes (saturation of the core-exit fluid and intermittent flow) were $\sim$10% slower than nominal, and the initiation of BCM was much delayed. This is attributable to the delay of AFW injection in this test, as has been described in section 6.4.

Two test sequences paralleled those of the Nominal Test. These are tests 5 (Cold Leg Discharge Leak) and 7 (Isolated Leak). The boundary conditions of Test 7 replicated those of the Nominal Test up to the time of leak isolation during interrupted flow; thus, its correspondence to the Nominal Test is expected. Test 5 used a CL discharge rather than a CL suction leak site. The point of HPI introduction and the leak site were immediately adjacent in this test, rather than being separated by the CL (pump site) spillover as in the remaining tests. This change in leak location was expected to affect the leak fluid temperature and, hence, the magnitude of HPI-leak cooling and the transient in general. As discussed in the description of Test 220503, the leak fluid temperature early in the transient did decrease more than was usually observed. But the relatively close correspondence between the Test 5 timing and that of the Nominal Test underlines the observation that the general leak temperature trends were similar between the two tests.

Test 3 (one-half of nominal HPI capacity) paralleled the Nominal Test through the actuation of the reactor vessel vent valve (RVVV), but then proceeded at a rate that became increasingly faster than nominal. The initial events -- pressurizer draining, saturation of the loop fluid, and RVVV actuation (as outer loop flow diminished) -- were apparently insensitive to the magnitude of the HPI flow rate. But the reduced HPI capacity of Test 5 obtained earlier saturation of the core exit fluid, indicating the impact of reduced HPI condensation capacity. Intermittent flow events occurred earlier in response to the faster depletion of system inventory with reduced HPI flow rate. The primary level descended to the elevation of the SG earlier and a primary condensing surface developed while the SG secondary refill was still in progress; hence, an "AFW BCM" developed (condensation of primary vapor at the AFW injection elevation with the primary liquid-vapor interface well above that of the SG secondary).

Tests 2 (15-cm^2 Leak) and 6 (Low-Head HPI) both proceeded more rapidly than nominal, also as shown in Figure 6.48. Their timing is sometimes coincident, indicating that the impact of a 50% increase in leak size (Test 2) was approximately the same as that of the altered HPI head-flow characteristics (Test 6), even though their integrated boundary system flow rates were quite different (cf. appended Plot 18). This observation is examined further in Figure 6.40.

Figure 6.40 presents system pressure versus transient time (after leak opening) for three tests: 220100, Nominal; 220201, 15-cm^2 Break Size; and 220604, Low-Head HPI. Each of the transients included pressurizer draining, depressurization to loop saturation, intermittent flow, and BCM. But the Nominal Test (the solid trace of Figure 6.40) repressurized to ∿1670 psia during reduced loop flow and then abruptly depressurized when the reactor level approached the elevation of the HL nozzle (point "Z" at 16-1/2 min). The other two transients were relatively insensitive to this nozzle uncovery event. The increased leak size of Test 2 (dotted trace) suppressed repressurization. The low-head HPI Test 6 (dashed trace) repressurized through the time of nozzle uncovery with a relatively small perturbation in pressure. Note that the HPI shutoff pressure in this test was 1630 psia, therefore, HPI was not observed until beyond 13 minutes, i.e., until after primary pressure had been reduced. The mechanism of pressure reduction is

clear from Figure 6.40. The accelerated rate of primary inventory loss (no HPI) drew the primary level down into the SG before 13 minutes (point "S"), while AFW refill of the SG secondary was still in progress (lowest curve). The resulting AFW BCM stopped the primary repressurization at 1740 psia and caused a dramatic depressurization. The larger-leak test (Test 2) attained a primary level within the SG slightly after Test 6, just as the SG secondary refill was being completed, therefore the AFW BCM depressurization was much less pronounced. "Pool BCM" (condensation with the steam generator primary level below the secondary level) ensued in the larger-break test at 25 minutes, and the primary depressurization continued down toward the SG secondary pressure. The primary level finally reached the SG elevation at ∿30 minutes in the Nominal Test, long after the SG secondary had been refilled. A non-sustaining AFW BCM obtained a gradual depressurization after 38 minutes.

The trends of these three tests merit review. The nominal conditions (10-cm^2 leak, high-head HPI) repressurized 150 psia until the uncovery of the HL nozzle allowed the venting of the core-generated steam which was in excess of the HPI-leak condensing capacity. An increased leak size suppressed the repressurizations accompanying interrupted flow. But the earliest depressurization occurred with no HPI (system pressure greater than shutoff pressure) because the enhanced rate of inventory depletion obtained a steam generator condensing surface while the SG secondary was still being refilled. The timing of the creation of a condensing surface versus that of the termination of AFW injection (after SG secondary refill) determined the transient pressure response.

General Pressure Trends

General pressure trends are illustrated in Figure 6.51. The ordinate is primary pressure, the abscissa is event timing in the Nominal Test 220100. The disparate response of Test 7 (Isolated Leak) is most apparent. This test replicated the Nominal Test until the leak was closed simulating leak isolation, at 21 minutes after leak initiation. In Test 7, the system quickly began to refill and repressurize, and completed HLUB refill in ∿1/2 hour.

The early pressures were similar among all the single-variable tests, cf. Figure 6.51. System pressures began to diverge during the repressurization accompanying flow interruptions, then diverged markedly as the primary level descended to the SG elevation. As previously discussed, the timing of this occurrence versus the completion of the AFW refill of the SG secondary had a pronounced impact on the subsequent pressure trends. The larger-leak Test 2 depressurized at 54 psi/min during pool BCM, following a rather weak AFW BCM. Test 3 (One-Half Capacity HPI) depressurized briefly at 250 psi/min during AFW BCM, then continued to depressurize in pool BCM. Tests 2 and 3 thus approached the SG secondary pressures during the BCM.

Test 6 (low-head HPI) depressurized relatively early, at 220 psi/min through the AFW BCM as previously discussed. But the primary depressurization had a greater-than-nominal effect on HPI flow rate because of the revised head-flow characteristics of this test. Therefore, in Test 6, refill started, and the BCM was terminated, at system pressures somewhat higher than nominal.

The pressure trends of Test 5 (CL discharge leak) paralleled those of the nominal test, but Test 4 (10-foot SG level) depressurized more than nominal during the BCM. The primary and secondary SG levels did not cross with the lowered SG secondary level, but the sustained AFW BCM (although delayed) depressurized the primary at 43 psi/min through the start of primary refill and the termination of the BCM.

Each of the tests repressurized during refill. This is attributable to the loss of heat transfer from the SG with refill, to the decreasing voided volume with which to suppress repressurization, and to the hotter metal at the higher system elevations. This last effect is addressed in detail in section 10.

Later Events

Figure 6.49 focuses on the later transient events. As in Figure 6.48, the ratio of event timing in the single-variable tests to the Nominal Test timing is plotted against the Nominal Test timing, i.e., ratios greater than unity indicate transients slower than nominal, and vice versa.

The onset of the BCM occurred earlier in tests with larger breaks or reduced HPI capacity, i.e., Test 2 (15 cm^2), 3 (One-Half Capacity HPI), and 6 (Low-Head HPI). Tests 2 and 3 took longer to begin refilling, and progressed more slowly through most of the subsequent events. Test 6 (Low-Head HPI) remained faster than nominal, however; system pressure remained well below 1325 psia, the pressure at and below which the capacity of the low-head HPI system exceeded that of the nominal HPI (cf. section 6.6 for a comparison of HPI characteristics). Test 4 (10-foot SG level) had its BCM delayed due to a malfunction of the AFW control system, but the AFW BCM quickly depressurized the system and brought the subsequent event timing back toward that of the Nominal Test.

The event timing trends of Figure 6.49 are noteworthy in that they became similar late in the test transients, even though the timing of the earlier events such as BCM and the start of refill differed by more than twofold. In several tests, spillover events occurred and refill appeared imminent before opening the HL high point vent (HLHPV). The HLHPV was opened at five hours in each test, however, to bring the tests to a timely conclusion. Refill (of the HL U-bend region) was not completed in any test, except the test with leak isolation, until after the HL vent had been opened. This would appear to indicate that the (OTIS) HL high point vent must be opened to complete refill. Also, the method of reactor vessel vent valve (RVVV) control may have had an impact. As discussed further in section 10, transfer of the RVVV control from manual-open to automatic may have allowed the valve to close periodically during refill spillovers; this would have enhanced the primary loop flow rate and primary-to-secondary heat transfer thereby obtaining HL U-bend refill. In each of the single-variable tests (except the isolated leak test) the RVVV was returned to automatic control only at or near the time of HL U-bend refill.

6.8.3 Summary

The single-variable tests were initialized at similar system conditions, each nearly identical to those of the Nominal Test. Differences between the actual initial conditions and those specified appear inconsequential. Steady-state energy balance at the initial conditions are consistent to within 0.2% of scaled full power, or 5% of the initial power level.

Test initiation was as planned in each of the single-variable tests. The simulated boundary systems were active before the loop fluid saturated. The earliest test sequence events, pressurizer draining and saturation of the loop fluid, occurred at virtually identical conditions in each of the tests.

Test conduct proceeded largely as planned, but several control system abnormalities adversely influenced test execution. These included AFW and SG level control, RVVV control (manual-open versus automatic), guard heating (cf. section 10) and HPI characteristics. The impact of these items has been previously addressed.

Measurement of the loop conditions paralleled the specified critical instruments. Exceptions included an SG thermocouple string and the metering of the primary discharge mass flow rates. This latter measuring difficulty prompted the introduction of redundant effluent measurements (weigh-tank data) to obtain mass closure. The aggregate measurements were generally sufficient to permit the examination of system interactions and to determine the causes underlying these interactions.

Observations from the single-variable tests have been given in section 6.8.2. Most of these tests experienced the major post-SBLOCA events: pressurizer draining, depressurization to loop saturation, repressurizations with intermittent circulation, depressurization through the BCM, refill and post-refill circulation, cooldown, and depressurization. The variations of the boundary conditions among these tests caused significant differences of the timing, magnitude, and even the occurrence of certain events. Of particular interest to the code benchmarking effect, the timing, type (AFW or Pool), and strength of the boiler-condenser mode (BCM) varied widely among the tests.

Table 6.1 Single-Variable Tests

Test number	Abbrev. test number	Section herein	Date performed	Chronological order	Variable	Value	Nominal Value (Test 220100)
220201	2	6.2	3/22/84	5	Leak size, scaled cm^2	15	10
220304	3	6.3	4/7	7	HPI capacity	1/2	full
220402	4	6.4	3/21	4	SG level, ft	10	38
220503	5	6.5	3/20	3	Leak location, cold leg-	Discharge	Suction
220604	6	6.6	3/19	2	HPI characteristics, shutoff head[a]	Low	High
220756	7	6.7	3/27	6	Leak isolation	Yes	No
(220100	1	5	3/15	1	Nominal)	---	---

[a]HPI head-flow characteristics, as well as the characteristic of the other boundary systems, are given in section 2 herein.

Table 6.2 Initial Conditions (Test 220201, 15 cm^2 Leak)

	Specified	Actual
o Core power (includes 0.5% for ambient losses), %	4.2±0.1	4.17
o Natural circulation	Yes	Yes
o Primary pressure, psia.	2200±50	2209
o Pressurizer liquid height, ft.	16.1 ± 2	17.0
o Pressurizer main and guard heaters adjusted for an approximately adiabatic pressure.	Yes	Yes
o RV and HL vents closed.	Yes	Yes
o RVVV in automatic (differential-pressure) control with open/close setpoints of 0.25 and 0.125 psid.	Yes	Yes
o AFW at 100F injected at the upper elevation using the minimum-wetting nozzle.	Yes	Yes
o SG secondary (collapsed) liquid level (constant level control), ft.	5 ± 1	5.6
o Hot leg fluid temperature, F.	610 ± 2	609
o HPI and leak systems are not yet in use.	Yes	Yes
Initialization is continued until a suitable system steady state is obtained:		
o Pressurizer metal temperatures, F.	650 ± 10	655-697
o The RVVV is not cycling.	Yes	Yes
o The SG fluid temperatures are varying than 20F/h (exception: cyclic secondary fluid temperature variations associated with high AFW injection, and with internal circulation within the secondary liquid pool, are acceptable).	Yes	Yes
Other initial conditions:	T_{cold} =571F, primary flow rate = 5.5%, SG pressure = 1202 psia, feed and steam flow rates = 2.3%, AFW temp = 113F	

Table 6.3 Selected Operator Actions (Test 220201, 15-cm^2 Leak Size)

Time	Time, min	Action
(March 22, 1984)		
0808	-12.8	Activated data acquisition system (DAS).
0821	(0)	Opened 15-cm^2 CL suction leak.
0822	1.6	HPI, AFW, core power actuated.
0832	13	SG secondary depressurization ramp activated.
Several	---	Transferred AFW control from automatic to manual-open.
1322	302	Opened HL high point vent.
1602	461	RVVV control changed from manual-open to automatic.
1606	465	HPI throttled to achieve 23 feet in the pressurizer.
1652	$\sim$ 515	Test completed, DAS de-energized.

Table 6.4 Unavailable Measurements (Test 220201, 15-cm^2 Leak).

SUMMARY OF VARIABLES DISCARDED ON INPUT, TEST 220201

NO.	VTAB	SYSTEM	INST.	ELEVATION	DESCRIPTION
1	155HLTC06	2HL	2FTC	50.00	HOT LEG FLUID TEMP (F)
2	262HLCP05	2HL	16 CP	41.00	HOT LEG CONDCTVTY (WET/DRY)
3	263HLCP06	2HL	16 CP	45.00	HOT LEG CONDCTVTY (WET/DRY)
4	264HLCP07	2HL	16 CP	49.00	HOT LEG CONDCTVTY (WET/DRY)
5	265HLCP08	2HL	16 CP	53.00	HOT LEG CONDCTVTY (WET/DRY)
6	266HLCP09	2HL	16 CP	57.00	HOT LEG CONDCTVTY (WET/DRY)
7	274HLCP17	2HL	23RCP	.50	HOT LEG REF. C.P.
8	273HLCP16	3SGP	16 CP	53.10	SG PRIMRY. CONDCTVTY (WET/DRY)
9	272HLCP15	3SGP	16 CP	56.90	SG PRIMRY. CONDCTVTY (WET/DRY)
10	223HPTM02	10HP1	13TMF	-999.00	HP INJECT. TURB.FLOW (LBM/SEC)
11	218HPAC01	10HPJ	19ACC	-999.00	HP INJECT. ACCD.FLOW (LBM)
12	221V2ACC2	12V2	19ACC	-999.00	2-PH VENT. ACCD.FLOW (LBM)
13	53SSTC13	22SGS	2FTC	32.30	SG SECOND.FLUID TEMP (F)
14	79SMTC02	22SGS	25MTC	26.30	SG SECOND. METAL TC (F)
15	76SMTC06	22SGS	25MTC	44.20	SG SECOND. METAL TC (F)
16	344V1TCC3	34CLD	2FTC	-999.00	CLD LEAK FLUID TEMP (F)

Table 6.5 Key Events (Test 220201, 15-cm^2 Leak Size)

Event	Time, Min
Leak opened.	0
HPI, AFW, core power controls initiated.	1.5
Pressurizer emptied.	1.2
HLUB saturated.	2.3
Primary flow interruption.	3.5
HLUB spillover.	6.1
SG secondary level approached control setpoint terminating AFW, SG secondary ramp depressurization initiated.	13
SG primary level reached SG secondary pool.	24
Leak and HPI flow equilibruim-refill began.	104
SG primary levels exceeded SG secondary level -- BCM ended.	200
HLHPV opened.	302
First refill spillover.	342
Loop refilled.	459
Test terminated.	∿515

Table 6.6 Initial Conditions (Test 220304, Half-Capacity HPI)

	Planned	Actual
o Core power (% of full power, 1% full power = 24.1 kW), includes 0.5% to replace losses to ambient, %.	4.2 ± 0	4.17
o Natural circulation.	X	X
o Primary pressure, psia.	2200 ± 50	2200
o Pressurizer liquid height, ft from SGLTSUF.	16.6 ± 2	19.6
o Presurizer main and guard heaters adjusted for an approximately adiabatic pressurizer.	X	X
o RV and HL vents closed.	X	X
o RVVV in automatic (differential-pressure) control with open/close setpoints of 0.24 and 0.125 psi.	X	X
o AFW at 100F injected at the upper elevation using the minimum-wetting nozzle.	X	X
o SG secondary (collapsed) liquid level (with constant level control), ft.	5 ± 1	5.8
o HL fluid temperature, F.	610 ± 2	608-610
o HPI and leak systems are not yet in use. Primary noncondensible gas additions are not to be tested.	X	X

Table 6.6 Initial Conditions (Cont'd)

	Planned	Actual
o Pressurizer metal temperatures, F.	650 ± 10	649-654
o The RVVV is not cycling.	X	X
o The SG fluid temperatures are varying less than 10F/h (exception: cyclic secondary fluid temperature variations associated with high AFW injection, and with internal circulation within the secondary liquid pool, are acceptable).	Yes	Yes

Other initial conditions: T_{cold} = 571F, primary flow rate = 5.5% SG pressure = 1200 psia, feed and steam flow rates = 2.2%, AFW temp = 117F.

Table 6.7 Selected Operator Actions Test 220304 (Half-Capacity HPI)

Time	Time, Min	Action
1009, April 7, 1984	-14.0	DAS started
1023	(0)	10-cm^2 CLS leak opened.
1025	2.5	HPI, AFW, and core power controls activated.
1036	13	SG secondary depressurization ramp initiated.
1041	18	AFW control valve (SFCV03) placed in manual control.
1044	21	SFCV03 valve switched to auto.
1152	89	RVVV to manual-open.
1418	235	HPI pump speed reduced from 30 to 10%. HPI flow control valve is fully opened.
1526	304	Opened HLHPV.
1640	377	Closed SFCV03 (AFW) manually, then back to auto.
1732	430	Pressurizer PORV opened.
1836	496	Core power ramped to sustaining power over 30-minute period beginning now.
1840	497	SG secondary steam control set for 100 psia.
1907	524	Core power reached sustaining power level.
2011	587	DAS stopped, test completed.

Table 6.8 HPI/LPI Flow Vs Pressure (Test 220304, Half-Capacity HPI)

	Flow, lbm/s	
Pressure, psia	Specified	Observed
233.0	0.1480	0.1157
234.0	0.1356	0.1041
235.0	0.1233	0.0856
237.1	0.0973	0.0627
239.5	0.0677	0.0610

Table 6.9 Key Events (Test 220304, Half-Capacity HPI)

Event	DAS Time, min.	Time After Leak Opened, min.
Leak Opened.	14.0	0
Pressurizer emptied.	16.3	2.3
HPI, AFW and core power ramp actuated.	16.3-16.5	2.3-2.5
HL Saturation.	17	3.0
HLUB spillover.	21	6.5
HL nozzle uncovered.	25	11
Secondary level approaches control setpoint terminating AFW SG secondary depressurization ramp initiated.	27	13
HL nozzle uncovery and spillover.	31	17
RV and DC partially refill.	31	17
High-elevation AFW BCM began (intermittent with AFW).	31	17.2
Pool BCM began.	101	87
Atypical HPI flow began.	140	126
Leak and HPI flows reached equilibrium -- refill began.	147	130
SG primary level exceeded secondary level -- Pool BCM ended.	192	178
SG primary level exceeded AFW injection elevation -- AFW BCM ended.	$\sim$209	$\sim$195
Atypical HPI flow ended.	249	235
HLHPV opened.	318	304
PORV opened.	444	430
Core power ramped down to sustaining power.	510-538	496-524
LPI flow began as primary pressure dropped below shutoff head.	548	534
Test terminated.	601	587

Table 6.10 Discarded Variables (Test 220304, Half-Capacity HPI)

SUMMARY OF VARIABLES DISCARDED ON INPUT, TEST 220304

NO.	VTAB	SYSTEM	INST.	ELEVATION	DESCRIPTION
1	155HLTC06	2HL	2FTC	50.00	HOT LEG FLUID TEMP (F)
2	262HLCP05	2HL	16 CP	41.00	HOT LEG CONDCTVTY (WET/DRY)
3	263HLCP06	2HL	16 CP	45.00	HOT LEG CONDCTVTY (WET/DRY)
4	264HLCP07	2HL	16 CP	49.00	HOT LEG CONDCTVTY (WET/DRY)
5	265HLCP08	2HL	16 CP	53.00	HOT LEG CONDCTVTY (WET/DRY)
6	266HLCP09	2HL	16 CP	57.00	HOT LEG CONDCTVTY (WET/DRY)
7	274HLCP17	2HL	23RCP	.50	HOT LEG REF. C.P.
8	273HLCP16	3SGP	16 CP	53.10	SG PRIMRY. CONDCTVTY (WET/DRY)
9	272HLCP15	3SGP	16 CP	56.90	SG PRIMRY. CONDCTVTY (WET/DRY)
10	103PRDT03	6PZR	10 DT	42.80	PRESURIZR. INSUL. DT (F)
11	223HPTM02	10HPI	13TMF	-999.00	HP INJECT. TURB.FLOW (LBM/SEC)
12	53SSTC13	22SGS	2FTC	32.30	SG SECOND.FLUID TEMP (F)
13	79SMTC02	22SGS	25MTC	26.30	SG SECOND. METAL TC (F)
14	76SMTC06	22SGS	25MTC	44.20	SG SECOND. METAL TC (F)
15	344V1TC03	34CLD	2FTC	-999.00	CLD LEAK FLUID TEMP (F)

Table 6.11 Initial Conditions (Test 220402, 10-foot SG Level)

	Specified	Actual
Core power (includes sustaining power of 0.51 %), % of full power.	4.21±0.1	4.17
Natural circulation.	Yes	Yes
Primary pressure, psia.	2200 ± 50	2198
Pressurizer liquid height, ft from SGLTSUF.	16.6 ± 2	18.9
Pressurizer main and guard heaters adjusted for an approximately adiabatic pressurizer.	Yes	Yes
RV and HL vents closed.	Yes	Yes
RVVV in automatic (differential-pressure) control with open/close setpoints of 0.25 and 0.125 psid.	Yes	Yes
AFW at 100F injected at the upper elevation using the minimum-wetting nozzle.	Yes	Yes (113F)
SG secondary (collapsed) liquid level, feet, with constant inventory or level control.	5 ± 1	6
Primary HL fluid temperature, F. (Use the model HL fluid temperature indication at 60 feet, HLTC07).	610 ± 2	609
HPI and leak systems are not yet in use.	Yes	Yes
Initialization is continued until a suitable system steady state is obtained:		
Pressurizer metal temperatures, F.	650 ± 10	652 - 692
The RVVV is not cycling.	Yes	Yes

Table 6.11 (Cont'd)

	Specified	Actual
The SG fluid temperatures are varying less than 10F/h (exception: cyclic secondary fluid temperature variation associated with high AFW injection, and with internal circulation within the secondary liquid pool, are acceptable).	Yes	Yes
Other inital conditions: T_{cold} = 571F, primary flow rate = 5.5%, SG pressure - 1204 psia, feed and steam flow rates = 2.2%, AFW temp = 113F.		

Table 6.12 Selected Operation Actions (Test 220402, 10-foot SG Level)

Time	DAS-T, min.	Action
March 21, 1984		
1114	-11.1	Started data acquisition system (DAS).
1125	0	10-cm^2 cold leg suction leak opened.
1127	2	HPI, AFW and core power ramp actuated.
1130	5	SG secondary on band level control.
1131	6	SG secondary depressurization ramp actuated.
1145 and several other times	20 and several other times	Transferred AFW control from automatic to manual and back to automatic. See Table 6.13.
1253	88	RVVV control changed from automatic to manual open.
1630	306	Opened HLHPV.
1828	424	Primary loop refilled.
1832	427	RVVV control changed from manual-open to automatic.
1837	432	HPI flow increased manually to obtained a 23-ft pressurizer level.
1930	484	Test completed.

Table 6.13 Operator Actions Associated With the AFW Control Valve[a] (Test 220402, 10-foot SG Level)

Time	Status of AFW control valve	Time after start of DAS, min.	Time after leak opened, min.
1147	Manually closed then back to automatic operation.	33	22
1202	Manually closed.	48	37
1221	Placed in automatic for 10 ft.	67	56
1302	Manually closed.	108	97
1334	Placed in automatic for 10 ft.	140	129
1355	Manually closed.	161	150
1411	Placed in automatic for 10 ft.	177	166
1425	Manually closed.	191	180
1434	Placed in automatic for 10 ft.	200	189
1449	Manually closed.	215	204
1501	Placed in automatic for 10 ft.	227	216
1530	Manually closed.	256	245
1545	Placed in automatic for 10 ft.	271	260
1609	Manually closed.	295	284
1713	Placed in automatic for 10 ft.	359	348
1755	Manually closed then back to automatic operation.	401	390
1828	Manually opened then back to automatic operation.	434	423
1910	Manually closed then back to automatic operation.	476	465

All times are based on operator log book entries.

[a]Valve Number SFCV03.

Table 6.14 Unavailable Measurements (Test 220402, 10-foot SG Level)

SUMMARY OF VARIABLES DISCARDED ON INPUT, TEST 220402

NO.	VTAB	SYSTEM	INST.	ELEVATION	D E S C R I P T I O N
1	155HLTC06	2HL	2FTC	50.00	HOT LEG FLUID TEMP (F)
2	262HLCPC5	2HL	16 CP	41.00	HOT LEG CONDCTVTY (WET/DRY)
3	263HLCP06	2HL	16 CP	45.00	HOT LEG CONDCTVTY (WET/DRY)
4	264HLCP07	2HL	16 CP	49.00	HOT LEG CONDCTVTY (WET/DRY)
5	265HLCP08	2HL	16 CP	53.00	HOT LEG CONDCTVTY (WET/DRY)
6	266HLCPC9	2HL	16 CP	57.00	HOT LEG CONDCTVTY (WET/DRY)
7	274HLCP17	2HL	23RCP	.50	HOT LEG REF. C.P.
8	273HLCP16	3SGP	16 CP	53.10	SG PRIMRY. CONDCTVTY (WET/DRY)
9	272HLCP15	3SGP	16 CP	56.90	SG PRIMRY. CONDCTVTY (WET/DRY)
10	223HPTM02	10HPI	13TMF	-999.00	HP INJECT. TURB.FLOW (LBM/SEC)
11	218HPACC1	10HPI	19ACC	-999.00	HP INJECT. ACCD.FLOW (LBM)
12	221V2AC02	12V2	19ACC	-999.00	2-PH VENT. ACCD.FLOW (LBM)
13	535STC13	22SGS	2FTC	32.30	SG SECOND.FLUID TEMP (F)
14	795MTCC2	22SGS	25MTC	26.30	SG SECOND. METAL TC (F)
15	765MTC06	22SGS	25MTC	44.20	SG SECOND. METAL TC (F)
16	289SSCP20	22SGS	32KCP	0.00	SG SECOND. UP.WET.CP (REF. FT)
17	344V1TC03	34CLD	2FTC	-999.00	CLD LEAK FLUID TEMP (F)

Table 6.15 Key Events (Test 220402, 10-foot SG Level)

Event	DAS time, min	Time after leak opened, min
Leak opened.	11.1	0
HPI, AFW, and core power ramp actuated.	13	2.1-2.2
Pressurizer empty.	13.3	2.2
HLUB saturation.	14.1	3.0
RVVV opened.	15.1	4.0
SG secondary level reaches band level control setpoint.	16.3	5.2
SG secondary depressurization ramp initiated.	17	6
Primary flow interruption.	∿18	∿7
HLUB spillover.	21.7	10.6
RVVV began cycling.	24.6	13.5
SG secondary on constant level control.	31	20
AFW BCM began.	77.7	66.6
Refill began.	85	74
RVVV control switched from automatic to manual.	99	88
First refill spillover.	311	300
HL HPV opened.	317	306
Loop refilled.	435	424
Test terminated.	495	484

Table 6.16 Initial Conditions[a] (Test 220503, Cold Leg Discharge Leak)

Condition	Actual	Specified[b]
Primary		
Core power, % (increased for ambient losses)	4.17	4.2 ± 0.1
Pressure, psia	2198	2200 ± 50
Flow rate, %	5.5	n.s.
HL fluid temperature, F	609	610 ± 2
CL fluid temperature, F	571	n.s.
Pressurizer level, ft	19.2	16.6 ± 2
Maximum Pzr metal temperature, F	684	650 ± 10
Secondary		
Pressure, psia	1199	n.s.
AFW flow rate, %	2.18	n.s.
AFW temeperature, F	121	n.s.
Level, ft.	6.1	5 ± 1

[a] 1% power = 21.4 kW
1% primary flow = 0.259 lbm/s
1% secondary flow = 0.0265 lbm/s

[b] Unspecified initial conditions are denoted by "n.s."

Table 6.17 Major Events and Operator Actions (Test 220503, Cold Leg Discharge Leak)

Time, min		Event
DAS	Leak	
0	--	Activated data acquisition system (DAS) at 0948, March 20, 1984.
10.6	0	Opened (10-cm^2 cold leg discharge) leak.
13	2.1-2.3	Actuated HPI, increased AFW, began core power ramp, adjusted pressurizer heaters.
13	3	HLUB fluid saturated (p = 1700 psia).
13	2.4	Pressurizer drained.
16	5.6	Core exit fluid saturated.
24	13	SG secondary refilled to control level, began depressurization ramp.
38	27.4	Primary level has decreased to elevation of the upper tubesheet.
52	41.6	AFW BCM began (p = 1470 psia).
64	53	RVVV control changed to manual-open.
76	65.5	Refill began.
117	106	End of BCM (p = 740 psia).
198	187	Maximum refill repressurization ($p \tilde{=} 900$ psia).
320	309	Opened HPV.
440	429	Loop full, RVVV control returned to automatic (valve closed) natural circulation began.
507	496	Test terminated.

Table 6.18 Unavailable Measurements (Test 220503, CLD Leak)

SUMMARY OF VARIABLES DISCARDED ON INPUT, TEST 220503

NO.	VTAB	SYSTEM	INST.	ELEVATION	DESCRIPTION
1	155HLTC06	2HL	2FTC	50.00	HOT LEG FLUID TEMP (F)
2	262HLCP05	2HL	16 CP	41.00	HOT LEG CONDCTVTY (WET/DRY)
3	263HLCP06	2HL	16 CP	45.00	HOT LEG CONDCTVTY (WET/DRY)
4	264HLCP07	2HL	16 CP	49.00	HOT LEG CONDCTVTY (WET/DRY)
5	265HLCP08	2HL	16 CP	53.00	HOT LEG CONDCTVTY (WET/DRY)
6	266HLCP09	2HL	16 CP	57.00	HOT LEG CONDCTVTY (WET/DRY)
7	274HLCP17	2HL	23RCP	.50	HOT LEG REF. C.P.
8	273HLCP16	3SGP	16 CP	53.10	SG PRIMRY. CONDCTVTY (WET/DRY)
9	272HLCP15	3SGP	16 CP	56.90	SG PRIMRY. CONDCTVTY (WET/DRY)
10	223HPTR02	10HPI	13TMF	-999.00	HP INJECT. TURB.FLOW (LBM/SEC)
11	218HPAC01	10HPI	19ACC	-999.00	HP INJECT. ACCD.FLOW (LBM)
12	221V2AC02	12V2	19ACC	-999.00	2-PH VENT. ACCD.FLOW (LBM)
13	79SMTC02	22SGS	25MTC	26.30	SG SECOND. METAL TC (F)
14	76SMTC06	22SGS	25MTC	44.20	SG SECOND. METAL TC (F)
15	343V1TC02	33CLS	2FTC	-999.00	CLS LEAK FLUID TEMP (F)

Table 6.19 Manual AFW Control[a] (Test 220503, Cold Leg Discharge Leak).

Start			End			
Clock	DAS, m	Leak, m	Clock	DAS, m	Leak m	Duration, min
1011	23	13	1011	23	13	-
1015	27	17	1015	27	17	-
1114	86	76	1114	86	76	-
1139	111	101	1149	121	111	10
1221	153	143	1228	160	150	7
1311	203	193	1316	208	198	5
1419	271	261	1428	280	270	9
1609	381	371	1621	393	383	12
1652	424	414	1657	429	419	5
1755	487	477	(1807)	499	489	(12)

[a]AFW control periods are from the operator's log. "Start" and "end" refer to the start and end of manual AFW control. "DAS" times are referenced to the time of data acquisition system activation, "leak" times are referenced to the time of leak opening.

Table 6.20 Initial Conditions (Test 220604, Low-Head HPI).

	Specified	Actual
Core power, % (1% of full power = 21.4 kW), including 0.5% losses to ambient.	4.2±0.1	4.17
Natural circulation.	Yes	Yes
Primary pressure, psia.	2200±50	2198
Pressurizer liquid height, ft from SGLTSUF.	16.6 ± 2	19.7
Pressurizer main and guard heaters adjusted for an approximately adiabatic pressurizer.	Yes	Yes
RV and HL vents closed.	Yes	Yes
RVVV in automatic (differential-pressure) control with open/close setpoints of 0.25 and 0.125 psid.	Yes Yes	Yes Yes
AFW at 100F injected at the upper elevation using the minimum-wetting nozzle.	Yes	Yes
SG secondary (collapsed) liquid level (with constant level control), ft	5 ± 1	5.5
SG secondary pressure adjusted to obtain a primary HL fluid temperature, F (Use the model HL fluid temperature indication at 60 ft, HLTC07.)	610 ± 2	609
HPI and leak systems are not yet in use. Primary noncondensible gas additions are not to be tested.	Yes	Yes
Initialization is continued until a suitable system steady state is obtained:		
Pressurizer metal temperatures are at saturation, F	650 ± 10	653-679
The RVVV is not cycling.	Yes	Yes
The SG fluid temperatures are varying less than 10/h (exception: cyclic secondary fluid temperature variations associated with high AFW injection, and with internal circulation within the secondary liquid pool, are acceptable).	Yes	Yes
Other initial conditions: T_{cold} = 571F, primary flow rate = 5.5%, SG pressure = 1203 psia, feed and steam flow rates = 2.2%, AFW temp = 112 F.		

Table 6.21 Selected Operator Actions (Test 220604, Low-Head HPI).

Time	Leak T, min.	Action
March 19, 1984		
1031	0	Data acquisition system (DAS) started.
1042	10.7	10-cm^2 cold leg suction leak opened.
1044	14	HPI, AFW, core power actuated.
1055	25	Steam pressure ramp activated.
Several (See Table 6.22)	--	Transferred AFW control from automatic to manual and back to automatic.
1101	30	RVVV control switched from automatic to manual-open.
1555	324	Opened HLHPV.
1715	405	RVVV control changed from manual-open to automatic.
1857	506	Test completed, DAS stopped.

Table 6.22 Manual AFW Valve (SFCV03) Actions (Test 220604, Low-Head HPI)

Time	Leak Time, min	Action
1043	-2	Set SFCV03 to manual at 39.5%
1055	10	Closed SFCV03 and placed on auto level at about 73%.
1059	14	Switched SFCV03 controller from auto to manual, closed valve, switched it back to auto.
1132	47	Switched SFCV03 to manual, closed valve, switched back to auto.
1147	62	Closed SFCV03 manually.
1150	65	Switched SFCV03 to auto.
1236	111	Closed SFCV03 manually, switched to auto.
1247	122	Closed SFCV03 manually, switched to auto.
1308	143	Closed SFCV03 manually, switched to auto.
1331	166	Closed SFCV03 manually until level drops.
1339	174	Switched back to auto.
1412	207	Closed SFCV03 manually.
1418	213	Switched back to auto.
1443	238	Closed SFCV03 manually, switched back to auto.
1451	246	Closed SFCV03 manually, switched back to auto.
1533	288	Closed SFCV03 manually.
1550	305	Switched SFCV03 to auto.
1609	324	Closed SFCV03 to auto.
1654	369	Switched SFCV03 to auto.
1750	425	Closed SFCV03 manually.

Table 6.23 Discarded Variables (Test 220604, Low-Head HPI)

SUMMARY OF VARIABLES DISCARDED ON INPUT, TEST 220604

NO.	VTAB	SYSTEM	INST.	ELEVATION	DESCRIPTION
1	155HLTC06	2HL	2FTC	50.00	HOT LEG FLUID TEMP (F)
2	262HLCP05	2HL	16 CP	41.00	HOT LEG CONDCTVTY (WET/DRY)
3	263HLCP06	2HL	16 CP	45.00	HOT LEG CONDCTVTY (WET/DRY)
4	264HLCP07	2HL	16 CP	49.00	HOT LEG CONDCTVTY (WET/DRY)
5	265HLCP08	2HL	16 CP	53.00	HOT LEG CONDCTVTY (WET/DRY)
6	266HLCP09	2HL	16 CP	57.00	HOT LEG CONDCTVTY (WET/DRY)
7	274HLCP17	2HL	23RCP	.50	HOT LEG REF. L.P.
8	273HLCP16	3SGP	16 CP	53.10	SG PRIMRY. CONDCTVTY (WET/DRY)
9	272HLCP15	3SGP	16 CP	56.90	SG PRIMRY. CONDCTVTY (WET/DRY)
10	223HPTM02	10HPI	13TMF	-999.00	HP INJECT. TURB.FLOW (LBM/SEC)
11	218HPACC1	10HPI	19ACC	-999.00	HP INJECT. ACCD.FLOW (LBM)
12	221V2ACC2	12V2	19ACC	-999.00	2-PH VENT. ACCD.FLOW (LBM)
13	79SMTC02	22SGS	25MTC	26.30	SG SECOND. METAL TC (F)
14	76SMTC06	22SGS	25MTC	44.20	SG SECOND. METAL TC (F)
15	344V1TC03	34CLD	2FTC	-999.00	CLD LEAK FLUID TEMP (F)

Table 6.24 Key Events (Test 220604, Low-Head HPI).

Event	DAS time, min	Leak time, min
Leak opened.	10.7	0
Pressurizer emptied.	12.9	2
HPI, AFW system, and core power ramp activated.	14	3
HL saturation.	14	2.5
HLUB spillover.	18	7
HL and CL nozzle uncovered, HL spillover, and CL void collapsed.	20	9
High elevation-BCM began.	24	12.9
HPI flow starts (P < shutoff head).	24	13.4
Secondary level reaches setpoint terminating AFW, Secondary system depressurization ramp initiated.	24.3	13.7
Leak and HPI flows reach equilibrium - refill began.	67	56
SG primary level exceeded the AFW site elevation.	111	100
HL spillover.	308	297 (and 371)
HLHPV opened.	324	313
Loop refilled, NC cooldown began.	400-411	389-394
Test terminated.	506	495

Table 6.25 Initial Conditions (Test 220756, Isolated Leak)

	Planned	Actual
Core power (% of full power, 1% full power - 24.1 kW), includes 0.5% to replace losses to ambient.	4.2 ± 0.1	4.17
Natural circulation.	X	X
Primary pressure, psia.	2200 ± 50	2199
Pressurizer liquid height, ft from SGLTSUF.	16.6 ± 2	18.6
Pressurizer main and guard heaters adjusted for an approximately adiabatic pressure.	X	X
RV and HL vents closed.	X	X
RVVV in automatic (differential-pressure) control with open/close setpoints of 0.25 and 0.125 psid.	X	X
AFW at 100F injected at the upper elevation using the minimum-wetting nozzle.	X	X
SG secondary (collapsed) liquid level (with constant level control), ft.	5 ± 1	5.9
Hot leg fluid temperature, F.	610 ± 2	609
HPI and leak systems are not yet in use. Primary NCG additions are not to be tested.	X	X
Initialization is continued until a suitable system steady state is obtained:		
Pressurizer metal temperatures, F.	650 ± 10	652 - 692
The RVVV is not cycling.	X	X
The steam generator fluid temperatures are varying less than 10F/h; exception cyclic secondary fluid temperature variations associated with high AFW injection, and with internal circulation within the secondary liquid pool, are acceptable.		
Other initial conditions: T_{cold} = 57F, primary flow rate = 5.5%, SG pressure = 1202 psia, feed and steam flow rates = 2.3%, AFW temp = 118F.		

Table 6.26 Selected Operator Actions and Key Events
(Test 220756, Isolated Leak)

Time	T, min.	Action
1042 March 27, 1984	-13	Data acquisition system (DAS) activated.
1054	0	Leak opened.
1056	2	HPI, AFW injection and core power ramp actuated.
1056	3	U-bend saturated.
1107	13	SG secondary pressure ramp actuated.
1116	21	Leak isolated -- refill began.
1127	34	Loop refilled.
1139	44	HPI throttled to maintain 23-foot level.
1143	48	HPI system turn off.
1156	61	HPI system turned on to maintain 23-foot presurizer level.
1254	117	DAS de-activated (test completed).

Table 6.27 Summary of Variables Discarded on Input (Test 220756, Isolated Leak).

SUMMARY OF VARIABLES DISCARDED ON INPUT, TEST 220756

NO.	VTAB	SYSTEM	INST.	ELEVATION	D E S C R I P T I O N
1	155HLTC06	2HL	2FTC	50.00	HOT LEG FLUID TEMP (F)
2	262HLCPC5	2HL	16 CP	41.00	HOT LEG CONDCTVTY (WET/DRY)
3	263HLCPC6	2HL	16 CP	45.00	HOT LEG CONDCTVTY (WET/DRY)
4	264HLCPC7	2HL	16 CP	49.00	HOT LEG CONDCTVTY (WET/DRY)
5	265HLCPC8	2HL	16 CP	53.00	HOT LEG CONDCTVTY (WET/DRY)
6	266HLCPC9	2HL	16 CP	57.00	HOT LEG CONDCTVTY (WET/DRY)
7	274HLCP17	2HL	23RCP	-50	HOT LEG REF. C.P.
8	273HLCP16	3SGP	16 CP	53.10	SG PRIMRY. CONDCTVTY (WET/DRY)
9	272HLCP15	3SGP	16 CP	56.90	SG PRIMRY. CONDCTVTY (WET/DRY)
10	223HPTMC2	10HPI	13TMF	-999.00	HP INJECT. TURB.FLOW (LBM/SEC)
11	220V2ACC1	12V2	19ACC	-999.00	2-PH VENT. ACCD.FLOW (LBM)
12	221V2ACC2	12V2	19ACC	-999.00	2-PH VENT. ACCD.FLOW (LBM)
13	318V2RF20	12V2	38FLD	-999.00	2-PH VENT. CALD.FLOW (LBM/SEC)
14	53SSTC13	22SGS	2FTC	32.30	SG SECOND.FLUID TEMP (F)
15	79SMTC02	22SGS	25MTC	26.30	SG SECOND. METAL TC (F)
16	76SMTC06	22SGS	25MTC	44.20	SG SECOND. METAL TC (F)
17	344V1TC03	34CLD	2FTC	-999.00	CLD LEAK FLUID TEMP (F)

Table 6.28 Initial Conditions (Single-Variable Tests 220201 through 220756)

Conversion factors: 1% (scaled) full power = 21.4 KW; 1% primary flow = 0.259 lbm/s; 1% secondary flow = 0.0265 lbm/s. Core power levels include 0.5% to replace losses to ambient. Elevations are referenced to the SG lower tubesheet upper face (SGLTSUF). Related Tests 2202AA and 2202BB are addressed in section 10. The Nominal Test 220100, described in section 5, is listed here for reference. Listed initial conditions are at steady state with primary boundary systems inactive.

Test Number Description Section (herein)	220100 Nominal 5.0	220201 15-cm^2 Leak Size 6.2	220304 1/2 HPI Capcity 6.3	220402 10-ft SG Level 6.4	220503 CLD 6.5	220604 Low-Head HPI 6.6	220756 Isolated Leak 6.7
Time DAS activated	0932, 15Mar84	0808, 22Mar84	1009, 7Apr84	1114, 21Mar84	0948, 20Mar84	1031, 19Mar84	1042, 27Mar84
PRIMARY							
Core power, %	4.17	4.17	4.17	4.17	4.17	4.17	4.17
Pressure, psia	2197	2209	2200	2198	2198	2198	2199
T_{hot}, F	609	609	609	609	609	609	609
T_{cold}, F	571	571	571	571	571	571	571
Flow rate, %	5.5	5.5	5.5	5.5	5.5	5.5	5.5
Pzr level, ft	20.6	17.0	19.6	18.9	19.2	19.7	18.6
[Level in Pzr, ft, rounded]	14	10	13	12	13	13	12
SECONDARY							
Pressure, psia	1201	1202	1200	1204	1199	1203	1202
Level, ft	5.5	5.6	5.8	6.0	6.1	5.5	5.9
Feed & steam flow rates, %	2.2	2.3	2.2	2.2	2.2	2.2	2.3
AFW temp., F	115	113	117	113	121	112	118
Time leak opened:							
Clock	1018	0821	1023	1125	0958	1042	1054
DAS time, m	46.8	12.8	14.0	11.1	10.6	10.7	12.8

Table 6.29 Early Events: Initiation, Saturation, and Intermittent Flow (Single-Variable Tests)

The first row of entries "leak opened (DAS-time)" gives the time (minutes) from Data Acquisition System (DAS) activation until leak opening; steady-state data at the (common) initial conditions were taken during this interval. The subsequent entries give the time (minutes) after leak opening. Additional notes follow the table. Entries referred to in the notes are marked by an asterisk(*).

Test Number	220100	220201	220304	220402	220503	220604	220756
Description	Nominal	15-cm^2 Leak Size	1/2 HPI Capacity	10-ft SG Level	CLD	Low-Head HPI	Isolated Leak
Section (herein)	5.0	6.2	6.3	6.4	6.5	6.6	6.7
Test Initiating Actions							
Leak opened, DAS time	46.8	12.8	14.0	11.1	10.6	10.7	12.8
AFW flow rate increased	2.7	1.5	2.5	2.2	2.3	3.2	2.1
Core power decreasing	2.6	1.5	2.5	2.1	2.1	2.7	2.0
HPI observed	2.5	1.5	2.3	2.2	2.3	13.4	2.1
Saturation							
Pzr drained	2.5	1.2	2.3	2.2	2.4	∿ 2	2.2
Pressure, psia	1920	2000	1950	1950	1930	1925	1970
Loop (HLUB) saturated	3.2	2.3	3.0	3.0	3.0	∿2.5	3.0
Pressure, psia	1700	1700	1710	1700	1700	1670	1700
Core-exit saturated	5.9	3.6	4.8	6.5	5.6	4.1	5.3
RVUH saturated	8.9	5.6	6.9	9.7	8.3	6.7	8.4
Intermittent Primary Flow							
RVVV actuated	4.2	3.1	4.0	4.0	4.2	4.1	3.8
Flow minimum (∿0)	6.9	(3.5)*	4.9	∿6*	6.3	(4.6)*	6
Initial flow interruption	8.0	3.5	6.1	∿7	(6.3)*	4.6	7
HLUB spillover	9.0	6.1	6.5	10.6	9.3*	6.7	9.4
Peak pressure, psia	1620	1670	1650	1670	1600	1670	1650
Subsequent Interruption	12.2	8	9	13.2	10.5	7.5	11
Spillover (RV liquid level ∿@ HL nozzle)	16.4	11	11	18	15	∿9*	15
Peak Pressure, psia	1660	1600	1650	1600	1650	1680	1620

Notes, Table 6-29 (Early Events)

- The times of "Test Initiating Actions" (AFW flow rate increase, decreasing core power, and HPI) are marked to the observation of each boundary condition, rather than to the time of operator control change.
- The first two "Saturation" timings are based on primary system pressure trends: Pressurizer draining is equated to the abrupt increase of the initial primary depressurization rate; loop saturation is equated to the subsequent abrupt decrease of primary depressurizaton rate. The remaining two saturation entries (core-exit and reactor vessel upper head) are based on local fluid temperature first reaching the saturation temperature.
- RVVV actuation is based on both the convergence of the bracketing fluid temperatures and on the divergence of the CL and downcomer flow rates.
- "Flow Minimum (>0)" refers to the initial minimum in CL flow rate which is often not quite zero. In Tests 220201 and 220604, the initial primary loop (CL) flow reduction did reach zero. There were multiple minimums in Test 220402.
- "Initial Flow Interruption" refers to the first occurrence of zero loop (CL) flow. In Test 220503, the indicated CL flow rate was not quite zero at the recorded event.
- The "HLUB Spillover" following flow interruption was relatively weak in Test 220503.
- "Spillover (RV liquid level @ HL nozzle)" denotes the loop flow increase and primary pressure decrease commonly associated with the descent of the RV (collapsed liquid) level to the vicinity of the HL nozzle elevation. This event was relatively weak in Test 220604, and was quickly followed by a strong BCM coupling and depressurization.

Table 6.30 BCM Conditions (Single-Variable Tests)

Test Number	220100	220201	220304	220402	220503	220604	220756
Description	Nominal	15-cm^2 Leak Size	1/2 HPI Capacity	10-ft SG Level	CLD	Low-Head HPI	Isolated Leak
Section (herein)	5.0	6.2	6.3	6.4	6.5	6.6	6.7
SG Secondary Control							
Depressurization started, min	13	11	13	6	13	14	13
Level reached control, min	12.8	13.1	23.8	5.2	12.8	13.7	44.4
AFW terminated, min	13	12.1	13.0	5.3	13.0	13.8	12.7
AFW BCM							NA
Primary level below tubesheet, min	29	13.1	17.1	29.1	27.4	12.8	
AFW BCM initiated, min	38	NA	17.2	66.6	41.6	12.9	
Maximum depress'n rate, psi/min	(weak)	(weak)	261	43	30	222	
Pool BCM				NA	NA	NA	NA
Pool BCM initiated, min	43	24	87				
Predominant depress'n rate, $\frac{psi}{min}$	37	54	3.4				
Refill: HPI $\geq$ leak flow, min*	70	104	130	74	66	56	20.8**
BCM terminated, min	105	200	195	97	106	89	NA

*The start of refill is defined as the time at which both the HL and SG primary levels begin to rise, with excess HPI flow rate.

**Leak isolated at 21 min, Test 220756.

Table 6.31 Later Events (Single-Variable Tests)

Test Number Description Section (herein)	220100 Nominal 5.0	220201 15-cm^2 Leak Size 6.2	220304 1/2 HPI Capacity 6.3	220402 10-ft SG Level 6.4	220503 CLD 6.5	220604 Low-Head HPI 6.6	220756 Isolated Leak 6.7
Start of Refill							
Time, min	70	104	130	74	66	56	21*
HL level, ft	43.6	15.6	37.2	32.4	46.2	50	65.5
Primary pressure, psia	747	509	430	∿1050	885	1050	1550
Refill Repressurization							
Maximum p, psia	795	∿400	389	829	876	992	1986
Time, min	243	298	246	193	187	160	45
HLHPV opened, min	305	302	304	306	309	313	NA
Refill Spillover: HLUB fluid desuperheats, min	365	358	276	300	309	371	25
HLUB liquid-filled, min	433	459	NA	424	428	389	34
RVVV control to auto, min	435	461	NA	427	429	394	NA
Natural circulation established, min	437	461	NA	428	429	394	33
PORV opened, min	NA	NA	430	NA	NA	NA	NA
Core power reduced, min	NA	NA	496	NA	NA	NA	NA
Test completed, min	600	515	587	484	496	495	117

*Leak isolated at 21 min in Test 220756.

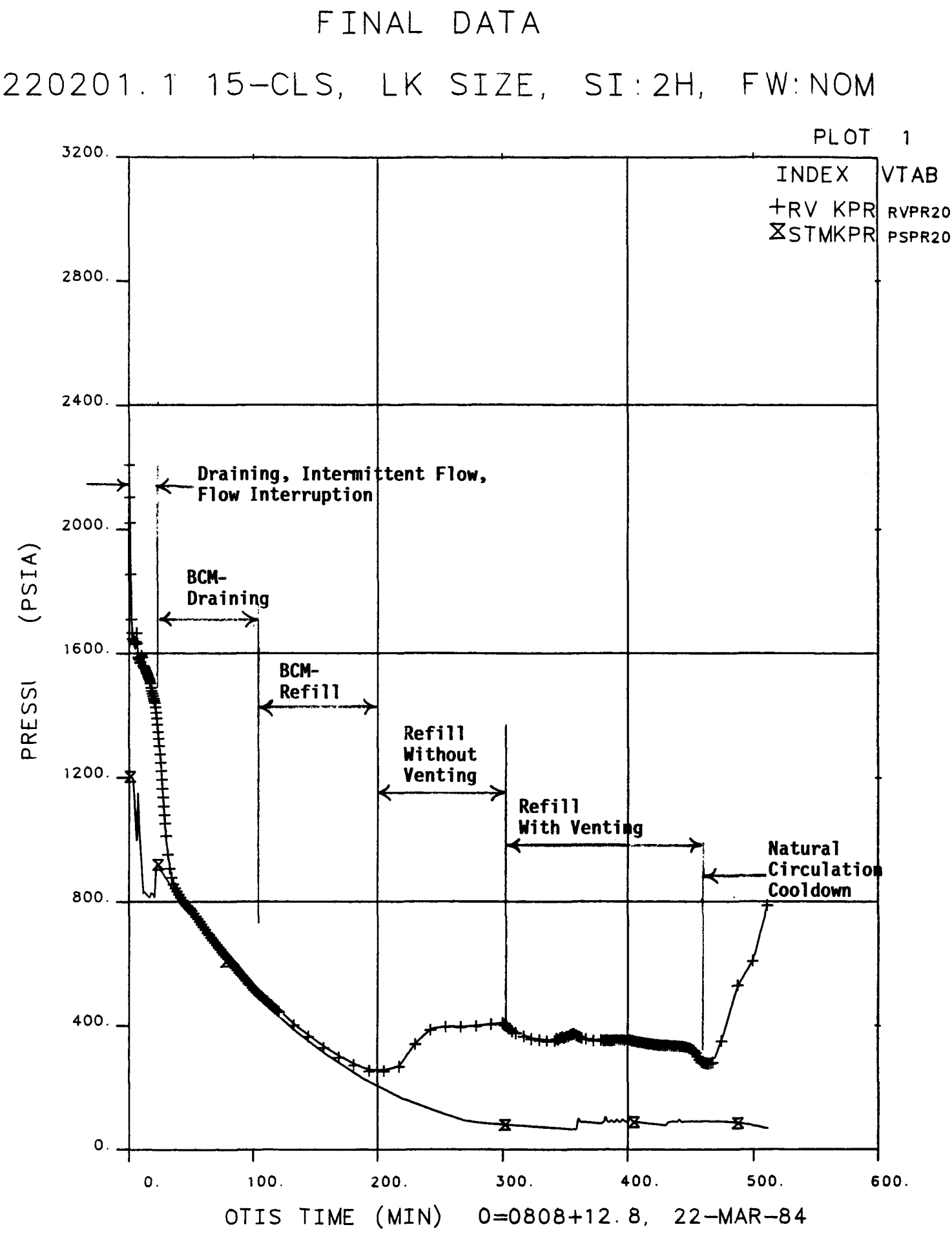

Figure 6.1 Primary and Secondary Pressure Versus Time Showing Key Events.

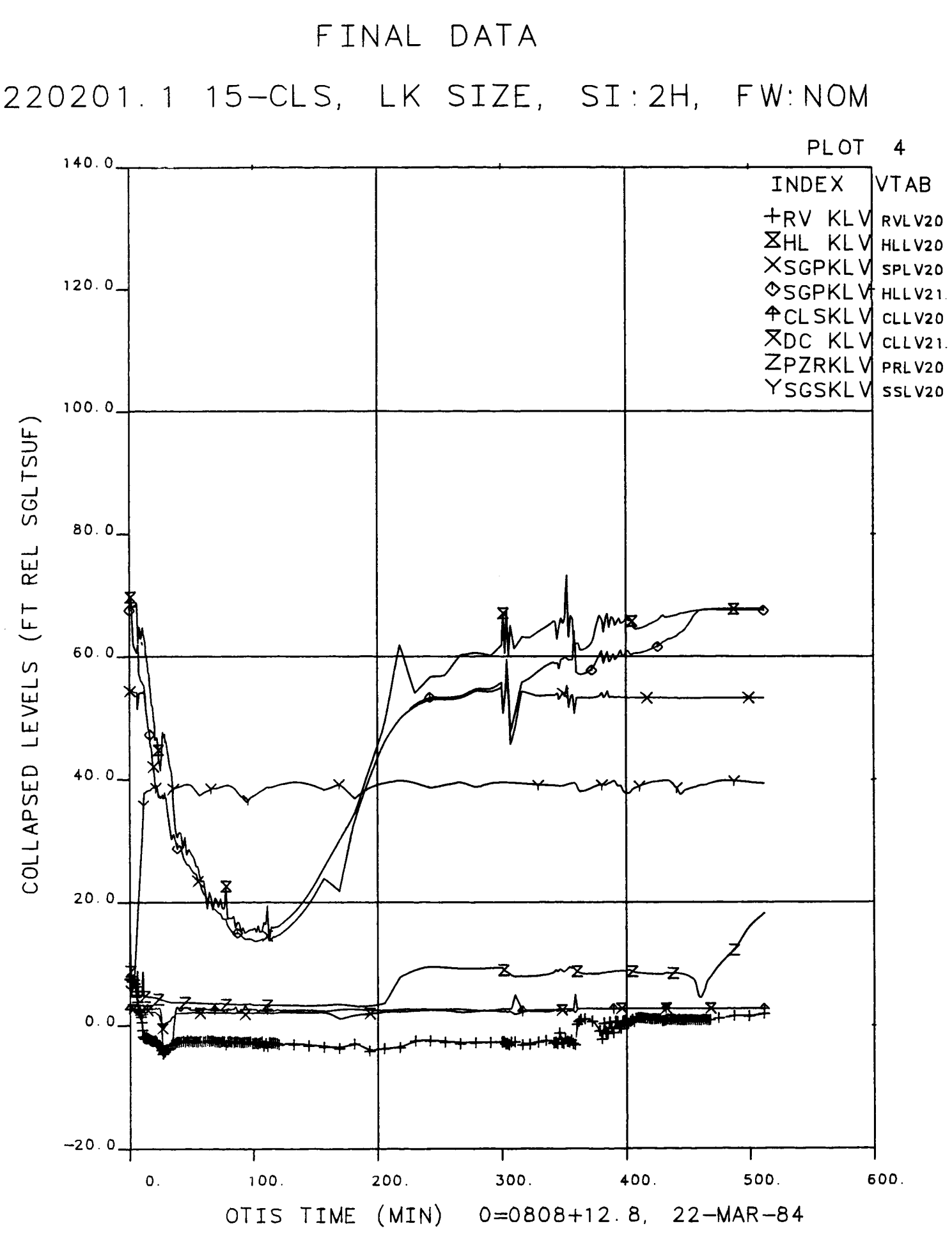

Figure 6.2 Collapsed Liquid Levels Versus Time.

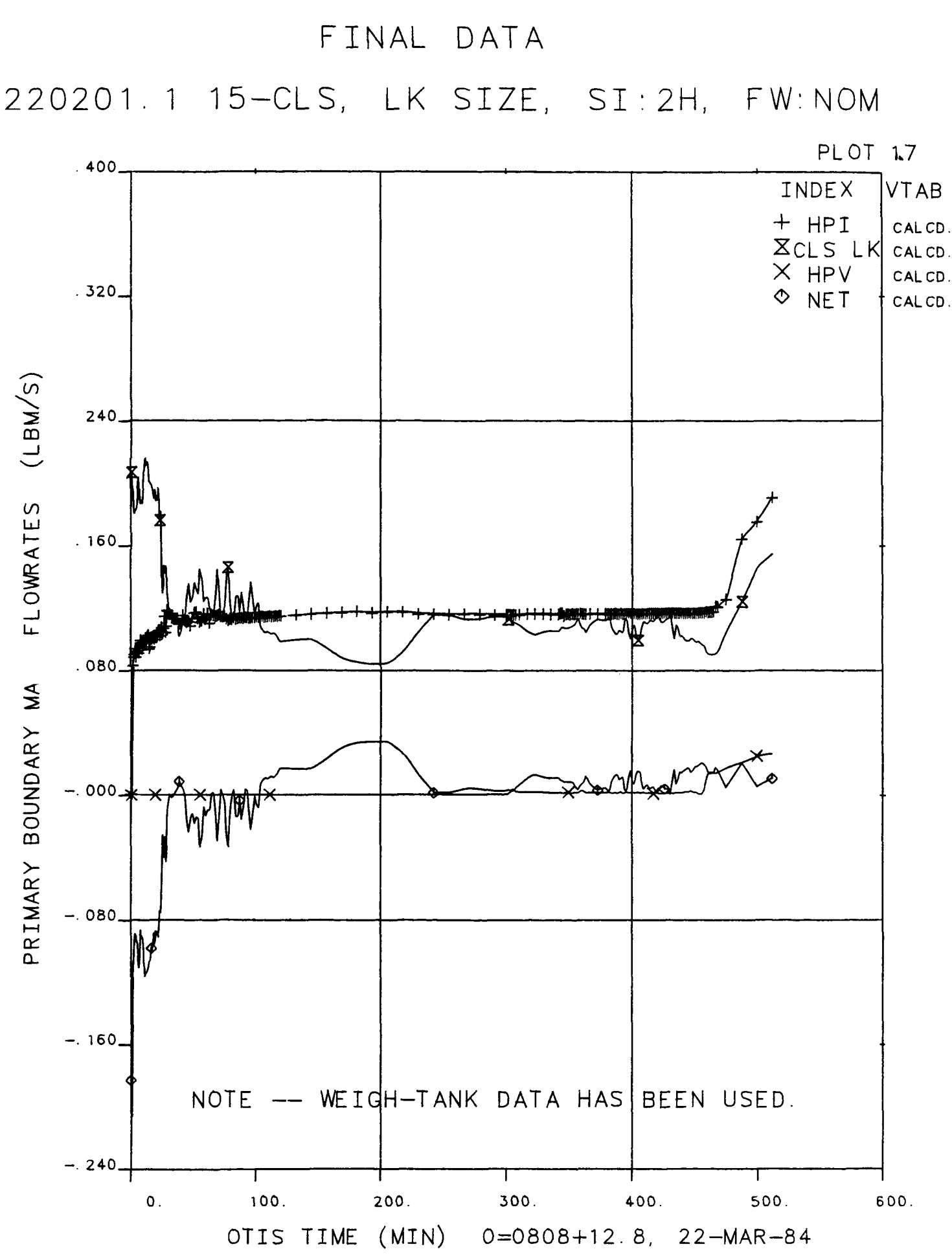

Figure 6.3 Primary Boundary Mass Flowrates Versus Time.

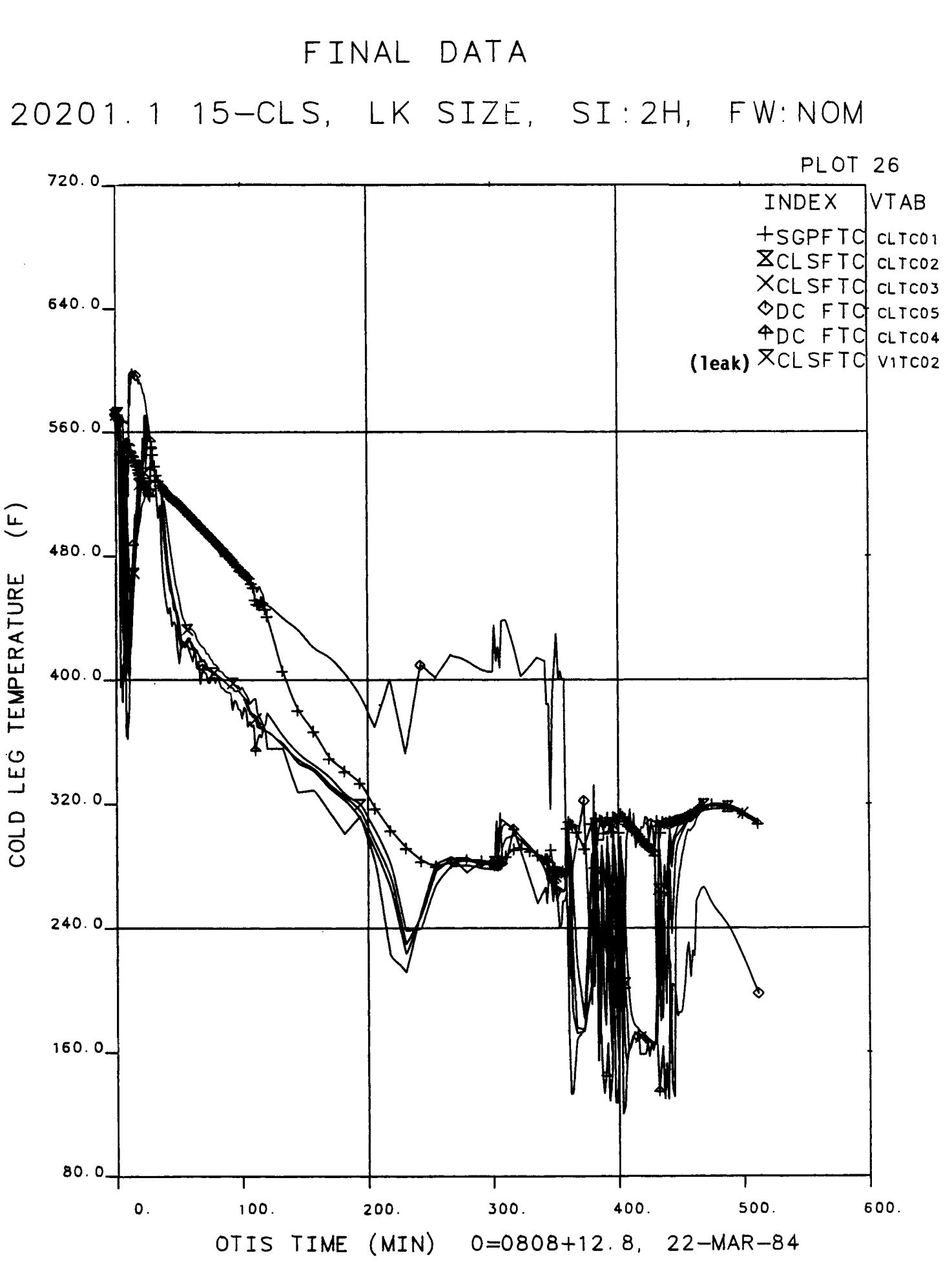

Figure 6.4 Cold Leg Temperatures Versus Time.

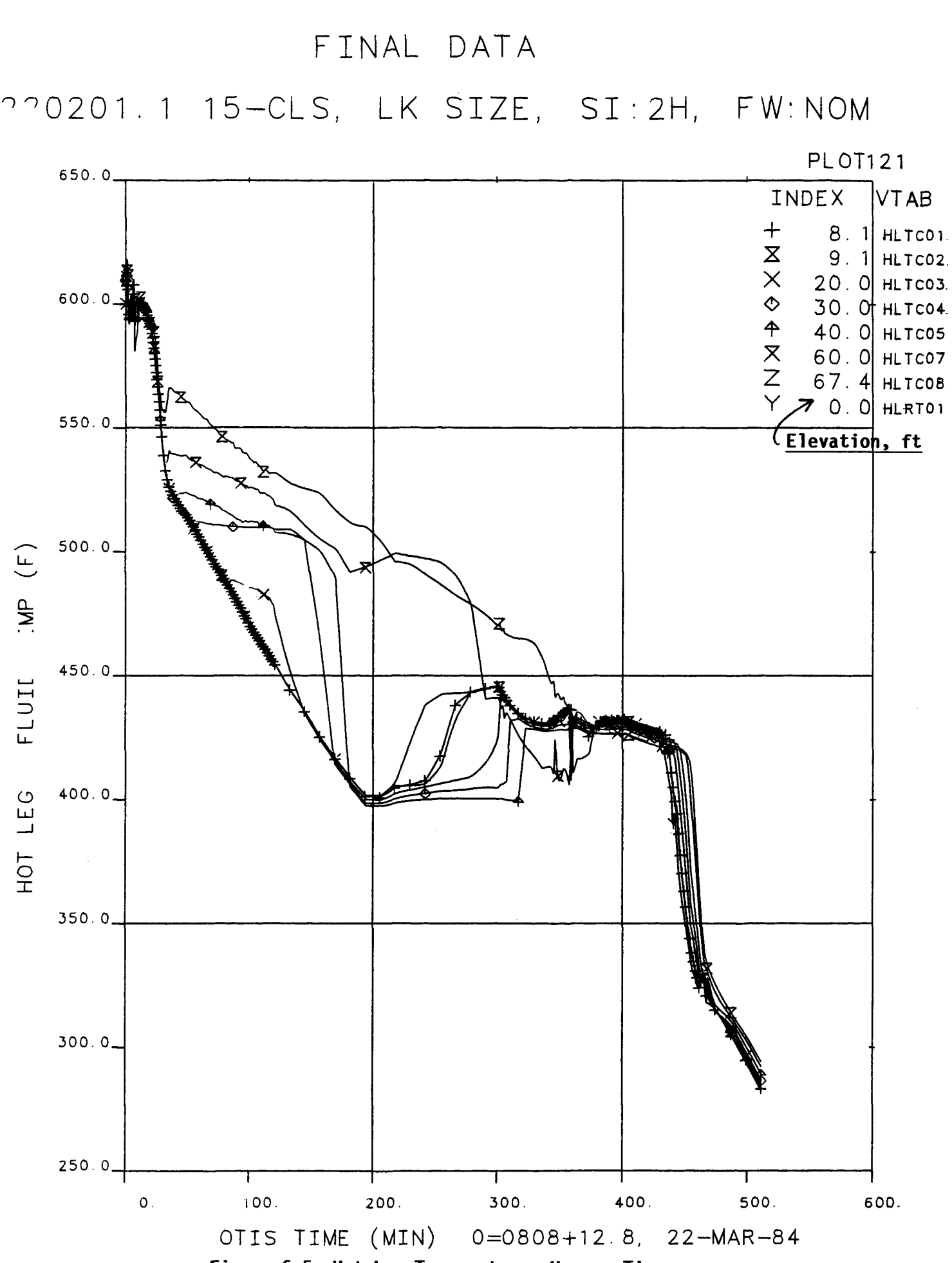

Figure 6.5 Hot Leg Temperatures Versus Time.

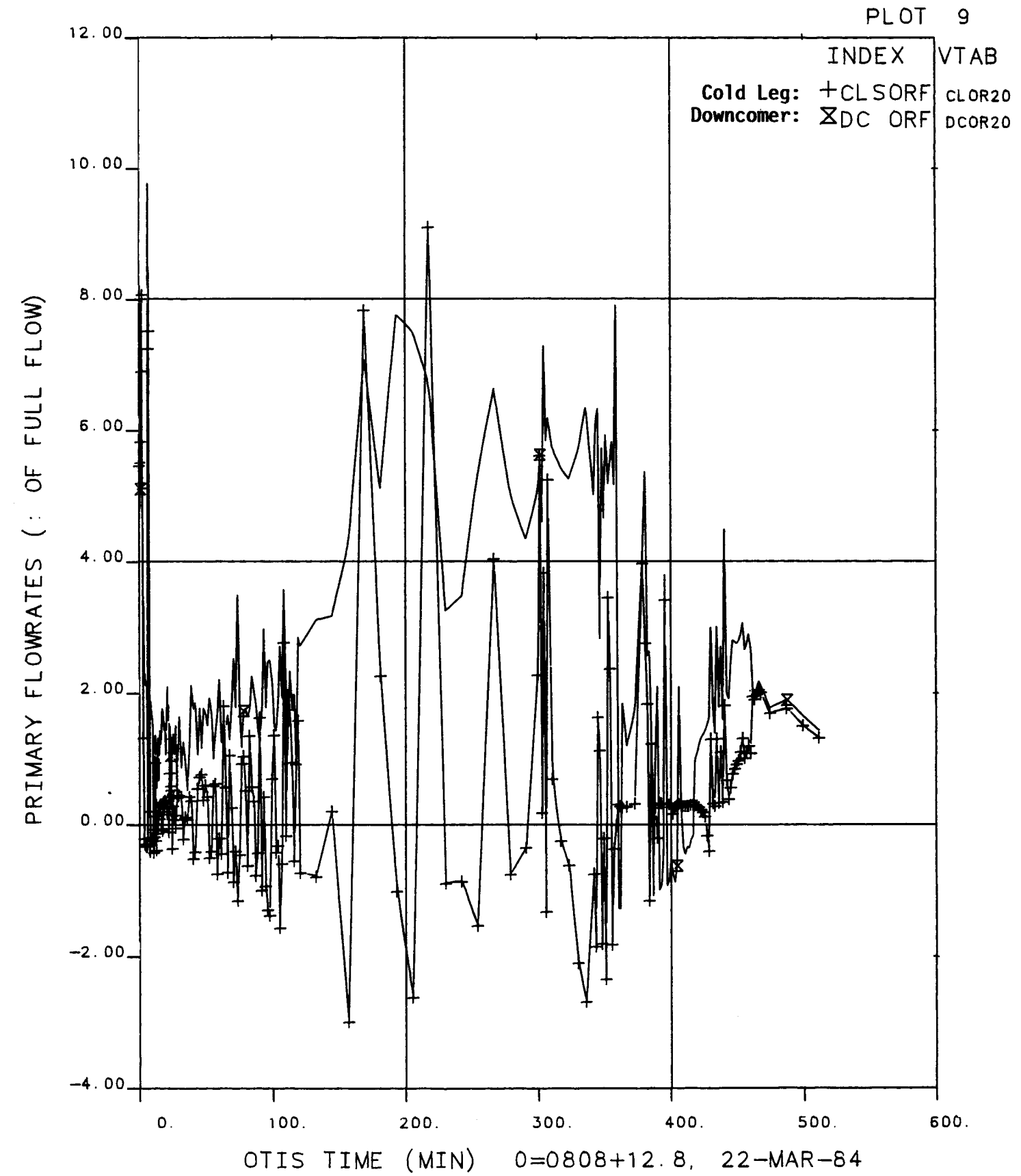

Figure 6.6 Primary Flowrates Versus Time.

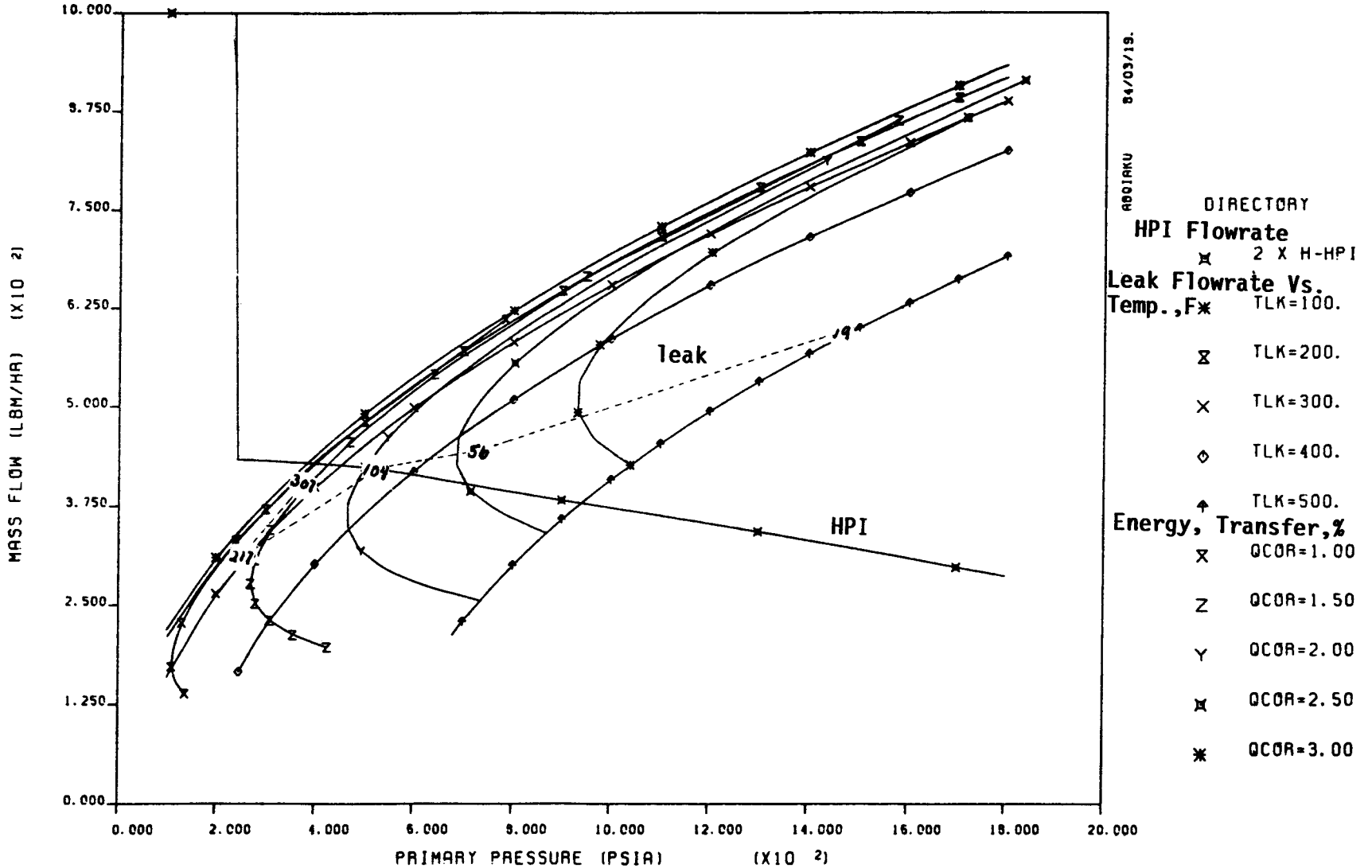

Figure 6.7 HPI and Leak Conditions, Test 220201 (15-cm^2 Leak).
See Appendix C for a description of this "equilibrium plot".

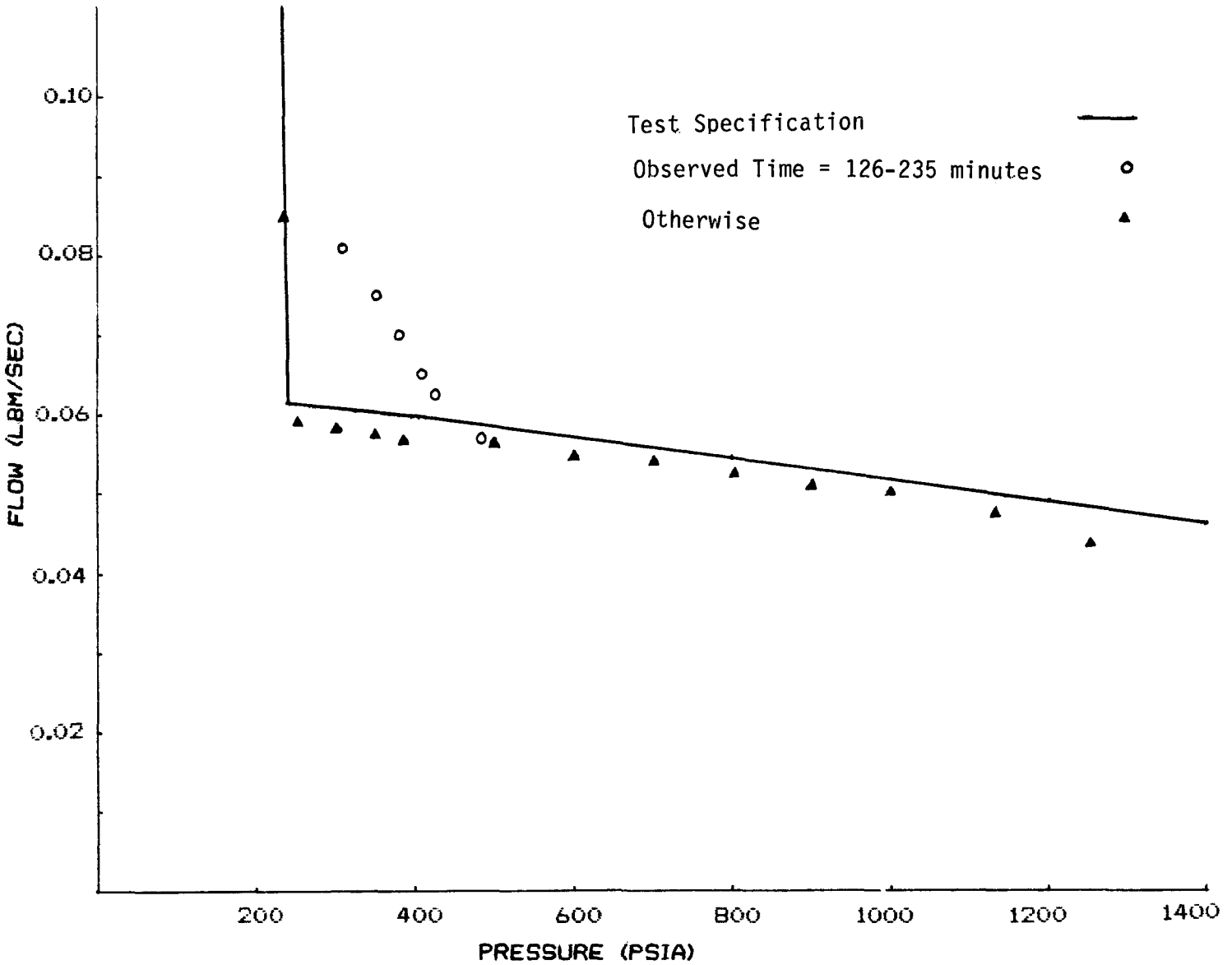

Figure 6.8 HPI Flow Versus Pressure (Test 220304, Half-Capacity HPI)

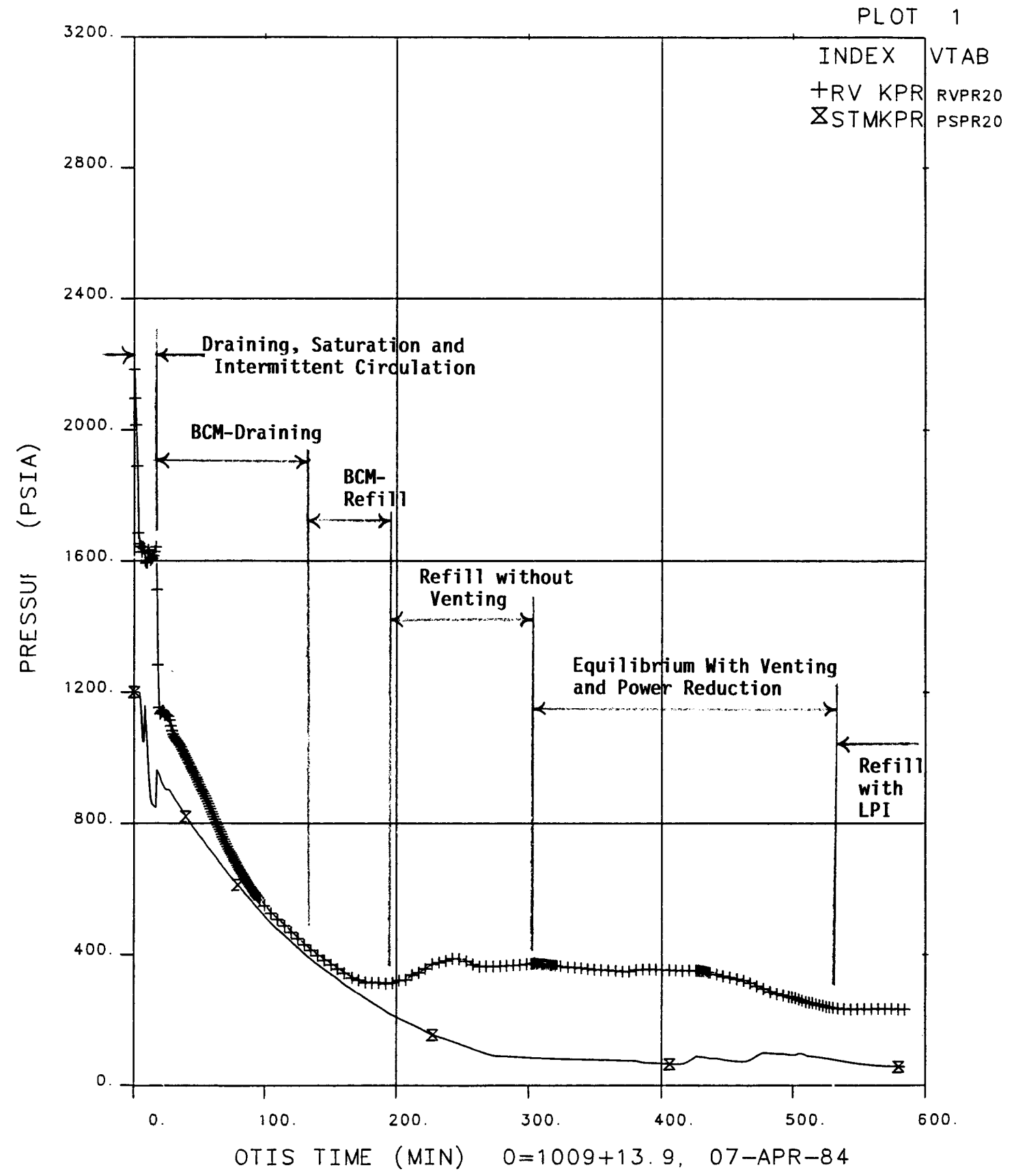

Figure 6.9 Primary and Secondary Pressure Versus Time Showing Key Events.

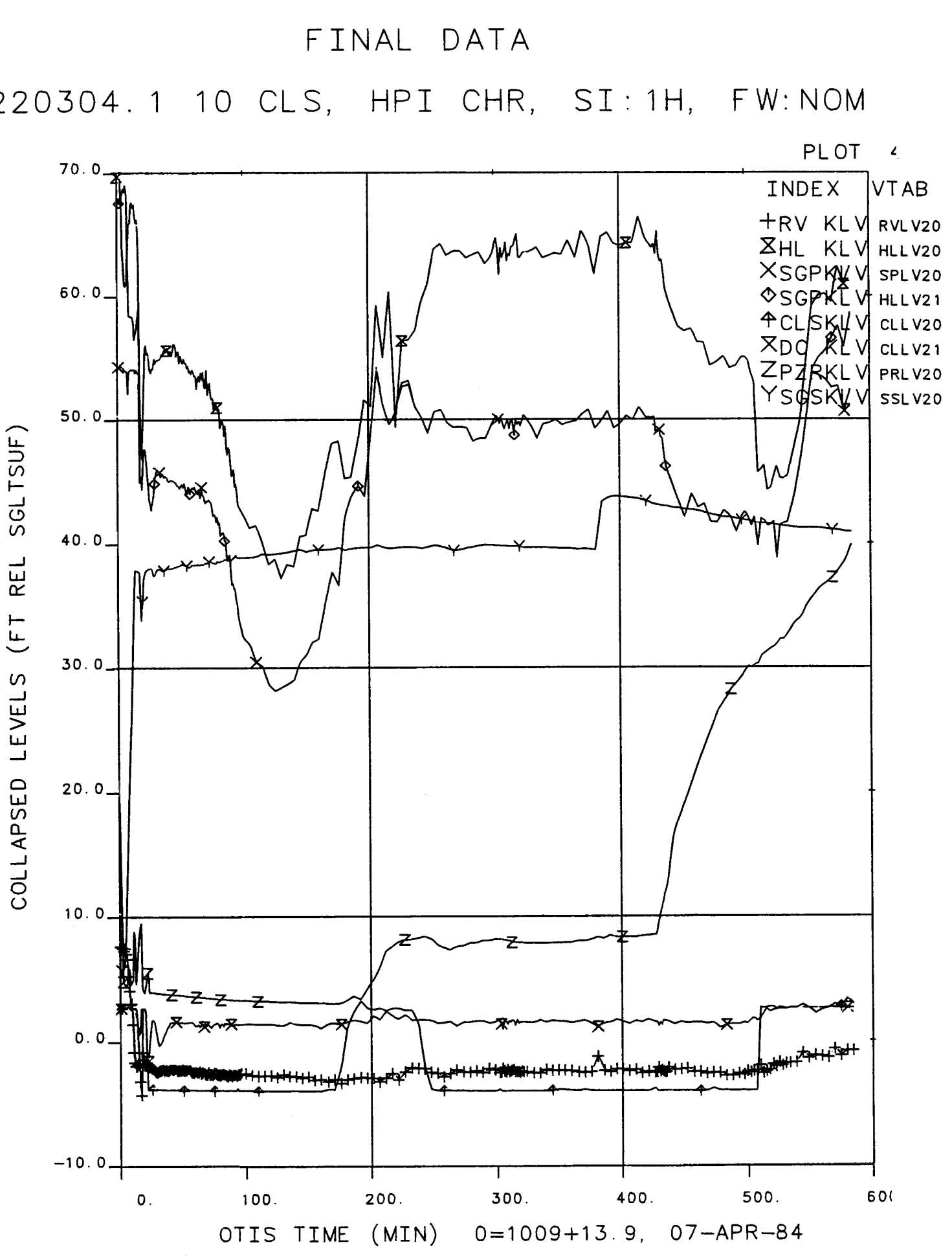

Figure 6.10 Collapsed Levels Versus Time

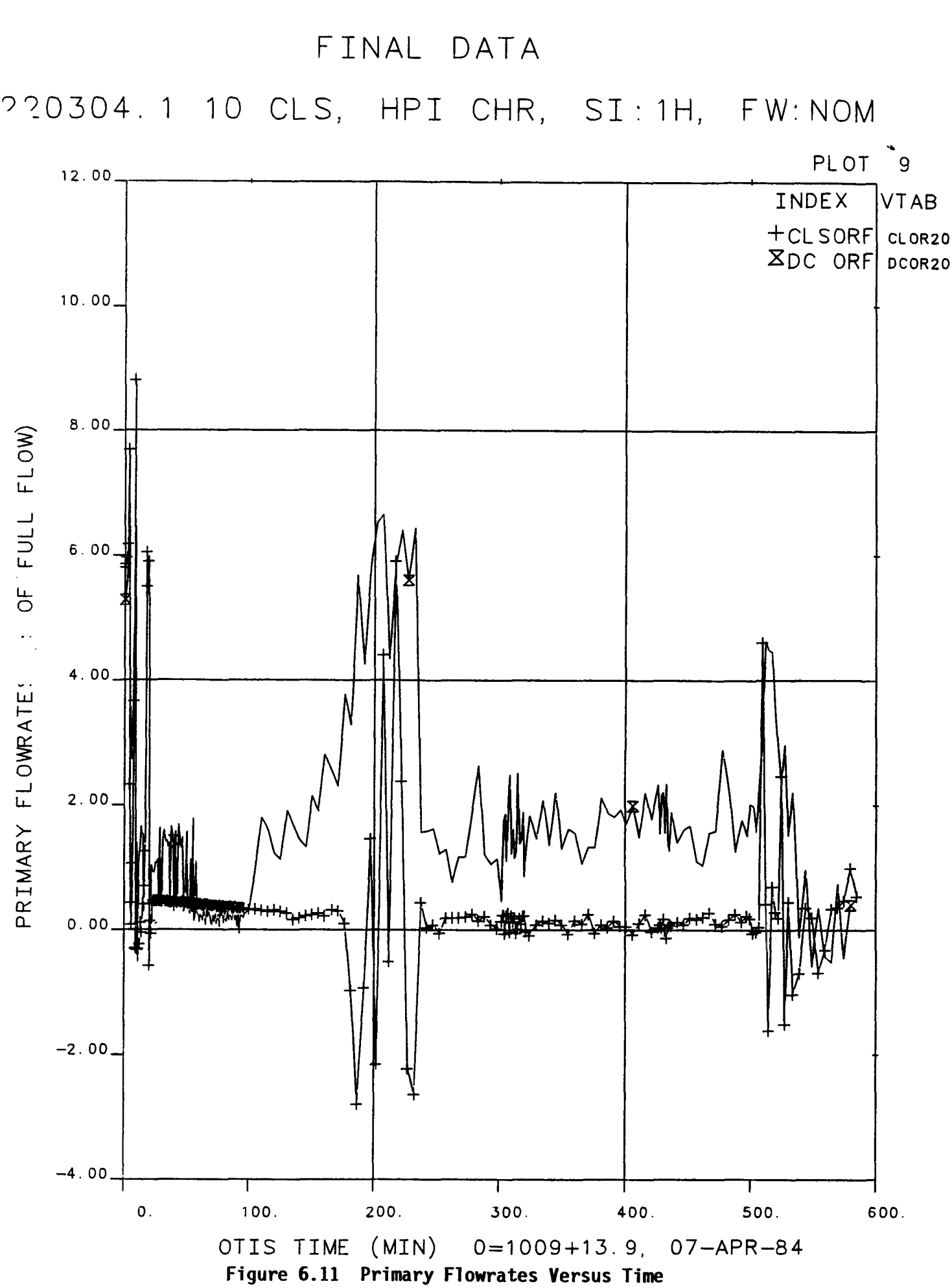

Figure 6.11 Primary Flowrates Versus Time

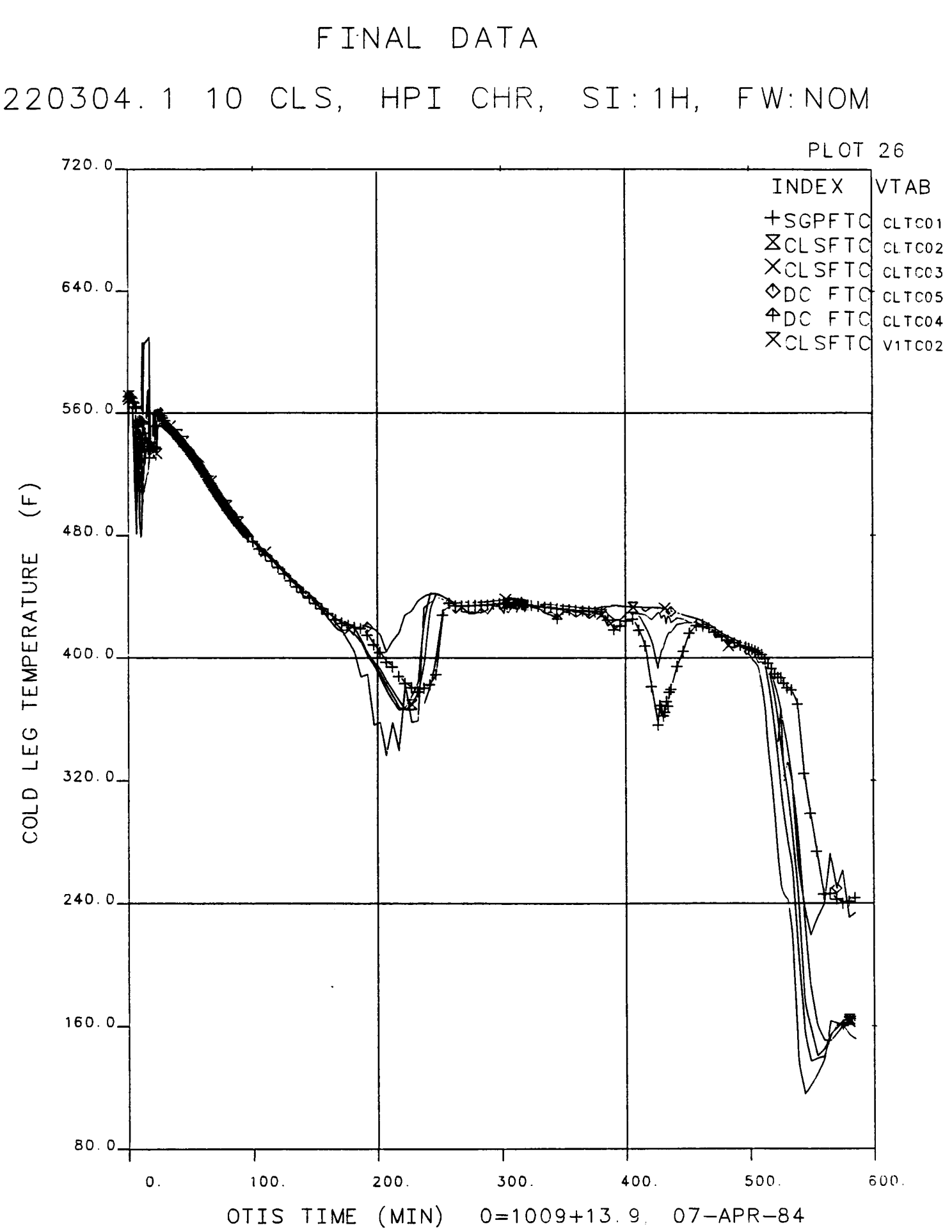

Figure 6.12 Cold Leg Temperatures Versus Time

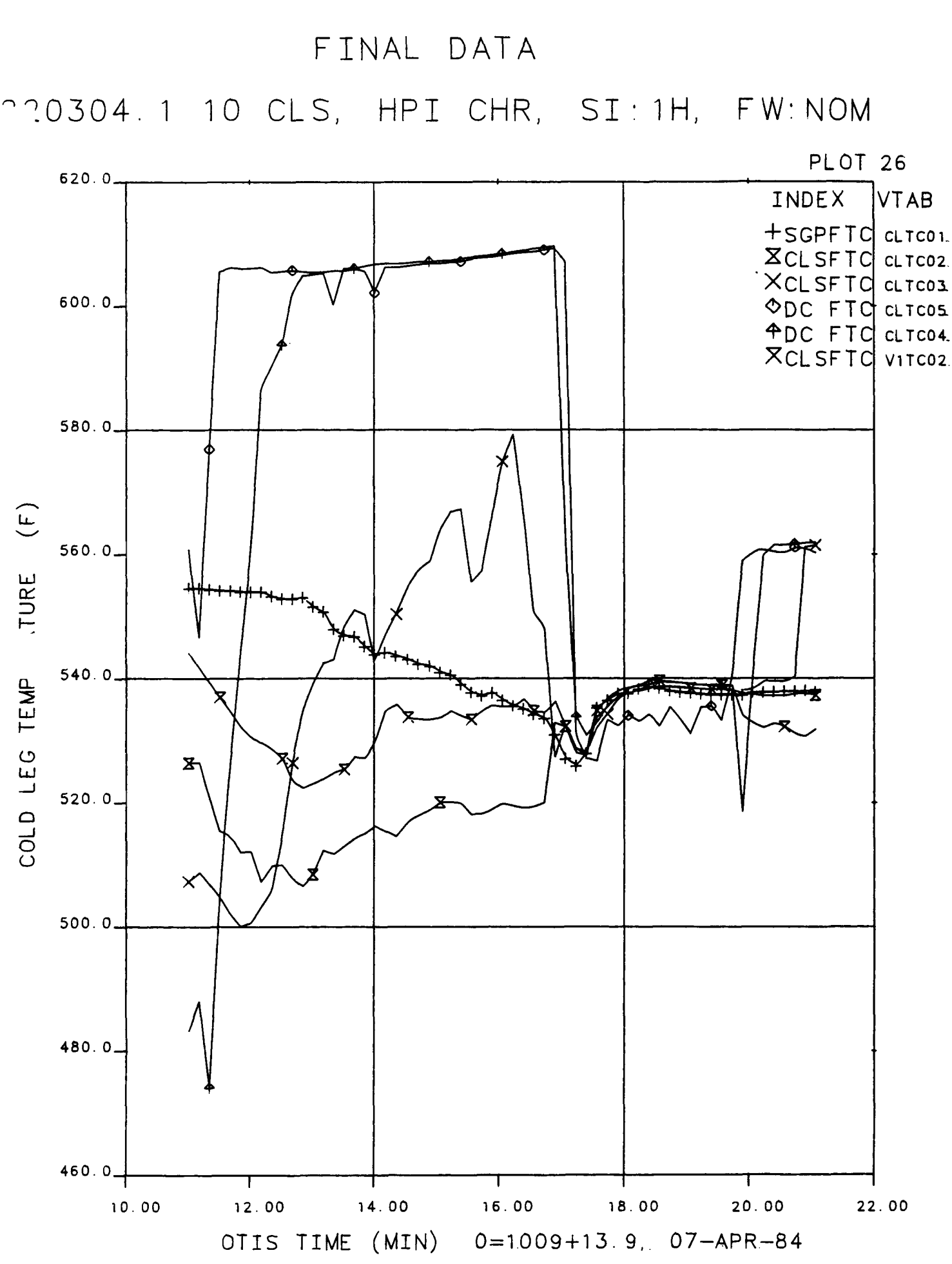

Figure 6.13 Cold Leg Temperatures Versus Time

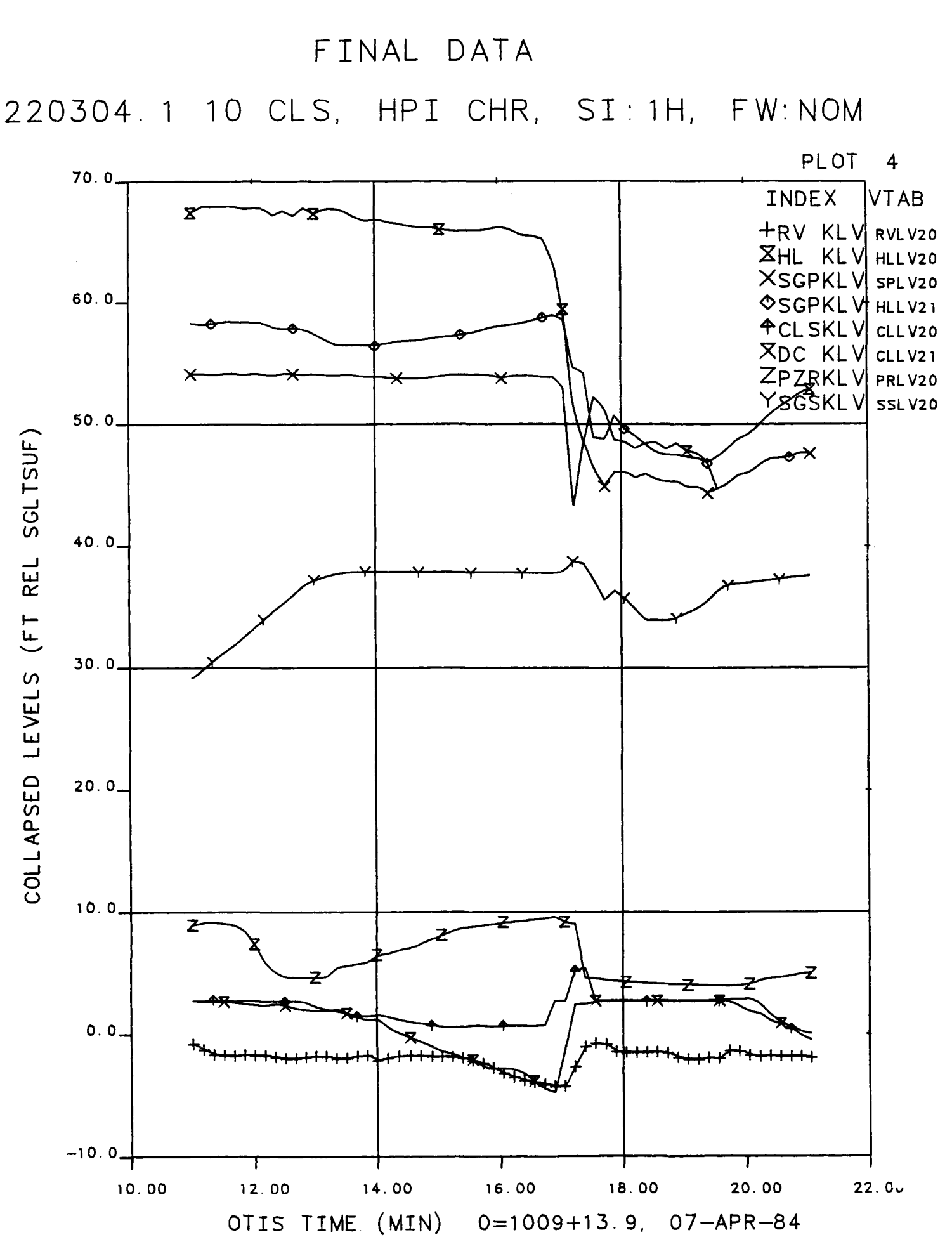

Figure 6.14 Collapsed Levels Versus Time

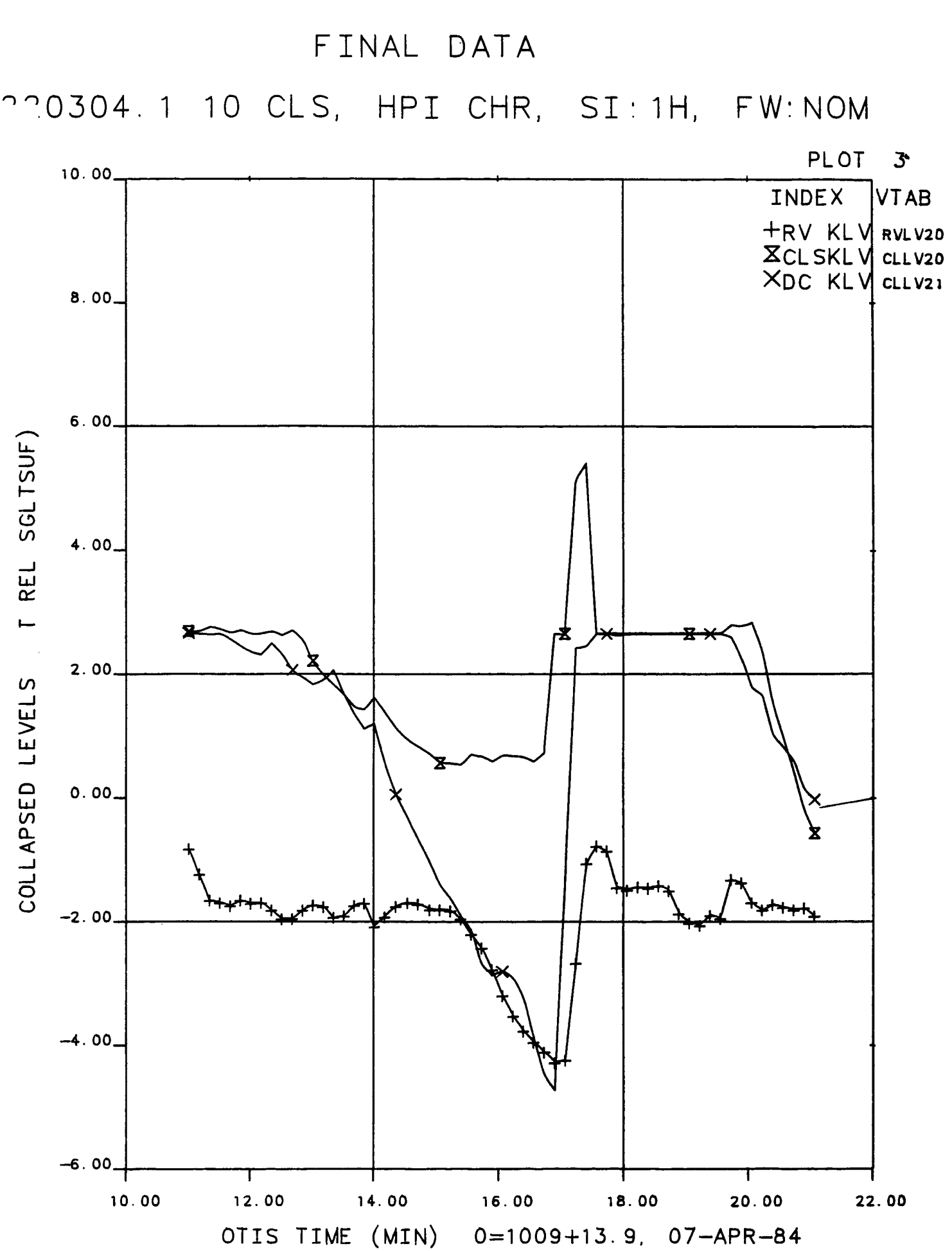

Figure 6.15 Collapsed Levels Versus Time

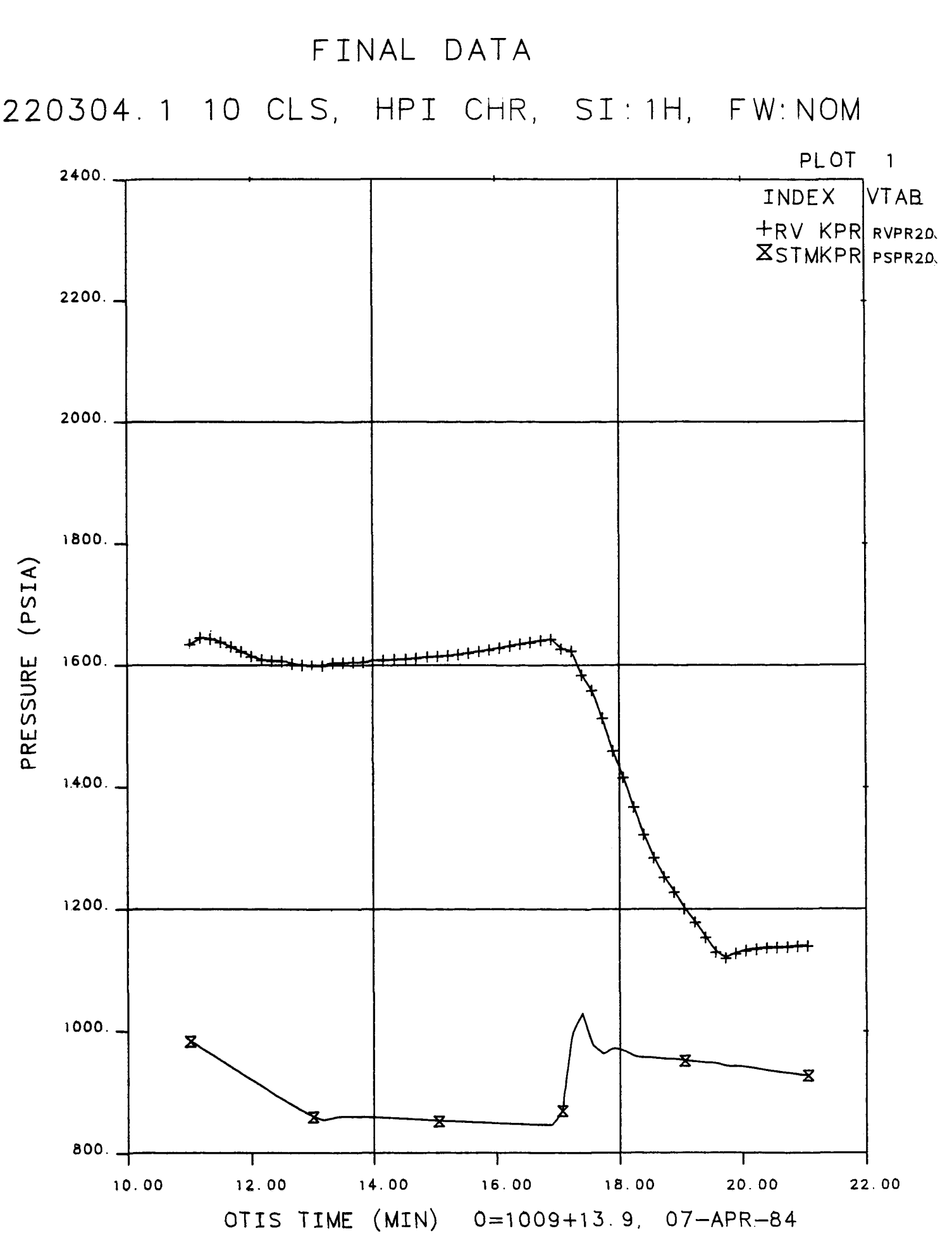

Figure 6.16 Primary and Secondary Pressure Versus Time

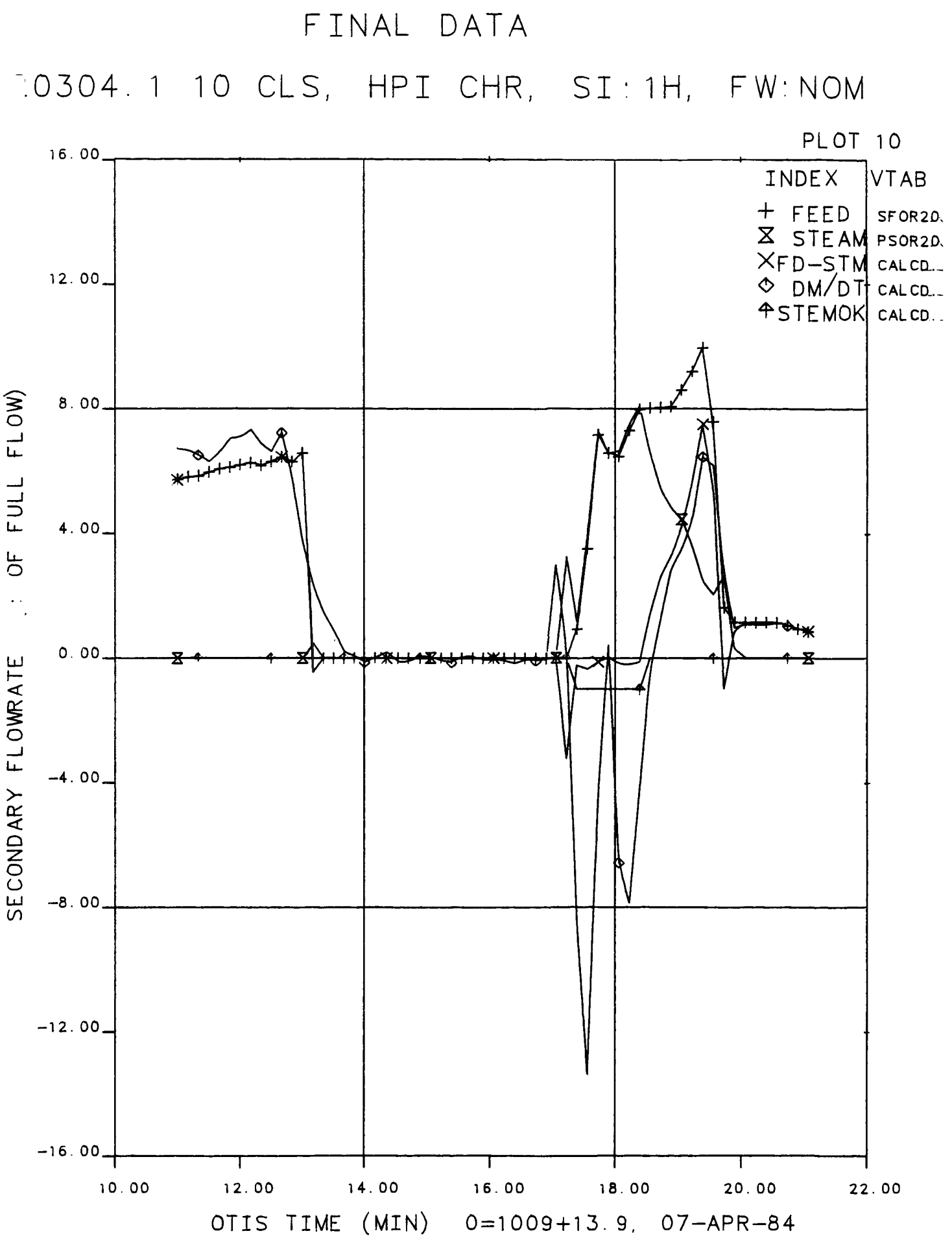

Figure 6.17 Secondary Flowrates Versus Time

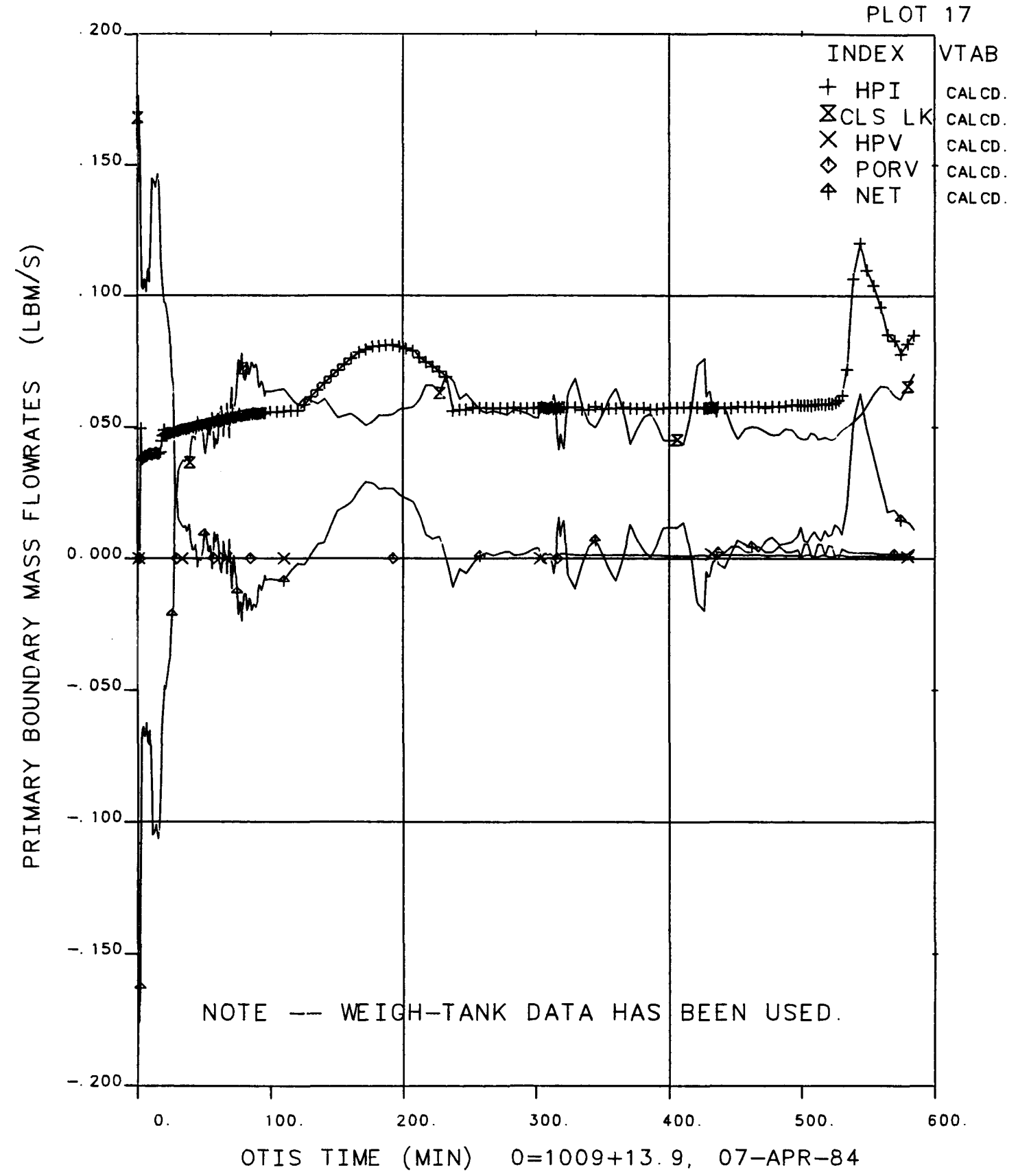

Figure 6.18 Primary Boundary Mass Flowrates Versus Time

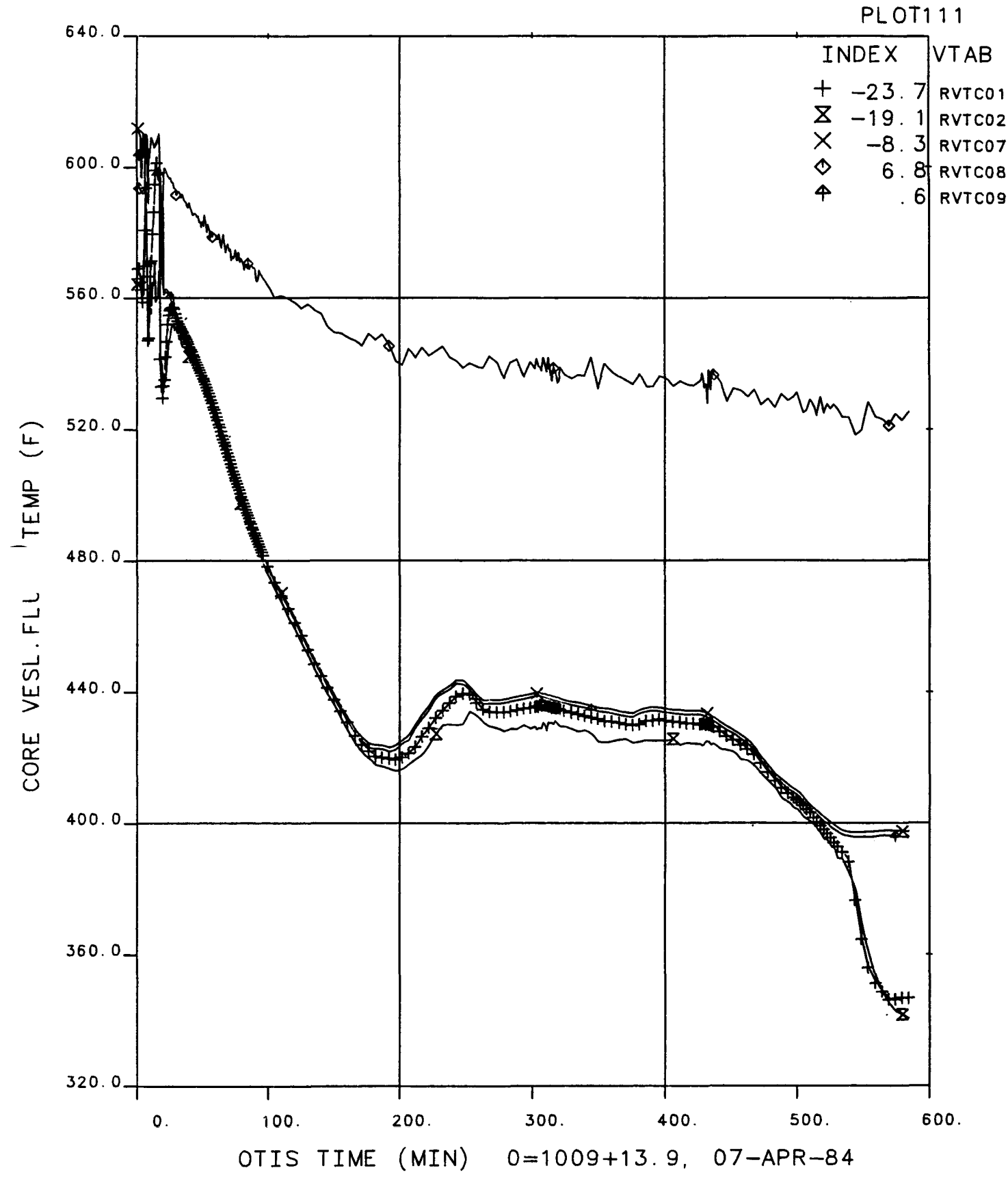

Figure 6.19 Core Vessel Fluid Temperatures Versus Time

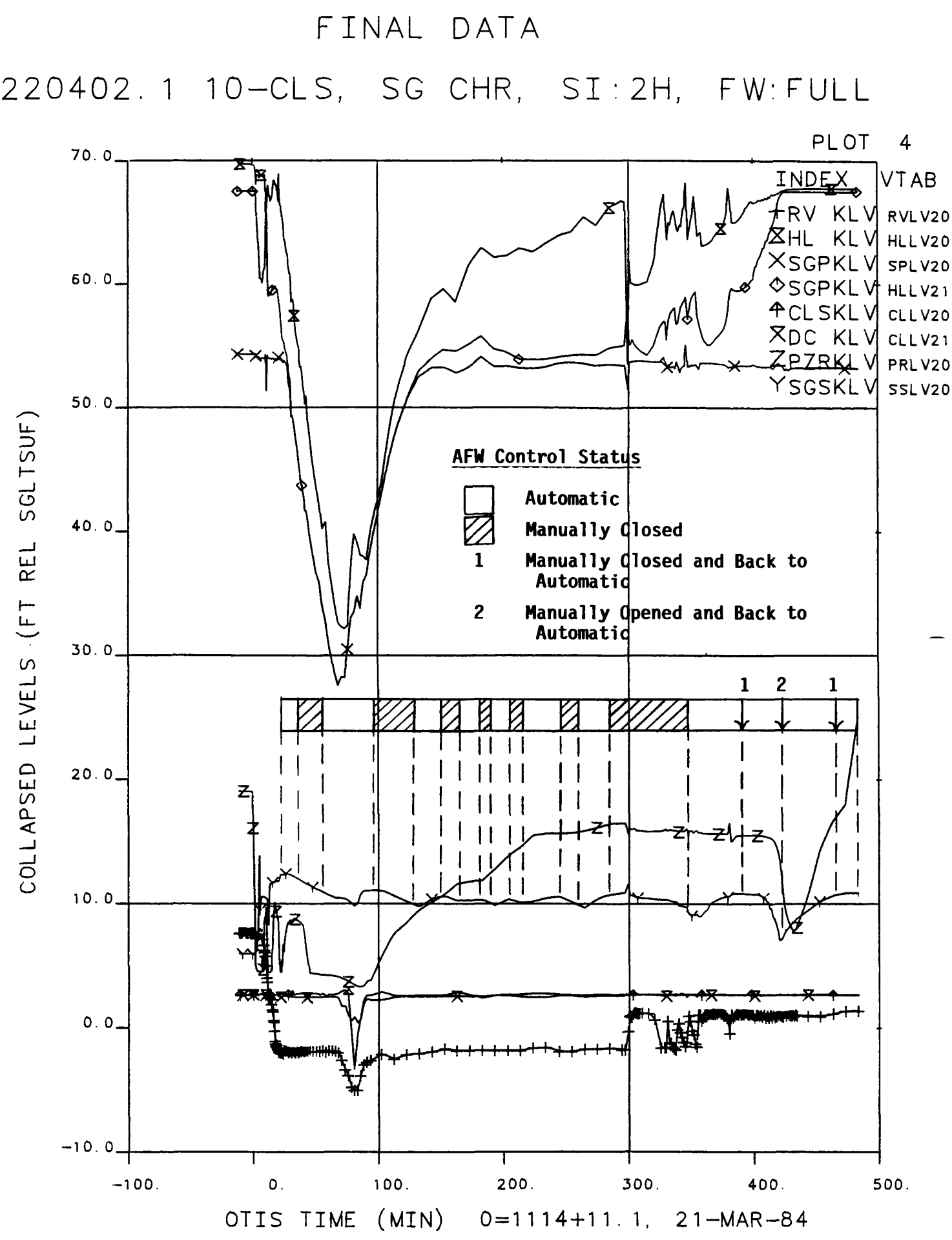

Figure 6.20 Collapsed Levels Versus Time

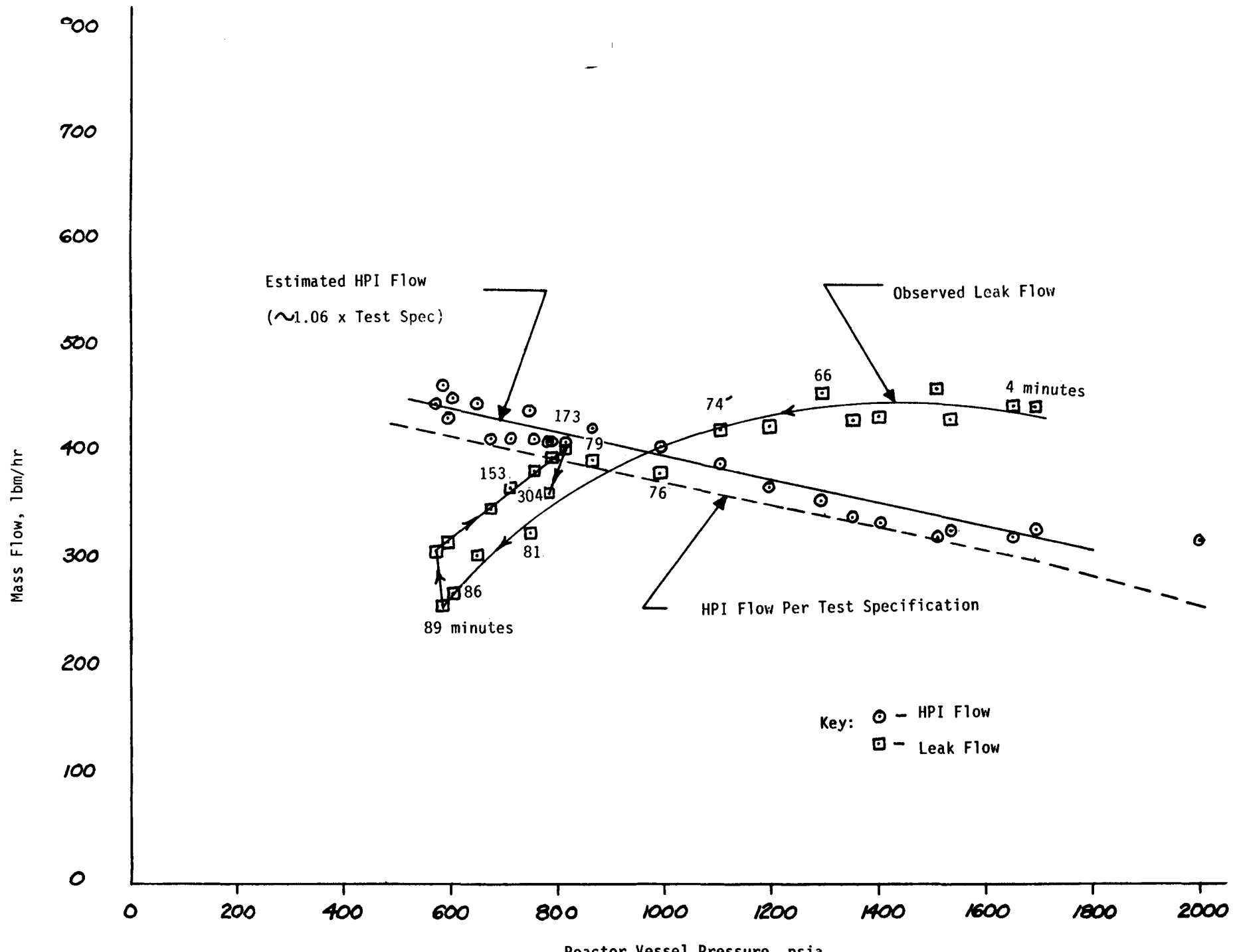

Figure 6.21 Mass Flow Vs Pressure OTIS Test 220402, 10-ft SG Level.

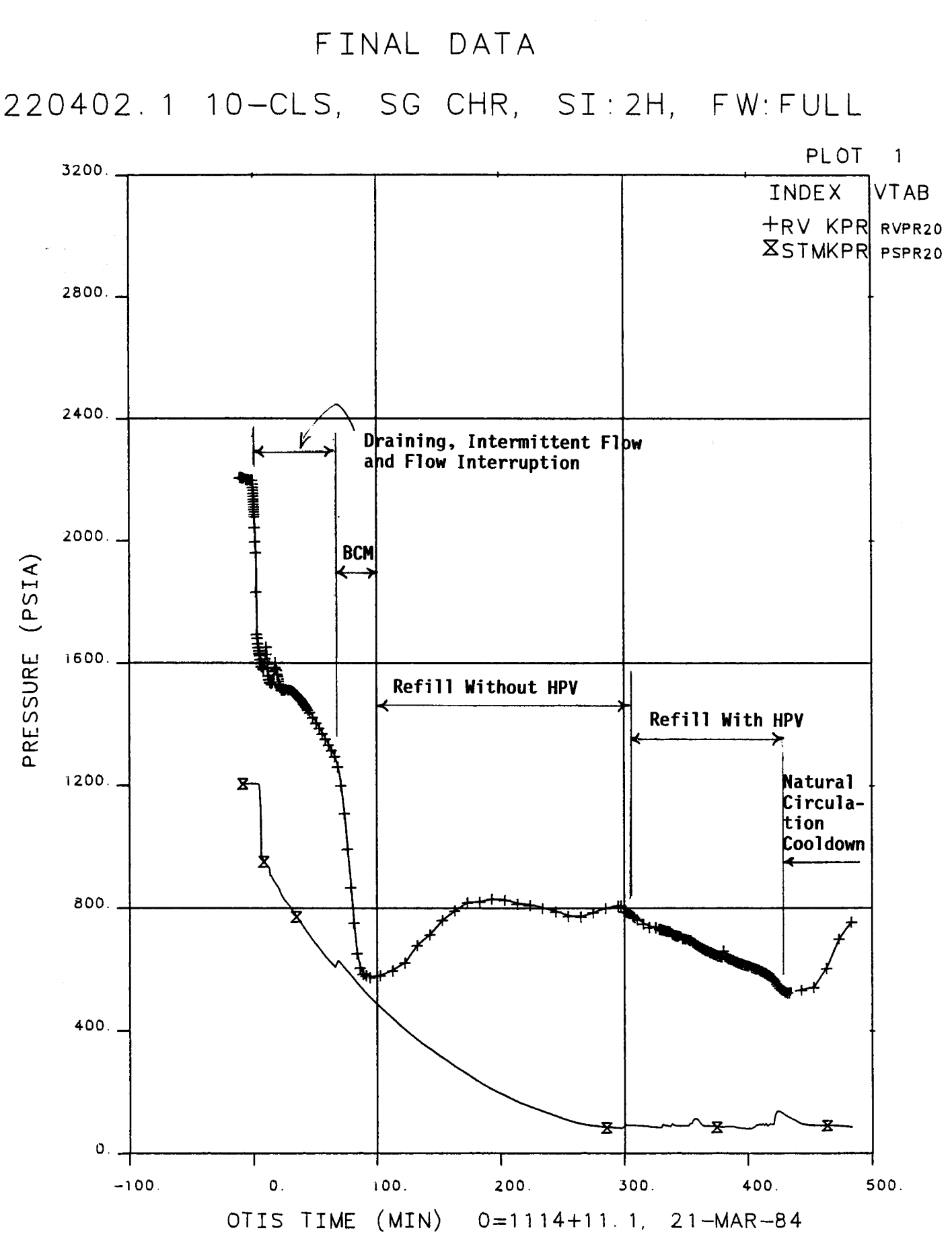

Figure 6.22 Primary and Secondary Pressure Versus Time Showing Key Events

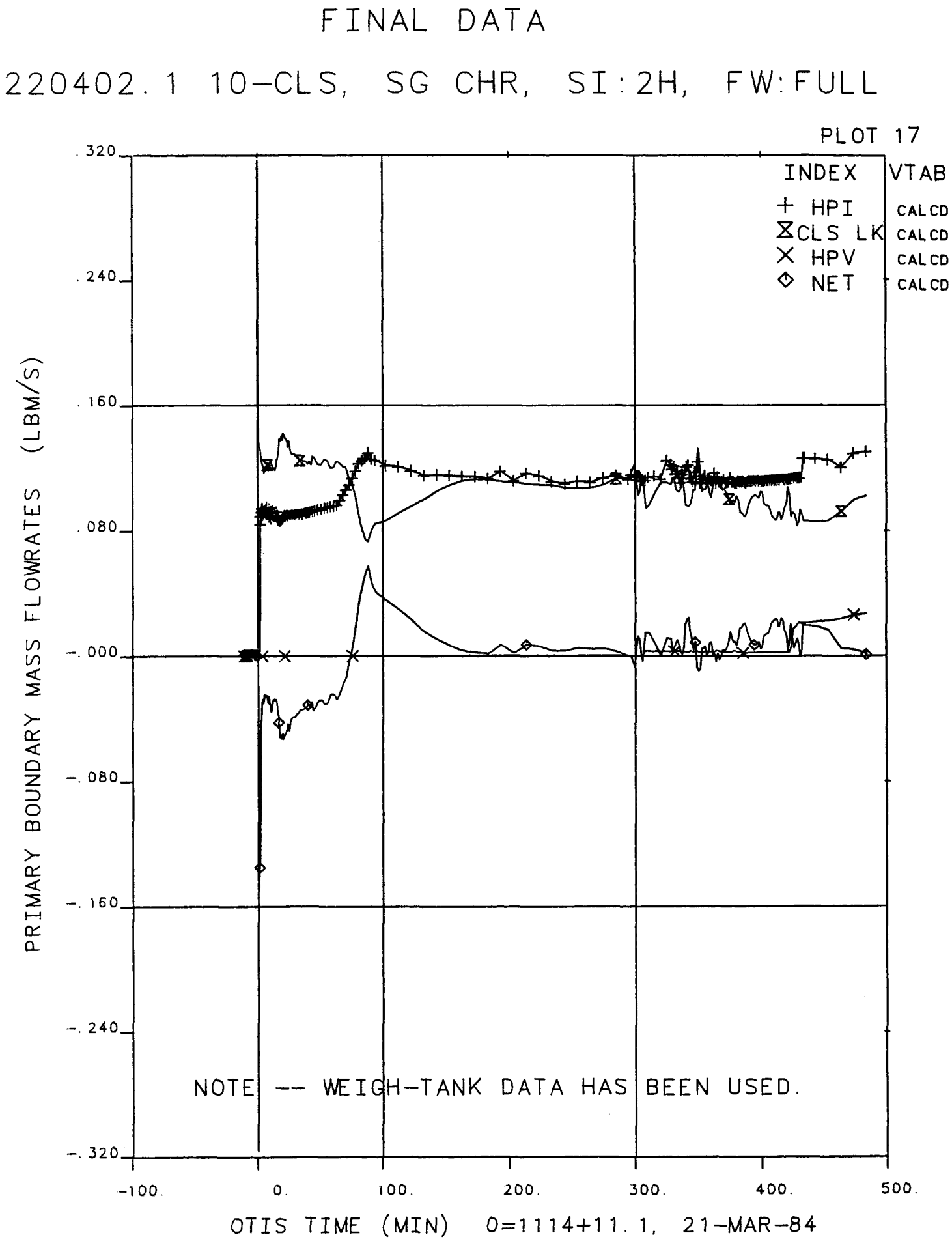

Figure 6.23 Primary Boundary Mass Flowrates Versus Time

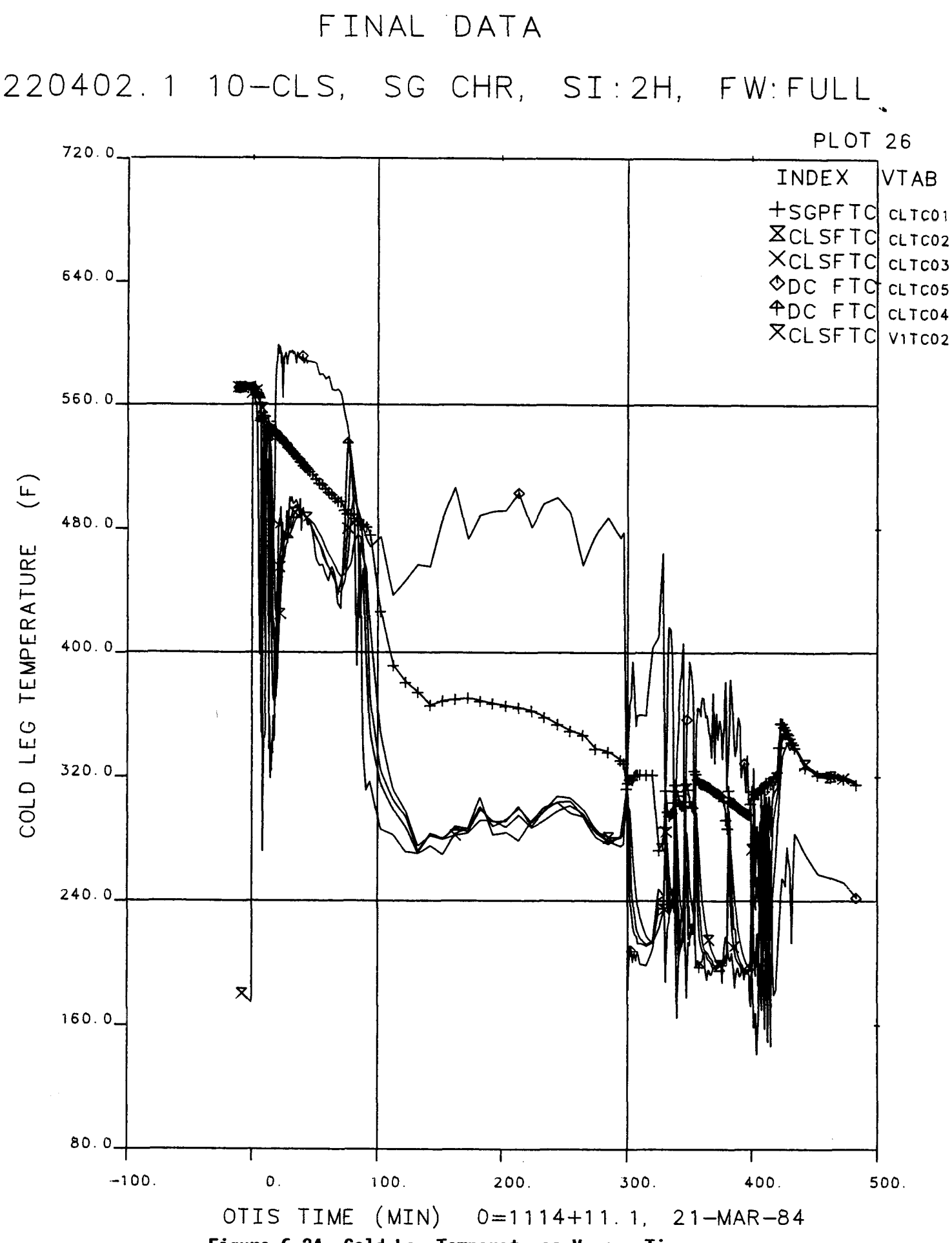

Figure 6.24 Cold Leg Temperatures Versus Time

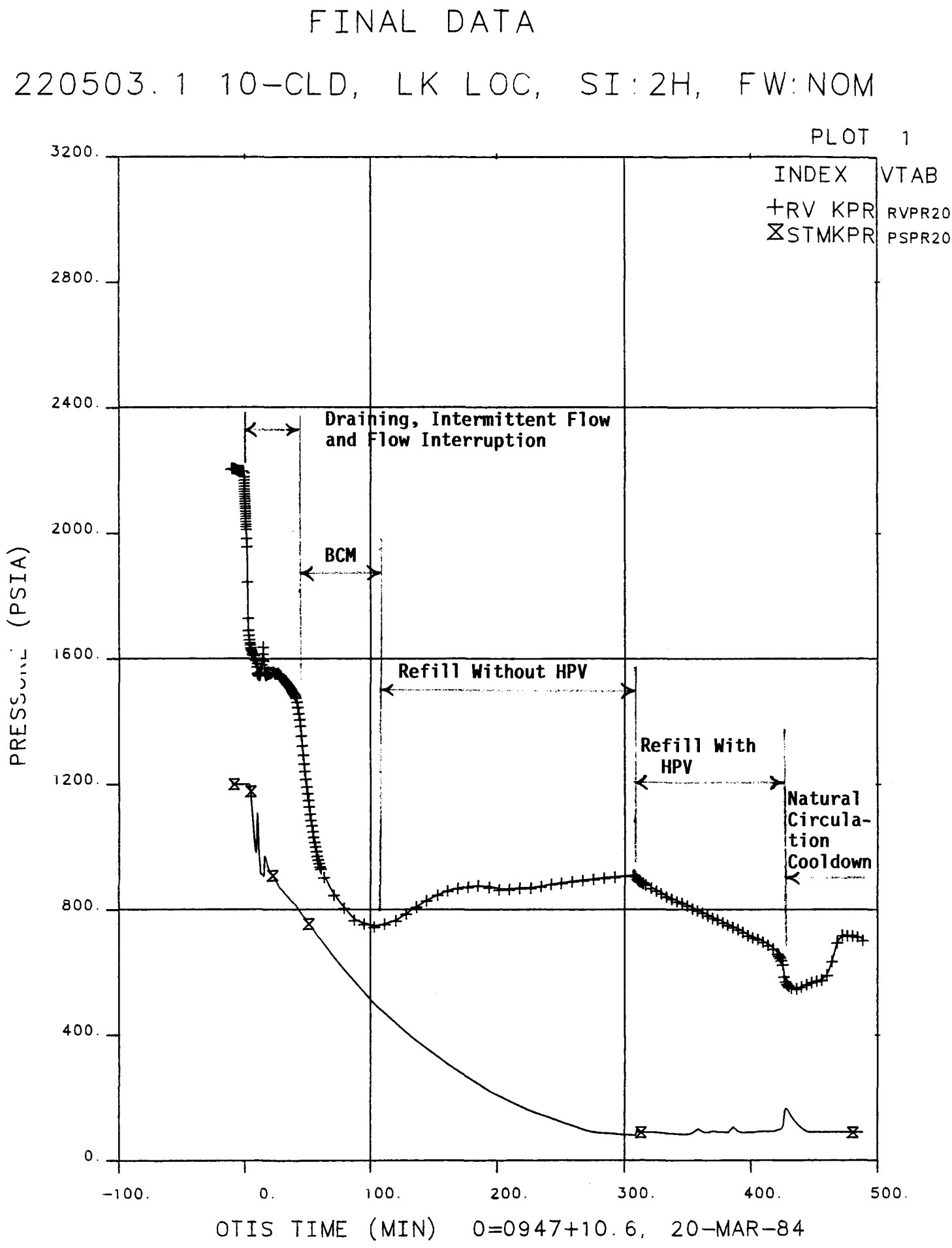

Figure 6.25 Primary and Secondary Pressure Versus Time Showing Key Events

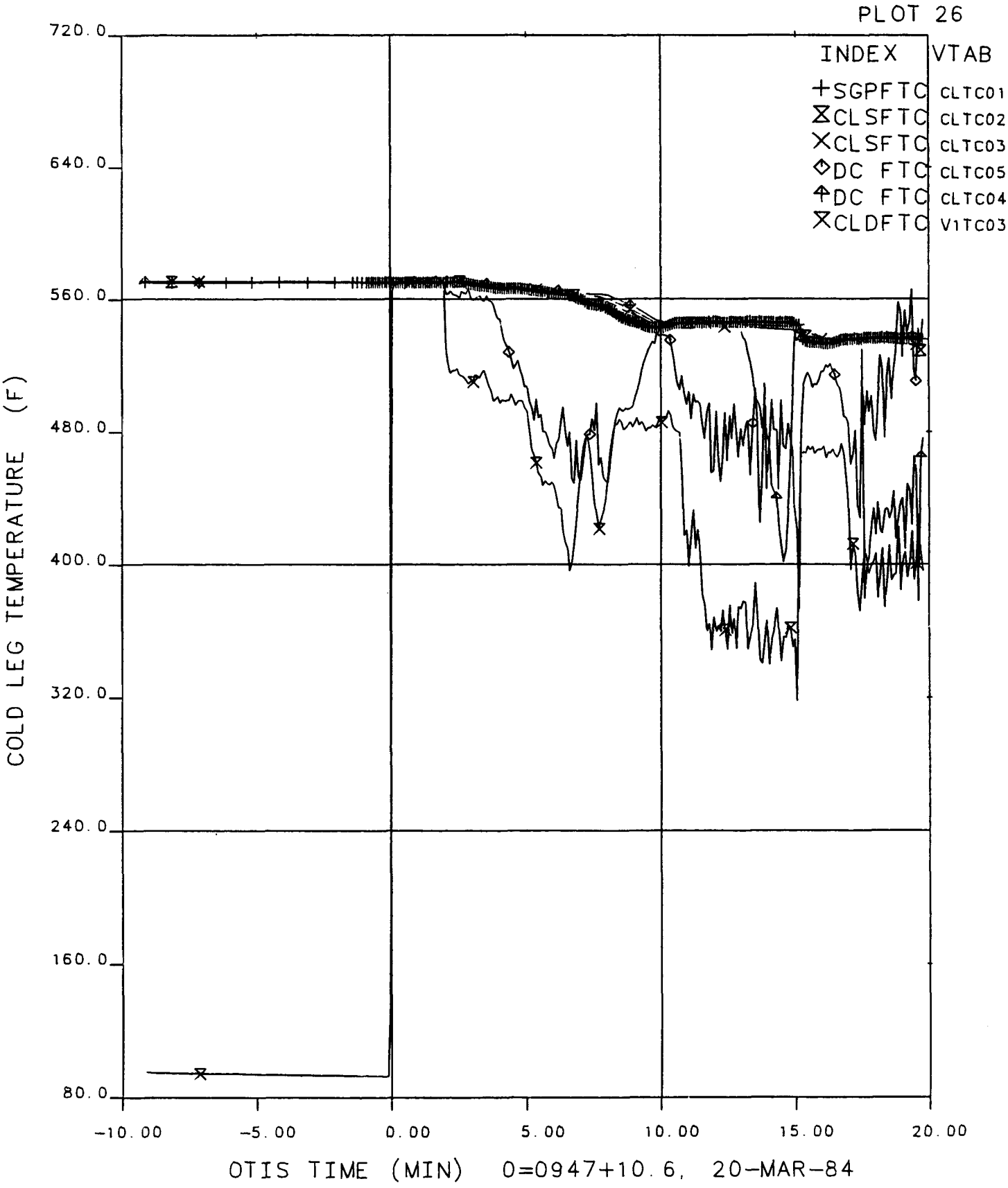

Figure 6.26 Cold Leg Temperatures Versus Time

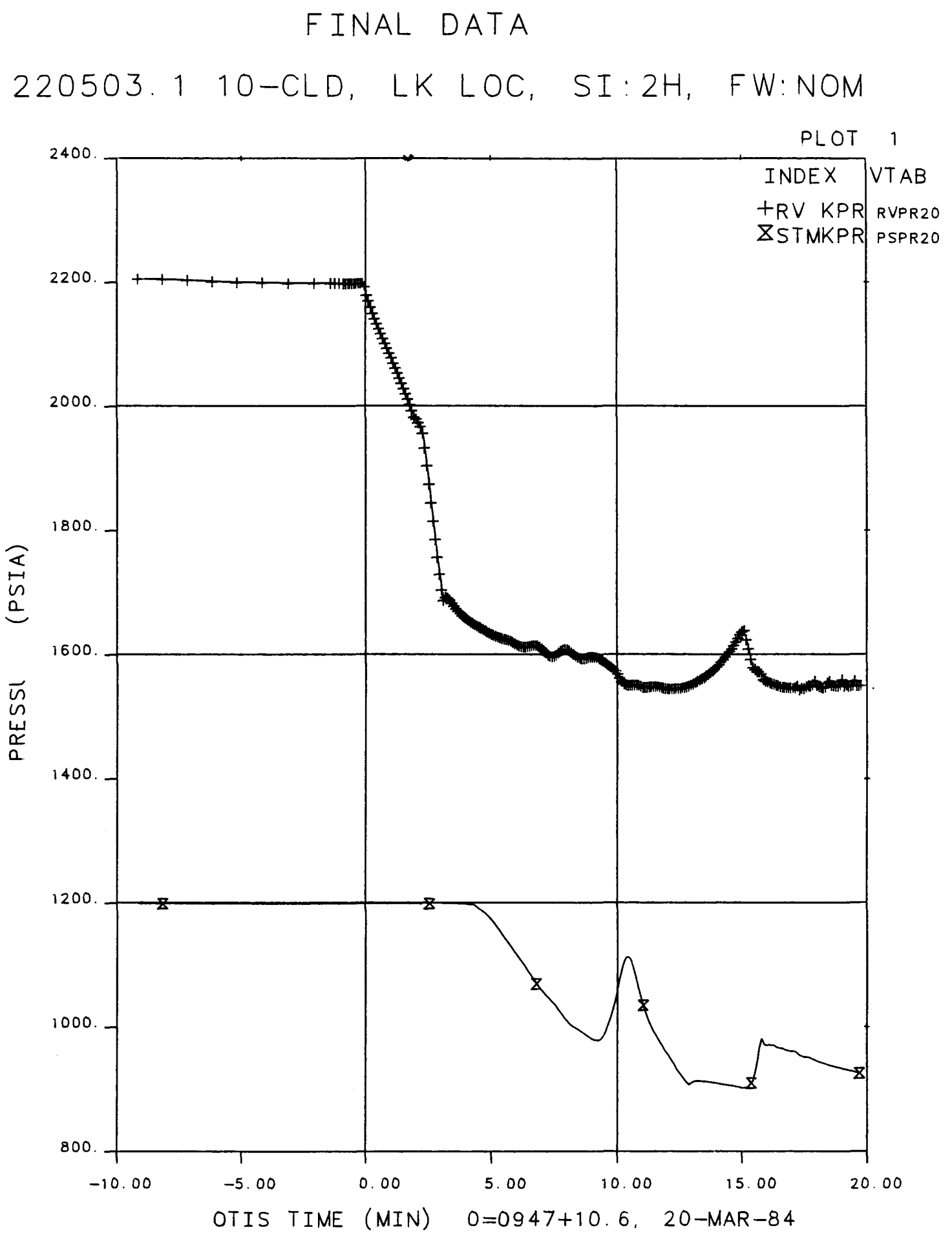

Figure 6.27 Primary and Secondary Pressure Versus Time

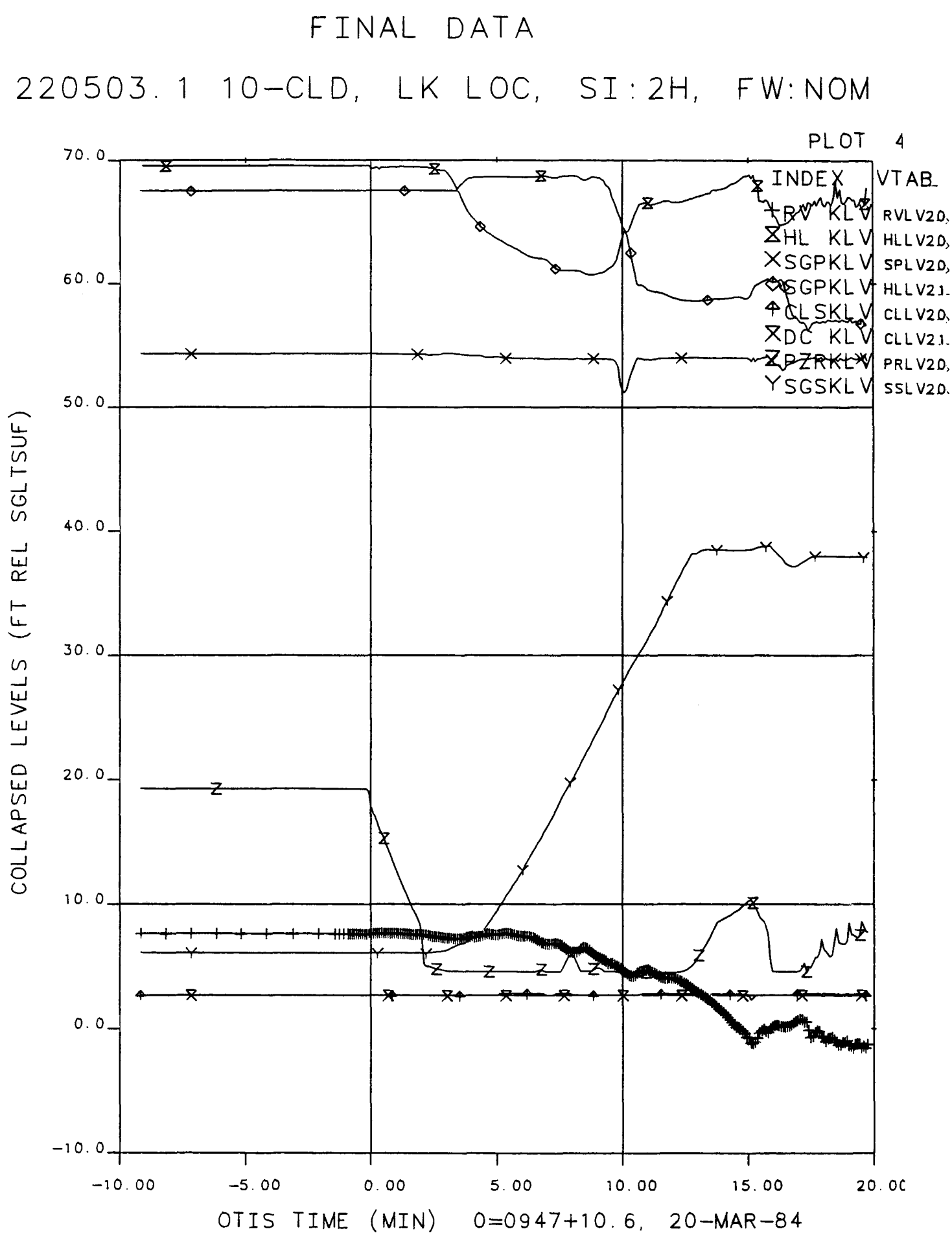

Figure 6.28 Collapsed Liquid Levels Versus Time

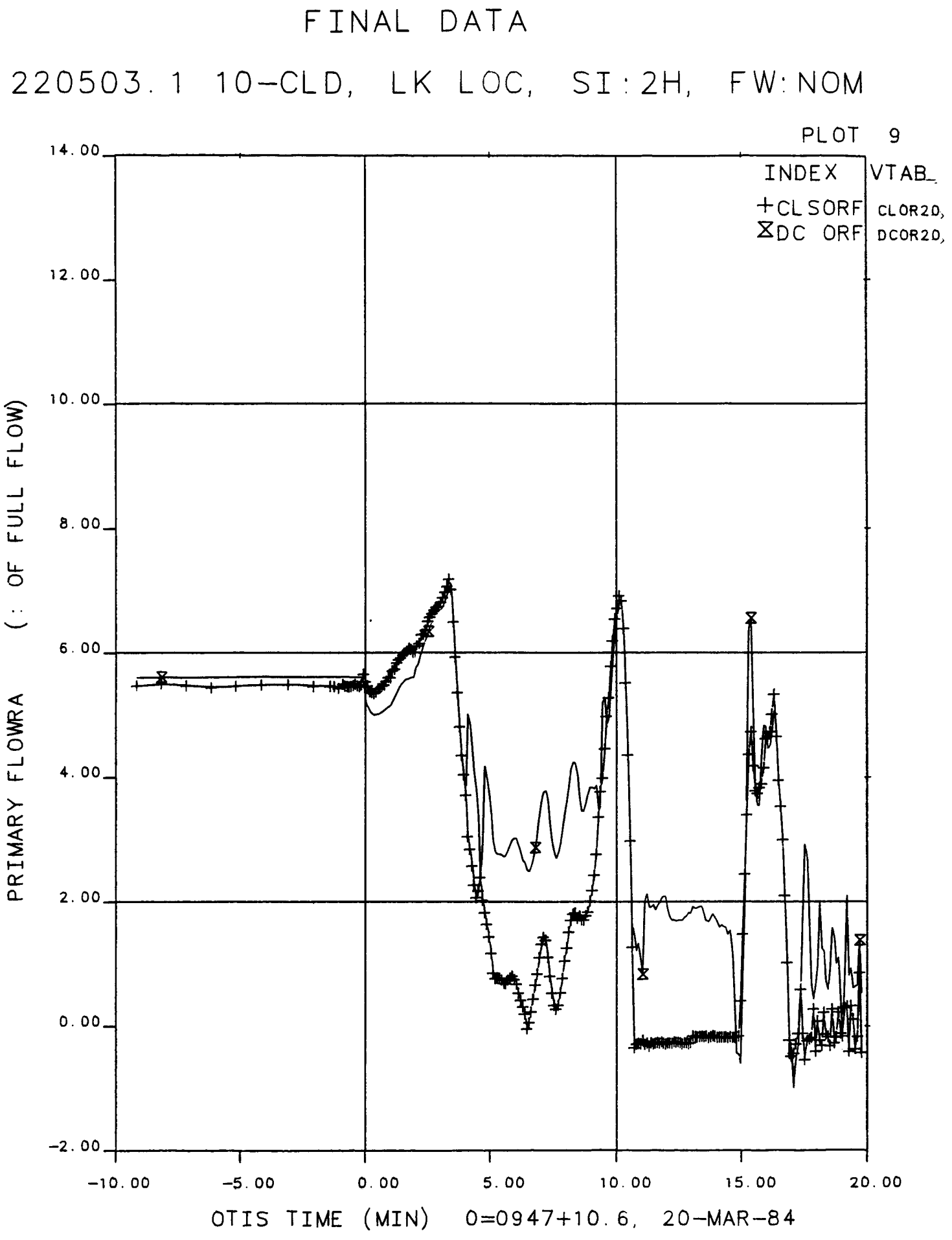

Figure 6.29 Primary FLowrates Versus Time

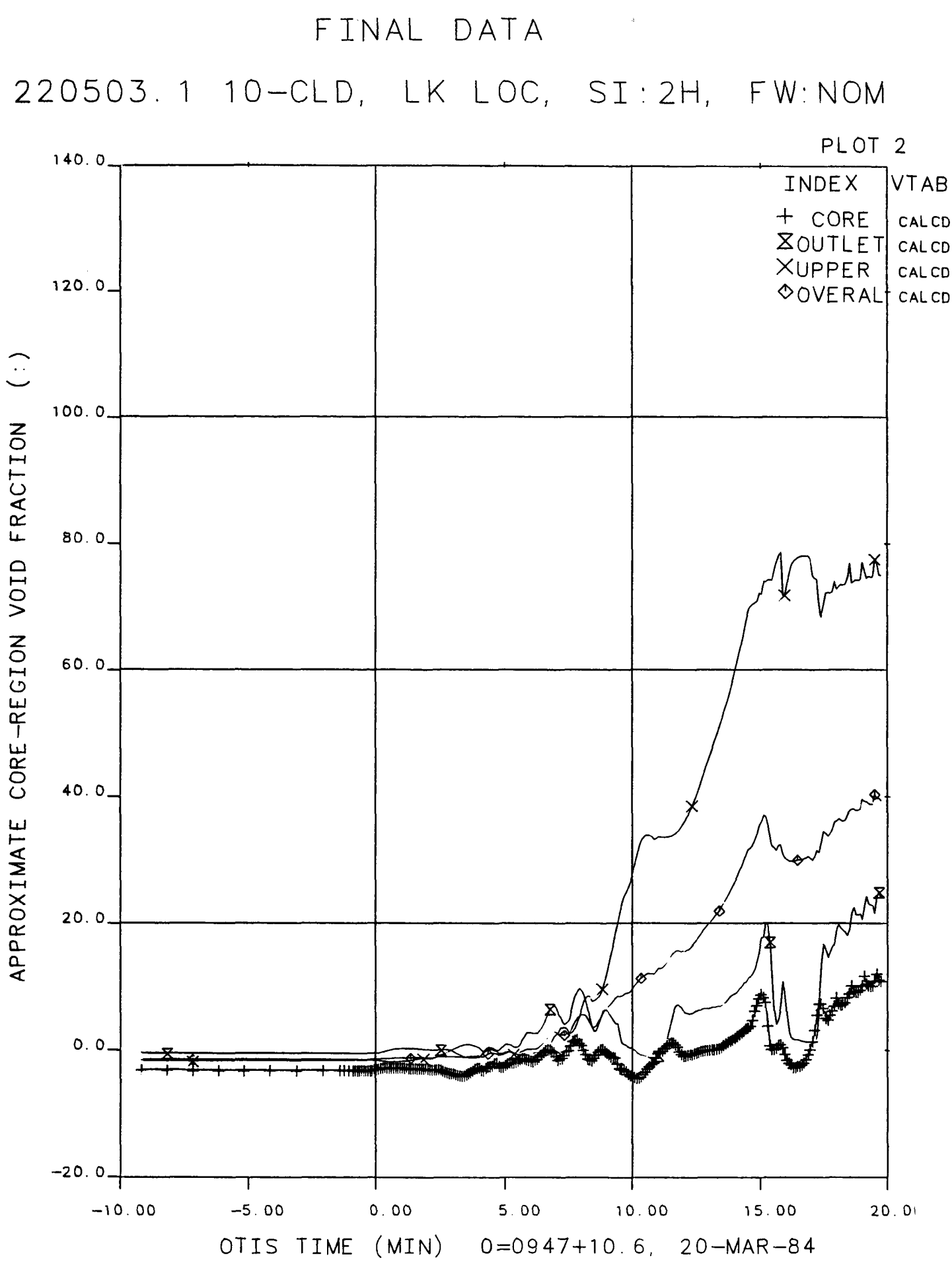

Figure 6.30 Core Region Void Fractions Versus Time

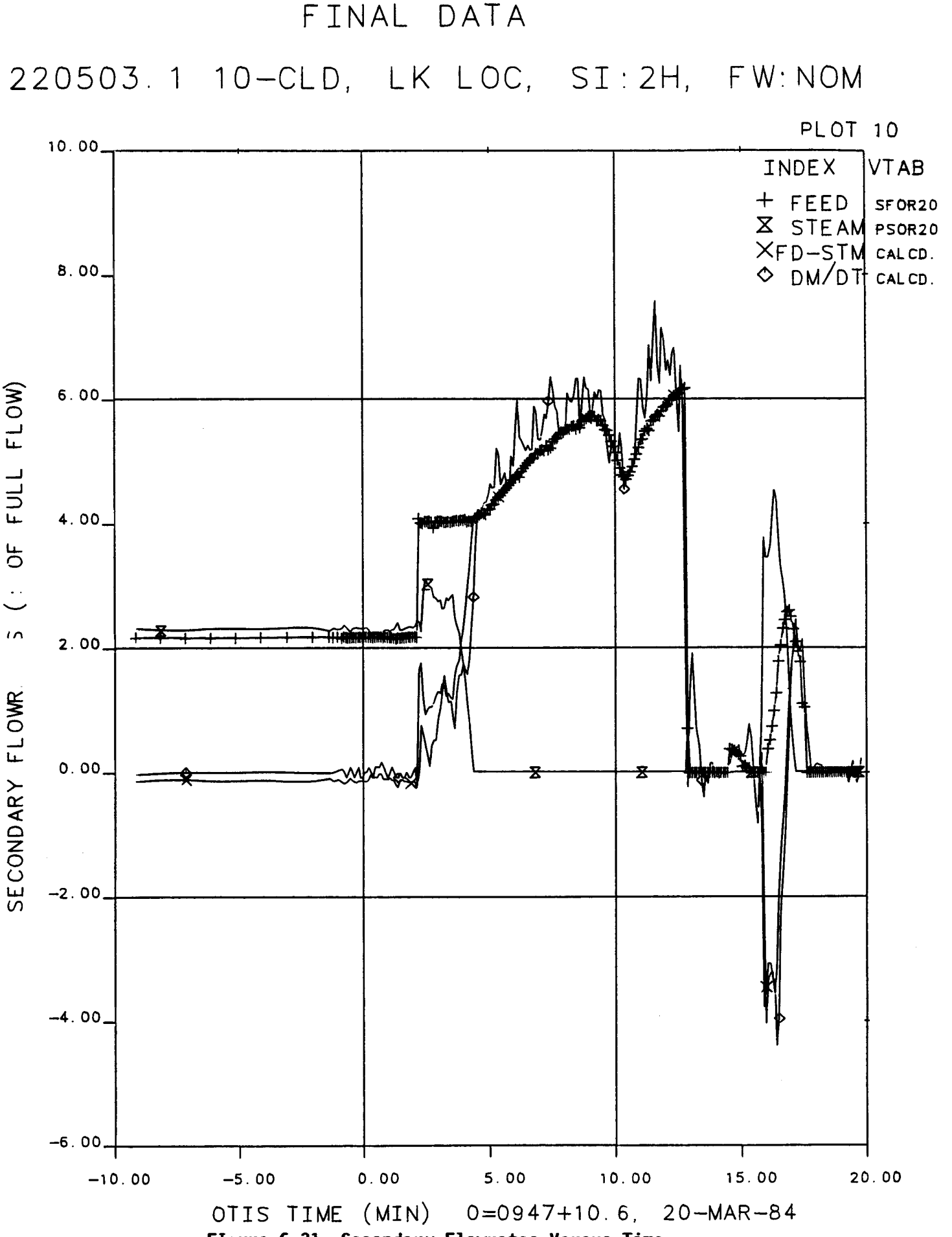

FIgure 6.31 Secondary Flowrates Versus Time

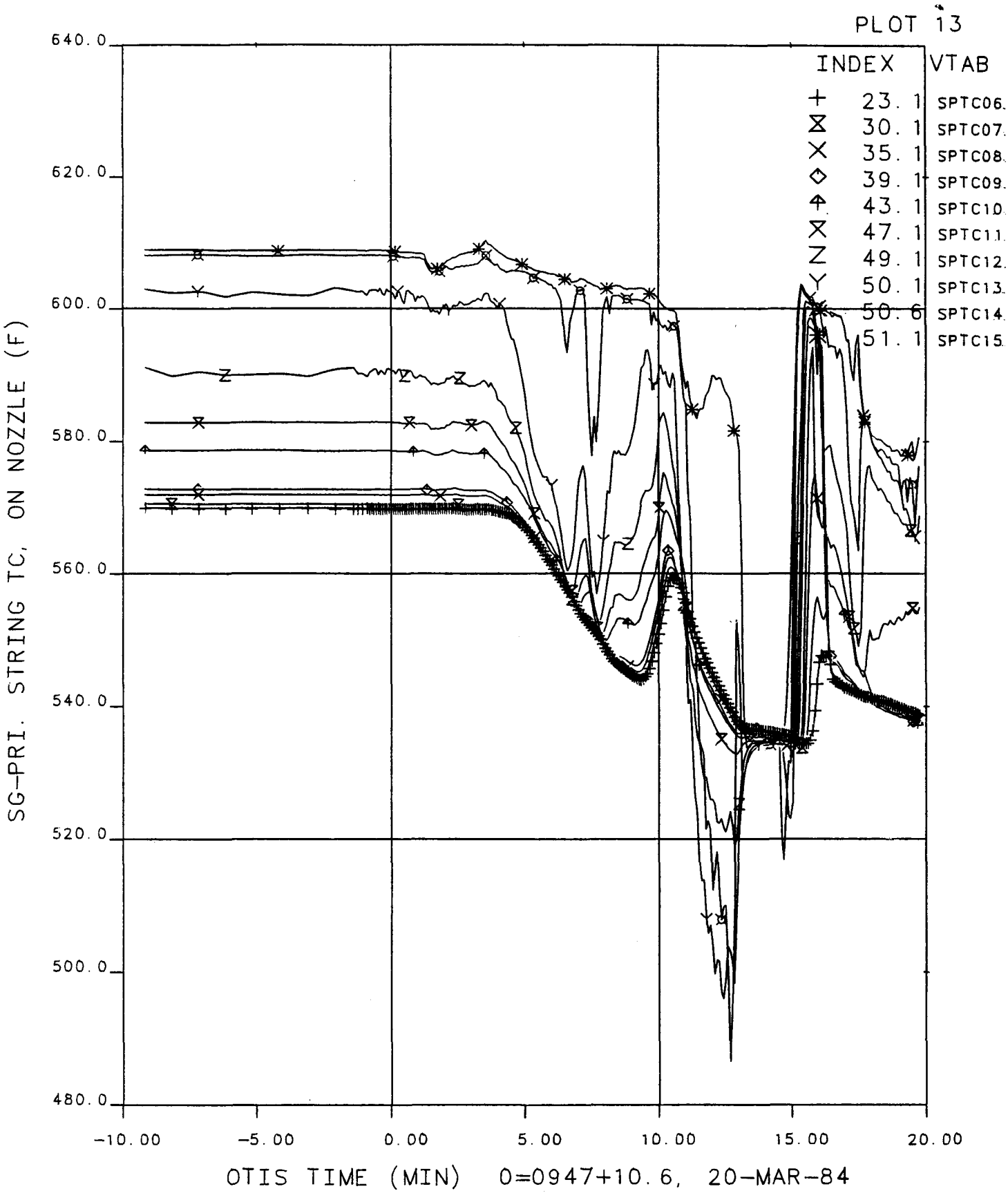

Figure 6.32 Steam Generator Primary Fluid Temperatures Versus Time

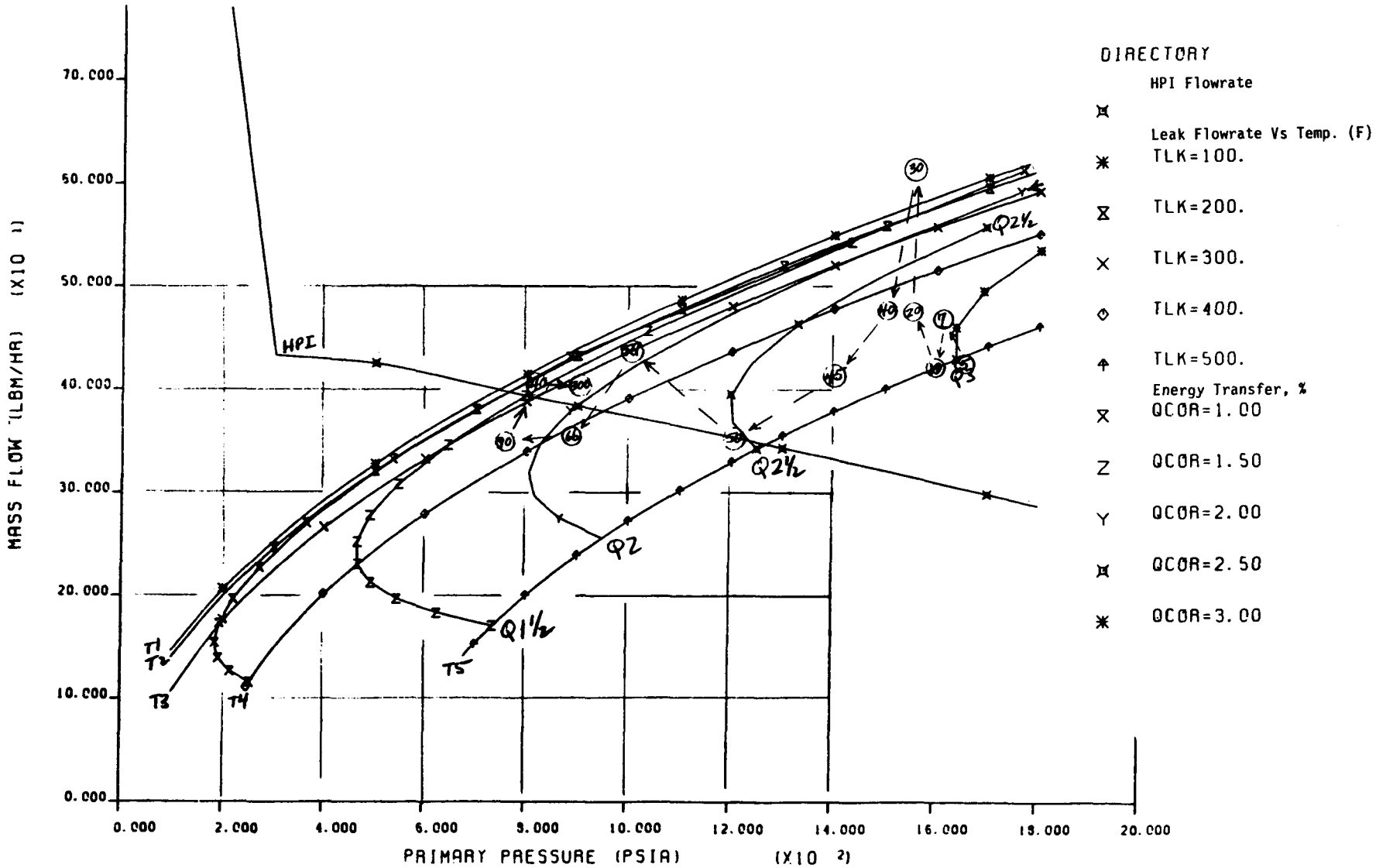

Figure 6.33 Transient Leak Flow Rate Vs System Conditions, Test 220503.
(Refer to Appendix C for an explanation of this "equilibrium plot")

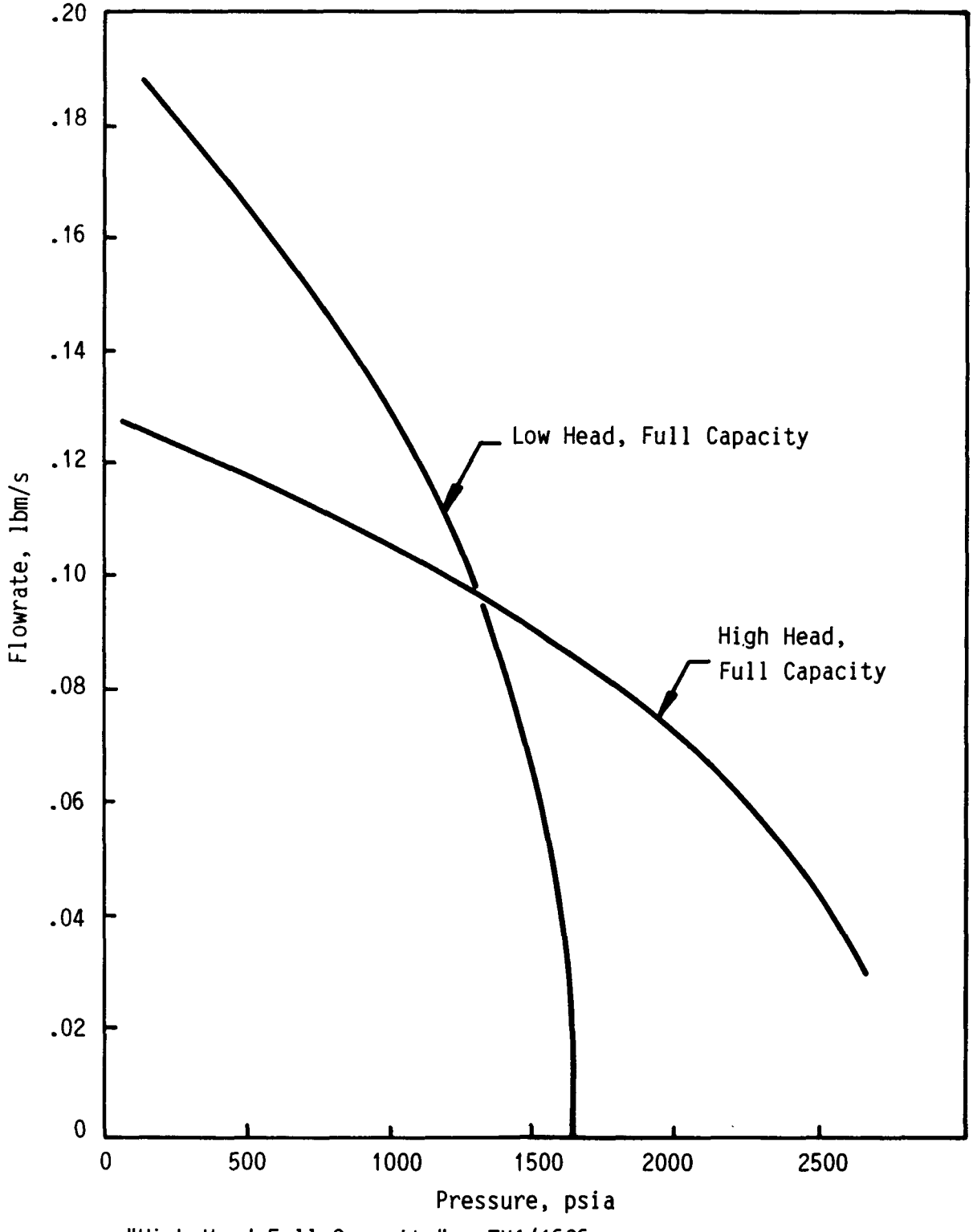

"High Head Full Capacity": TVA/1686
"Low Head, Full Capacity": DB/1300

Full Capacity Denotes the Simulation of Two Plant HPI Pumps

Figure 6.34

HPI Characteristics

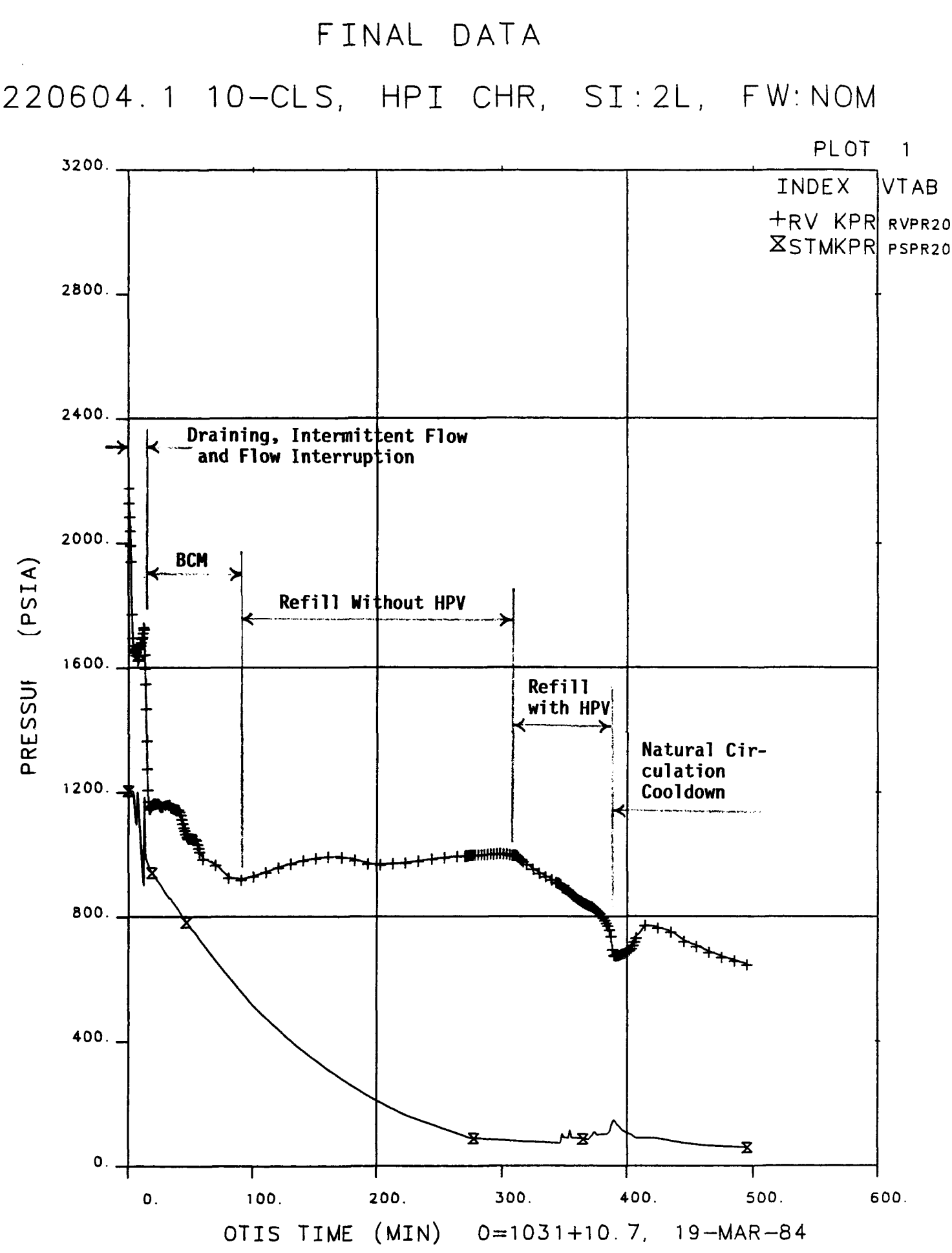

Figure 6.35 Primary and Secondary Pressure Versus Time Showing Key Test Phases

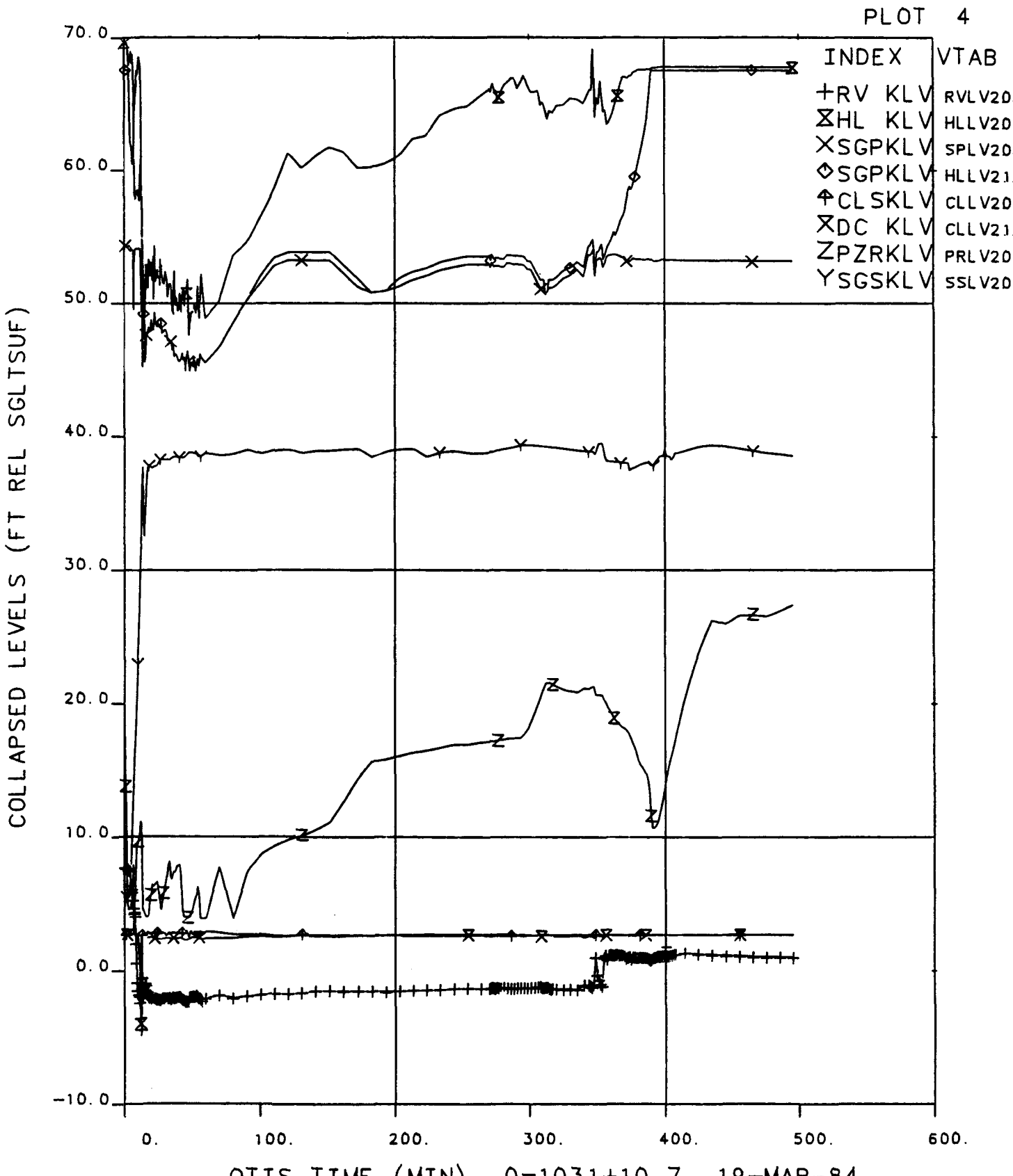

Figure 6.36 Collapsed Levels Versus Time

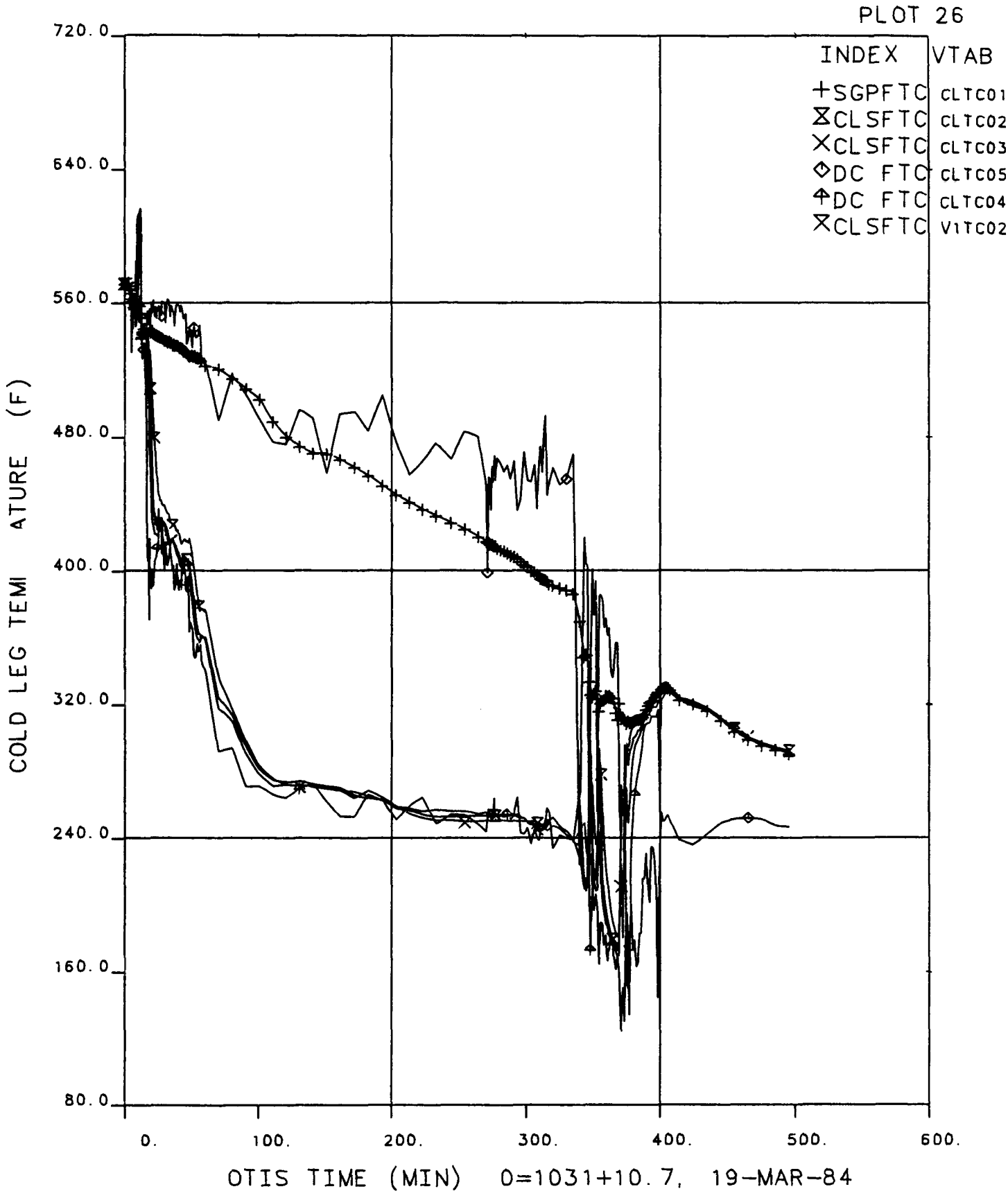

Figure 6.37 Cold Leg Temperatures Versus Time

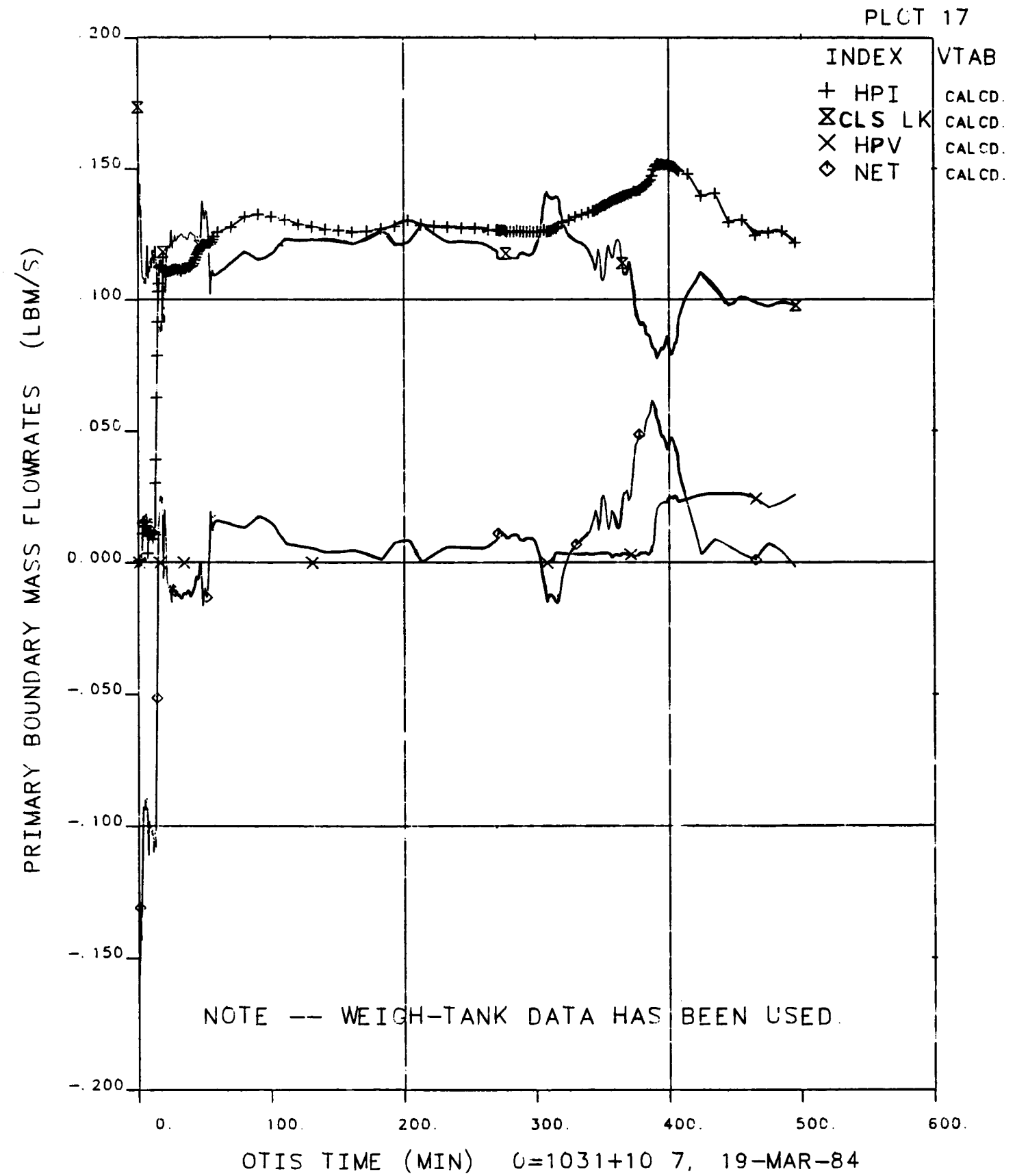

Figure 6.38 Primary Boundary Mass Flowrates Versus Time

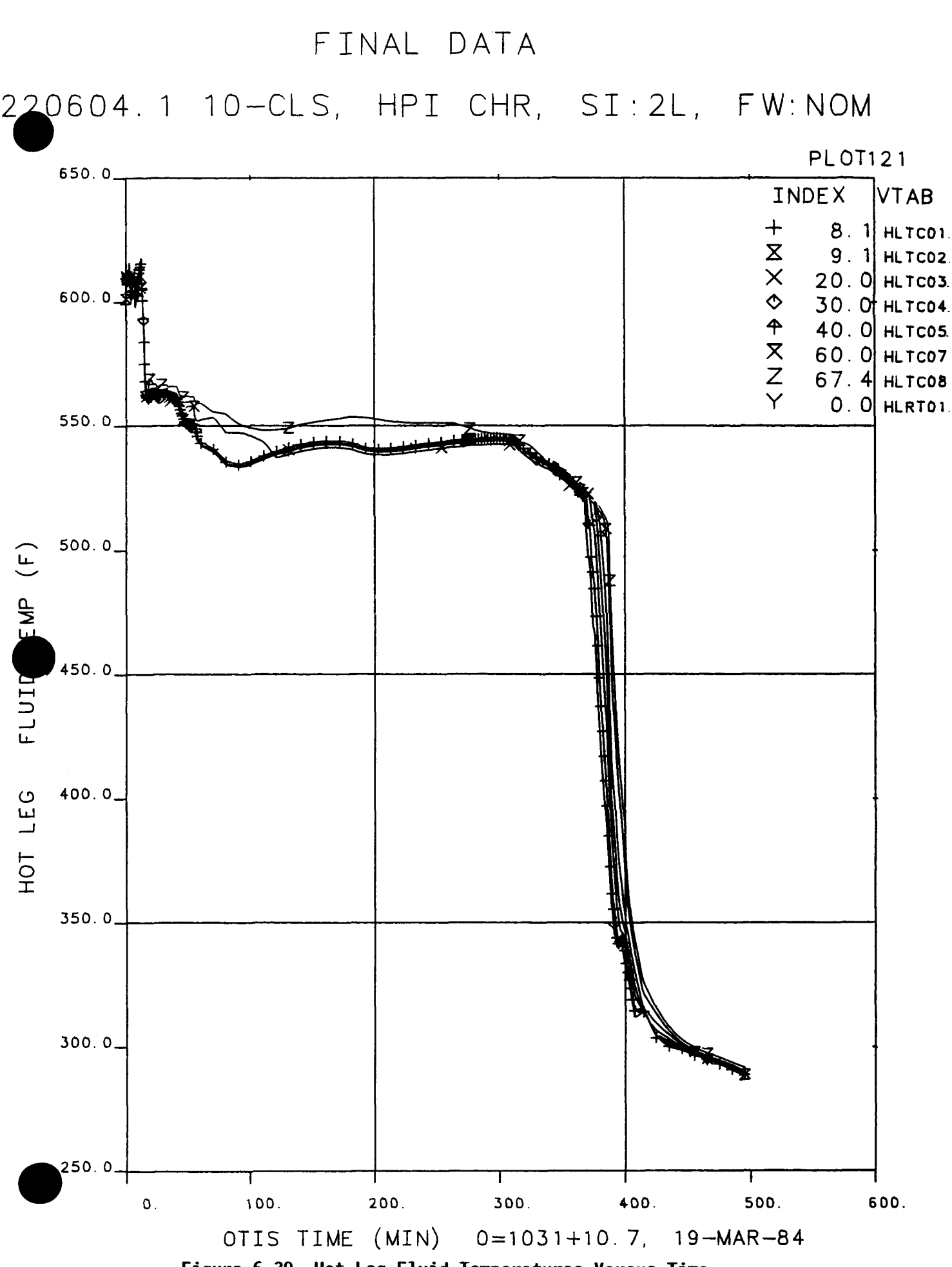

Figure 6.39 Hot Leg Fluid Temperatures Versus Time

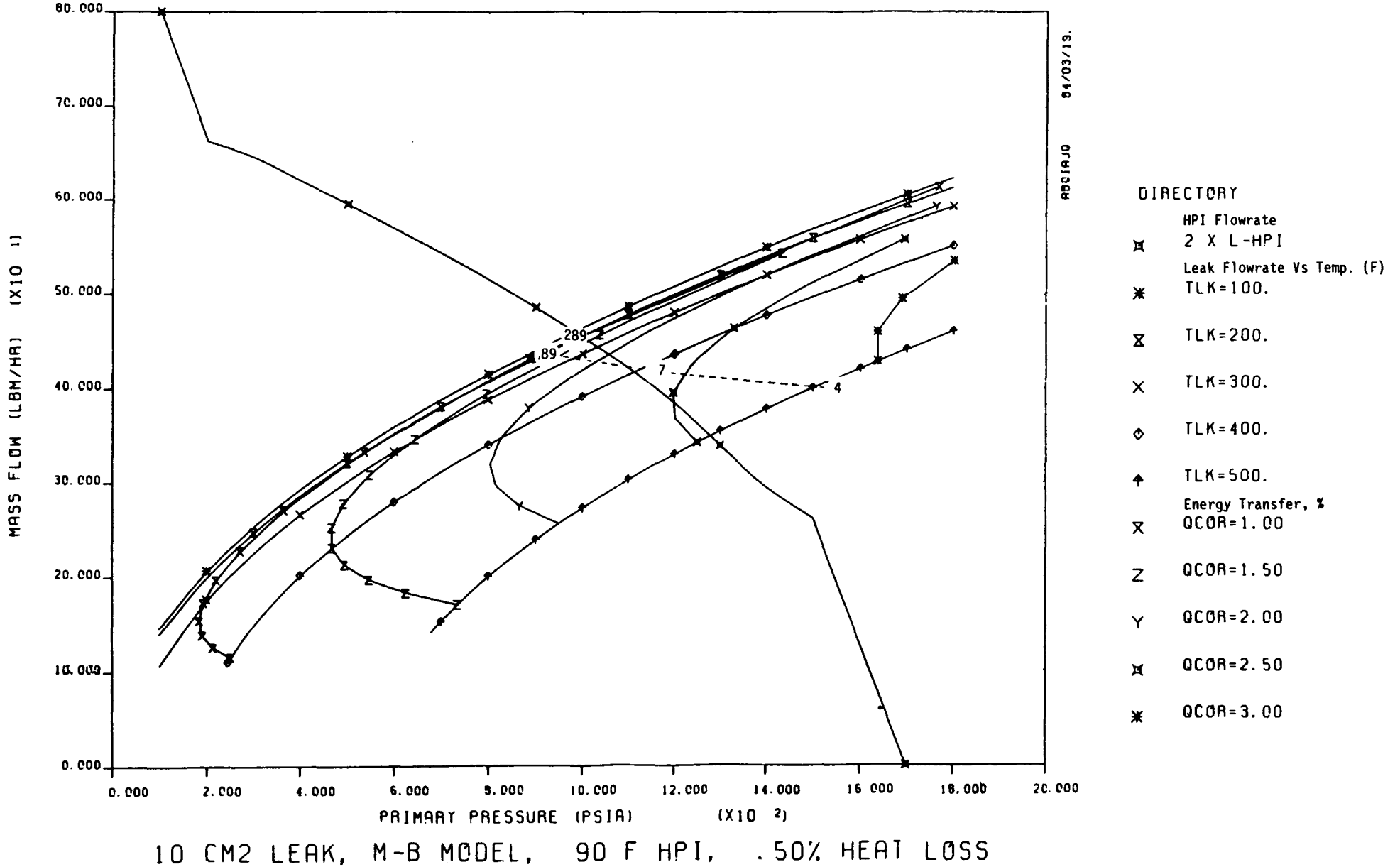

Figure 6.40 Critical Flow Vs Pressure at Several Temperatures Test 220604, Low-Head HPI (Refer to Appendix C for a description of this "equilibrium plot").

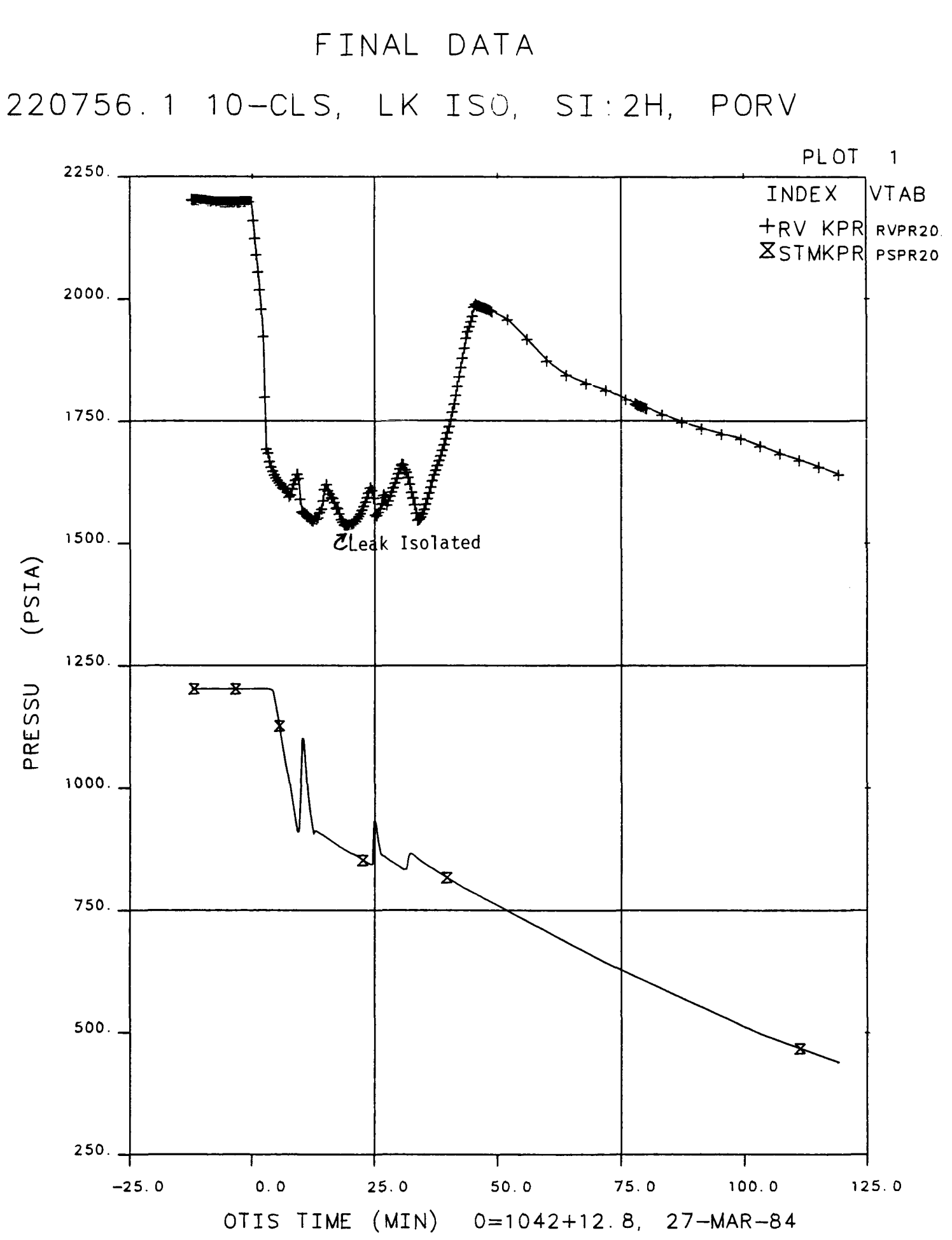

Figure 6.41 Primary and Secondary Pressure Versus Time

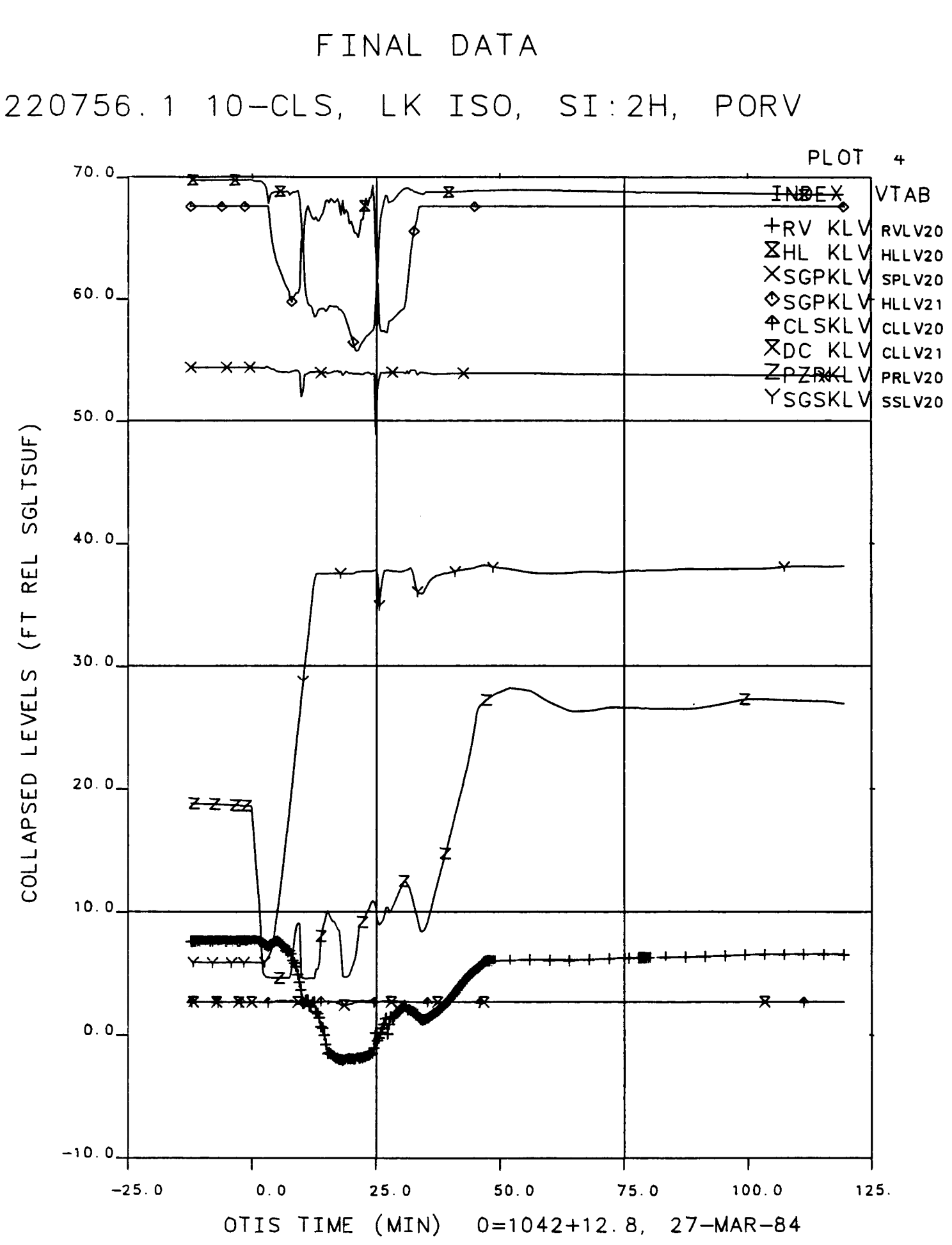

Figure 6.42 Collapsed Levels Versus Time

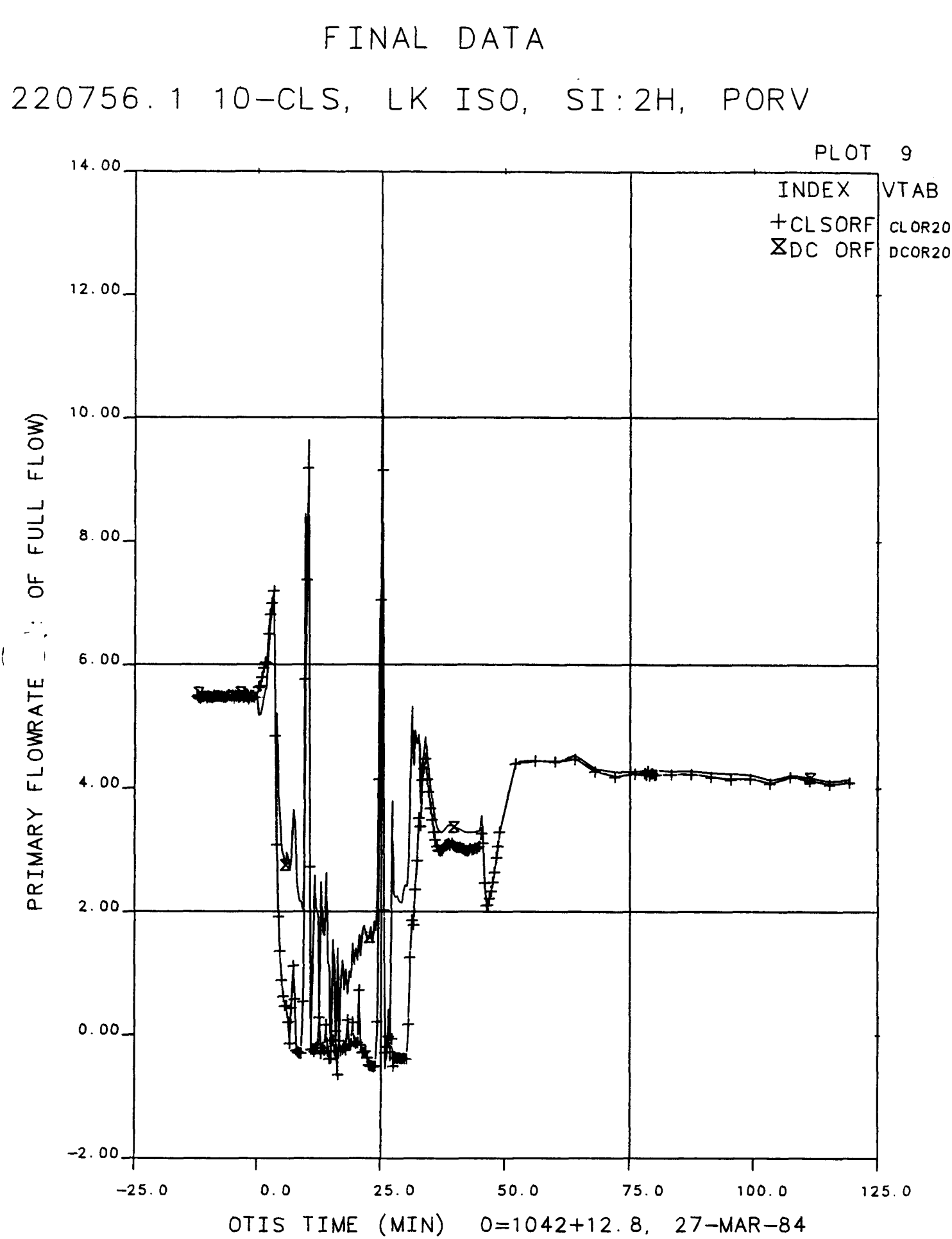

Figure 6.43 Primary Flowrates Versus Time

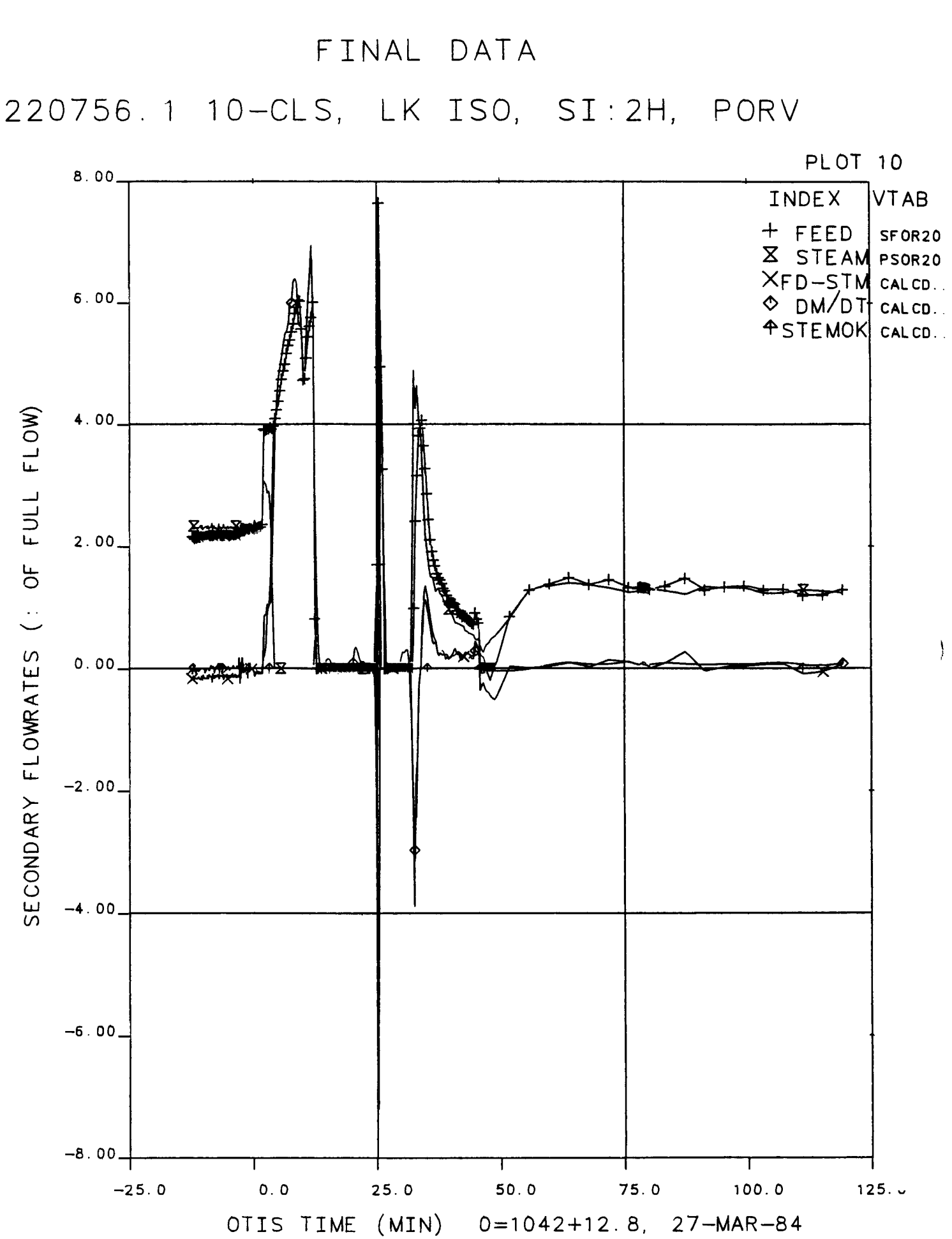

Figure 6.44 Secondary Flowrates Versus Time

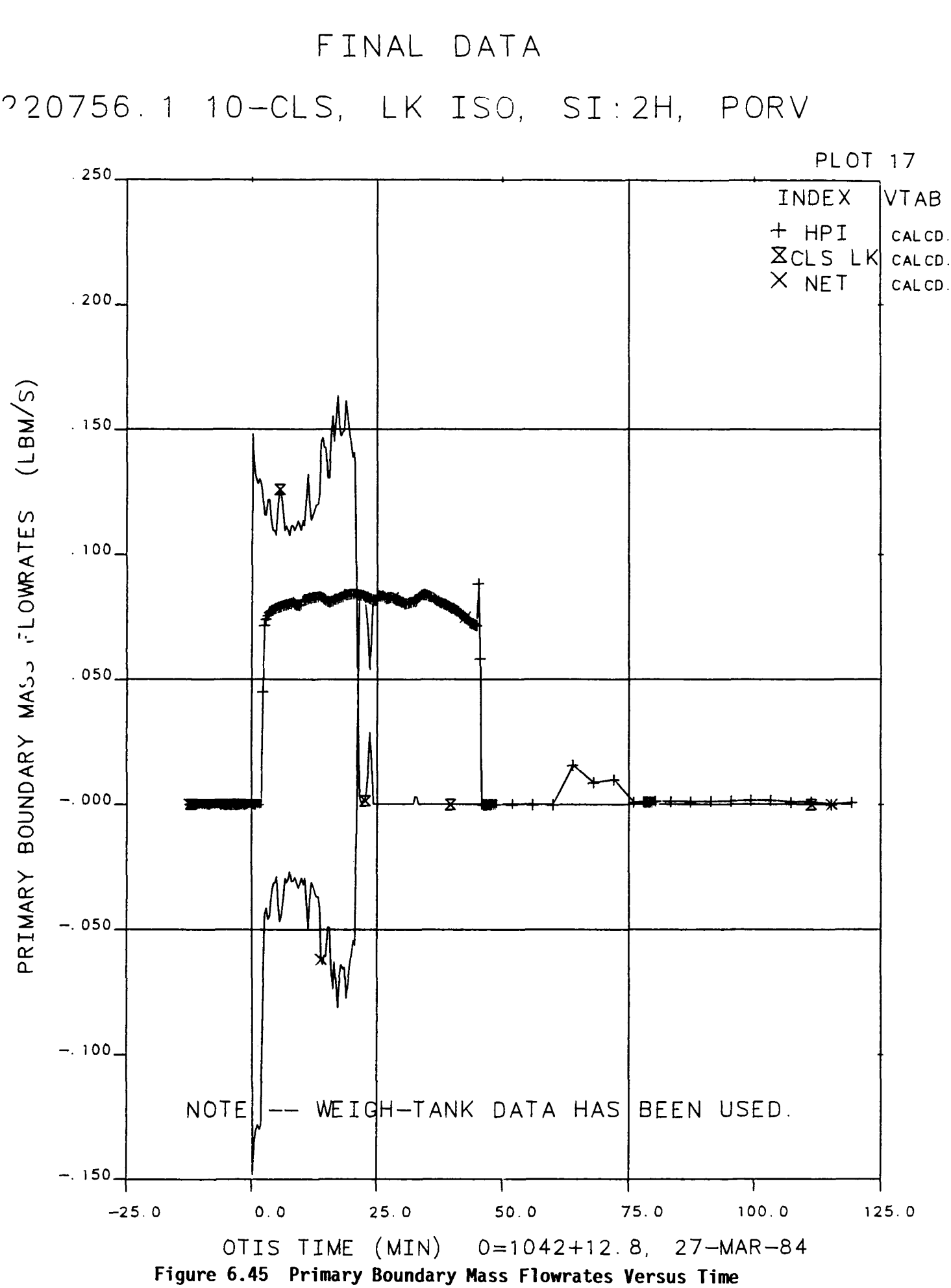

Figure 6.45 Primary Boundary Mass Flowrates Versus Time

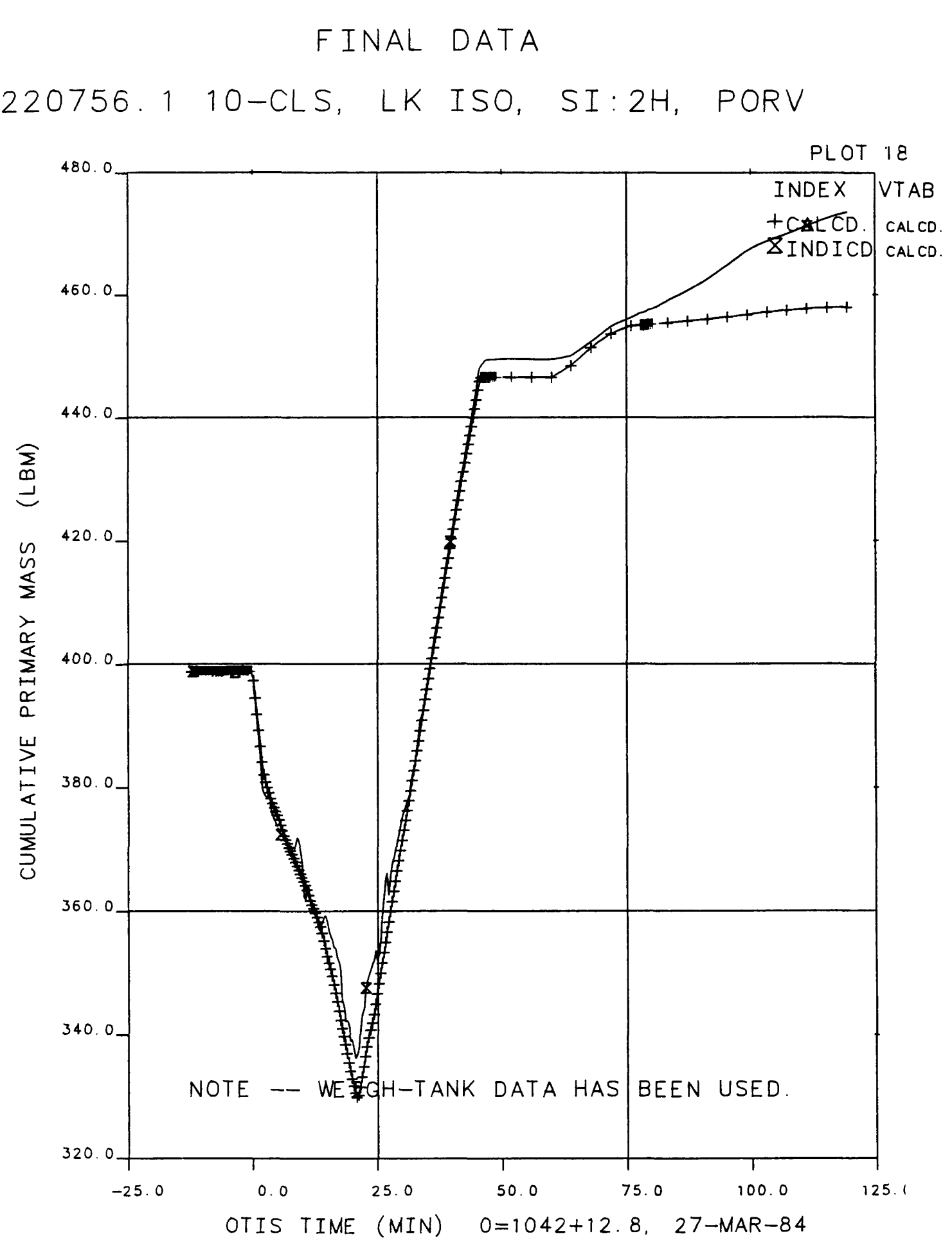

Figure 6.46 Cumulative Primary Mass Versus Time

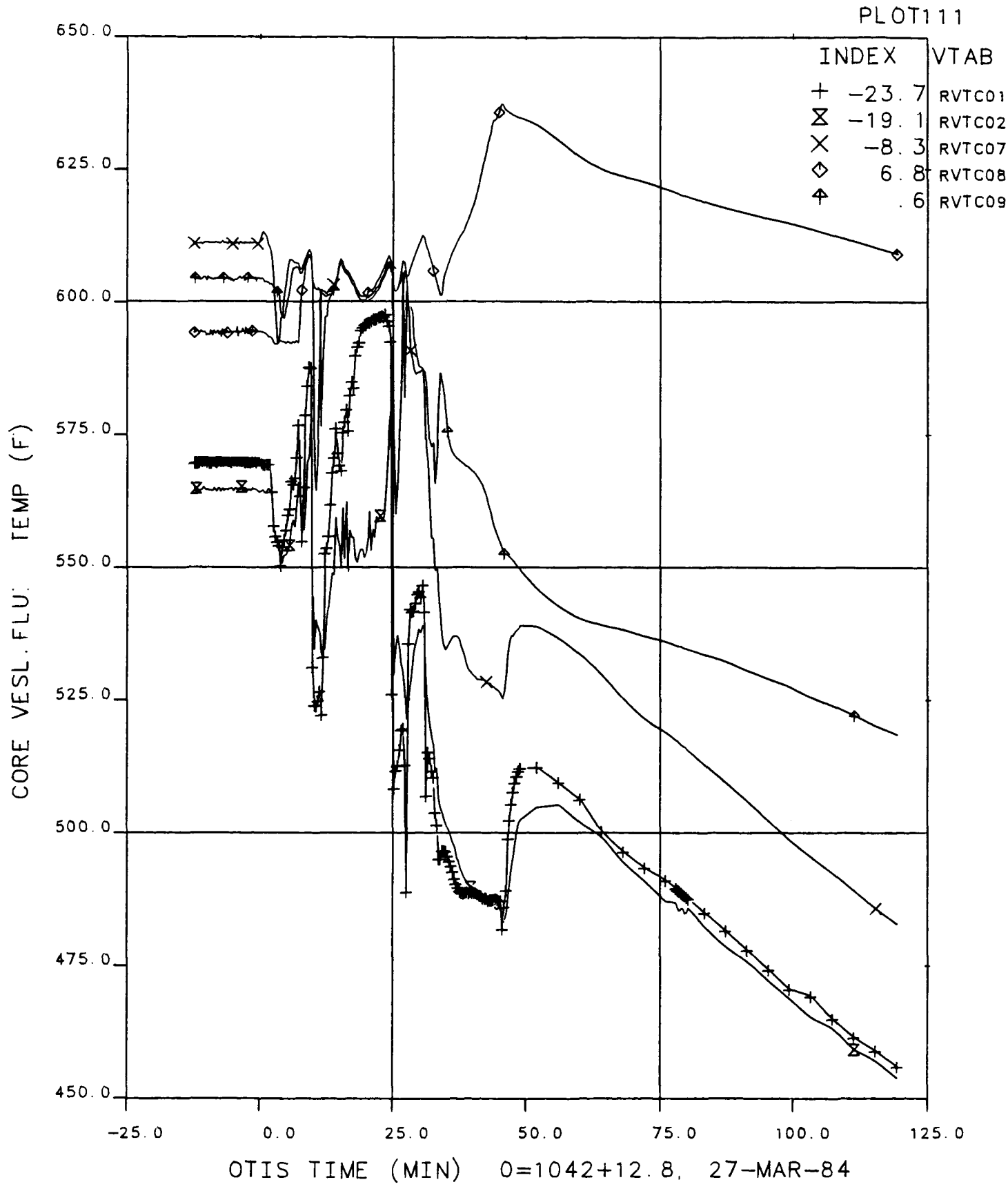

Figure 6.47 Core Vessel Fluid Temperatures Versus Time

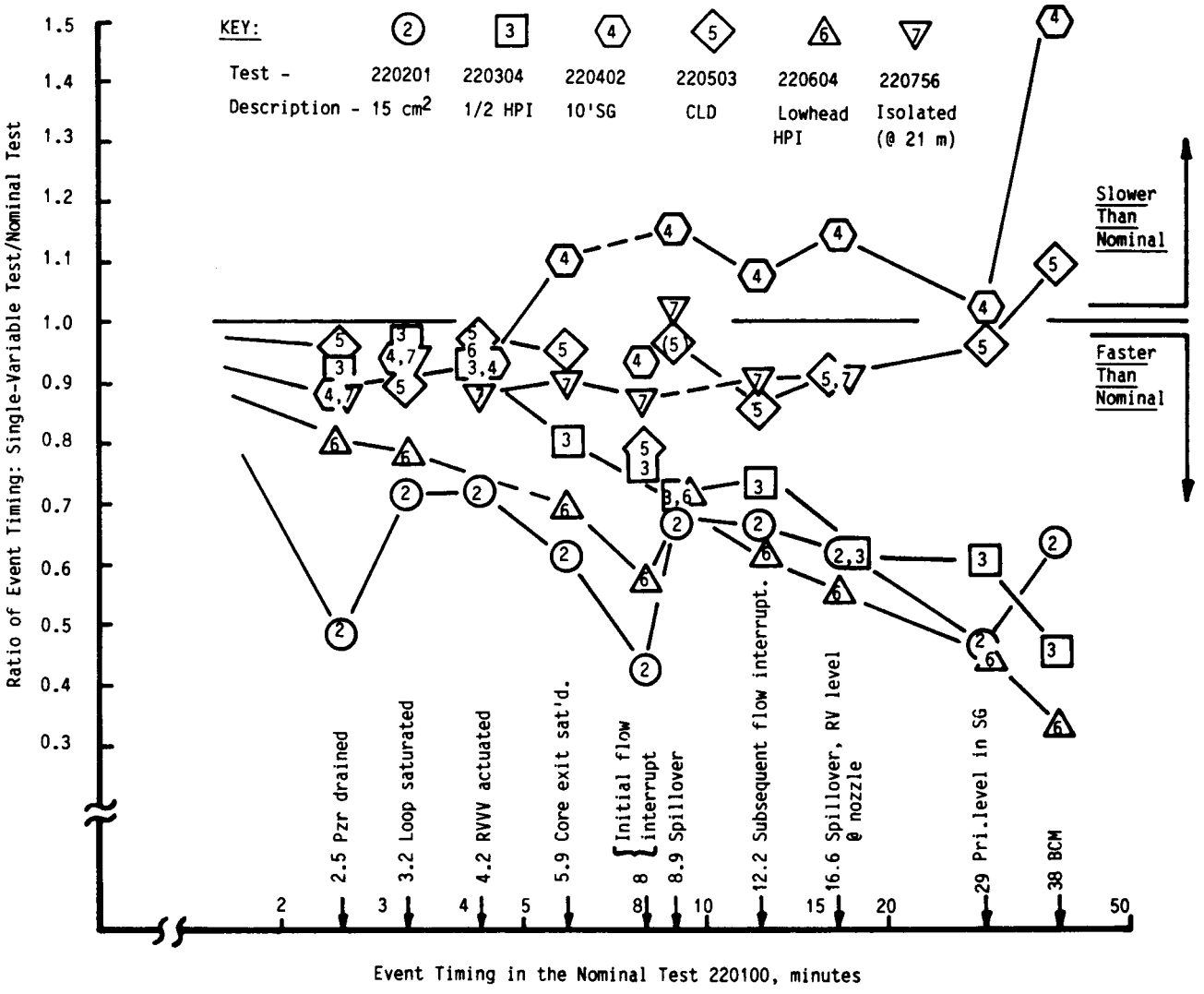

Figure 6.48 Event Timing (Earlier Events) Single-Variable Tests Vs Nominal Test

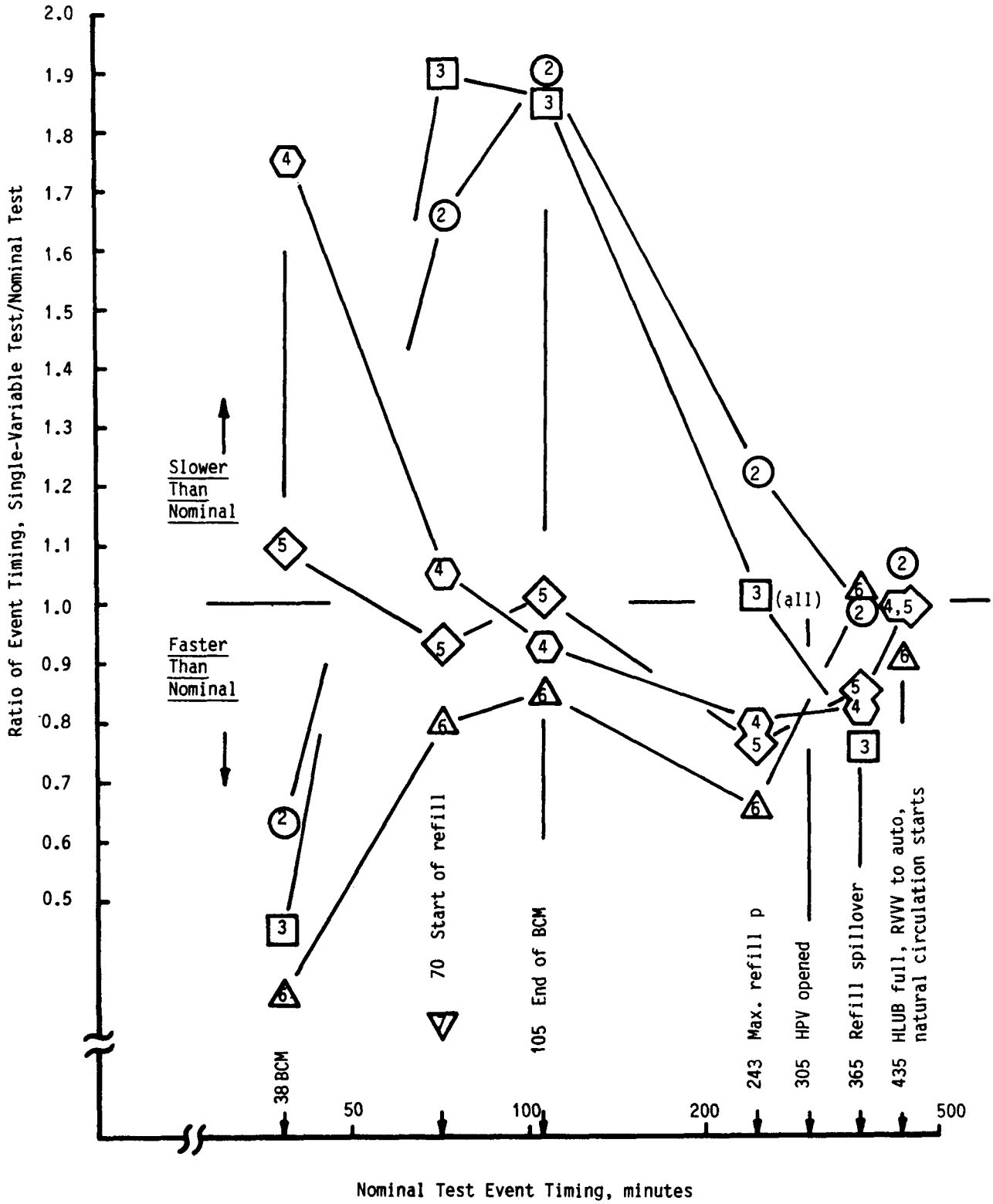

Figure 6.49 Event Timing (Later Events) Single-Variable Tests Vs Nominal Test (Key on Fig. 6.48)

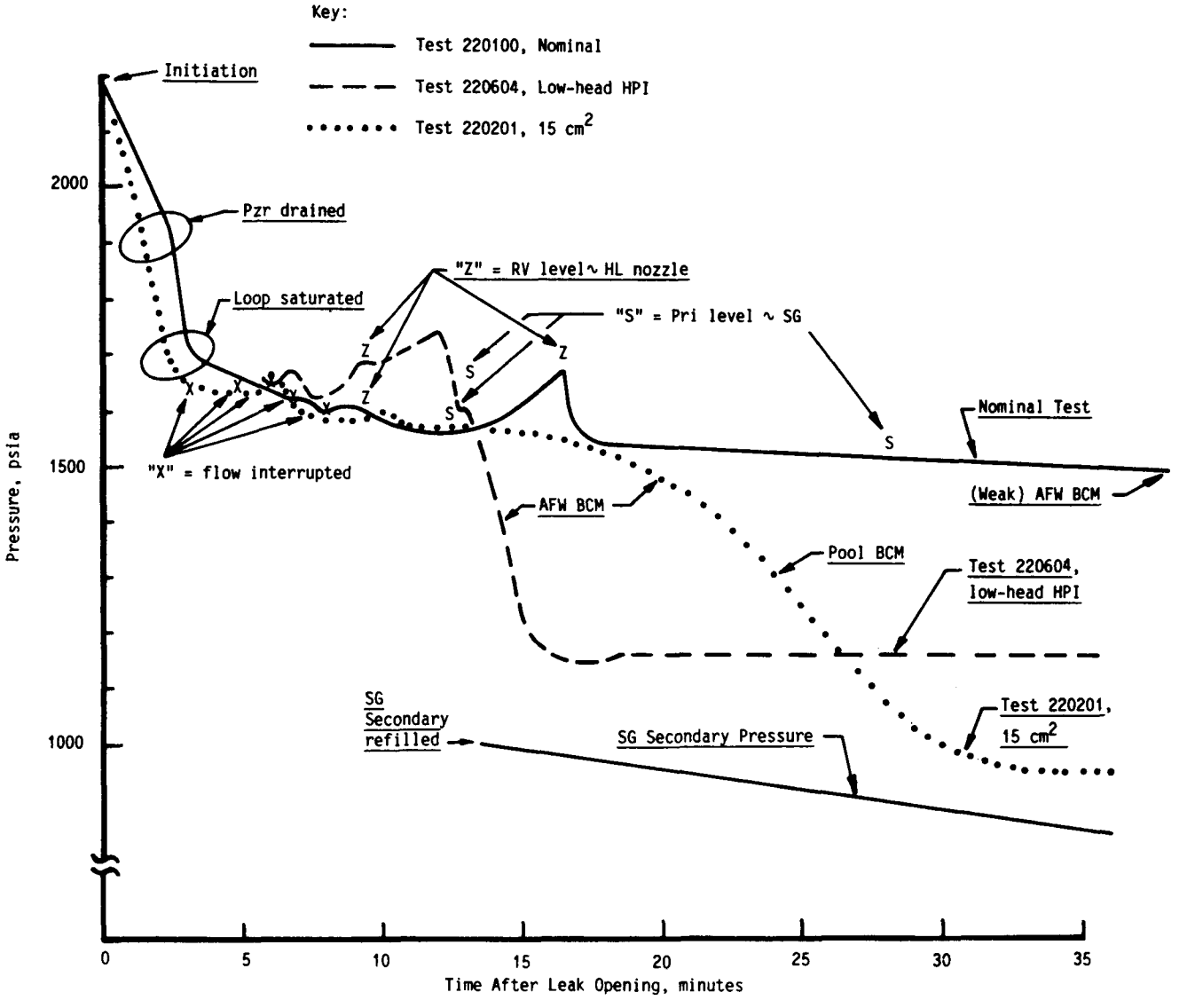

Figure 6.50 Early Events p(t)

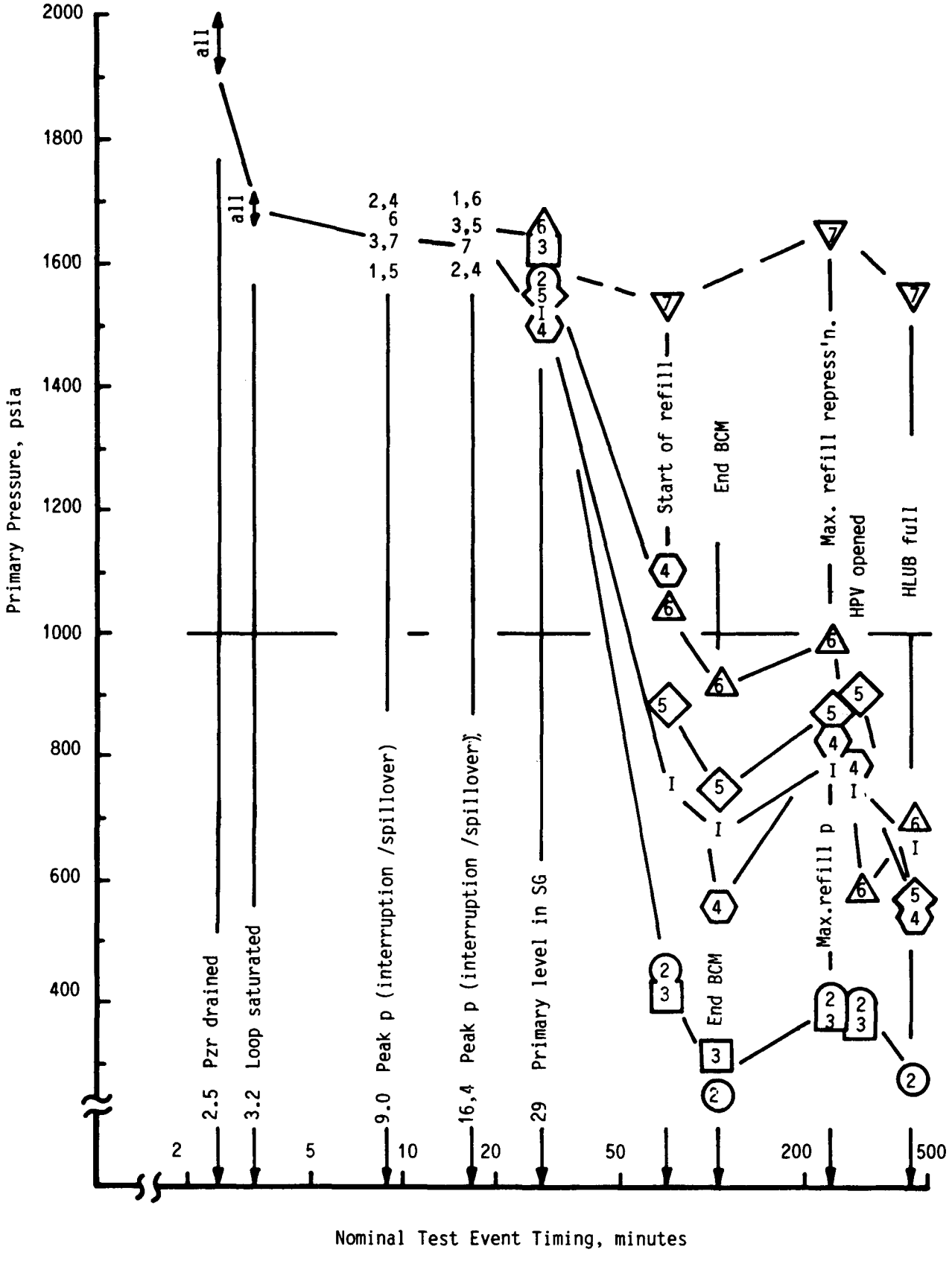

Figure 6.51 Pressure Trends
Pressure in Single-Variable Tests Vs
Event Timing of Nominal Test ("I")

7. HPI-PORV COOLING TEST

7.1 Introduction

Test 220899 examined an HPI-PORV cooldown without auxiliary feedwater. Test initialization was like that of the Nominal Test, but test initiation was different and test conduct most closely resembled that of the leak isolation test (2207). The test specifications, outlined below, are given in Section 3.

Initiation

No leak was to be simulated in this test, therefore the customary leak initiation step preceding test initiation was not applicable. This test was to be initiated by three simultaneous actions:

1. Actuate high-pressure injection (full capacity, full head).
2. Stop auxiliary feedwater.
3. Begin the usual core power decay ramp.

The steam generator (SG) secondary was to be kept isolated throughout the test, except as required to assure model generator integrity. As primary inventory and pressure increased at test initiation, the simulated PORV would actuate at 2300 psia on overpressure. Upon automatic actuation, the PORV control mode was to be transferred from automatic (actuation on overpressure) to manual-open. The PORV was to be held open for the duration of the test. The primary would then be cooled by HPI-PORV flow. Testing was to be continued through primary refill plus one hour of cooling.

7.2 Performance

The test was initiated, controlled, and terminated as specified. The AFW flow rate was reduced at test initiation (10 minutes after activation of the data acquisition system) and indicated zero flow by 2 minutes. Feed and steam flow rates were periodically reactivated throughout the test to control secondary pressure; these active periods were brief, and had maximum flow rates of 1/2% of full secondary flow (1% = 0.0265 lbm/s).

Initialization

The system was initialized in subcooled natural circulation at 2180 psia and 4.2% of full power (1% = 21.4 kW). These initial conditions are summarized in Table 7.1. Each of the specified control conditions was obtained. The specified loop conditions were also met, except that the pressurizer metal temperatures ranged from 650 to 690F, versus 650 ± 10F; this deviation is not perceived to have affected the test.

Measurements

Unavailable measurements are listed in Table 7.2. This list is predominated by the HL conductivity probes and the SG primary string thermocouples. The unavailability of these indications did not impede the analysis of the test.

The PORV effluent measurement should be noted, cf. appended Plots 17 and 18. Referring first to the time-integrated rates combined in Plot 18, the PORV discharge flow rate measurements caused no major inaccuracy in cumulative mass. Turning to the individual flow rates, Plot 17, the oscillatory nature of the PORV discharge rate is immediately apparent. As addressed in section 7.3 herein, the oscillations are attributable to the metering system rather than to sporadic PORV flow. Average PORV discharge rates derived from the weigh-tank measurements have been included on Plot 17 -- these average flow rates indicate the trends of the PORV discharge. The variability of the PORV discharge rate invalidates the system energy closure calculations. This is because the PORV discharge enthalpy is keyed to discharge mass flow rate (as well as to pressurizer liquid level and fluid temperature), to determine fluid state. But the available pressurizer fluid indications and the PORV discharge rates obtained from weigh-tank measurements permit the analysis of the major system interactions despite the lack of system energy closure. However, the indicated rate of the PORV discharge was neither quantitatively nor qualitatively correct.

7.3. Observations

Observed system behavior is described according to the following test phases:

- Initialization.
- Initiation (0 to 3 minutes).
- Cooldown with the pressurizer filling (3 to 13 minutes).
- Cooldown with decreasing loop flow (13 to 70 minutes).
- Cooldown with HL U-bend saturation (70 to 128 minutes).

These key test phases are shown on Figure 7-1. Tables 7.3 and 7.4 provide the operator's comments and key test events.

7.3.1 Initialization

The loop was initialized in subcooled natural circulation. Primary pressure was 2180 psia ($T_{sat} \tilde{=}$ 650F), and secondary pressure was 1200 psia (567F saturation). Core power was 4.2% of scaled full power (or 3.7% plus losses to ambient, 1% = 21.4 kW). The primary flow rate was 5-1/2% of the scaled full flow (1% = 0.259 lbm/s); the HL and CL fluid temperatures were 610 and 571F. The pressurizer liquid level was 18 feet. The reactor vessel vent valve was on automatic actuation on differential pressure. The SG secondary was on constant level control at 5-1/2 feet collapsed liquid level. The data acquisition system was activated at 1801 on 26 March 1984.

7.3.2 Initiation (0 to 3 minutes)

This test was initiated approximately 10 minutes after data acquisition was begun. The initiation actions included isolation of the SG secondary, and activation of the high-pressure injection system and the core power ramp. When the PORV actuated on high pressure, it was manually maintained open. These test initiation events are described in the following paragraphs. Figures 7.2 through 7.9 display the system response to these initiating actions.

Steam Generator Isolation (Figures 7.2 through 7.5)

The test initiation steps were begun after ten minutes of steady state data had been acquired. The SG steam flow was stopped (by increasing the SG secondary control pressure to 1350 psia), and the SG secondary level control point was reduced to 3 feet; feed flow was thereby reduced to zero over about a two-minute period. Within ten seconds, the effects of interrupted SG heat transfer became apparent: the SG heat transfer rate diminished, the SG secondary pressure began to increase, the wetted tube primary fluid temperatures (down to 23.1 feet, well above the secondary liquid level) rapidly heated toward T_{hot} (see appended Plot 13), the primary flow rate began to decrease, the primary system pressure rose, and a pressurizer insurge began.

Activation of High-Pressure Injection (HPI) and
the Core Power Ramp (Figures 7.6 through 7.8)

At 0.7 minutes, HPI was activated to the cold leg discharge piping (this action was also one of the test-initiating actions). The primary mass balance immediately responded and the CL fluid temperature downstream of the HPI point (CLTC05) dropped about 10F. The RVVV differential pressure increased causing a momentary valve actuation at 1 minute, which raised the fluid temperature downstream of the valve and caused the downcomer and CL flow rates to diverge to 6-1/2% and 4% of full flow, respectively. By this time, the HPI flow rate had reached $\sim$0.06 lbm/s; this injection rate caused a pressurizer level rise and a sustained excess of downcomer flow rate over that of the CL (0.06 lbm/s is equivalent to a 0.2% loop flow rate difference). The core power decay ramp was activated at 1 minute. The power removed by heating the HPI fluid, roughly 1-1/2% of scaled full power, was less than the current core power of 4%; hence, the primary system pressure continued to rise.

Power Operated Relief Valve (PORV) Actuation
(Figures 7.2, 7.3, 7.6 and 7.7)

Primary pressure reached 2300 psia at 3 minutes, triggering the final test initiation action. As the PORV actuated, the operator changed its control to manual-open (for the duration of the test). Primary pressure immediately decreased, and the rate of pressurizer level rise slowed (at

∿25 feet). However, the PORV discharge metering systems did not respond until ∿5 minutes. The measured PORV discharge rate was cyclic, indicating a brief period of relatively high flow, followed by a period of zero flow that was roughly three times as long as the flow period. Further examination of these indicated flow rates confirms that this apparent cyclic behavior was erroneous. The indicated flow during the "on" cycles far exceeded the predicted vapor flow rate, and the zero indicated flow during the "off" cycles also disagreed with predicted critical flow. A comparison of the "calculated" and "indicated" fluid mass (of Figure 7.7) yields further insight. (The calculated primary mass is based on the mass contained in each primary component using level measurements; the indicated value uses the primary boundary mass flow rates, viz. measured HPI and PORV mass flow rates.) The measured PORV flow rate being examined caused perturbations of the calculated total mass. But the calculated and indicated "cumulative" trends coincided. Thus, although the measured PORV discharge flow rates were aphysical, their integral over time was not. Evidently, the actual PORV discharge behaved as expected. The discharge metering system accurately measured this PORV flow but registered the flow in a discontinuous fashion. This PORV flow metering difficulty was caused by the coarseness of the control of the level in the PORV discharge separator. Rather than maintaining a nearly-constant level and thereby causing the flow rate from the separator to reflect the PORV discharge flowrate, the separator level control system functioned in a band level control mode. Refer to the loop functional specifications[2] for additional details.

Behavior of the Isolated Steam Generator (Figures 7.2, 7.3, 7.5 and appended Plot 13)

The SG secondary had been isolated to accentuate the HPI-PORV cooling mode. By 5 minutes, the secondary pressure had approached the elevated SG secondary pressure control point (1350 psia) and the SG secondary pressure control system began to release steam from the SG secondary. The indicated steam flow was 1/2% of the scaled full secondary flow rate (1% = 0.0265 lbm/s) and, although feed flow rate indicated zero, a minor feed actuation at 4 minutes was evidenced by a momentary reduction of the SG primary fluid temperatures. (The operator transferred AFW injection from high elevation

to low elevation at test initiation, and closed the high-elevation AFW manual isolation valve at 23 min). The SG heat transfer was approximately 1% of scaled full power during this time; HPI-PORV cooling thus remained the predominant mode of primary system heat removal. The secondary pressure was maintained near the control setpoint by regulated SG steam discharges, and the secondary steam flow rate gradually decreased as the primary flow rate continued to decrease. In response to this steaming, the SG secondary liquid level slowly diminished, from 6-1/2 feet at 5 minutes to 4-1/2 feet by 12 minutes. Beyond this time, the primary mode of SG secondary heat removal was by losses to ambient. Indeed, beyond 70 minutes, the SG secondary was cooled by the primary, as described below. Although the SG heat loss to ambient was estimated to be only 0.3% of scaled full power, its impact on loop flow was not inconsequential. The natural circulation flow rate may be estimated using the following thumbrule*:

$$F\ (\%\ \text{flow}) = 4 \times [Q(\%\ \text{power}) / 2]^{**}1/3 \qquad (7\text{-}1)$$

(for stable, single-phase loop flow with the raised-loop plant configuration). By this relation, 0.3% power obtains approximately 2% flow, which parallels the observed loop flow rate. Thus, although the SG was isolated as intended, it had a lingering effect on the transient for the initial hour of testing.

7.3.3 Cooldown With the Pressurizer Filling (3 to 13 minutes)

The initial portion of the cooldown from 3 to 13 minutes was characterized by steam venting out the PORV. The energy transfer by HPI-PORV cooling was slightly less than core power, but the PORV vapor discharge caused rapid primary depressurization. This depressurization lead to voiding in the reactor vessel. The RVVV (internals vent valve simulation) actuated. These interactions are addressed below. Figures 7.2 through 7.9 provide time-expanded displays through this time frame.

---

*The general expression relates the mass flow rate in natural circulation directly to the one-third power of the fluid density squared, the flow ara squared, the fluid thermal expansion coefficient, the (core) power level, the vertical distance between thermal centers, and the inverse of the loop hydraulic resistance and the fluid specific heat. The thumbrule is thus an approximate evaluation of the general relation at customary cooldown conditions.

Energy Balance (Figures 7.2, 7.3, and 7.6)

During this period of PORV actuation with the pressurizer filling, the PORV ostensibly vented near-saturated vapor (the uppermost pressurizer fluid temperature was 2OF superheated at the time of PORV actuation, decreasing to saturation by 13 minutes). The power offset through the heating and vaporization of HPI fluid to match critical steam flow out the relief was 1.3% of scaled full power, while heating the excess HPI (which refilled the pressurizer) accommodated almost 1% power. Core power was decreasing toward 2-1/2% by 15 minutes. The average primary fluid specific energy was also decreasing during this time. The primary continued to depressurize, mainly in response to the vapor volume reduction due to the PORV discharge.

Reactor Vessel Voiding and RVVV Actuation (Figures 7.3, 7.4, and 7.9)

The reactor vessel (RV) outlet and top plenum fluid temperatures had remained relatively constant, cooling from 610F initially to 607F at 11 minutes. Thus, the continuing primary depressurization saturated the upper RV fluid. The RV collapsed liquid level began to decline at 12 minutes (the uppermost RV-region void fraction grew toward 15%), reducing the rate of primary depressurization. The RVVV differential pressure increased slowly due to the cooling of the uppermost (stagnant) downcomer fluid, and due to the changing loop flow rate and fluid densities. The RVVV actuated at 12-1/2 minutes. This single actuation was significant because, in contrast to subsequent actuations, it did not accompany loop oscillations (pressure, temperature, and flow). Actuation was signaled by the vent valve limit switch, by the heatup of the fluid downstream of the valve, and by a momentary divergence of the cold leg loop flow rate from that metered in the downcomer. [The RVVV flow rate of single-phase liquid at 1/4 psi differential pressure was ∿2-1/2% of the scaled full loop flow rate (1% = 0.259 lbm/s) which roughly corresponded to the observed downcomer versus cold leg flow rate difference.]

The behavior of the reactor vessl (RV) level during this RVVV actuation was of particular interest -- this type of response is observed repeatedly

during the subsequent cyclic operation of the RVVV. The RV level had been subsiding slowly before this valve actuation at 12-1/2 minutes. The magnitude of the RV mass reduction rate roughly corresponded to the rate of vapor discharge from the PORV, $\sim$0.02 lbm/s. When the valve opened, "inner-loop" flow (downcomer to core to RVVV to downcomer) was abruptly enhanced. The core outlet temperature plummeted accordingly, as did the core-region average fluid temperature. This obtained a reduced coefficient of fluid thermal expansion and, thus, a net fluid contraction. The rate of RV level decline was therefore augmented. The RV-to-pressurizer pressure difference dropped, confirming that the rate of fluid displacement from the RV to the pressurizer was reduced.

The subsequent closure of the RVVV reversed the transient: core flow decreased, the RV liquid level stabilized as the core-region liquid expanded, and the RV-to-pressurizer pressure difference briefly increased.

7.3.4 Cooldown With Decreasing Loop Flow (13 to 70 minutes)

At 13 minutes (10 minutes after PORV actuation), the pressurizer filled and the PORV began to discharge liquid periodically; hence, the system conditions during cooldown changed distinctly. The primary depressurization rate and the rate of increase of total primary fluid mass slowed. The loop flow rate diminished as HPI-PORV cooling (and SG losses to ambient) began to offset core power, and as the HPI flow was diverted out the PORV. The RVVV began to actuate periodically, and the near-zero loop flow rate began to fluctuate and then to periodically reverse. The loop fluid temperatures continued to diverge with cooldown (reflecting the lengthening loop transit time with reduced loop flow). The core region fluid continued to cool. These events from 13 to 70 minutes are addressed in the following paragraphs. Figures 7.10, and 7.12 through 7.19, provide selected data plots on an expanded time scale.

The PORV Began to Discharge Liquid (Figures 7.2, 7.3 and 7.10)

Beyond 13 minutes, the reactor vessel (RV) displaced liquid to the pressurizer at a rate of $\sim$0.08 lbm/s, driven by the excess pressure differential from the RV to the pressurizer. This mass transfer rate, plus

a similar rate from the HPI, was far in excess of the PORV vapor discharge rate (and was roughly twice the predicted critical flow rate of liquid from the PORV). The pressurizer had been filling at a nearly constant rate, and was approaching full according to several indications: it filled beyond its upper level tap (40.5 ft) at 11 minutes, the uppermost pressurizer fluid temperature (at 46.5 ft) saturated at 13.3 minutes, and linear extrapolation of the level-time trace predicted a time to refill of roughly 14 minutes. Fluid conditions indicated that liquid reached the PORV at 13.5 minutes. At this time the RV-to-pressurizer differential pressure subsided, the rate of change of system pressure abruptly reversed from -20 psi/min to +6 psi/min and back toward zero, and the RV level stabilized at 6.4 feet. The characteristics of the PORV discharge flow rate trace also changed at this time, cf. appended Plot 17.

The PORV discharge of liquid plus the primary fluid contraction with cooling now exceeded the HPI flow rate, but the HPI rate greatly exceeded the rate of critical discharge of vapor. Thus, the PORV discharge fluid state became variable. It was generally liquid, but experienced brief periods of vapor discharge; this was evidenced by the correlation between the predicted critical liquid flow rate and the observed flow rate, cf. Figure 7.11. Referring to Figure 7.11, note the increase of the PORV discharge flow rate toward the predicted critical discharge of liquid, at and beyond 25 minutes after test initiation. (The basis for the equilibrium plot of Figure 7.11 is given in Appendix C.) System conditions, notably pressure and RV level, were responsive to these fluid conditions at the PORV. The overall primary system depressurization rate slowed markedly from that before pressurizer refill. The RV level, although generally declining, periodically increased.

The system response to a hypothetical pressure reduction may be used to illustrate the effects of the PORV discharge fluid state: the saturated fluid at the PORV and in the RV upper head flashes, retarding the depressurization. The RV level subsides, displacing liquid into the system (viz., the pressurizer). The PORV discharge mass flow rate abruptly decreases from critical liquid flow to critical vapor flow. The HPI flow rate (plus the liquid displaced from the RV) exceeds this reduced rate of discharge. The pressurizer refills, compressing its vapor volume and

elevating system pressure. When liquid reaches the PORV, the critical discharge mass flow rate abruptly increases, and the process is repeated.

The Reactor Vessel Vent Valve (RVVV) Began to Actuate Periodically (Figures 7.12 through 7.15)

The cooldown proceeded regularly until 20 minutes. But, the upper downcomer fluid (cf. RVTC10, Figure 7.12) had been cooling more rapidly than the lower downcomer fluid following the momentary RVVV actuation at 13 minutes. The increasing upper downcomer fluid density gradually raised the RVVV differential pressure, as did the dwindling SG heat transfer (by lessening the outer-loop flow rate). At 20 minutes, the RVVV differential pressure reached the actuation point, the valve opened, and cyclic interactions began. Warmer core-region fluid was admitted to the upper downcomer, the decreasing downcomer fluid density immediately began to depress the "inner-loop" manometric balance (downcomer to core to RVVV), and hence, the RVVV differential pressure.

Loop Flow Rate Began to Oscillate (Figures 7.16 and 7.17)

Upon RVVV actuation, the enhanced inner loop flow rate suppressed (outer) loop flow both directly by flow diversion and indirectly by the downcomer fluid density reduction mentioned previously. The subsequent reclosure of the vent valve interrupted the inner loop flow while the outer loop flow rate was substantially less than that compatible with the prevailing loop conditions (i.e., core power level and thermal center elevations). Core fluid density began to decrease, loop flow began to increase, and conditions realigned toward those preceding the initiating vent valve actuation. This outlines the interactions underlying the cyclic loop behavior which began at 20 minutes.

Loop Fluid Temperature Differences Are Amplified
(Figures 7.12, and 7.18 through 7.20)

The concurrent loop fluid temperature trends provide additional insight. Because of the intermittent actuation of the RVVV, the lower downcomer fluid was alternately heated by flow through the vent valve and then cooled by enhanced loop flow.

As loop flow was depressed upon RVVV actuation, the high-pressure injection (HPI) cooling of the cold leg discharge fluid was accentuated. Simultaneously, the hotter core exit fluid discharged into the upper downcomer through the RVVV, plus the brief reduction of HPI cooling in the downcomer, formed a column of relatively warm fluid in the upper downcomer. Also at the time of RVVV actuation, the enhanced inner loop flow briefly reduced the temperature difference across the core, and hence, depressed the core exit fluid temperatures. These fluid temperature changes first occurred at 20.2 minutes (upon RVVV actuation). The CL exit fluid cooled until 20.4 minutes (Figure 7.18). The movement of the relatively warm downcomer fluid was evidenced by the progression of the successive maximums of the downcomer fluid temperature indications: -3 feet at 20.2 minutes, -10 feet at 20.4 minutes, and -20 feet at 20.8 minutes (Figure 7.12); the core inlet fluid temperature peaked at about the same time, the core outlet at 21 minutes, and the HL beginning at 21.5 minutes (the magnitude of these temperature changes gradually subsided with distance up the HL, Figures 7.19 and 7.20). Recall that the core outlet fluid temperature (followed by the HL) had first cooled with enhanced inner loop flow -- the core outlet fluid temperature reached a minimum at 20.5 minutes, at which time warmer fluid was passing down the downcomer. Both these temperature changes tended to suppress the (outer loop) natural circulation driving force. This augmented the previously mentioned RVVV differential pressure reduction that occurred shortly after RVVV actuation. The cyclic loop flow rate calculated from whole-loop fluid densities and flow resistance was in coarse agreement with the indicated flow rate (cf. Figure 7.17), confirming that the observed flow perturbations were directly related to the accompanying fluid density redistributions. (The derivation of the calculated flow rates of Figure 7.17 is given in Appendix A.)

The Cooldown Continued (Figure 7.11)

The system cooldown continued unabated through the perturbations just described. The cooldown rate of the core exit fluid was approximately 60F/h. The primary system total fluid mass grew slowly with the gradual fluid contraction upon cooling (the primary was full except for the uppermost reactor vessel volume). As core power was continually reduced to simulate post-trip decay, and with the continuing HPI-PORV cooling, the

equilibrium primary loop flow rate gradually slowed, reaching roughly 1-1/2% of the full scaled flow rate by 30 minutes.

The general loop cooldown continued through 65 minutes. By this time, the core outlet fluid temperature had cooled to 550F. The pressurizer fluid temperature had cooled correspondingly; thus, the PORV critical flow had gradually increased and the primary pressure had decreased (reaching ∿1150 psia by 80 minutes) for approximately equal HPI and PORV flow rates. The RV level stabilized near the elevation of the upper plenum orifice plate (1.4 ft) at approximately 55 minutes; thus, the rate of increase of total primary fluid mass was enhanced. (This orifice plate simulated the plant upper plenum cover plate.) Primary loop flow rate had continued to diminish, at times approaching zero flow beyond 48 minutes.

Loop Flow Rate Dwindled and Reversals Occurred
(Figures 7.21 through 7.28)

At 48 minutes, the diminishing and oscillating (outer) loop flow momentarily indicated zero (appended Plot 9). This loop flow decay was attributable to the offset of core power by HPI-PORV cooling, as previously described. The whole-loop perturbations were related not only to the RVVV cycling (which has also been previously discussed), but also to the continual reorientation of the loop thermal centers. Forward flow drew HPI-cooled fluid up the HL, and the resulting elevation of the heating thermal center caused flow to reverse. These reversals were brief -- they depressed the heating thermal center elevation and also moved cold HPI fluid up the cold leg discharge sloping section.

The flow reversals gradually became more pronounced. With little overall forward loop flow the higher elevation fluid became less responsive to lower elevation cooling. The HL fluid temperatures thus began to diverge. The enhanced HL fluid temperature gradient itself suppressed forward loop flow by, in effect, increasing the long-term elevation of the heating thermal center. The development of these periodic displacements of loop fluid was clearly indicated by the behavior of the CL fluid temperatures. The trend of each of the (five) CL temperature indications was to gradually decrease with the continuing cooldown. But the indication upstream of the

HPI site (CLTC04) and of that downstream (CLTC05) alternately and abruptly dropped ∿100F. This reflected the periodic displacement of the cold HPI fluid with the changing loop flow direction.

The CL fluid temperature indication upstream of the CL spillover (the high point simulating the discharge elevation of the plant pump) was at first just barely cooled during loop flow reversals. But beginning at 63 minutes, the heightened responsiveness of this indicator (CLTC03) attested to the amplification of the flow reversals. The reversal at 65 minutes completely traversed the CL; even the cold leg suction thermocouple at the SG outlet was cooled. The lower elevation SG primary fluid temperatures responded similarly; they had been approximately 5F greater than the SG secondary saturation temperature, but with this reversal they cooled ∿45F. This introduction of relatively cold primary fluid into the SG accelerated the rate of secondary depressurization. Downflow in the HL drew relatively warm fluid from the upper HL elevation into the pressurizer surgeline, heating the surgeline metal.

The HL fluid temperatures at each elevation increased as warmer fluid was drawn downward with backflow. But the highest-elevation HL fluid also heated, albeit less than at the lower elevations. Comparing the uppermost HL metal and fluid temperatures, it is apparent that the ∿3F heatup of the HL fluid was due both to the backflow of slightly warmer fluid from beyond the U-bend and to the heat transfer from the warmer HLUB metal. These subtle changes in HL fluid temperature were significant because the upper elevation fluid was approaching saturation.

7.3.5. Cooldown With HLUB Saturation (70 to 128 minutes)

The relatively stagnant upper elevation loop fluid approached saturation at 70 minutes. This caused a change in system interactions with continued cooldown. Primary pressure was reduced only slowly as the upper elevation fluid and metal slowly cooled. The core region fluid continued to cool at the previous rate; thus, the loop fluid temperatures diverged with elevation. These trends persisted for the duration of the cooldown test, as described below. Figures 7.21 through 7.28 provide time-expanded information for the beginning of this period, and the appended plots may be used to examine the remainder of the cooldown.

The HL U-bend Fluid Saturated (Figures 7.21, 7.25, and 7.26)

A relatively strong loop flow reversal occurred at 70 minutes. The upper-elevation HL metal temperature was at or just above the primary saturation temperature, and the uppermost fluid temperature was just less than saturation. From this time on, the primary system pressure was apparently governed by saturation near the HLUB (although the facility operator did not observe voids at the HL viewports).

Loop Fluid Temperature Diverged

The primary depressurization rate slowed markedly as the primary saturation temperature paralleled the slowly decreasing fluid temperature at the HLUB. The HL and SG primary fluid temperatures increasingly diverged according to their elevation -- the lower-elevation SG primary fluid temperatures were cooled by HPI during recurring backflow. The lower-elevation HL temperatures cooled as HPI-PORV cooling continued. Concurrent with this apparent HLUB saturation, the reactor vessel void fraction stabilized following a prolonged growth -- the roughly constant void fraction corresponded to a reactor vessel liquid level near the elevation of the RVVV and the upper plenum orifice plate. At this time, too, the pressurizer fluid unmistakably subcooled -- the saturation temperature after 65 minutes decreased slowly toward 550F, while the pressurizer fluid temperatures continued to cool in response to HPI-PORV cooling.

The Cooldown Progressed

The cooldown of the lower region primary fluid continued unabated through test termination (after two hours of testing). The overall cooldown rate remained remarkably constant, even with loop flow cessation and apparent HL U-bend fluid saturation. The cooldown rate of the core exit fluid remained at roughly 60F/h.

Also, there was a close correspondence between SG secondary saturation temperature and core exit fluid temperature. The isolated SG had been cooled by the primary since the relatively pronounced primary flow reversals began at 70 minutes. The CL fluid drawn back into the SG during flow reversals was alternately transported into the downcomer and core with forward flow, and hence, their temperatures were interrelated. The primary fluid

temperatures at the termination of the cooldown ranged from as low as 250F in the CL to 550F (saturation) in the HL U-bend region. The core outlet, lower HL, and lower SG primary fluid temperatures were within approximately 10F of the secondary saturation temperature, 460F. The CL temperatures were not only the lowest but also the most variable. They changed by more than 100F every few minutes.

Figure 7.29 depicts the overall cooldown and the divergence of the HL and core-exit fluid temperatures as the HL U-bend fluid approached saturation. Figure 7.11 compares the high-pressure injection (HPI) and PORV discharge flow rates through the transient. Testing was completed at 138 minutes, after more than two hours of HPI-PORV cooling.

7.4 Results

OTIS Test 220899 investigated HPI-PORV cooling. The test was conducted as specified. Measurements were sufficient to permit the analysis of loop behavior, but the discontinuous metering of the PORV discharge flow rate necessitated substitution of the weigh-tank measurements. Although individual phenomena were readily understood, the causal events were sometimes uncertain. During loop condition oscillations, for example, the cause-and-effect relationship was indiscernible among RVVV operation, inter-component pressure differences, and the changing PORV discharge fluid state.

Three phases of HPI-PORV cooling were observed: (1) pressurizer filling with relatively rapid primary depressurization (from 3 to 13 minutes after test initiation); (2) PORV discharging liquid with brief periods of vapor discharge, reduced primary depressurization rate, and diminishing and oscillating loop flow (from 13 to 70 minutes after initiation); and (3) the upper-elevation loop fluid approaching saturation, the primary depressurization rate slowing markedly, and the lower elevation fluid continuing to cool while the upper elevation fluid cooling decreases (from 70 minutes after test initiation through the completion of testing at 128 minutes). The cooldown rate of the core-region fluid remained nearly constant at approximately 60F/h throughout these cooldown phases. The test data appears useful and challenging for code benchmarking.

Table 7.1. Initial Conditions, HPI-PORV Cooling Test 220899.

Specified Control Conditions

Pressurizer heaters adjusted for approximately adiabatic conditions.

Boundary systems (vents, HPI, leaks) not in use.

RVVV on differential-pressure control with 0.25/0.125 psi to open/close.

Auxilairy feedwater at approximately injected at the upper elevation using a minimum-wetting nozzle.

Specified Loop Conditions	Specified	Actual
Core power, % of full power, (1% = 21.4 kW, includes 0.5% increase for ambient losses)	4.2 ± 0.1	4.2
Primary pressure, psia	2200 ± 50	2180
Pressurizer liquid level, ft	16.6 ± 2	18.3
SG secondary level, ft	5 ± 1	5.4
Hot leg fluid temperature, F	610 ± 2	610
Pressurizer metal temperatures, F	650 ± 10	650 to 690
SG fluid temperatures varying less than 10F/h	--	--

Derived System Conditions	Value
Natural circulation flow rate (% of full flow, 1% = 0.259 lbm/s)	5.5
Cold leg fluid temperature, F	571
SG secondary flow rate, (% of full secondary flow, 1% = 0.0265 lbm/s)	
Steam flow	∿2.3
AFW flow	∿2.2
SG secondary pressure, psia	1200
AFW temperature, F	117

Table 7.2. Unavailable Measurements, HPI-PORV Cooling Test 220899.

SUMMARY OF VARIABLES DISCARDED ON INPUT, TEST 220899

NO.	VTAB	SYSTEM	INST.	ELEVATION	DESCRIPTION
1	155HLTC06	2HL	2FTC	50.00	HOT LEG FLUID TEMP (F)
2	262HLCP05	2HL	16 CP	41.00	HOT LEG CONDCTVTY (WET/DRY)
3	263HLCP06	2HL	16 CP	45.00	HOT LEG CONDCTVTY (WET/DRY)
4	264HLCP07	2HL	16 CP	49.00	HOT LEG CONDCTVTY (WET/DRY)
5	265HLCP08	2HL	16 CP	53.00	HOT LEG CONDCTVTY (WET/DRY)
6	266HLCP09	2HL	16 CP	57.00	HOT LEG CONDCTVTY (WET/DRY)
7	274HLCP17	2HL	23RCP	.50	HOT LEG REF. C.P.
8	273HLCP16	3SGP	16 CP	53.10	SG PRIMRY. CONDCTVTY (WET/DRY)
9	272HLCP15	3SGP	16 CP	56.90	SG PRIMRY. CONDCTVTY (WET/DRY)
10	223HPTM02	10HPI	13TMF	-999.00	HP INJECT. TURB.FLOW (LBM/SEC)
11	219V1AC01	11V1	19ACC	-999.00	1-PH VENT. ACCD.FLOW (LBM)
12	317V1RF20	11V1	38FLO	-999.00	1-PH VENT. CALD.FLOW (LBM/SEC)
13	220V2AC01	12V2	19ACC	-999.00	2-PH VENT. ACCD.FLOW (LBM)
14	53SSTC13	22SGS	2FTC	32.30	SG SECOND.FLUID TEMP (F)
15	795MTC02	22SGS	25MTC	26.30	SG SECOND. METAL TC (F)
16	763MTC06	22SGS	25MTC	44.20	SG SECOND. METAL TC (F)
17	289SSCP20	22SGS	32KCP	0.00	SG SECOND. UP.WET.CP (REF. FT)
18	344V1TC03	34CLD	2FTC	-999.00	CLD LEAK FLUID TEMP (F)

Table 7.3. Operator's Comments, HPI-PORV Cooling Test 220899

Time	Comment
18:02	Reset pressurizer guard heaters for 0.2 bias.
18:11:30	SG pressure control to 90%, (1350 psia). SG level control to 6% (3 ft). Switch to low-elevation AFW. HPI to auto/cascade.
18:12	Core power ramp started.
18:14	PORV opened on auto.
18:16	Reset SFCV03 control for low-elevation AFW settings.
18:25	DCDP01 and CLDP02 in service.
18:34	Closed FPHV03 (manual HI AFW).
18:39	DCDP01 out of service.
19:59	DCDP01 in service.
20:21	Stop data save for run 220899.

Table 7.4. Test Events, HPI-PORV Cooling Test 220899

Time, min		Event
DAS	Initiation[a]	
0	--	Data acquisition system (DAS) activated at 1801, 26 March 1984.
10	0	Test initiation: Isolated the SG secondary, activated HPI, began the core power (decay) ramp.
13	3	PORV actuated, valve control changed to manual-open. HPI-PORV cooling began. Pressurizer filling.
21	11	RV upper plenum fluid saturated, RVVV actuated.
23	13	Pressurizer filled, PORV discharged liquid, the primary system depressurization rate slowed.
30	20	The RVVV began to actuate periodically. Loop flow rates began to oscillate.
60	50	The decreasing primary loop flow rate reached zero. Brief loop flow reversals occurred. Cooling of the higher elevation primary fluid decreased.
73	63	Flow reversals became sufficiently robust to transport cold HPI fluid back to the SG primary exit.
80	70	Uppermost primary fluid approached saturation. The primary system depresurization rate decreased markedly. Cooldown of the lower elevation primary fluid continued.
138	128	Testing completed, DAS deactivated.

[a]"DAS" time is from activation of the Data Acquisition System. "Initiation" time is measured from the start of the test-inititation events.

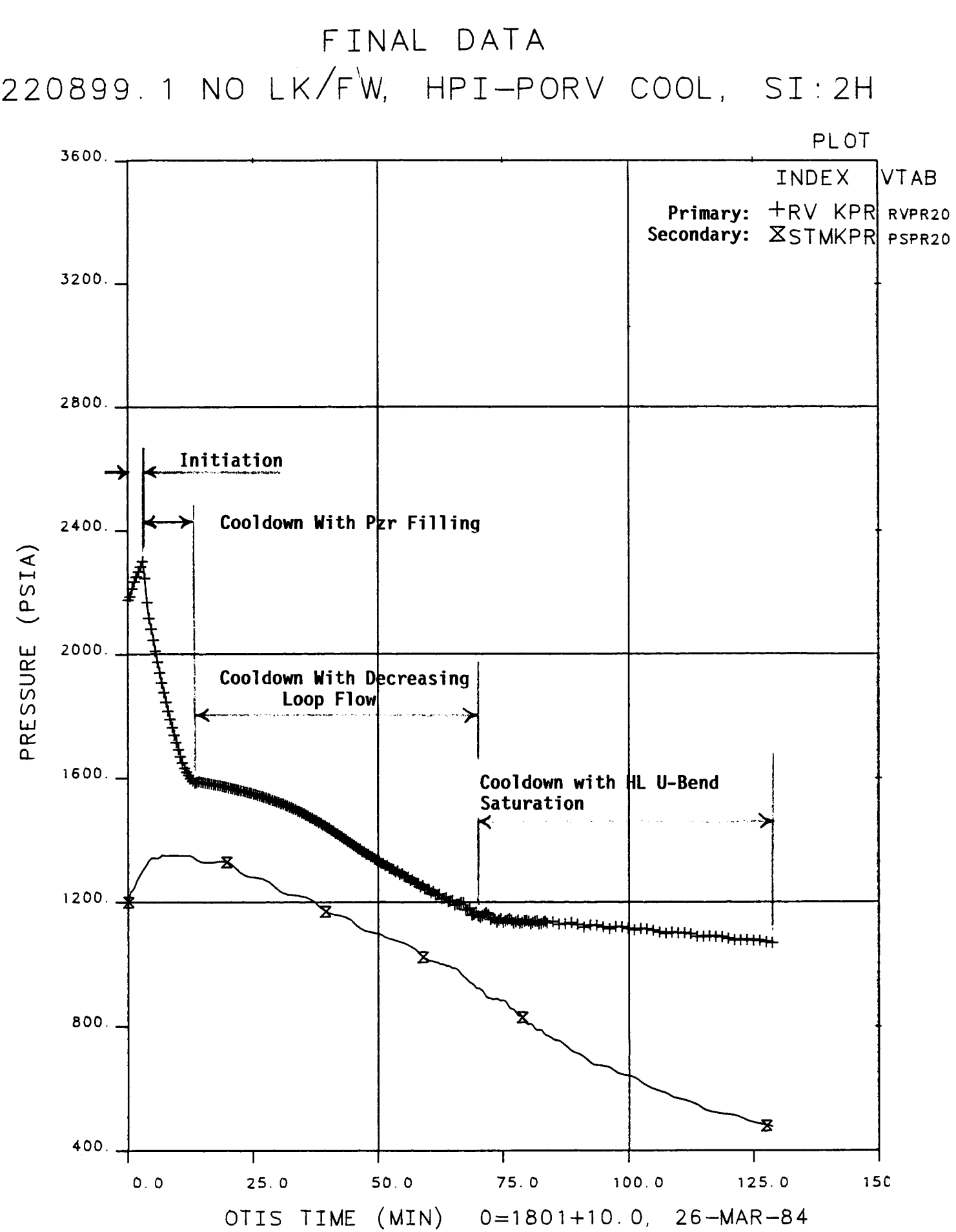

Figure 7.1 Primary and Secondary Pressure Versus Time Showing Key Events

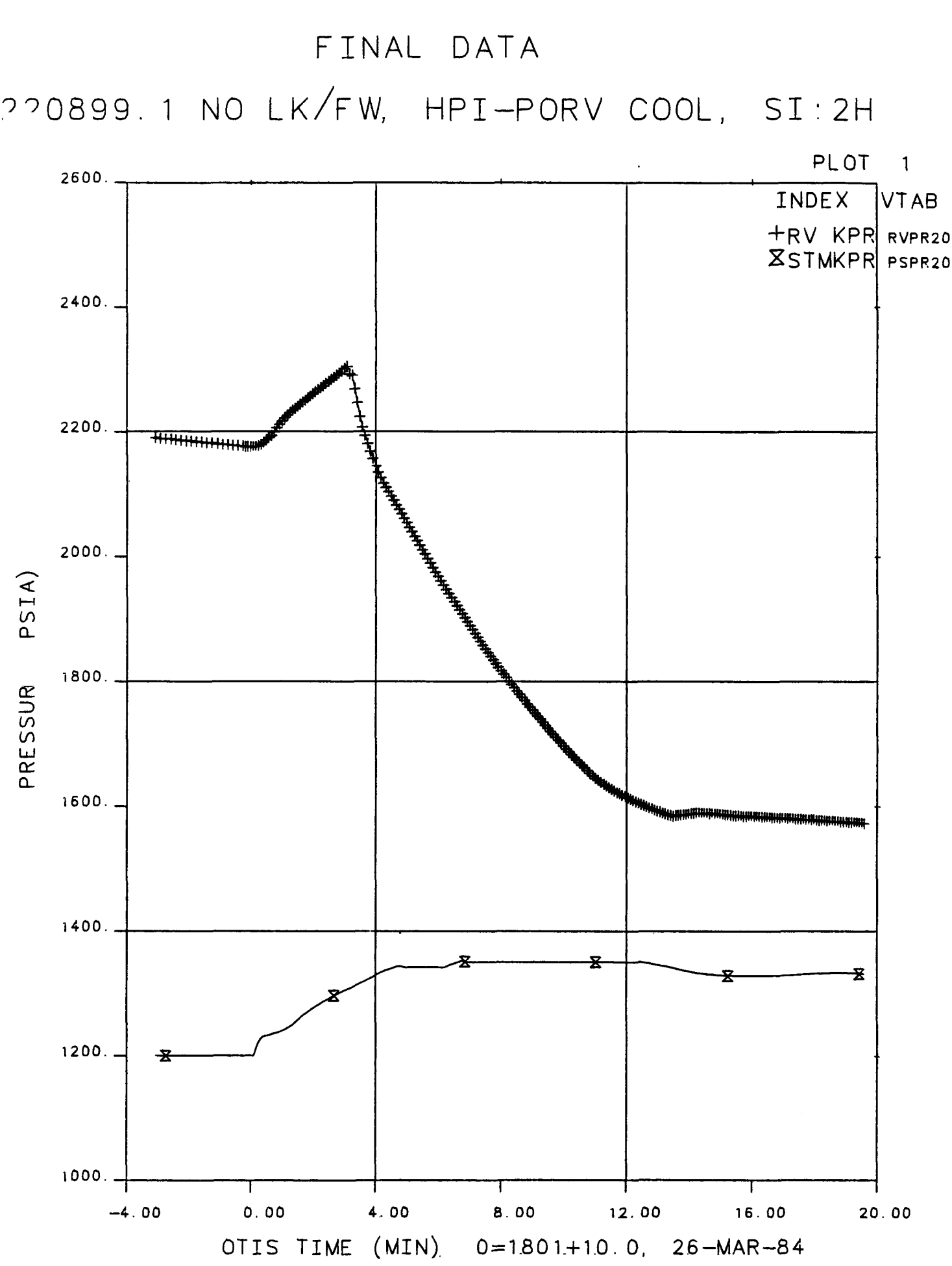

Figure 7.2 Primary and Secondary Pressures, 0 to 20 Minutes

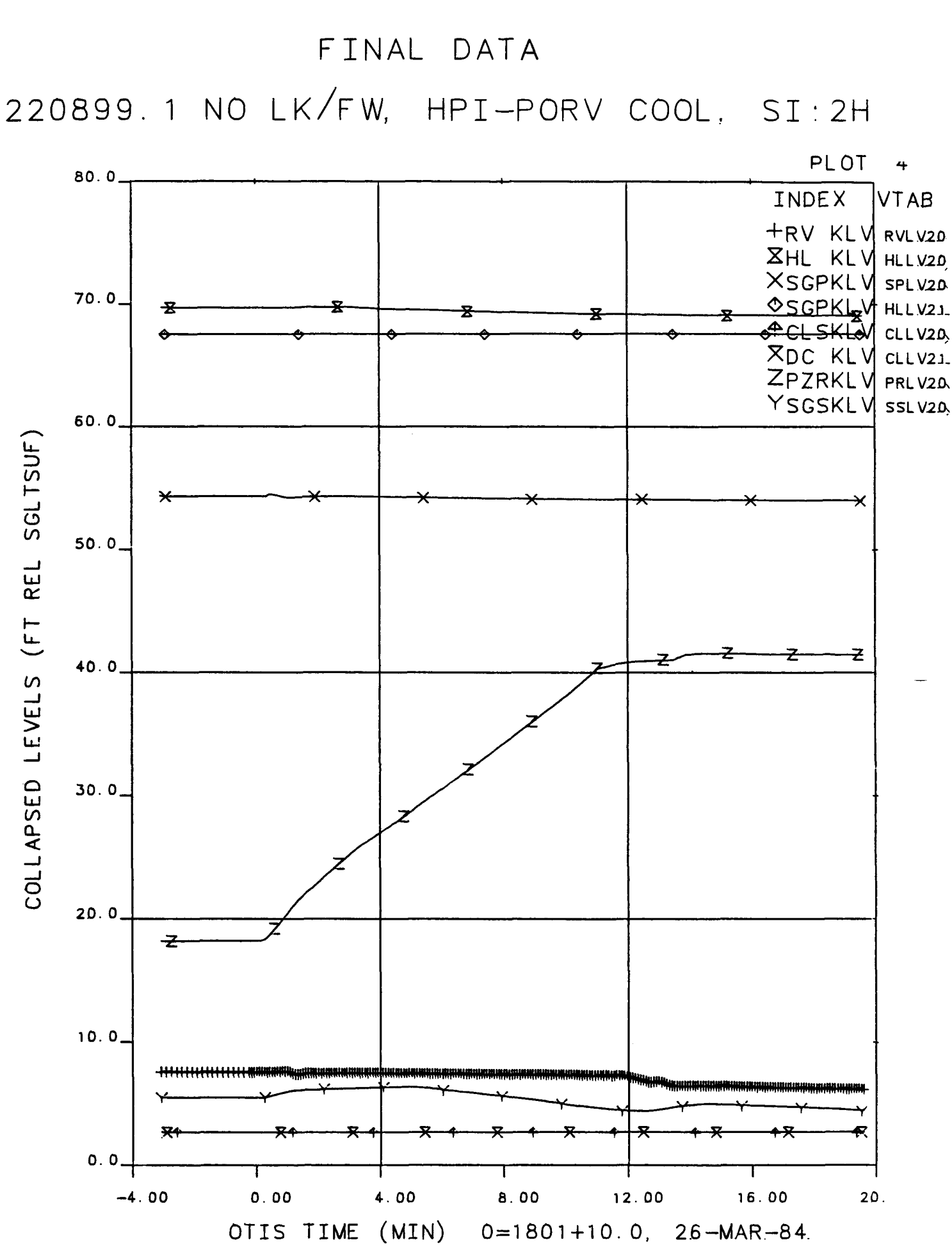

Figure 7.3 Collapsed Liquid Levels, 0 to 20 Minutes

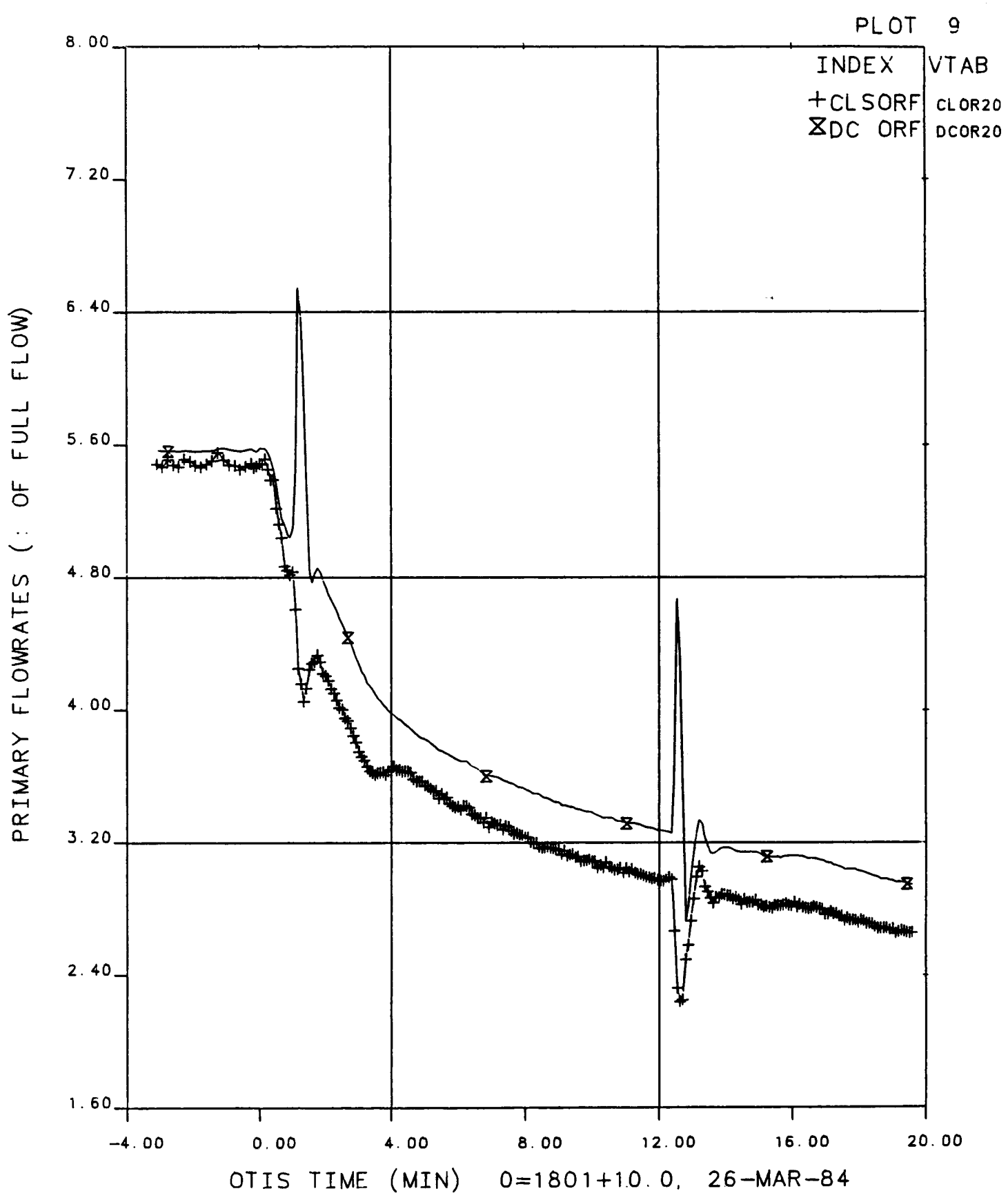

Figure 7.4 Primary Flowrates, 0 to 20 Minutes

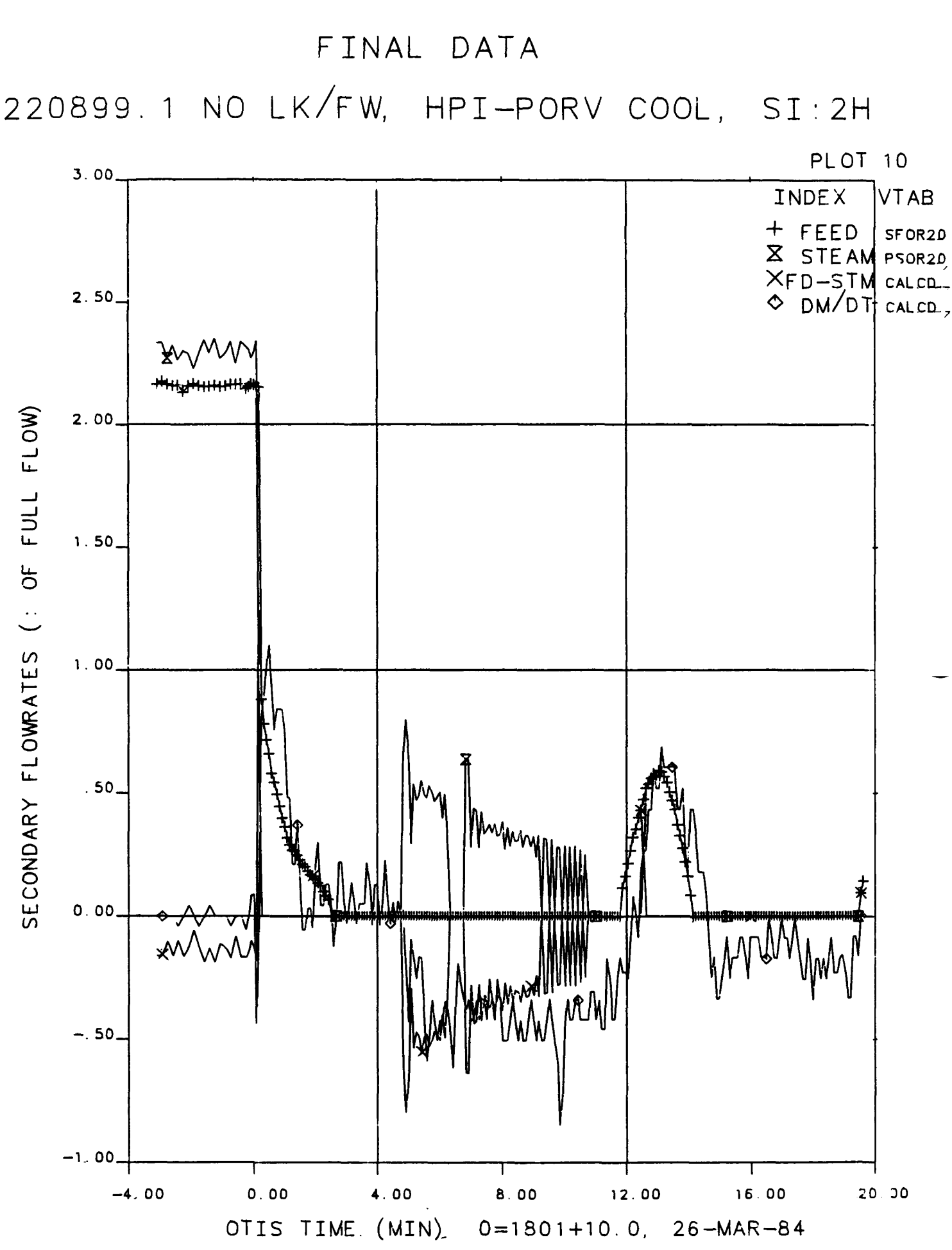

Figure 7.5 Secondary Flowrates, 0 to 20 Minutes

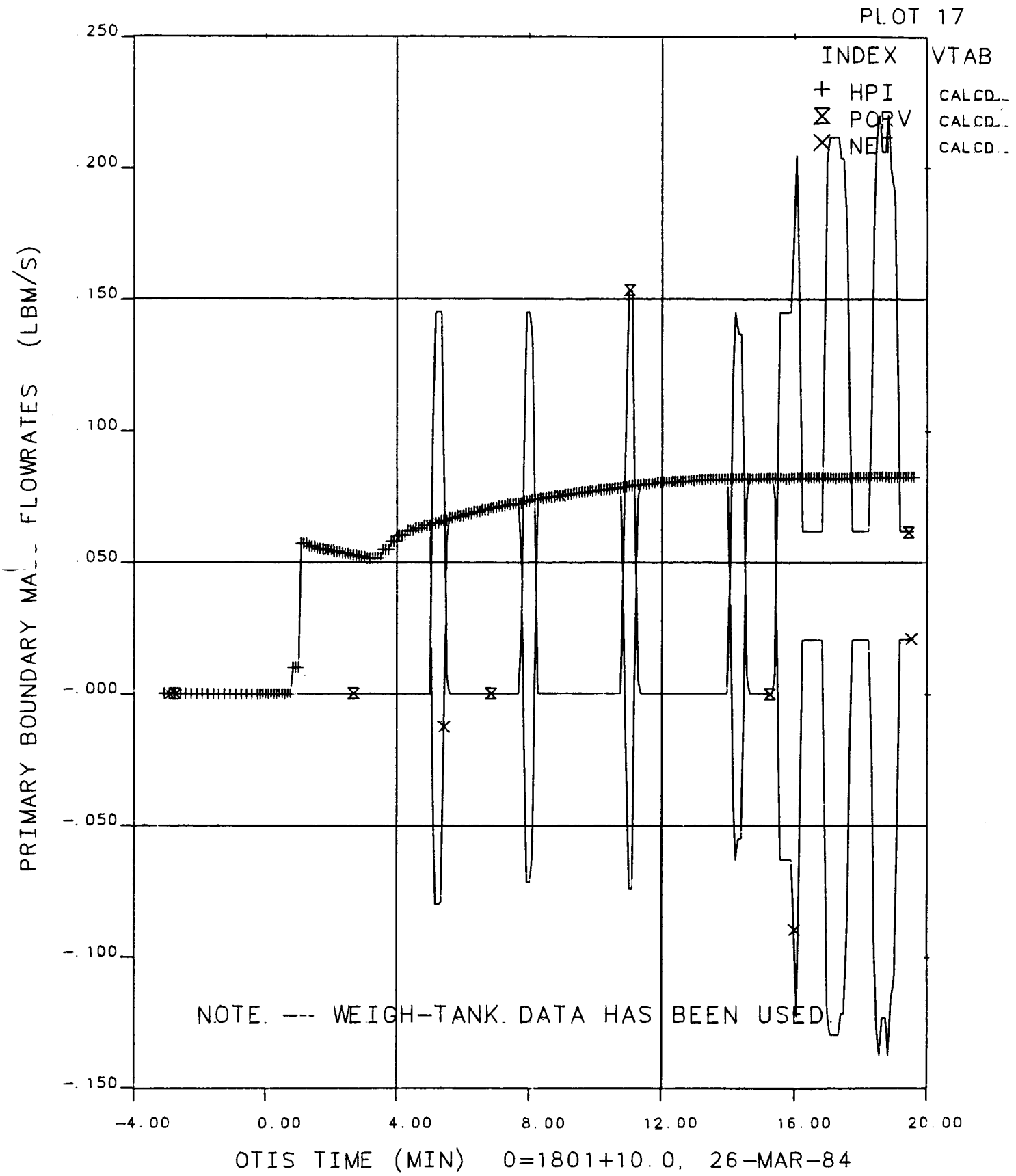

Figure 7.6 Primary Boundary Mass Flowrates, 0 to 20 Minutes

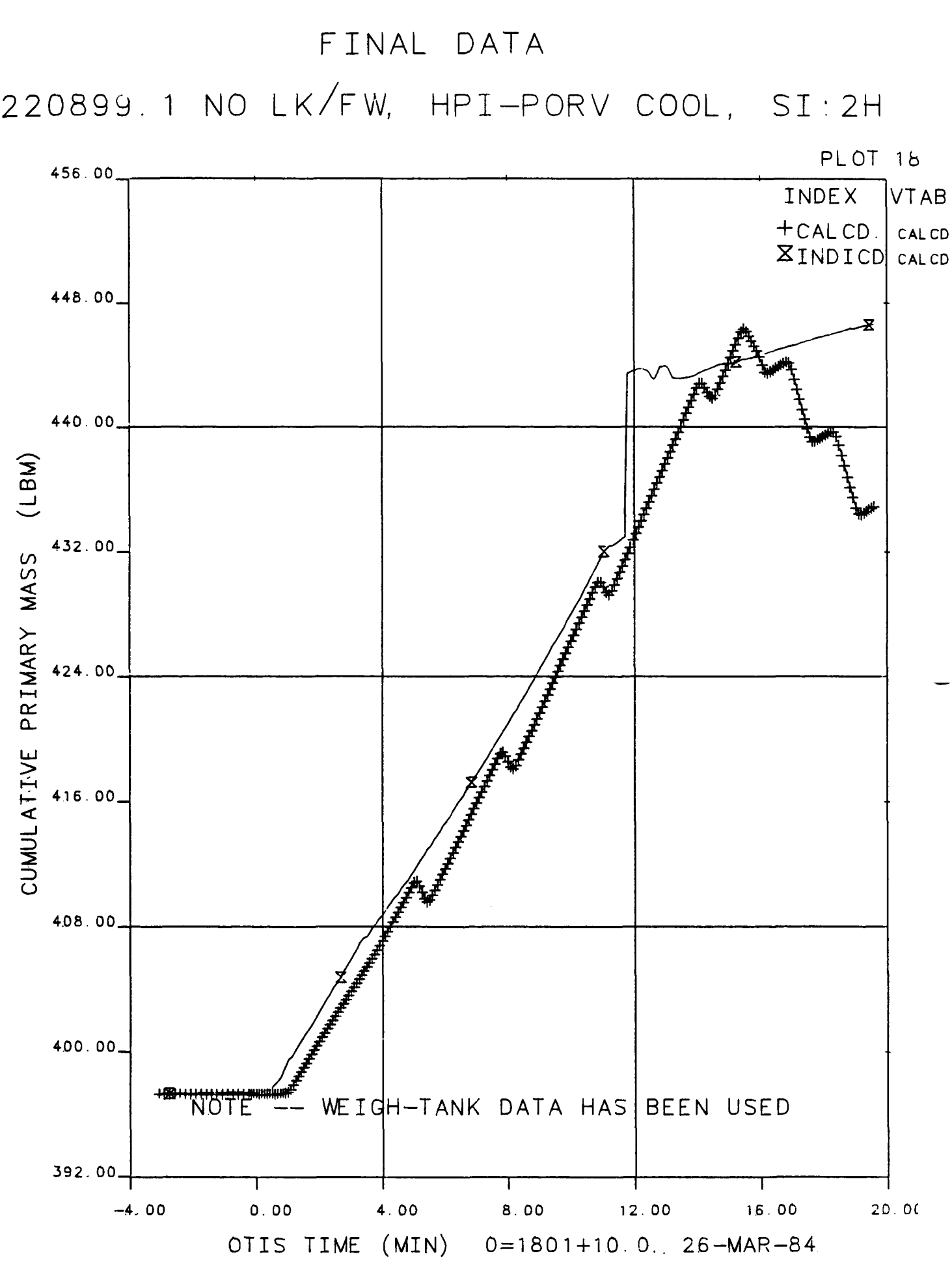

Figure 7.7 Cumulative Primary Fluid Mass, 0 to 20 Minutes

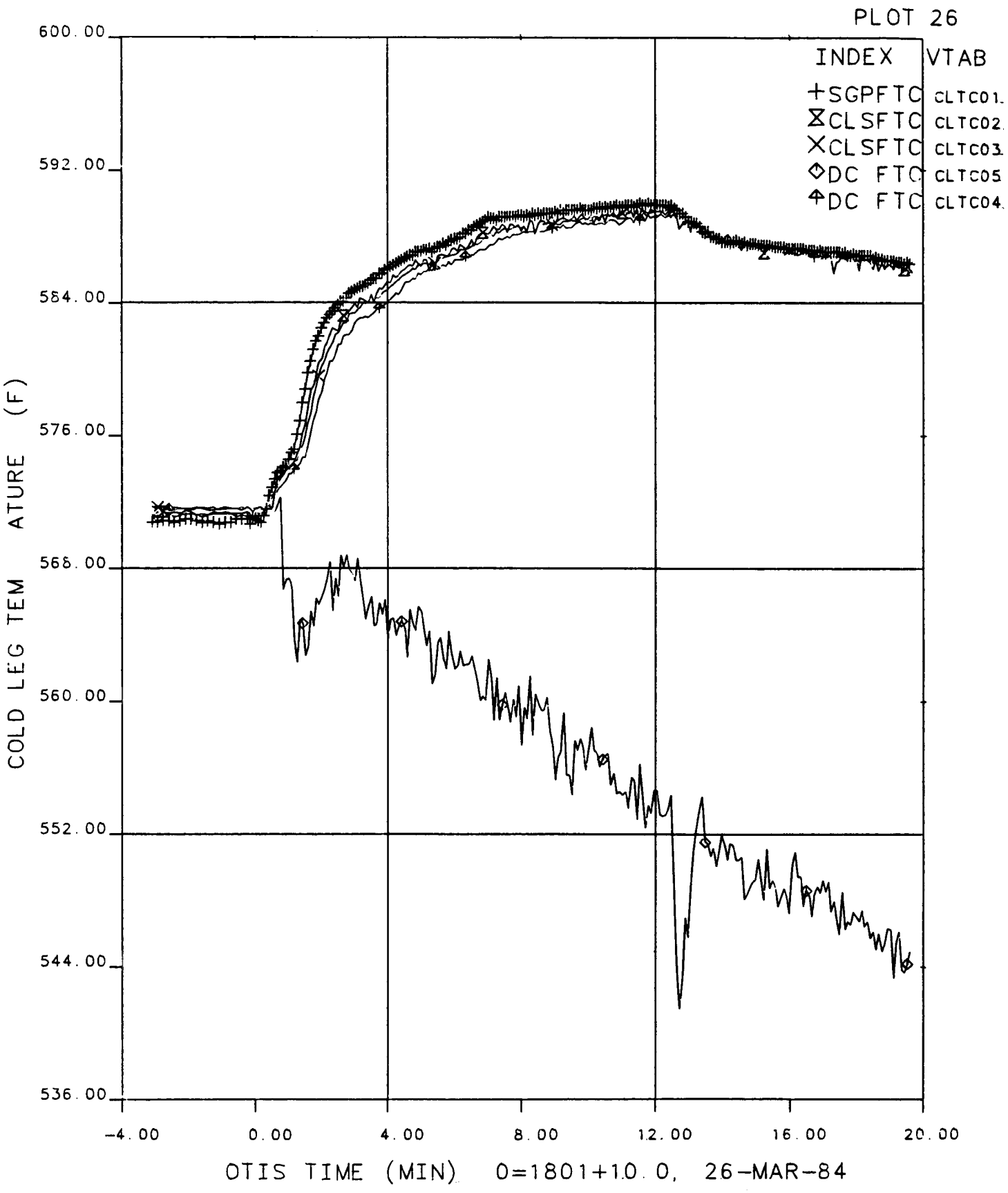

Figure 7.8 Cold Leg Temperatures, 0 to 20 Minutes

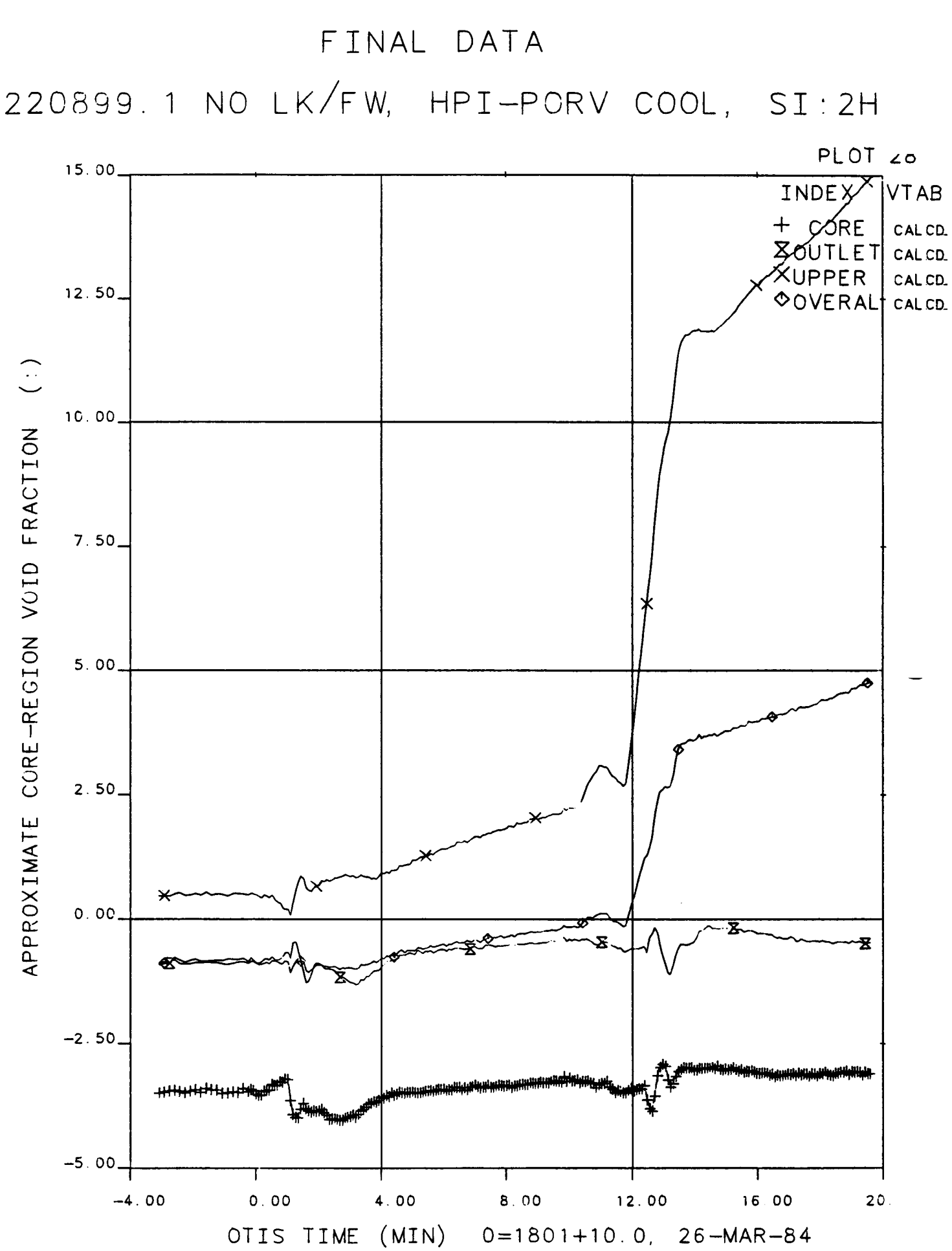

Figure 7.9 Core Region Void Fractions, 0 to 20 Minutes

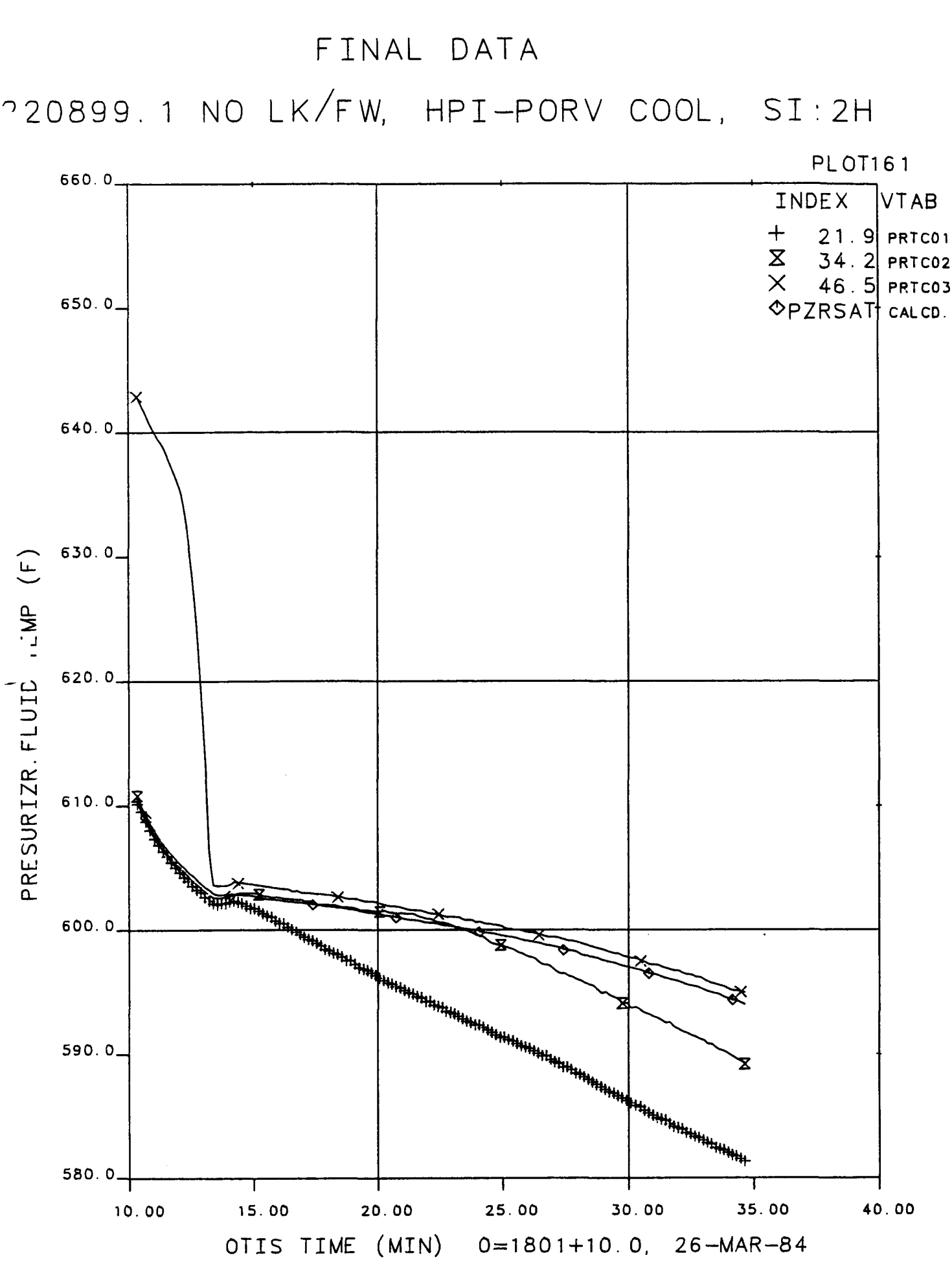

Figure 7.10 Pressurizer Fluid Temperatures, 10 to 35 Minutes

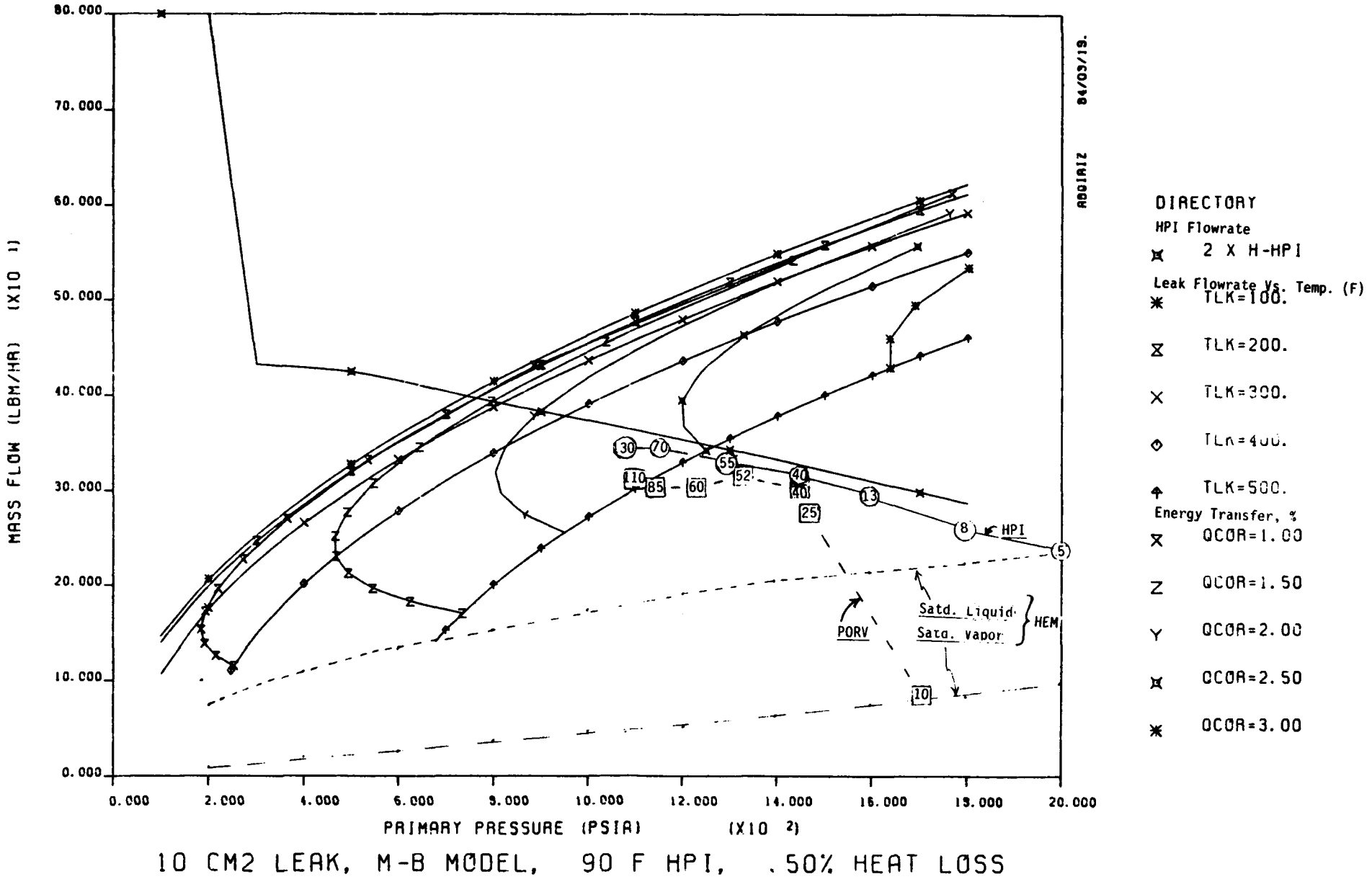

Figure 7.11 HPI and PORV Flow Rates Vs. System Conditions
Refer to Appendix C for a discussion of this equilibrium plot.

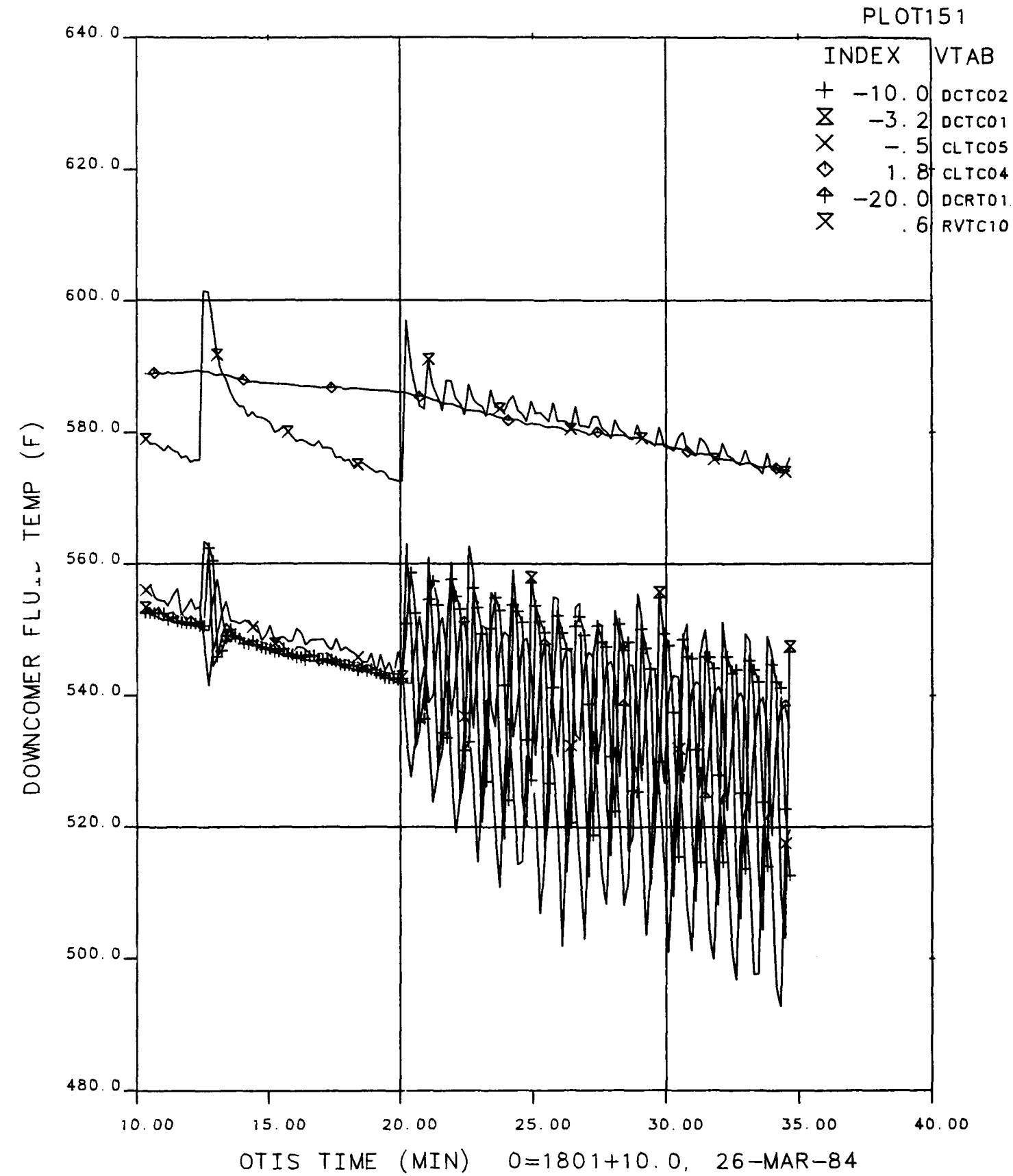

Figure 7.12· Downcomer Fluid Temperatures, 10 to 35 Minutes

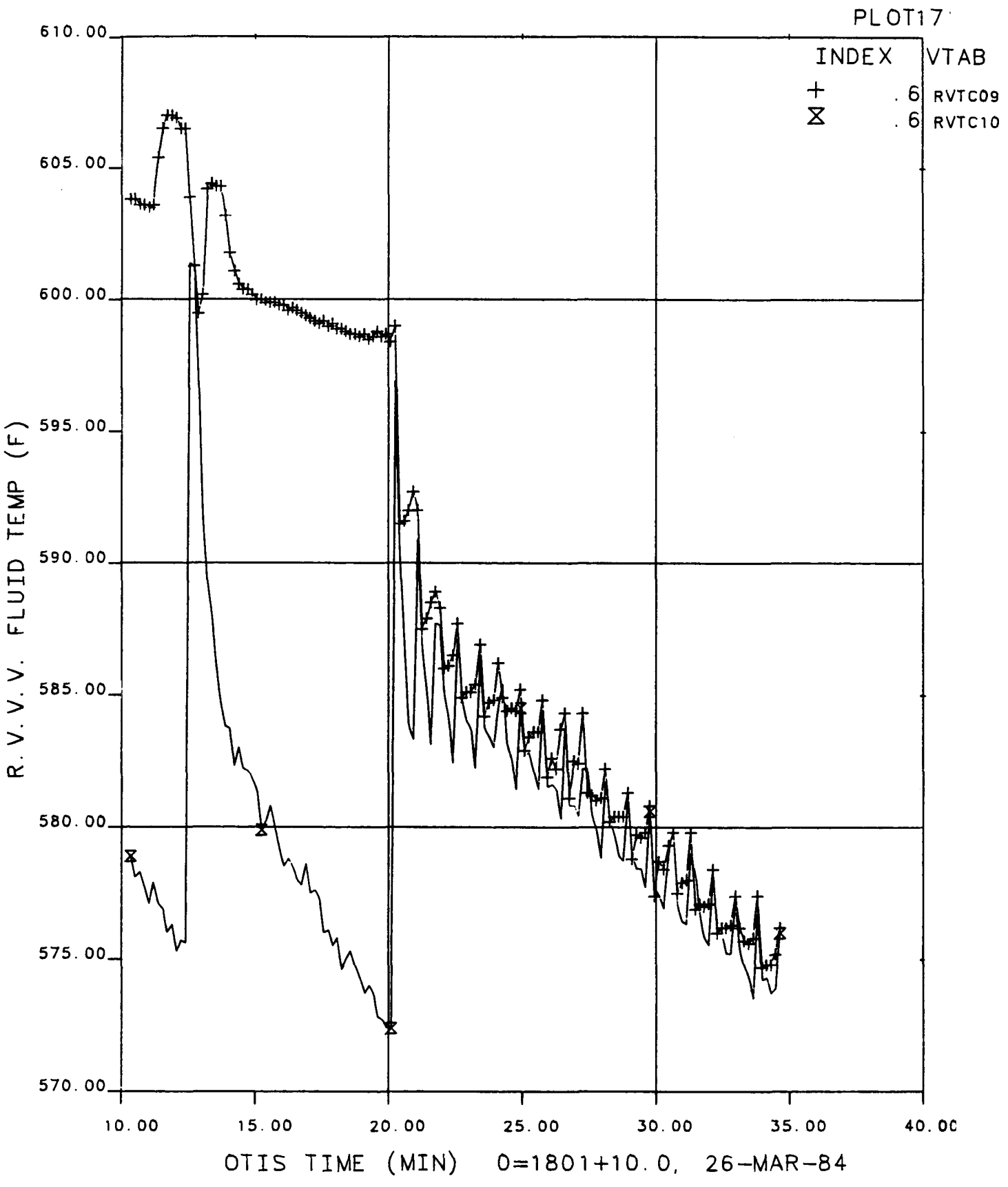

Figure 7.13 Reactor Vessel Vent Valve Fluid Temperatures, 10 to 35 Minutes

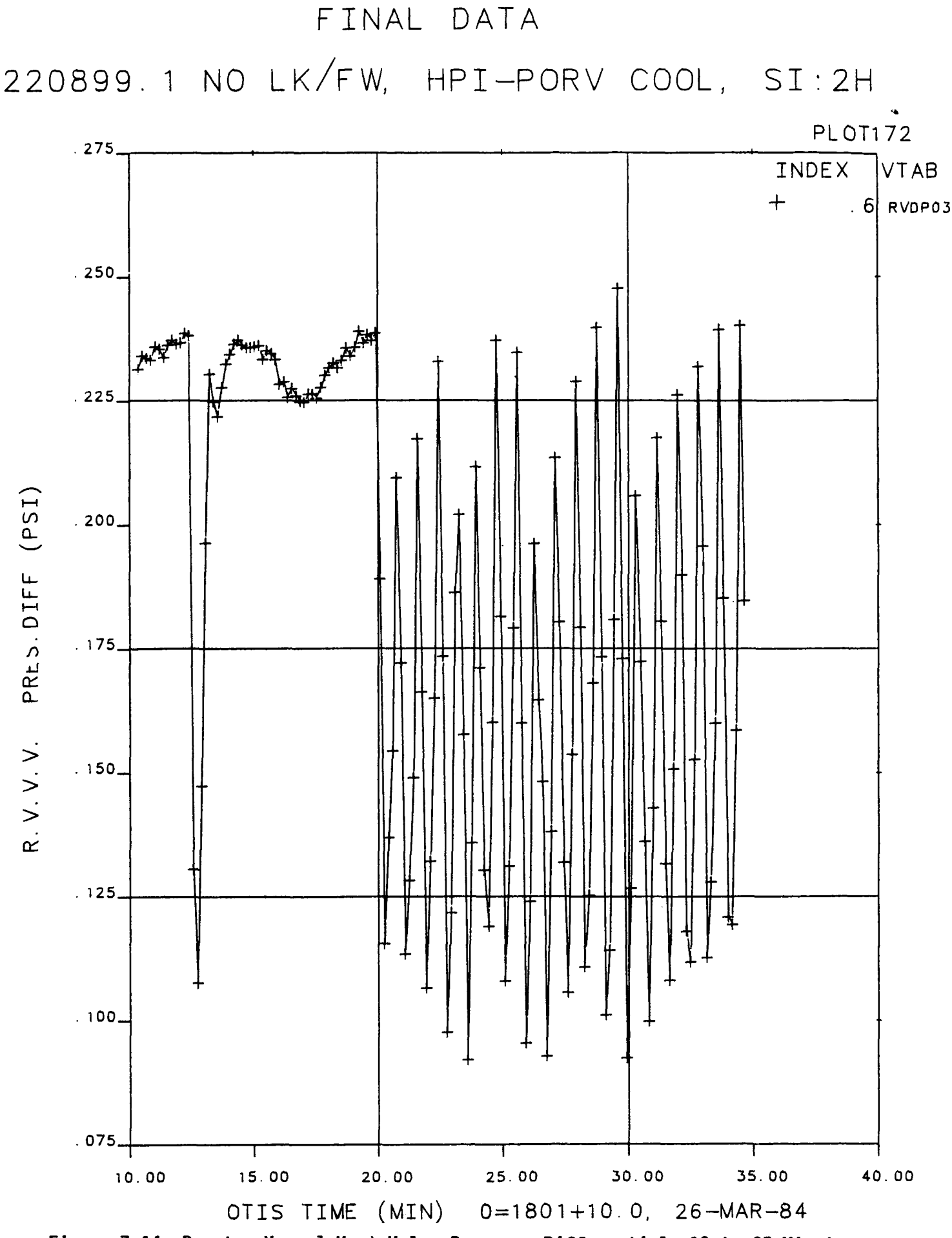

Figure 7.14 Reactor Vessel Vent Valve Pressure Differential, 10 to 35 Minutes

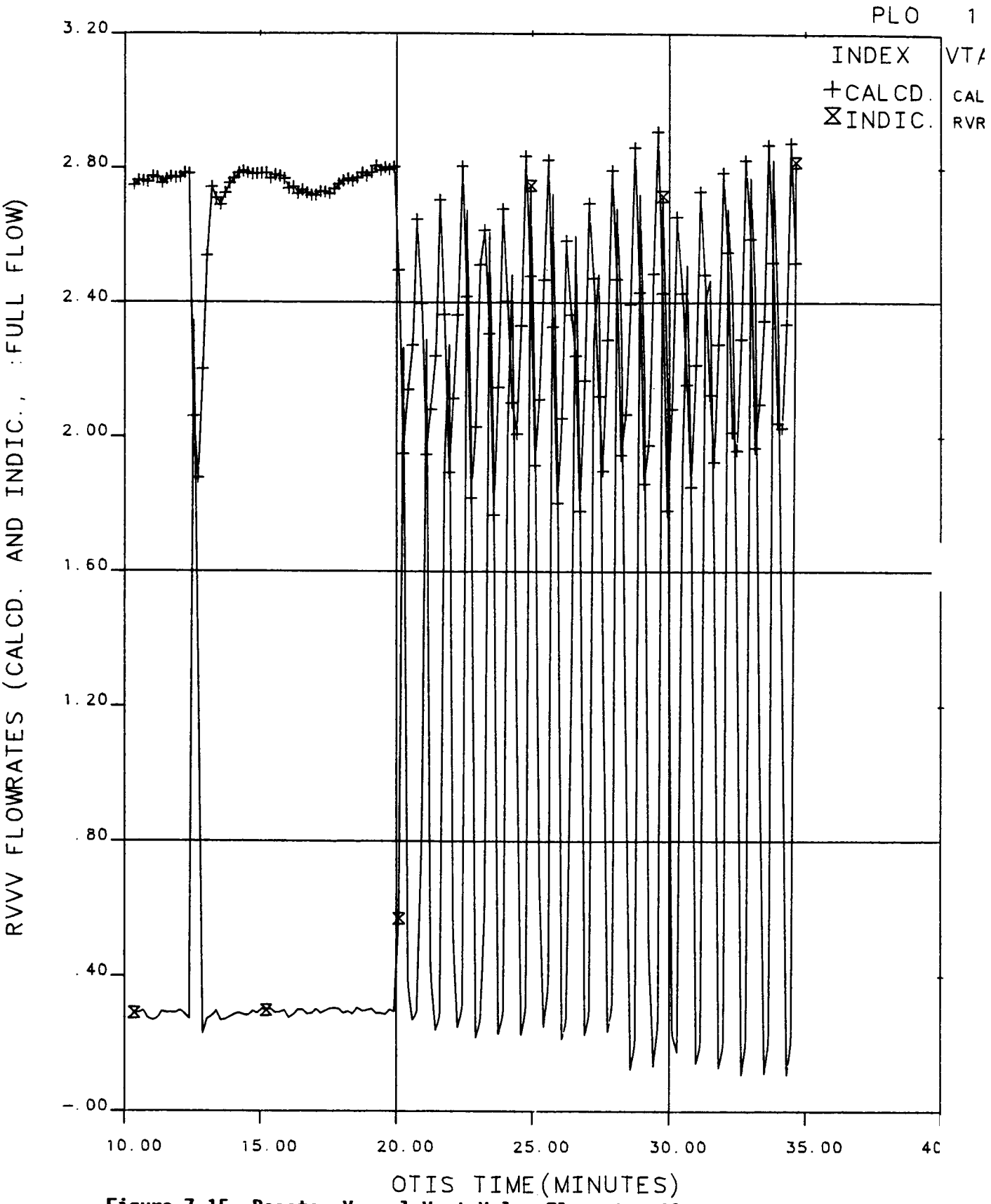

Figure 7.15 Reactor Vessel Vent Valve Flowrate, 10 to 35 Minutes

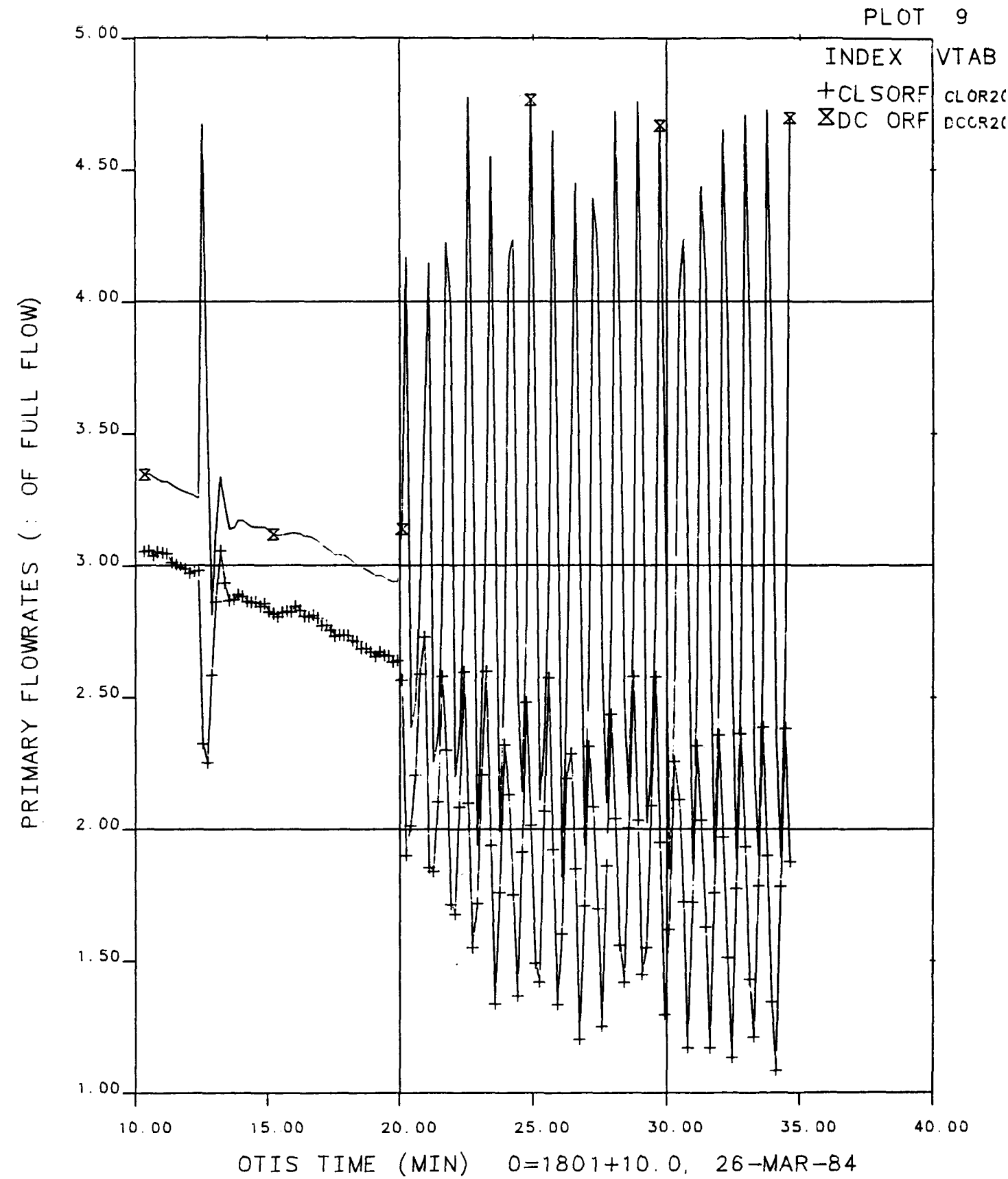

Figure 7.16 Primary Flowrates, 10 to 35 Minutes

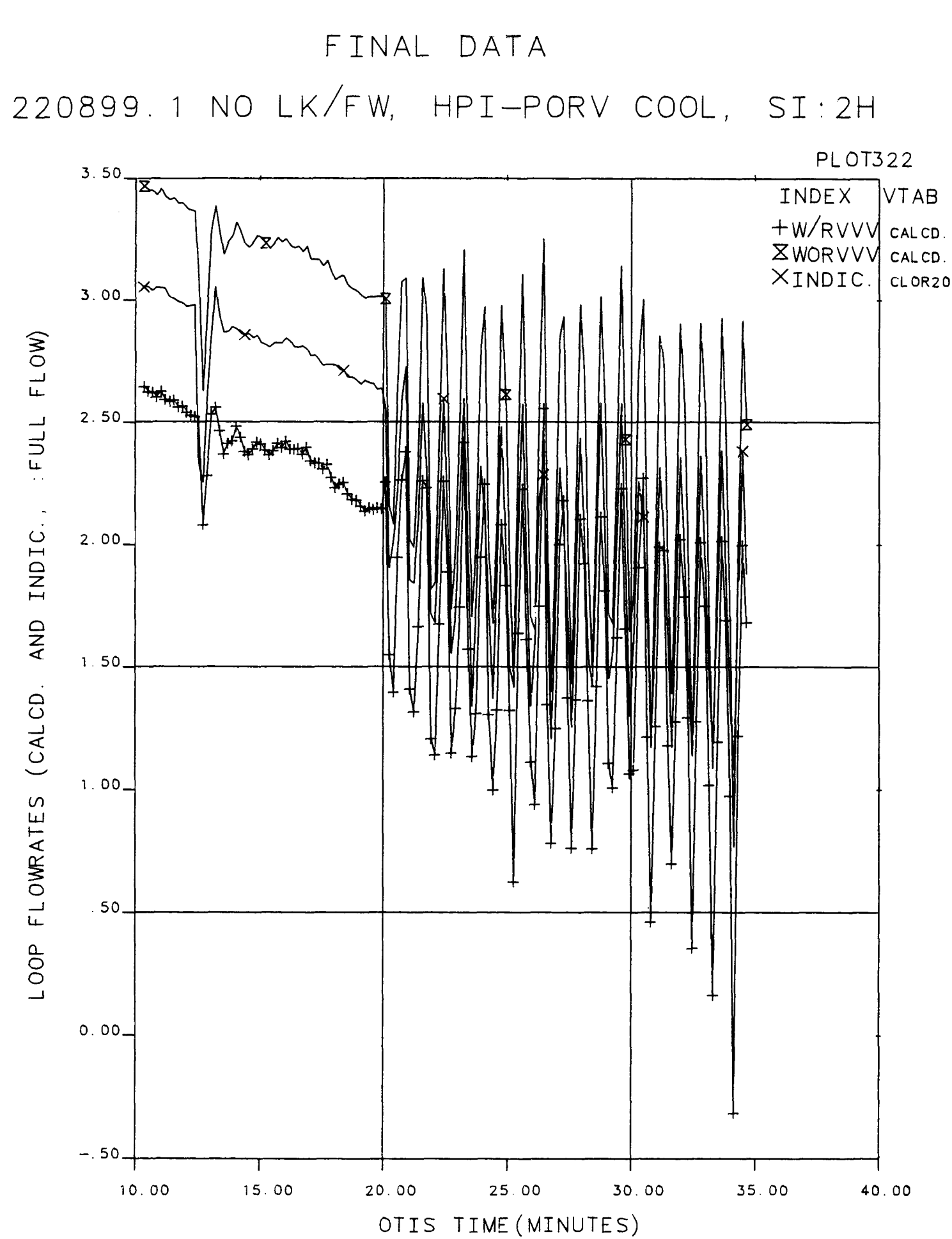

Figure 7.17 Loop Flowrate, 10 to 35 Minutes

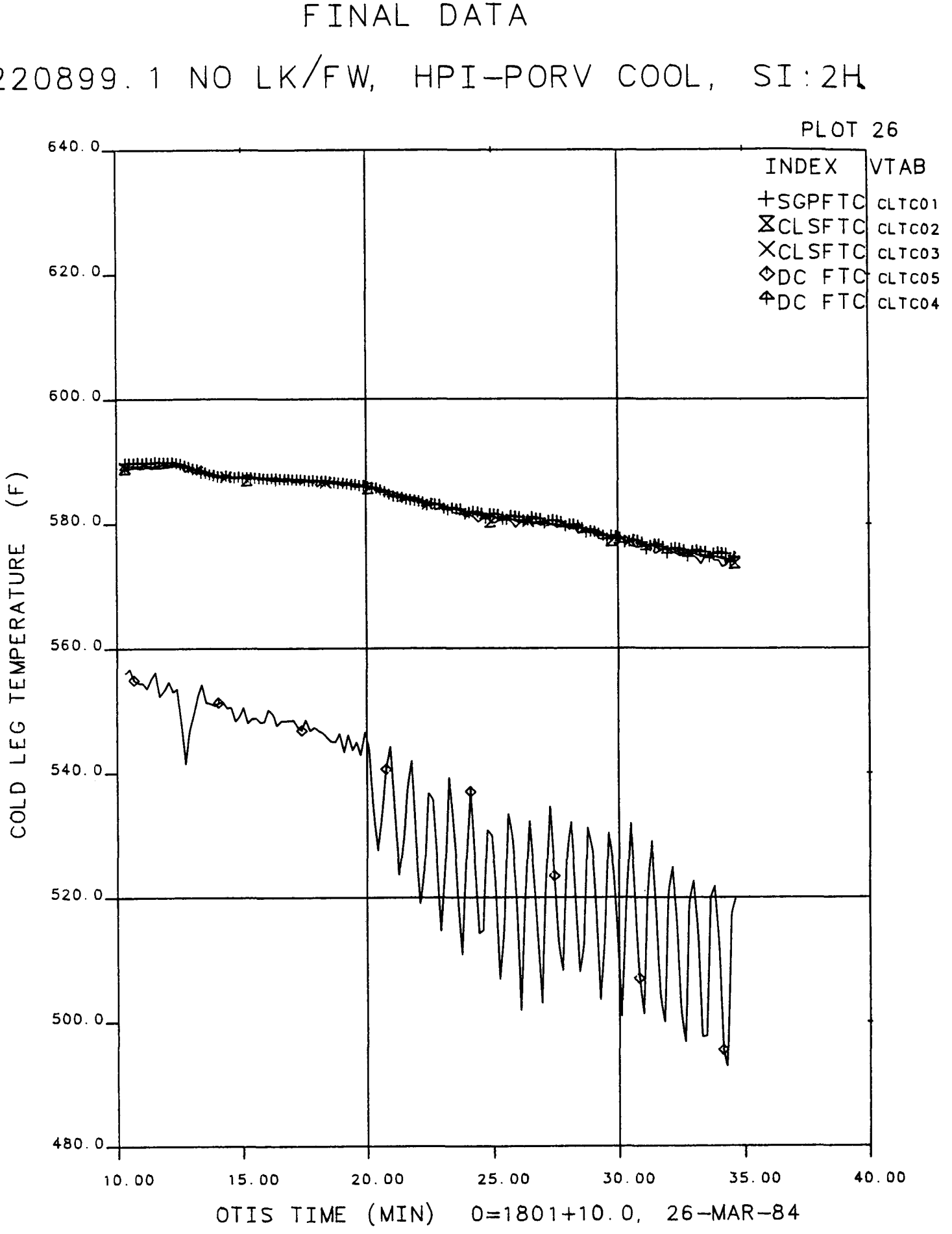

Figure 7.18 Cold Leg Temperatures, 10 to 35 Minutes

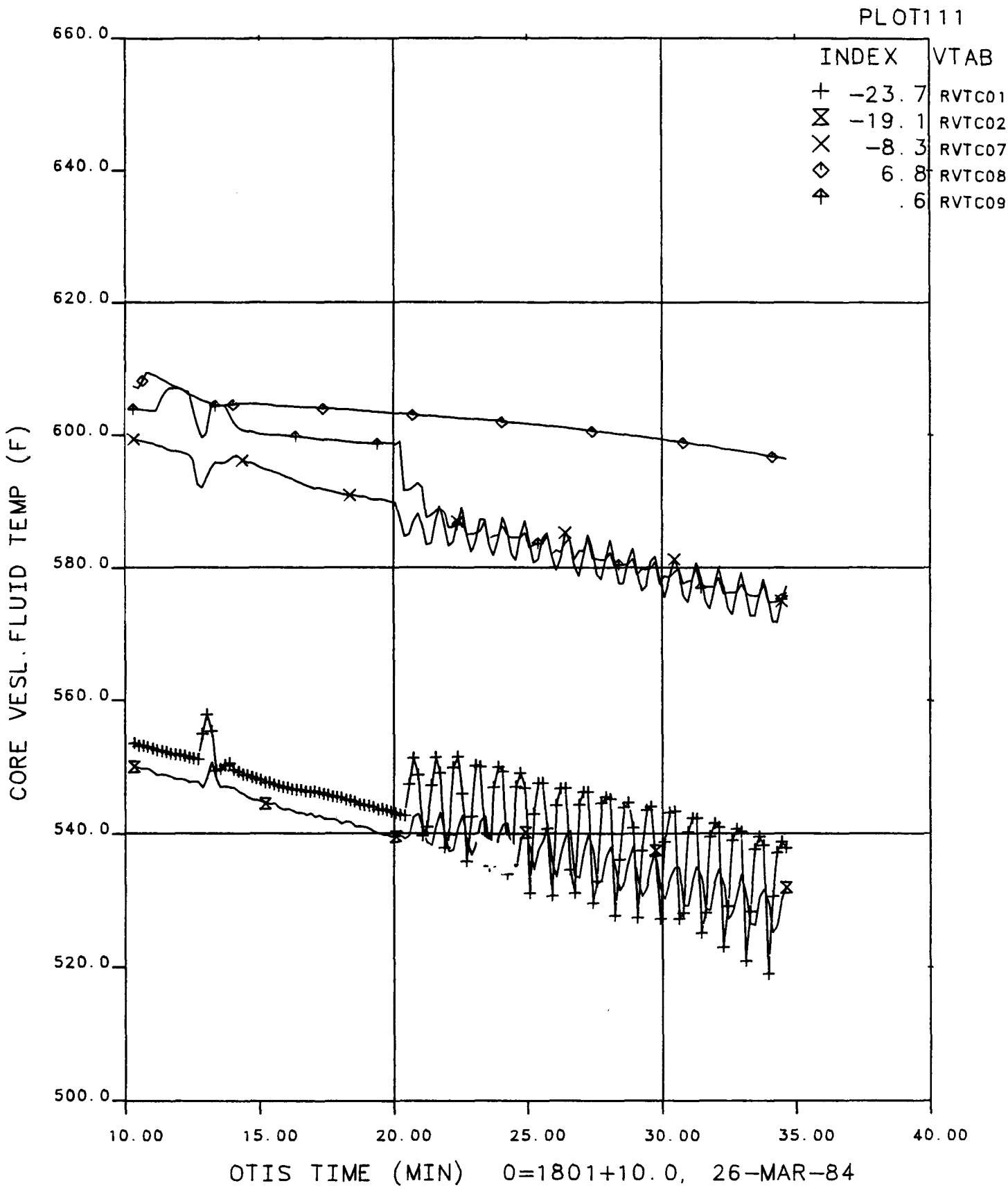

Figure 7.19 Core Vessel Fluid Temperatures, 10 to 35 Minutes

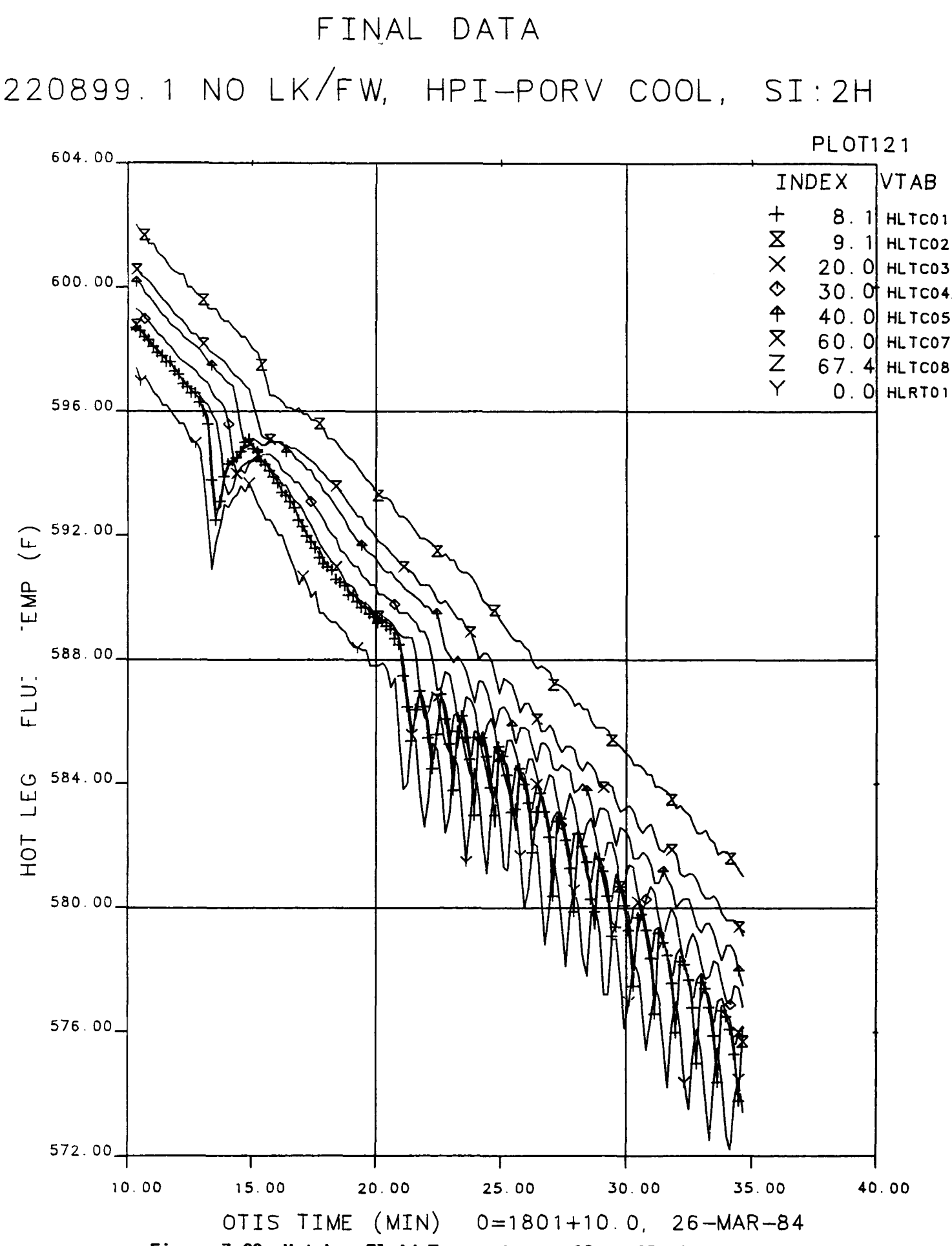

Figure 7.20 Hot Leg Fluid Temperatures, 10 to 35 Minutes

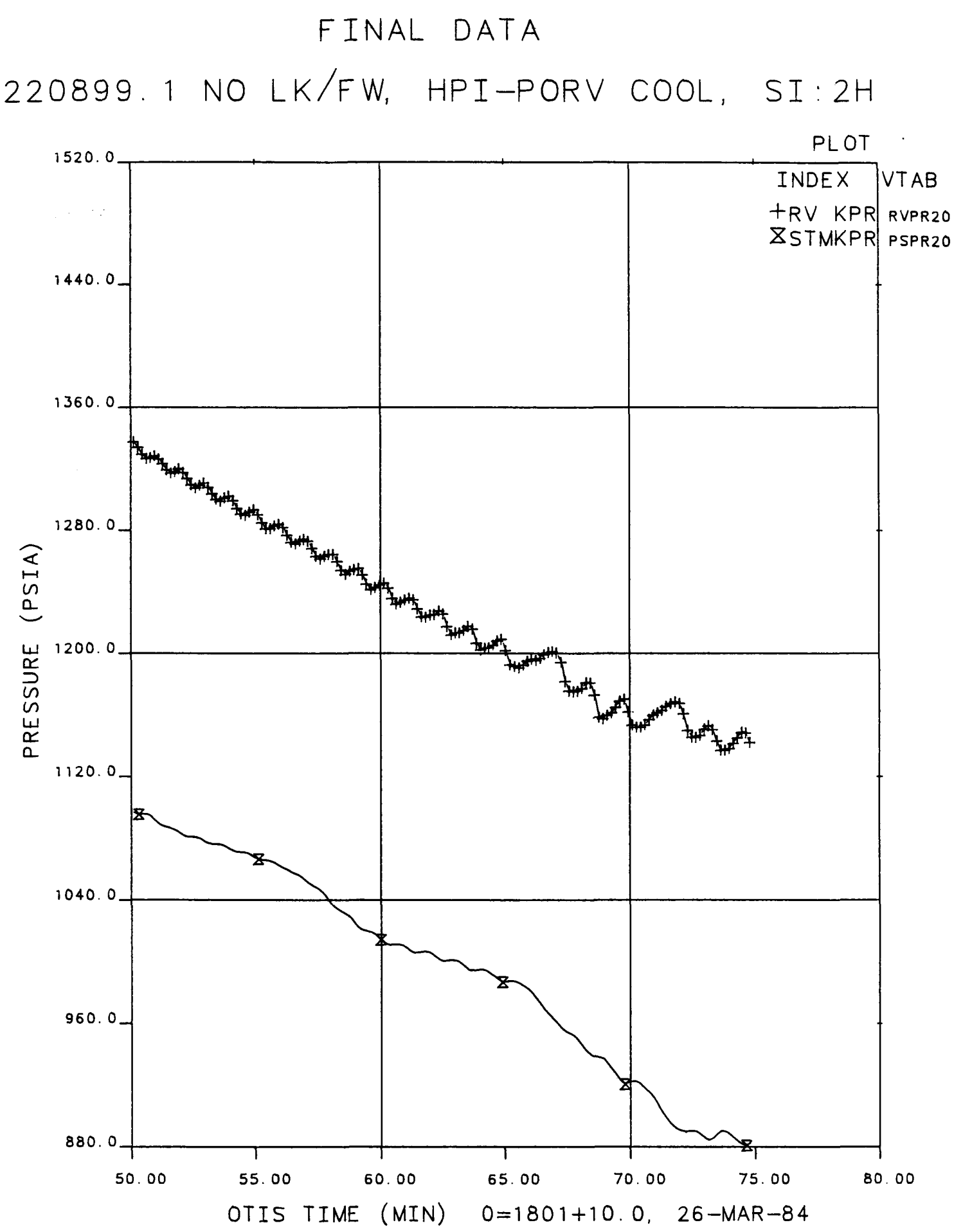

Figure 7.21 Primary and Secondary Pressure, 50 to 75 Minutes

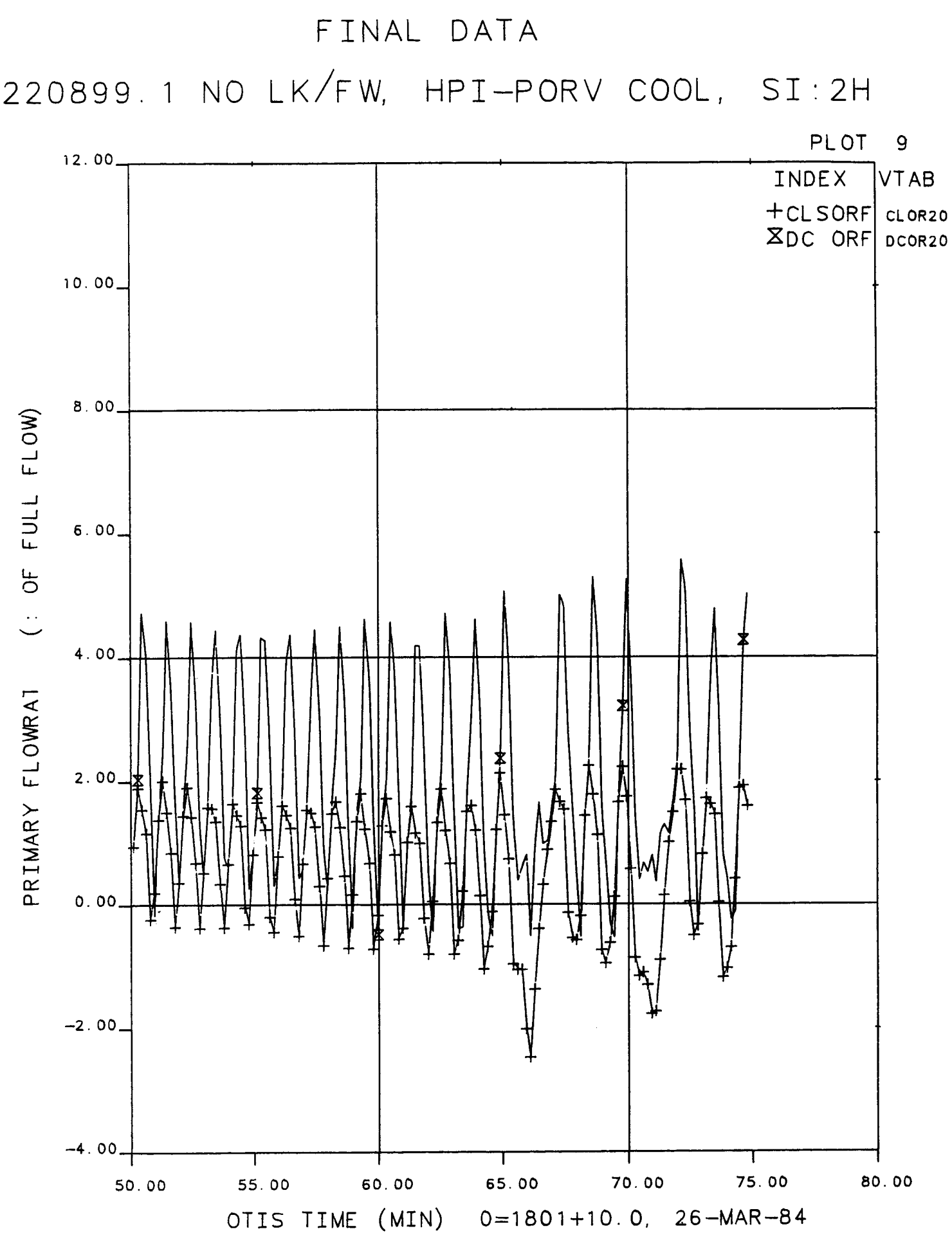

Figure 7.22 Primary Flowrates, 50 to 75 Minutes

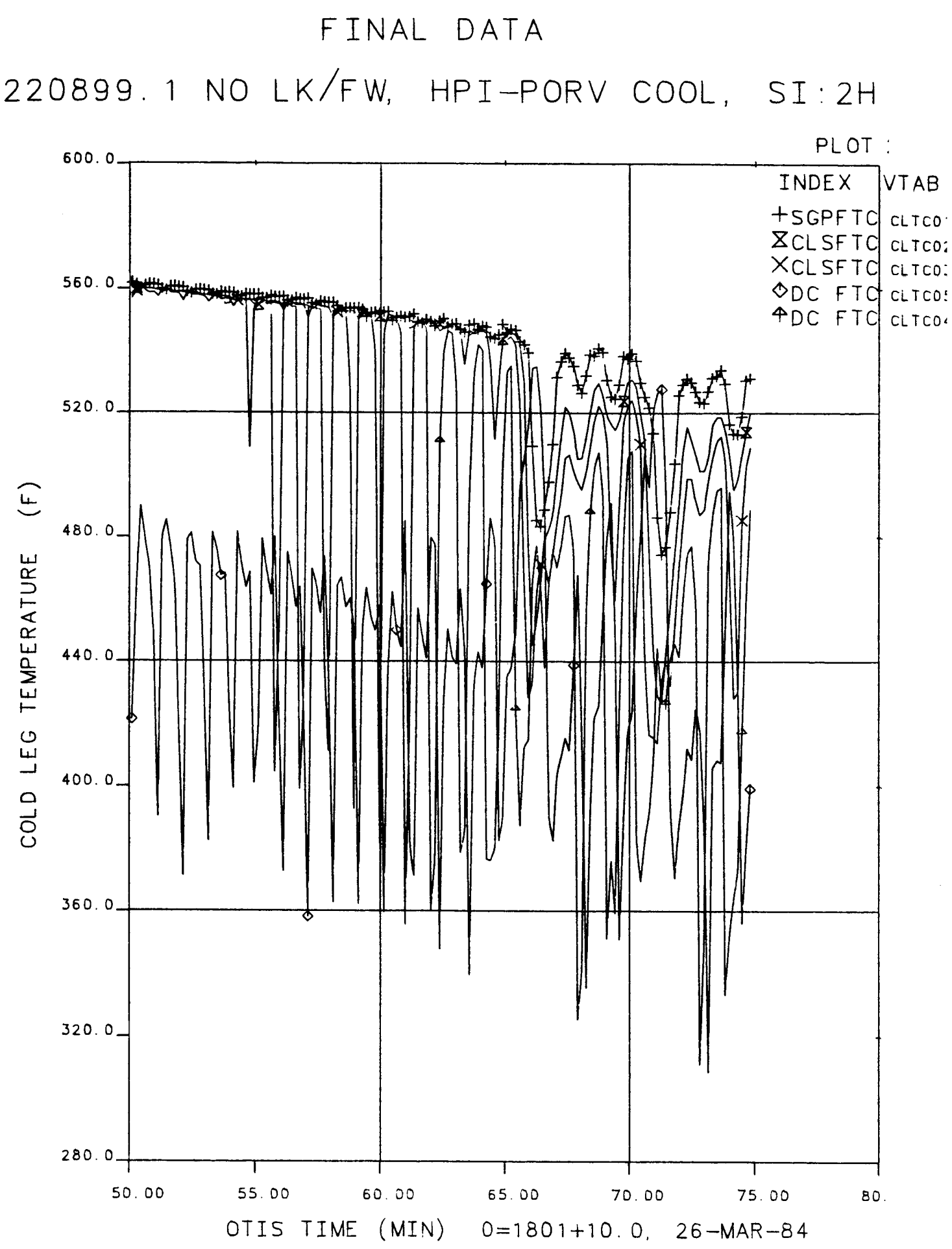

Figure 7.23 Cold Leg Temperatures, 50 to 75 Minutes

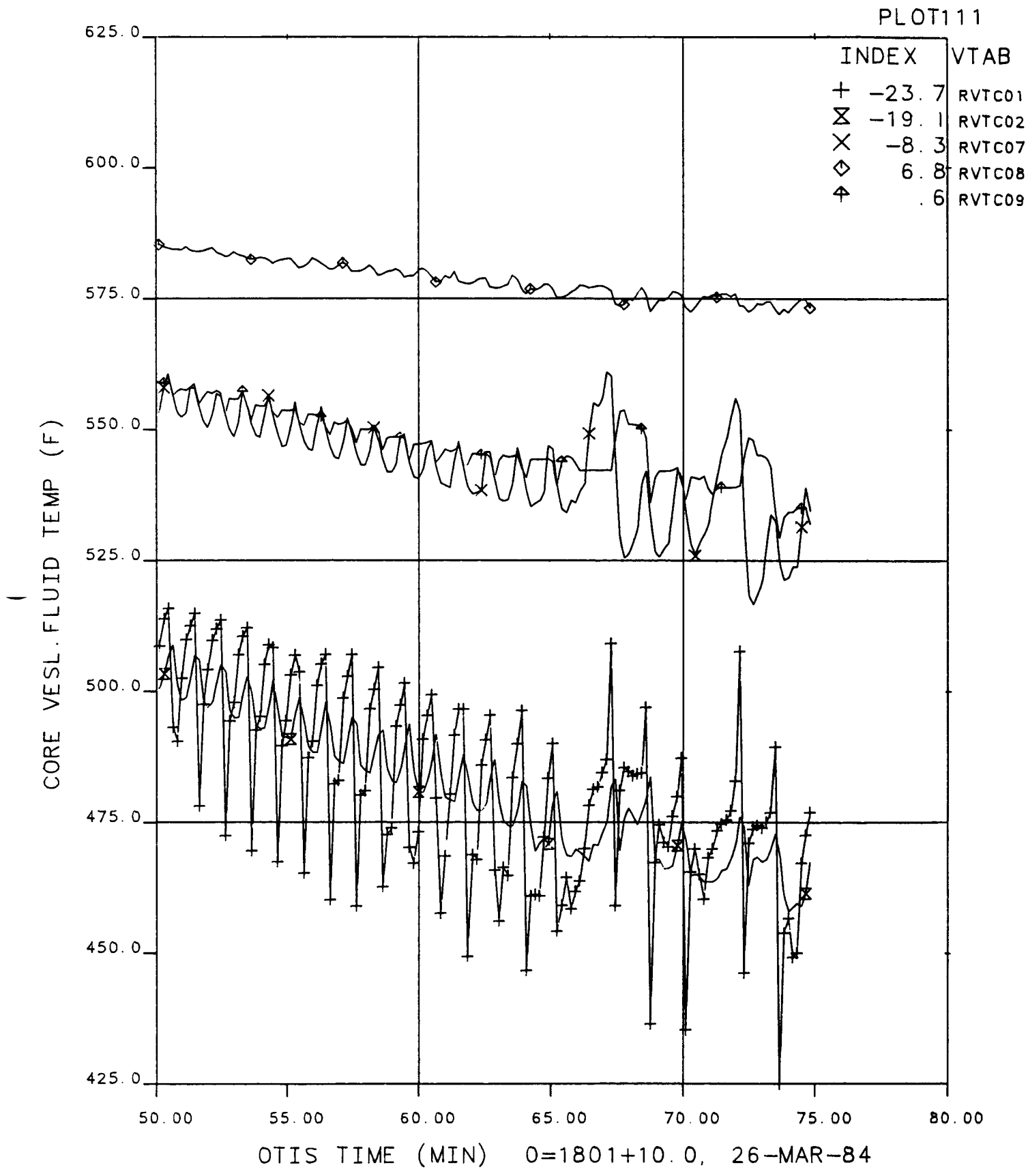

Figure 7.24 Core Vessel Fluid Temperatures, 50 to 75 Minutes

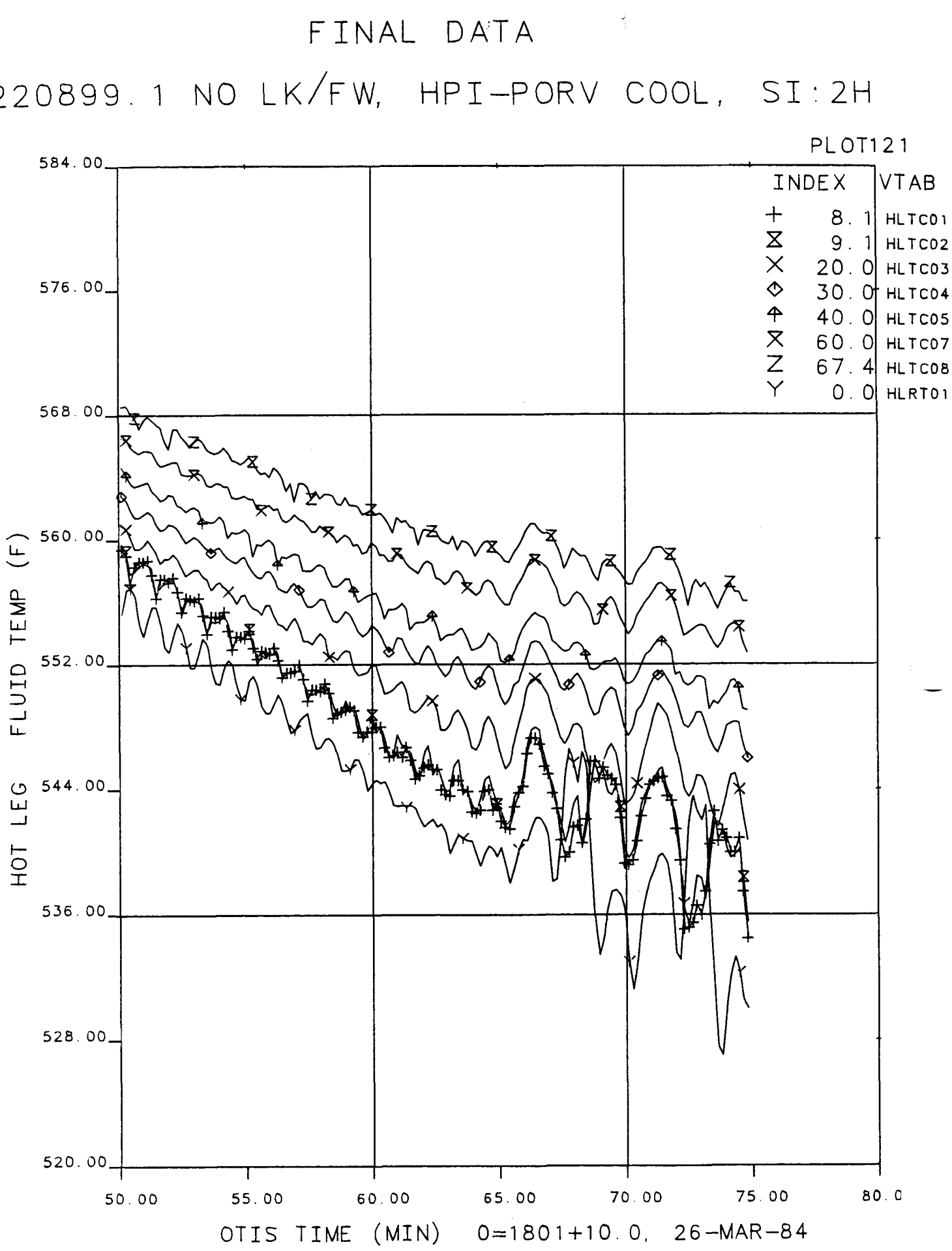

Figure 7.25 Hot Leg Fluid Temperatures, 50 to 75 Minutes

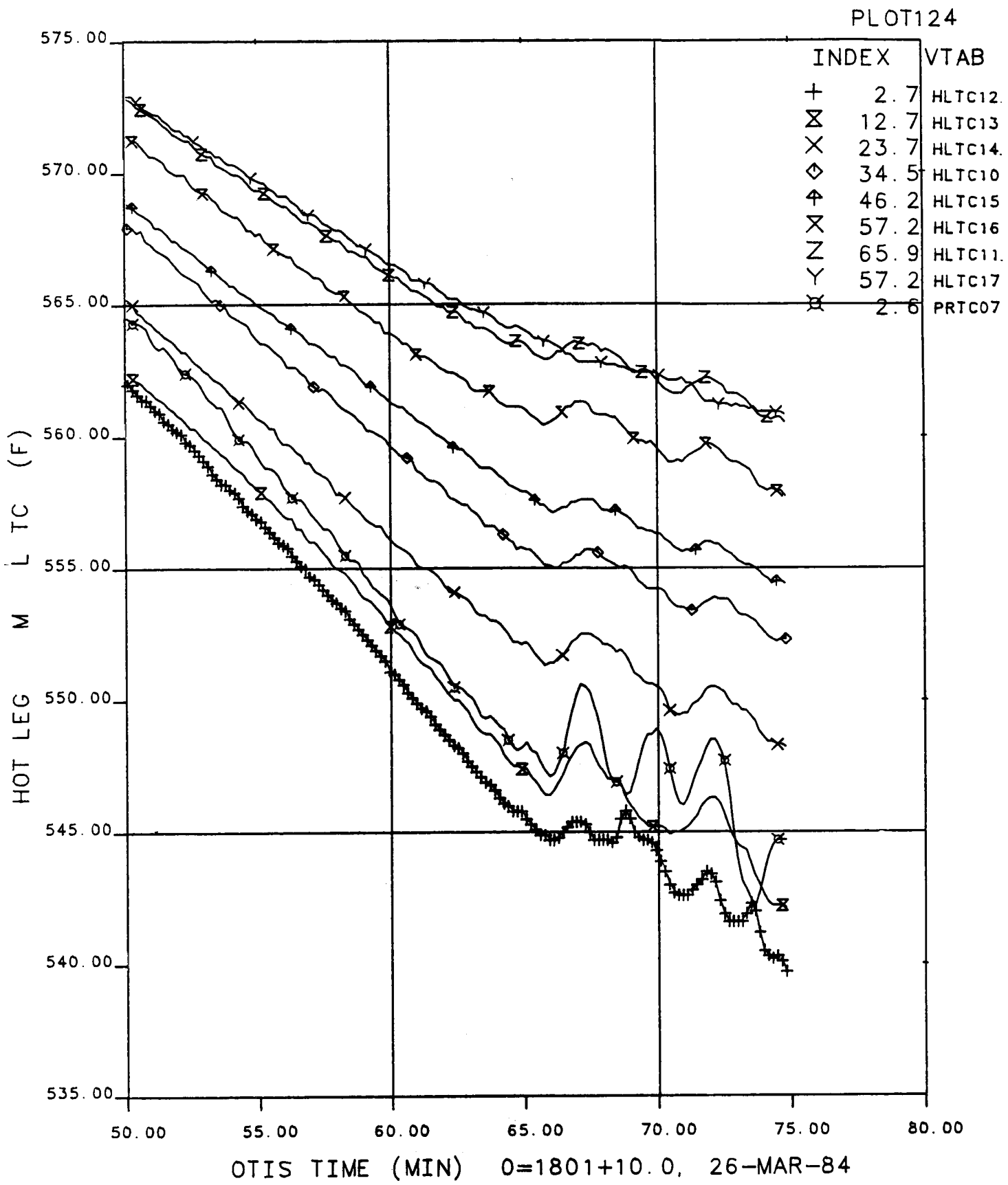

Figure 7.26 Hot Leg Metal Temperatures, 50 to 75 Minutes

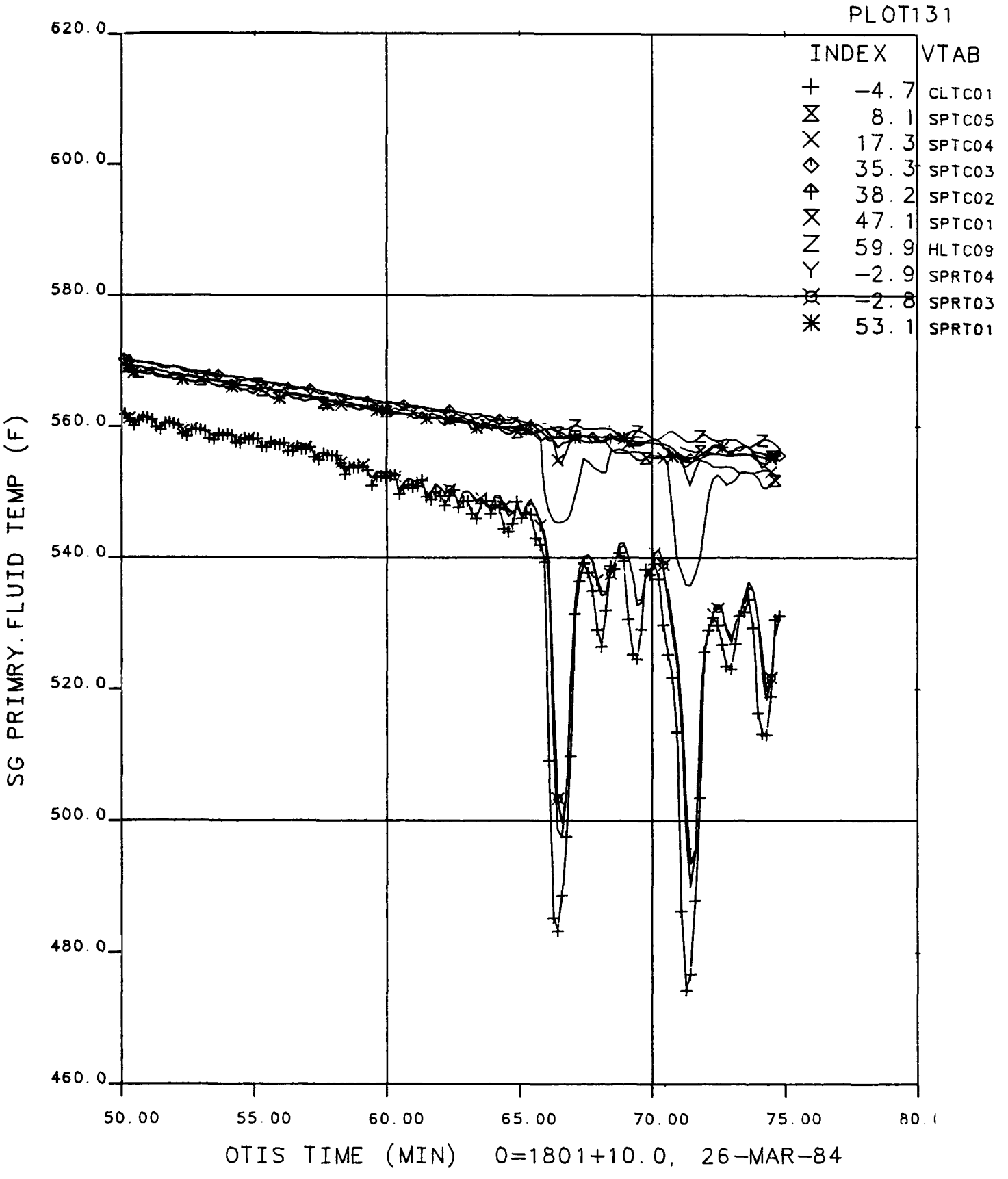

Figure 7.27 Steam Generator Primary Fluid Temperatures, 50 to 75 Minutes

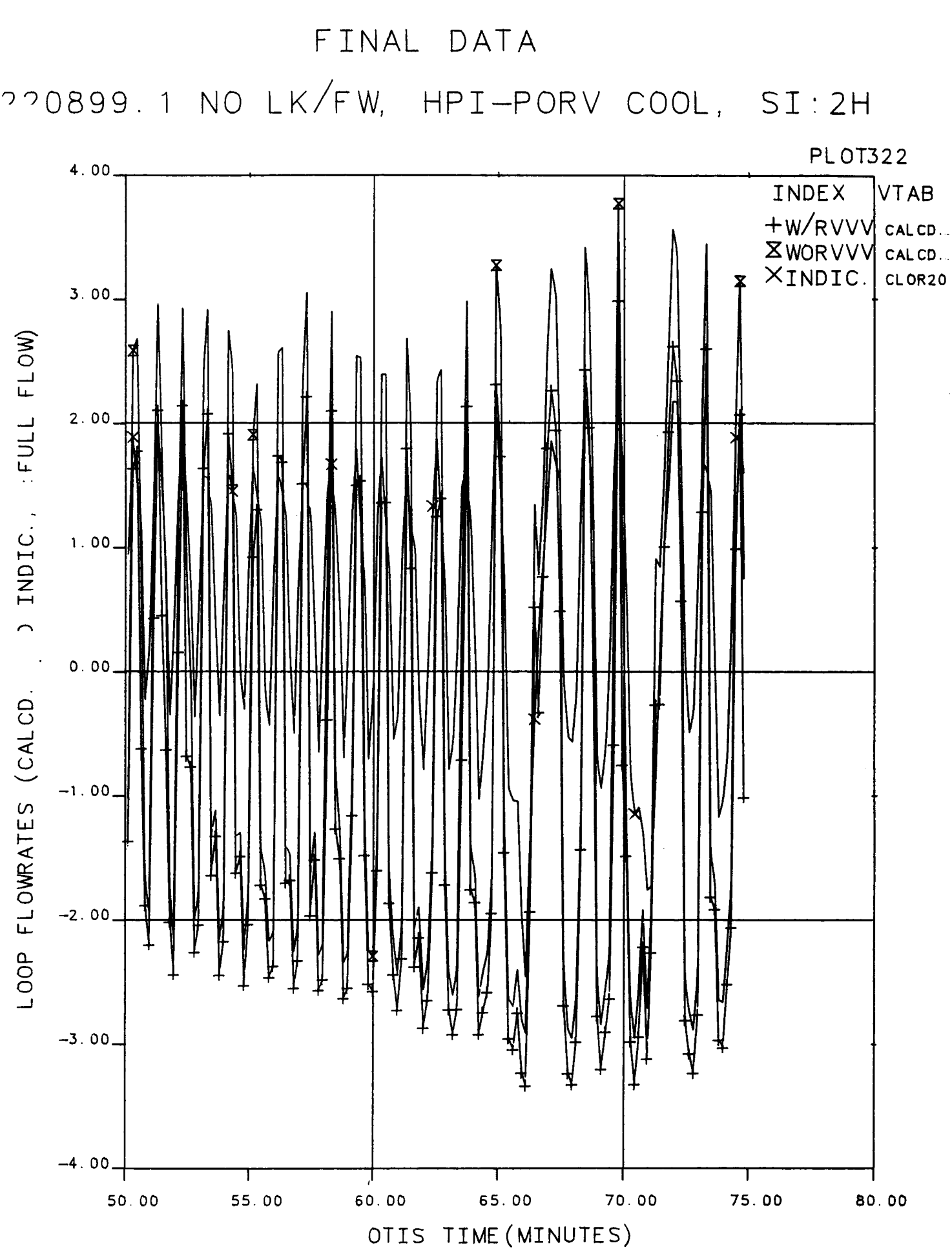

Figure 7.28 Loop Flowrates, 50 to 75 Minutes

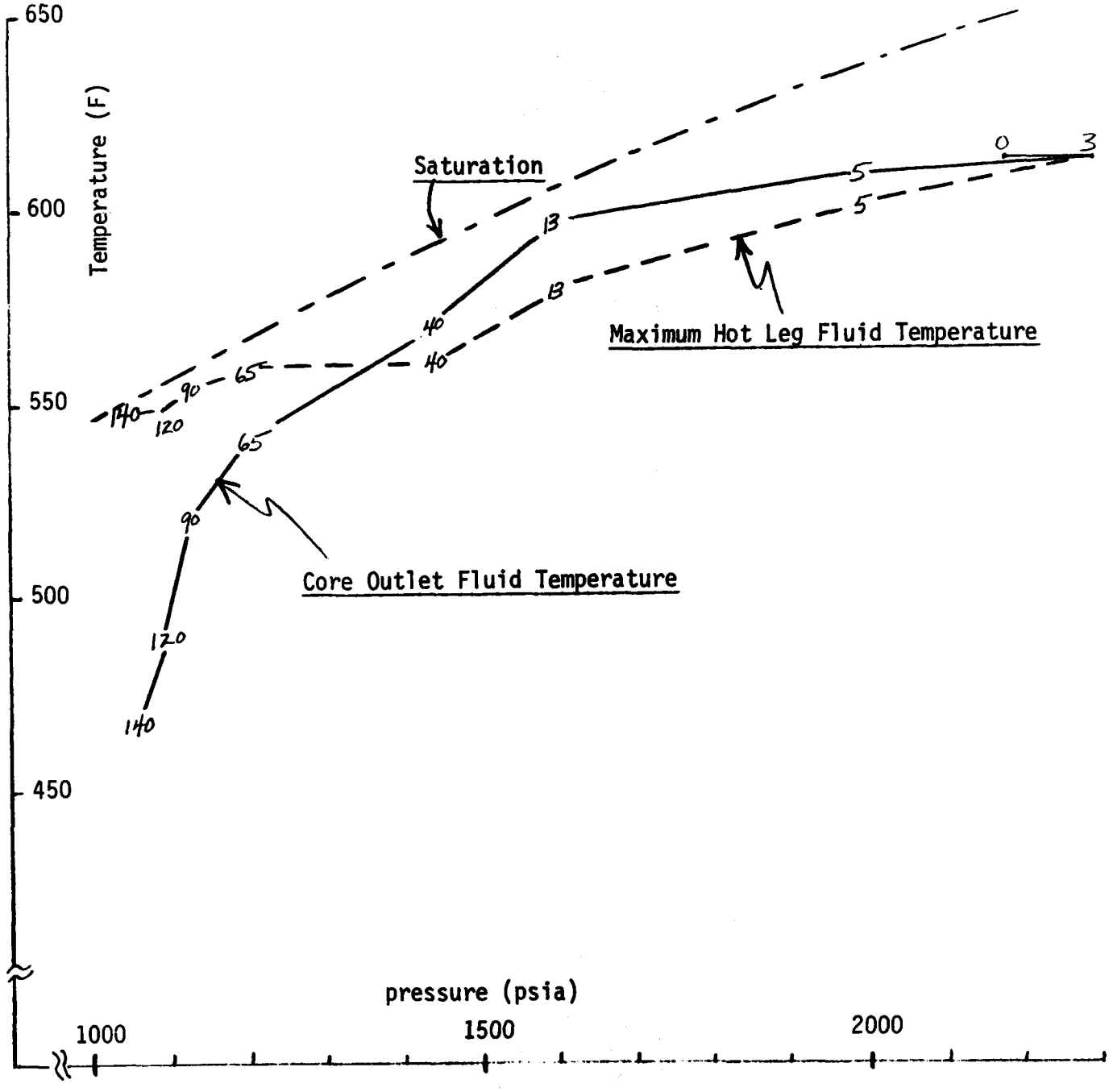

Figure 7.29 Core Outlet and Maximum Hot Leg Fluid Temperature Vs System Pressure.
(Plotted Numbers Denote Time After Test Initiation, in Minutes.)

8. NATURAL CIRCULATION COOLDOWN TESTS 220999 and 221099

8.1 Introduction

Natural Circulation Cooldown Tests 220999 and 221009 were similar to each other, but were quite unlike the other OTIS "single-variable" tests. The primary was cooled using the steam generator and adhering to the pressure-temperature envelope. There was no controlled leak, and core power was held constant. Test 220999 used no venting, but the reactor vessel head vent was actuated in Test 221099 after the upper head had voided due to system depressurization, to clear the void and to cool the upper head.

8.2 Test 220999 (Natural Circulation Cooldown Without Venting)

8.2.1 Conduct

OTIS Test 220999 was conducted on 6 April 1984. The test was performed as specified in the OTIS Test Specification[3] and the Alliance Research Center (ARC) Technical Procedure[5]. The conditions designated for the test were as follows:

- o No leak.
- o Constant core power -- 1% of scaled full power plus ambient heat loss.
- o Cooldown by depressurizing the stream generator secondary system at 50F/h.
- o Depressurize the primary system with the pressurizer relief valve while using high-pressure injection to maintain the pressurizer level.
- o Primary temperature and pressure were to be maintained within pressure-temperature (P-T) envelope limits (shown in Figure 8.1 and described in section 3).
- o No reactor vessel or hot leg vent actuation.
- o Terminate the test 30 minutes after minimum secondary pressure has been reached.

The initial conditions observed versus those specified are compared in Table 8.1. All observed conditions were as specified. The initial steam generator pressure of 1300 psia was revised (in Revision 2 of the Test Procedure[5] and verbally agreed to before test conduct) to bring the hot leg fluid to near normal plant operating temperatures (∿600F). The test was initiated following a period of steady-state operation, by the actuation of the secondary depresurization ramp (50F/h), followed thereafter by numerous

manual pressurizer relief valve actuations. The key operator actions and pressurizer relief valve actuation times are shown in Tables 8.2 and 8.3. Instruments discarded from the data base are listed in Table 8.4. As with preceding OTIS tests, the HL conductivity probes and off-nozzle string thermocouples dominate the list of unavailable instruments.

8.2.2 Observations

Figures 8.1 through 8.10 pertain to this discussion of Test 220999, cooldown without venting. Unlike the previous OTIS tests, Test 220999 exhibited only one mode of operation -- single-phase natural circulation. The data acquisition system was activated at 1107 on 6 April 1984. Steady-state data was accumulated for 12.4 minutes before test initiation. At time "0", the secondary system depressurization ramp was activated, as can be observed on Figure 8.2. Approximately two minutes later, the high-pressure injection system was started, resulting in a brief pressurization of the primary system as the high-pressure injection flow reached 0.10 lbm/s (Figure 8.3). The high-pressure injection fluid temperature influence is observable on Figure 8.4. The activation of high-pressure injection caused the initial primary flow rate of 3.6% to increase abruptly to 4.3%, then decrease to 2.9%, before returning to 3.75% (Figure 8.5). The relatively high primary flow maintained the reactor vessel vent valve in the closed position throughout the cooldown, cf. Figure 8.6. The effect of the secondary depressurization and cooldown can be observed on numerous plots. Figure 8.7 and the appended temperature plots show a linear cooldown rate of 50F/h from test initiation until approximately 400 minutes. The primary loop cooldown, in parallel with that of the secondary system, illustrated strong inter-system coupling.

At 42 minutes, the first of seventeen power-operated relief valve (PORV) actuations resulted in a primary depressurization of approximately 125 psi (Figure 8.2). The system depressurization resulted in increased high-pressure injection flow (Figure 8.3) and caused a slight oscillation in primary flow (Figure 8.5). Numerous PORV actuations followed (Table 8.3), resulting in a sawtooth primary pressure trace (Figure 8.2). Figure 8.8 shows the core inlet temperature (RVTC01) and the core outlet

temperature (RVTC07) decreasing together at a rate of approximately 50F/h. However, the upper head region temperatures (RVTC09 and RVTC08) indicated a reduced rate of decrease because they were isolated from the loop flow path.

Figure 8.8 shows the core temperature difference increasing somewhat as a result of slightly reduced primary loop flow. The decrease in primary loop flow was the result of the decreasing natural circulation driving head (Figure 8.9); this reduction was caused by a thermal center shift within the steam generator, as the ratio of heat transfer at the high (AFW) injection elevation versus the pool elevation decreased with decreasing primary-to-secondary temperature difference. That is, initially 100F auxiliary feedwater (AFW) was sprayed onto the primary tubes which were at 600F (500F ΔT), whereas at 368 minutes, the primary inlet temperature was only 300F (200F ΔT), thereby reducing the AFW cooling effect. The reduced fluid thermal expansion coefficient with lower average fluid temperature also contributed to the gradual flow reduction.

Continued primary depressurization ultimately caused the saturation and flashing of the upper head region fluid at 375 minutes. As shown on Figure 8.8, RVTC09 indicates a sharp increase to the saturation temperature as the liquid interface moves by. Figure 8.10 (collapsed liquid levels) indicates a step decrease in reactor vessel level at this time. The pressurizer level response changed markedly as the reactor vessel voided, cf. Figure 8.10. Whereas the pressurizer level had decreased roughly one foot during the previous PORV depressurizations, it increased abruptly by 3 to 5 feet as the reactor vessel level descended.

At approximately 388 minutes the secondary pressure reached 31 psia, ending the depressurization ramp. The component temperature plots indicate a leveling trend and nearly constant temperatures beyond 388 minutes (Figure 8.7). After 388 minutes, the duration of PORV opening was increased, resulting in an increase in the rate of primary depressurization (Figure 8.2). The accelerated depressurization was permitted as the RCS temperature decreased below the P-T envelope "knee" at 365F on Figure 8.1. Numerous PORV actuations occurred until 638 minutes, when the primary

pressure reached 300 psia. At 638 minutes, the test was terminated according to procedure, with the loop temperature below 300F and primary flow approximately 3.1%.

8.3 Test 221099, Natural Circulation Cooldown With Upper Head Venting

8.3.1 Conduct

OTIS Test 221009 was conducted on 5 April 1984. Test performance was as specified by the OTIS Test Specification[3] and the ARC Techncial Procedure[5]. The conditions for this test were identical to those of Test 220999 except that the reactor vessel head vent was to be utilized to refill the voided upper head region during the transient. The observed versus specified conditions are compared in Table 8.1. All conditions except the pressurizer level were as specified. However, this discrepancy is not perceived to have affected the test results. The secondary pressure was initialized at 1300 psia as it was in Test 220999 in order to establish primary loop fluid at plant-typical temperatures. With the reactor vessel head vent closed, Test 221009 was initiated by actuating the secondary depressurization ramp. The key operator actions and poweroperated relief valve actuation times are shown in Tables 8.5 and 8.6. The reactor vessel head vent actuations are shown in Table 8.7. Instruments discarded from the data base are listed in Table 8.8. As with preceding OTIS tests, the hot leg conductivity probes and off-nozzle string thermocouples dominated the list of unavailable instruments. The primary pressure was controlled during cooldown and was maintained within the envelope shown on Figure 8.1. According to procedure, the test was conducted for 615 minutes and was terminated after ten hours of natural circulation cooldown.

8.3.2 Observations

Figures 8.11 through 8.20 pertain to this discussion of Test 221099, cooldown with venting. As with Test 220999, Test 221099 remained in subcooled natural circulation the entire time. The data acquisition system was activated at 1016 on 5 April 1984. Steady-state data was accumulated

until 1029, when the steam pressure ramp was activated (time "0", Figure 8.11). The high-pressure injection (HPI) system was activated approximately four minutes later. The operator immediately throttled HPI, limiting its flowrate to 0.012 lbm/s (Figure 8.12) versus 0.1 lbm/s initially in test 220999 (Figure 8.3). Whereas the primary loop flowrate increased and then decreased before stabilizing at an intermediate value in test 220999 (Figure 8.5), it increased and then stabilized in test 221099 (Figure 8.13) illustrating the reduced impact of HPI with initial HPI throttling. The relatively high loop flow maintained the reactor vessel vent valve in the closed position for the entire test (Figure 8.14). The secondary depressurization and cooldown rate of 50F/h is observable on Figure 8.15 and the appended plots.

The primary pressure was reduced by manual actuations of the power-operated relief valve (Figure 8.11), which began at 43 minutes and continued throughout the test (Table 8.6). Loop cooldown and depressurization continued regularly until approximately 312 minutes, when a dysfunction of the steam flow control system caused a decrease in steam and feed flow in the secondary system. The dysfunction was caused by the loss of steam pressure control valve rangeability (the valve was at its full open position) using the low steam flow circuit. Control was regained when the operator transferred to the high flow circuit. As a result, a 15-minute period of reduced primary-to-secondary coupling caused an undulation in the normally linear component temperature curves at 317 minutes (Figure 8.15 and the appended plots). Recovery of the steam flow control system led to a feed flow spike (Figure 8.16) at 322 minutes and a primary flow spike (Figure 8.17) at 324 minutes. A brief period of cooldown in excess of 50F/h followed until approximately 330 minutes, when the normal rate resumed. At 361 minutes, the upper head region of the reactor vessel saturated and voided as in Test 220999. The reactor vessel level decreased from 6 to 5 feet initially, but with additional power-operated relief valve actuations, it ultimately fell to 0.0 feet by 410 minutes (Figure 8.18). Saturated temperatures were apparent on Figures 8.14 and 8.19 (core vessel and reactor vessel vent valve fluid temperatures) at this time. At 411 minutes, the operator manually opened the reactor vessel head vent (RVUHV). The vent open for 10 minutes during which time the reactor vessel level increased to 8 feet (full), Figure 8.18. Continued primary depressurization again

resulted in upper reactor vessel head region flashing at 423 minutes. Numerous openings of the RVUHV over the next 60 minutes (Table 8.7) according to the test procedure eventually resulted in sufficient cooldown of the upper head metal (RVTC11 and 12 on Figure 8.20) to preclude further flashing. Therefore, subcooled conditions were maintained for the remainder of the test. At 410 minutes, the secondary system depressurization was completed (Figure 8.11), and the rate of system cooldown slowed dramatically (Figure 8.15). Power-operated relief valve actuations continued to depressurize the primary system, which reached 300 psia at 602 minutes. The test was terminated at 602 minutes with primary temperatures below 300F (Figure 8.15) and a primary flow rate of 3.1% of scaled full flow (Figure 8.17).

8.4 Results

OTIS Tests 220999 and 221099 both remained in subcooled natural circulation for their entirety. Both tests exhibited approximately 400 minutes of cooldown at a rate of 50F/h before the secondary pressure reached its minimum and the cooldown ceased. In both tests, the upper head region voided at approximately 360 to 380 minutes. Upper head voiding did not lead to loop flow interruption or even to saturation of the core-exit fluid. In Test 221009, the reactor vessel head vent was effective in cooling and refilling the voided region. Both tests were ended after approximately 10 hours of testing with loop temperatures at or below 300F, a primary pressure of approximately 300 psia, and a primary flow rate of 3.1%.

Table 8.1 Initial Conditions, Natural Circulation Cooldowns

	Test 220999		Test 221099	
	Planned	Actual	Planned	Actual
Core power (% of full power, 1% full power = 24.1 kW), includes 0.5% to replace losses to ambient.	1 ± 0.1	1	1 ± 0.1	1
Natural circulation.	X	X	X	X
Primary pressure, psia.	2200 ± 50	2200	2200 ± 50	2200
Pressurizer liquid height, ft from SGLTSUF.	21.6 ± 2	24	21.6 ± 2	26
Pressurizer main and guard heaters adjusted for an approximately adiabatic pressure.	X	X	X	X
RVUHV ("open" after RVUH voiding, Test 221099).	CLOSED	CLOSED	CLOSED	CLOSED
HLHPV.	CLOSED	CLOSED	CLOSED	CLOSED
RVVV in automatic (differential-pressure) control with open/close setpoints of 0.25 and 0.125 psid.	X	X	X	X
AFW at 100F injected at the elevation using the minimum-wetting nozzle.	X	X	X	X
SG secondary (collapsed) liquid level (with constant level control).	12 ± 1	12	12 ± 1	12
SG secondary pressure.	1300 ± 10	1300	1300 ± 10	1300
HPI and leak systems are not yet in use. Primary non-condensible gas additions are not to be tested.	X	X	X	X
Initialization is contined until a suitable system steady state is obtained:				
Pressurizer metal temperatures, F.	650 ± 10	650	650 ± 10	650
RVVV is not cycling.	X	X	X	X

Table 8.1 (Cont'd)

	Test 220999		Test 221099	
	Planned	Actual	Planned	Actual
The SG fluid temperatures are varying less than 10F/h: cyclic secondary fluid temperature variations associated with high AFW injection, and with internal circulation within the secondary liquid pool, are acceptable.	X	X	X	X
Other initial conditions:				
T-cold, F		580		580
Primary flow rate, % (1% = 0.259 lbm/s)		3.6		3.6
Steam/feed flow rate, %, approx. (1% = 0.0265 lbm/s)		0.4		0.35
AFW temperature, F		103		102

Table 8.2. Selected Operator Actions -- Natural Circulation Cooling Without Venting, Test 220999

Time	T, min.	Action
1107	-12	DAS starts (6 April 1984).
1119	0	Began SG secondary depressurization ramp.
1121	2	Activated HPI.
1201 and beyond	42 and beyond	PORV opened. (PORV actuations are summarized in Table 8.3).
2157	638	Test completed, deactivated DAS.

Table 8.3 PORV Actuations -- Natural Circulation Cooldown Without Venting, Test 220999

PORV opening times (min.) from the start of the secondary depressurization, which occurred 12.4 min. after DAS activation. Durations and integrated flow from log entries.

PORV open, min	Duration, s	Integrated flow, lbm
42.	50.	2.0
61.	50.	3.5
79.	70.	5.25
134.	75.	7.0
188.	60.	7.0
216.	45.	8.75
250.	50.	8.75
288.	55.	10.5
325.	80.	12.25
355.	115.	14.0
375.	265.	17.75
395.	340.	21.0
419.	315.	24.5
446.	420.	26.25
471.	620.	29.5
505.	1050.	34.5
564.	780.	38.0

Table 8.4 Summary of Variables Discarded on Input, Natural Circulation Cooldown Without Venting, Test 220999

SUMMARY OF VARIABLES DISCARDED ON INPUT, TEST 220999

NO.	VTAB	SYSTEM	INST.	ELEVATION	D E S C R I P T I O N
1	155HLTC06	2HL	2FTC	50.00	HOT LEG FLUID TEMP (F)
2	262HLCP05	2HL	16 CP	41.00	HOT LEG CONDCTVTY (WET/DRY)
3	263HLCP06	2HL	16 CP	45.00	HOT LEG CONDCTVTY (WET/DRY)
4	264HLCP07	2HL	16 CP	49.00	HOT LEG CONDCTVTY (WET/DRY)
5	265HLCP08	2HL	16 CP	53.00	HOT LEG CONDCTVTY (WET/DRY)
6	266HLCP09	2HL	16 CP	57.00	HOT LEG CONDCTVTY (WET/DRY)
7	274HLCP17	2HL	23RCP	.50	HOT LEG REF. C.P.
8	273HLCP16	3SGP	16 CP	53.10	SG PRIMRY. CONDCTVTY (WET/DRY)
9	272HLCP15	3SGP	16 CP	56.90	SG PRIMRY. CONDCTVTY (WET/DRY)
10	103PRDT03	6PZR	10 DT	42.80	PRESURIZR. INSUL. DT (F)
11	323RVLS01	7RVV	29ETC	.60	R.V.V.V. MISCELLAN (VARIOUS)
12	324RVLS06	7RVV	29ETC	.60	R.V.V.V. MISCELLAN (VARIOUS)
13	223HPTM02	10HPI	13TMF	-999.00	HP INJECT. TURB.FLOW (LBM/SEC)
14	219V1AC01	11V1	19ACC	-999.00	1-PH VENT. ACCD.FLOW (LBM)
15	317V1PF20	11V1	36FLO	-999.00	1-PH VENT. CALD.FLOW (LBM/SEC)
16	220V2AC01	12V2	19ACC	-999.00	2-PH VENT. ACCD.FLOW (LBM)
17	53SSTC13	22SGS	2FTC	32.30	SG SECOND.FLUID TEMP (F)
18	79SMTC02	22SGS	25MTC	26.30	SG SECOND. METAL TC (F)
19	76SMTC06	22SGS	25MTC	44.20	SG SECOND. METAL TC (F)
20	289SSCP20	22SGS	32KCP	0.00	SG SECOND. UP.WET.CP (REF. FT)
21	344V1TC03	34CLD	2FTC	-999.00	CLD LEAK FLUID TEMP (F)

Table 8.5 Selected Operator Actions -- Natural Circulation Cooldown With Venting, Test 221099

Time	ΔT, min.	Action
1016	-13	DAS started.
1029	0	Began SG secondary depressurization ramp.
1033	4	Activated HPI.
1112 and beyond	43 and beyond	Opened PORV. (PORV actuations are summarized in Table 8.6).
1720	411	Opened RVUHV.
1730	421	Closed RVUHV.
1734 and beyond	425 and beyond	Opened RVUHV for 1 min. (RVUHV actuations are summarized in Table 8.7).
2033	602	Test complete, deactivated DAS.

Table 8.6 PORV Actuations -- Natural Circulation Cooldown With Venting, Test 221099

PORV (power-operated relief valve) opening times from the start of the secondary depressurization (min.), which occurred 13 min. after DAS activation. Durations and integrated flows from log entries.

PORV opened, min	Duration, s	Integrated flow, lbm
43.	54.	-
58.	97.	3.5
80.	120.	7.5
102.	120.	9.0
138.	130.	12.5
172.	145.	14.75
213.	120.	18.75
234.	70.	
253.	140.	22.25
282.	100.	24.0
322.	180.	27.75
344.	180.	29.50
362.	250.	33.0
381.	360.	38.0
403.	330.	40.25
426.	540.	43.0
474.	840.	50.25
520.	1080.	55.25
561.	1380.	60.5

Table 8.7 RVUHV Actuations -- Natrual Circulation Cooldown With Venting, Test 221099

RVUHV (reactor vessel head vent) opening times from the start of the secondary depressurizaton (min.), which occurred 13 min. after DAS activation. Durations and integrated flows (when available) from operator log entries.

RVUHV opened, min	Duration, min.	Integrated flow, lbm
411.	10.	
425.	1.	
430.	1.	
436.	1.	2.5
441.	1.	
446.	1.	
451.	1.	
456.	1.	
461.	1.	
466.	1.	
471.	1.	
476.	1.	
481.	1.	
486.	1.	12.5
491.	1.	
496.	1.	
502.	1.	
507.	1.	
512.	1.	
517.	1.	
522.	1.	
527.	1.	
532.	1.	
537.	1.	23.5
542.	1.	
547.	1.	
552.	1.	

Table 8.7 (Cont'd)

RVUHV opened, min	Duration, min.	Integrated flow, lbm
557.	1.	
562.	1.	
567.	1.	
572.	1.	
577.	1.	
582.	1.	
588.	1.	33.0
592.	1.	
597.	1.	
602.	1.	36.5

Table 8.8 Summary of Variables Discarded on Input, NC Cooldown With Venting, Test 221099

SUMMARY OF VARIABLES DISCARDED ON INPUT, TEST 221099

NO.	VTAB	SYSTEM	INST.	ELEVATION	DESCRIPTION
1	155HLTC06	2HL	2FTC	50.00	HOT LEG FLUID TEMP (F)
2	262HLCP05	2HL	16 CP	41.00	HOT LEG CONDCTVTY (WET/DRY)
3	263HLCP06	2HL	16 CP	45.00	HOT LEG CONDCTVTY (WET/DRY)
4	264HLCP07	2HL	16 CP	49.00	HOT LEG CONDCTVTY (WET/DRY)
5	265HLCP08	2HL	16 CP	53.00	HOT LEG CONDCTVTY (WET/DRY)
6	266HLCP09	2HL	16 CP	57.00	HOT LEG CONDCTVTY (WET/DRY)
7	274HLCP17	2HL	23RCP	.50	HOT LEG REF. C.P.
8	273HLCP16	3SGP	16 CP	53.10	SG PRIMRY. CONDCTVTY (WET/DRY)
9	272HLCP15	3SGP	16 CP	56.90	SG PRIMRY. CONDCTVTY (WET/DRY)
10	103PRDT03	6PZR	10 DT	42.80	PRESURIZR. INSUL. DT (F)
11	323RVLS01	7RVV	29ETC	.60	R.V.V.V. MISCELLAN (VARIOUS)
12	324RVLS06	7RVV	29ETC	.60	R.V.V.V. MISCELLAN (VARIOUS)
13	223HPTM02	10HPI	13TMF	-999.00	HP INJECT. TURB.FLOW (LBM/SEC)
14	220V2AC01	12V2	19ACC	-999.00	2-PH VENT. ACCD.FLOW (LBM)
15	53SSTC13	22SGS	2FTC	32.30	SG SECOND.FLUID TEMP (F)
16	79SMTC02	22SGS	25MTC	26.30	SG SECOND. METAL TC (F)
17	76SMTC06	22SGS	25MTC	44.20	SG SECOND. METAL TC (F)
18	289SSCP20	22SGS	32KCP	0.00	SG SECOND. UP.WET.CP (REF. FT)
19	344V1TC03	34CLD	2FTC	-999.00	CLD LEAK FLUID TEMP (F)

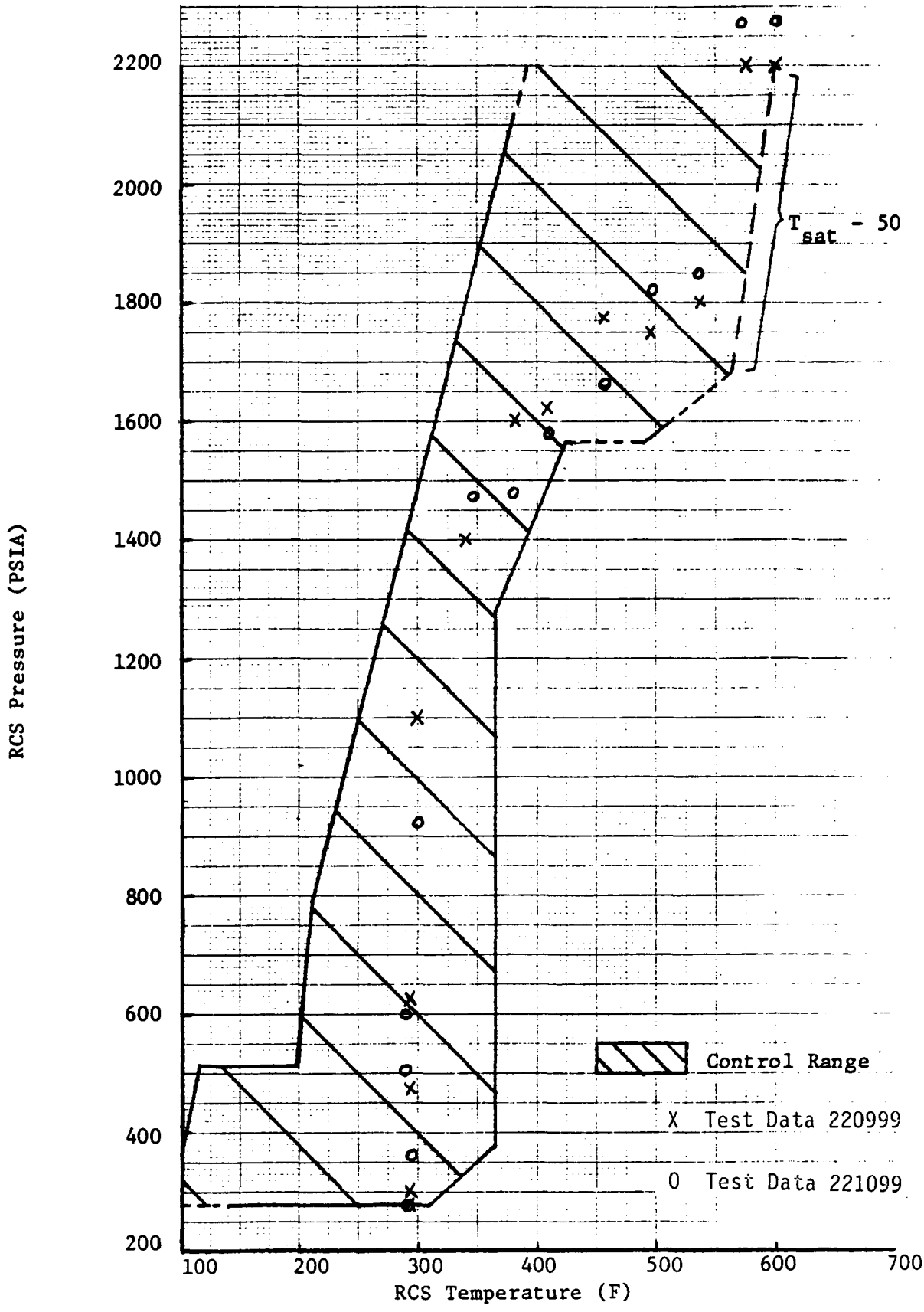

Figure 8.1 Pressure-Temperature Envelope

Refer to Section 2 for a description of the envelope

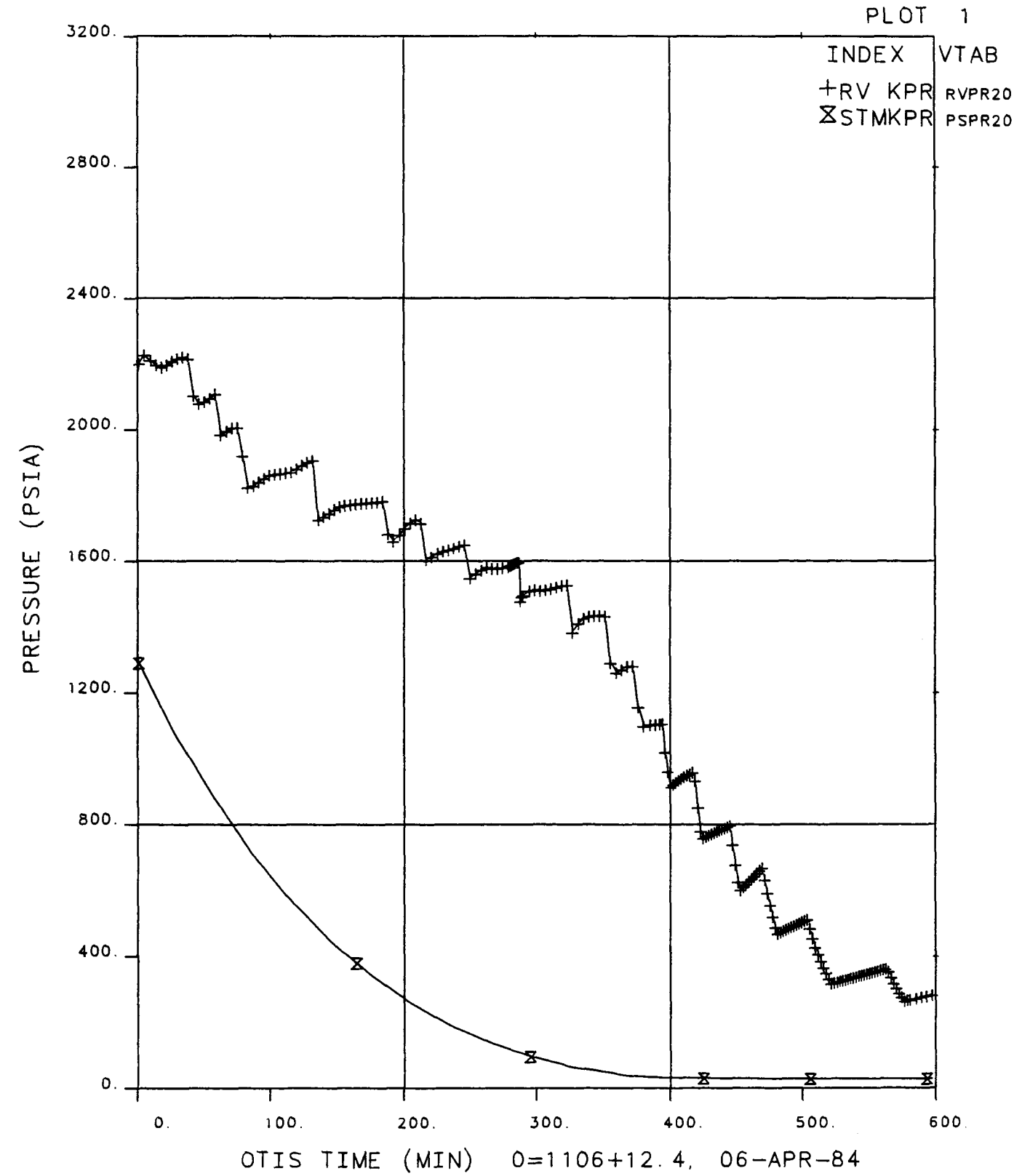

Figure 8.2 Primary and Secondary System Pressures (NC Cooldown Without Venting, Test 220999).

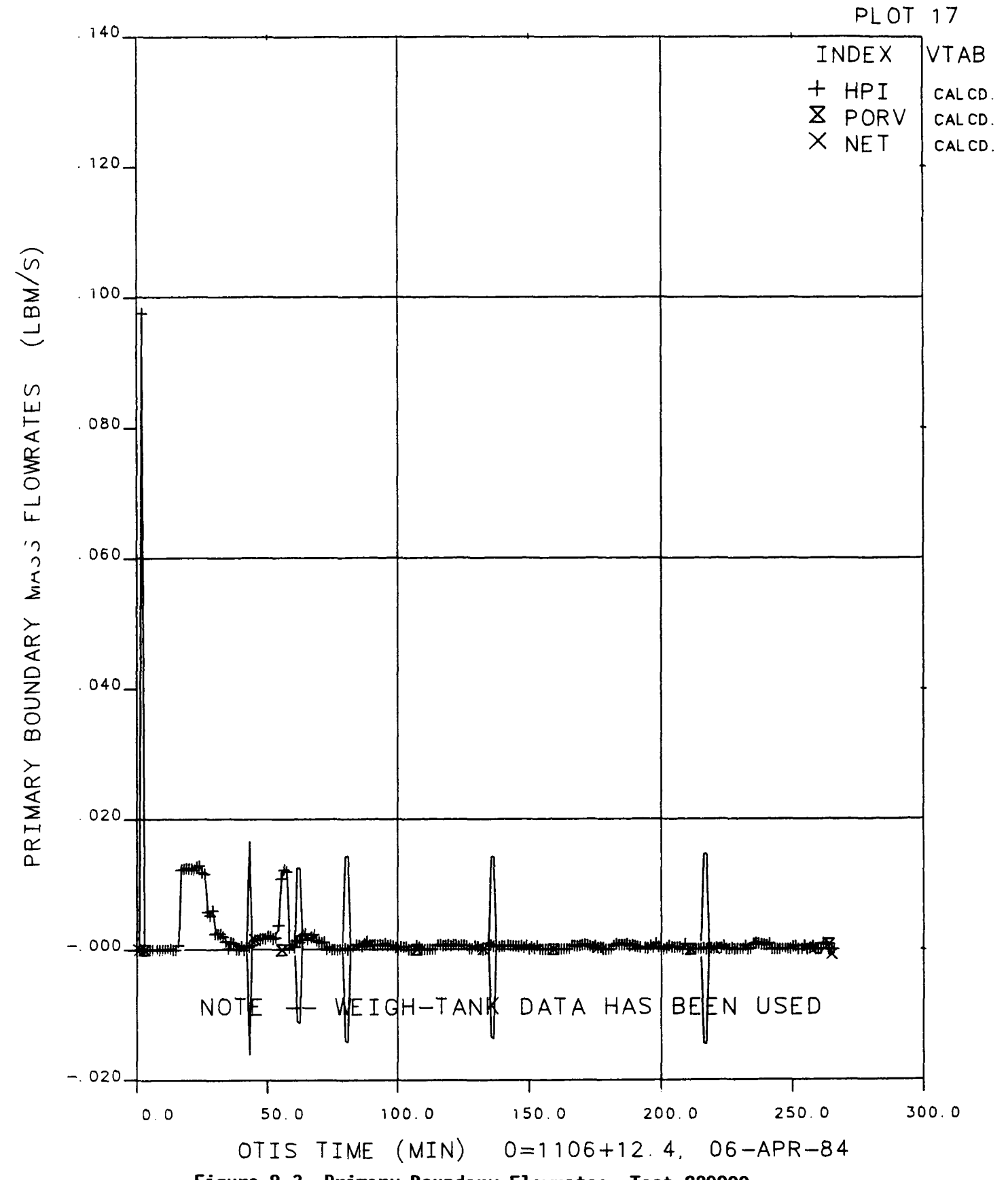

Figure 8.3 Primary Boundary Flowrates, Test 220999.

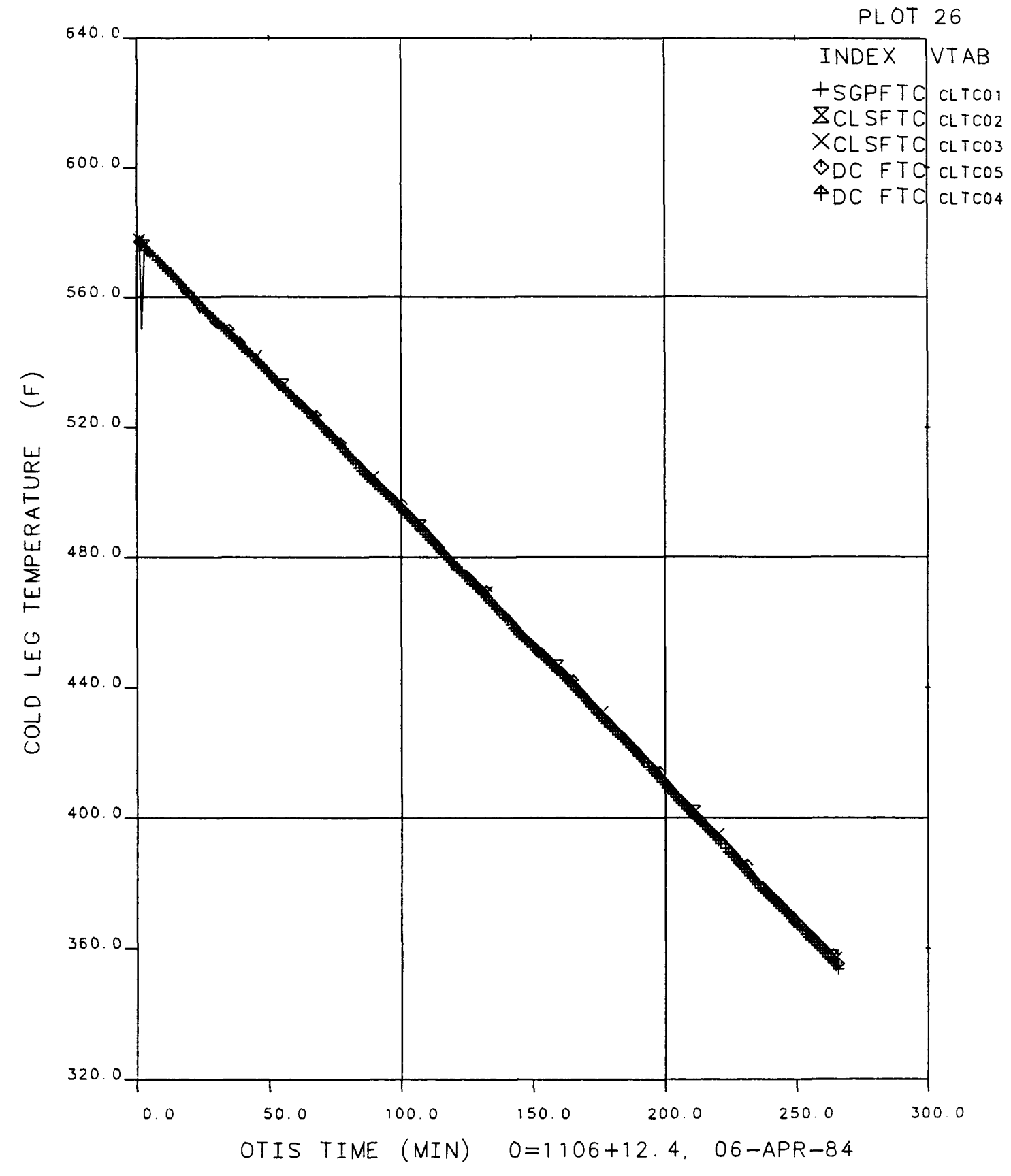

Figure 8.4 Cold Leg Fluid Temperatures, Test 220999.

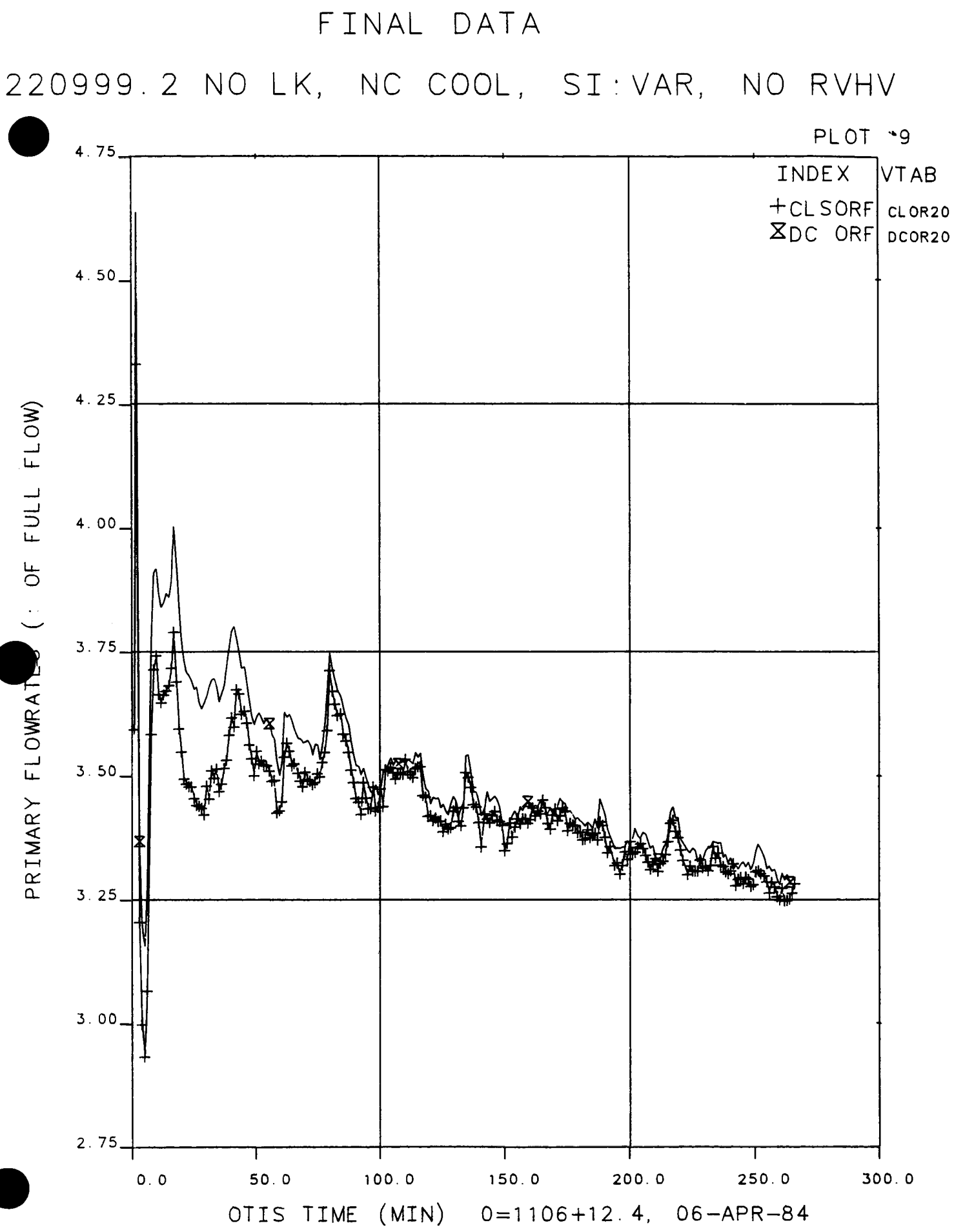

Figure 8.5 Primary Flowrates, Test 220999.

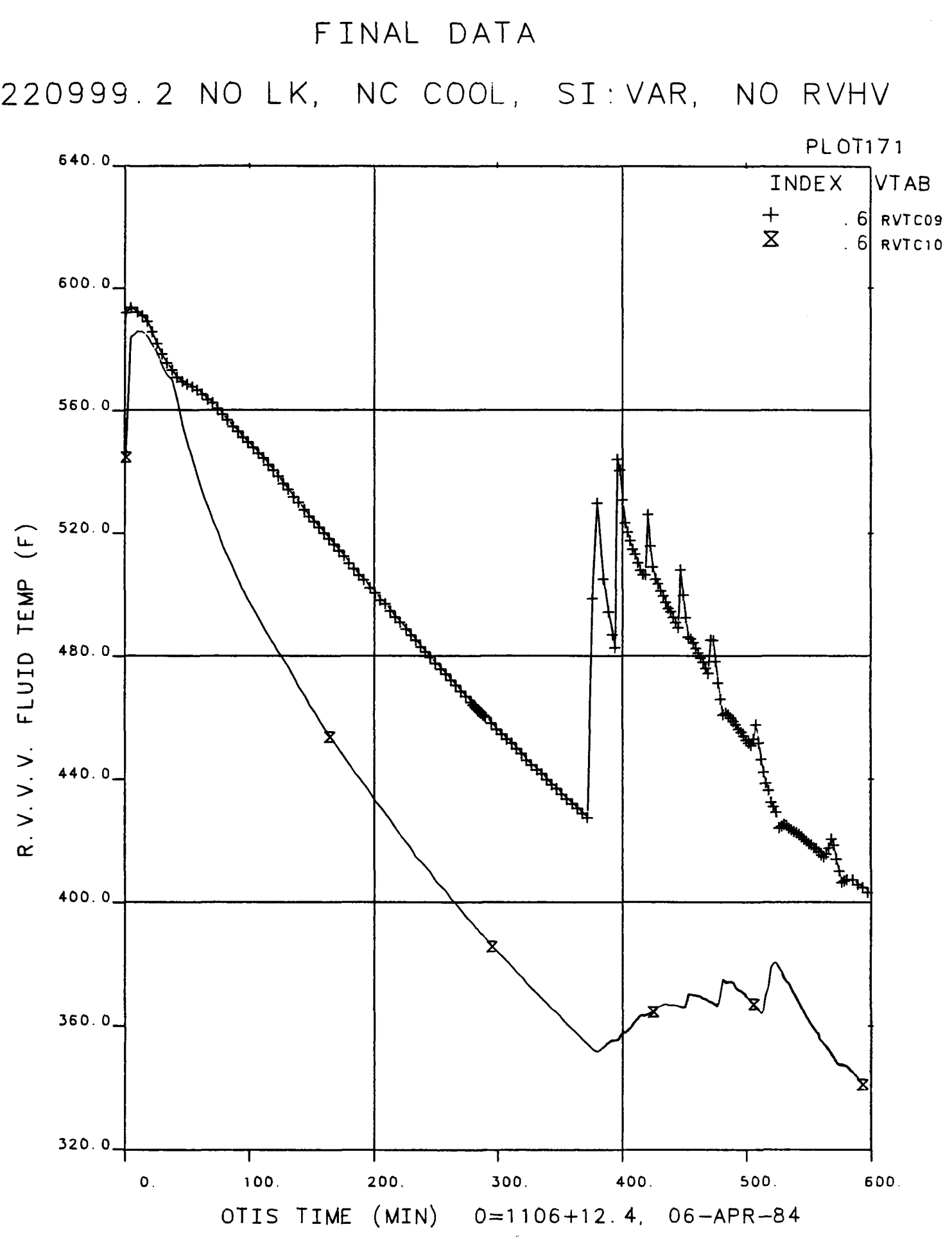

Figure 8.6 RVVV Fluid Temperatures, Test 220999.

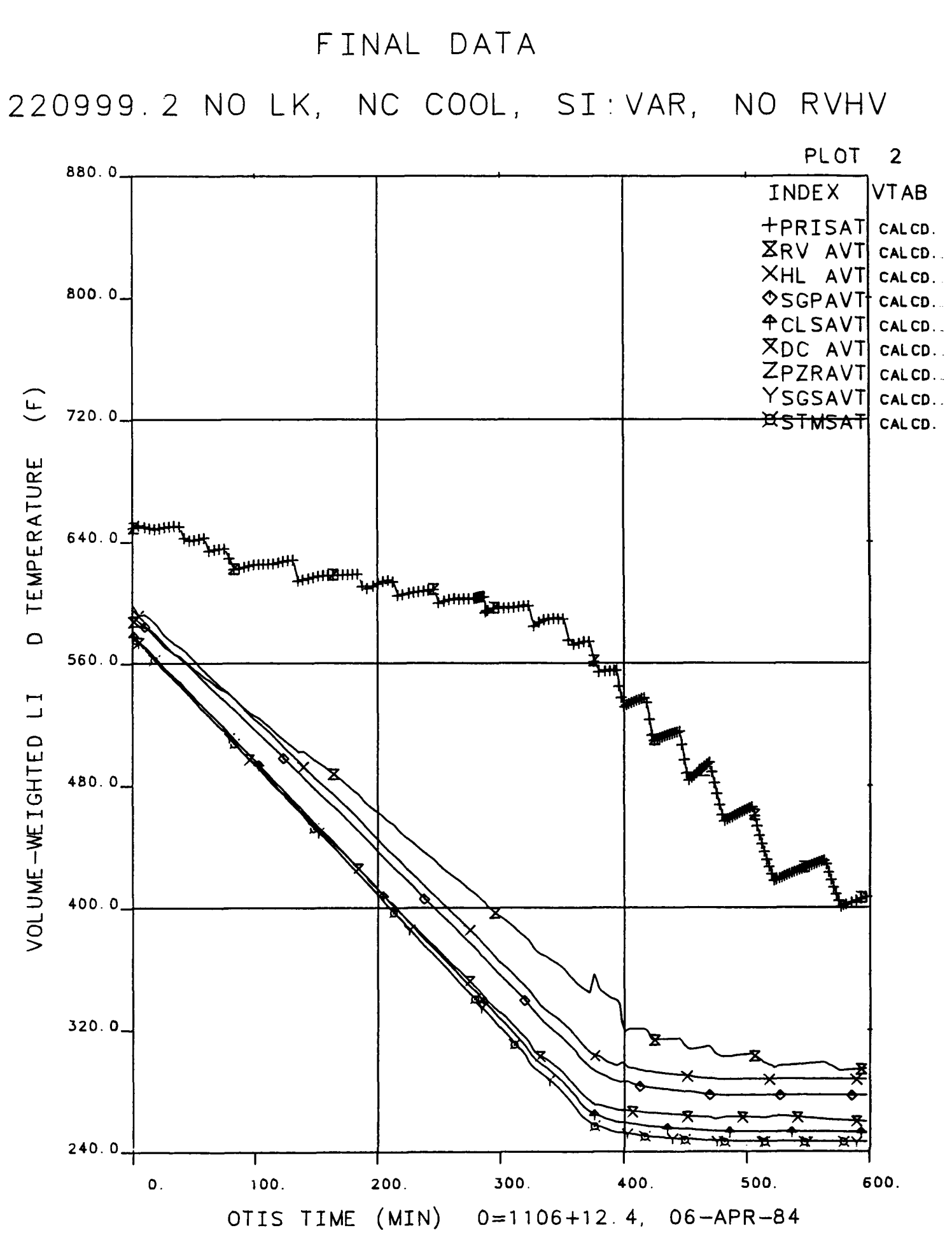

Figure 8.7 Volume-Weighted Fluid Temperatures, Test 220999.

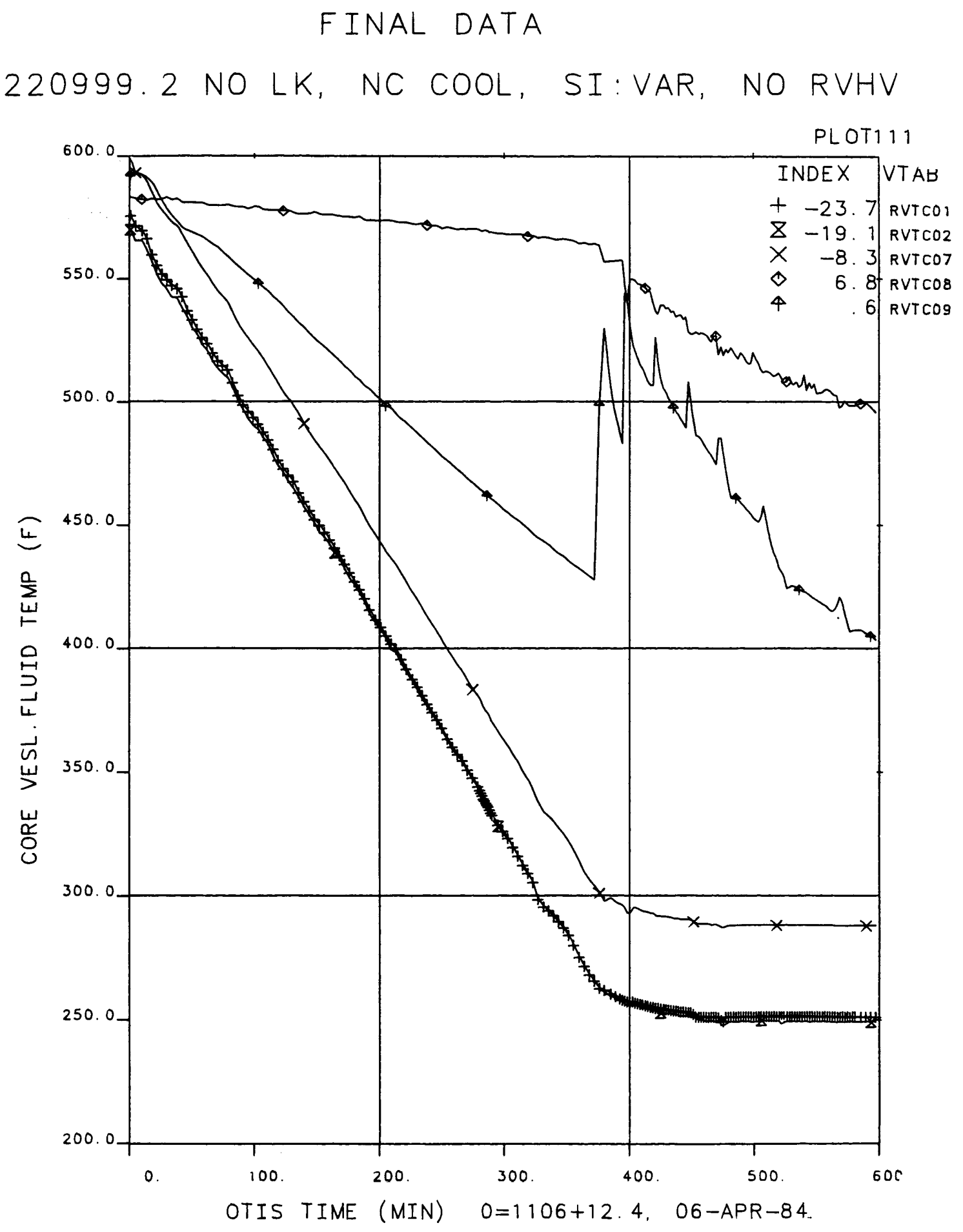

Figure 8.8 Reactor Vessel Fluid Temperatures, Test 220999.

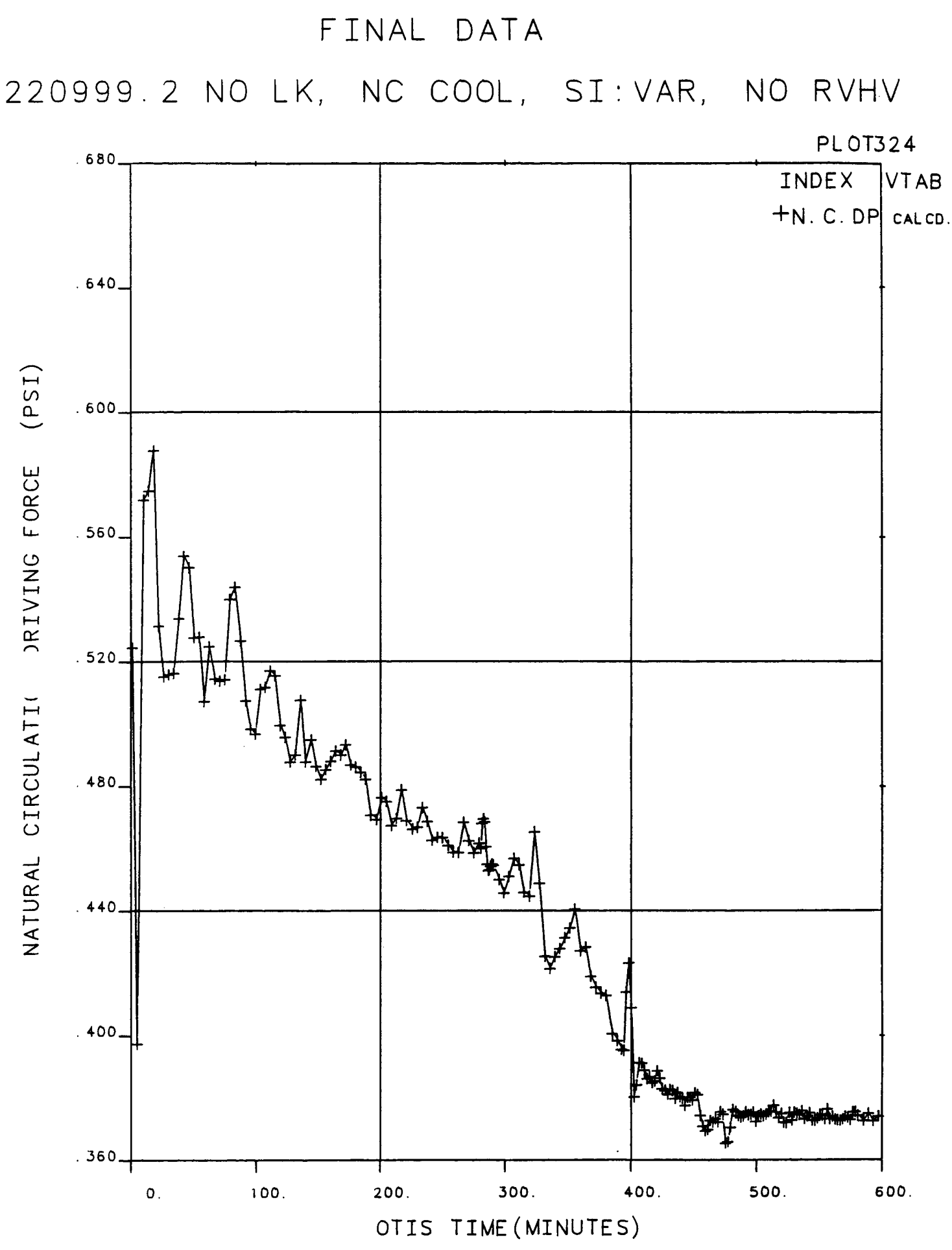

Figure 8.9 Natural Circulation Driving Force, Test 220999.

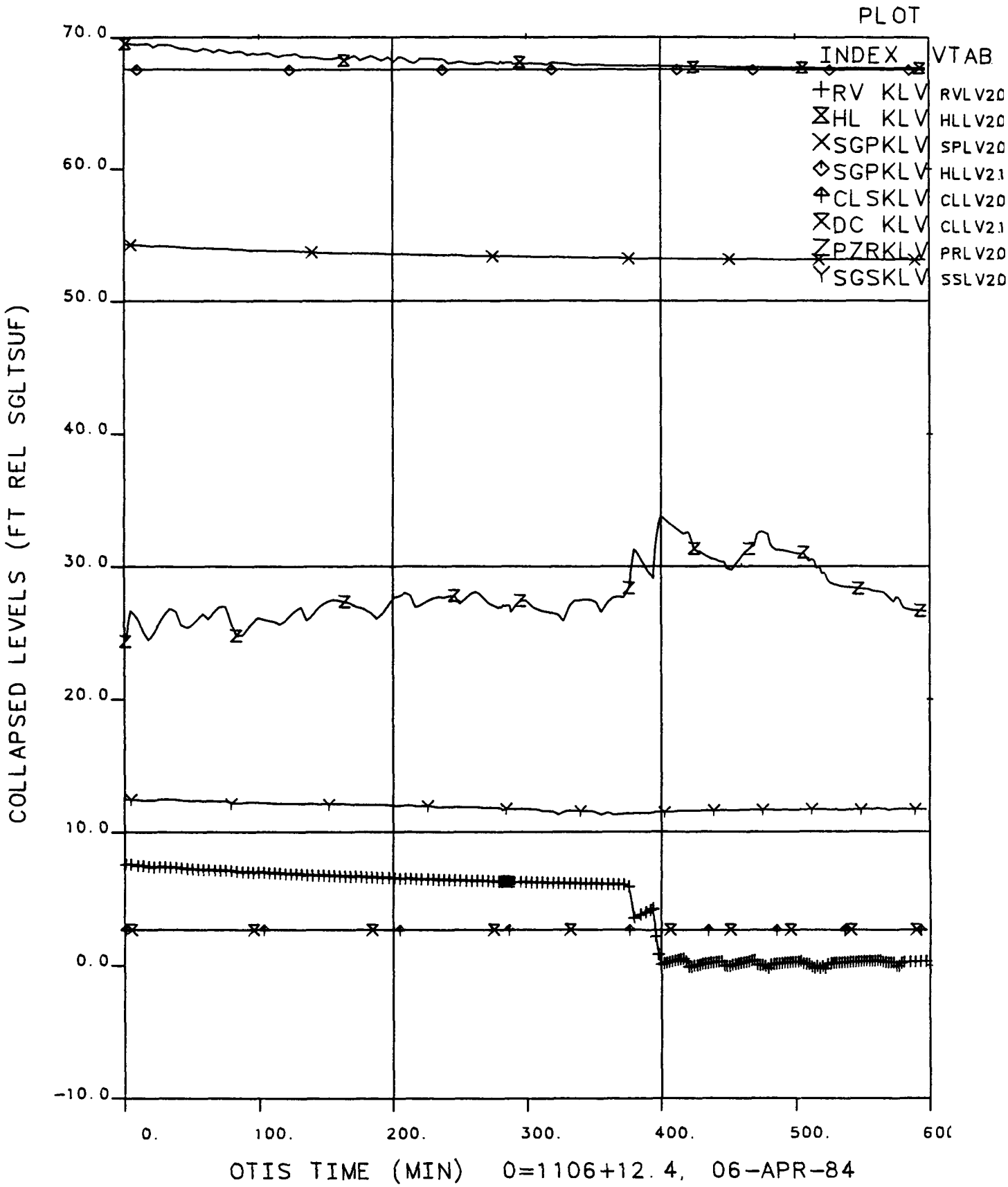

Figure 8.10 Collapsed Liquid Levels, Test 220999.

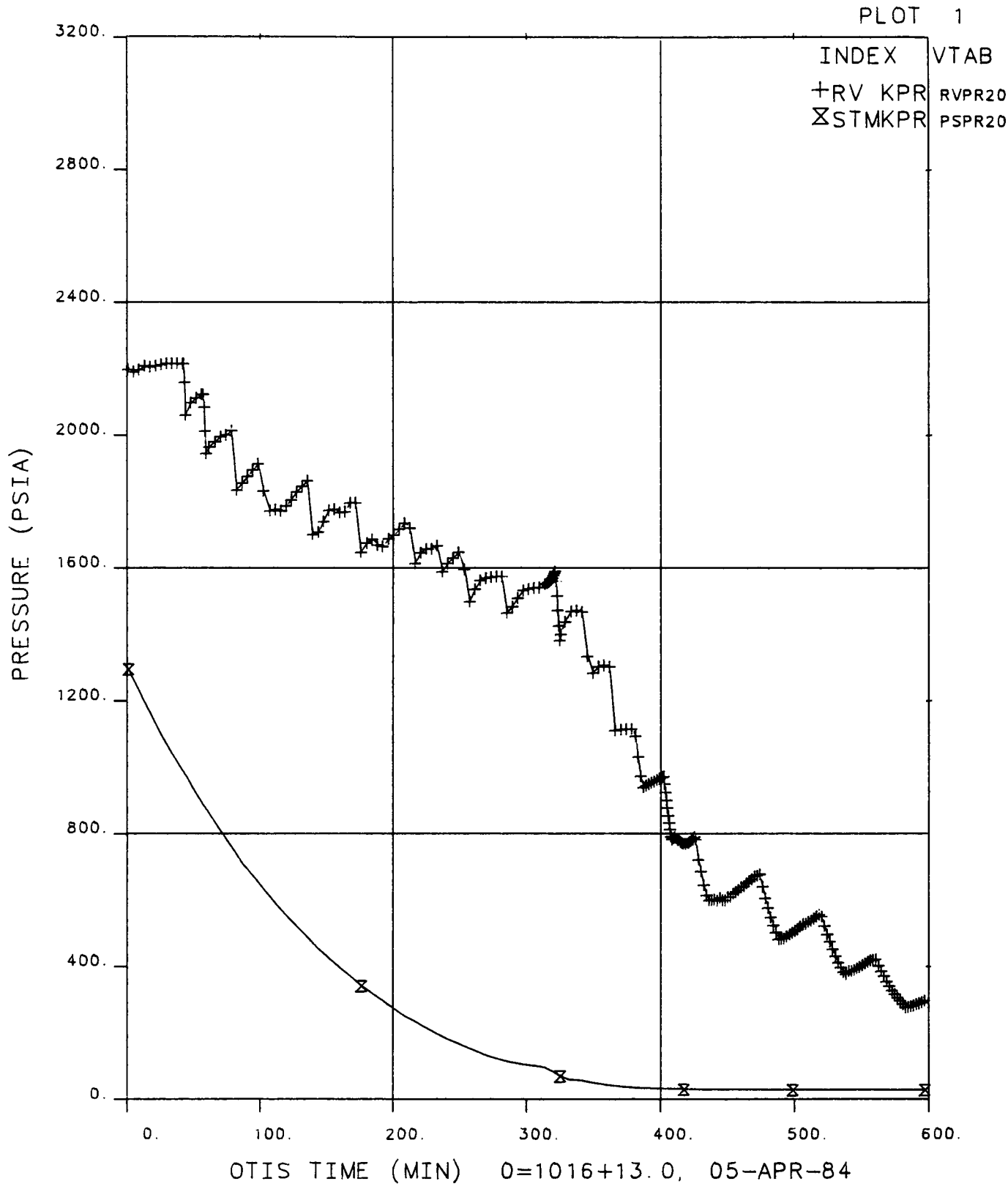

Figure 8.11 Primary and Secondary System Pressures (Test 221099, Natural Circulation Cooldown with Venting).

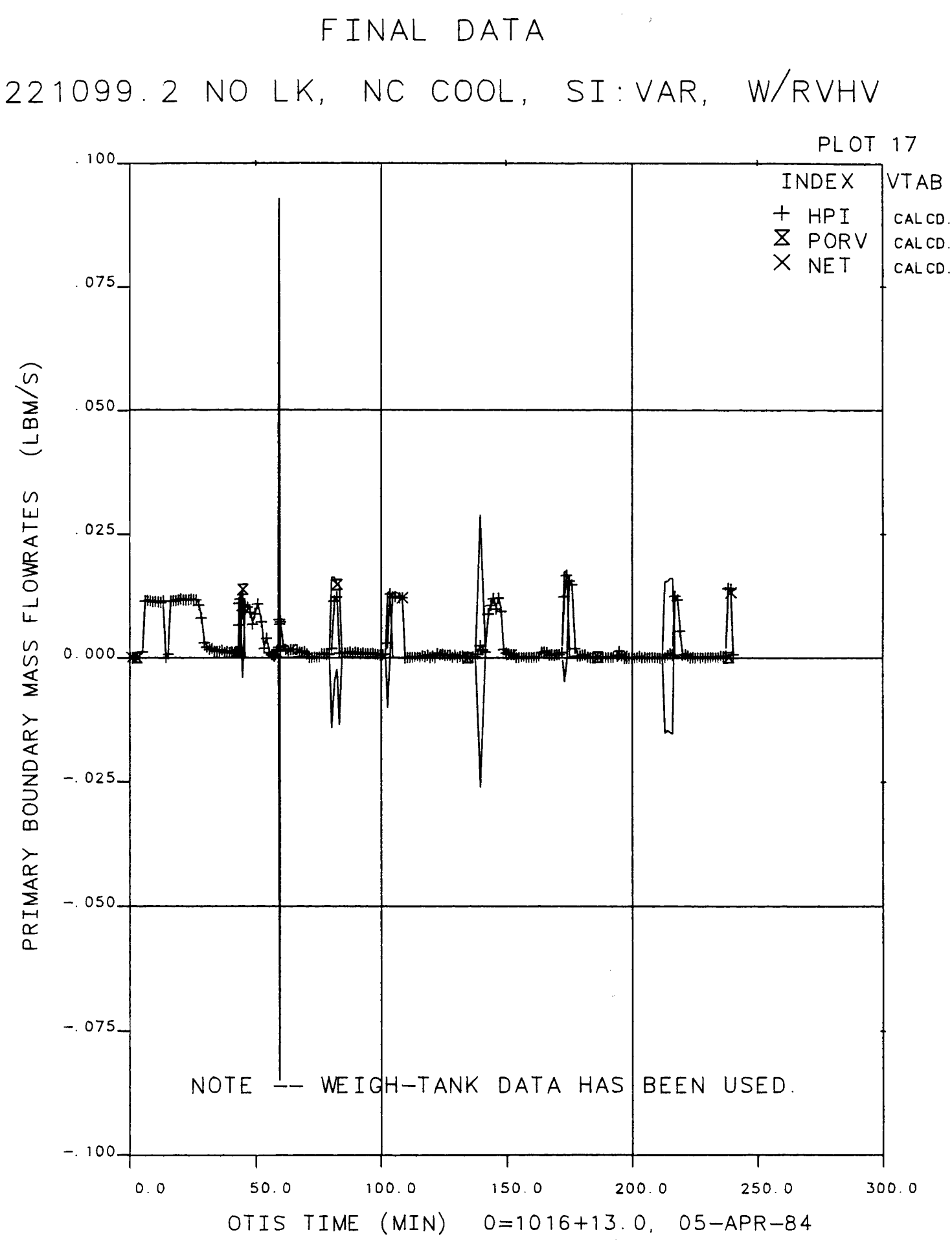

Figure 8.12 Primary Boundary Flowrates, Test 221099.

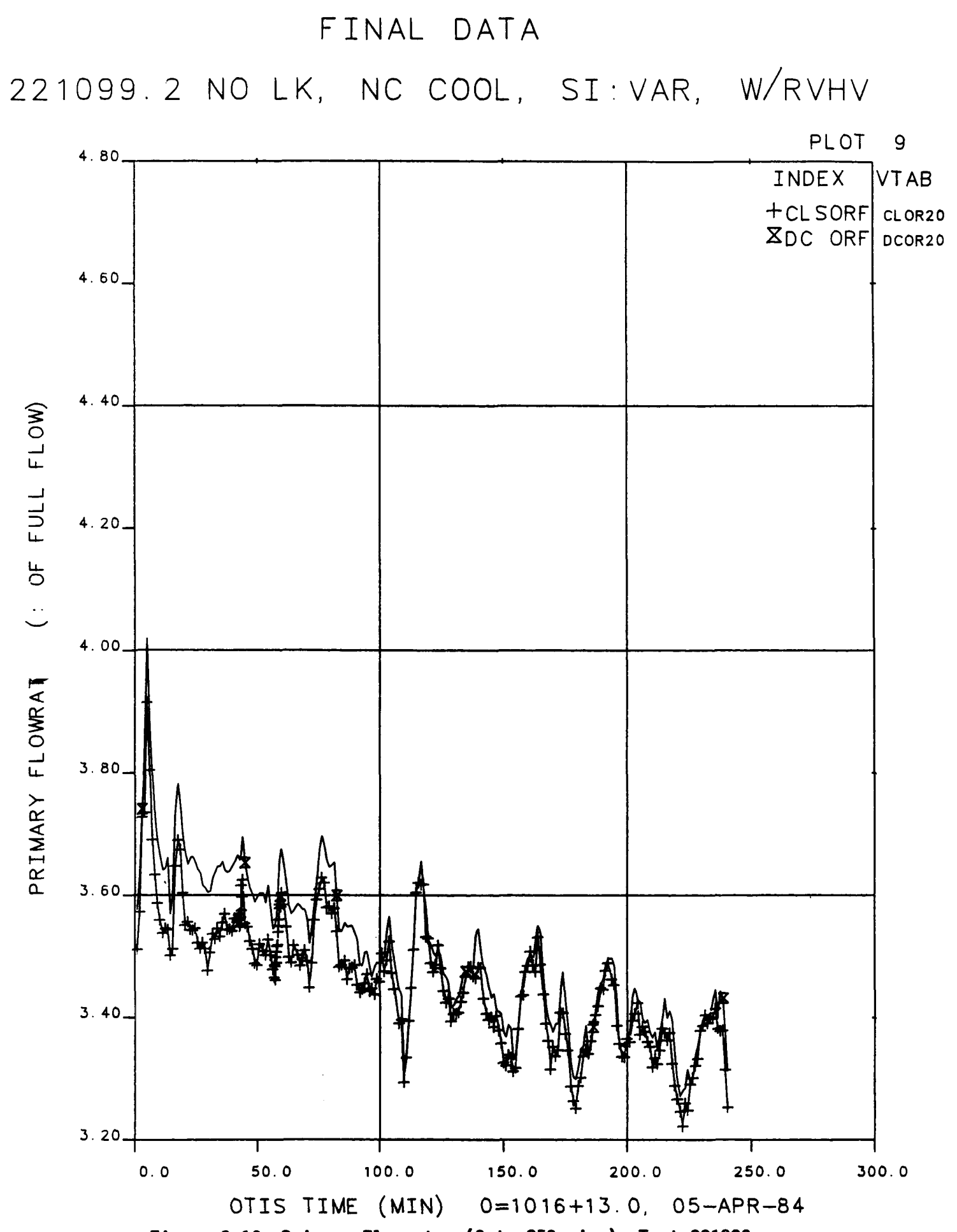

Figure 8.13 Primary Flowrates (0 to 250 min.), Test 221099.

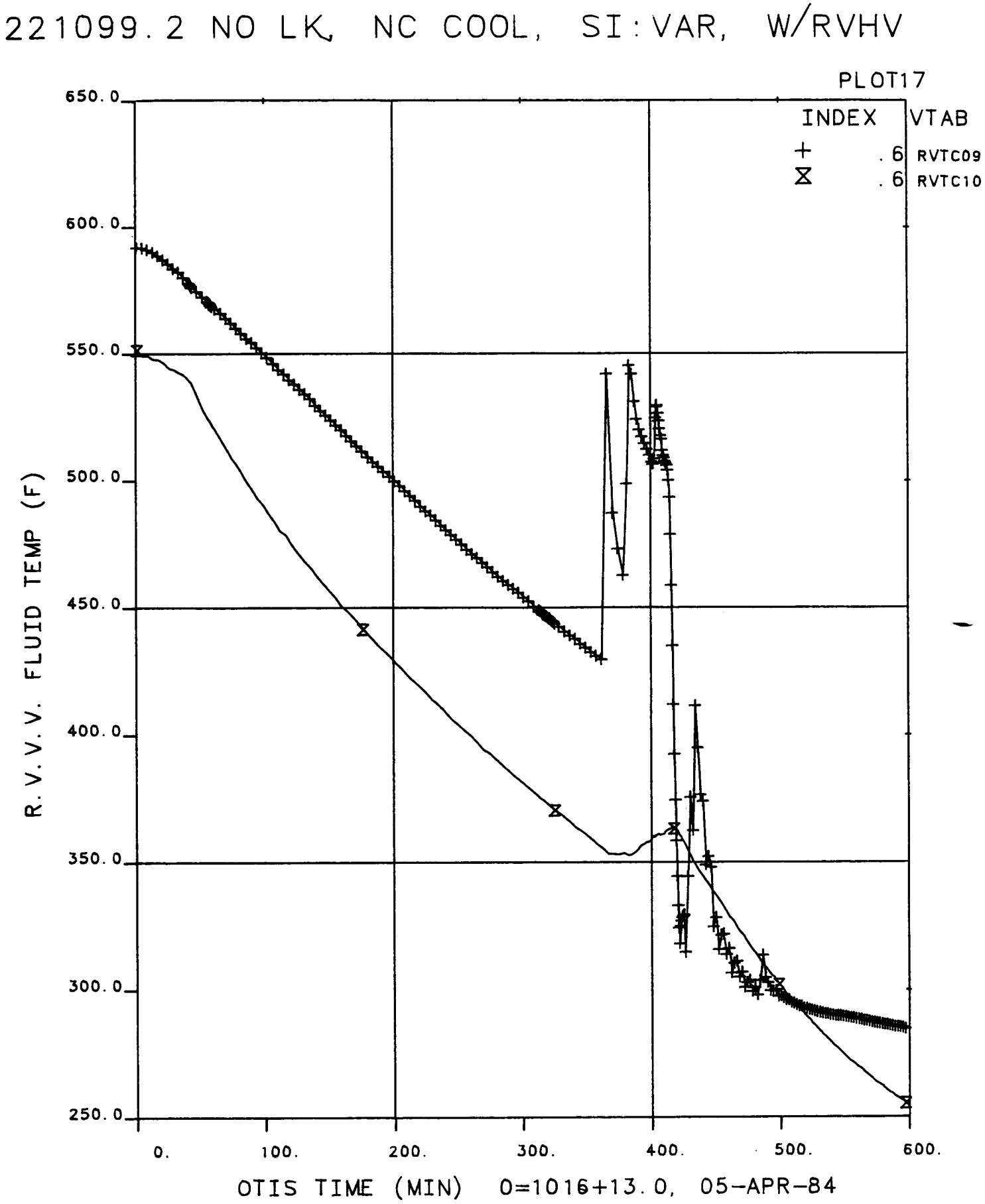

Figure 8.14 RVVV Fluid Temperatures, Test 221099.

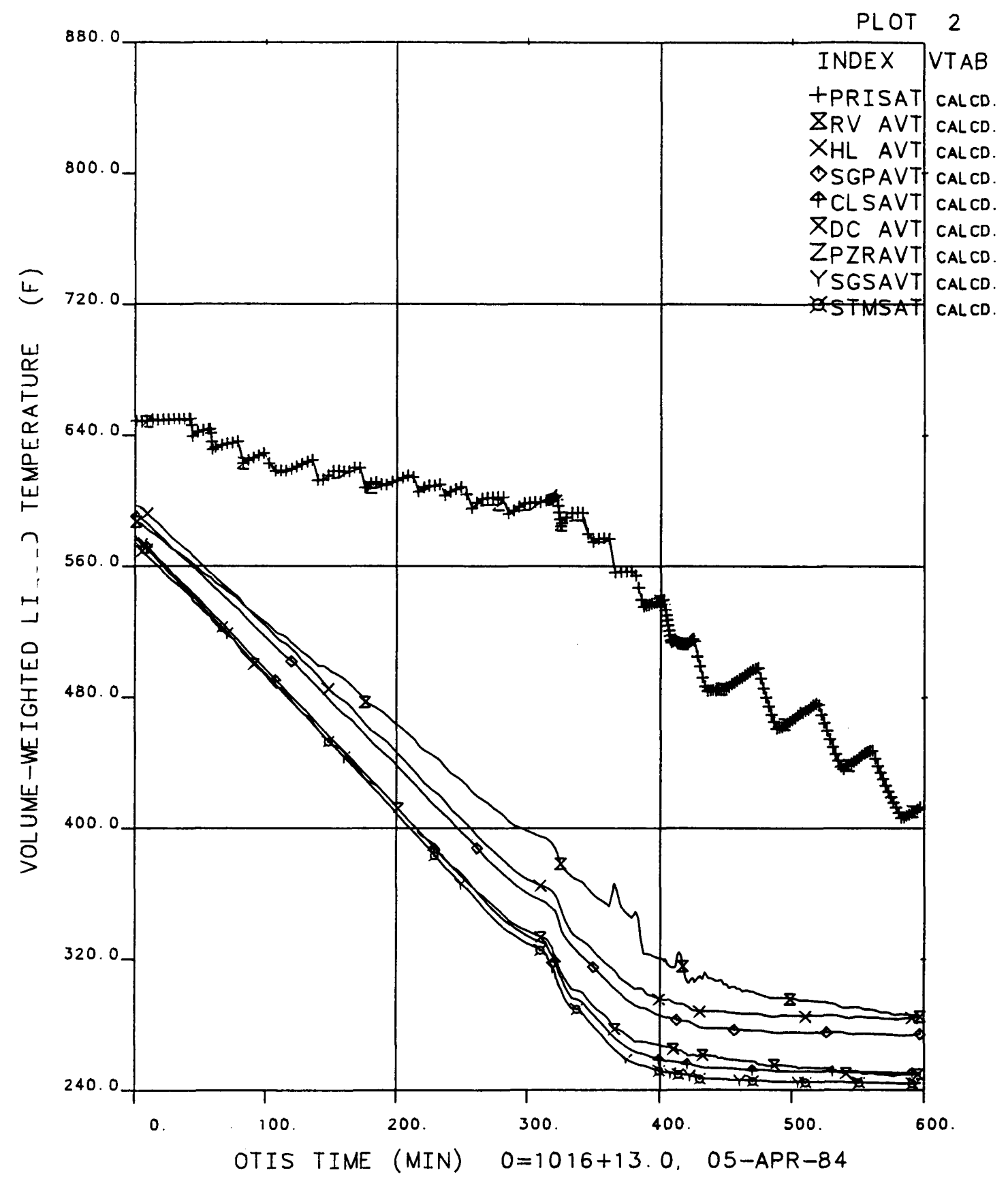

Figure 8.15. Volume-Weighted Liquid Temperatures, Test 221099.

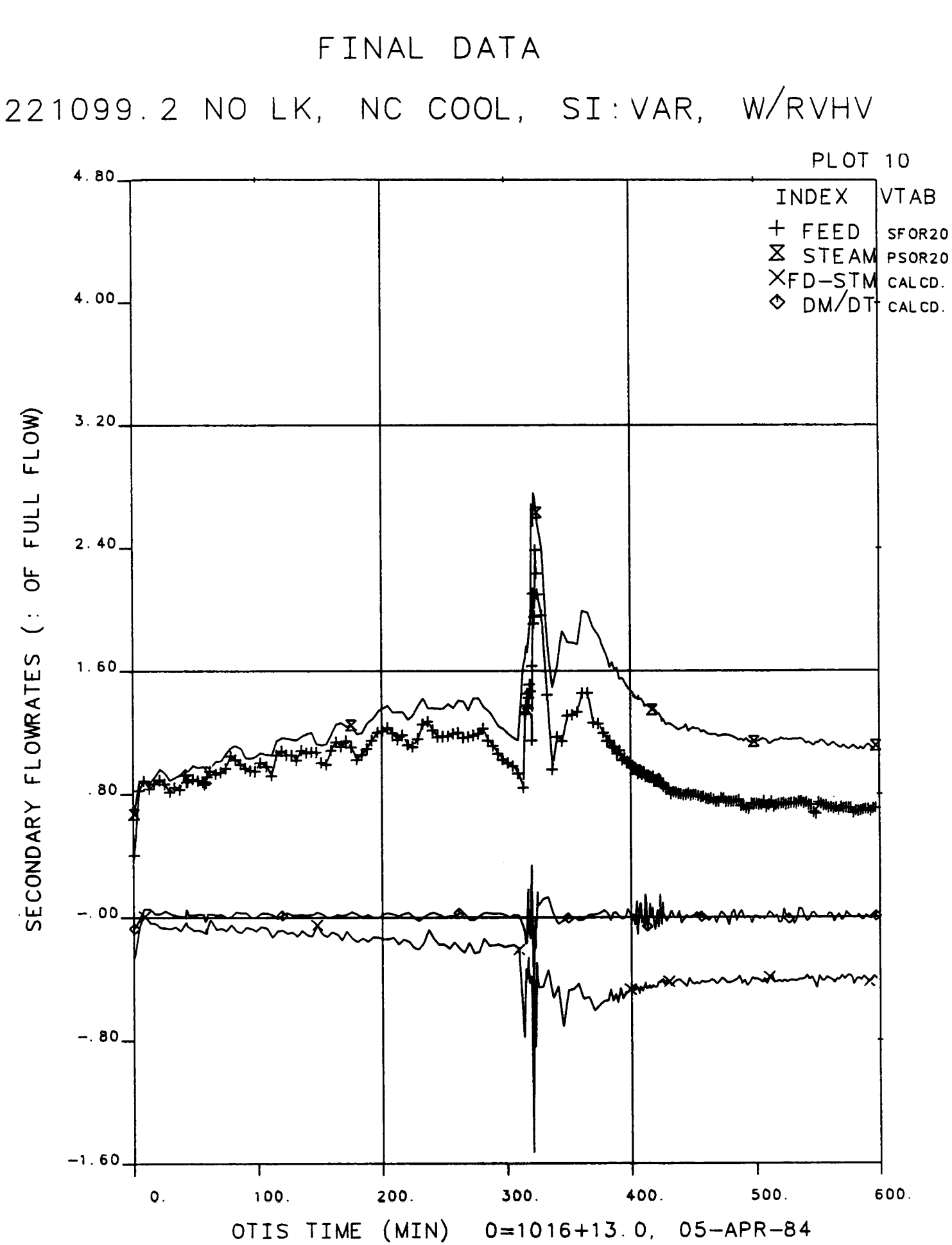

Figure 8.16 Steam Generator Secondary Flowrates, Test 221099.

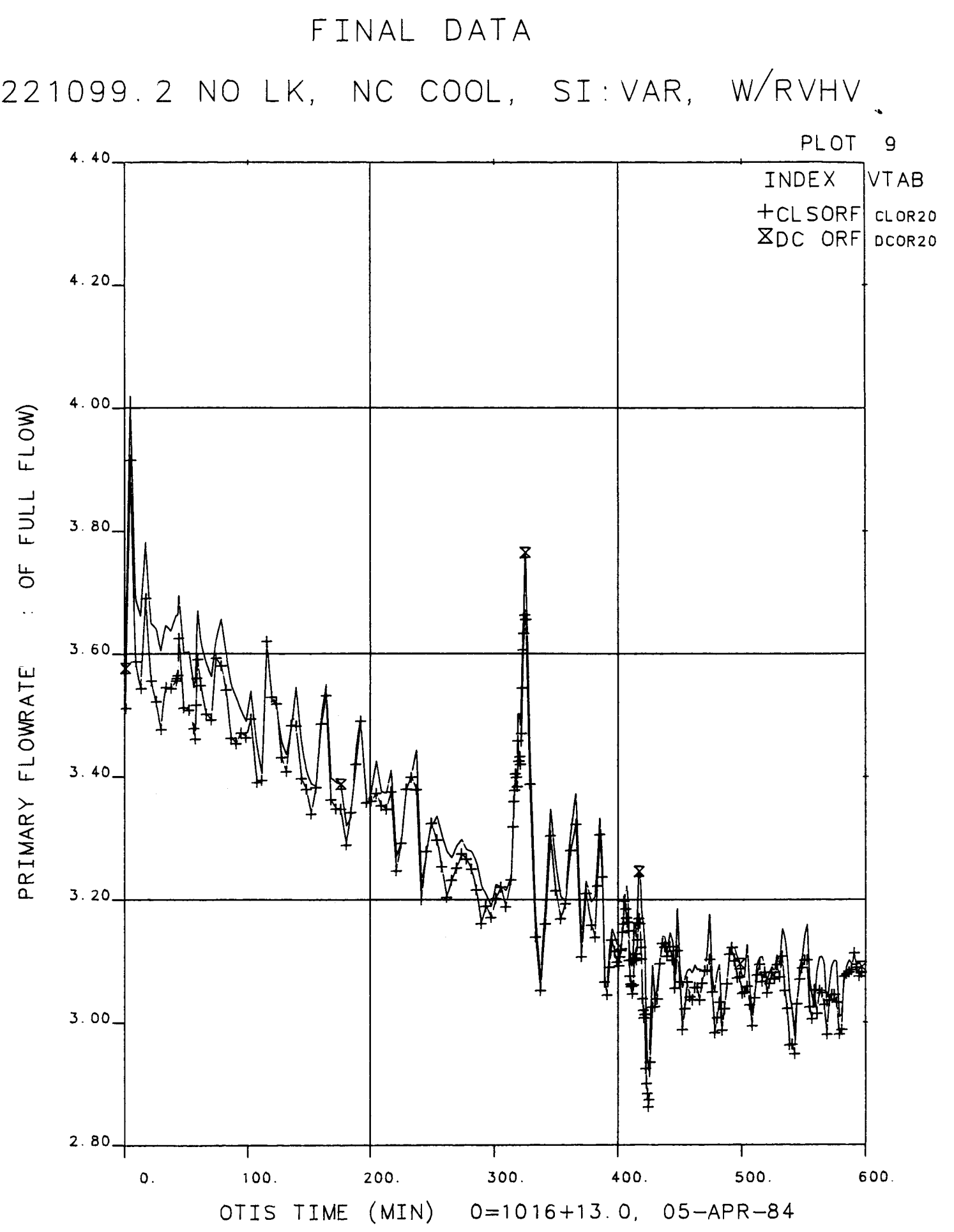

Figure 8.17 Primary Flowrates (0 to 600 min.), Test 221099.

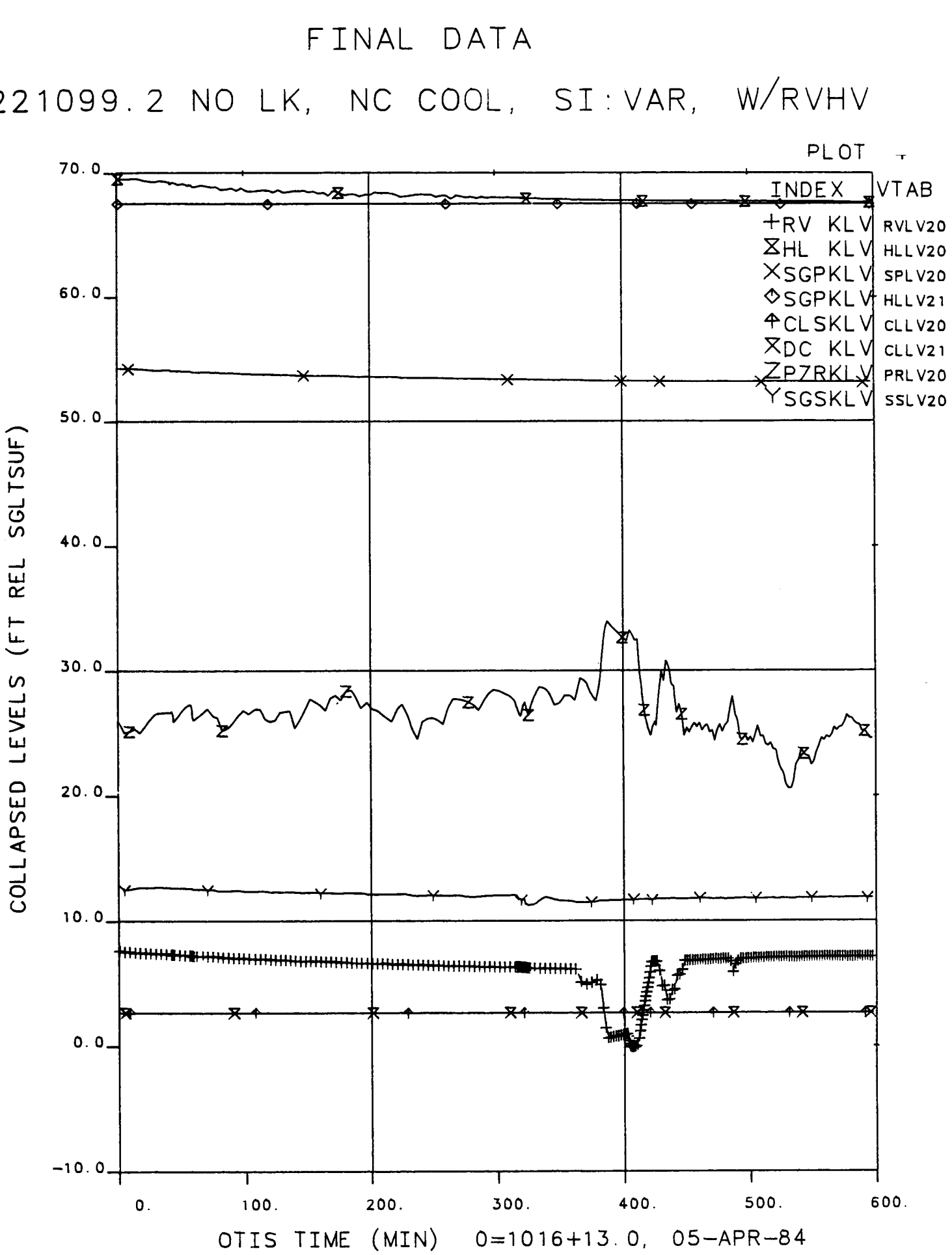

Figure 8.18 Collapsed Liquid Levels, Test 221099.

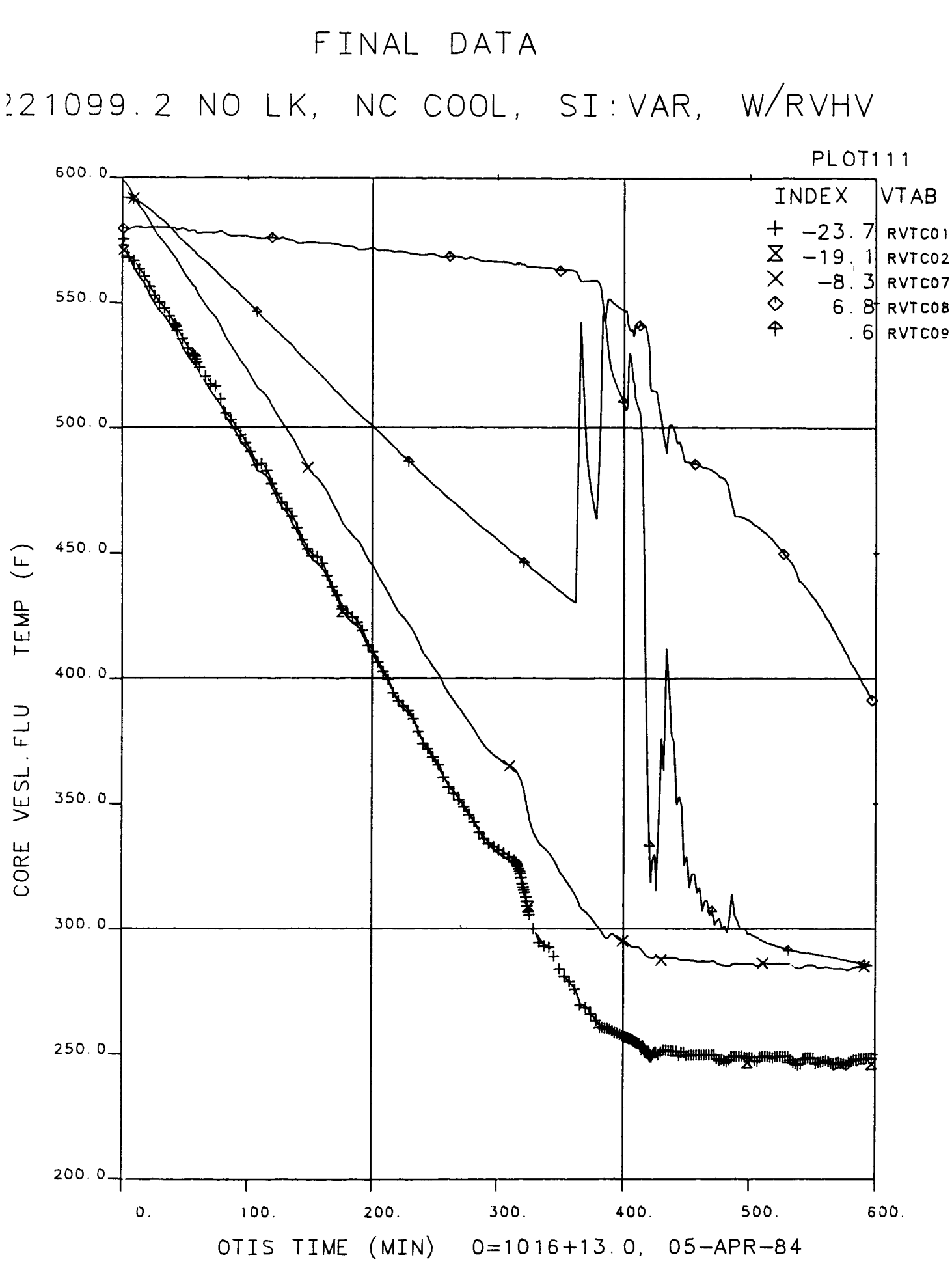

Figure 8.19 Reactor Vessel Fluid Temperatures, Test 221099.

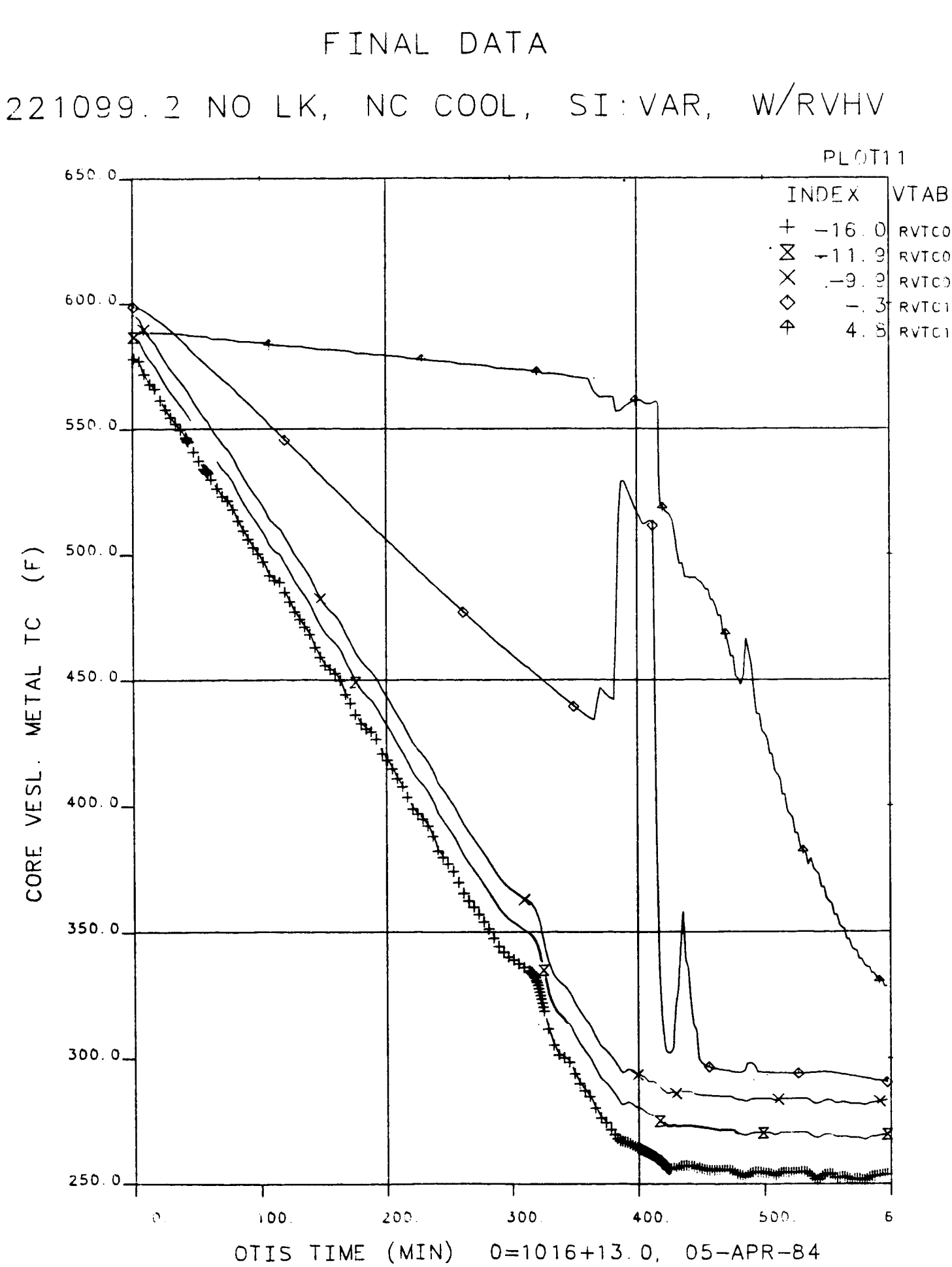

Figure 8.20 Reactor Vessel Metal Temperatures, Test 221099.

9. COMPOSITE TESTS

9.1 Introduction

OTIS Tests 230199 and 230299 employed a plant-trained operator to direct loop control through a post-SBLOCA transient. Operator actions were maximized, in contrast to the preceding OTIS tests. Both tests specified leak isolation at 30 minutes after leak opening, and auxiliary feedwater was unavailable for a significant portion of the transient (the duration was set by several loop-conditions criteria). High-head high-pressure injection characteristics were simulated in Test 230199 and low-head characteristics (with low-pressure injection assist) in 230299 (Figure 9.1). The auxiliary feedwater characteristics and steam generator secondary refill level were also varied between the two tests.

9.2 Test 230199, Nominal High-Pressure Injection

The test conduct and observations for OTIS Test 230199 are briefly discussed in the following sections. The data traces of Figures 9.2 through 9.6 supplement these discussions. References are also made to the appended data plots.

9.2.1 Test Conduct and Background

OTIS Test 230199 was conducted on 4 April 1984. Test performance was as specified. The conditions for this test were as follows:

- 10-cm^2 cold leg suction leak (isolated at 30 minutes).
- Full high-pressure injection capacity with high-head pumps.
- Auxiliary feedwater termination at test initiation.
- A loop operator available to interact with the system.

Auxiliary feedwater was to be reintroduced with a relatively low primary inventory. This led to the development of a hot leg level criterion for auxiliary feedwater reactivation. To preclude premature test termination by automatic core heater trip, auxiliary feedwater reactivation criteria were also specified based on reactor vessel collapsed liquid level and outlet fluid temperature. A default auxiliary feedwater reactivation criterion based on test duration was also specified to be used should the primary not void sufficiently to trigger the preceding criteria. The auxiliary feedwater reactivation criteria, each of which was separately sufficient to trigger the reactivation of auxiliary feedwater during both of the composite

tests, are listed below (all elevations are with respect to the steam generator lower tubesheet):

1. Hot leg collapsed liquid level less than 20 feet.
2. With a reactor vessel collapsed liquid level less than -1 foot, core outlet fluid temperature (indicated by RVTC07 at -8.3 ft) greater than 625F.
3. Reactor vessel collapsed liquid level less than -6 feet.
4. Test duration (after leak initiation) greater than one hour.

The composite tests introduced a wide range of operator actions to post-SBLOCA loop control. Whereas the ten single-variable tests minimized operator interaction to highlight the effects of the off-nominal variables, the composite tests maximized operator-system interactions to examine their effects. An engineer versed in plant operator guidelines was on site during these two tests. This engineer was furnished model loop conditions and directed the test loop operator throughout the evolutions needed to control system cooldown using the Abnormal Transient Operating Guidelines (ATOG).

Only the following indications were to be available to simulate those in or anticipated to be in the plant:

- Pressure-temperature envelope (Figure 9.7): Saturation temperature, (T_{sat} - 50F), and current T_{hot}, T_{core}, and T_{cold}, all versus primary pressure.
- Collapsed liquid levels: reactor vessel head*, hot leg*, and pressurizer.
- Flow rates: high-pressure injection and auxiliary feedwater.
- Secondary pressure, fluid temperature, and level.
- Primary system pressure.

The following model measurements were appropriate for these indications:

- Primary pressure -- PRPR20, pressurizer pressure at 40.5 ft.
- T_{HOT} -- HLTC07, hot leg fluid temperature at 60 ft.
- T_{COLD} -- CLTC03, cold leg suction fluid temperature at -0.1 ft.
- T_{CORE} -- RVTC07, core outlet fluid temperature at -8.3 ft.

The loop was to be cooled within the prescribed pressure-temperature envelope (Figure 9.7). Any model boundary system simulating that of a plant, i.e., high-pressure injection, relief valve (PORV), hot leg and reactor vessel vents, pressurizer heaters, and secondary system steam and feed controls, were to be used at the discretion of the loop operator.

*Not used during the test.

The initial conditions obtained versus those specified are compared in Table 9.1. Other conditions were as follows: (1) a primary flow rate of 5.4% of full flow, (2) a secondary flow rate of 2.2% of full flow, and (3) an auxiliary feedwater temperature of 118F. All observed conditions were as specified except the pressurizer level and metal temperatures. However, these discrepancies are not perceived to have affected the test results. The test was initiated following a nine-minute period of steady-state operation. The key operator actions are provided in Table 9.2. Instruments discarded from the data base are listed in Table 9.3. As with the preceding OTIS tests, the hot leg conductivity probes and off-nozzle string thermocouples dominate the list of unavailable instruments.

9.2.2 Observations

In Test 230199, four major SBLOCA phases were observed: (1) draining, saturation, and intermittent circulation, (2) auxiliary feedwater boiler-condenser mode (BCM), (3) refill, and (4) post-refill natural circulation cooldown (Figure 9.2).

Draining, Saturation, and Intermittent Circulation

The data acquisition system was activated at 2131 on 4 April 1984. Following a nine-minute period of steady-state operation, the 10-cm^2 cold leg suction leak was opened. Two minutes later, the high-pressure injection system was activated, the core power decay ramp was initiated, and the auxiliary feedwater flow was terminated. The primary pressure decreased from 2255 psia at 0 minutes to approximately 1650 psia at 5 minutes (Figure 9.2). At the same time, the steam generator secondary pressure increased from 1200 to 1310 psia as the control pressure was increased to 1350 psia. Primary-to-secondary coupling was relatively strong until flow interrupted at 7 minutes (Figure 9.3). Immediately, primary pressure began to increase, causing the pressurizer level to increase at 7 minutes (Figure 9.4). A relatively weak recoupling of the primary and secondary systems began at 8 minutes; apparently the hot leg level upstream of the hot leg U-bend briefly swelled as the upper reactor vessel fluid began to void, cf. Figures 9.2 and 9.4. The leak mass flow exceeded the high-pressure injection flow (Figure 9.5). Flow re-interrupted at 13 minutes and primary pressure again began to

increase. The pressurizer level increased to 12 feet as a result. The inventory required for this level increase was displaced from the reactor vessel, as indicated by its coincident level decrease (Figure 9.4). A marked spillover recoupling occurred at 15 minutes when the reactor vessel level uncovered the hot leg nozzle. Primary flow spiked to 8% of full flow, primary pressure decreased, and secondary pressure increased. At ∿20 minutes, the hot leg and steam generator levels indicated a rapid decrease (Figure 9.4).

At 30 minutes, the operator closed the leak (Figure 9.5) as instructed by the test procedure. The pressurizer, hot leg, and steam generator primary levels began to increase as the high-pressure injection continued to add inventory to the system. System pressure rose as the vapor regions of the pressurizer and hot leg U-bend were compressed and pressurizer fluid was heated by the metal. At 37 minutes, the operator opened the pressurizer relief valve, venting the steam space in the pressurizer. The pressurizer level rose rapidly (Figure 9.4). The primary pressure and the hot leg and steam generator primary levels decreased at the same time. Although the primary pressure decrease was small due to hot leg saturation, the effect of opening the relief valve was evident from the core vessel fluid temperatures (Figure 9.6). As the pressurizer relief valve was opened, a flow path from the high-pressure injection system to the relief valve through the reactor vessel was established. The core inlet temperature decreased from ∿590F at 37 minutes to 500F at 60 minutes. However, the core outlet temperature remained saturated. At 45 minutes, the pressurizer filled, and the hot leg and steam generator primary levels reached plateaus near 58 and 50 feet respectively as liquid was discharged from the relief valve. Even though the auxiliary feedwater injection had been interrupted, the uncovery of primary tubes within the steam generator at 45 minutes allowed hotter U-bend vapor (appended Plot 13) to further superheat the secondary steam (appended Plot 193). With primary flow stalled, the hot leg and steam generator temperatures were nearly constant until 60 minutes.

Auxiliary Feedwater Boiler-Condenser Mode (AFW BCM)

At one hour after test initiation, the operator activated the auxiliary feedwater system (as directed by criterion 4 of the auxiliary feedwater reintroduction procedure, viz. test duration greater than one hour). Boiler-condenser heat transfer occurred; the primary pressure decreased from 1575 to 1400 psia by 65 minutes (Figure 9.2). The steam generator primary level rose at 61 minutes, ending the boiler-condenser mode. Also at 61 minutes, the operator decreased secondary pressure by 25 psia (Table 9.2) with little impact.

Refill

At 64 minutes, the operator closed the pressurizer relief valve. Almost immediately, the hot leg and steam generator primary levels began to increase. At 66 minutes, the operator decreased steam control pressure to 625 psia, again with little impact to the loop because the cold auxiliary feedwater was already depressing the steam pressure below 625 psia. By 69 minutes, the secondary level reached the control setpoint (38 feet), auxiliary feedwater injection automatically terminated, and the steam generator level was controlled at this setpoint for the remainder of the test (Figure 9.4).

Post-Refill Natural Circulation Cooldown

At 73 minutes, the hot leg level reached the hot leg U-bend, and the steam generator primary quickly refilled. Primary loop flow increased abruptly (Figure 9.3). Primary-to-secondary coupling was established as indicated by the steam generator fluid temperature (appended Plots 13, and 191 through 194). The primary pressure began to decrease while secondary pressure increased. At 76 minutes, the loop was completely refilled, and the operator adjusted and then terminated high-pressure injection (Figure 9.5). At 79 minutes, the primary-to-secondary pressure difference was $\sim$700 psi and increasing. As a result, the operator increased the steam pressure to 750 psia to reduce the loop cooldown rate. At 90 and 92 minutes, the reactor

vessel head vent was opened for 5 and 10 seconds. At 94 minutes, the reactor vessel head vent was reopened. The reactor vessel upper head filled immediately. At 97 minutes, the operator energized the pressurizer main heaters to provide pressure control. The pressurizer level began to decrease due to loop cooldown while the primary pressure slowly increased. The upper reactor vessel head was approximately full when the operator closed the reactor vessel head vent at 98 minutes (Figure 9.5). All upper head thermocouples indicated subcooled conditions (Figure 9.6) at 113 minutes. For the remainder of the test, the operator cooled the loop through a series of secondary pressure reductions (Table 9.2 and Figure 9.2). The loop temperature decreases are indicated on the fluid temperature versus time plots, cf. appended Plots 2, 13, 26, 111, 121, 131, 132, 141, 151, and 191 through 194.

While the loop was cooling, the energized pressurizer heaters were slowly elevating the primary pressure, which reached 1550 psia at 211 minutes. As the pressurizer steam space increased in volume, the pressurizer level decreased to 17 feet by 212 minutes. The operator raised the pressurizer level to 25.5 feet by actuating high-pressure injection for seven minutes, starting at 212 minutes (Figures 9.4 and 9.5). At 241 minutes into the test, the transient was terminated by the operator. The final conditions were as follows: primary pressure approximately 1600 psia, primary flow rate approximately 4%, secondary pressure 300 psia, and loop temperatures cooling at approximately 25F/h.

Figure 9.7 shows the results of the test on the pressure-temperature envelope. For the initial 30 minutes of the test, there were no operator actions and the loop conditions followed the saturation line. While the loop fluid was saturated (until 73 minutes), pressure and temperature could not be controlled independently; thus, the loop conditions did not move toward the envelope. Once the leak was isolated and the auxiliary feedwater was actuated, the primary system refilled and natural circulation cooldown commenced. Continued secondary side depressurization by the operator resulted in system cooldown and loop conditions within the envelope during the final hour of the test.

9.3 Test 230299, Low-Head High-Pressure Injection

The test conduct and observations for OTIS Test 230299 are briefly discussed in the following sections. The data traces of Figures 9.8 through 9.12 supplement these discussions, references are also made to the appended data plots.

9.3.1 Test Conduct

OTIS Test 230299 was conducted on March 29, 1984. Test performance was as specified. The conditions for this test were identical to those of Test 230199 with the following exceptions:

1. Low-head full capacity high-pressure injection with low-pressure injection assist were simulated (the "piggyback mode").
2. The steam generator secondary control level was to be 10 feet following auxiliary feedwater reinitiation.
3. Auxiliary feedwater flow-versus-head was to simulate the Davis-Besse characteristics (which are described in section 2).

The observed versus specified initial conditions are compared in Table 9.2. Other initial conditions were as follows: (1) a primary flow rate of 5.5%, (2) a cold leg temperature of 570F, (3) a secondary flow rate of 2.2%, and (4) an auxiliary feedwater temperature of 111F. All observed conditions except pressurizer metal temperatures and level were as specified. These discrepancies are not perceived to have affected the test results. The key operator actions are provided in Table 9.4. Instruments discarded from the data base are listed on Table 9.5. As with preceding OTIS tests, the hot leg conductivity probes and off-nozzle string thermocouples dominated the list of unavailable instruments. The test was terminated after 243 minutes of transient data acquisition, as specified.

9.3.2 Observations

Test 230299 exhibited four major SBLOCA phases: (1) draining, saturation, and intermittent circulation, (2) high-elevation AFW BCM (auxiliary feedwater boiler-condenser mode), (3) refill, and (4) post-refill natural circulation cooldown (Figure 9.8).

Draining, Saturation and Intermittent Circulation

The data acquisition system was activated at 1528 on 29 March 1984. Following a ten-minute period of steady-state operation, the scaled 10-cm^2 cold leg suction leak was opened. Approximately two minutes later, the high-pressure injection system was activated. At 3 minutes, the steam pressure control was increased to 1350 psia, the secondary control level was reduced to 3 feet (and maintained using low-elevation auxiliary feedwater injection), and the core power decay ramp was initiated. From 0 to 5 minutes, the primary pressure decreased rapidly from 2200 to 1650 psia (Figure 9.8). The loop saturated at 3 minutes and the hot leg and steam generator primary levels began to decrease (Figure 9.9). The primary flow was interrupted as a result, but was followed by a spillover at 6 minutes. This spillover was apparently caused by voiding in the reactor vessel. The intermittent primary flow in combination with low-head HPI resulted in a rapid decrease of the hot leg and steam generator primary levels beyond 6 minutes. At 10 minutes, the primary system began to repressurize, increasing from 1650 to 1750 psia in two minutes. The repressurization was halted by a strong spillover which occurred at 13 minutes, as indicated by the flow spike on Figure 9.10. This recoupling was concident with the uncovery of the hot leg nozzle. The brief coupling of primary-to-secondary caused steam pressure to increase.

The leak flow continued to exceed the HPI flow (Figure 9.11) and the loop rapidly lost inventory. The cold leg, downcomer, and core fluid temperatures increased as core heat generation exceeded the high-pressure injection cooling capacity, leading to sustained saturation of the core inlet fluid beyond 20 minutes. The hot leg and steam generator primary levels showed a step decline until 30 minutes (Figure 9.9). A comparison of appended Plot 18 of Test 230199 with appended Plot 18 of Test 230299 illustrates the faster rate of primary inventory decrease that occurred in Test 230299 as a result of the low-head high-pressure injection. At 30 minutes into the test, with the hot leg level at 51 feet and the steam generator primary level at 45 feet, the operator isolated the leak (Figure 9.11) by procedure. The hot leg and steam generator primary levels began to increase as did the primary pressure. The brief refill was halted at 33 minutes when the pressurizer relief valve was opened and the pressurizer

began to fill, removing liquid inventory from the hot leg and steam generator. The pressurizer level rose rapidly (Figure 9.9) as steam was vented from the pressurizer. By 40 minutes the pressurizer had filled and the relief valve began to vent liquid. With the pressurizer relief valve open, primary pressure decreased and the high-pressure injection flow increased. High-pressure injection flow through the core and out of the relief valve cooled the core inlet rapidly (Figure 9.12).

AFW BCM (Auxiliary Feedwater Boiler-Condenser Mode) and Refill

At 60 minutes auxiliary feedwater injection was actuated as specified (AFW reactivation criteria 4: test duration greater than one hour). With the steam generator primary level at 34 feet, approximately 18 feet of primary condensing length was exposed to the effects of auxiliary feedwater.

A significant high-elevation boiler-condenser mode ("AFW BCM") occurred and primary pressure decreased from 1500 to 1200 psia in 3 minutes (Figure 9.8). At the same time that auxiliary feedwater was initiated, the operator closed the pressurizer relief valve (appended Plot 16). The pressurizer level decreased rapidly (Figure 9.9). By 64 minutes, the hot leg and steam generator primary levels had increased to 63 and 53 feet, respectively. With the secondary level control at 10 feet, the auxiliary feedwater injection terminated at 65 minutes with the secondary level at 14 feet. The reduction in primary pressure during the boiler-condenser mode resulted in a step increase in high-pressure injection flow. As a result, the pressurizer, hot leg, and steam generator primary inventories increased rapidly. At 70 minutes, the operator energized the pressurizer main heaters to maintain pressure control.

Post-Refill Natural Circulation Cooldown

By 75 minutes, the hot leg level had reached the hot leg U-bend and the steam generator primary quickly began to fill (Figure 9.9). The primary flow rate increased to $\sim$ 6%, then fell to $\sim$1% (Figure 9.10). Primary-to-secondary coupling was evident from the string thermocouple temperature increase (appended Plot 13), as well as from the feed and steam flow increases (appended Plot 10). As coupling was established, the operator reduced secondary pressure (see Table 9.4) and primary-to-secondary heat transfer was maintained, cooling the loop. At 80 minutes, with the

loop full of liquid and the pressurizer level at 30 feet, the operator terminated HPI (Figure 9.11). Numerous secondary pressure decreases occurred from 80 to 190 minutes (Table 9.4) and the loop continued to cool (appended Plots 2, 13, 26, 111, 121, 131, 132, 135, 141, 151 and 191 through 194). The core outlet temperature reached 450F (75F subcooled) at 190 minutes (Figure 9.12). With the pressurizer main heaters operating, the primary pressure stayed virtually constant from 95 to 190 minutes even though a cooldown was occurring. Pressurizer level fell from 30 to 15 feet during this time as a result of primary inventory contraction. At 198 minutes, high-pressure injection was actuated to raise pressurizer level (Figure 9.11). The high-pressure injection was terminated again at 204 minutes with the pressurizer level at 20 feet. Numerous secondary pressure reductions occurred until 231 minutes, maintaining the loop cooldown. At 243 minutes, the test was terminated according to procedure. Figure 9.13 shows the test results on the pressure-temperature envelope. The results are similar to those of Test 230199 and indicate that loop conditions were approaching the envelope at test termination.

9.4 Results*

OTIS Tests 230199 and 230299 both exhibited four major SBLOCA phases: (1) saturation, draindown, and intermittent circulation, (2) the boiler-condenser mode, (3) refill, and (4) natural circulation cooldown. The low-head high-pressure injection system used in Test 230299 led to a greater draindown in comparison to Test 230199. Even though more inventory was lost before leak isolation, in Test 230299, the larger primary condensing surface within the steam generator resulted in a more-pronounced boiler-condenser mode depressurization. Test 230199 depressurized to 1400 psia whereas, in Test 230299, primary pressure decreased to 1200 psia during the boiler-condenser mode. This pressure difference resulted in differing high-pressure

*Additional information regarding these operator-controlled transients is contained in the following paper: D. P. Birmingham, R. L. Black, and G. C. Rush, "An Experimental Study of the Application of Abnormal Transient Operating Guidelines (ATOG) To the Babcock & Wilcox Nuclear Steam Supply System During a Small Break Loss-of-Coolant Accident," (Paper presented at the 23rd ASME/AICHE/ANS National Heat Transfer Conference, Denver, August 6-9, 1985).

injection flow characteristics and, during this time frame, the low-head high-pressure injection system produced greater flow in Test 230299 than the high-head system in Test 230199. As a result of the pressurizer outsurge at the time of auxiliary feedwater actuation in Test 230299, the system inventory depletion difference was offset, causing refill to occur at approximately the same time in the two tests. Since a high-elevation boiler-condenser mode occurred in both tests, the difference in pool elevations (38 feet for Test 230199 versus 10 feet for Test 230299) appeared to have little influence on the results. The differences between the two tests following refill may have been caused by the operator-controlled steam generator depressurization rate. Test 230199 entered post-refill natural circulation with a steam pressure of ∿700 psia, versus 550 psia in Test 230299. This resulted in fluid temperatures that were approximately 50F higher in Test 230199 than in Test 230299 at test termination.

Table 9.1 Initial Conditions, Composite Tests.

	Test 230199		Test 230299	
	Planned	Actual	Planned	Actual
Core power (% of full power, 1% full power = 24.1 kW), includes 0.5% to replace losses to ambient.	4.2 ± 0.1	4.17	4.2 ± 0.1	4.17
Natural circulation.	x	x	x	x
Primary pressure, psia.	2200 ± 50	2250	2200 ± 50	2200
Pressurizer liquid height, ft from SGLTSUF.	16.6 ± 2	18.6	16.6 ± 2	19.0
Pressurizer main and guard heaters adjusted for an approximately adiabatic pressurizer.	x	x	x	x
Reactor vessel and hot leg vents closed.	x	x	x	x
Reactor vessel vent valve in automatic (differential-pressure) control with open/close setpoints of 0.25 and 0.125 psid.	x	x	x	x
Auxiliary feedwater at 100F injected at the upper elevation using the minimum-wetting nozzle.	x	x	x	x
Steam generator secondary (collapsed) liquid level.	5 + 1	5.3	5 ± 1	5.7
Hot leg fluid temperature, F.	610 ± 2	608-610	610 ± 2	608-610
High-pressure injection and leak systems are not yet in use . Primary noncondensible gas additions are not to be tested.	x	x	x	x

Table 9.1 (Cont'd)

		Test 230199		Test 230299	
		Planned	Actual	Planned	Actual
Initialization is continued until a suitable system steady state is obtained:					
Pressurizer metal temperatures, F.		650 ± 10	646-709	650 ± 10	652-681
The reactor vessel vent valve is not cycling.		x	x	x	x
The steam generator fluid temperature are varying less than 10F/h (exception: cyclic secondary fluid temperature variations associated with high-elevation AFW injection, and with internal circulation within the secondary liquid pool, are acceptable).		x	x	x	x
Other initial conditions:	T-COLD, F	-	572	-	572
	Primary flow rate, %	-	5.6	-	5.6
	SG pressure, psia	-	1200	-	1200
	Feed/steam flow rate, %	-	2	-	2.2
	AFW temperature, F	100	118	100	111

Table 9.2 Selected Operator Action and Key Events -- Composite Test 230199 (High-Head HPI)

Time	Δ T, min	Action
April 4, 1984		
2132	-9	Started the data acquisition system.
2141	0	Opened 10-cm^2 cold leg suction leak.
2143	2	HPI and core power ramp actuated. SG level control to 3 feet. AFW injection off.
2211	30	Leak isolated.
2218	37	PORV opened.
2241	60	Actuated AFW injection.
2244	63	Decreased SG secondary pressure 25 psi.
2245	64	PORV closed.
2247	66	Decreased SG secondary pressure to 615 psia.
2251	70	AFW level control at 38 feet.
2254	73	Loop refilled.
2258	77	Throttled HPI.
2259	78	Turned off HPI.
2300	79	Raised SG secondary pressure to 750 psia.
2306	85	Set SG secondary pressure to 742 psia.
2311	90	Opened RVUHV for 5s.
2313	92	Opened RVUHV for 10s.
2315	94	Opened RVUHV (left open).
2318	97	Turned on pressurizer main heaters.
2319	98	Closed RVUHV.
2320	99	Decreased SG secondary pressure to 700 psia.
2325	104	Decreased SG secondary pressure to 675 psia.
2353	132	Decreased SG secondary pressure to 617 psia.
0003	142	Decreased SG secondary pressure to 564 psia.
0014	153	Decreased SG secondary pressure to 545 psia.
0020	159	Decreased SG secondary pressure to 496 psia.
0031	170	Decreased SG secondary pressure to 445 psia.
0046	185	Decreased SG secondary pressure to 395 psia.
0102	201	Decreased SG secondary pressure to 349 psia.

Table 9.2 (Cont'd)

Time	ΔT, min	Action
0113	212	Actuated HPI.
0120	219	Stopped HPI.
0127	226	Reduced SG secondary pressure to 298 psia.
0142	241	DAS stopped. Test terminated.

Table 9.3 Summary of Variables Discarded on Input, Composite Test 230199

SUMMARY OF VARIABLES DISCARDED ON INPUT, TEST 230199

NO.	VTAB	SYSTEM	INST.	ELEVATION	D E S C R I P T I O N
1	155HLTC06	2HL	2FTC	50.00	HOT LEG FLUID TEMP (F)
2	262HLCP05	2HL	16 CP	41.00	HOT LEG CONDCTVTY (WET/DRY)
3	263HLCP06	2HL	16 CP	45.00	HOT LEG CONDCTVTY (WET/DRY)
4	264HLCP07	2HL	16 CP	49.00	HOT LEG CONDCTVTY (WET/DRY)
5	265HLCP08	2HL	16 CP	53.00	HOT LEG CONDCTVTY (WET/DRY)
6	266HLCP09	2HL	16 CP	57.00	HOT LEG CONDCTVTY (WET/DRY)
7	274HLCP17	2HL	23RCP	.50	HOT LEG REF. C.P.
8	273HLCP16	3SGP	16 CP	53.10	SG PRIMRY. CONDCTVTY (WET/DRY)
9	272HLCP15	3SGP	16 CP	56.90	SG PRIMRY. CONDCTVTY (WET/DRY)
10	103PRDT03	6PZR	10 DT	42.80	PRESURIZR. INSUL. DT (F)
11	223HPTM02	10HPI	13TMF	-999.00	HP INJECT. TURB.FLOW (LBM/SEC)
12	22CV2AC01	12V2	19ACC	-999.00	2-PH VENT. ACCD.FLOW (LBM)
13	53SSTC13	22SGS	2FTC	32.30	SG SECOND.FLUID TEMP (F)
14	79SMTC02	22SGS	25MTC	26.30	SG SECOND. METAL TC (F)
15	76SMTC06	22SGS	25MTC	44.20	SG SECOND. METAL TC (F)
16	344V1TC03	34CLD	2FTC	-999.00	CLD LEAK FLUID TEMP (F)

Table 9.4 Selected Operator Actions and Key Events -- Composite Test 230299

Time	ΔT, min	Action
29 March 1984		
1528	-10	DAS started.
1538	0	Opened 10-cm^2 CLS leak.
1540	2	Main pressurizer heaters off. HPI system activated.
1541	3	Increased SG secondary pressure to 1350 psia. Lowered SG secondary level to 3 feet. Changed AFW injection from high to low elevation. Core power ramp actuated.
1608	30	Leak isolated.
1611	33	PORV opened.
1638	60	Decreased SG secondary pressure to 750 psia.
1640	62	Actuate high elevation AFW injection. PORV closed.
1642	64	Decreased SG secondary pressure to 700 psia.
1648	70	Decreased SG secondary pressure 650 psia. Turned on pressurizer main heaters.
1649	71	Decreased SG secondary pressure to 600 psia.
1651	73	Decreased SG secondary pressure to 550 psia.
1653	75	Loop refilled.
1658	80	HPI stopped.
1702	84	Decreased SG secondary pressure to 525 psia.
1706	88	Decreased SG secondary pressure to 500 psia.
1710	92	Decreased SG secondary pressure to 475 psia.
1719	101	Decreased SG secondary pressure to 450 psia.
1722	104	Decreased SG secondary pressure to 425 psia.
1742	124	Decreased SG secondary pressure to 413 psia.
1753	135	Decreased SG secondary pressure to 400 psia.
1801	143	Decreased SG secondary pressure to 375 psia.
1817	159	Decreased SG secondary pressure to 350 psia.
1822	164	Decreased SG secondary pressure to 325 psia.
1833	175	Decreased SG secondary pressure to 300 psia.
1847	189	Decreased SG secondary pressure to 250 psia.
1856	198	HPI actuated.

Table 9.4 (Cont'd)

Time	ΔT, min	Action
1902	204	HPI turned off.
1910	212	Decreased SG secondary pressure to 225 psia.
1915	217	Decreased SG secondary pressure to 300 psia.
1925	227	Decreased SG secondary pressure to 175 psia.
1929	231	Decreased SG secondary pressure to 150 psia.
1941	243	DAS stopped. Test terminated.

Table 9.5 Summary of Variables Discarded on Input, Composite Test 230299

SUMMARY OF VARIABLES DISCARDED ON INPUT, TEST 230299

NO.	VTAB	SYSTEM	INST.	ELEVATION	DESCRIPTION
1	155HLTCC6	2HL	2FTC	50.00	HOT LEG FLUID TEMP (F)
2	262HLCPC5	2HL	16 CP	41.00	HOT LEG CONDCTVTY (WET/DRY)
3	263HLCPC6	2HL	16 CP	45.00	HOT LEG CONDCTVTY (WET/DRY)
4	264HLCPC7	2HL	16 CP	49.00	HOT LEG CONDCTVTY (WET/DRY)
5	265HLCPC8	2HL	16 CP	53.00	HOT LEG CONDCTVTY (WET/DRY)
6	266HLCP09	2HL	16 CP	57.00	HOT LEG CONDCTVTY (WET/DRY)
7	274HLCP17	2HL	23RCP	.50	HOT LEG REF. C.P.
8	273HLCP16	3SGP	16 CP	53.10	SG PRIMRY. CONDCTVTY (WET/DRY)
9	272HLCP15	3SGP	16 CP	56.90	SG PRIMRY. CONDCTVTY (WET/DRY)
10	223HPTMC2	10HPI	13TMF	-999.00	HP INJECT. TURB.FLOW (LBM/SEC)
11	220V2AC01	12V2	19ACC	-999.00	2-PH VENT. ACCD.FLOW (LBM)
12	53SSTC13	22SGS	2FTC	32.30	SG SECOND.FLUID TEMP (F)
13	79SMTCC2	22SGS	25MTC	26.30	SG SECOND. METAL TC (F)
14	76SMTCC6	22SGS	25MTC	44.20	SG SECOND. METAL TC (F)
15	344V1TCC3	34CLD	2FTC	-999.00	CLD LEAK FLUID TEMP (F)

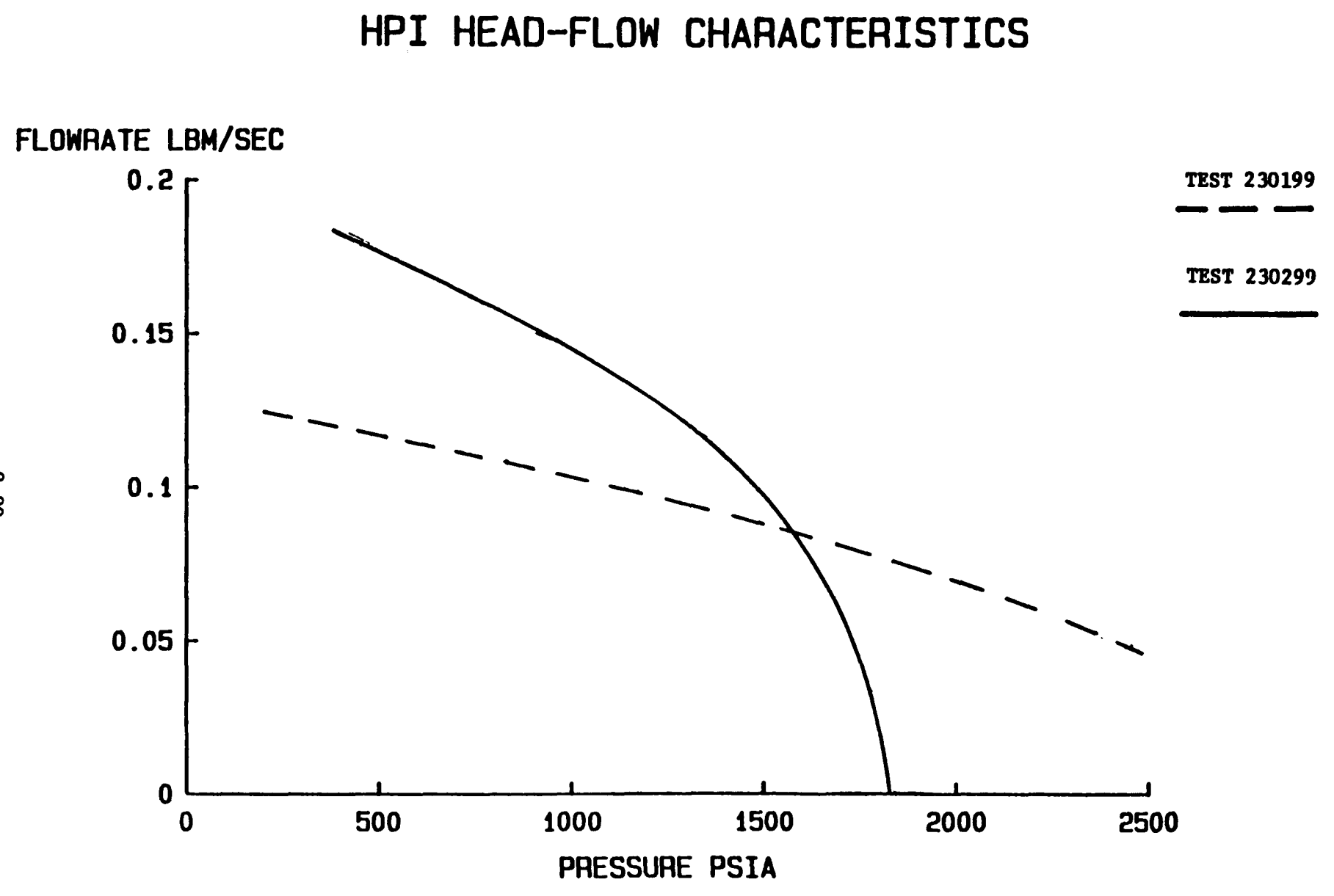

Figure 9.1 High-Pressure Injection Head-Flow Characteristics, Composite Tests 231099 and 230299.

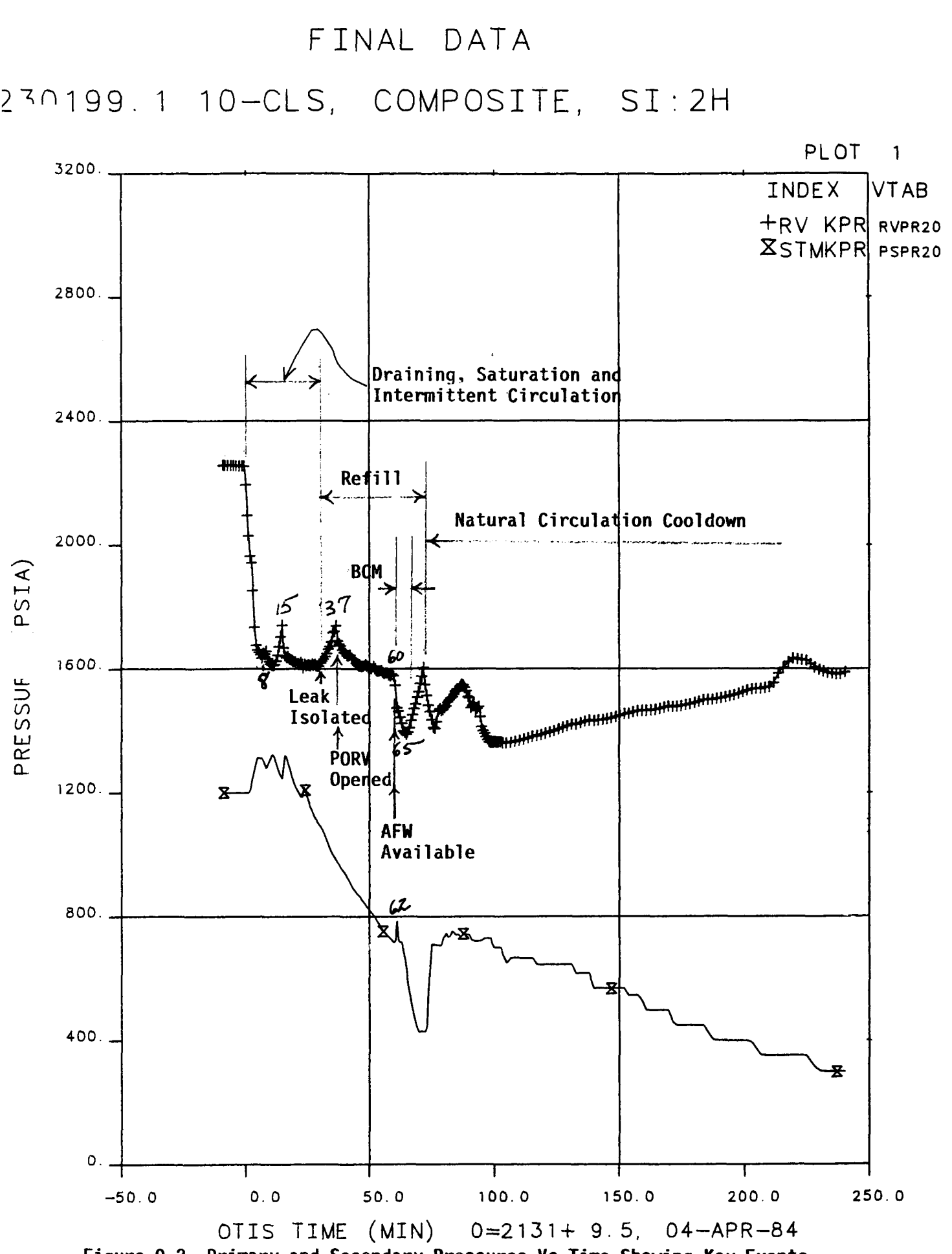

Figure 9.2 Primary and Secondary Pressures Vs Time Showing Key Events

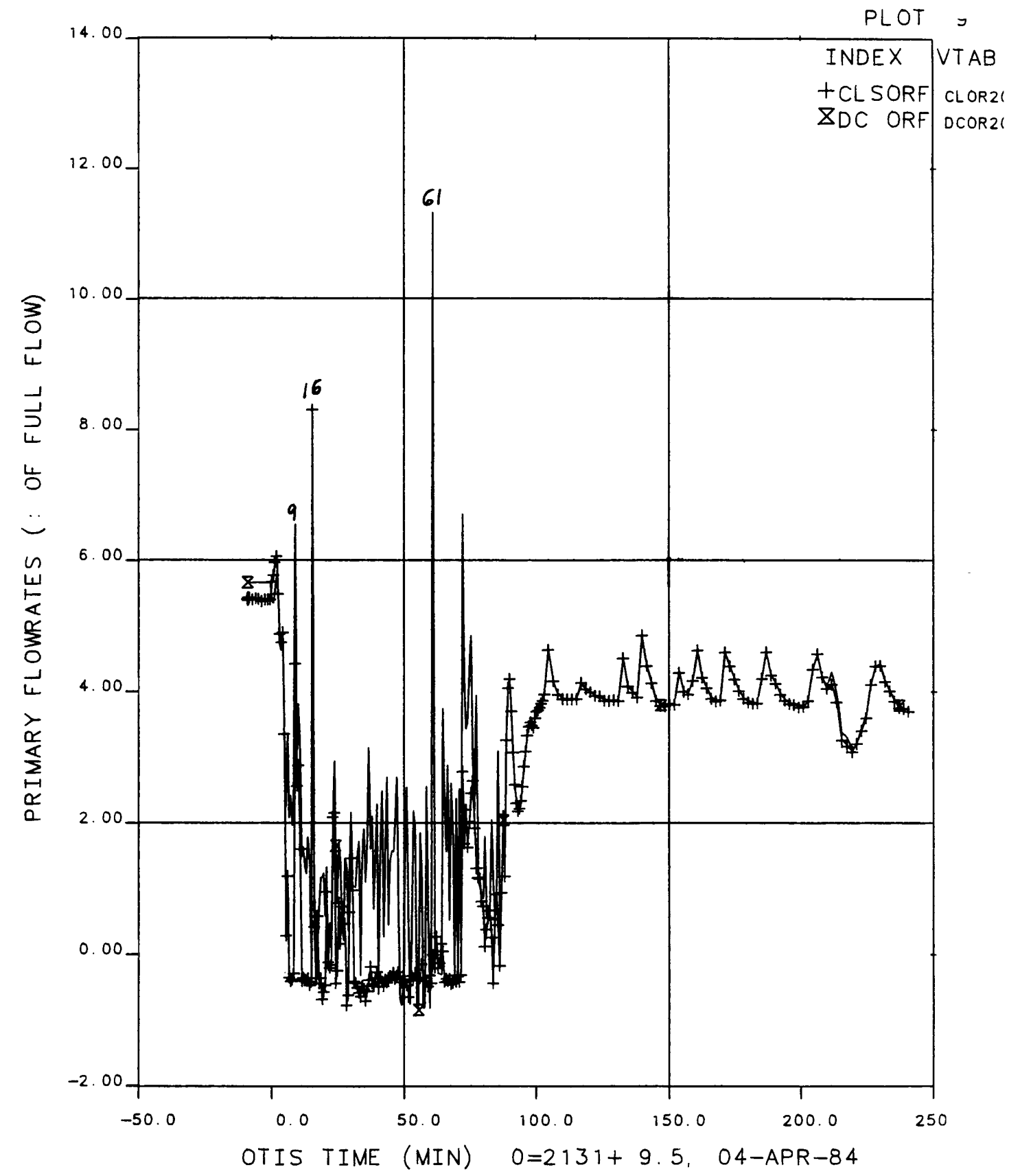

Figure 9.3 Primary Flowrates Versus Time.

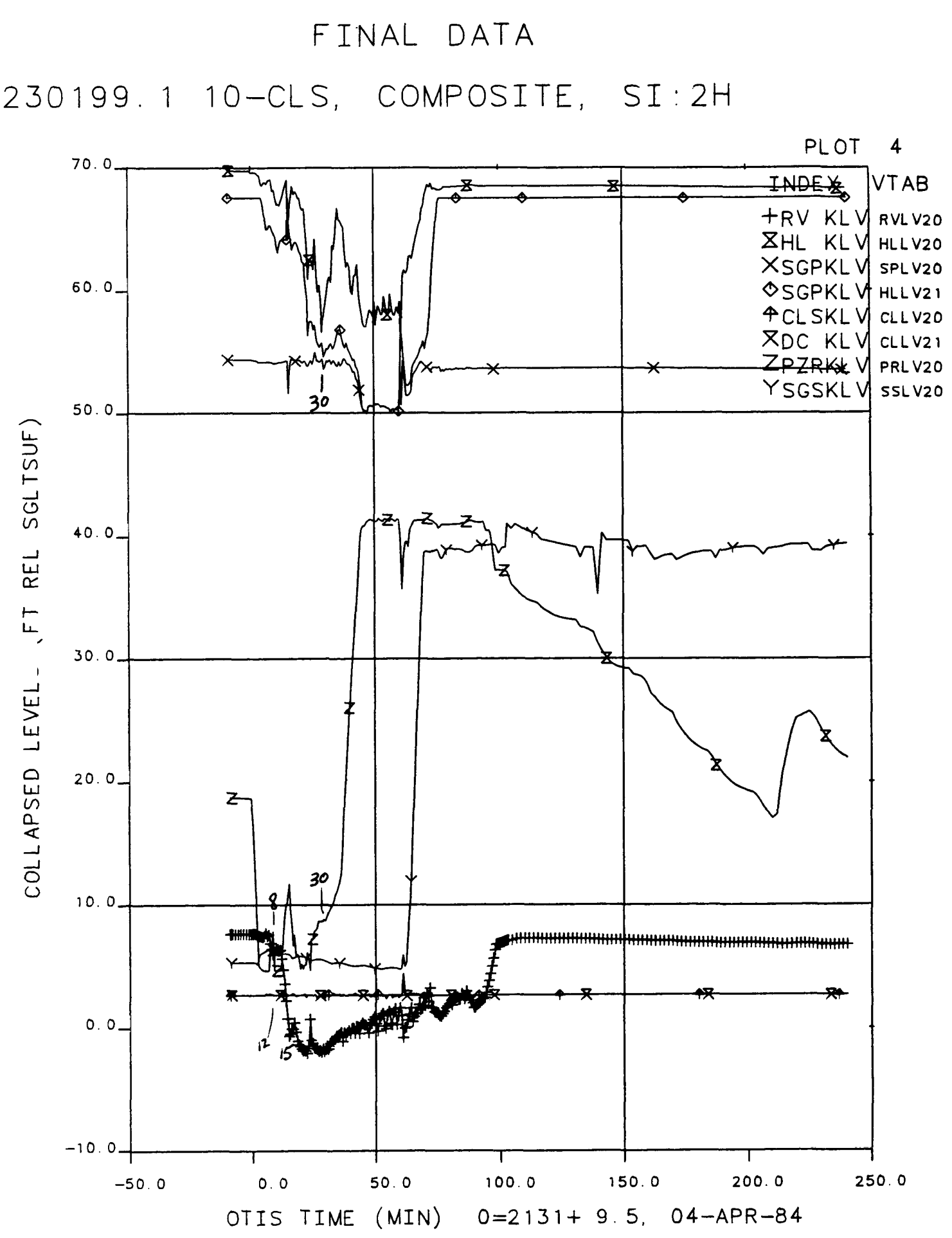

Figure 9.4 Collapsed Liquid Levels Versus Time

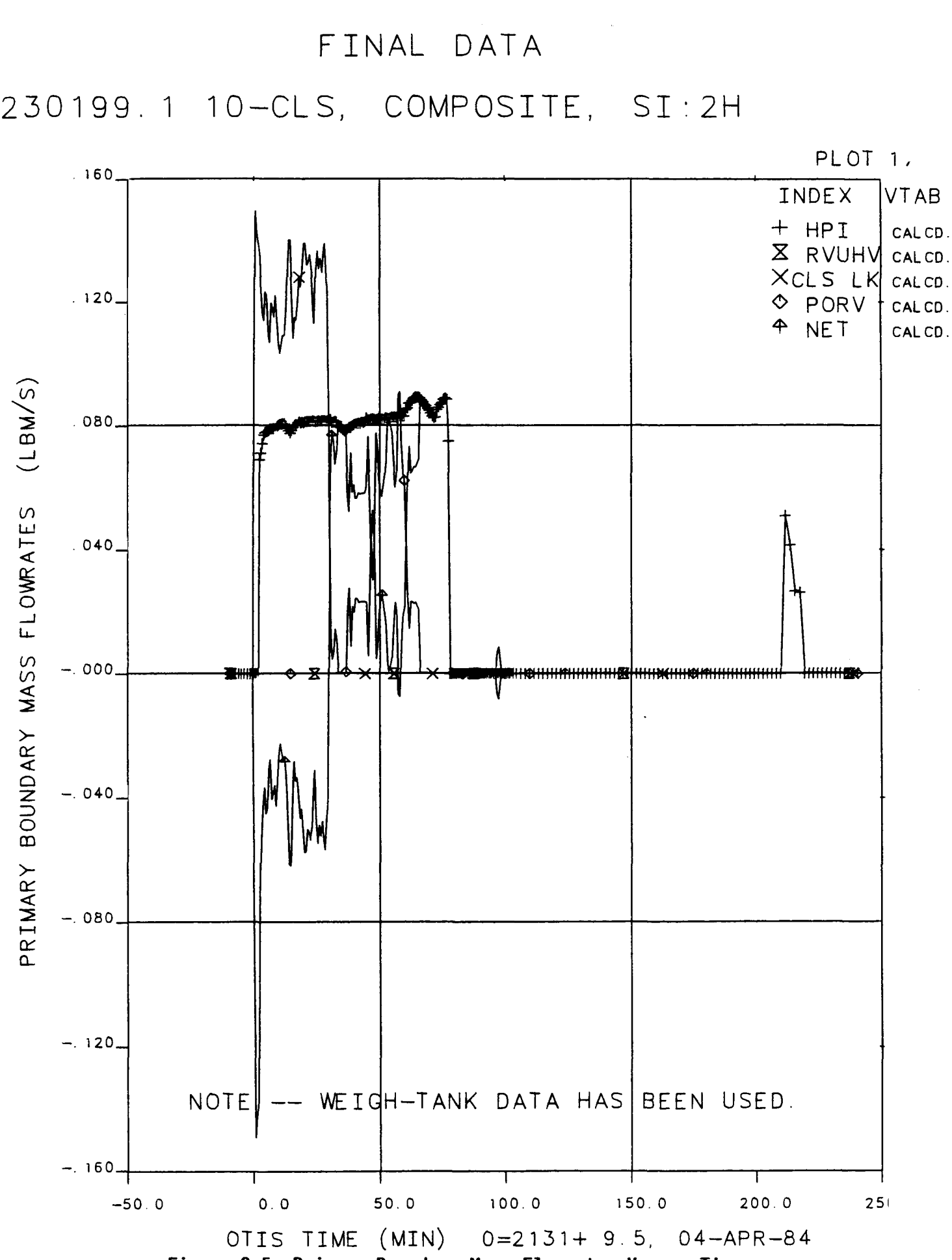

Figure 9.5 Primary Boundary Mass Flowrates Versus Time

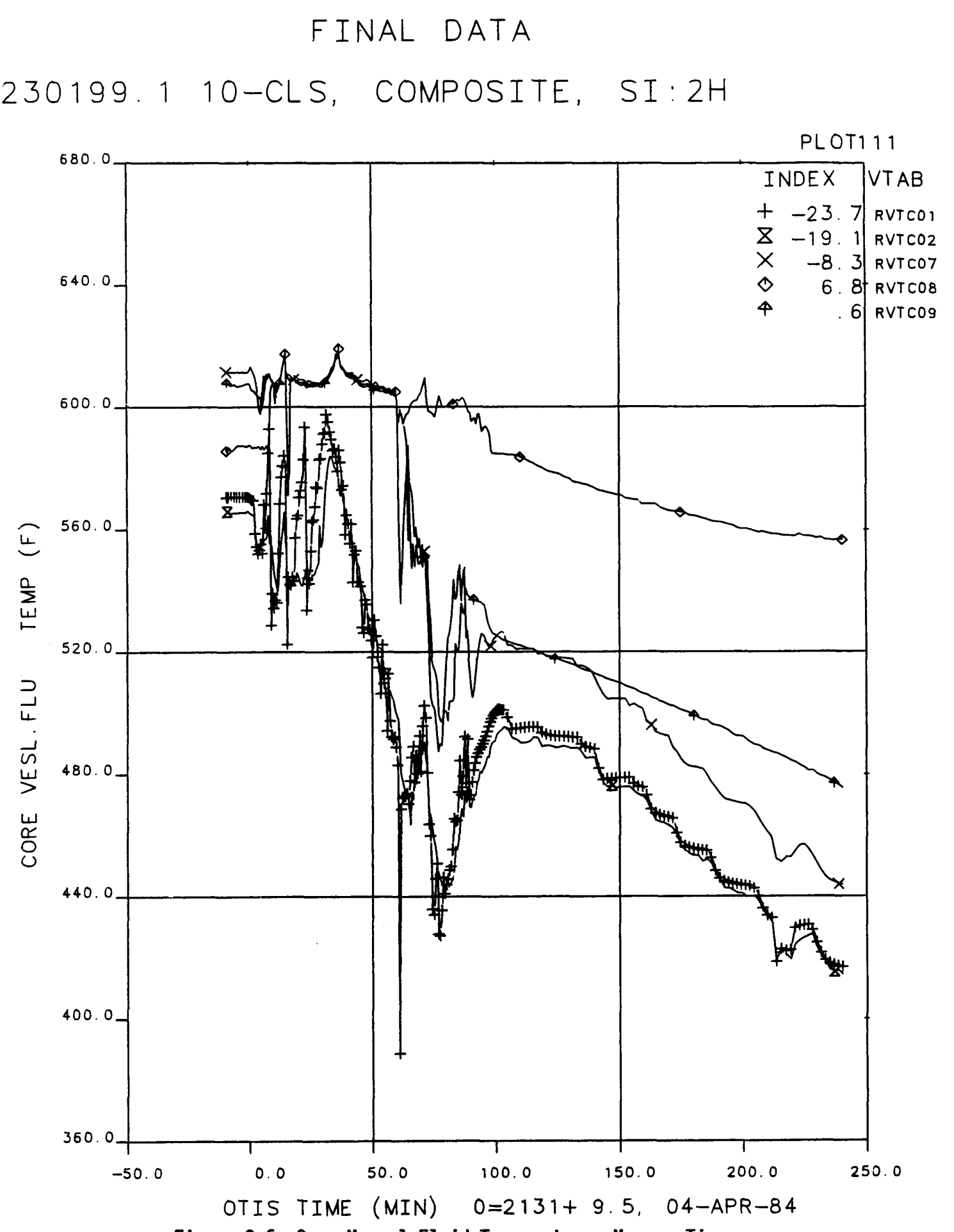

Figure 9.6 Core Vessel Fluid Temperatures Versus Time

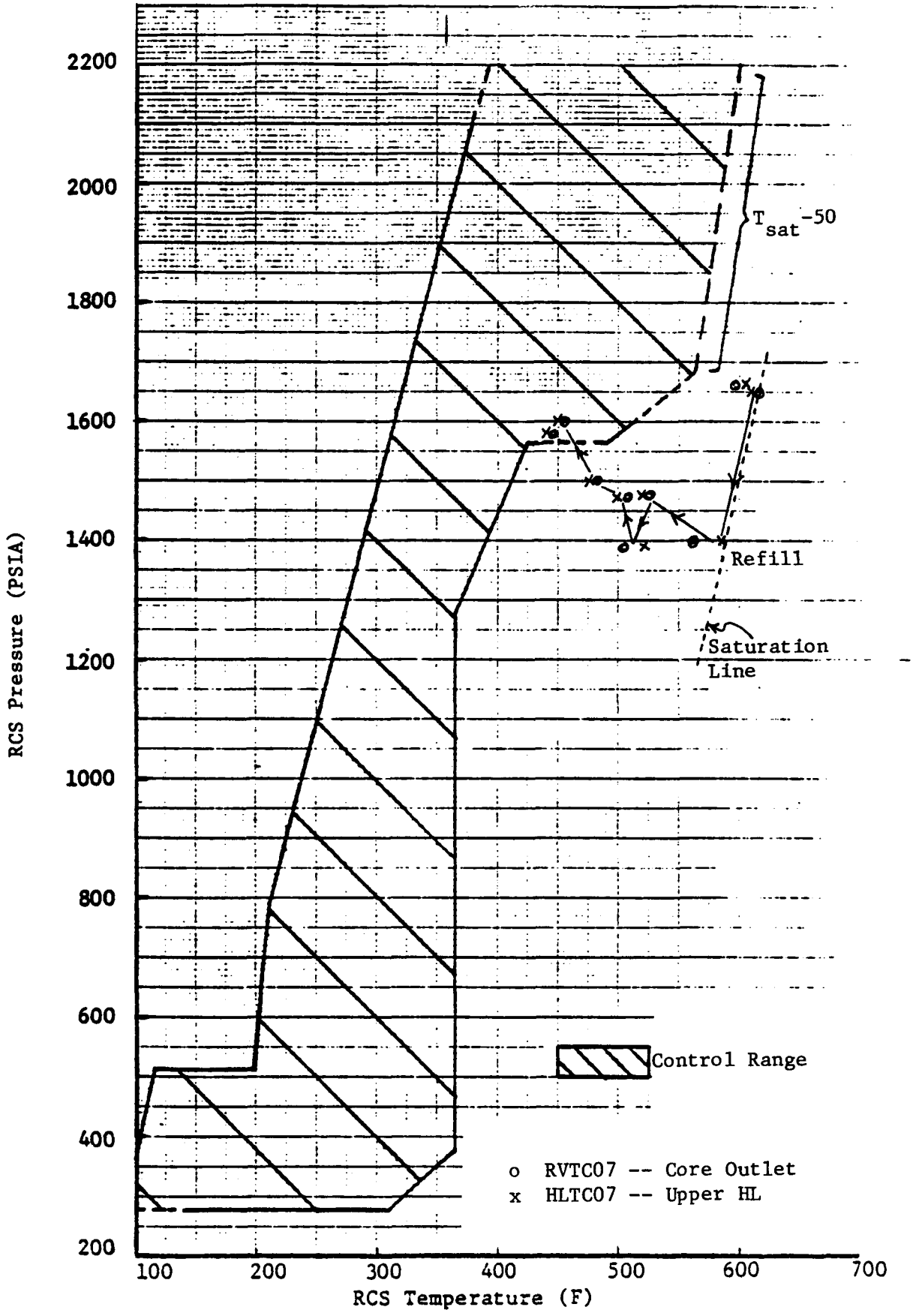

Figure 9.7 Pressure-Temperature Envelope and Primary System Conditions, Composite Test 230199.

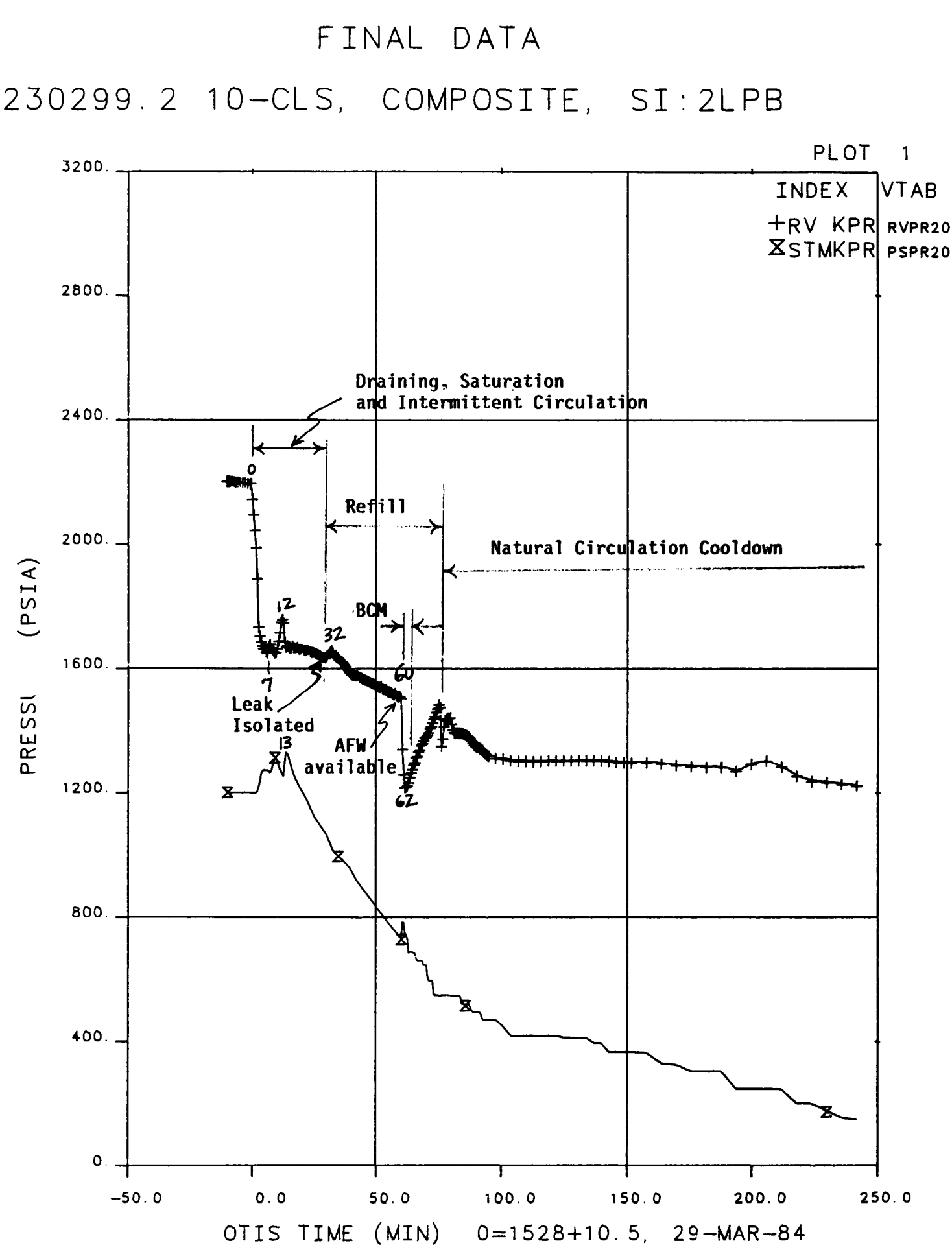

Figure 9.8 Primary and Secondary Pressures Vs Time Showing Key Events.

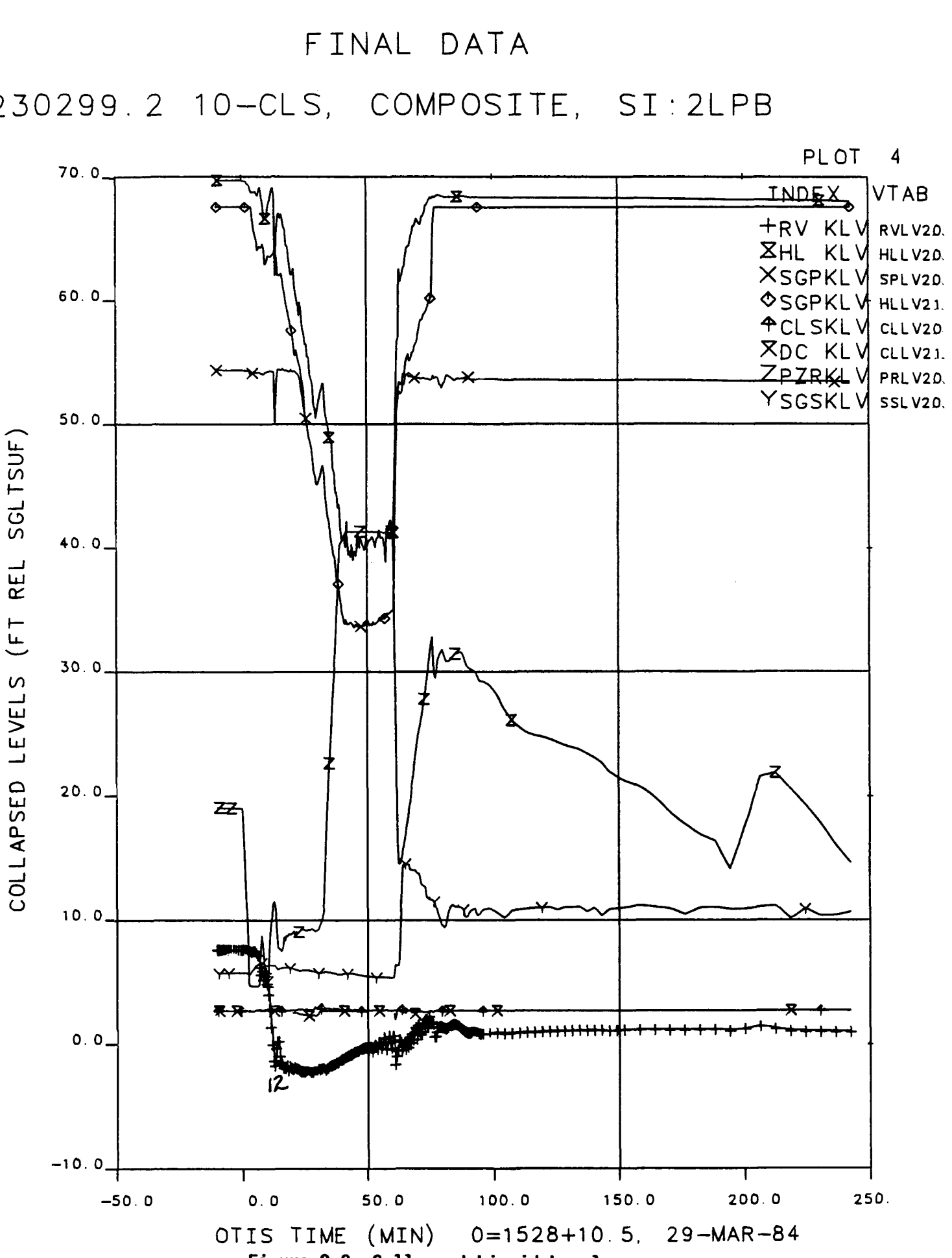

Figure 9.9 Collapsed Liquid Levels.

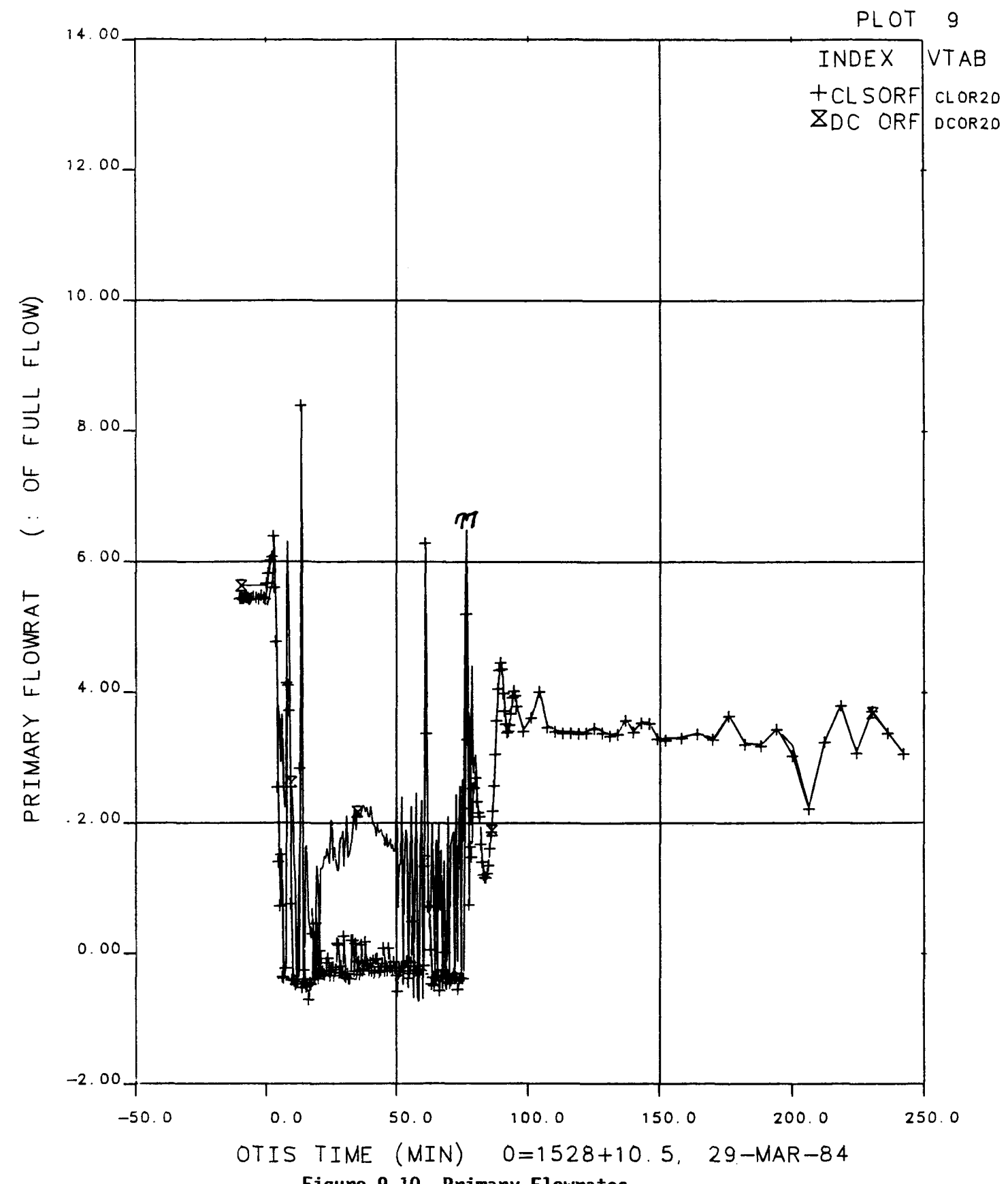

Figure 9.10 Primary Flowrates.

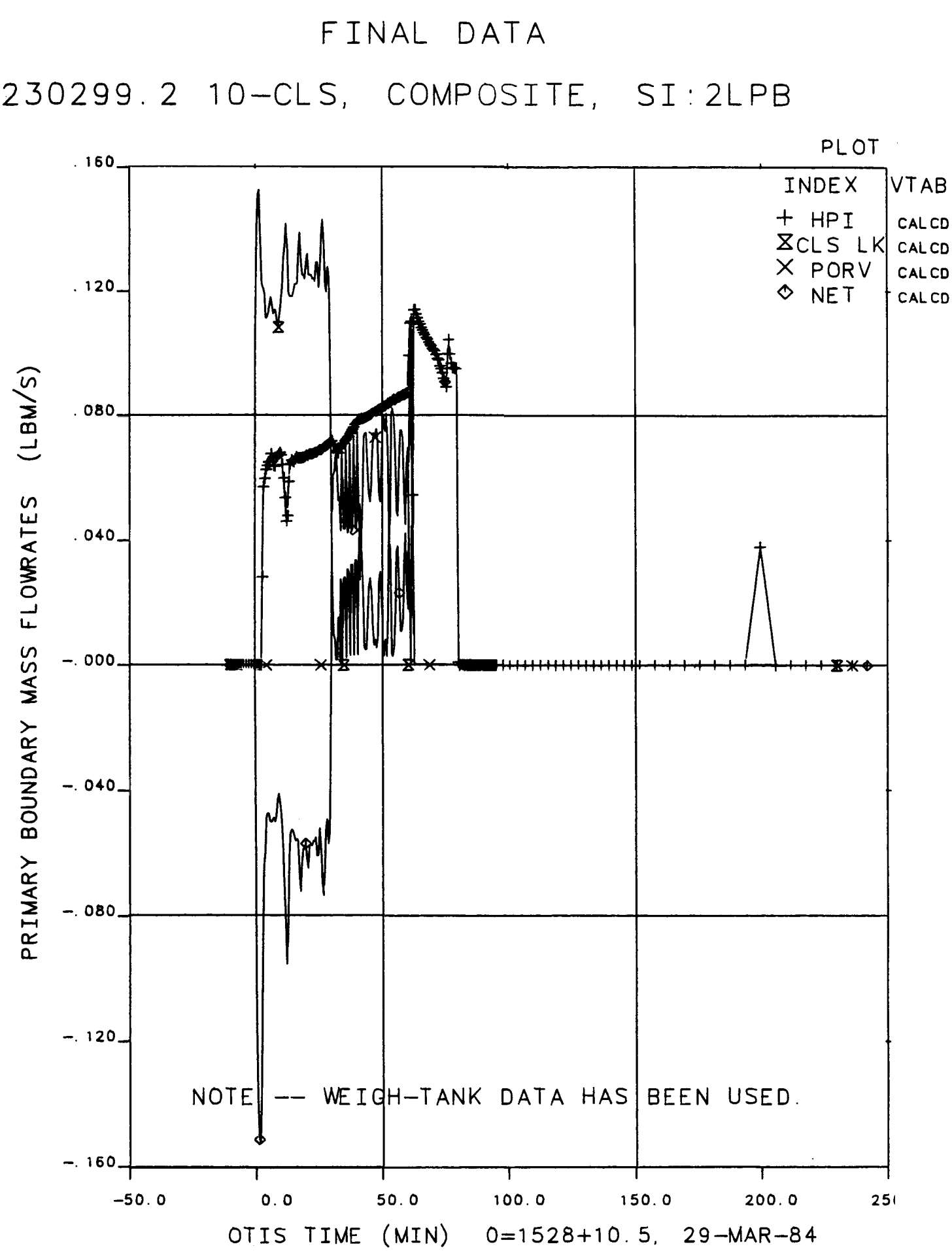

Figure 9.11 Primary Boundary Mass Flowrates.

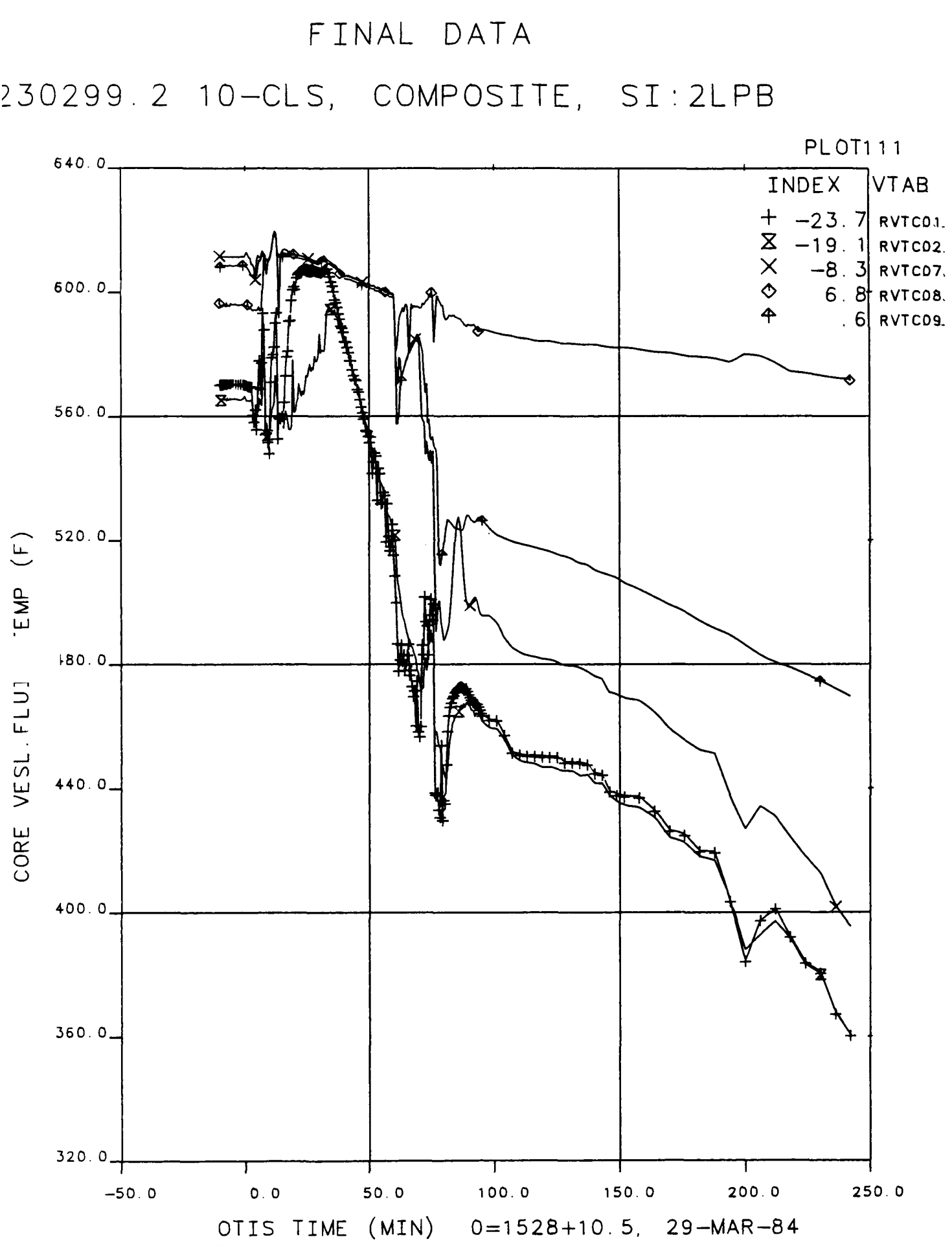

Figure 9.12 Core Vessel Fluid Temperatures.

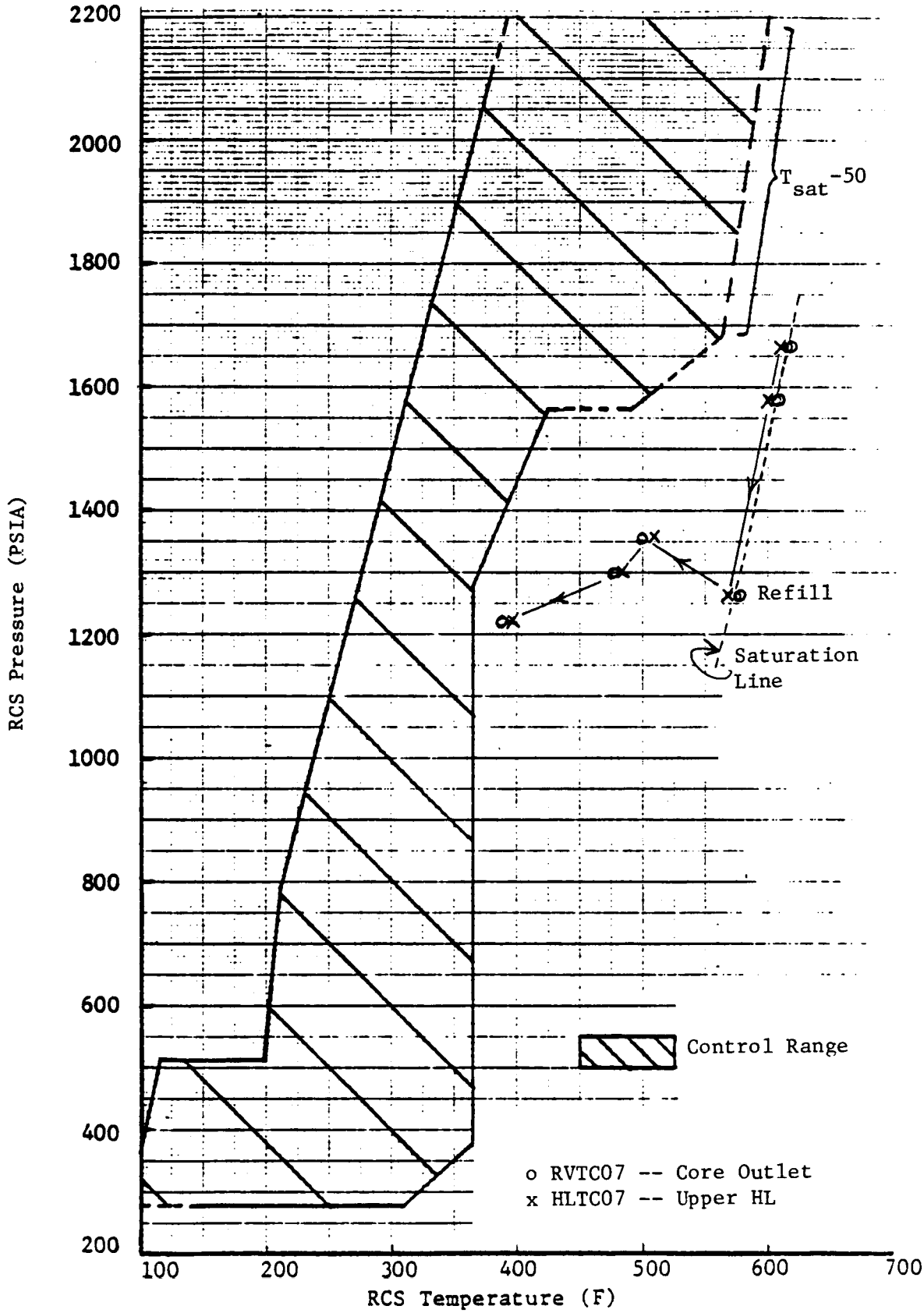

Figure 9.13 Pressure-Temperature Envelope and Primary System Conditions, Composite Test 230299.

10. GUARD HEATER TESTS

10.1 Introduction

OTIS Tests 2202AA and 2202BB were conducted to determine the effect of the guard heaters on the transient response of the system. These tests were added to the original scope of the OTIS test program and are of the single-variable test type.

The OTIS hot leg, pressurizer (including the surge line), and reactor vessel upper head were guard heated. The guard heaters are described in section 2 and in the OTIS Functional Specification. The purpose of these guard heaters was to compensate for the (atypically large) model heat losses to ambient. Guard heater control was based on the radial temperature gradient through the insulation (shown in Figure 2.4). If the model heat losses were distributed uniformly over the guard-heated region, then the guard heater power should have been controlled to minimize the radial temperature gradient. Regions of increased heat loss, such as viewports and fittings, required that the control temperature be biased somewhat from zero. The guard heaters then deposited more energy than was lost to ambient near the control thermocouples, thereby compensating for the increased losses away from the control thermocouples. Using this biasing technique, the guard-heated region was, on a regional average, approximately adiabatic. The appropriate bias was established at one set of system conditions. As the system conditions deviated from those at which the optimum bias had been established, the guard heater control bias (and hence input power) became less appropriate.

The guard heater control insulation differential temperatures indicate negative with the guard heaters functioning, cf. appended plots 112, 122, and 162 showing the reactor vessel, hot leg, and presssurizer differential temperatures (DT), respectively. These negative DTs reflect the aforementioned bias. If the local fluid temperature decreased (such as during refill) or if the local metal temperature increased (such as by excess guard heating), then the corresponding insulation DT became more negative than its setpoint. This deviation of the sensed DT from its control value automatically caused the guard heater power to be reduced, thus countering

the perturbing temperature changes and driving the insulation DT back towards it control point. To illustrate this performance, examine any of the plots of insulation DT. The curves of the individual control DTs remain at or near one (negative) value for the duration of each test (this reflects the control bias). Each individual DT trace usually evidences marked spikes. Each spike is a deviation from the control point due to changes in system conditions, followed by the return to the control point as the system perturbation subsides and the guard heater power control circuit takes effect. This sort of operation is most clearly visible in the plots of hot leg control DT (appended Plot 122) during refill.

Test 2202AA was identical to Test 220201 (15-cm^2 leak) except that during the initiation of the test the pressurizer was to be isolated from the primary system and kept isolated. Test 2202BB was identical to Test 2202AA except that the loop guard heaters were to be de-energized during and after the initiation of the test. These tests are of the single-variable test type; their specifications have been given in section 3. The initializations of these tests were to be identical to that of the Nominal Test (220100). The initiation of both tests involved two steps designed to obtain similar plant conditions at the time of (model and plant) loop fluid saturation. The initial step was simply to open the 15-cm^2 cold leg suction leak (starting the pressurizer drain and the primary system depressurization).

All previous single-variable tests involved actions that were keyed to the depletion of the pressurizer liquid inventory. Test 2202AA required an additional action which was also keyed to the depletion of the pressurizer liquid inventory, namely the isolation of the pressurizer. Test 2202BB was to be identical to Test 2202AA except that the hot leg and the reactor vessel head guard heaters were to be de-energized during the initiation of the test.

The conduct of these tests was to be identical to Test 220201 except that after the loop piping has been refilled, attempts should be made to maintain approximately 5OF subcooling in the hot leg by varying the high-pressure injection flow rate. Test termination was to be identical to that of Test 220201, except that if the hot leg U-bend had not refilled in two hours after the hot leg vent was opened, testing should be continued for an additional hour with the hot leg vent open (total elapsed time with the vent

open would therefore be three hours). Since the pressurizer was to be isolated, the pressurizer relief valve was not to be used for these tests.

10.2 Performance

The initialization, conduct, and measurements of Tests 22202AA and 2202BB are discussed in the following paragraphs.

10.2.1 Initialization

Test initial conditions are summarized in Tables 10.1 and 10.2 for Tests 2202AA and 2202BB, respectively. Actual initial conditions corresponded to those specified, with the exception of the pressurizer level for both tests and the pressurizer metal temperature for Test 2202AA.

The initial liquid inventory in the pressurizer, in conjunction with the amount of draindown from the pressurizer before isolating it, affected the liquid inventory transferred to the primary loop. This slight difference in the initial pressurizer level is not perceived to have had a significant influence on test behavior.

One pressurizer metal TC was observed to be out of specification with a reading of 672F (PRTC10 on appended Plot 163) for Test 2202AA. This reading is not important to the test conclusions, because the pressurizer was isolated from the primary loop shortly after the leak was opened.

10.2.2 Conduct

Test conduct is summarized in Tables 10.3 and 10.4 for Tests 2202AA and 2202BB, respectively. Additional information is available in the operator's log (not included herein) and by reviewing the accompanying data plots. The following operator actions were performed as specified by the test procedures:

- Actuated 15-cm^2 cold leg suction leak.
- Actuated the simulation of two high-head high-pressure injection pumps.
- Actuated the core power ramp.
- Actuated auxiliary feedwater.
- Isolated the pressurizer.
- De-energized the hot leg and reactor vessel guard heaters (Test 2202BB only).

- Actuated the steam generator depressurization ramp.
- Increased the high-pressure injection pump speed before automatic low-pressure injection actuation.*
- Actuated the hot leg vent.
- Adjusted the core power to obtain sustaining power late in the transient (Test 2202AA only).

10.2.3 Measurements

Measurements unavailable are listed in Tables 10.5 and 10.6 for Tests 2202AA and 2202BB, respectively. The majority of these instruments were not critical to testing, e.g., hot leg conductivity probes (cf. section 3 for the identification of critical instruments). The unavailable string thermocouple steam generator primary fluid temperature measurements did reduce the steam generator primary instrumentation below the minimum level; this string thermocouple failure was caused by a steam leak through the string sheath. This entire string was subsequently severed and sealed to prevent leakage from the primary system.

10.3 Observations

The observed transient performance of Tests 2202AA and 2202BB are described separately in the following paragraphs. These relatively brief descriptions are supplemented by the detailed inter-test comparisions given in section 10.4. The key transient events are listed in Table 10.7 and 10.8, the major test phases are indicated on Figures 10.1 and 10.2.

10.3.1 Test 2202AA, Isolated Pressurizer

The scaled 15-cm^2 cold leg suction leak was actuated after 11.4 minutes of steady-state data collection. The pressurizer level descended to two feet in the pressurizer and the following test-initiating actions were taken between 1 and 2.3 minutes after leaking opening: the pressurizer was isolated (by closing its surge line isolation valves), high-pressure

*Although the simulated low-pressure injection was automatically actuated at approximately 240 psi, operator action was required in anticipation of the low-pressure injection actuation. This was due to the simulation of both high-pressure injection and low-pressure injection with one system in the OTIS test facility, thus requiring an increase in the high-pressure injection pump speed to accommodate the increase in flow when low-pressure injection actuates.

injection was activated, the steam generator secondary level control setpoint was increased to 38 feet, and the core power decay ramp was activated. (The isoloation of the pressurizer distinguishes this test from Test 220201.) The primary system pressure quickly fell to 1630 psia, and then stabilized as the hot leg U-bend fluid saturated. The continuing decrease of the primary fluid inventory caused a flow interruption due to voiding at the hot leg U-bend at 3 minutes. The resulting repressurization was interrupted as voiding in the reactor vessel region caused a spillover at 3.4 minutes. Primary-to-secondary heat transfer was then again inhibited, until the hot leg nozzle was uncovered by the descending level in the reactor vessel. This uncovery and attendant recoupling occurred at approximately 8 minutes, and halted the primary repressurization at 1675 psia. After this recoupling, the primary system pressure held constant at approximately 1600 psia.

The steam generator primary level reached the elevation of the auxiliary feedwater injection point at 11 minutes. The auxiliary feedwater (AFW) was still being injected to refill the steam generator secondary to 38 feet, therefore an "AFW BCM" occurred (the condensation of primary vapor at the AFW injection location). This BCM (boiler-condensor mode) rapidly depressurized the primary, and caused the steam generator secondary pressure to increase momentarily. The auxiliary feedwater injection rate was reduced at 15 minutes, as the secondary level approached its control point; therefore, the rate of primary depressurization was correspondingly reduced. The primary depressurization rate increased again at 22 minutes, however, as the steam generator primary level dropped below that of the secondary pool level and the Pool BCM became active. The primary pressure approached the secondary pressure at 31 minutes, and then paralleled the secondary pressure as the Pool BCM continued.

The primary continued to depressurize with the secondary until approximately 200 minutes, descending to 225 psia. The hot leg and steam generator primary levels decreased to as low as 4 feet during this BCM depressurization, until the high-pressure injection flowrate exceeded the leak flowrate at 123 minutes (and refill began). The primary system depressurization was rather abruptly interrupted after the low-pressure injection system became active at 199 minutes. The rising steam generator primary

liquid level precluded Pool BCM; the auxiliary feedwater system was inactive, thus the primary system repressurized (and deactivated the low-pressure injection system) beginning at 206 minutes.

The leak flowrate increased due to the primary system repressurization, therefore, the primary system fluid conditions approached equilibrium at 250 minutes. The leak and high-pressure injection flowrates were approximately equal at a primary system pressure of roughly 350 psia. The hot leg high-point vent was opened at 304 minutes. The primary system pressure decreased following vent actuation, but then slowly increased back toward equilibrium conditions (these events are discussed in detail in the comparison between Tests 2202AA and 2202BB which follows). The rising hot leg and steam generator primary levels obtained a (hot leg U-bend) spillover, primary-to-secondary heat transfer, and a weak primary system depressurization at 371 minutes. Although many spillovers subsequently occurred, refill (of the hot leg U-bend) was not completed and the primary system pressure stayed virtually constant. At 487 minutes the scheduled reduction of core power to sustaining power was begun. The spillovers began to occur more frequently. The hot leg vent began to discharge liquid at 557 minutes, 3 minutes after the reactor vessel vent valve control was transferred from manual-open to automatic. The loop fluid conditions were slowly realigning toward those which support natural circulation when the test was terminated at 615 minutes.

10.3.2 Test 2202BB, Guard Heaters Deenergized

The 15-cm^2 cold leg suction leak was opened after acquiring steady-state data for 12 minutes. The pressurizer level reached 2 feet in the pressurizer in 1.3 minutes, and the following test-initiation actions were performed in rapid succession: the pressurizer was isolated, the high-pressure injection system was activated, the steam generator secondary level control setpoint was increased to 38 ft (increasing the auxilary feedwater flowrate), the core power ramp was activated, and the loop guard heaters were deenergized. (This deactivation of the loop guard heaters distinguished Test 2202BB from the comparison Test 2202AA.) The initial events of Test 2202BB were almost identical to those of Test 2202AA: the hot leg U-bend fluid saturated at 1.7 minutes as the primary depressurized

to 1630 psia, the primary loop flow interrupted at 4.5 minutes with the continuing reduction of primary fluid inventory, and the subsequent primary system repressurization was interrupted at 6 and 9 minutes. The first recoupling of the primary and secondary systems occurred when the HL level briefly reattained the elevation of the hot leg U-bend spillover, due to voiding in the reactor vessel and hence the displacement of reactor vessel liquid to the hot leg. The second recoupling was due to the increased vapor flow up the hot leg as the reactor vessel level dropped below the elevation of the hot leg nozzle.

A precipitous primary depressurization began at 12 minutes, when the primary level entered the steam generator while auxiliary feedwater (AFW) injection was still active. This AFW BCM depressurization was quickly reduced when the steam generator secondary level approached its control level and the auxiliary feedwater flowrate was reduced; but the rate of primary depressurization increased again at 23 minutes, when the primary level descended below the elevation of the secondary pool and the Pool BCM became active.

The primary level remained below that of the steam generator secondary pool, and hence the primary depressurized with the secondary, until 208 minutes. During this depressurization phase, the hot leg and steam generator primary levels attained minimums of approximately 4 feet, at 120 minutes. Then the high-pressure injection flowrate began to exceed the leak flowrate, but the primary system continued to be depressurized through (Pool) boilercondenser mode heat transfer. The low-pressure injection system shutoff head was attained at 200 minutes. The rate of primary system refill was then greatly enhanced, and the Pool BCM was precluded after 207 minutes by the rising steam generator primary level. The auxiliary feedwater system was inactive at this time, thus the primary system began to gradually repressurize, reaching approximately 290 psia by 250 minutes.

At 277 minutes the hot leg level reached the elevation of the hot leg U-bend spillover, a spillover was observed, and the operator transferred the control of the reactor vessel vent valve from manaual-open to automatic. The primary and secondary systems then remained coupled through intermittent spillovers. The hot leg high point vent was opened at 301 minutes, and continuing natural circulation (with spillover flow) began at 306 minutes.

The primary system depressurized sufficiently to actuate the low-pressure injection system at 309 minutes, and the refill of the loop was completed almost immediately. The operator throttled the injection flowrate to maintain 50F subcooling, beginning at 318 minutes. The test was terminated at 370 minutes, after one hour of natural circulation cooldown. At test termination, the natural circulation flowrate was approximately 2.5% of scaled full flow. The primary system pressure was 180 psia. The primary system components were full and subcooled, except for the reactor vessel head and the pressurizer.

10.4 Inter-Test Comparisons

The interactions of Tests 2202AA and 2202BB are examined and compared in the following paragraphs, with special emphasis on guard heater effects. These inter-test comparisons are grouped according to the following tests phases:

1. Draining, saturation, intermittent circulation, and interruption.
2. Boiler-Condenser Mode (BCM).
3. Transition between low-pressure injection actuation (loss of BCM) and repressurization.
4. Repressurization phase.
5. Continued refill before opening the hot leg vent.
6. Refill after opening the hot leg vent to the end of each test.

The key events of Tests 2202AA and 2202BB are summarized in Tables 10.7 and 10.8. The phases are also indicated on Figures 10.1 and 10.2. Key data plots are included in Figures 10.1 through 10.54. To facilitate this discussion of test evolutions, Tests 2202AA and 2202BB are hereinafter referred to as Tests "A" and "B".

10.4.1 Draining, Saturation, Intermittent Circulation, and Interruption, 0 to 11 Minutes

Following a period of steady-state loop operation, the transients were initiated at nearly the same DAS (data acquisition system) times (Test A was initiated at 11.4 minutes, and Test B was initiated at 12.0 minutes relative to the start of data collection). The scaled 15-cm^2 cold leg suction leak was opened at these times. When the pressurizer liquid level had descended to approximately 9 feet above the steam generator lower tubesheet upper face, the pressurizer was isolated, the high-pressure injection system was

actuated, the core power ramp was initiated, and the auxiliary feedwater was actuated to increase the steam generator secondary level to 38 feet. In addition to these actions, Test B also required de-energizing all the guard heaters. The primary pressure responses for both tests were virtually identical during this period (Figures 10.3 and 10.4). The primary pressures decreased and then stabilized at approximately 1630 psia (Figures 10.3 and 10.4), the hot leg U-bend voided (HLTC07 and -08, appended Plot 121 indicate saturated conditions), and the hot leg levels began to decrease (Figures 10.5 and 10.6). This occurred between approximately 1 and 2 minutes for both tests. The voiding of the hot leg U-bend region resulted in the interruption of flow to the steam generator. This decoupling of the primary and secondary systems caused an increase in the primary pressure at approximately 3 and 4.5 minutes for Tests A and B, respectively. Almost immediately, a spillover occurred, observable on Figures 10.5 and 10.6 as an increase in steam generator primary level. Steam pressure (Figures 10.3 and 10.4) increased as primary-to-secondary heat transfer was momentarily established because of the spillover. Flow interrupted subsequent to this spillover and a second primary-to-secondary decoupling/repressurization/spillover occurred at approximately 8 (A) and 9 (B) minutes. Additional spillovers were precluded by the continued decrease of the hot leg and steam generator primary levels well below the hot leg U-bend region; thus, primary flow was interrupted.

10.4.2 Boiler-Condenser Mode (BCM), 11 to 200 Minutes

At approximately 11 minutes (Test A) and 12 minutes (Test B), the steam generator primary level reached the high-elevation auxiliary feedwater injection site (approximately 51 feet). Since the steam generator secondary level was still below the control setpoint of 38 feet (Figures 10.5 and 10.6), a high-elevation auxiliary feedwater boiler-condenser mode (AFW BCM) was established. This is observable on Figures 10.3 and 10.4 as a rapid decrease in primary pressure and a rapid increase in secondary pressure at these times. This AFW BCM continued at a decreasing rate, due to the reduction in the auxiliary feedwater flow as the steam generator secondary level approached the control setpoint of 38 feet, until auxiliary feedwater terminated at 15 (A) and 17 (B) minutes (appended Plot 10). As the steam generator secondary continued to steam following the steam generator

depressurization ramp, both tests exhibited a weak primary-to-secondary coupling for roughly the next 6 minutes, as indicated on Figures 10.3 and 10.4.

The hot leg and steam generator primary levels continued to decrease and, at approximately 22 (A) and 22.5 minutes (B), reached the steam generator secondary pool level (cf. Figures 10.5 and 10.6). Pool BCM occurred as indicated by the increased depressurization rate occurring at these times (Figures 10.3 and 10.4). The primary pressure approached and then paralleled the secondary pressure at approximately 31 minutes. During this phase of the BCM, a downcomer and cold leg level perturbation was caused by the flashing of liquid as the pressure decreased (Figures 10.5 and 10.6). The BCM continued with the primary pressure coupled to the secondary pressure until approximately 200 minutes for both tests. During this phase of the transient, the hot leg and steam generator primary levels reached minimums of approximately 4 feet at approximately 120 minutes for both tests (appended Plot 4). At this time, the primary loop pressure had decreased to approximately 450 psia (Figures 10.1 and 10.2), the leak flow had decreased sufficiently so that the high-pressure injection flow began to exceed the leak flow (Figures 10.7 and 10.8) and the refill process started.

During the initial 200 minutes of these transients, no discernible differences in the primary system pressure response were observed between the tests with and without guard heaters. This indicated that the guard heaters had no impact on the system pressure response (provided primary-to-secondary heat transfer existed, i.e., fluid was flowing up the hot leg to the steam generator). Discernible differences in the hot leg and fluid temperatures were apparent, however.

Guard Heater Effects As the Boiler-Condenser Mode (BCM) Subsided

Near the termination of the AFW BCM (at approximately 15 minutes), the hot leg metal temperatures began to respond differently for these tests. During the initial portion of the AFW BCM, the vapor flow rate was sufficient to cool the hot leg piping. This can be observed by the similar temperature response of the hot leg metal and fluid thermocouples from approximately 11 to 13 minutes (Test A) and 12 to 14 minutes (Test B), cf. Figures 10.9 through 10.12.

As the auxiliary feedwater flow rate began to decrease due to the steam generator secondary level control approaching the 38-foot setpoint, the primary-to-secondary heat transfer decreased. As a result, the fluid (steam) flow rate in the hot leg decreased and the heat transfer between the hot leg piping and the fluid decreased. When this occurred, the stored heat in the hot leg piping was not as readily transferred to the fluid; the hot leg metal temperatures in the upper region began to diverge [at approximately 13 (Test A) and 14 minutes (Test B), cf. HLTC11 and HLTC17, Figures 10.10 and 10.12]. Approximately one minute later, the fluid temperature in the hot leg stub (that portion of the hot leg piping from the U-bend downward to the steam generator inlet) increased. After one additional minute, the U-bend fluid temperature also increased. This indicated that pipe stored heat was being transferred to the fluid. Both tests (with and without hot leg guard heaters) responded in a very similar manner through this portion of the transient. Their responses were similar because the guard heaters in Test A were de-energized as they followed the cooldown, thereby duplicating the test without guard heaters through this portion of the transient.

Distinct differences between the hot leg metal and fluid temperature response for these tests can be observed during the remainder of the transient. Figures 10.10 and 10.12 show that the guard heaters (Test A) maintained higher hot leg metal temperatures in the upper regions of the hot leg during the next approximately 6 minutes, when there was a weak coupling between the primary and secondary system. The resulting hot leg metal temperatures in the upper regions of the hot leg for Test A were approximately 10 to 12F higher than those observed in the test without guard heaters (B). The increase in primary-to-secondary heat transfer, which occurred when the steam generator primary level reached the steam generator secondary level (i.e., pool BCM occurred) resulted in an increase in the primary steam flow. This increase in flow again resulted in increased heat transfer from the pipe to the fluid. This was reflected in a decrease in the hot leg fluid temperatures followed by a decrease in metal temperatures in the upper regions of the hot leg, cf. Figures 10.9 through 10.12, at approximately 22 minutes. The excess metal temperatures resulted in a more negative temperature difference across the hot leg insulation, which was the control temperature difference for the guard heaters; thus, in Test A, the

guard heaters were de-energized during this phase of the transient (see appended Plot 122 from 22 to 28 minutes).

As the primary-to-secondary temperature difference decreased, the primary-to-secondary heat transfer also decreased, reducing the steam flow and, consequently, the heat transfer in the upper regions of the hot leg. Stored pipe heat was still transferred to the hot leg fluid in the test with guard heaters (Test B) as indicated by the increasing fluid temperatures between approximately 29 and 34 minutes (HLTC07 and -08, Figure 10.11 and HLTC09, appended Plot 131). Beyond this time, the primary and secondary systems were coupled. Steam was flowing up the hot leg and was being condensed in the steam generator. The hot leg metal and fluid temperatures indicated that the pipe stored heat continued to be transferred to the fluid, as evidenced by the metal temperatures in the steam region being greater than the fluid temperatures, throughout the remaining time when the primary and secondary were coupled (until approximately 200 minutes). A general cooling of the pipe metal temperatures was occurring, and the trend of these temperatures followed the trend of the decreasing saturation temperature of the primary system for the test without guard heaters (Test B). This implies that the pipe metal temperature was being driven by the fluid conditions and not by the ambient heat loss. Fluid temperatures during this period indicated approximately 35 to 50F of superheat for Test B.

The hot leg metal temperatures in Test A differed considerably from those of the test without guard heaters during this phase of the transient. At approximately 30 minutes, the metal temperatures in the U-bend and in the hot leg stub (HLTC11 and -17, Figure 10.10) leveled out between approximately 577 and 584F, while the metal temperature approximately 57 feet up the hot leg (HLTC16) continued on a decreasing trend. As the hot leg collapsed liquid level continued to decrease, more of the hot leg pipe was exposed to steam. At approximately 32 minutes, the hot leg metal temperature at the 46-foot level (the collapsed liquid level was approximately 41 feet at this time) began increasing (HLTC15, Figure 10.10). An examination of the hot leg insulation differential temperatures in those regions of the hot leg where steam was present indicated that, in general, the hot leg metal temperatures were maintained or began to increase when the insulation temperature difference exceeded its initial value, cf. HLDT08,

appended Plot 122 and HLTC17, Figure 10.10, at approximately 15 minutes; also see HLDT05, appended plot 122 and HLTC15, Figure 10.10 at 31 minutes. As the collapsed liquid level continued to decrease, more of the hot leg pipe was exposed to steam flow. A hot leg metal temperature, HLTC10, initially decreased but then increased in a similar manner. This hot leg metal thermocouple was located near the hot leg viewport and may have been influenced by the high local heat loss. A comparison of the hot leg metal and fluid temperatures indicated that the fluid temperatures followed the metal temperature response and that the metal temperatures were higher than the fluid temperatures, with the exception of HLTC10.

Figures 10.13 through 10.16 display the hot leg metal and fluid temperature versus the traversed hot leg distance, from the hot leg inlet resistance temperature detector, HLRT01, to the steam generator inlet RTD, SPRT01. These figures depict specific times during the depressurization phase of these transients and provide a comparison of the hot leg temperature response for the tests with (Test A) and without (B) guard heaters.

Since the primary system response for both tests was identical during the depressurization phase of the transient, virtually identical times (after leak opening) can be compared. The times chosen confirm the identical response of both tests when the reactor vessel pressure and hot leg levels are compared. During the depressurization phase of the transient, primary-to-secondary heat transfer occurred through the BCM of heat transfer. Steam flowed up the hot leg and was condensed in the steam generator.

Figure 10.13 shows the hot leg temperature distributions for these tests at approximately 42.5 minutes after the leak was opened. The reactor vessel pressure was approximately 817 psia and the hot leg collapsed liquid level was approximately 28 ft for both tests. All temperatures approximated the saturation temperature up to an elevation that was slightly above the collapsed liquid level. Beyond this point, increasing temperatures were observed, with the fluid temperatures at the steam generator inlet indicating approximately 54 and 36F of superheat for the tests with (A) and without (B) guard heaters. The metal temperatures for both tests were consistently higher than the fluid temperatures, indicating heat input to the fluid. A distinct difference in the hot leg metal temperatures for

these tests is observable in the upper regions of the hot leg. Test A, with guard heaters, indicated metal temperatures of approximately 580F at the hot leg U-bend and stub, whereas Test B, without guard heaters, indicated metal temperatures that were approximately 20F lower, $\sim$ 560F. Corresponding differences in the fluid temperature were also observed between the tests.

As the depressurization continued through the draindown (Figures 10.14 and 10.15) and the initial portion of the refill phase (Figure 10.16), the hot leg metal temperatures were generally greater than the fluid temperature for both tests. The exception to this was the hot leg metal temperature at the 34.5-foot elevation, HLTC10. This thermocouple was located near the hot leg viewport and may have been affected by local heat losses.

Certain guard heaters apparently energized during the depressurization phase of Test A. The impact of the guard heaters is apparent from Figures 10.13 through 10.16. As the primary loop depressurized, the fluid entering the hot leg followed the saturation temperature. Since the primary and secondary systems were coupled, fluid flow up the hot leg to the steam generator was expected. The steam generator inlet temperature for the test without guard heaters (B) responded to the decreasing saturation temperature. This was indicated by the almost constant superheat (approximately 36 to 52F) over the time investigated in Figures 10.13 through 10.16. However, in Test A (with guard heaters) the steam generator inlet conditions did not respond to the decreasing saturation temperature. A relatively constant fluid temperature of approximately 550 to 575F was maintained and a corresponding increase in superheat at the steam generator inlet was obtained (approximately 54 to 156F). Figure 10.17 shows the steam generator inlet superheat condition versus the time after the break was opened.

In summary, during the depressurization phase of the transient, the guard heaters affected only the local conditions in the hot leg and had no impact on the overall transient response of the primary system.

10.4.3 Refill: Transition Between Low-Pressure Injection Activation (Loss of Boiler-Condenser Mode) and Repressurization, 200 to 235 Minutes

The coupling of the primary and secondary systems during the BCM resulted in a continuously decreasing primary system pressure. When the reactor vessel pressure reached approximately 228 psia at 199 minutes (Test A) and 226 psia

at 200 minutes (Test B), the simulated low-pressure injection system actuated, Figures 10.18 and 10.19. At approximately 204 minutes, the reactor vessel inlet temperatures indicated subcooled conditions. A significant increase in the refill rate of the hot leg and steam generator primary was also observed, Figures 10.20 and 10.21. At approximately 206 minutes (Test A) and 207 minutes (Test B), the steam generator primary level reached the secondary pool elevation (see Figures 10.20 and 10.21), thereby terminating pool BCM. The relatively small temperature difference between the primary and secondary side did not cause a significant amount of heat transfer, therefore auxiliary feedwater flow was not initiated and AFW BCM did not occur. This resulted in a decoupling of the primary and secondary systems leading to the repressurization of the primary system and eventual termination of the low-pressure injection. The initial seven minutes of the repressurization were identical for both tests (Figures 10.22 and 10.23). However, in Test B, low-pressure injection again actuated at 212 minutes at relatively low flow rate, whereas in Test A, low-pressure injection did not actuate a second time (see Figures 10.18 and 10.19). This second low-pressure injection actuation appeared to be due to both the slightly greater amount of low-pressure injection during the first low-pressure injection system actuation in Test B (which appears to be confirmed by the slightly lower reactor vessel inlet temperature) and possibly the low-pressure injection system control sensitivity. In Test B, the primary depressurized approximately 6 psi as a result of this low-pressure injection actuation and then began to repressurize at approximately 218 minutes (Figure 10.23). Low-pressure injection terminated at approximately 226 minutes (Figure 10.19).

Test 2202AA, during this same period, exhibited an increasing primary system pressure. A decrease in the repressurization rate can be observed at approximately 217 minutes, Figure 10.22. During the time from 217 to 227 minutes, slight SG secondary level oscillations (appended Plot 8) and intermittent AFW actuations (appended Plot 10) can be observed. This indicates a weak coupling of the primary and secondary systems, which reduced the repressurization rate.

From approximately 230 until 235 minutes, both tests exhibited an identical repressurization rate. Their primary system liquid mass inventories were

nearly equal. This implies that the differences in low-pressure injection had very little impact on the overall primary system pressure response and the mass inventory. The low-pressure injection actuation only resulted in an increased refill rate that terminated the BCM of heat transfer.

The atypical LPI injection location, the high-pressure injection nozzle in the cold leg discharge piping, caused the termination of low-pressure injection when the steam in the cold leg and the downcomer (below the cold leg nozzle) was condensed in conjunction with the loss of primary-to-secondary heat transfer*.

Guard Heater Effects With Weak Primary-to-Secondary Coupling.

The hot leg metal and fluid temperatures for these two tests continued to exhibit distinct differences through this phase of the transient. Figure 10.24 is a plot of the hot leg metal and fluid temperatures versus the hot leg distance, from the hot leg inlet resistance temperature detector, HLRT01, to the steam generator inlet resistance temperature detector, SPRT01. This figure shows the temperatures during the early portion of the repressurization phase of the transient (at approximately 230 minutes) and provides a comparison of the hot leg temperatures with and without guard heaters (Tests A and B). The conditions for both tests at this time were as follows: the reactor vessel pressure was approximately 248 psia, the primary system was uncoupled from the secondary system, the primary system was repressurizing, and the hot leg liquid level was increasing. Figure 10.24 shows decreasing fluid and metal temperatures as a function of the hot leg elevation in the liquid-filled portion of the hot leg (up to approximately 45 ft). This decreasing temperature trend was a result of the decrease in the saturation temperature caused by the change in elevation head.

The reactor vessel pressure, measured at +7.1 ft above the steam generator lower tubesheet, was approximately 248 psia and the steam generator primary pressure, measured at +53.1 ft above the steam generator lower tubesheet,

---

*Had the low-pressure injection location been more prototypical, i.e., at the top of the downcomer above the reactor vessel vent valve elevation, it is anticipated that LPI-induced steam condensation would have continued until the reactor vessel outlet subcooled. This would have resulted in a continued depressurization of the primary system.

was approximately 224 psia. The corresponding reactor vessel and steam generator primary saturation temperatures were approximately 400 and 391F, respectively. The Test A fluid temperature profile correlated well with these saturation temperatures, confirming that the previously discussed intermittent auxiliary feedwater actuations were caused by flow up the hot leg during the initial portion of the repressurization. Test B shows a similar decreasing fluid temperature; however, the fluid temperatures were subcooled by approximately 10F. A portion of this temperature difference can be attributed to the slightly greater amount of low-pressure injection during Test B. (This is the previously discussed second low-pressure injection actuation. This caused an approximately 6F lower core outlet and hot leg inlet temperature than those observed during Test A.) The remaining fluid temperature difference (approximately 4F) can be attributed to heat loss. This is implied by the relationship of the metal and fluid temperatures in the liquid-filled region of the hot leg: Test A, with guard heaters, had metal temperatures approximately 2F less than the fluid temperatures. These differences in the hot leg liquid temperatures were relatively small, indicating that the heat loss in the liquid-filled portion of the hot leg for the test without guard heaters (Test B) was insignificant.

The steam-filled portion of the hot leg continued to display significant metal and fluid temperature differences between these tests. In both tests, the metal temperatures were generally higher than the fluid temperatures, indicating heat transfer from the pipe to the fluid. Test A, with guard heaters, had maintained the previously established high metal temperatures in the upper portion of the hot leg, see Figures 10.16 and 10.24. The fluid temperatures at traversed lengths of 60 (HLTC07) and 75 feet (HLTC09) have approached the pipe metal temperature, indicating that a stagnant condition existed in this portion of the hot leg. The temperature at 67.5 feet (at the U-bend) did not respond in a similar manner. This different response may have been entirely due to the susceptibility of this thermocouple, HLTC08, to local heat losses (this thermocouple was located near the U-bend viewport, which was a region of high local heat loss).

A comparison of the hot leg fluid temperatures in the steam-filled portion of the hot leg continued to show a significantly higher degree of superheat for the test with guard heaters. The greatest amount of superheat (150F in

Test A and 27F in Test B) at this time occurred in the stub portion of the hot leg rather than at the steam generator inlet. This was a result of the steam generator primary level increasing and thereby exposing the steam generator inlet resistance temperature detector to colder fluid.

In summary, during this portion of the transient, the guard heaters affected only the local conditions in the hot leg and had no impact on the overall transient response of the primary system.

10.4.4 Refill: Repressurization Phase of the Transient, 235 to 258 Minutes

As the refill process continued during the repressurization phase of the transient, the core outlet temperature and, subsequently, the hot leg inlet temperature, increased as a result of the rise in saturation temperature. At approximately 235 minutes, the primary system responses for these two tests began to differ. Figures 10.22 and 10.23 show that the repressurization rate for Test A (with guard heaters) began to increase, while it remained virtually constant in Test B. The maximum reactor vessel pressure attained in Test A was approximately 361 psia, at 258 minutes. The maximum reactor vessel pressure attained in Test B was approximately 293 psia, at 248 minutes.

During this phase of the repressurization, the core outlet temperature and the hot leg inlet temperature increased as they followed saturation. The liquid in the hot leg, having been near the saturation temperature before the repressurization (it had become saturated at a lower pressure), and being nearly stagnant, now became subcooled for both tests. The free convection mixing process within the hot leg appears ineffective in heating the liquid in the higher elevations of the hot leg. Therefore, a relatively slow heating process occurred.

Figure 10.25 shows hot leg metal and fluid temperatures versus the traversed length of the hot leg at approximately 251 minutes (near the time when the maximum pressure occurred). Comparing the liquid region temperatures at 251 minutes with those at 230 minutes (Figure 10.24), the hot leg metal and fluid temperatures have remained almost constant. The exception to this was the temperature near the inlet to the hot leg that reflected the increasing saturation temperature due to the repressurization of the primary system. The temperatures in the steam-filled portion of the hot leg again showed

significant differences between the tests with (A) and without (B) guard heaters. Test A continued to maintain high metal temperatures and corresponding high fluid temperatures in the upper portions of the hot leg. These temperatures remained relatively constant for the duration of this test. The degree of superheat in the steam-filled portion of the hot leg remained high, but decreased because of the increase in the saturation temperature. The metal temperatures remained higher than the fluid temperatures, indicating heat transfer from the pipe to the fluid.

In Test B, the fluid temperature in the steam-filled portion of the hot leg was almost saturated (approximately 407F based on the steam generator primary pressure). The relationship between the metal and fluid temperature was not as well-defined as earlier in the transient, i.e., certain portions of the hot leg pipe appeared colder than the fluid, while others appeared hotter, cf. Figure 10.25 at 57 and 77 feet. The fluid thermocouple at the 50-foot elevation had failed for these tests, therefore the interpretation of the fluid temperature profile between the 40- and 60-foot elevations is imprecise when the HL level resided within this range. The steam generator inlet fluid was subcooled in Test B indicating that the steam generator primary level was above this elevation (this is confirmed by the divergence of HLLV21 and SPLV20 at approximately 248 minutes, Figure 10.21).

The termination of the repressurization phase in Test A occurred when the leak flow rate increased to that of the high-pressure injection flow, Figure 10.18 and an equilibrium pressure was attained. An equilibrium pressure was not attained in Test B. This test (B) reached a maximum pressure at approximately 248 minutes, and then began a very gradual depressurization while maintaining high-pressure flow greater than the leak flow, cf. Figure 10.19. As discussed previously, the steam-filled portion of the hot leg had saturated by this time. The reactor vessel head also approached saturation at this time. The portion of the high-pressure injection flow that was directed towards the downcomer was apparently sufficient to quench the steam supplied to the downcomer by the open reactor vessel vent valve, and to subcool the fluid. Therefore there was excess high-pressure injection cooling in Test B, which resulted in a depressurization of the primary system.

10.4.5 Continued Refill Prior to Opening the Hot Leg High Point Vent, 258 to 300 Minutes

The conditions in Test A (with guard heaters) remained near equilibrium during this time (258 to 300 minutes). The injection flow was approximately equal to the leak flow (Figure 10.7), the reactor vessel pressure remained approximately constant (Figure 10.1), and the refill rate was nearly zero.

In Test B (without guard heaters) the primary continued to depressurize gradually as a result of the previously discussed high-pressure injection cooling, reaching approximately 280 psia by 276 minutes (Figure 10.26). The HPI flow continued to exceed the leak flow (Figure 10.27) and the refill process continued at approximately 0.3 ft/min (Figure 10.28).

Subsequent to attaining the maximum repressurization, the primary pressure in both tests exhibited periodic oscillations of ±2.5 psi. Figure 10.26 shows these pressure oscillations for Test B. Two candidate explanations exist for these pressure oscillations: (1) the covering-uncovering of the hot leg nozzle as discussed in the description of the Nominal Test and (2) the characteristics of the OTIS high-pressure injection system. This system consisted of a variable-speed positive displacement pump (three pistons), bypass line with a control valve, and an accumulator. The interaction of these components and the high-pressure injection system controller may have caused the observed high-pressure injection flow variations (of approximately ±3%, Figure 10.27). These flow variations may in turn have caused primary system level and pressure oscillations. Although the magnitude of these pressure oscillations was small, they were large enough to have affected the reactor vessel vent valve operation and may have caused the observed cyclical behavior of the reactor vessel vent valve when the controller was in automatic.

At approximately 277 minutes, a weak spillover was observed in Test B, as evidenced by the increasing steam generator inlet temperature (appended Plot 131). At approximately 277 minutes, the loop operator transferred the reactor vessel vent valve control from manual open to automatic (as specified by the Test Procedure). The reactor vessel vent valve closed due to the low differential pressure across the valve. Prior to the reactor vessel vent valve closing, the hot leg level was near the U-bend. When the

reactor vessel vent valve closed, the inner loop flow path (core-RVVV-downcomer) was removed. More steam then entered the hot leg, causing its level to swell and resulting in a spillover at the hot leg U-bend. The spillover is verified by the decrease in the primary system pressure (approximately 20 psi), the increase in the steam pressure (approximately 40 psi), the hot leg temperature response, the increase in the steam generator inlet and outlet temperatures, the increase in the steam generator on-nozzle fluid temperatures, and the decrease in the downcomer fluid temperatures. The sudden increase in primary loop flow, combined with the decreased downcomer and reactor vessel inlet fluid temperature, subcooled the reactor vessel outlet fluid. These subcooled reactor vessel outlet fluid conditions propagated into the lower regions of the hot leg, which altered the manometric balance and caused a flow interruption. This flow interruption resulted in an increasing core outlet temperature, which returned to saturation at approximately 281 minutes (a corresponding pressure increase also occurred). The core region began to void, resulting in a sufficient differential pressure across the reactor vessel vent valve to cause it to momentarily open fully. Subcooled liquid, apparently residing in the upper plenum region, was discharged into the downcomer. This event was confirmed by the indicated wetting of those conductivity probes located near the vent valve line. A momentary increase in the downcomer flow also occurred. The conductivity probes near the vent valve line quickly returned to an unwetted condition and the temperatures upstream and downstream of the vent valve returned to saturation. This indicates that the reactor vessel vent valve position was oscillating between closed and partially open.

A weak coupling of the primary and secondary system occurred between 277 and 279 minutes. Secondary steam flow was indicated; however, very little or no auxiliary feedwater flow was observed. At approximately 279 minutes, the steam generator secondary level had dropped to approximately 37 feet and auxiliary feedwater actuated. Loop flow had subsided by this time and the auxiliary feedwater actuation did not sustain loop flow. The only discernible impact was to subcool the primary fluid in the on-nozzle tube (i.e., the steam generator tube wetted by auxiliary feedwater).

Between approximately 281 and 300 minutes, intermittent primary loop flow was established (indicated by numerous spillovers resulting in primary-to-secondary recoupling). The occurrence at approximately 289 minutes resulted in increased primary loop flow and a subsequent subcooling of the reactor vessel outlet temperature. The primary loop flow interrupted again and the reactor outlet temperature increased toward saturation.

Figure 10.29 shows the hot leg metal and fluid temperature versus the traversed hot leg length at approximately 287 minutes for both tests. The upper hot leg fluid remained highly superheated in Test A, with guard heaters. The steam generator inlet temperature subcooled indicating that the collapsed liquid level was within the stub portion of the hot leg (the steam generator collapsed liquid level was approximately 53 feet). In Test B, without guard heaters, the fluid in the upper regions of the hot leg was saturated and the metal and fluid temperatures were nearly equal. The refill spillover process observed in Test B (and discussed previously) had quenched the metal in the upper regions of the hot leg and the hot leg refill rate increased. The steam generator collapsed liquid level was approximately 61 feet.

The primary and secondary remained uncoupled until approximately 304 minutes in Test A, at which time the hot leg vent was opened. In Test B, the systems remained coupled with intermittent flow and spillovers until approximately 301 minutes, at which time the hot leg vent was opened.

10.4.6 Refill After Opening the Hot Leg High Point Vent, 300 Minutes to the End of Each Test

At approximately 300 minutes, the hot leg vent was opened in both tests. In Test A (with guard heaters) the reactor vesssel pressure decreased from approximately 369 to 324 psia during the 19 minutes following the opening of the hot leg vent (Figure 10.1). The hot leg vent was discharging superheated steam, and no primary-to-secondary coupling was observed. The interactions in Test B (without guard heaters) showed almost no effect when the hot leg vent was opened (Figure 10.2). The primary and secondary systems remained weakly coupled, and spillovers and intermittent flow continued.

At this time the refill process was nearly completed in Test B. Therefore, the remaining phenomena occurring during this transient are discussed in the following paragraphs, before resuming the discussion of Test A.

Completion of Test B

The previously-established high-pressure injection cooling mode continued in Test B. At approximately 301 minutes, the core outlet fluid subcooled, and remained subcooled for the remainder of the transient. The sustained subcooling of the reactor vessel outlet was a result of the spillovers. Additional high-pressure injection fluid was directed towards the reactor vessel, thereby decreasing the reactor vessel inlet temperature. The combination of the increased flow and the decreased inlet temperature subcooled the core outlet fluid temperature.

At approximately 306 minutes, a major continuous spillover occurred. This was indicated by the rapid decrease in the reactor vessel pressure (Figure 10.30), the cold leg temperature response (Figure 10.31), the increase in primary loop flow (Figure 10.32), and the closure of the reactor vessel vent valve as evidenced by the temperature difference across the vent valve (Figure 10.33). At approximately 309 minutes the reactor vessel pressure had decreased to 220 psia, thus causing the actuation of low-pressure injection (Figure 10.34). The low-pressure injection flow immediately caused an increase in the reactor vessel level, and the hot leg vent flow rate indicated liquid flow. The primary loop refilled and natural circulation flow was established. The increasing reactor vessel level compressed the steam in the reactor vessel head, resulting in a repressurization of the primary system and subsequent termination of low-pressure injection, at approximately 312 minutes. The reactor vessel head at this time contained the only voided volume in the primary system; thus, it governed the primary system pressure response (neglecting loop operator actions), i.e., the primary system pressure followed the saturation pressure established by conditions in the reactor vessel head. At approximately 318 minutes, after having met the specified requirements (refill complete and natural circulation flow established), the loop operator throttled high-pressure injection flow in an attempt to maintain the specified 5OF subcooling in the hot leg. The high-pressure injection

flow was throttled to approximately half its capacity, obtaining a leak flow rate in excess of the high-pressure injection flow rate (Figure 10.34); the primary system depressurized to approximately 162 psia at 328 minutes (Figure 10.30). The high-pressure injection flow was then increased. The primary system repressurized to 192 psia and further injection flowrate adjustments resulted in a gradual depressurization until test termination at 370 minutes, after approximately one hour of natural circulation cooldown. At test termination, the primary system pressure was 180 psia; the primary system with the exception of the reactor vessel head was liquid full; all primary fluid temperatures were stable and subcooled, except for the reactor vessel head which remained saturated; and stable natural circulation flow rate of approximately 2.5% of full flow was established.

Completion of Test A

In Test A (with guard heaters), the reactor vessel pressure stabilized at approximately 322 psia until 336 minutes; then it began a gradual rise to 328 psia at 352 minutes (Figure 10.35). A more rapid increase in reactor vessel pressure followed. The total increase in pressure was approximately 42 psia. However, two distinct increases, each reaching a plateau, can be observed. The first occurred at approximately 353 minutes and reached 344 psia. The second occurred at approximately 360 minutes and reached 370 psia (see Figure 10.35). The number of fluid and metal thermocouples in the U-bend region was too sparse to firmly identify the phenomena; however, the following discussion is a possible explanation for the observed pressure increases. From 327 to 334 minutes, the level in the hot leg stub increased sufficiently to quench the hot leg pipe (HLTC17, Figure 10.36) in the region of the "zone 8" guard heater control thermocouples. The zone 8 guard heater, which extended from the top of the steam generator upward 8.25 feet into the stub, had its control thermocouples located at the same elevation as HLTC17. The pipe metal temperature, HLTC17, decreased from approximately 560 to 422F (saturation) during this period and de-energized the zone 8 guard heater (as indicated by the decrease in HLDT08, Figure 10.37). At 334 minutes, the hot leg stub fluid temperature contained within guard heater zone 8 (HLTC09, Figure 10.38) began to decrease (as a result of the decreased guard heater power) after being essentially constant at 555F. At 350 minutes, the stub fluid temperature (HLTC09) had decreased approximately

15F (to 540F). The hot leg U-bend fluid temperature (HLTC08, Figure 10.39) decreased approximately 12F, from 481 to 469F. This thermocouple (HLTC08) was located within guard heater zone 7 (which covered the upper 5 feet of the hot leg, the U-bend, and the upper 6 feet of the stub). Therefore, the reduced zone 8 guard heater power caused a decrease in the fluid temperature at the U-bend. The hot leg metal temperature (HLTC11, Figure 10.36), located within heater zone 7, remained almost constant during this time. The fluid temperature at the U-bend, as previously mentioned, may have been affected by heat loss in this region, and may not have been representative of the actual fluid temperature in the U-bend and in the upper portion of the stub.

The location of the metal thermocouple within guard heater zone 7 was approximately 1.4 feet upstream of the U-bend and was influenced by the fluid in the hot leg. This fluid, which was approximately 2 feet below the beginning of guard heater zone 7, was approximately 20F subcooled (HLTC07, Figure 10.39); the fluid in the lower portion of the stub was approximately 100F subcooled. This indicates that if steam generated in the core region was entering the hot leg, it was condensed before it reached the hot leg U-bend. Therefore, the steam which was being discharged through the hot leg vent was that which was contained or generated in the U-bend region piping. The heat source for this steam production was the guard heater and the energy stored in the metal mass of the pipe. An estimate was made to determine if the zone 7 guard heater could have generated the volume of steam being discharged through the hot leg vent. Using the observed fluid conditions in the U-bend region at approximately 344 minutes and the HEM (Homogeneous Equilibrium Model) critical flow correlation, it was determined that approximately 60% of the zone 7 guard heater power would have been sufficient to generate the observed fluid conditions and steam flow rate. No stored heat from the metal mass was considered because no change in the metal temperature was observed at this time.

At approximately 353 minutes, the hot leg metal temperature 1.4 feet upstream of the U-bend (HLTC11, Figure 10.40) decreased rapidly. This occurrence corresponded to the initial observed pressure increase at 353 minutes. This pressure rise was attributed to the quenching of the pipe metal and the resulting flashing of liquid in the hot leg and the stub. The

pressure rise appeared to cause level fluctuations in the primary system that resulted in alternating increased and decreased wetting at certain elevations in the hot leg U-bend region, cf. the hot leg conductivity probes, Figure 10.41; the stub fluid temperature response, HLTC09, Figure 10.42; and HLTC08, Figure 10.43. At approximately 353 minutes, the zone 7 guard heater control temperature difference increased (HLDT07, Figure 10.44). (The pipe metal temperature used for the guard heater temperature difference was obtained from a thermocouple which was at the same elevation but across the pipe from HLTC11.) This increase in the control temperature difference, caused by either an increase in the pipe metal temperature (however, HLTC11 indicated a decreasing metal temperature, cf. Figure 10.40) or a decrease in the insulation temperature, resulted in an increase in the zone 7 guard heater power. Therefore, local flow phenomena may have been affecting the temperature distribution within the hot leg and causing the guard heater to activate, when the available indication from HLTC11 would imply that a decrease in guard heater power was required. This increase in guard heater power would have augmented the repressurization process.

At approximately 359 minutes another rapid hot leg metal temperature decrease was observed (cf. HLTC11, Figure 10.40). Phenomena similar to those which occurred at 353 minutes were also observed at this time. At approximately 371 minutes, a spillover occurred as indicated by the hot leg levels (cf. Figure 10.45). This spillover was confirmed by a decrease in primary pressure, by an increase in secondary pressure (primary-to-secondary coupling), and by the primary fluid temperature responses. The coupling of the primary and secondary systems apparently resulted in an increased demand for auxiliary feedwater even though the steam generator secondary level was relatively constant during this time (Figure 10.46). At approximately 372 minutes, a rapid increase of 2 feet in the steam generator secondary level was observed. The loop operator noted this increased steam generator secondary level and manually terminated auxiliary feedwater flow at approximately 374 minutes. The spillover at 371 minutes resulted in a brief period of forward loop flow which quenched the metal in the U-bend (Figure 10.40) and rapidly cooled the downcomer and reactor vessel inlet fluid temperatures (Figures 10.47 and 10.48). The reactor vessel outlet temperature subcooled at approximately 372.5 minutes. Downcomer flow was interrupted and the core outlet temperature increased (Figure 10.48). The

increasing core temperature caused swelling of the liquid in the reactor vessel; the level increased sufficiently to subcool the reactor vessel vent valve elevation (RVTC09, Figure 10.48), resulting in the discharge of subcooled fluid through the reactor vessel vent valve and into the downcomer. The hotter fluid discharged through the reactor vessel vent valve increased the downcomer fluid temperatures (Figure 10.47). The core outlet fluid saturated momentarily and then subcooled again as downcomer flow was established. The reactor vessel level continued to remain near the vent valve elevation, hot liquid continued to be discharged through the reactor vessel vent valve, and the reactor vessel inlet temperature continued to increase. At approximately 387 minutes, the reactor vessel inlet temperature had increased sufficiently such that, in combination with the core power level and flow rate, the core outlet and the reactor vessel vent valve fluid saturated, cf. Figure 10.48. During this entire period (after the spillover until the reactor vessel vent valve fluid reached saturation), the primary system (with the exception of the reactor vessel and the downcomer) was cooling, thus a gradual decrease in primary pressure was observed (Figure 10.35). When the core outlet and the reactor vessel vent valve fluid saturated, the primary system pressure increased rapidly (Figure 10.35), the reactor vessel level decreased, the hot leg level increased (Figure 10.45), and a relatively high inner-loop (downcomer) flow was established (Figure 10.49). The reactor vessel vent valve control had been placed in the manual-open position at approximately 143 minutes but had not been placed into the automatic control mode through this time in the transient. The potential effect of cyclical closures of the reactor vessel vent valve on the refill process have, therefore, been disallowed.

Leak-HPI (High-Pressure Injection) Equilibrium

Subsequent to this pressure increase, the primary system again attained a leak-HPI equilibrium condition. Between approximately 400 and 470 minutes, nine distinct spillovers were observed (primary-to-secondary coupling, indicated by the pressure responses shown on Figure 10.50). The spillovers resulted in a decrease in the reactor vessel inlet temperature, which was followed by an increase in its temperature (Figure 10.51) when the primary loop flow was interrupted. During the first three spillovers, the core outlet and the reactor vessel vent valve fluid temperatures remained

saturated. The fourth through the ninth spillovers resulted in an alternating subcooled and saturated core outlet fluid temperature (as primary system flow was alternately established and interrupted). During this time the reactor vessel inlet temperature, which oscillated in a similar manner with the flow, was generally decreasing from 420 to 250F. During these spillovers, the reactor vessel level was generally increasing. At approximately 475 minutes, the core outlet subcooled, the downcomer flow decreased, and the downcomer and reactor vessel inlet fluid temperatures increased. At approximately 476 minutes, the reactor vessel vent valve fluid subcooled, the reactor vessel level reached the vent valve elevation (Figure 10.52), and liquid was discharged through the vent valve. The downcomer and reactor vessel inlet fluid temperatures continued to increase but at a slower rate after liquid was being discharged through the vent valve. At approximately 484 minutes, the core outlet temperature began to increase. At approximately 486 minutes, the operator initiated the specified core power reduction to attain sustaining power. The core inlet and outlet temperatures continued to increase. The core outlet and the reactor vessel vent valve region fluid eventually saturated and voided, resulting in a primary pressure increase at approximately 499 minutes (Figure 10.50). The hot leg level increased, precipitating a spillover. The core outlet fluid subcooled and the reactor vessel level decreased, thus permitting the reactor vessel vent valve to momentarily discharge steam into the downcomer. The reactor vessel level then increased and subcooled liquid discharge was indicated at the reactor vessel vent valve. The reactor vessel inlet temperature increased. However, due to the reduced core power level, the core outlet fluid temperature decreased and remained subcooled for the remainder of the test. The hot leg and steam generator primary levels continued to increase at a gradual rate during this period (Figure 10.53). From 523 to 549 minutes relatively frequent spillovers were observed (Figure 10.50). The hot leg fluid temperatures decreased rapidly during this time. At approximately 551 minutes, the hot leg and steam generator primary levels became equal (Figure 10.53), signifying that a continuous spillover was occurring and that refill was nearly complete. At approximately 554 minutes, the reactor vessel vent valve control was placed in automatic and the vent valve closed immediately. The reactor vessel pressure had decreased to approximately 280 psia; subsequent to the closure of the reactor vessel vent valve, the downcomer flow decreased substantially. The

decreased downcomer flow increased the core outlet temperature, which apparently caused a swelling of the fluid in the reactor vessel (as indicated by the increase of approximately one foot in the reactor vessel level, cf. Figure 10.52) and an increase in the fluid temperature at the hot leg inlet (indicated by the increase in HLRT01, Figure 10.39). At approximately 557 minutes, the hot leg vent indicated liquid discharge (Figure 10.54). The reactor vessel pressure increased slightly to 290 psia following the discharge of liquid through the hot leg vent. The conditions at 569 minutes were: The hot leg U-bend, the hot leg stub, and the steam generator inlet fluid were saturated; the reactor vessel upper head fluid temperature was approximately 10OF superheated; and the remaining loop fluid temperatures were subcooled. (The reactor vessel head was also guard heated; the upper portion of the head, which contained steam, indicated an almost constant metal temperature of approximately 622F.)

Test A was terminated at 615 minutes, before establishing natural circulation. The primary loop was approaching natural circulation near the end of the test. This was evidenced by the intermittent opening and closing of the reactor vessel vent valve, the increasing core inlet and outlet fluid temperatures, and the increasing hot leg fluid temperatures. All of these observations indicated a lowering of the hot leg thermal center, which eventually would have obtained natural circulation.

10.5 Results

Tests 2202AA and 2202BB were additions to the original test matrix. These tests were conducted to provide insight into the effects of guard heating on the progression of the OTIS SBLOCA transient response. Certain guard heater effects were discernible from these tests. The major impact of guard heating occurred after the loss of BCM heat transfer, i.e., during the repressurization phase and in the later portion of the refill phase.

Tests 2202AA ("A", with guard heaters) and 2202BB ("B", without guard heaters) were based on OTIS Test 220201, increased leak size (see section 6.2 herein). A comparison of some key events of each of these transients is presented in Table 10.9. These events and their differences are described below.

All three tests exhibited a strong similarity during the major portion of the depressurization phase of the transient. The primary system pressure responses were virtually identical for all three tests until the repressurization phase of the transient. The depressurization phase ended slightly earlier in Test 220201 ("1") (∿6 min), and resulted in a slightly higher minimum pressure than in Tests A and B. This difference was due to the differences in the high-pressure injection flow rates. As discussed previously, the turbine meter used to control the high-pressure injection flow rate was degraded during Test 220201. The degraded turbine meter was replaced after Test 220201 and before Tests A and B. This turbine meter caused the addition of more high-pressure injection fluid during the initial approximately 100 minutes of Test 220201. The higher high-pressure injection flow rate obtained a higher minimum hot leg level and a higher minimum primary system pressure during the depressurization phase of Test 220201 (see Table 10.9).

The high-pressure injection flow rate difference partially accounts for the earlier (25 to 29 minutes) initiation of refill and for the lack of low-pressure injection actuation in Test 220201. In Test A, the low-pressure injection actuation apparently added a sufficient amount of liquid to the system to counteract the difference in the high-pressure injection flow rates. This is evidenced by the similarity in the time when the steam generator inlet fluid saturated and subcooled the first time (261 minutes in Test 220201 and 273 minutes in Test A). The maximum fluid temperatures (542F in Test 220201 and 549F in Test A) and maximum pipe metal temperatures (554F in Test 220201 and 559F in Test A) in the stub region were nearly identical. The maximum pressure attained (397 psia in Test 220201 and 361 psia in Test A), the time when it occurred (254 minutes in Test 220201 and 258 minutes in Test A), and the occurrence of the first hot leg spillover (356 minutes in Test 220201 and 372 minutes in Test A) all confirm the HPI/LPI difference and indicate the similarity between these two tests. The impact of the pressurizer on these test results appears negligible. Test A had the pressurizer isolated early in the transient, after it had drained from approximately 20 to 10 feet (relative to the SG lower tubesheet upper face). The pressurizer was not isolated in Test 220201. This allowed the complete draining of the pressurizer (from an initial level approximately 17 feet above the SGLTSUF). The more complete draining of the pressurizer

partially accounts for the earlier initiation of refill. The pressurizer remained empty during the long-term depressurization phase of Test 220201. As the primary system repressurized, the pressurizer level increased to approximately 9 feet and remained roughly constant for the duration of the refill phase of the test. Therefore, because of the rather subdued pressurizer response in Test 220201, Tests A and B do not unequivocally establish the impact of the pressurizer (guard heating) on the transient response of the system.

Test B (without guard heaters) showed significant differences from the other tests subsequent to the low-pressure injection actuation. The steam generator inlet fluid first saturated and subcooled approximately 27 and 39 minutes earlier in Test B, compared to Tests 220201 and A (Table 10.9). As discussed previously, the low-pressure injection actuations did not cause primary system liquid mass inventory differences between Tests A and B. Therefore, the difference in time when the liquid level entered the stub region between these two tests is attributable to the slightly higher high-pressure injection rate due to the lower repressurization rate in Test B. The lower repressurization rate and resulting greater refill rate of Test B was therefore a direct result of the interactions occurring in the voided regions of the hot leg. The higher hot leg pipe metal temperatures for Tests 220201 and A appear to have impeded the refill process in these tests. Referring to Table 10.9, in Test B the maximum pressure attained during the repressurization phase was approximately 68 to 104 psi lower than that in the tests with guard heaters; the hot leg stub region began refilling before the maximum pressure occurred, whereas both tests with guard heaters showed the opposite; the first hot leg spillover occurred 79 to 95 minutes earlier than in the tests with guard heaters; the maximum pipe metal temperature in the stub, when the maximum pressure was attained, was 138 to 143F lower than in the tests with guard heaters; the maximum fluid temperature in the stub when the maximum pressure was attained was 131 to 138F lower than the tests with guard heaters; the fluid temperatures in the voided region of the hot leg, when the maximum pressure was attained, were saturated whereas the guard heater tests indicated significant superheat.

Reactor Vessel Vent Valve (RVVV) Control

A major difference in the conduct of these tests and its impact on the remaining transient is apparent in Table 10.9. This table shows that in the test without guard heaters (B), the RVVV control was transferred from manual-open to automatic (0.25 psi to open, 0.125 psi to close) at approximately 277 minutes after the leak was opened. This was approximately the same time as the first hot leg spillover. Several rapidly occurring spillovers were observed and, approximately 30 minutes later, loop refill was completed and sustained natural circulation was established. For both tests with guard heaters, the reactor vessel vent valve control was not transferred from manual-open to automatic when the first hot leg spillover was observed, but rather approximately 105 minutes (Test 220201) and 182 minutes (Test A) after the first observed hot leg spillover. During this time, numerous hot leg spillovers occurred; the hot leg U-bend fluid temperature indicated saturated conditions at or shortly after the first observed spillover. The hot leg metal temperature near the U-bend also indicated that the pipe metal had been quenched. Thus, the pipe metal was no longer a heat source and should no longer have impeded refill. When the reactor vessel vent valve control was switched to automatic in Test 220201 (whereupon the vent valve closed), the hot leg and stub levels were indicating liquid full, and natural circulation began. When the reactor vessel vent valve control was switched to automatic in Test A and the vent valve closed, the hot leg and stub levels indicated full approximately two minutes later. However, sustained natural circulation was not established before the test was terminated (this may have been due to the reduction of core power to the sustaining level during this time interval, which reduced the driving head for natural circulation). The similarity between Tests 220201 and A through the initial refill spillover (as previously discussed) suggests that refill and the initiation of natural circulation should also have been similar. The dissimilarity in the time required to refill and to initiate natural circulation between these two tests, therefore appears to be directly related to the time at which the reactor vessel vent valve control was placed in automatic.

When a spillover occurs, a relatively low pressure differential can exist across the vent valve. If the vent valve control is in the automatic position, it may close and terminate the inner loop flow. Valve closure increases flow up the hot leg. When the hot leg level is near the U-bend, this diversion of flow to the hot leg may be sufficient to maintain a continuous spillover, to complete the loop refill, and to initiate natural circulation. The time required to refill the primary loop for the guard heated tests must, therefore, be interpreted considering the control mode of the RVVV, i.e., the observed refill time is not entirely a result of the guard heaters*.

---

*Had the RVVV been placed into the automatic control mode for Tests 220201 and A in a manner similar to that done for Test B, i.e., approximately one minute after the first hot leg spillover was observed, the hot leg U-bend region is expected to have saturated and the piping to quench shortly thereafter. Once this occurred, the guard heater in the U-bend region would have de-energized, thus the time required to establish sustained natural circulation would have been similar to that observed in the test without guard heaters (Test B). Based upon this scenario, it is estimated that sustained natural circulation may have occurred approximately 29 minutes after the first hot leg spillover occurred, i.e., at 385 minutes (in Test 220201) and at 401 minutes (in Test A) after leak opening. Therefore, it can be concluded that the tests with guard heaters would have required only 79 minutes (Test 220201) and 95 minutes (Test A) longer to refill than in the test without guard heaters (Test B), rather than the observed times of 151 and 248 minutes. This supposition does not invalidate the observed guard heater effects, but rather indicates the contributing effects of RVVV operation.

Summary

The following specific conclusions were obtained from the comparisons of the tests with and without guard heating:

- The guard heaters did not affect the primary system pressure response during the depressurization phase of the transient. During this phase, the initially established guard heater control settings affected the local conditions (temperature) in the voided regions of the primary system. The metal mass of the OTIS test facility hot leg and stub and the associated stored energy were large enough to maintain superheated fluid conditions in the upper regions of the hot leg and at the steam generator inlet throughout the major portion of the depresurization phase and during a portion of the refill phase, with no guard heating (Test B).

- The tests with guard heating (Tests 220201 and A) had higher superheated fluid conditions throughout the major portion of the depressurization and refill phases of the transient than in the test without the guard heating. The tests with guard heating also had considerably higher HL hot leg and stub metal temperatures (which produced these highly superheated fluid conditions) than the test without guard heating.

- The local conditions which existed in the hot leg and the stub upon termination of the boiler-condenser mode (BCM) established the repressurization rate as well as the magnitude of the pressure attained during the repressurization phase of the transient. Higher hot leg and stub metal temperatures increased the time required to refill the primary system. The refill process required the quenching of the entire metal mass in the hot leg and the stub region. For Tests 220201 and A, the guard heaters attempted to maintain a nearly constant pipe metal temperature, which extended the quenching process and the time required to refill compared to the test without guard heating. The quenching of the metal mass encompassed by a guard heater zone was accelerated when the elevation of the guard heater control thermocouples was quenched, thereby decreasing the heat input from that particular guard heater zone. The quenching of the metal mass in the hot leg and stub provided an additional source of steam production. The temperature and stored energy of this metal mass established the amount of steam produced. During

the final phase of the refill process (when the steam generator primary level was above the steam generator upper tubesheet elevation), the steam produced by the metal mass in the upper regions of the hot leg and the hot leg vent capacity affected the repressurization and the refill of the primary loop. This quenching process may have caused primary system pressure increases, pressure oscillations, and hot leg and steam generator primary level oscillations.

- The method of reactor vessel vent valve control during refill, in particular during the later portion (subsequent to the termination of the boiler-condenser mode), had a significant impact on the time required to refill and initiate natural circulation.

These tests have indicated that the time required to refill the primary system is dependent upon the use of guard heaters, the metal mass of the piping from the hot leg inlet to the steam generator inlet, and the method used to control the reactor vessel vent valve.

Table 10.1. Initial Conditions Test 2202AA, Pressurizer Isolated

	Specified	Actual
Core power (includes sustaining power of 0.51%), % of full power	4.21±0.1	4.17
Natural circulation flow rate, % of full flow	Yes	Yes (5.5%)
Primary pressure, psia	2200±50	2207
Pzr liquid height, ft from SGLTSUF	16.6±2	20.3
Pzr main and guard heaters adjusted for an approximately adiabatic Pzr	Yes	Yes
Reactor vessel and hot leg vents closed	Yes	Yes
RVVV in automatic (differential-pressure) control with open/close setpoints of 0.25 and 0.125 psi	Yes	Yes
AFW at 100F injected at the upper elevation using the minium-wetting nozzle	Yes	Yes (113F)
SG secondary (collapsed) liquid level with constant level control, ft	5±1	5.7
Primary HL fluid temperature, F (use the model HL fluid temperature indication at 60 ft HLTC07.)	610±2	609.2
Primary CL fluid temperature, F (from the model CL fluid temperature indication at the CL discharge CLTC05.)	NA	571.2
HPI and leak systems not yet in use	Yes	Yes
Initialization is continued until a suitable system steady state is obtained:		
Pzr metal temperatures, F	650±10	651-672
The RVVV is not cycling	Yes	Yes
The SG fluid temperature are varying less than 10F/h (exception: cyclic secondary fluid temperature variations associated with high-elevation AFW injection, and with internal circulation within the secondary liquid pool, are acceptable).	Yes	Yes
Steam flow rate, % of full flow	NA	2.3
Steam pressure, psia (adjusted to obtain specificed HL temperature)	∿ 1000	1202

Table 10.2. Initial Conditions Test 2202BB, Without Guard Heating.

	Specified	Actual
Core power (includes sustaining power of 0.51%), % of full power	4.21±0.1	4.16
Natural circulation flow rate, % of full flow	Yes	Yes (5.5%)
Primary pressure, psia	2200±50	2200
Pzr liquid height, ft from SGLTSUF	16.6±2	18.7
Pzr main and guard heaters adjusted for an approximately adiabatic Pzr	Yes	Yes
RVUHV and HLHPV closed	Yes	Yes
RVVV in automatic (differential-pressure) control with open/close setpoints of 0.25 and 0.125 psi	Yes	Yes
AFW at 100F injected at the upper elevation using the minium-wetting nozzle	Yes	Yes (115F)
SG secondary (collapsed) liquid level with constant inventory or level control, ft	5±1	5.7
Primary HL fluid temperature, F (from the model HL fluid temperature indication at 60 ft HLTC07.)	610±2	609.0
Primary CL fluid temperature, F (Use the model CL fluid temperature indication at the CL discharge CLTC05.)	NA	571.0
HPI and leak systems are not yet in use	Yes	Yes
Initialization is continued until a suitable system steady state is obtained:		
Pzr metal temperatures, F	650±10	649-653
The RVVV is not cycling	Yes	Yes
The SG fluid temperature are varying less than 10F/h (exception: cyclic secondary fluid temperature variations associated with high-elevation AFW injection, and with internal circulation within the secondary liquid pool, are acceptable).	Yes	Yes
Steam flow rate, % of full flow	NA	2.3
Steam pressure, psia (adjusted to obtain specified HL fluid temperature)	~1000	1201

Table 10.3. Selected Operator Actions and Observations Observations For Test 2202AA, Pressurizer Isolated

Clock Time	Elapsed Time, min.	Action/observation
April 19, 1984		
0755	-11	Data acquisition system started.
0806	0	15cm^2-CLS leak opened.
0808	2	Pzr isolated, HPI actuated.
0809	3	Core power ramp and AFW actuated.
0819	13	SG secondary depressurization ramp actuated, AFW control then placed into automatic level control.
1018	132	RVVV control changed from automatic to manual-open.
1125	199	Safety injection is controlling on the LPI head-flow curve.
1239	273	AFW control valve manually closed.
1253	287	AFW control valve placed in automatic operation to control at 38 ft.
1309	303	HLHPV opened.
1321	315	AFW control valve manually closed.
1354	348	AFW control valve placed in automatic operation to control at 38 ft.
1419	373	Spillover at HLUB, steam valve choked.
1420	374	AFW control valve manually closed.
1444	398	AFW control valve placed in automatic operation to control at 38 ft.
1448	402	Spillover at HLUB.
1450	404	AFW control valve manually closed.
1456	410	AFW control valve placed in automatic operation to control at 38 ft.
1505	419	Spillover at HLUB.
1513	427	Spillover at HLUB.
1517	431	AFW control valve manually closed.
1519	433	Spillover at HLUB.
1520	434	Steam valve choked.
1527	441	Steam valve choked.

Table 10.3. (Cont'd)

Clock Time	Elapsed Time, min.	Action/observation
1528	442	AFW control valve placed in automatic operation to control at 38 ft.
1534	448	Spillover at HLUB, steam valve chokes.
1541	455	Spillover at HLUB, steam valve chokes.
1556	470	Spillover at HLUB, steam valve chokes.
1613	487	Start core power ramp to achieve sustaining power (11 kW) in 30 minutes.
1628	502	Spillover at HLUB, steam valve chokes.
1645	519	Core power reduction to sustaining power (11 kW) completed.
1720	554	System refilling at HLUB viewport, RVVV control changed from manual-open to automatic control, RVVV closes.
1721	555	Loop refilled.
1724, 1738, 1742, 1749, 1755, 1801, and 1806	558 572 576 583 589 595 600	RVVV cycles (closed-open-closed) once at each indicated time.
1821	615	Test terminated.

Table 10.4. Selected Operator Actions and Observations for Test 2202BB, Without Guard Heating.

Clock Time	Elapsed Time, min.	Action/observation
April 18, 1984		
1232	-12	DAS activated.
1244	0	15-cm^2 CLS leak opened.
1245	1	Pzr isolated, all guard heaters turned off, HPI actuated.
1246	2	Core power ramp and AFW actuated.
1257	13	SG secondary depressurization ramp actuated, manually closed AFW control valve then placed into automatic level control.
1342	58	RVVV control changed from automatic to manual open.
1440	116	Hot leg level at 4 ft.
1600	196	LPI actuated.
1610 through 1636	206	Safety injection flow oscillating between the simulated HPI and LPI head-flow curves.
1636	232	RV pressure increasing approximately 260 psia, safety injection flow oscillations damping out, and flow following simulated HPI head-flow curve.
1721	277	Spillover at HLUB, RVVV control changed from manual-open to automatic control, steam valve choked.
1725	281	RVVV cycling, mostly in the closed position.
1728	284	Spillover at HLUB.
1730	286	Spillover at HLUB.
1732	288	RVVV cycling mostly in the closed position.
1733	289	Spillover at HLUB, RVVV closed.
1736	292	RVVV cycling.
1739	295	Spillover at HLUB.

Table 10.4. (Cont'd)

Clock Time	Elapsed Time, min.	Action/observation
1742	298	RVVV cycling.
1744	300	HLHPV opened.
1747	303	Slight spillover at HLUB.
1749	305	Steam valve opening.
1752	308	Spillover at HLUB, system refilled.
1758	314	Hot leg 30F subcooled (HLTC07).
1801	317	HPI on manual control to hold 50F subcooling in the HL.
1809	325	RVVV cycling.
1854	370	Test completed.

Table 10.5. Unavailable Measurements for Test 2202AA, Isolated Pzr.

SUMMARY OF VARIABLES DISCARDED ON INPUT, TEST 2202AA

NO.	VTAB	SYSTEM	INST.	ELEVATION	DESCRIPTION
1	155HLTC06	2HL	2FTC	50.00	HOT LEG FLUID TEMP (F)
2	262HLCPC5	2HL	16 CP	41.00	HOT LEG CONDCTVTY (WET/DRY)
3	263HLCPC6	2HL	16 CP	45.00	HOT LEG CONDCTVTY (WET/DRY)
4	264HLCPC7	2HL	16 CP	49.00	HOT LEG CONDCTVTY (WET/DRY)
5	265HLCPC8	2HL	16 CP	53.00	HOT LEG CONDCTVTY (WET/DRY)
6	266HLCPC9	2HL	16 CP	57.00	HOT LEG CONDCTVTY (WET/DRY)
7	274HLCP17	2HL	23RCP	.50	HOT LEG REF. C.P.
8	273HLCP16	3SGP	16 CP	53.10	SG PRIMRY. CONDCTVTY (WET/DRY)
9	272HLCP15	3SGP	16 CP	56.90	SG PRIMRY. CONDCTVTY (WET/DRY)
10	103PPDTC3	6PZR	10 DT	42.80	PRESURIZR. INSUL. LT (F)
11	223HPTPC2	10HPI	13TMF	-999.00	HP INJECT. TURB.FLOW (LBM/SEC)
12	221V2ACC2	12V2	19ACC	-999.00	2-PH VENT. ACCD.FLOW (LBM)
13	53SSTC13	22SGS	2FTC	32.30	SG SECOND.FLUID TEMP (F)
14	79SMTCC2	22SGS	25MTC	26.30	SG SECOND. METAL TC (F)
15	76SMTCC6	22SGS	25MTC	44.20	SG SECOND. METAL TC (F)
16	344V1TC03	34CLD	2FTC	-999.00	CLD LEAK FLUID TEMP (F)

Table 10.6. Unavailable Measurements for Test 2202BB, Without Guard Heating.

SUMMARY OF VARIABLES DISCARDED ON INPUT, TEST 2202BB

NO.	VTAB	SYSTEM	INST.	ELEVATION	D E S C R I P T I O N
1	155HLTC06	2HL	2FTC	50.00	HOT LEG FLUID TEMP (F)
2	262HLCP05	2HL	16 CP	41.00	HOT LEG CONDCTVTY (WET/DRY)
3	263HLCP06	2HL	16 CP	45.00	HOT LEG CONDCTVTY (WET/DRY)
4	264HLCP07	2HL	16 CP	49.00	HOT LEG CONDCTVTY (WET/DRY)
5	265HLCP08	2HL	16 CP	53.00	HOT LEG CONDCTVTY (WET/DRY)
6	266HLCP09	2HL	16 CP	57.00	HOT LEG CONDCTVTY (WET/DRY)
7	274HLCP17	2HL	23RCP	.50	HOT LEG REF. C.P.
8	273HLCP16	3SGP	16 CP	53.10	SG PRIMRY. CONDCTVTY (WET/DRY)
9	272HLCP15	3SGP	16 CP	56.90	SG PRIMRY. CONDCTVTY (WET/DRY)
10	103PRDT03	6PZR	10 DT	42.80	PRESURIZR. INSUL. DT (F)
11	223HPTM02	10HPI	13TMF	-999.00	HP INJECT. TURB.FLOW (LBM/SEC)
12	221V2AC02	12V2	19ACC	-999.00	2-PH VENT. ACCD.FLOW (LBM)
13	53SSTC13	22SGS	2FTC	32.30	SG SECOND.FLUID TEMP (F)
14	79SMTC02	22SGS	25MTC	26.30	SG SECOND. METAL TC (F)
15	76SMTC06	22SGS	25MTC	44.20	SG SECOND. METAL TC (F)
16	344V1TC03	34CLD	2FTC	-999.00	CLD LEAK FLUID TEMP (F)

Table 10.7. Key Events, Test 2202AA, Pressurizer Isolated

Event	DAS time, min.	Time after leak opened, min.
Leak opened	11.4	0.0
Pzr isolated	12.7	1.3
HPI, AFW, and core power ramp actuated	12.4-13.7	1.0-2.3
HLUB saturated (based on pressure stabilization	∿13	∿1.6
RVVV opened	13.7	2.3
Primary flow interruption	14.8	3.4
HLUB spillover	16.1	4.7
RVVV began cycling	16.3	4.9
SG secondary depressurization ramp initiated	24.0	13.0
SG primary level reached secondary side pool level	35.4	24.0
SG secondary level reached 38 ft	43.2	31.8
Refill began	134.	123.
RVVV switched from automatic to manual open (from operator's log)	143.	132.
LPI actuation	210.	199.
Primary loop repressurization began (BCM ended)	218.	206.
SG primary level exceeded secondary pool height	220.	209.
LPI termination	221.	211.
HLHPV opened	315.	304.
First refill spillover	383.	372.
Began core power reduction to sustaining power	498.	487.
Core power attained sustaining power level	532.	521.
RVVV switched from manual-open to automatic	565.	554.
Loop refilled	567.	556.
Natural circulation established	NA	NA
Test terminated	626.	615.

Table 10.8. Key Events, Test 2202BB, Without Guard Heating

Event	DAS time, min.	Time after leak opened, min.
Leak opened	12.0	0.0
Pzr isolated	13.3	1.3
HPI, AFW, and core power ramp actuated	14.2-14.4	∿2
Guard heaters de-energized	14.2-15.2	2-3
HLUB saturated (based on pressure stabilization)	∿13.7	∿1.7
RVVV opened	14.9	2.9
Primary flow interruption	15.4	3.4
RVVV began cycling	17.6	5.6
HLUB spillover	17.7	5.7
Began SG secondary depressurization ramp	25.0	13.0
SG secondary level reached 38 ft	30	18
SG primary level reached secondary side pool level	35	23
RVVV switched from automatic to manual open (from operator's log)	70.	58.
Refill began	141.	129.
LPI actuation/termination	212/223 224/238	200/211 212/226
Primary loop repressurization began (BCM ended)	219.	207.
SG primary level exceeded secondary pool height	220.	208.
First refill spillover, RVVV switched from manual open to automatic	289.	277.
HLHPV opened	313.	300.
Natural circulation established	319.	306.

Table 10.8. (Cont'd)

Event	DAS time, min.	Time after leak opened, min.
Loop refilled	321.	308.
LPI actuated/terminated	321/324	309/312
HPI throttled	330.	318.
Test terminated	382.	370.

Table 10.9. Comparison of Key Events

Event	OTIS test number		
	220201	2202AA	2202BB
Minimum RV pressure attained during the depressurization phase, psia	252	218	218
Time when minimum pressure attained, min.	200	206	207
Minimum HL level attained during the draindown phase, ft	14.9	3.8	3.6
Time when minimum HL level attained, min.	93	118	122
LPI actuation	NO	YES	YES
Maximum pressure attained during the repressurization phase, psia	397	361	293
Time when maximum pressure attained, min.	254	258	248
Maximum pipe metal temperature in HL when maximum pressure was attained, F	554	559	416
Maximum fluid temperature in HL when maximum pressure was attained, F	542 (SH)*	549 (SH)*	411 (SAT)*
Time when SPRT01 saturated and subcooled first time during refill (indicating SG primary liquid level in stub), min.	261	273	234
HLHPV opened, min.	302	304	300
Time when first HL spillover was observed	356	372	277
Time when U-bend fluid temperature indicated saturated conditions, min.	358	372	235
Time when RVVV control switched from manual open to automatic, min.	461	554	277
Time when HL levels indicated full, min.	459	556	308
Time when sustained natural circulation was established, min.	461	NA	306

Note: All times are based on time after leak opening. The DAS times when the leaks were opened are: 220201 -- 12.9 min, 2202AA -- 11.4 min, and 2202BB -- 12.4 min.

*"SH" and "SAT" denote superheated and saturated.

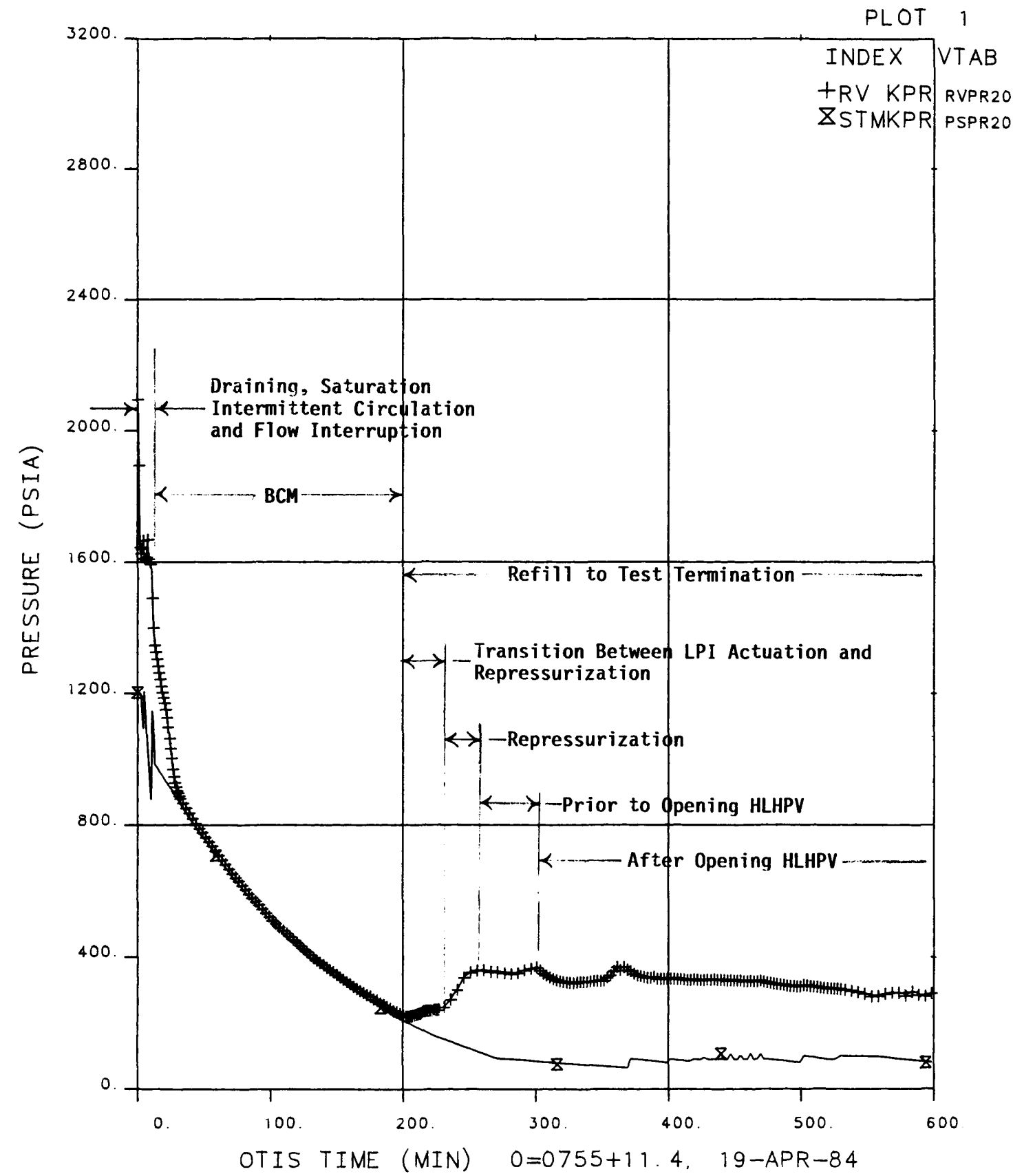

Figure 10.1 Primary and Secondary Pressure Versus Time, Test 2202AA, Showing Key Test Phases

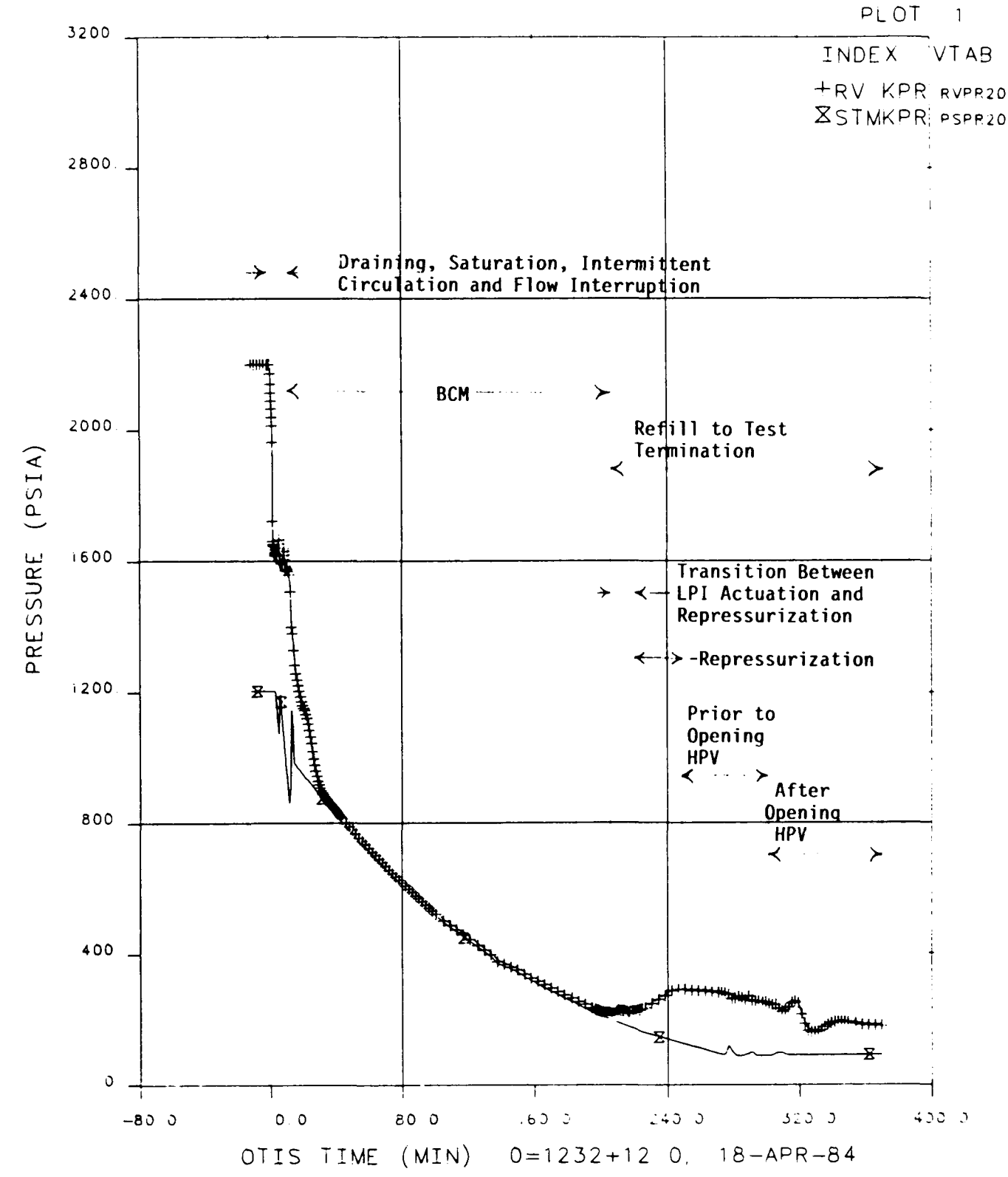

Figure 10.2 Primary and Secondary Pressure Versus Time, Test 2202BB, Showing Key Test Phases

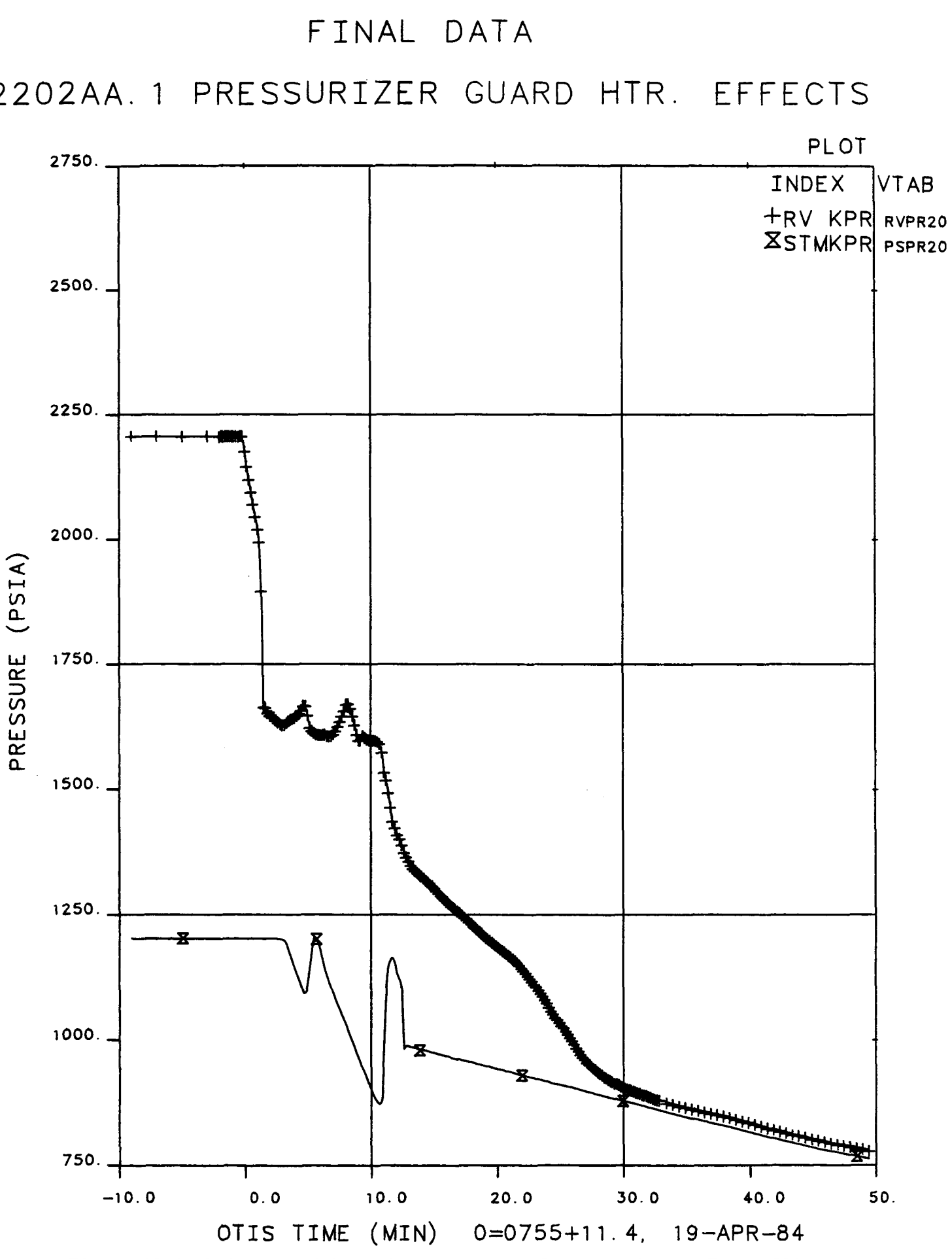

Figure 10.3 Primary and Secondary Pressure, 0 to 50 Minutes Test 2202AA

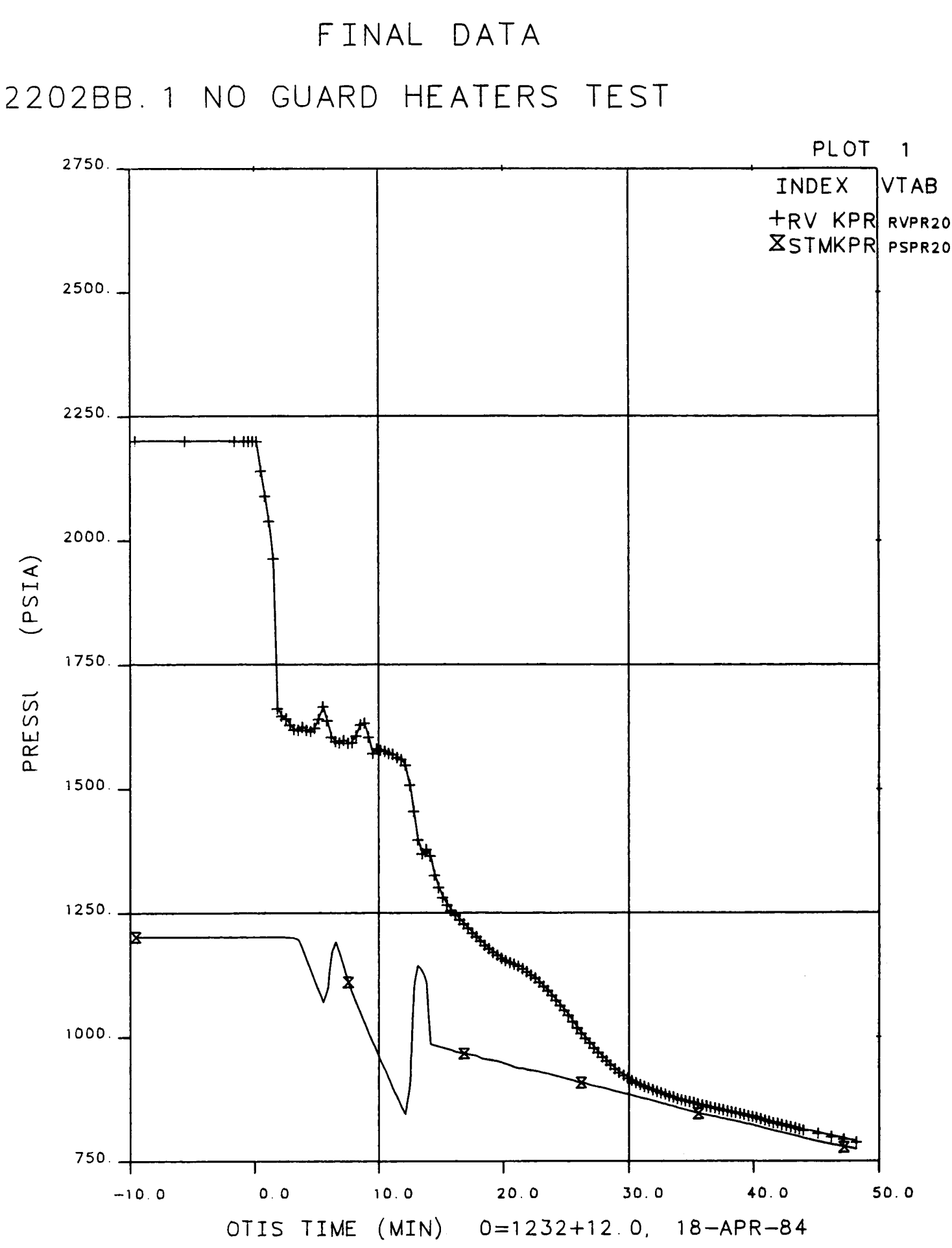

Figure 10.4 Primary and Secondary Pressure, 0 to 50 Minutes, Test 2202BB

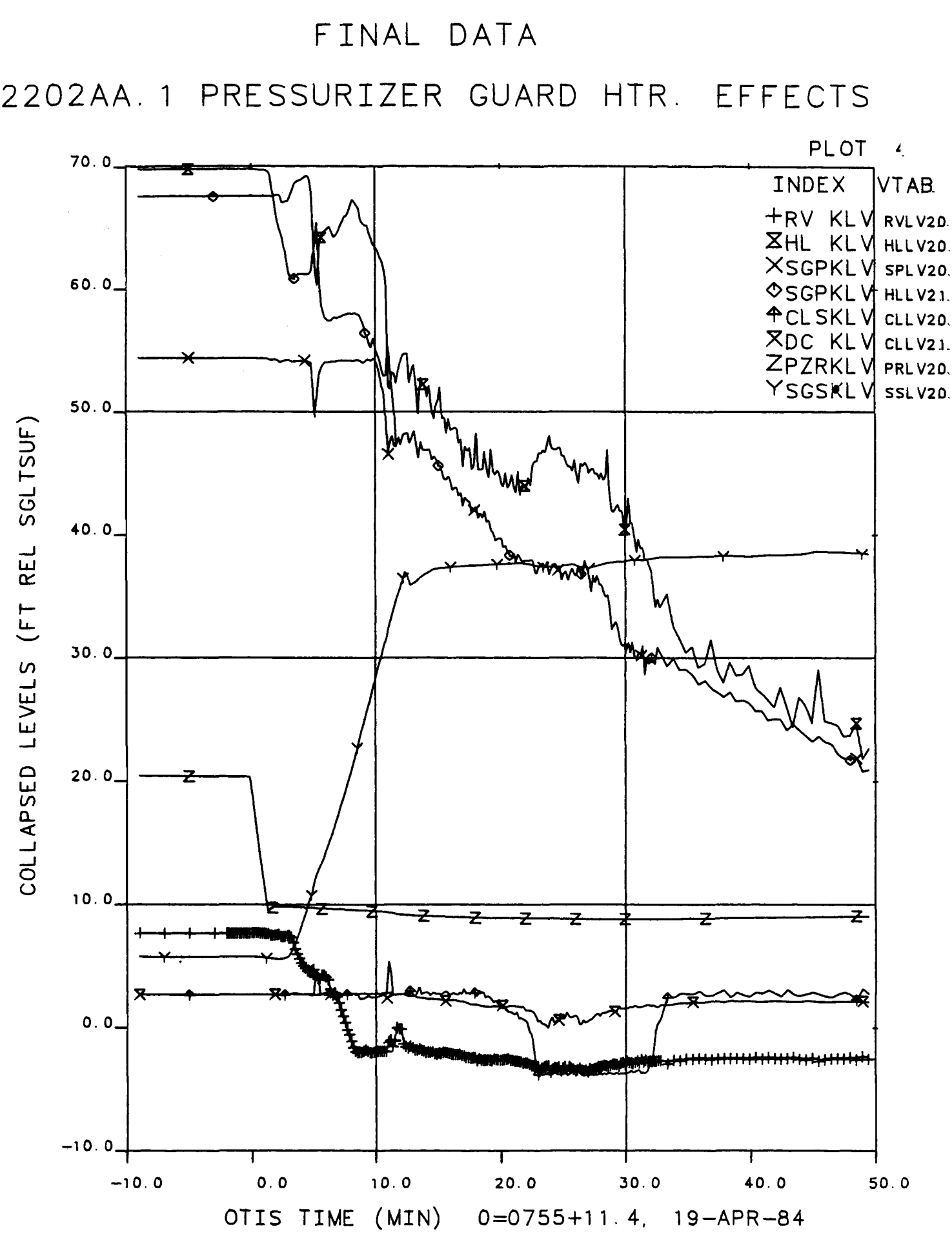

Figure 10.5 Collapsed Liquid Levels, 0 to 50 Minutes, Test 2202AA

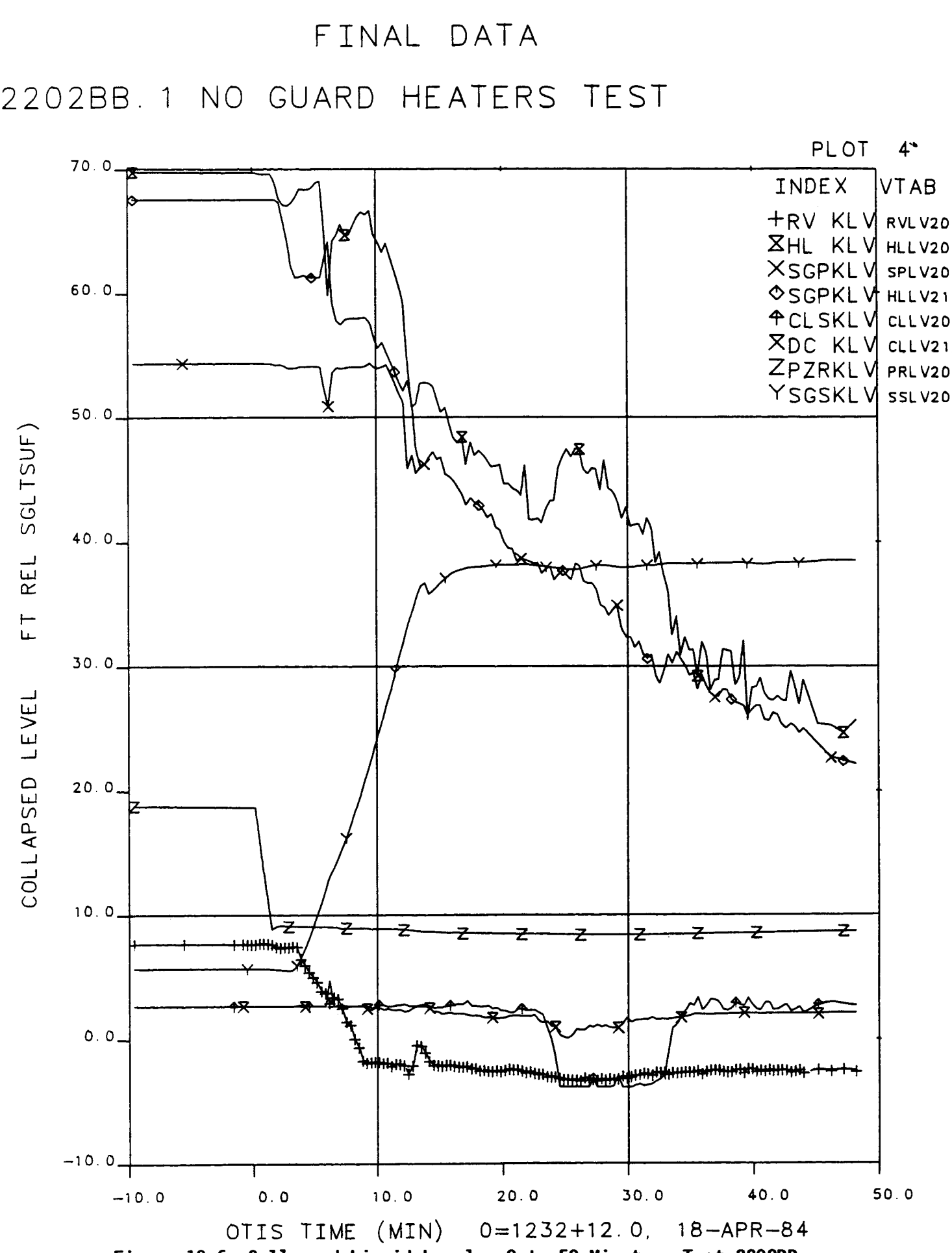

Figure 10.6 Collapsed Liquid Levels, 0 to 50 Minutes, Test 2202BB

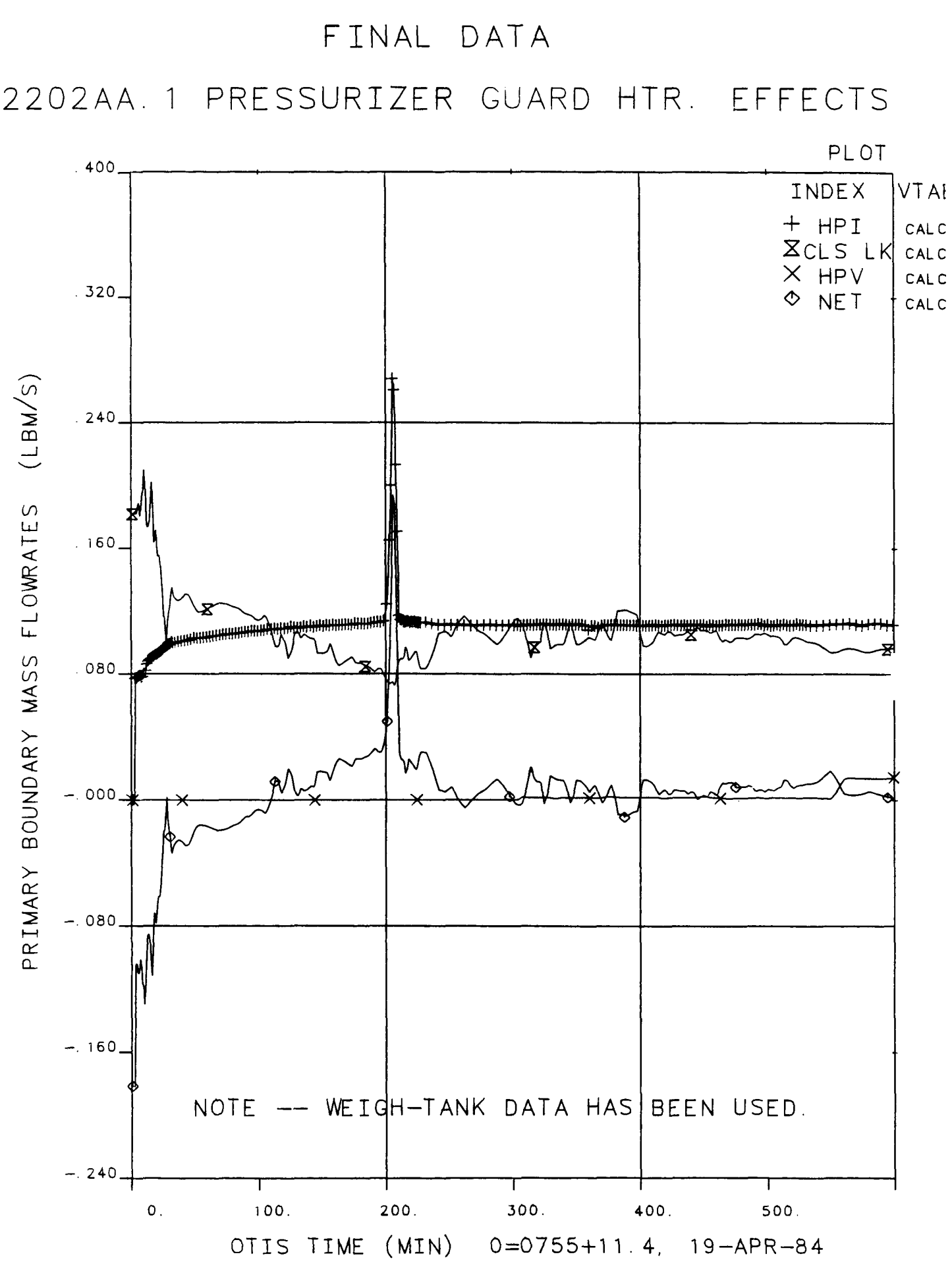

Figure 10.7 Primary Boundary Mass flowrates, Test 2202AA

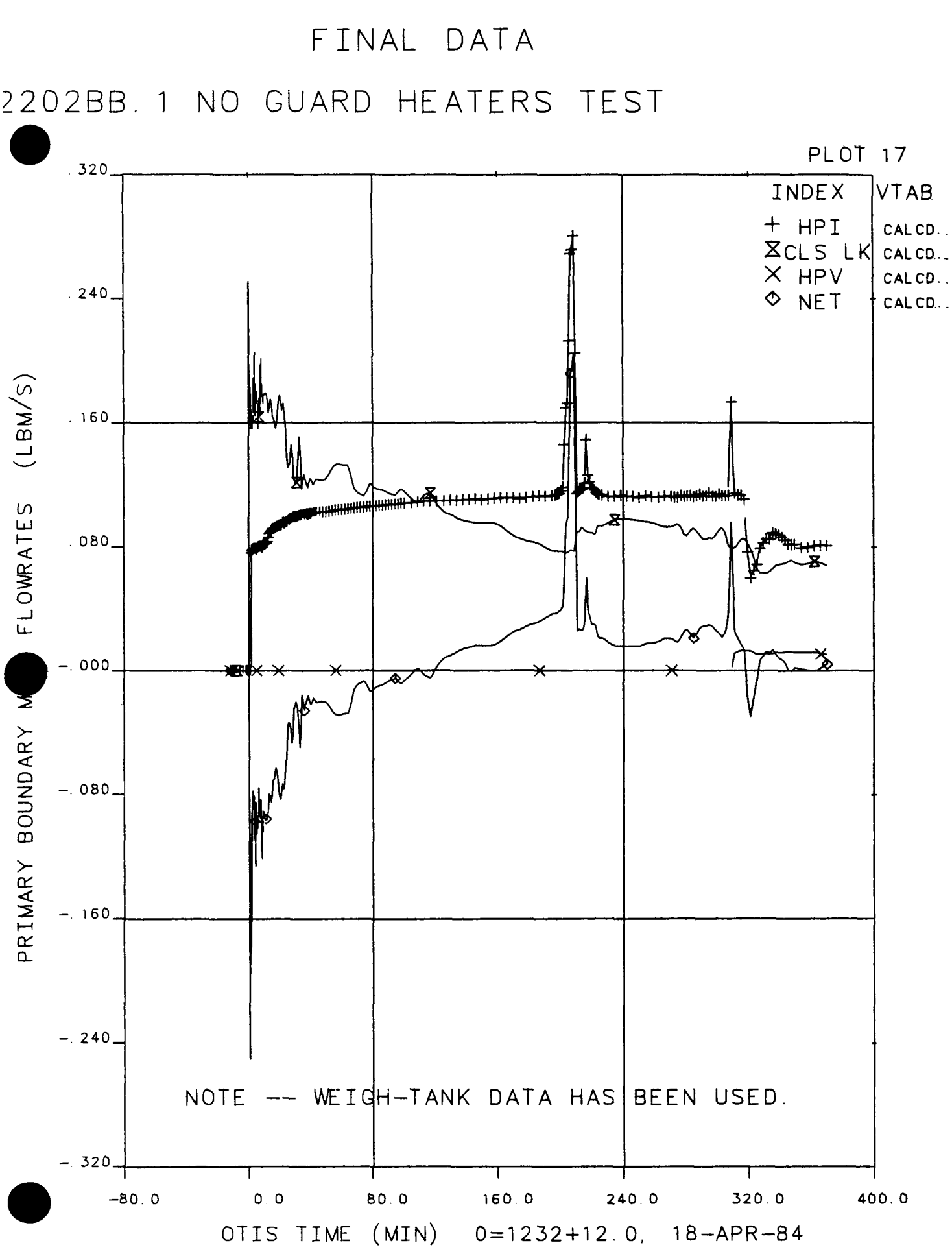

Figure 10.8 Primary Boundary Mass Flowrates, Test 2202BB

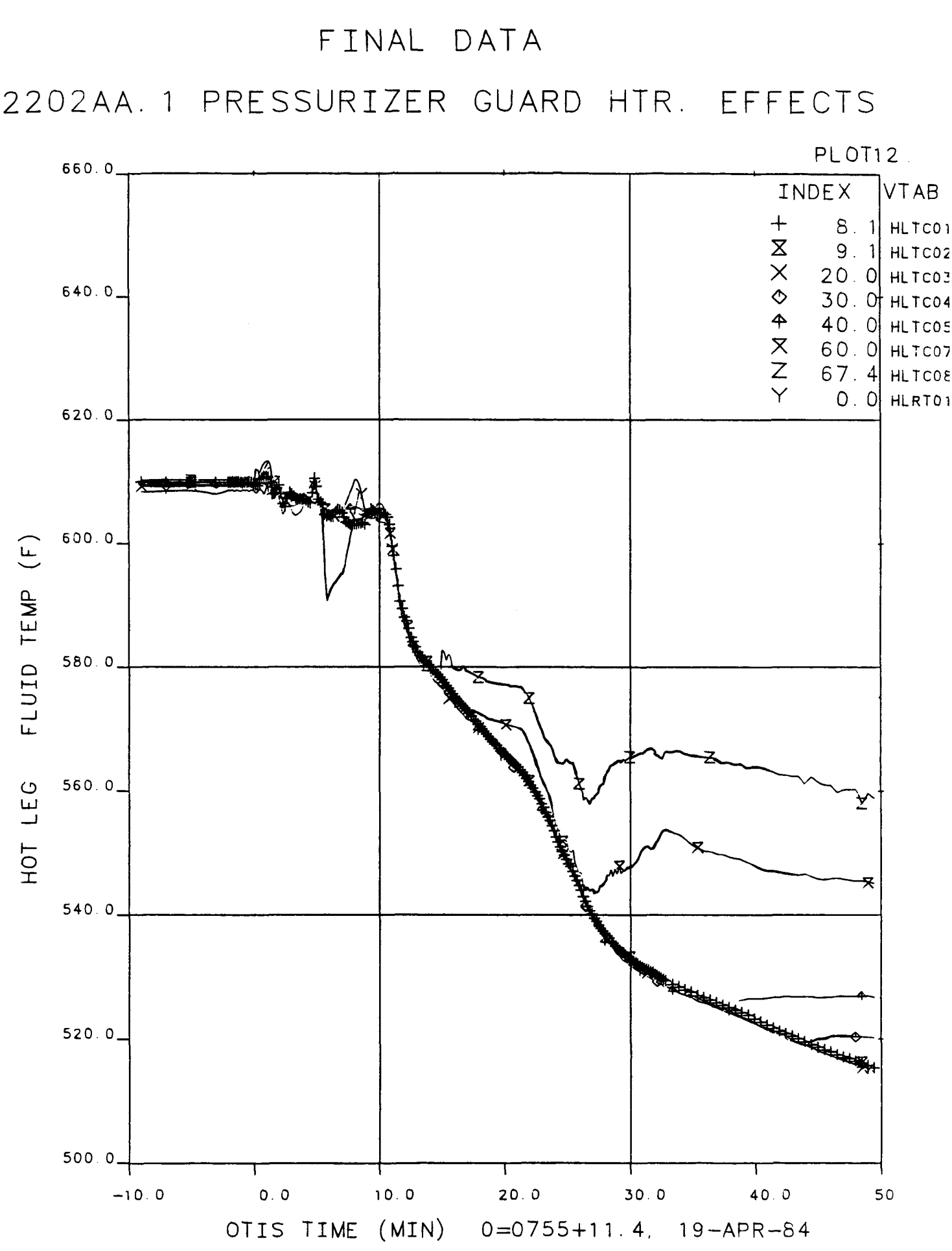

Figure 10.9 Hot Leg Fluid Temperatures, Test 2202AA

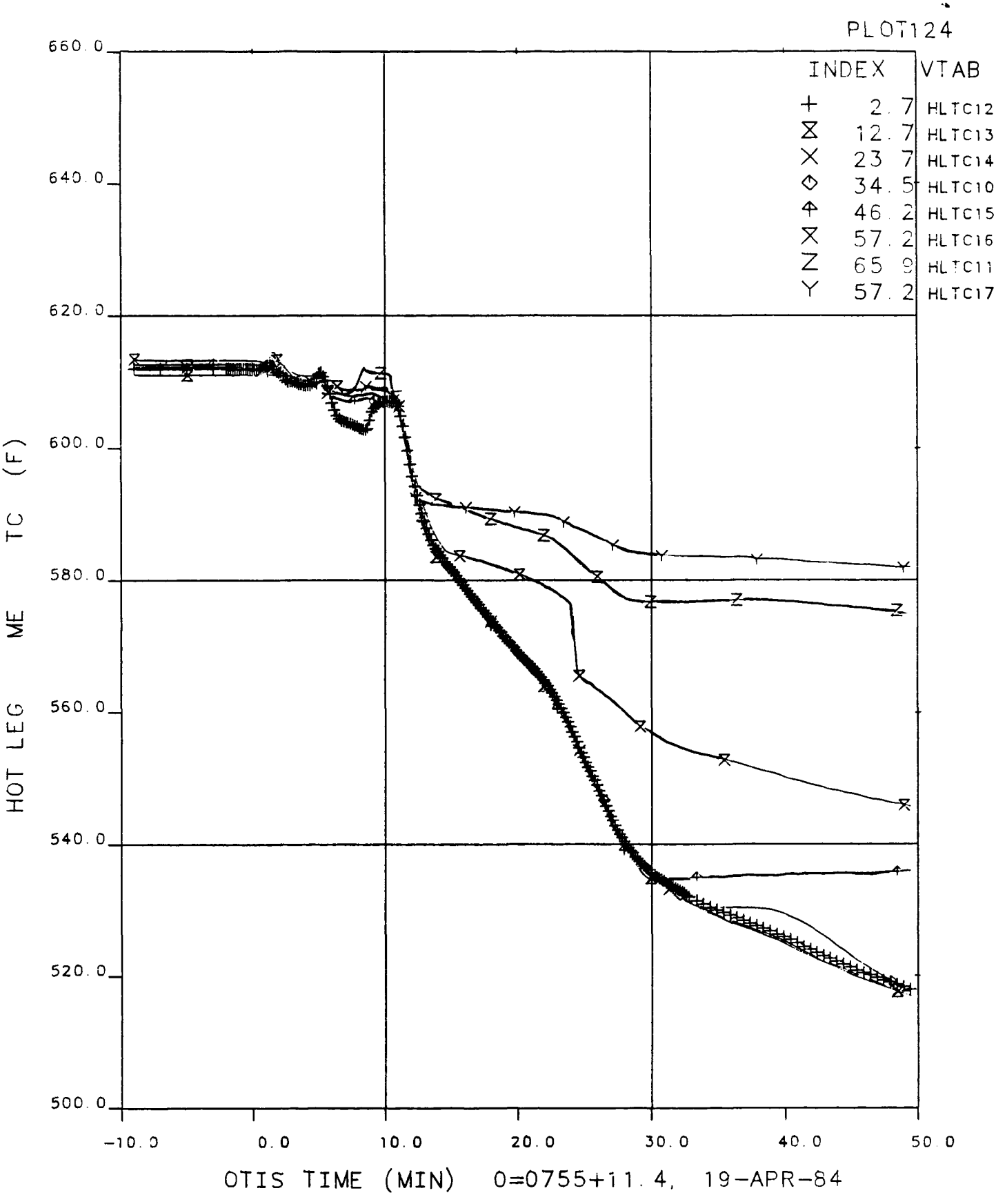

Figure 10.10 Hot Leg Metal Temperatures, Test 2202AA

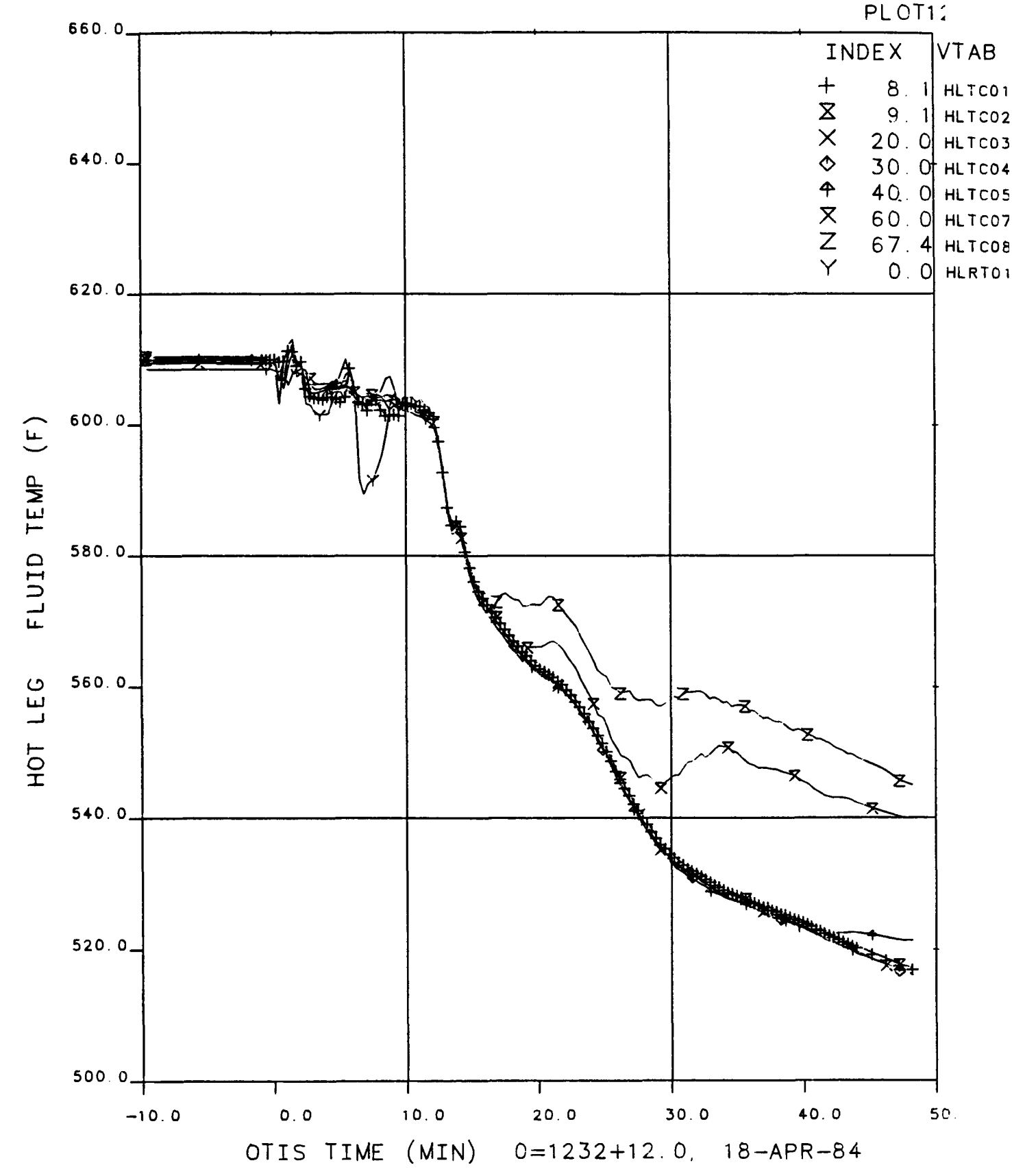

Figure 10.11 Hot Leg Fluid Temperatures, Test 2202BB

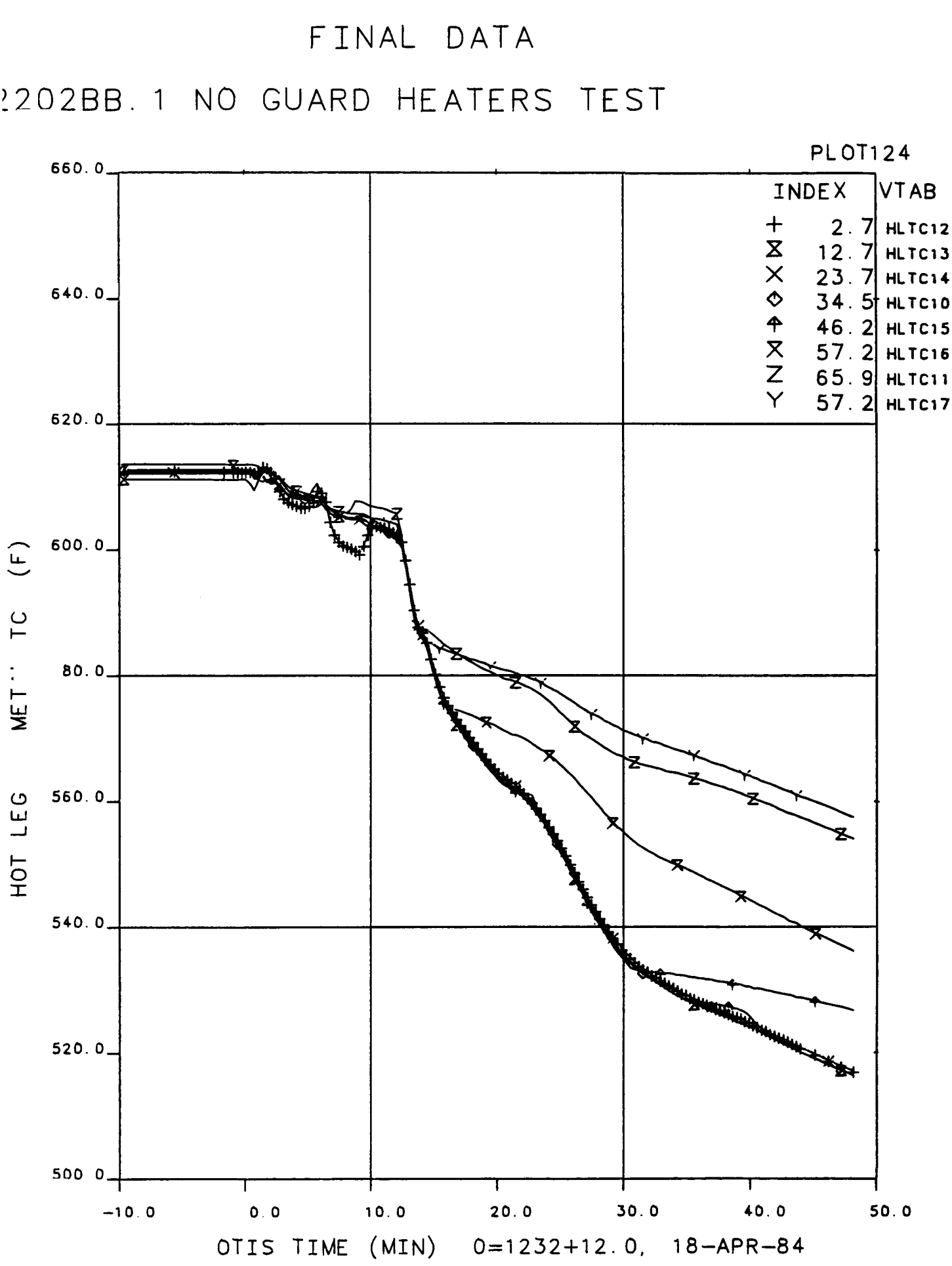

Figure 10.12 Hot Leg Metal Temperatures, Test 2202BB

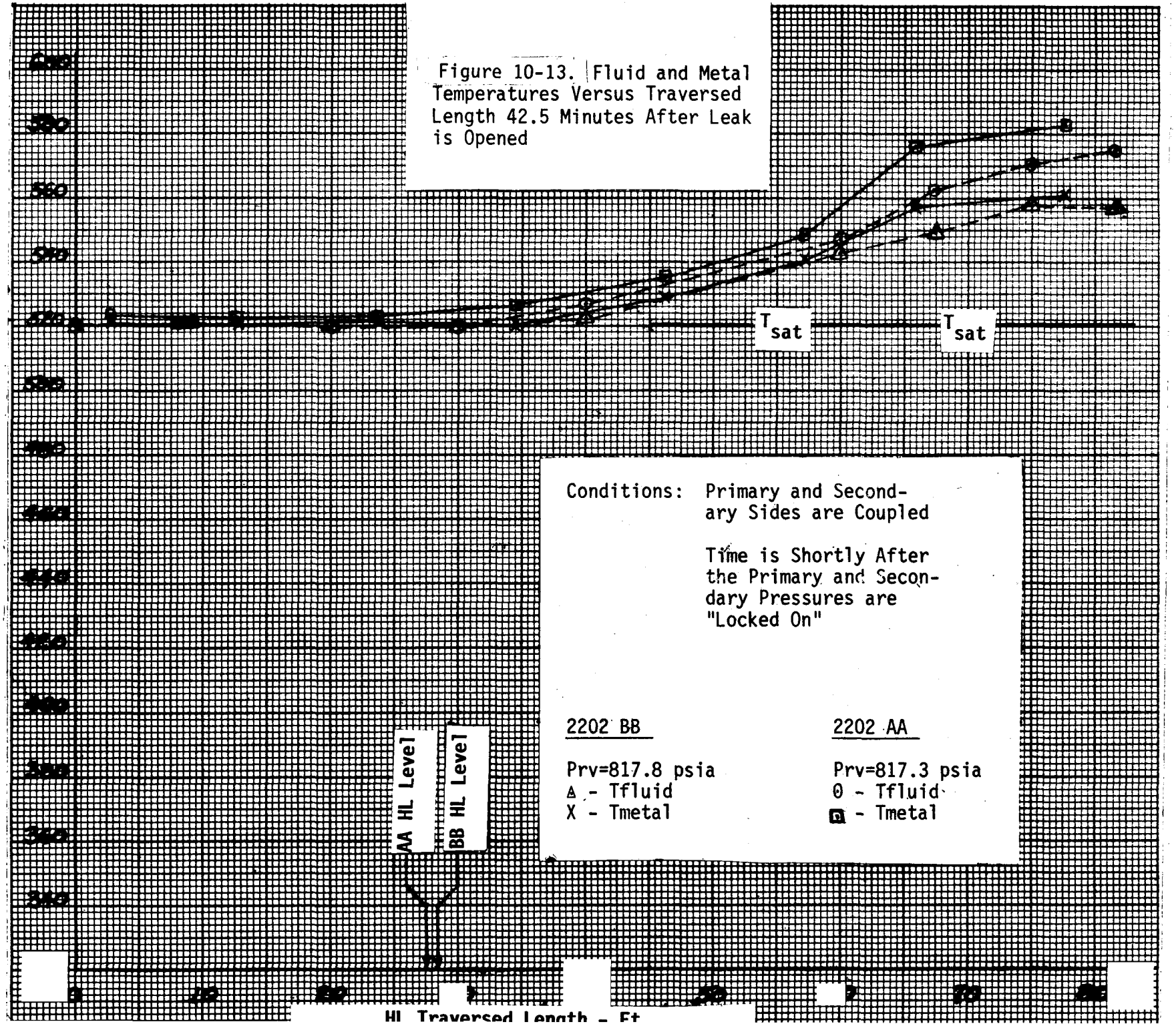
Figure 10-13. Fluid and Metal Temperatures Versus Traversed Length 42.5 Minutes After Leak is Opened
HL Temperature - °F
HL Traversed Length - Ft
AA HL Level
BB HL Level
T_{sat}
T_{sat}
Conditions: Primary and Secondary Sides are Coupled
Time is Shortly After the Primary and Secondary Pressures are "Locked On"
2202 BB
Prv=817.8 psia
Δ - Tfluid
X - Tmetal
2202 AA
Prv=817.3 psia
0 - Tfluid
□ - Tmetal

Figure 10 Fluid and Metal Temperatures Versus Traversed Length 69 Minutes After Leak is Opened

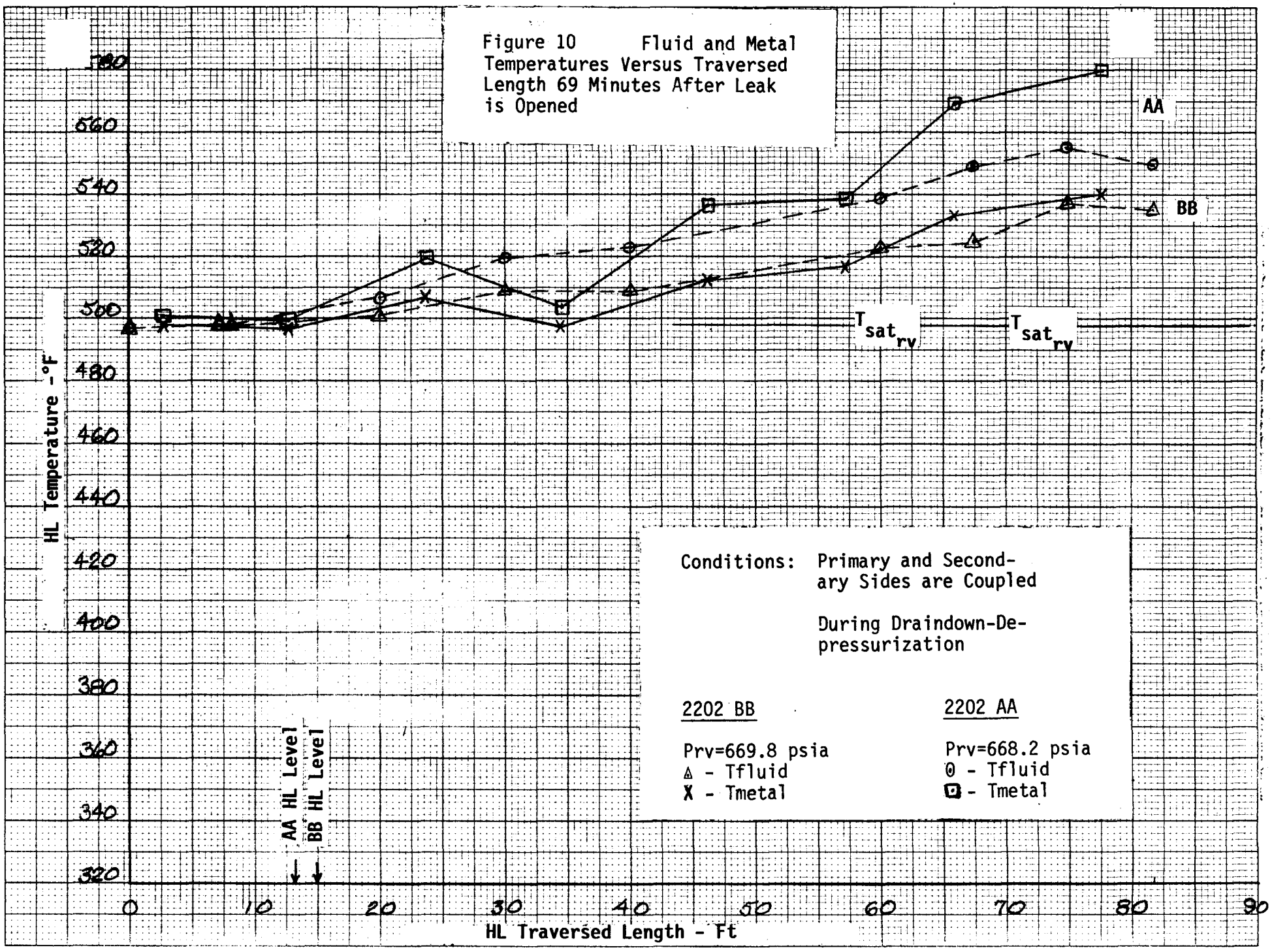

Figure 10.15. Fluid and Metal Temperatures Versus Traversed Length 133 Minutes After Leak is Opened

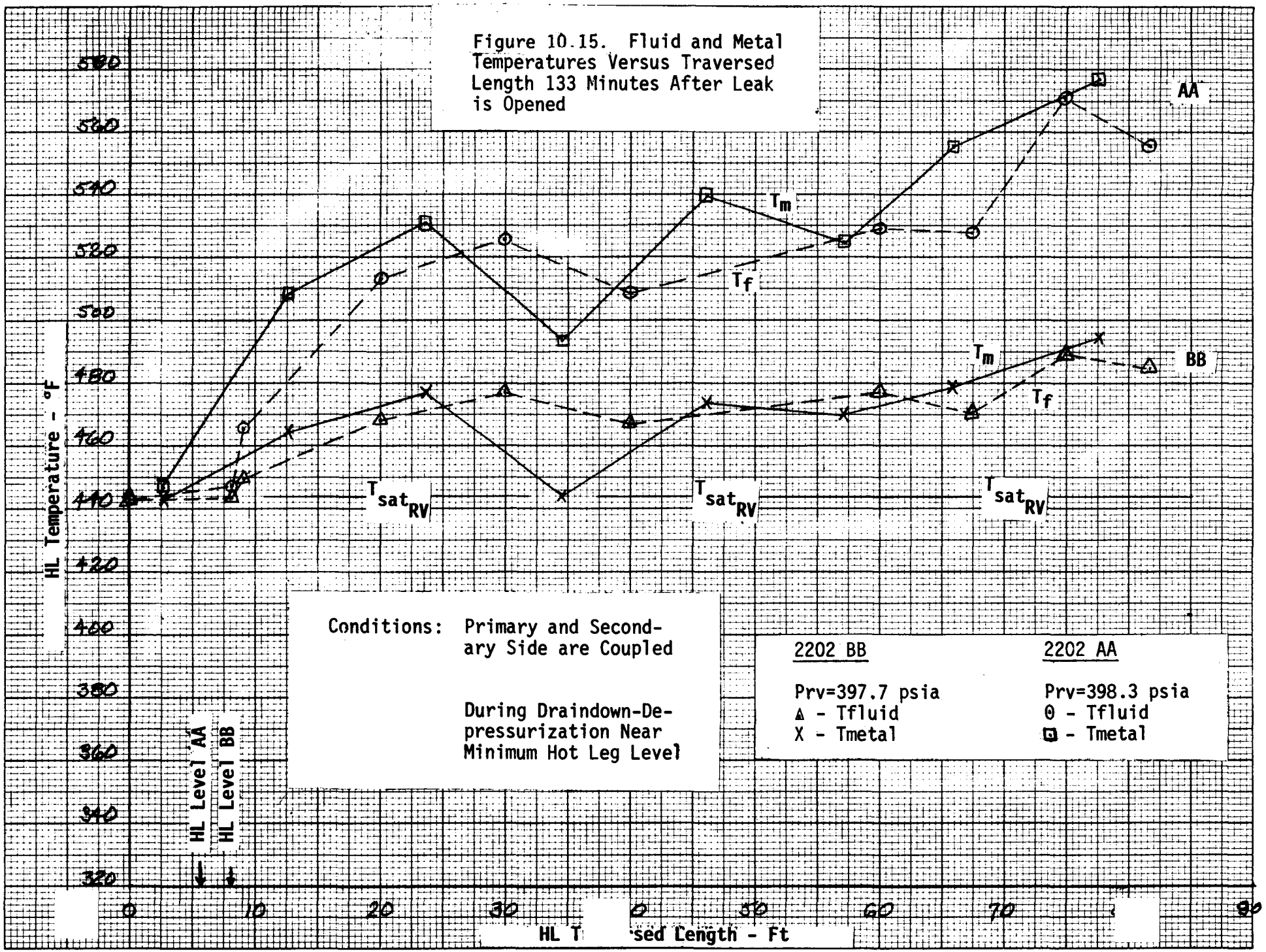

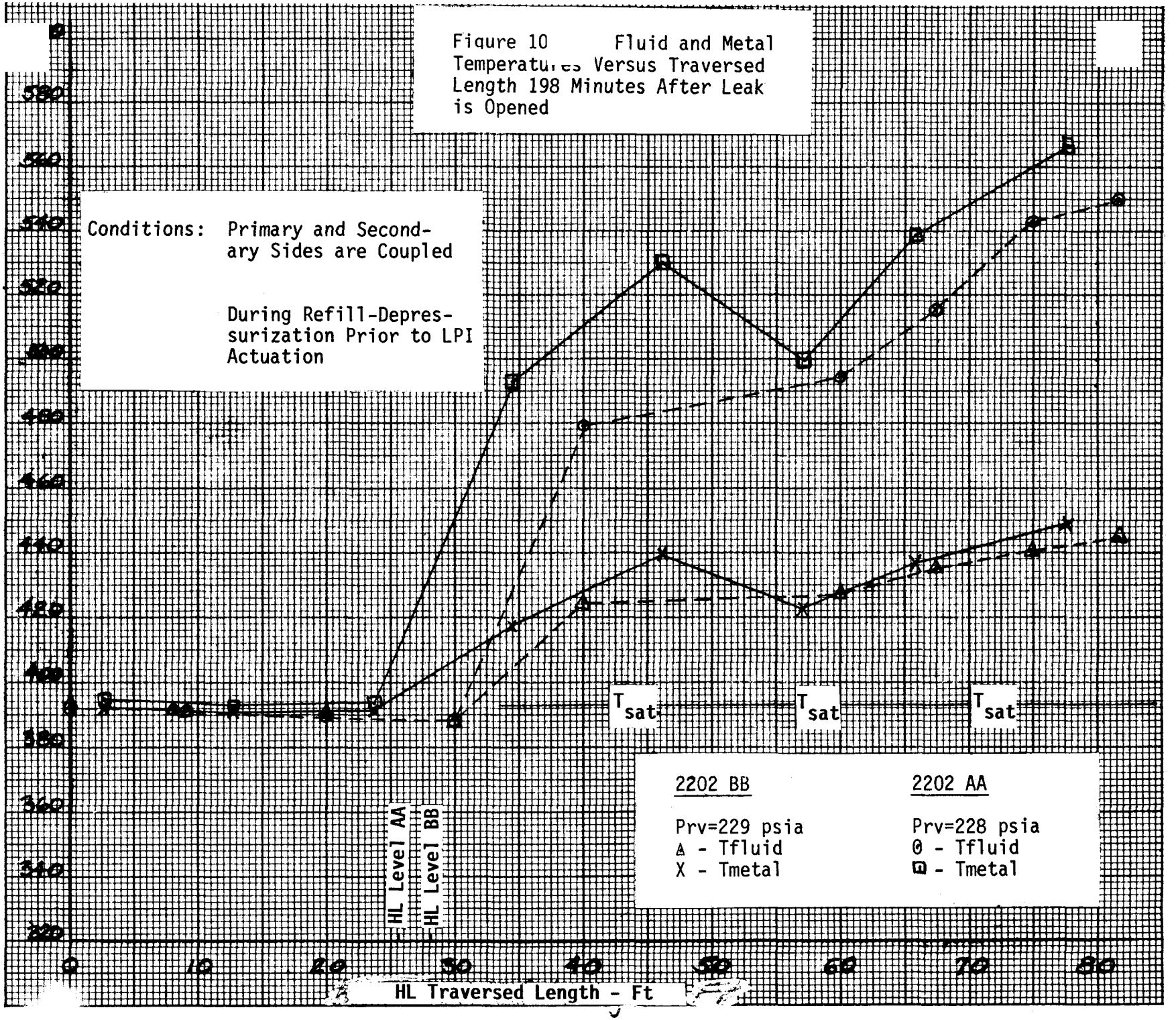
Figure 10 Fluid and Metal Temperatures Versus Traversed Length 198 Minutes After Leak is Opened
Conditions: Primary and Secondary Sides are Coupled
During Refill-Depressurization Prior to LPI Actuation
HL Temperature - °F
HL Traversed Length - Ft
HL Level AA
HL Level BB
T_{sat}
T_{sat}
T_{sat}
2202 BB
Prv=229 psia
Δ - Tfluid
X - Tmetal
2202 AA
Prv=228 psia
0 - Tfluid
□ - Tmetal

Figure 10.17. Degrees of Superheat at Steam Generator Inlet Versus Time After Leak Opened

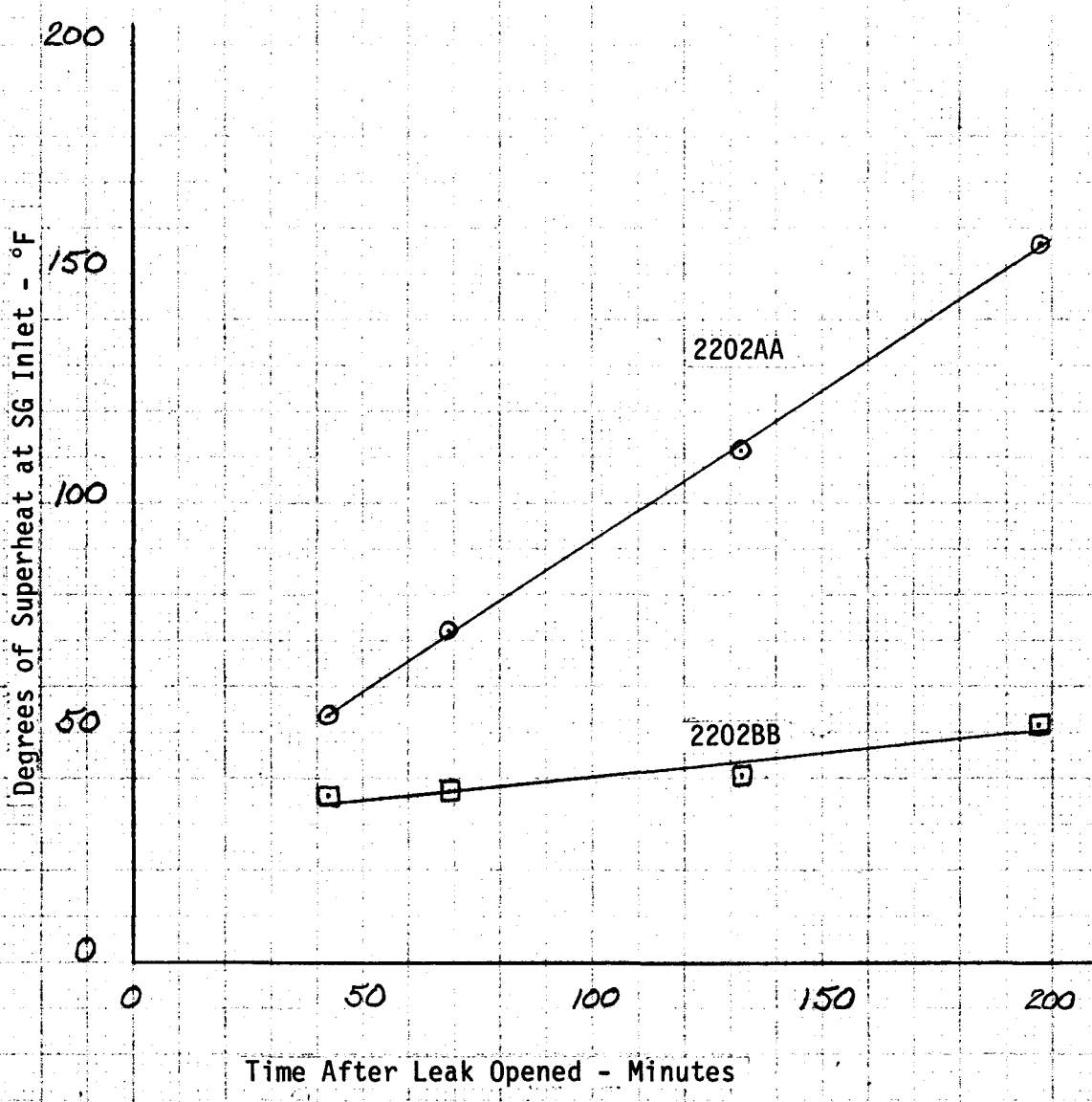

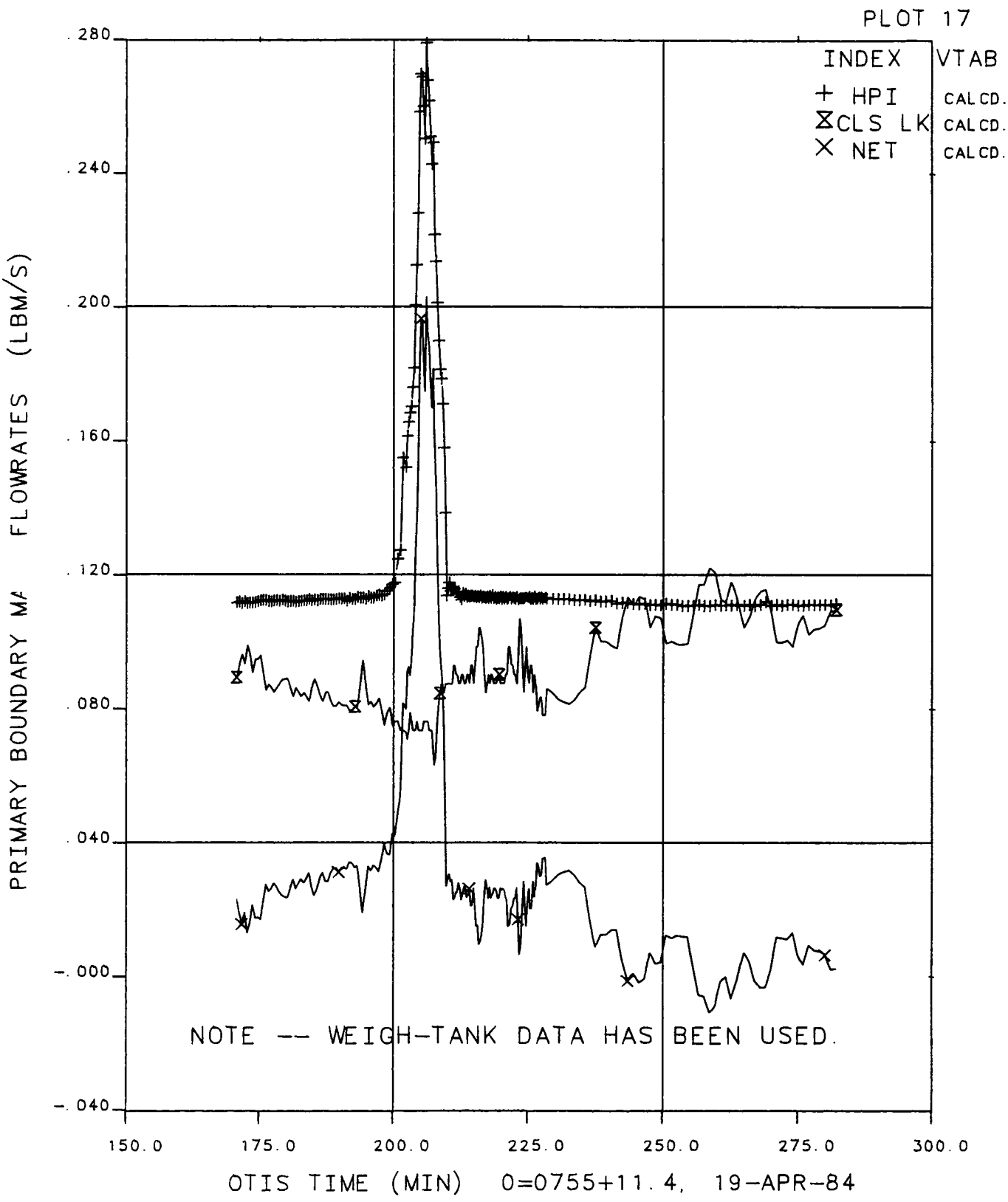

Figure 10.18 Primary Boundary Mass Flowrate, 175 to 275 Minutes, Test 2202AA

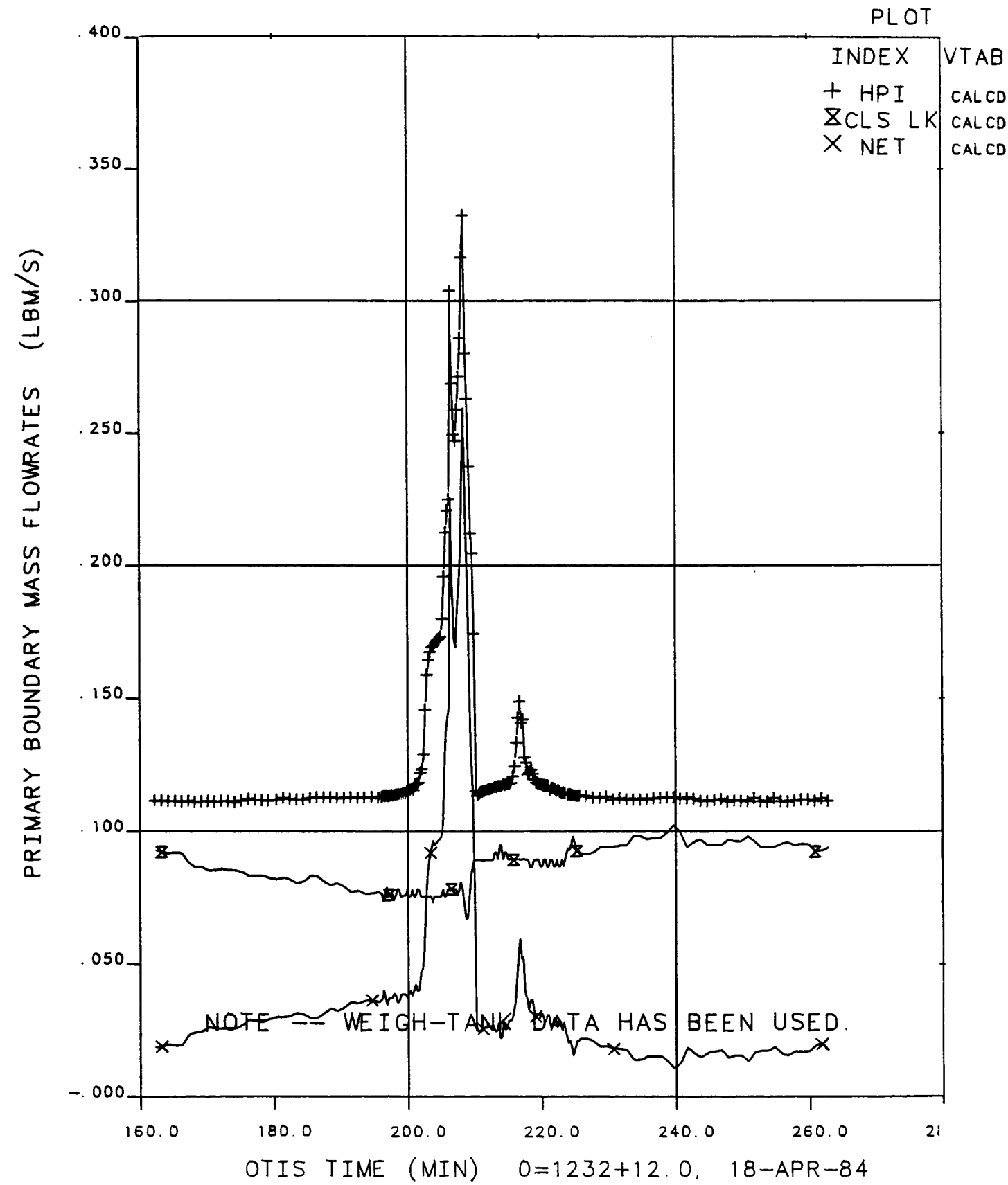

Figure 10.19 Primary Boundary Mass Flowrates, 160 to 260 Minutes, Test 2202BB

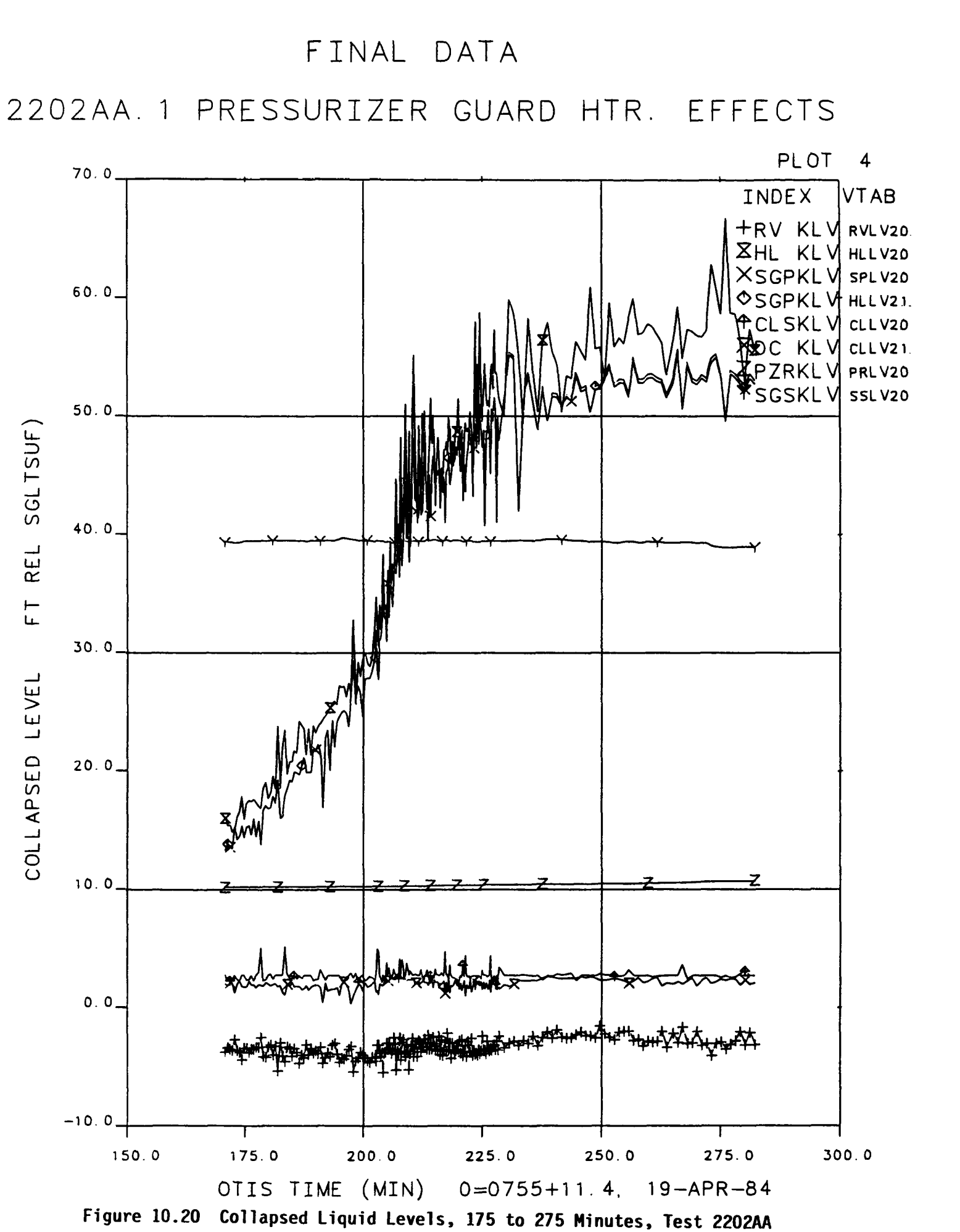

Figure 10.20 Collapsed Liquid Levels, 175 to 275 Minutes, Test 2202AA

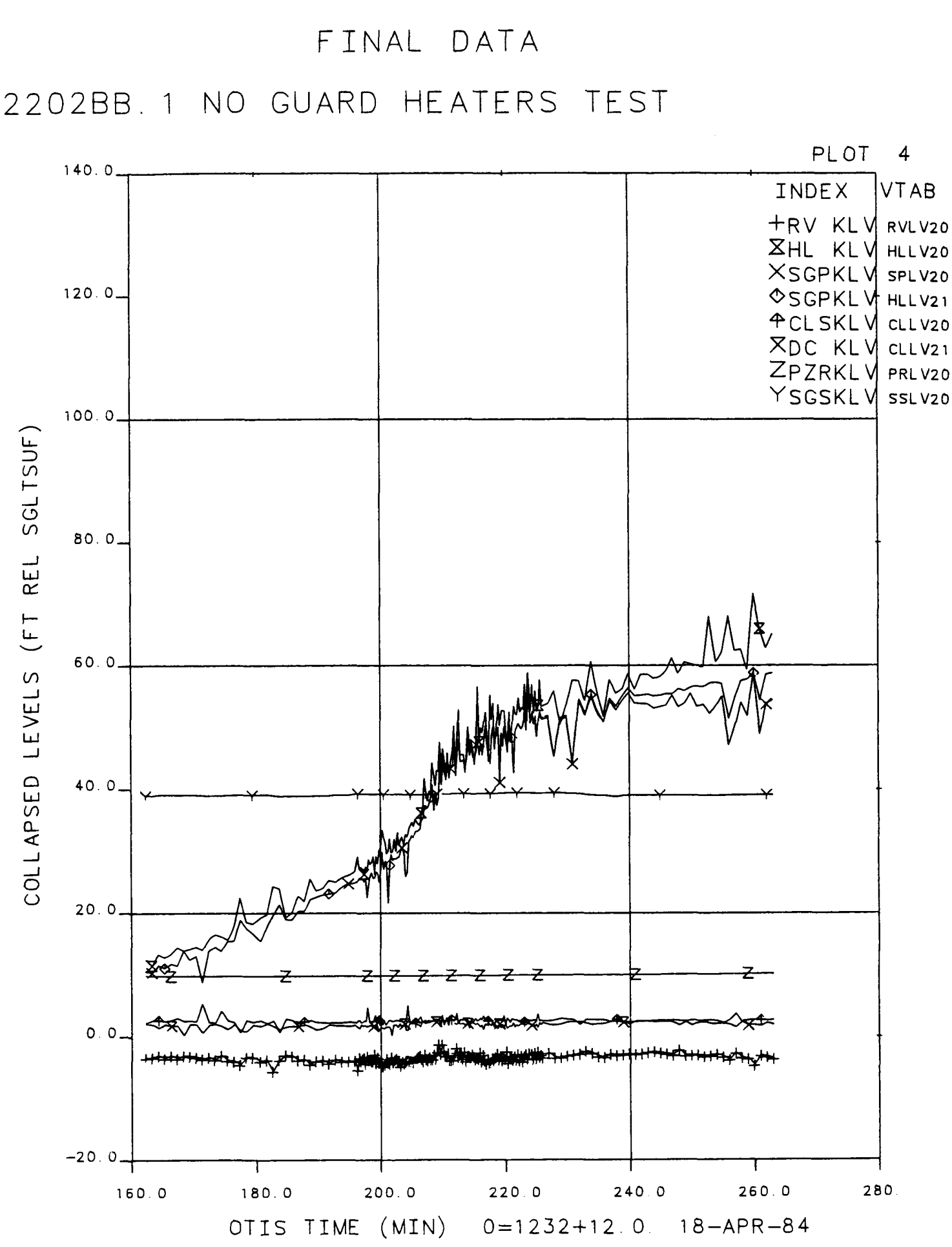

Figure 10.21 Collapsed Liquid Levels, 160 to 260 Minutes, Test 2202BB

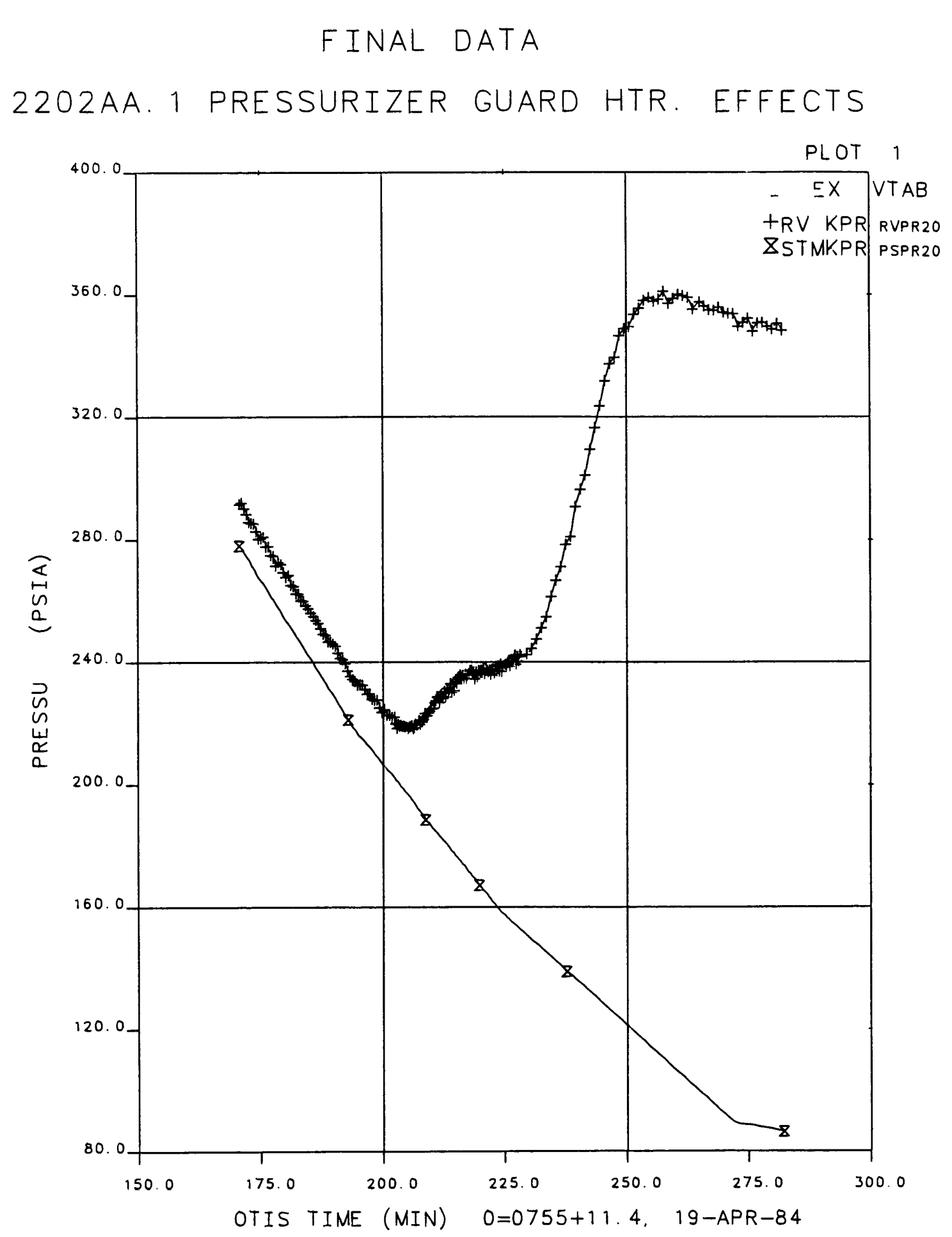

Figure 10.22 Primary and Secondary Pressure, 175 to 275 Minutes, Test 2202AA

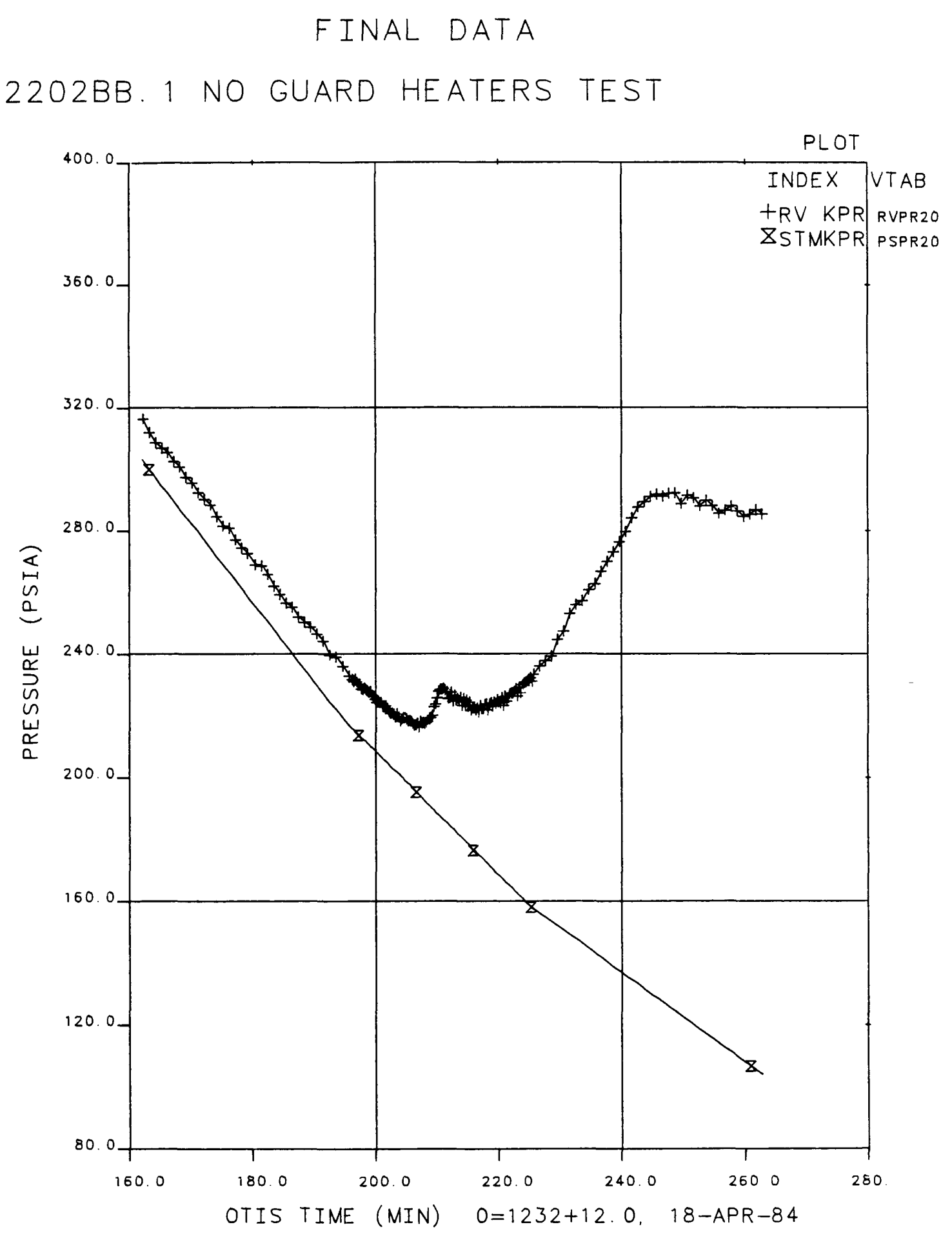

Figure 10.23 Primary and Secondary Pressure, 160 to 260 Minutes, Test 2202BB

Figure 10.24. Fluid and Metal Temperatures Versus Traversed Length 230 Minutes After Leak is Opened

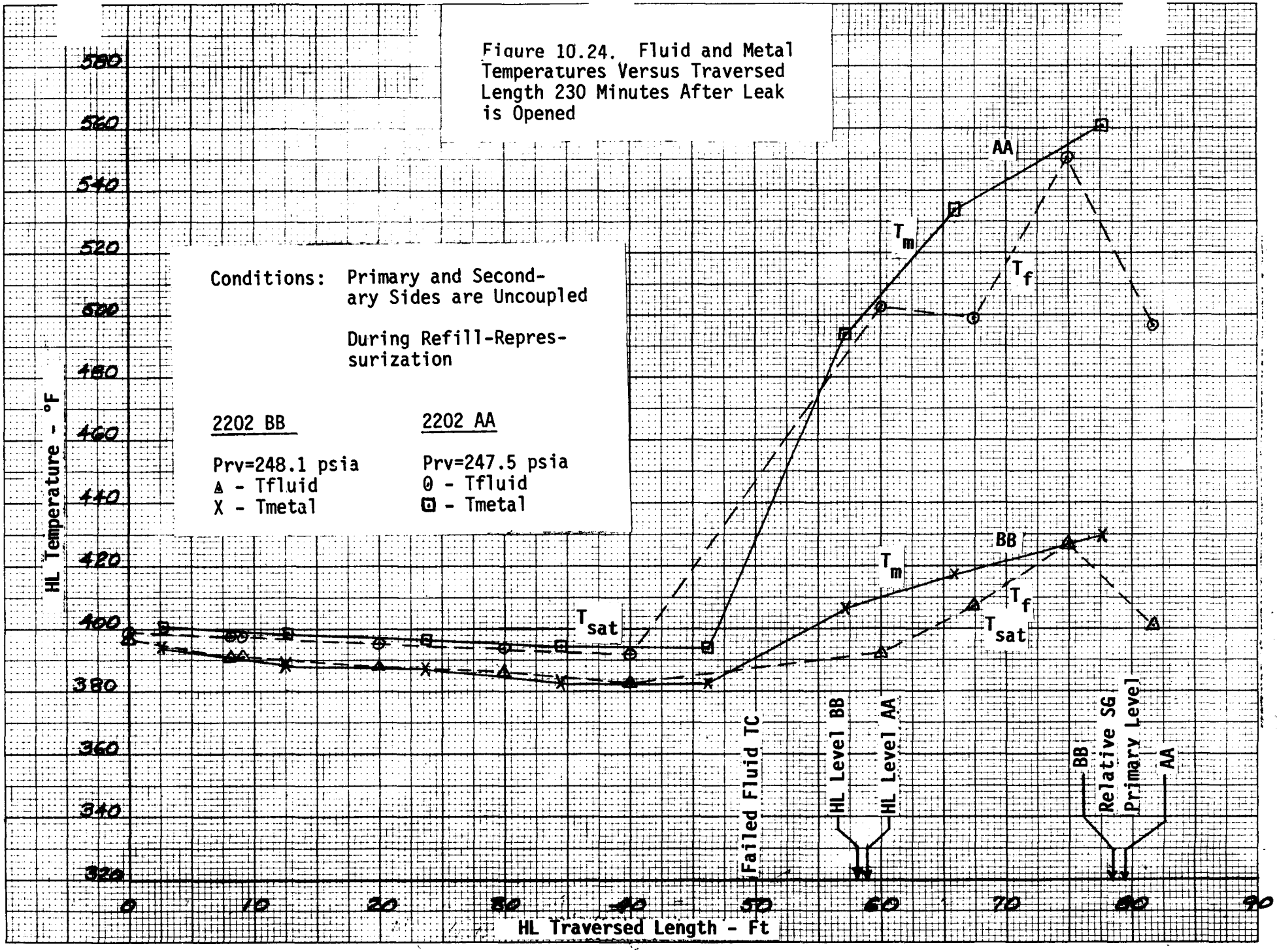

Figure 10.25 Fluid and Metal Temperatures Versus Traversed Length 251 Minutes After Leak is Opened

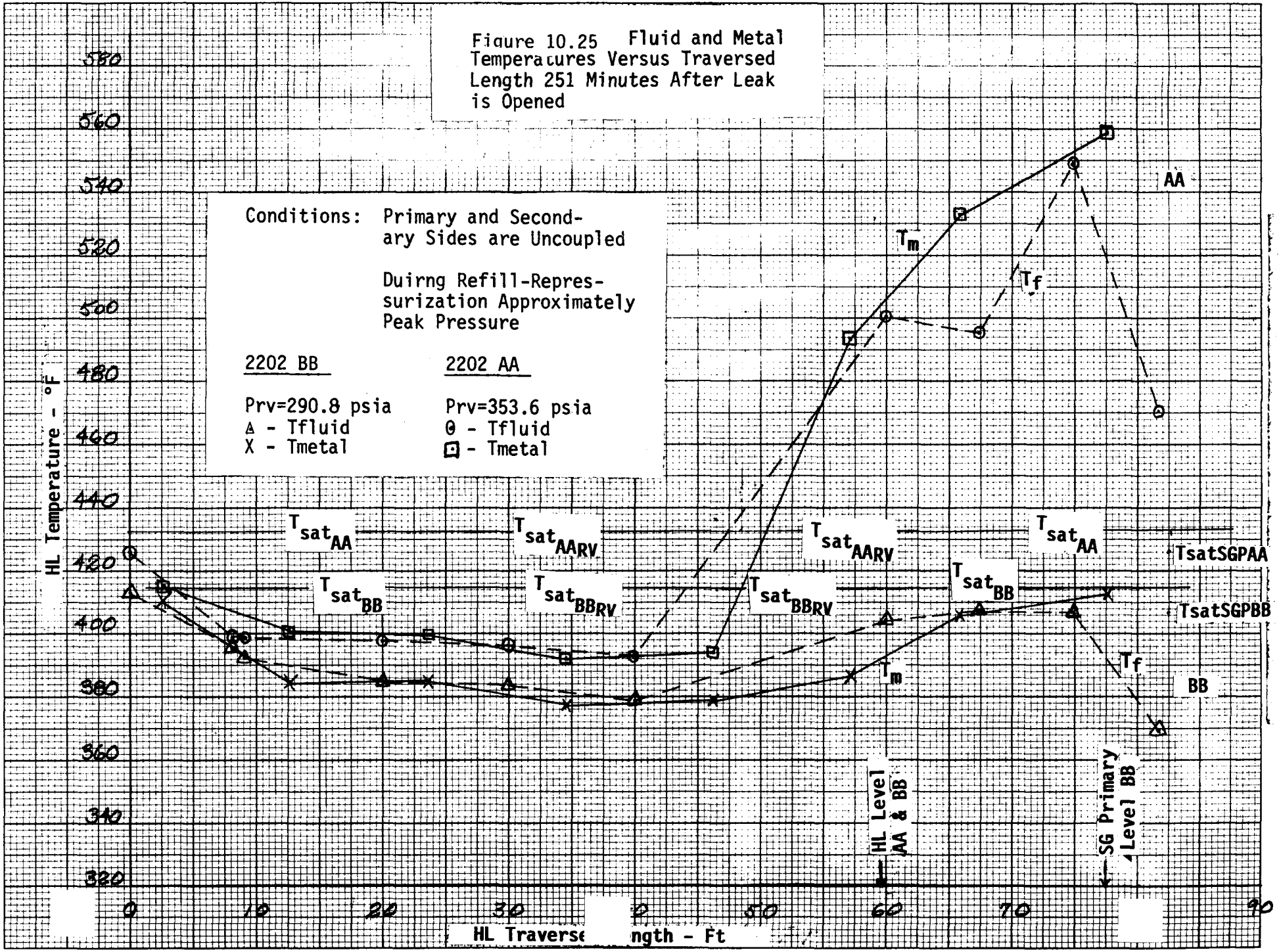

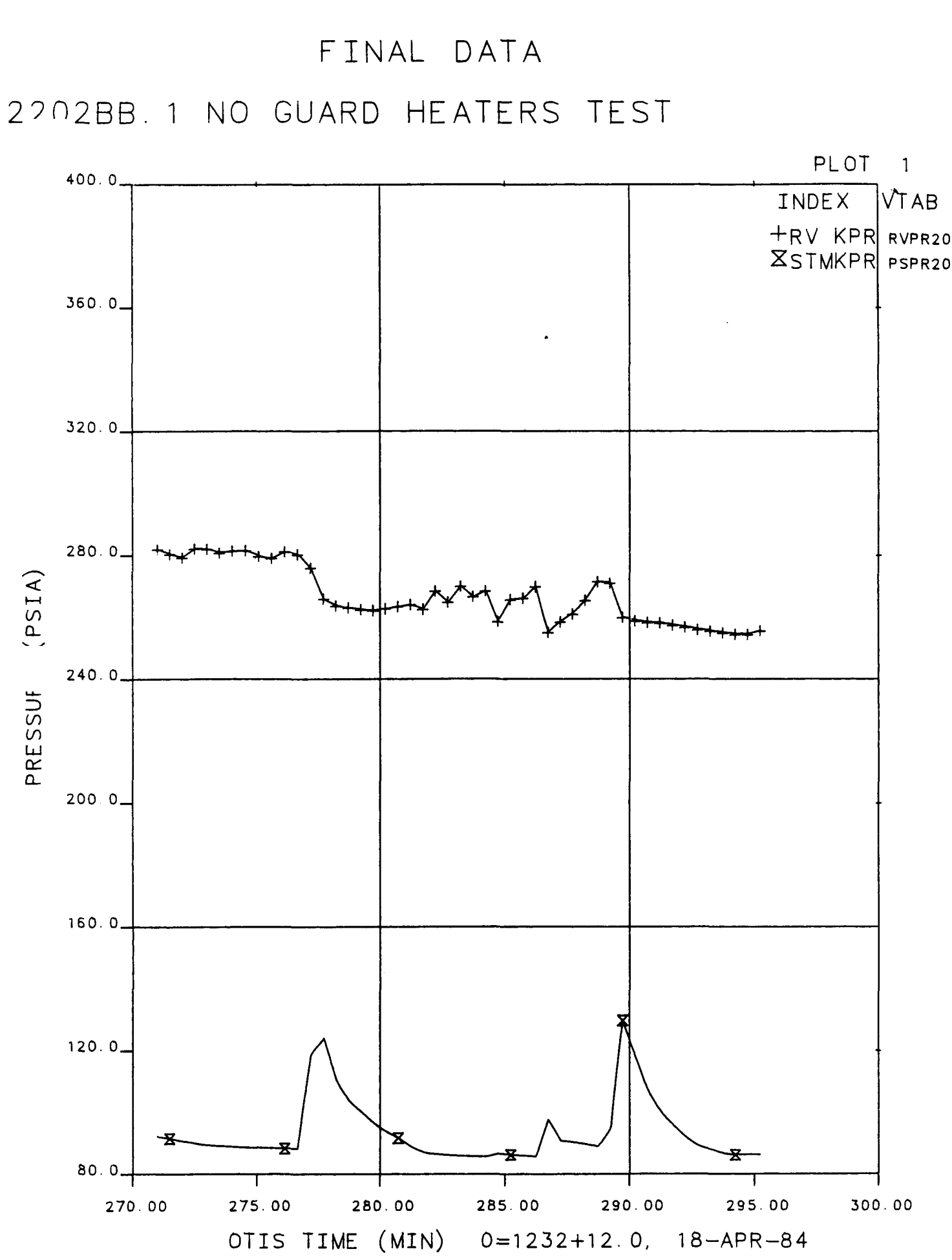

Figure 10.26 Primary and Secondary Pressure, 270 to 295 Minutes, Test 2202BB

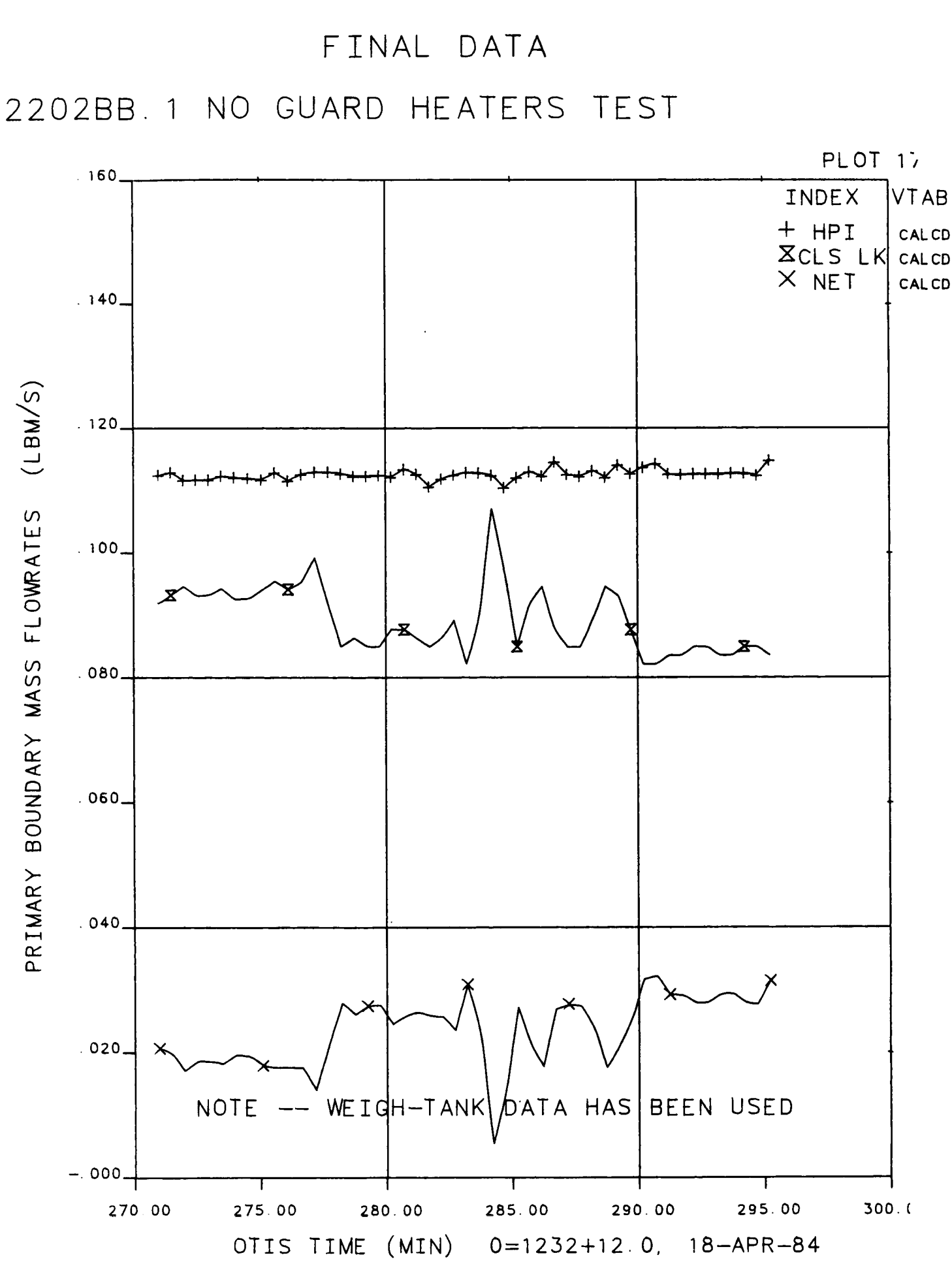

Figure 10.27 Primary Boundary Mass Flowrates, 270 to 295 Minutes, Test 2202BB

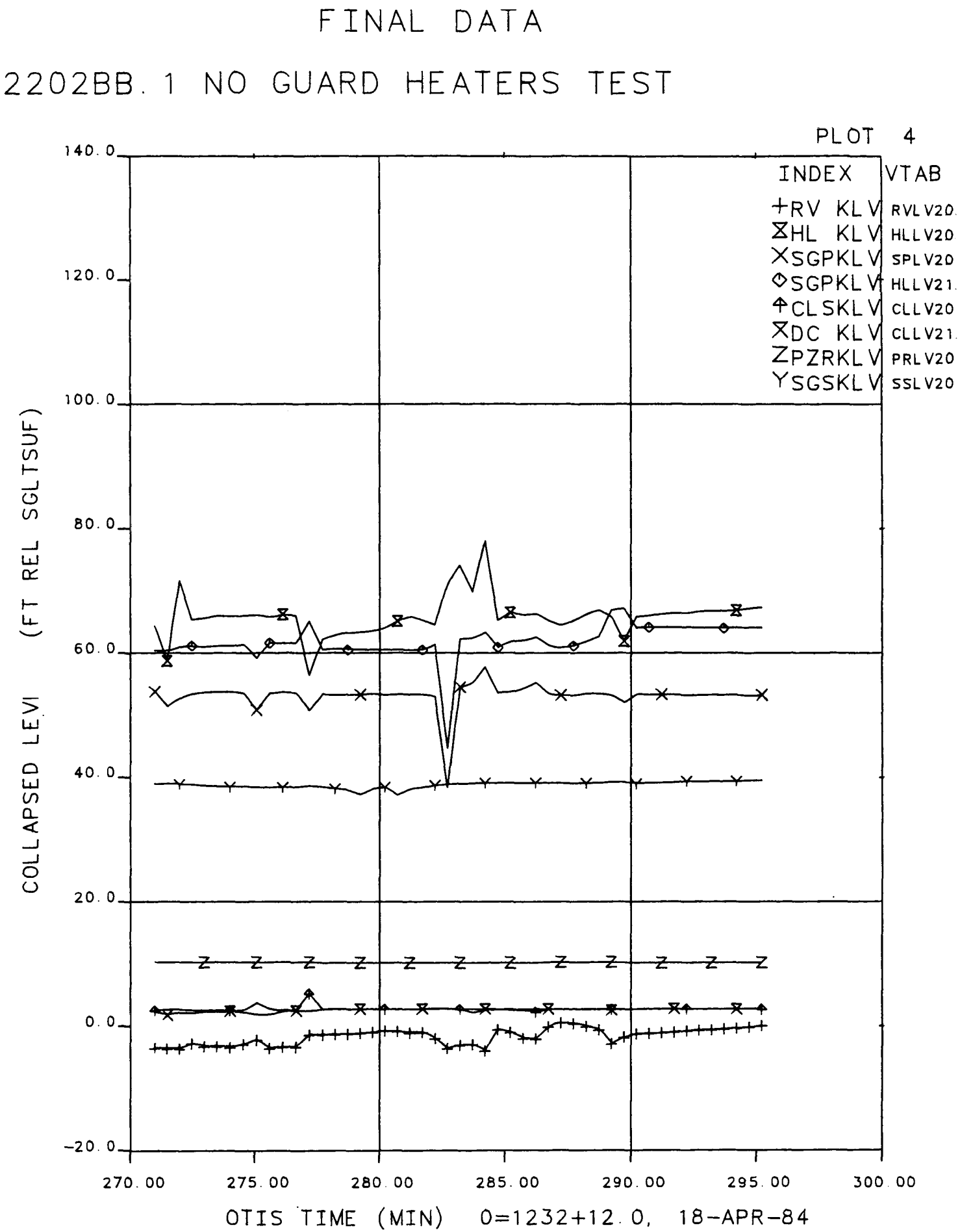

Figure 10.28 Collapsed Liquid Levels, 270 to 295 Minutes, Test 2202BB

Figure 10.29. Fluid and Metal Temperature Versus Traversed Length 287 Minutes After Leak Is Opened

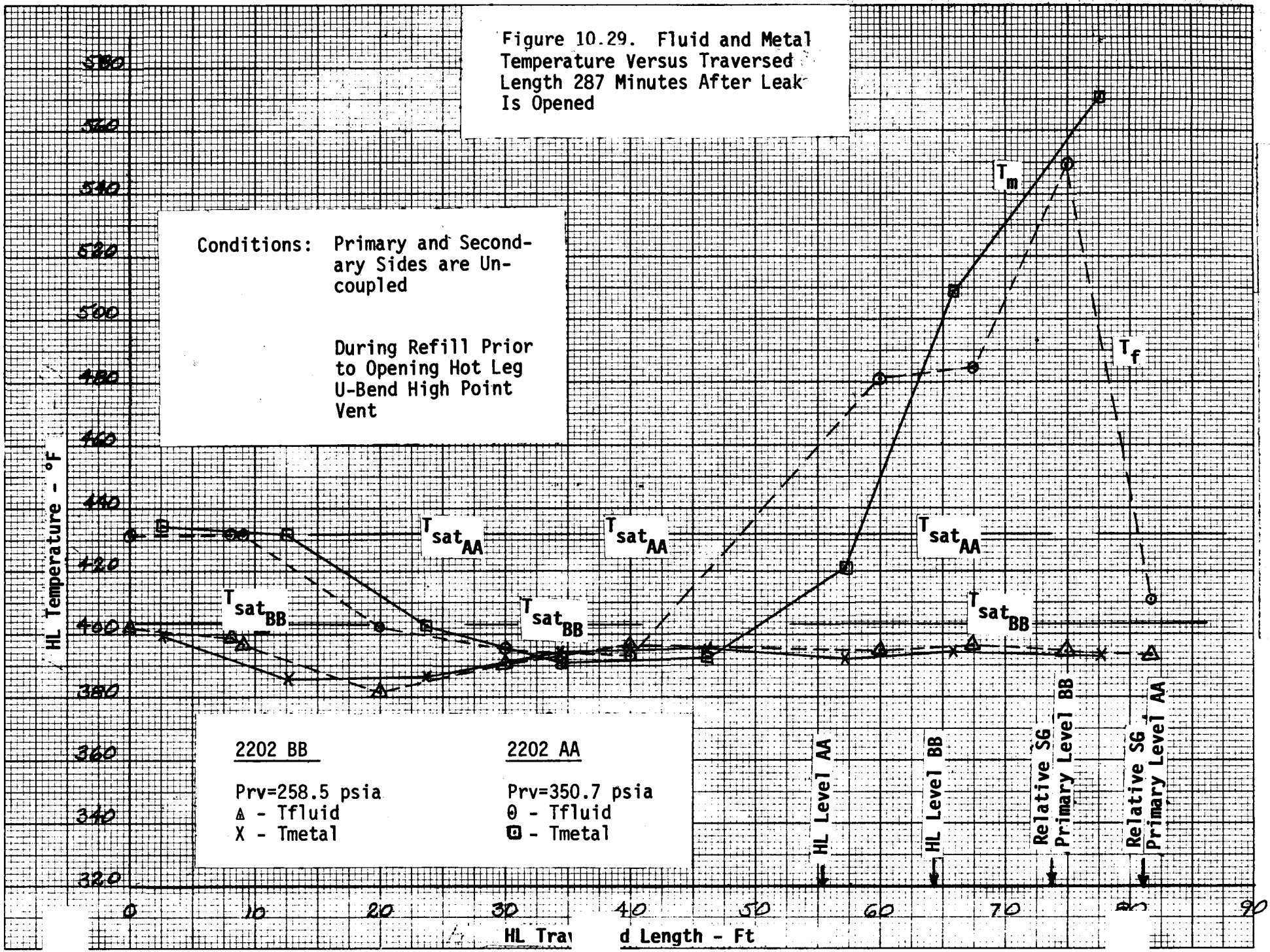

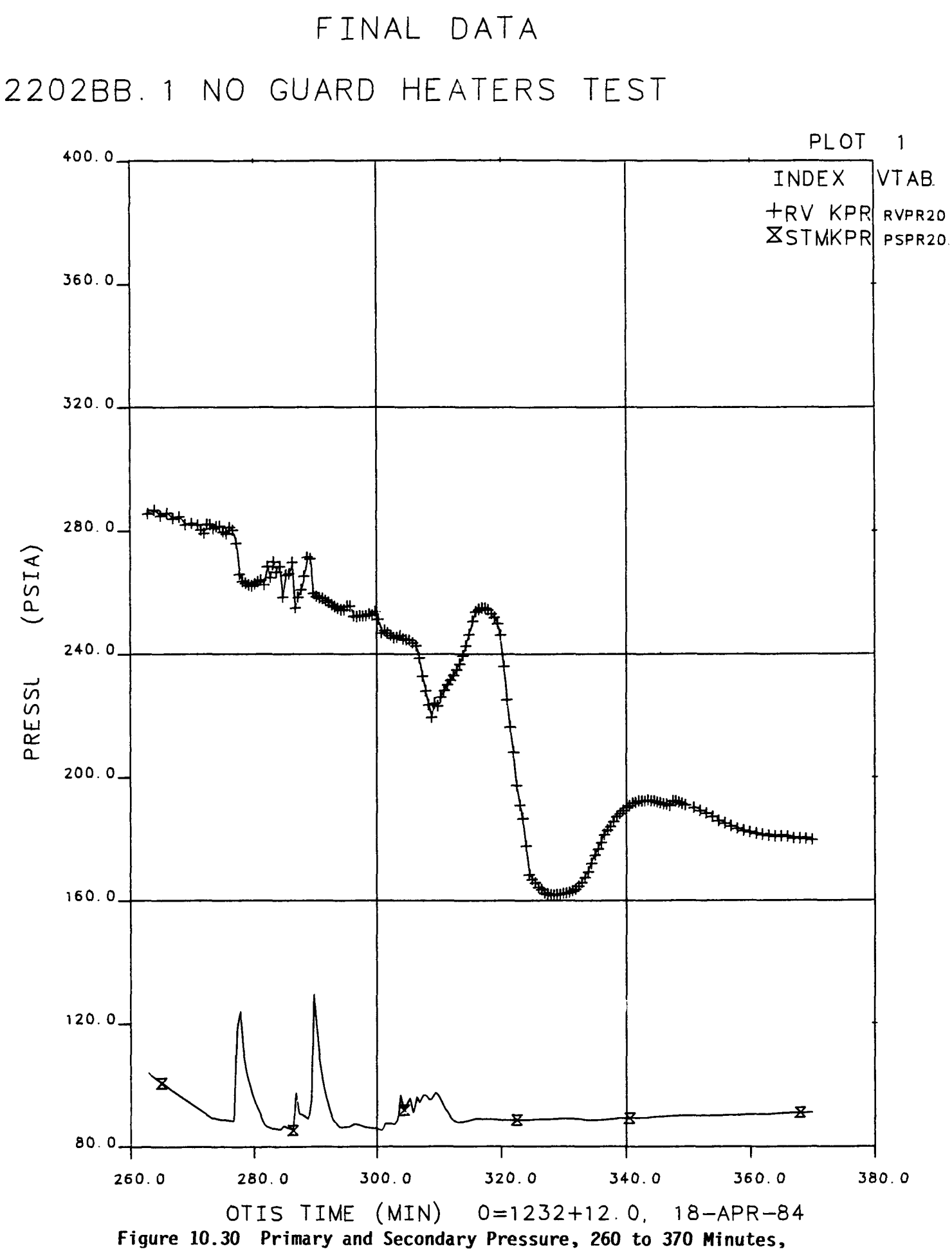

Figure 10.30 Primary and Secondary Pressure, 260 to 370 Minutes, Test 2202BB

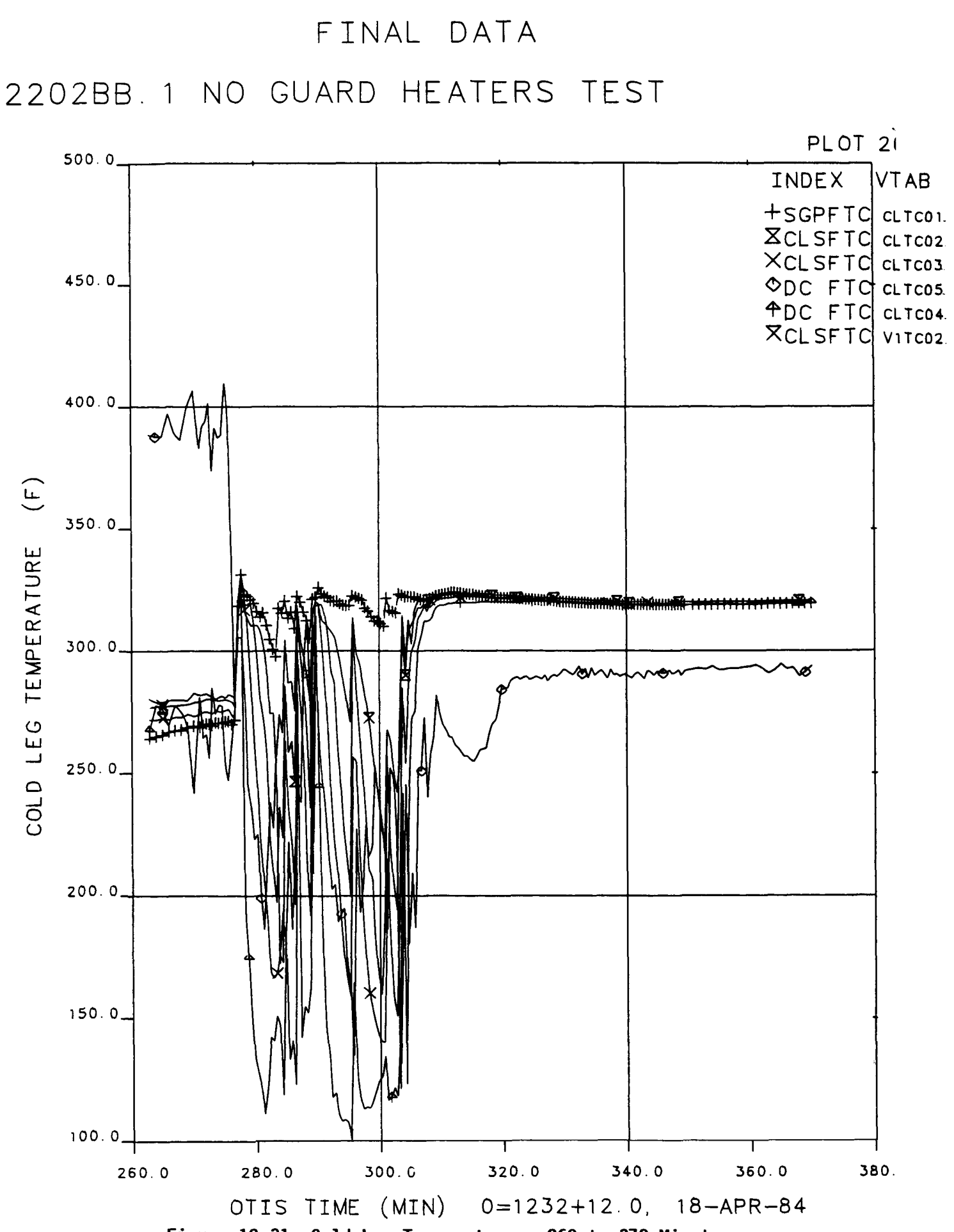

Figure 10.31 Cold Leg Temperatures, 260 to 370 Minutes, Test 2202BB

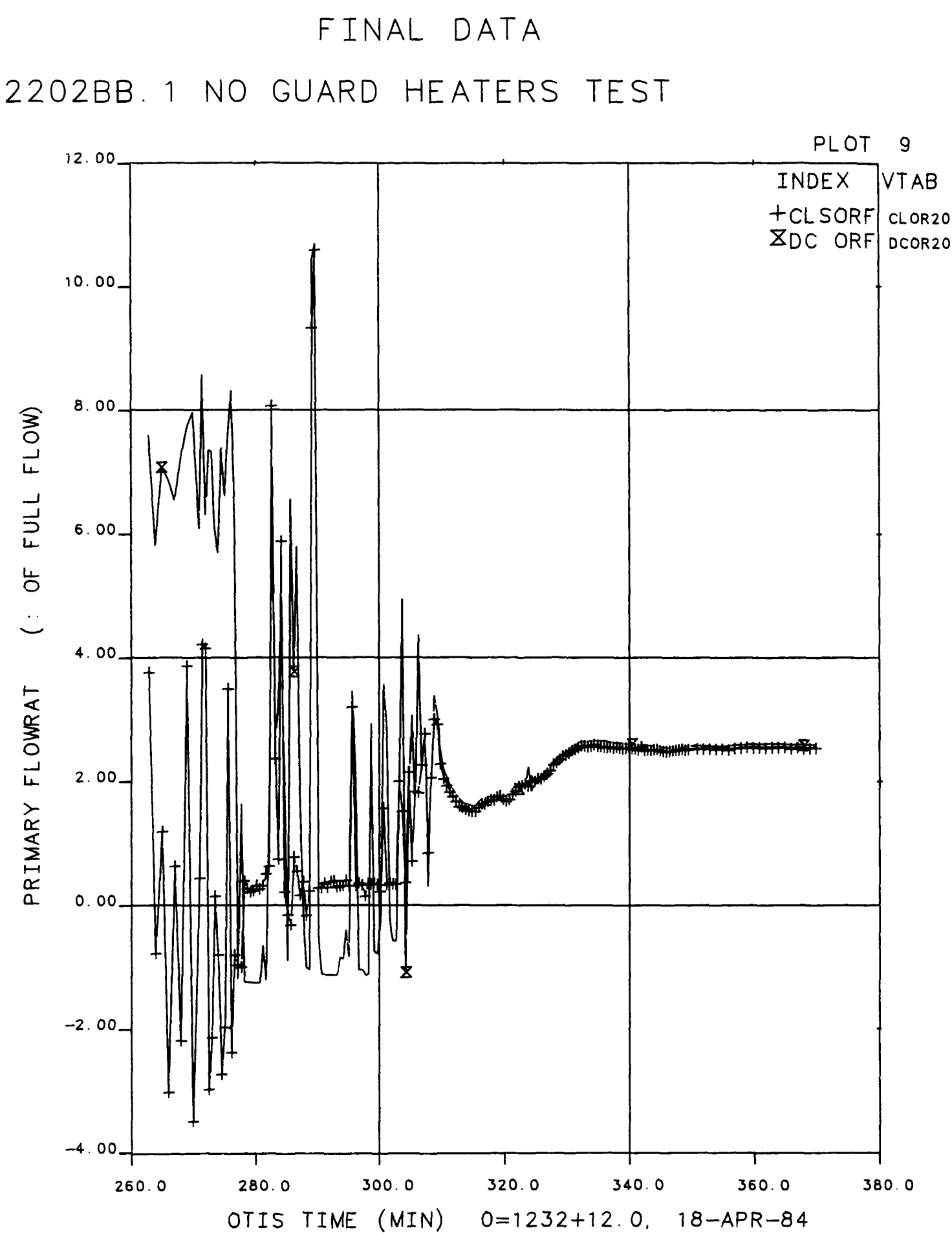

Figure 10.32 Primary Flowrate, 260 to 370 Minutes, Test 2202BB

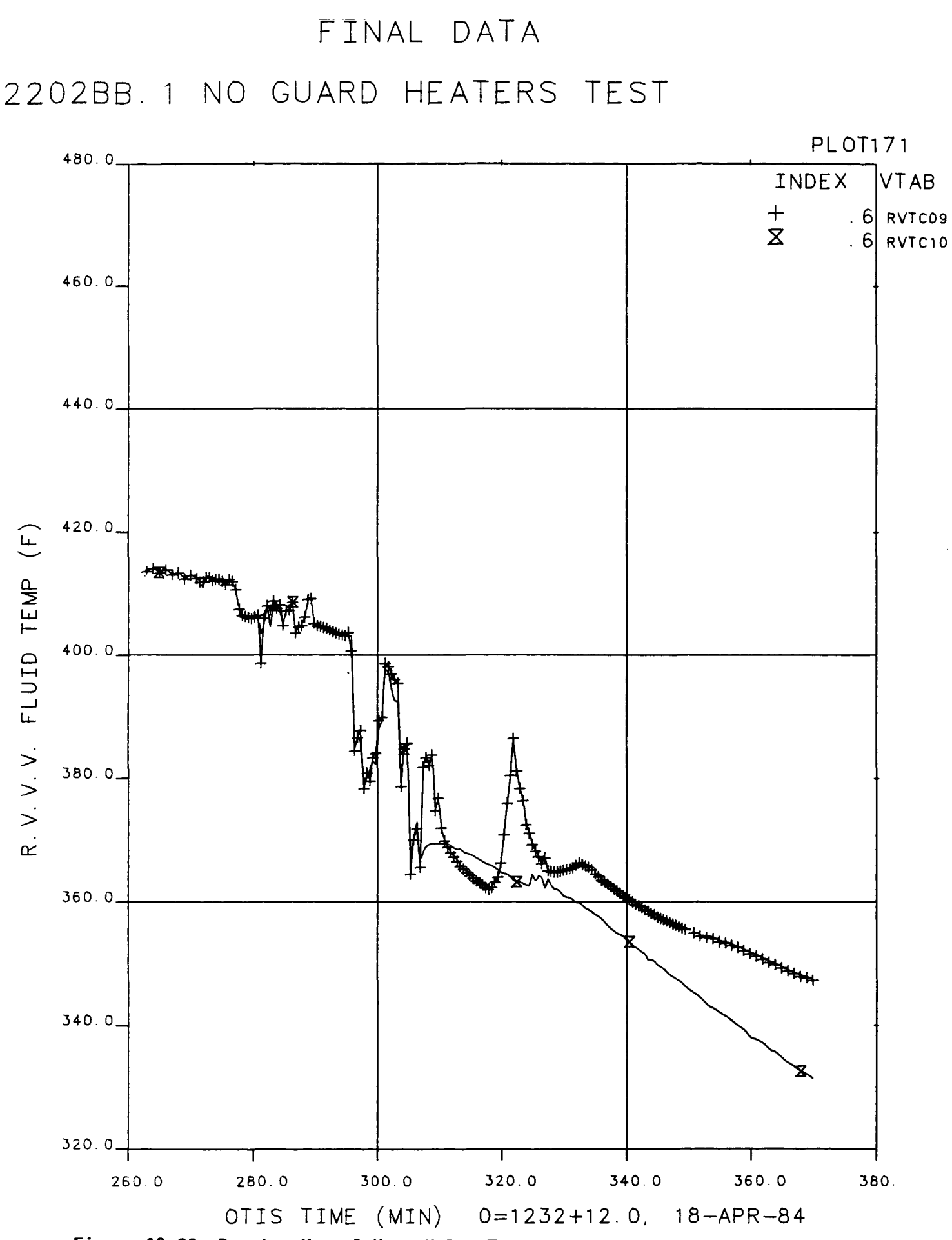

Figure 10.33 Reactor Vessel Vent Valve Temperatures, 260 to 370 Minutes, Test 2202BB

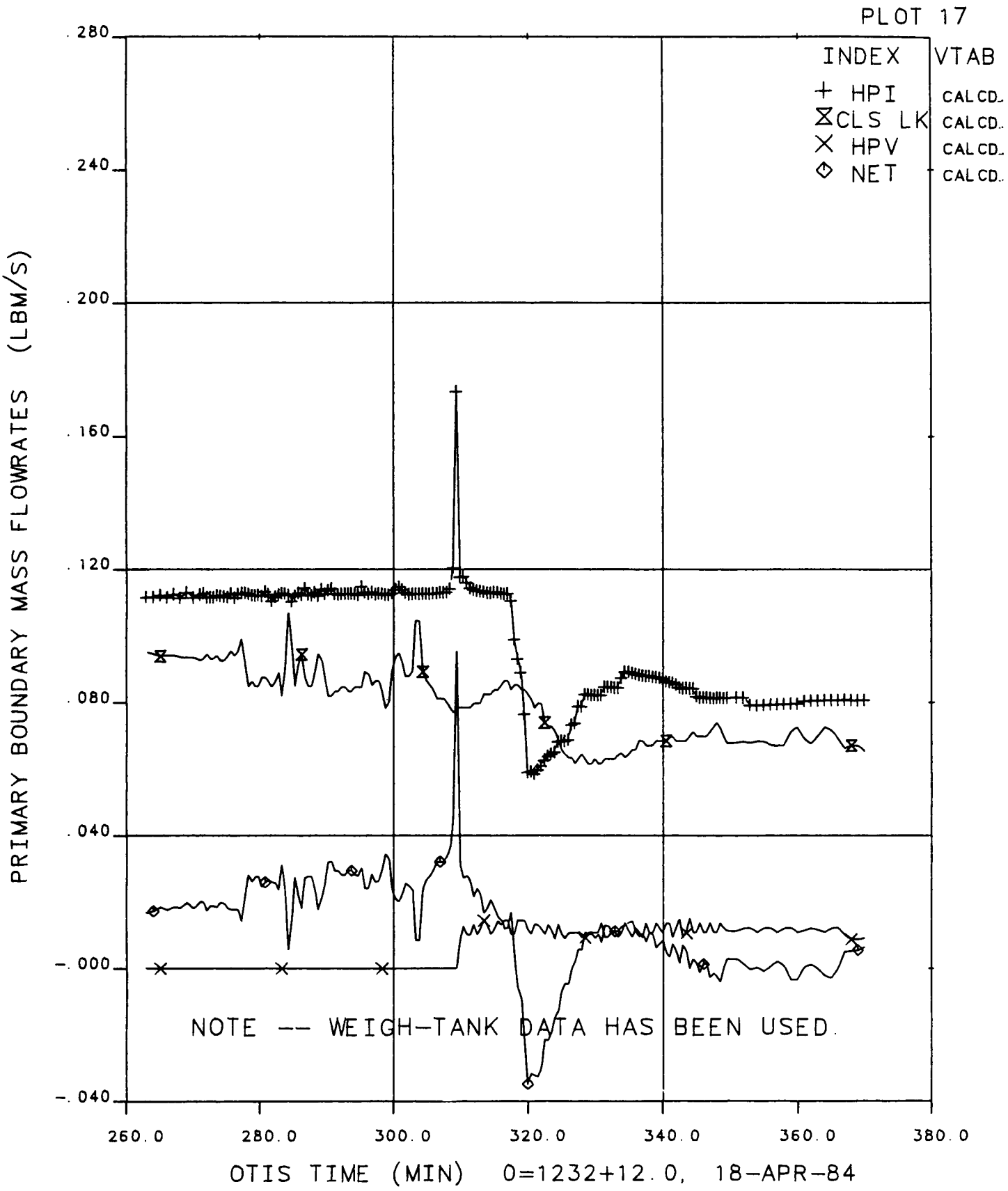

Figure 10.34 Primary Boundary Mass Flowrates, 260 to 370 Minutes, Test 2202BB

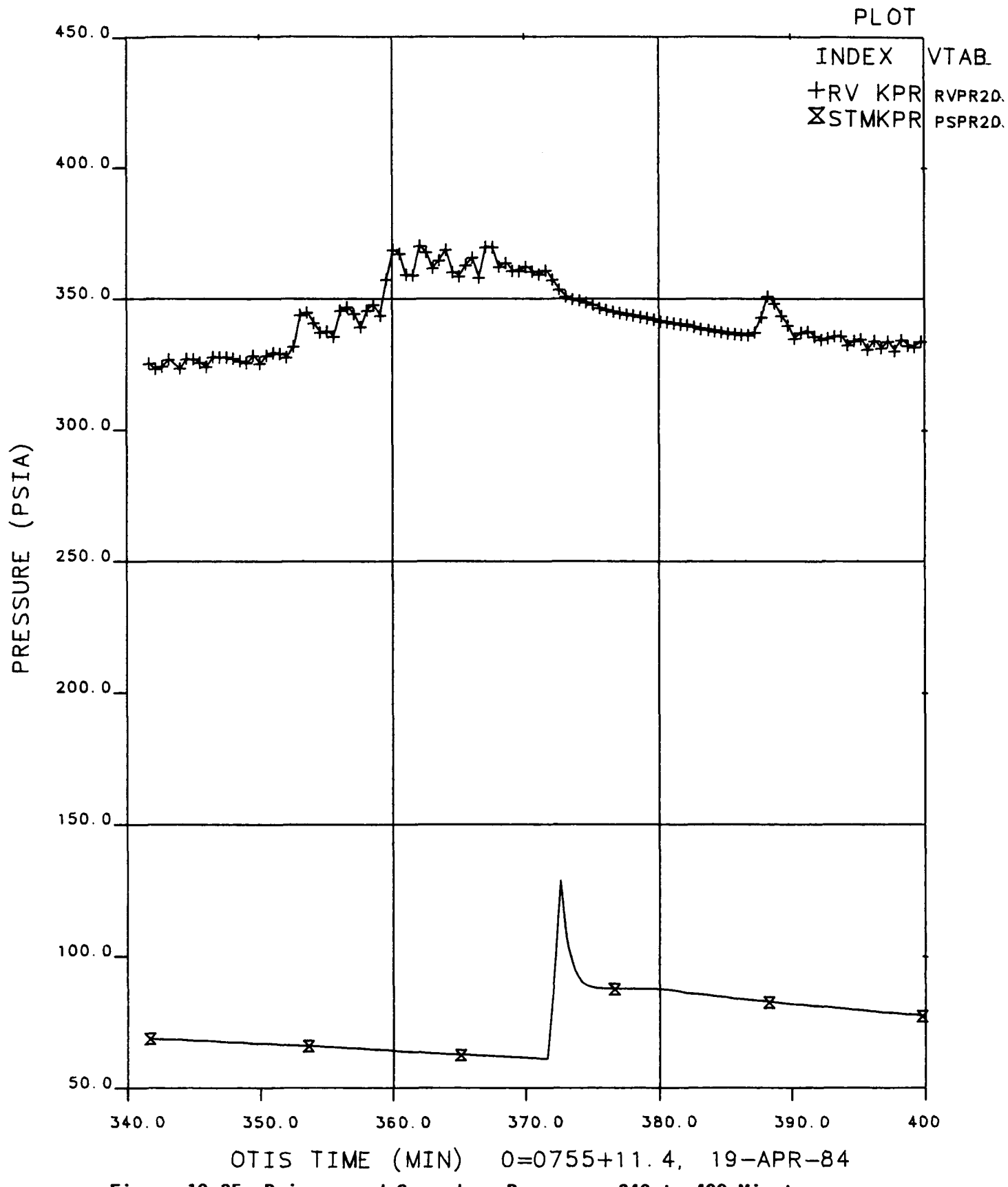

Figure 10.35 Primary and Secondary Pressure, 340 to 400 Minutes, Test 2202AA

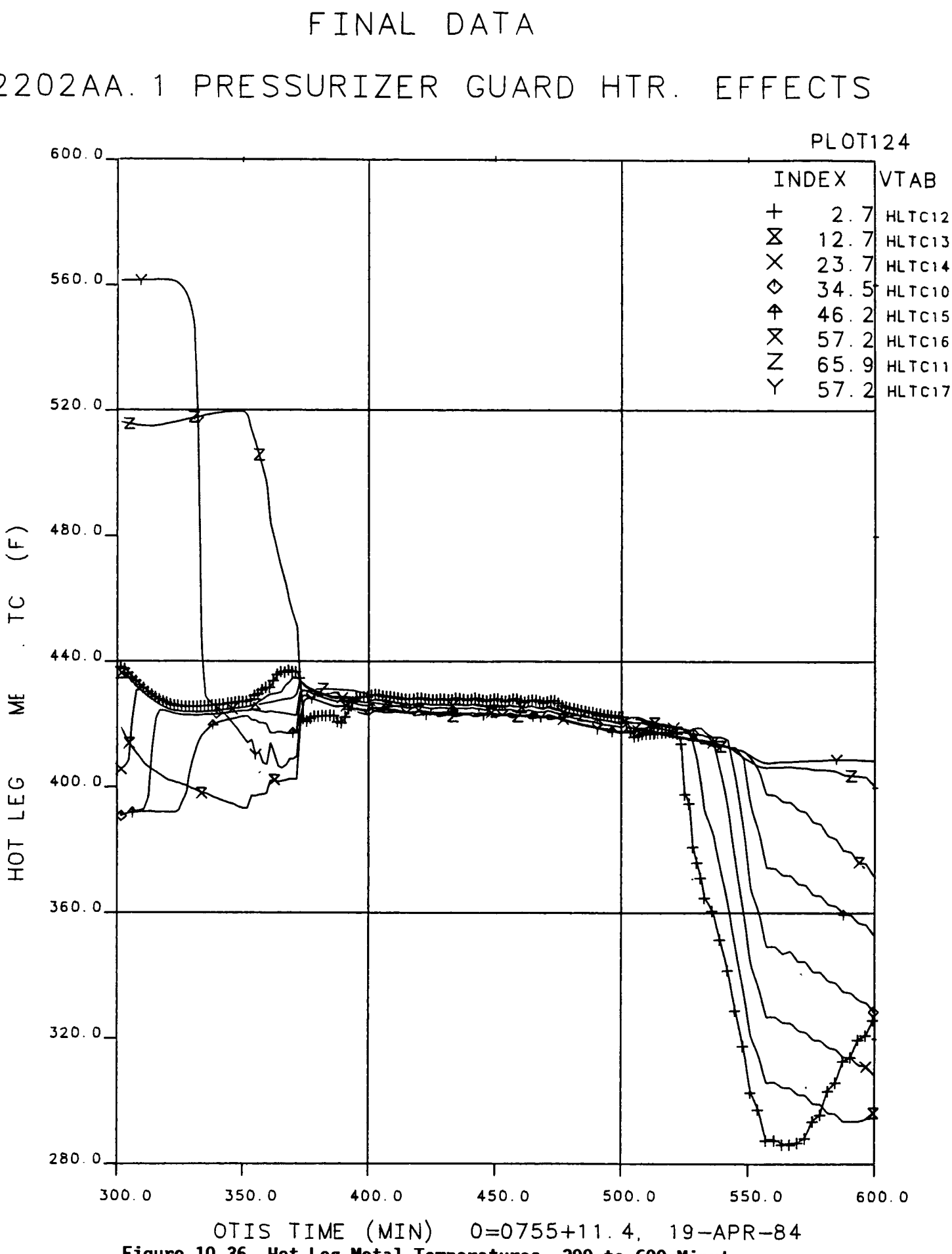

Figure 10.36 Hot Leg Metal Temperatures, 300 to 600 Minutes, Test 2202AA

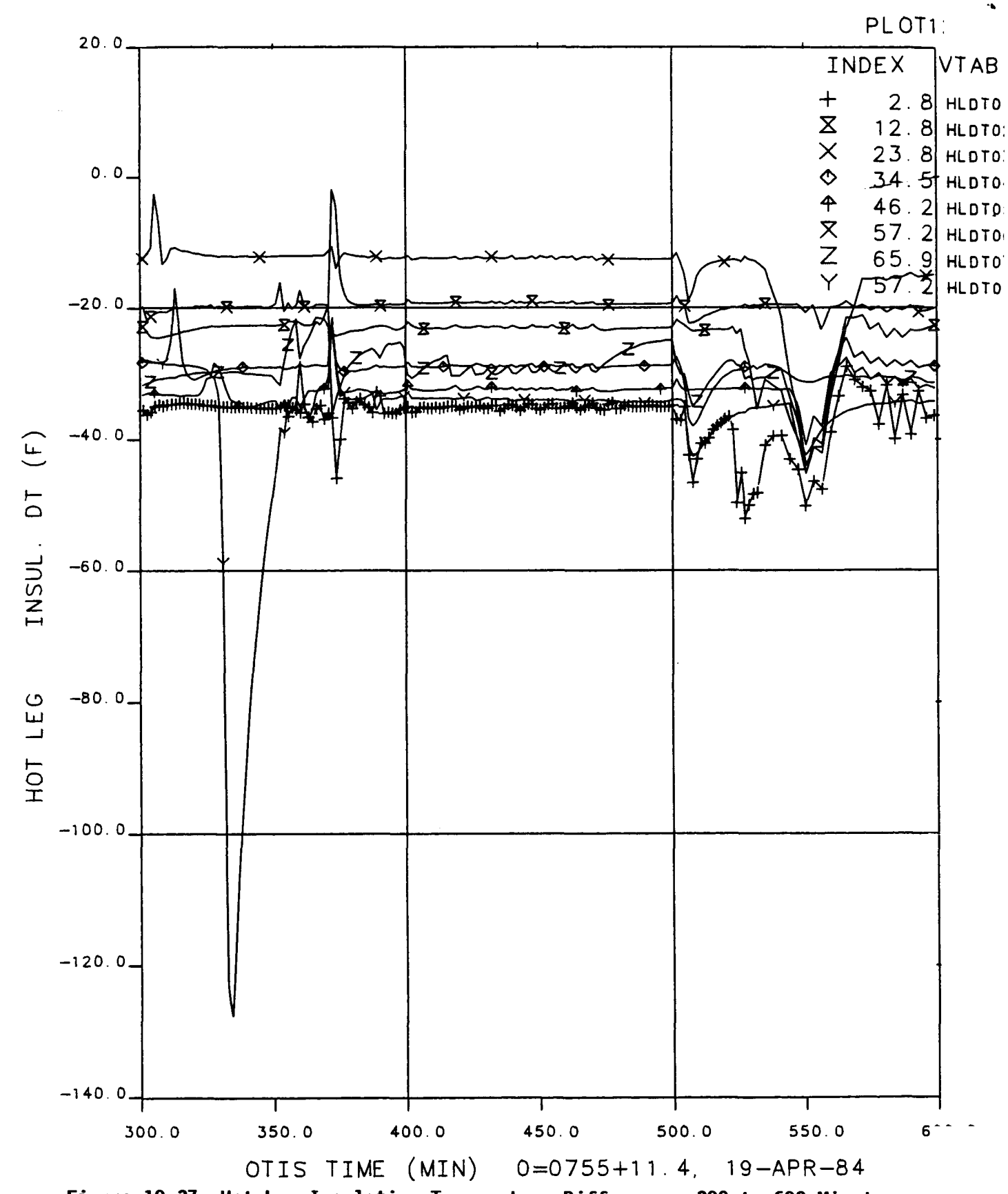

Figure 10.37 Hot Leg Insulation Temperature Difference, 300 to 600 Minutes, Test 2202AA

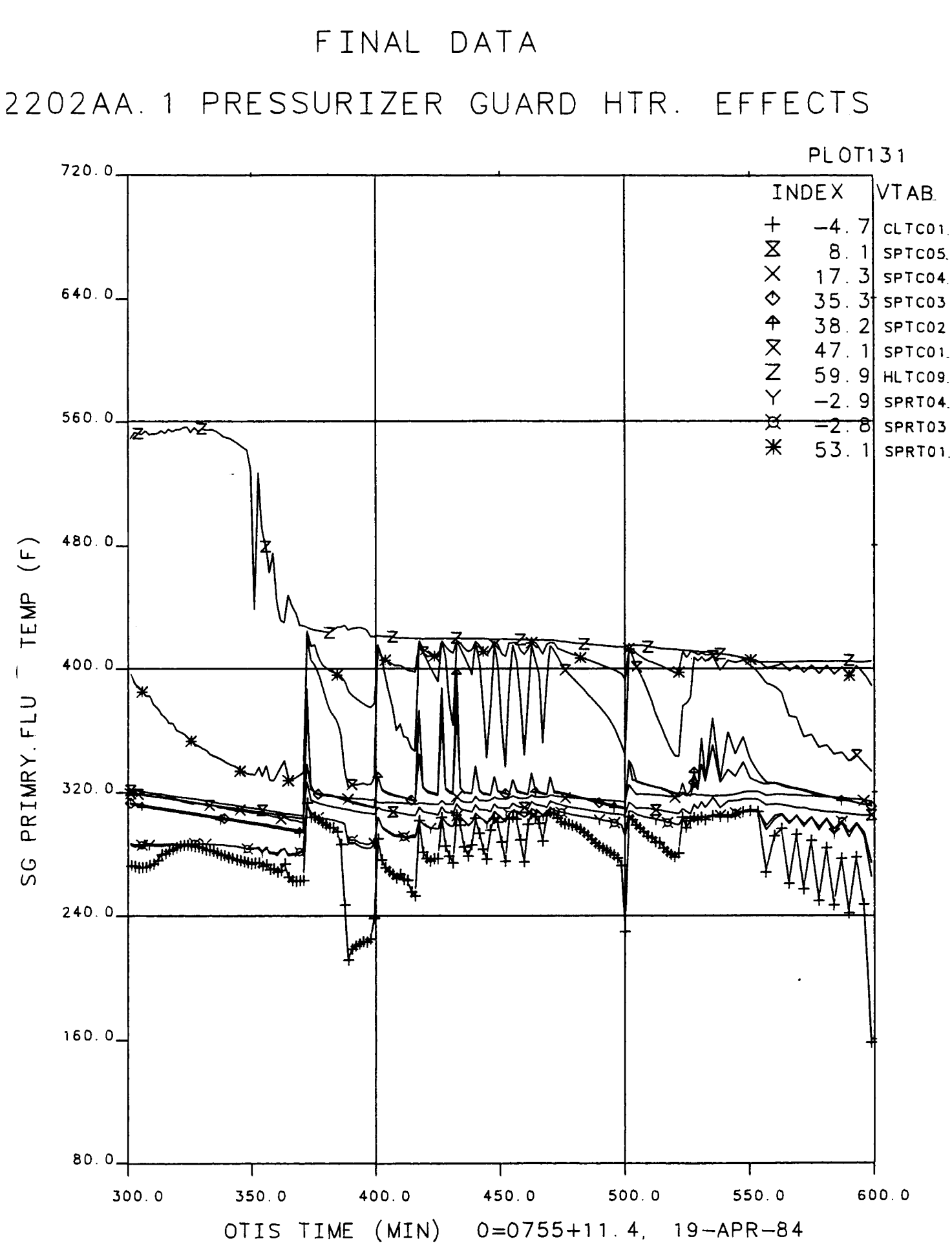

Figure 10.38 Steam Generator Primary Fluid Temperatures, 300 to 600 Minutes, Test 2202AA

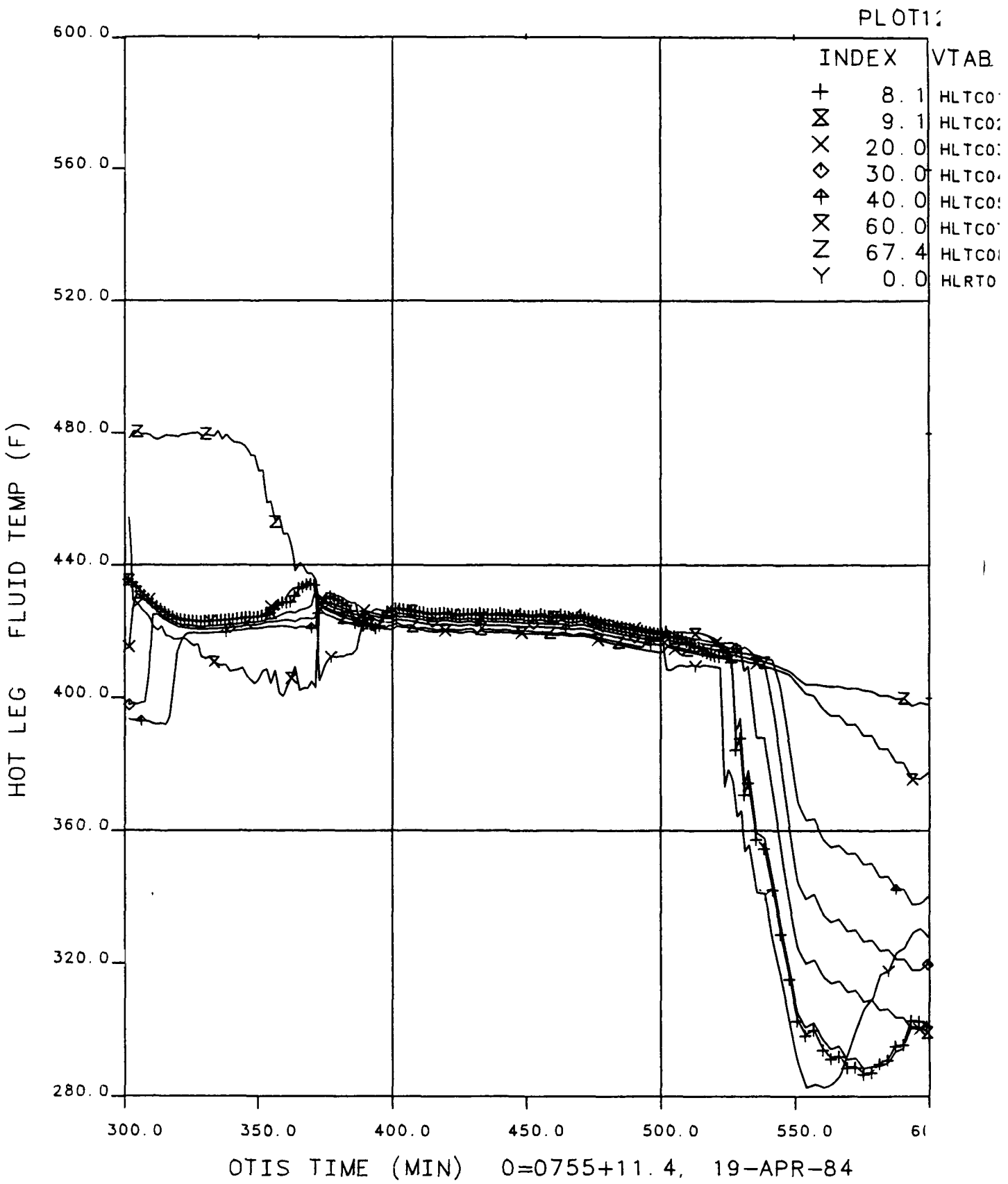

Figure 10.39 Hot Leg Fluid Temperatures, 300 to 600 Minutes, Test 2202AA

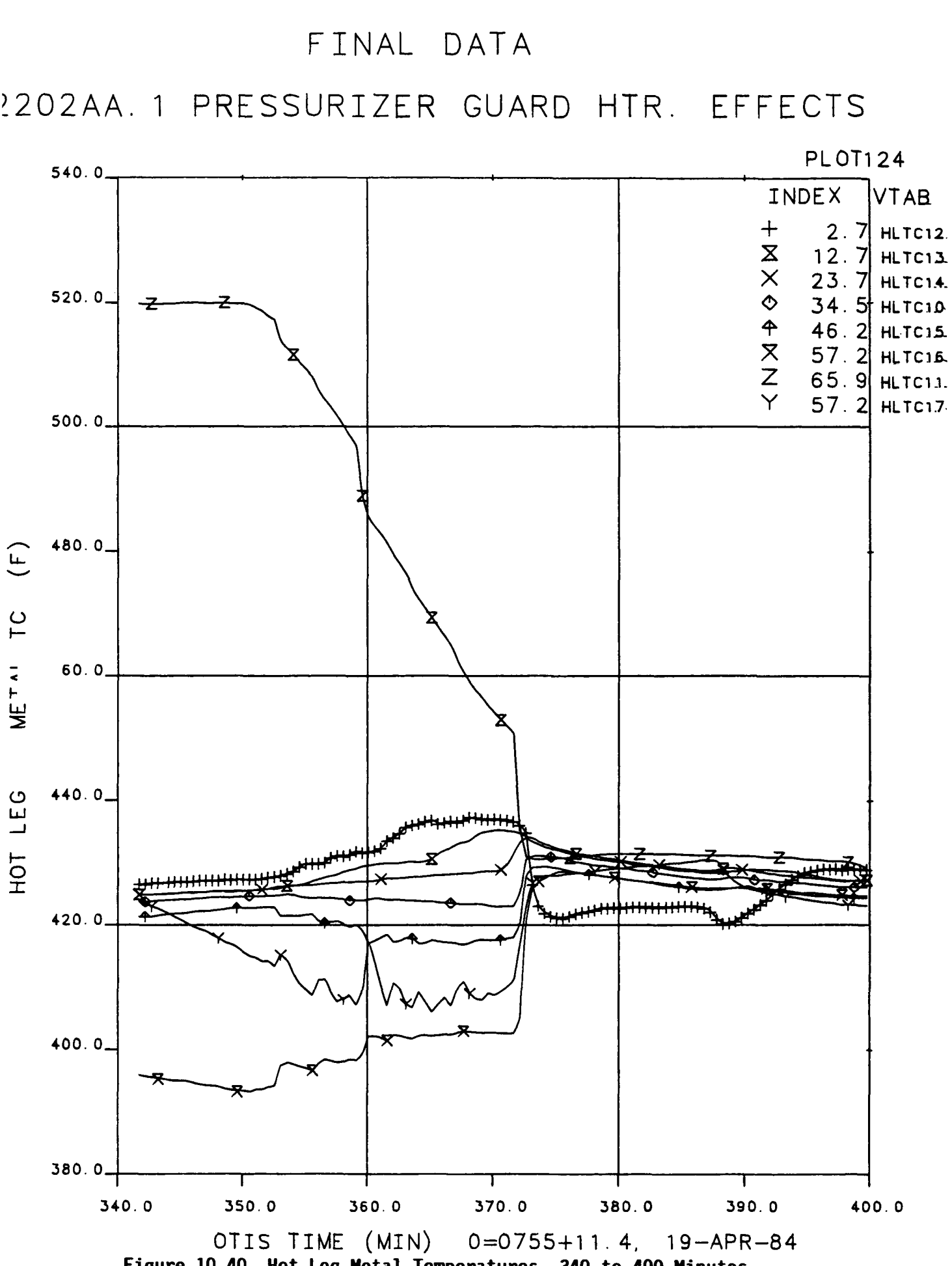

Figure 10.40 Hot Leg Metal Temperatures, 340 to 400 Minutes, Test 2202AA

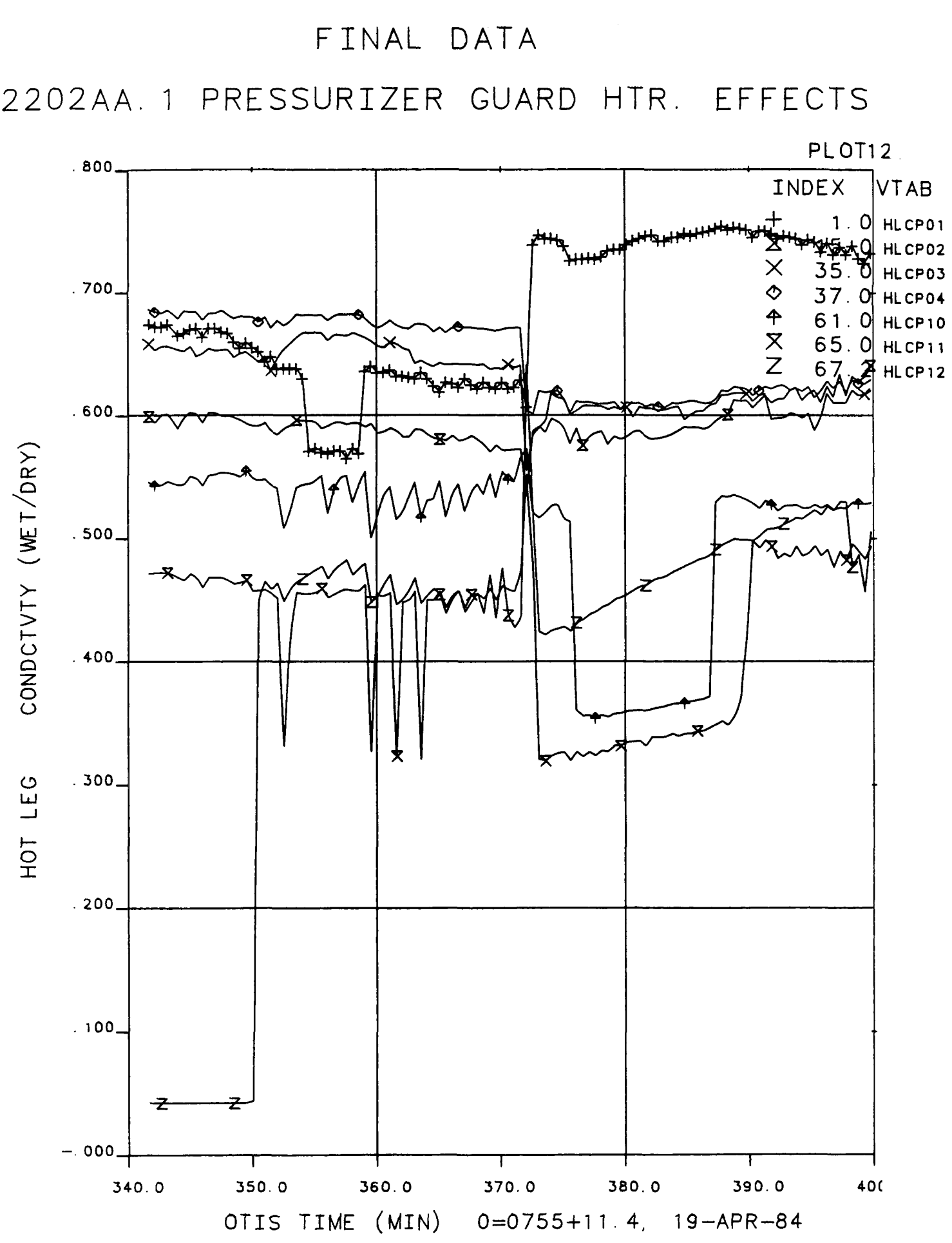

Figure 10.41 Hot Leg Conductivity Probe Responses, 340 to 400 Minutes, Test 2202AA

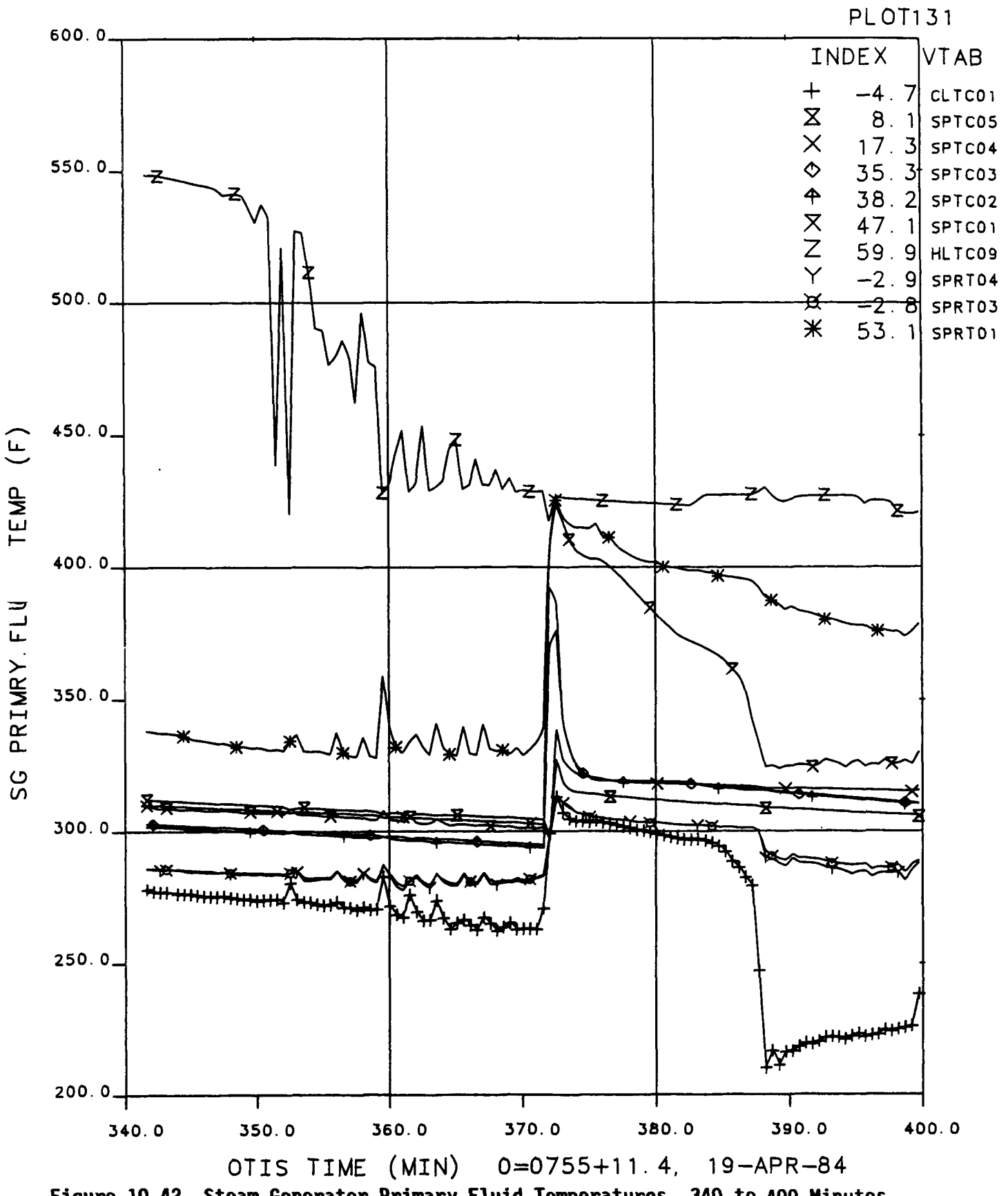

Figure 10.42 Steam Generator Primary Fluid Temperatures, 340 to 400 Minutes, Test 2202AA

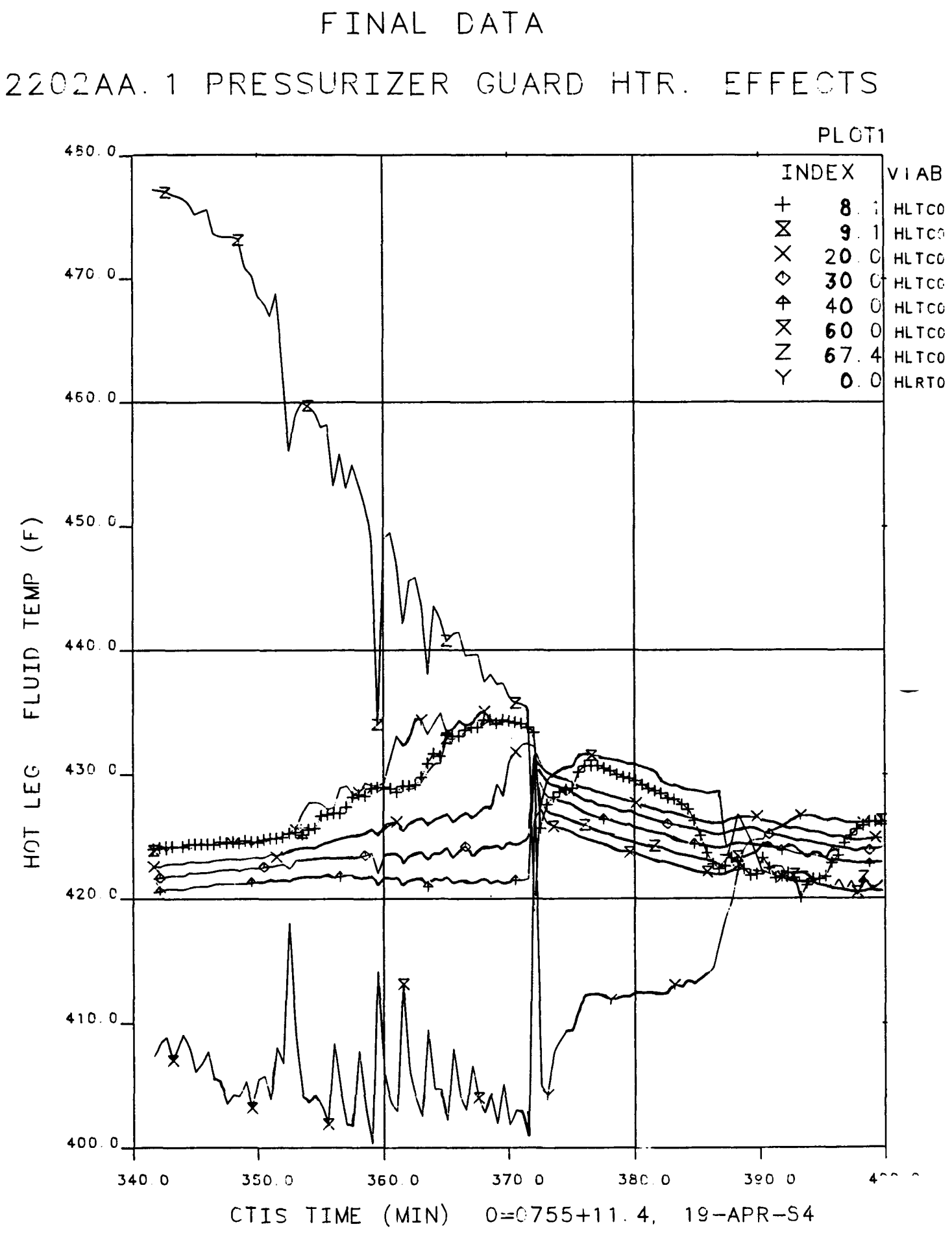

Figure 10.43 Hot Leg Fluid Temperatures, 340 to 400 Minutes, Test 2202AA

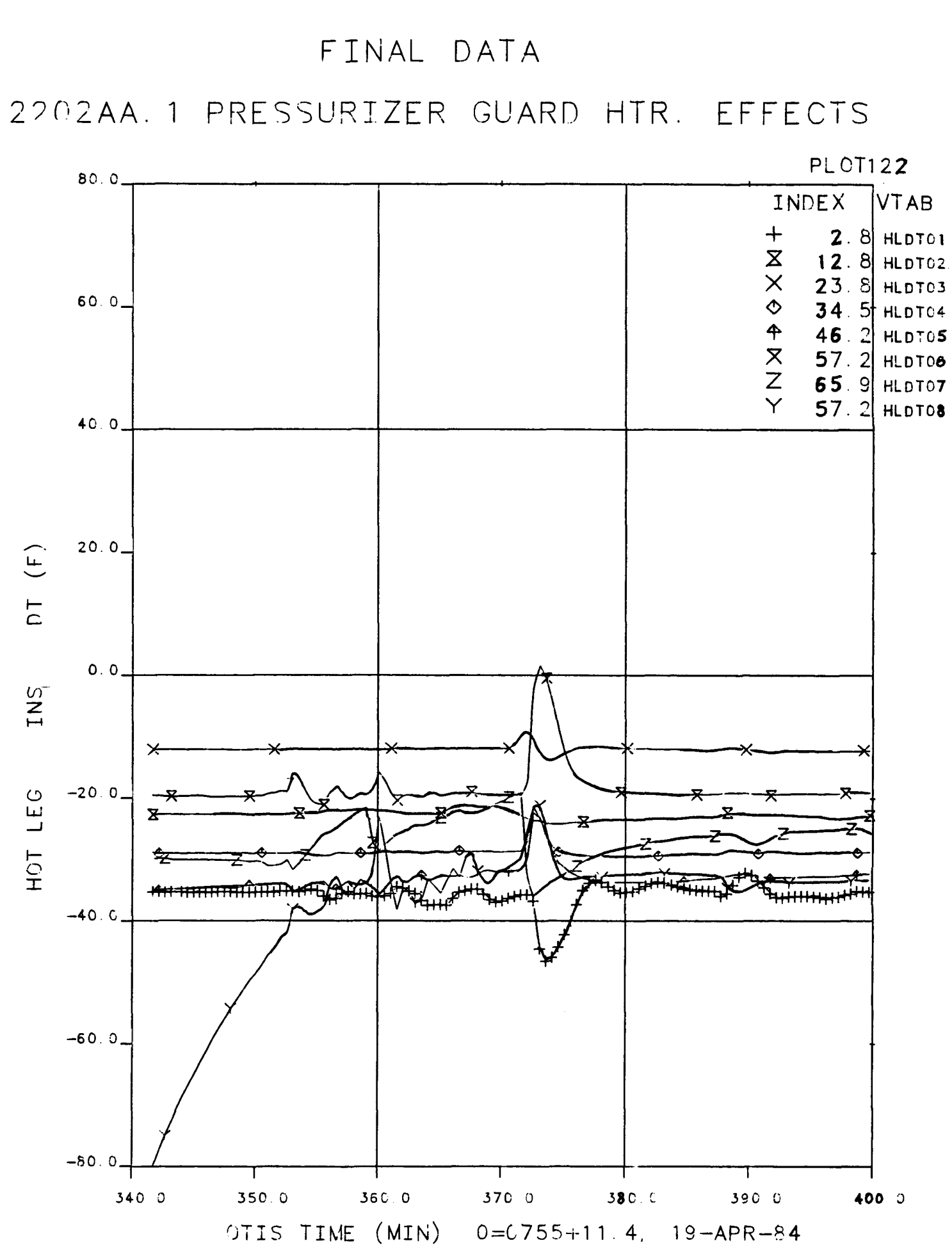

Figure 10.44 Hot Leg Insulation Temperature Difference, 340 to 400 Minutes, Test 2202AA

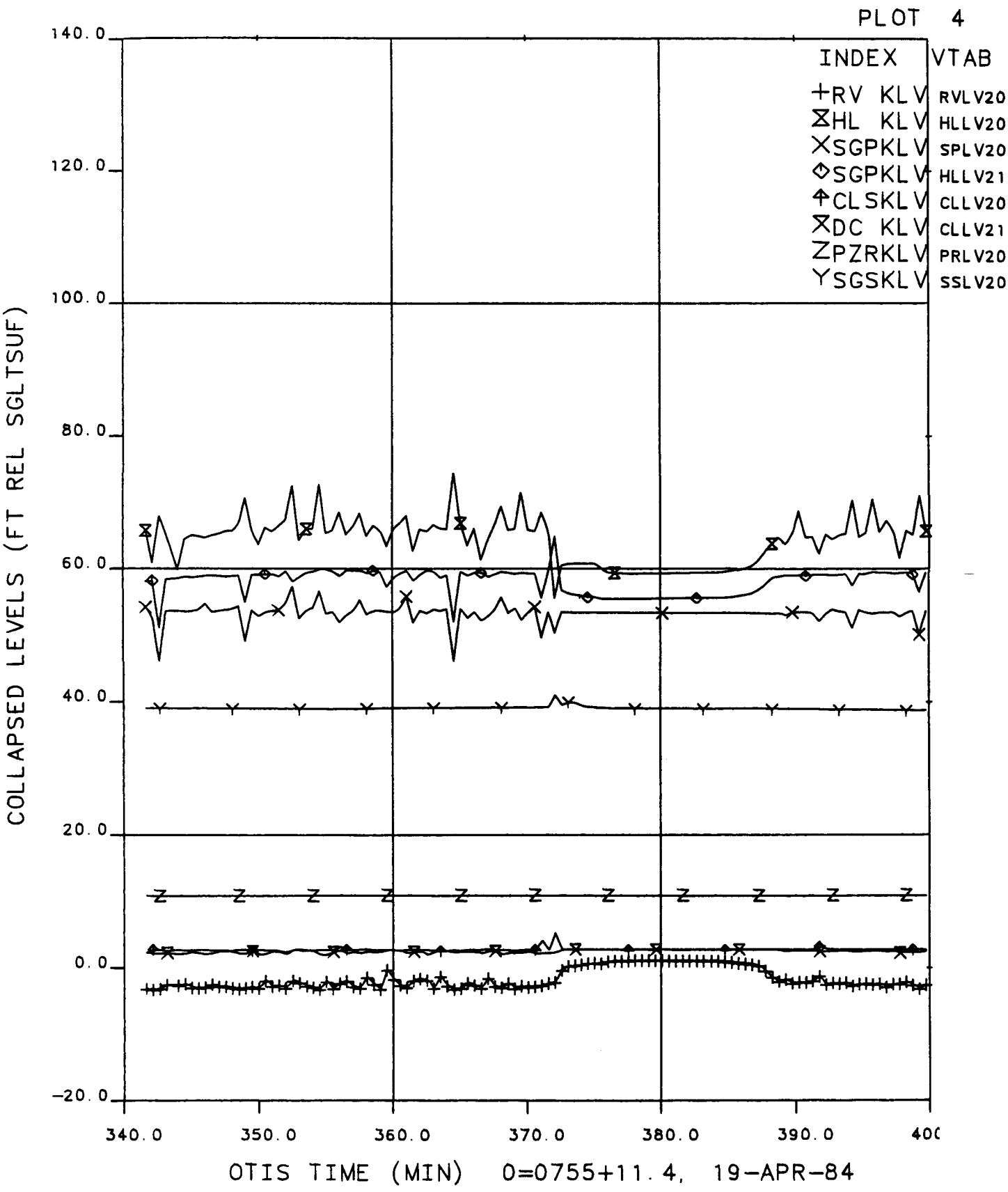

Figure 10.45 Collapsed Liquid Levels, 340 to 400 Minutes, Test 2202AA

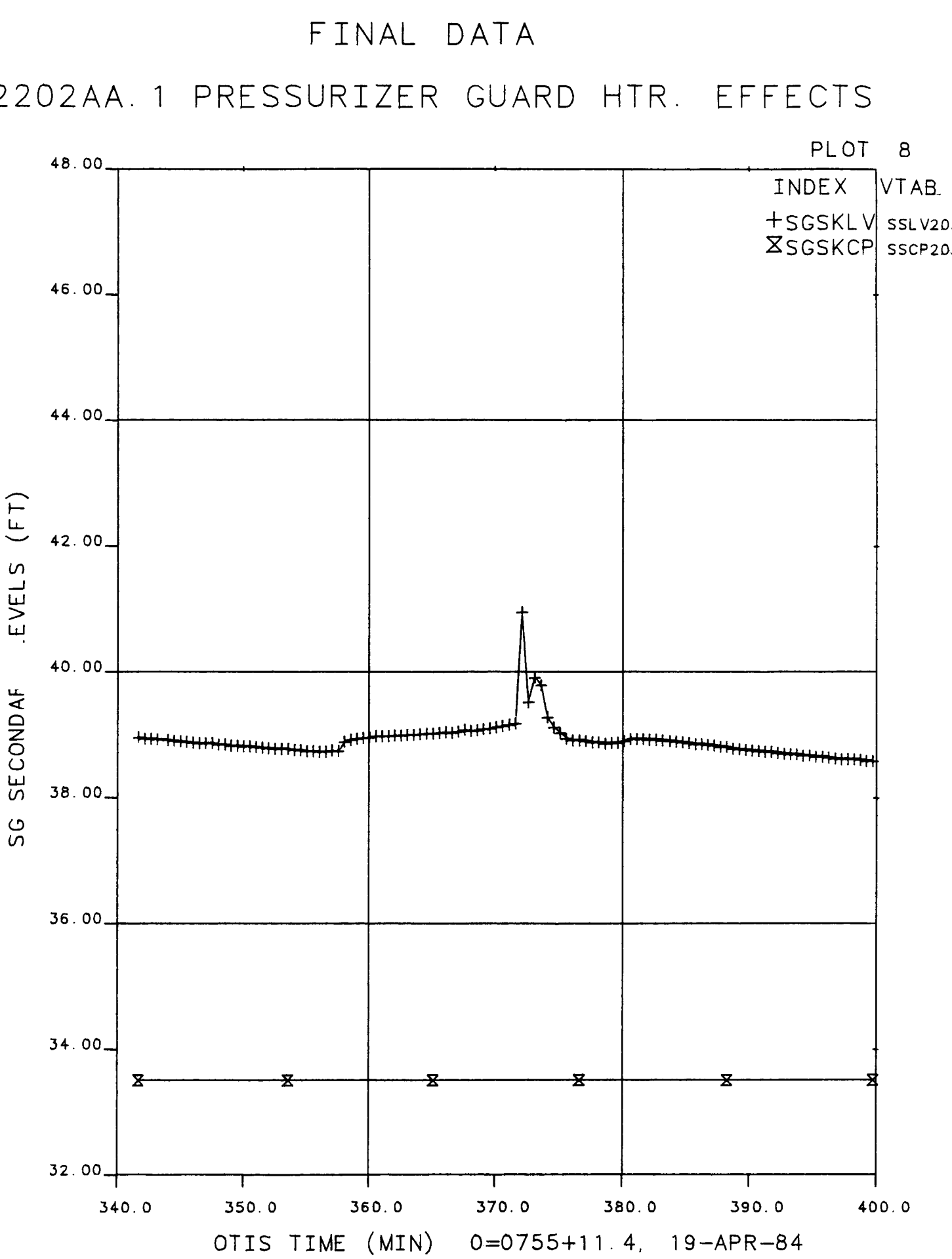

Figure 10.46 Steam Generator Secondary Level, 340 to 400 Minutes, Test 2202AA

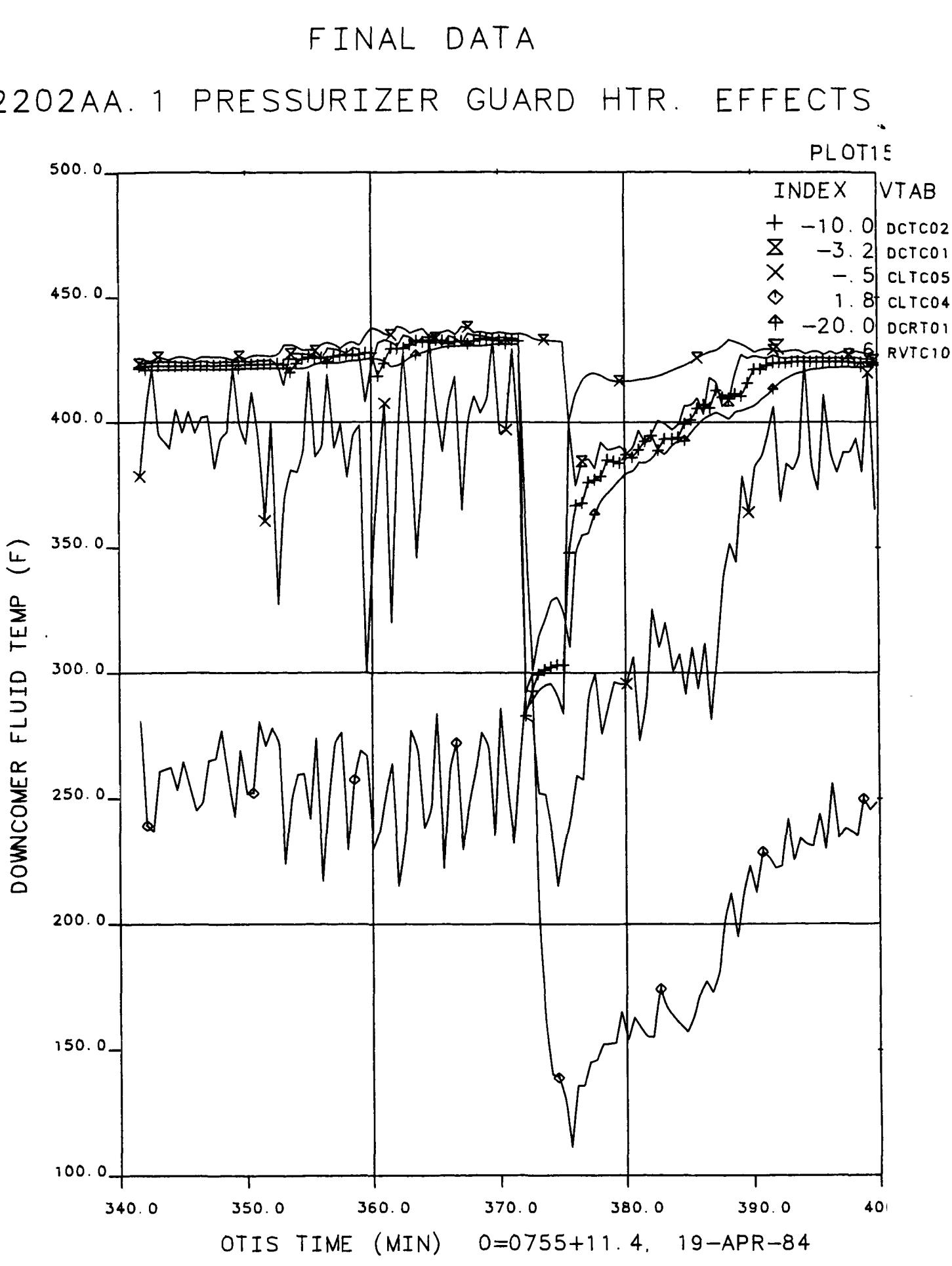

Figure 10.47 Downcomer Fluid Temperatures, 340 to 400 Minutes, Test 2202AA

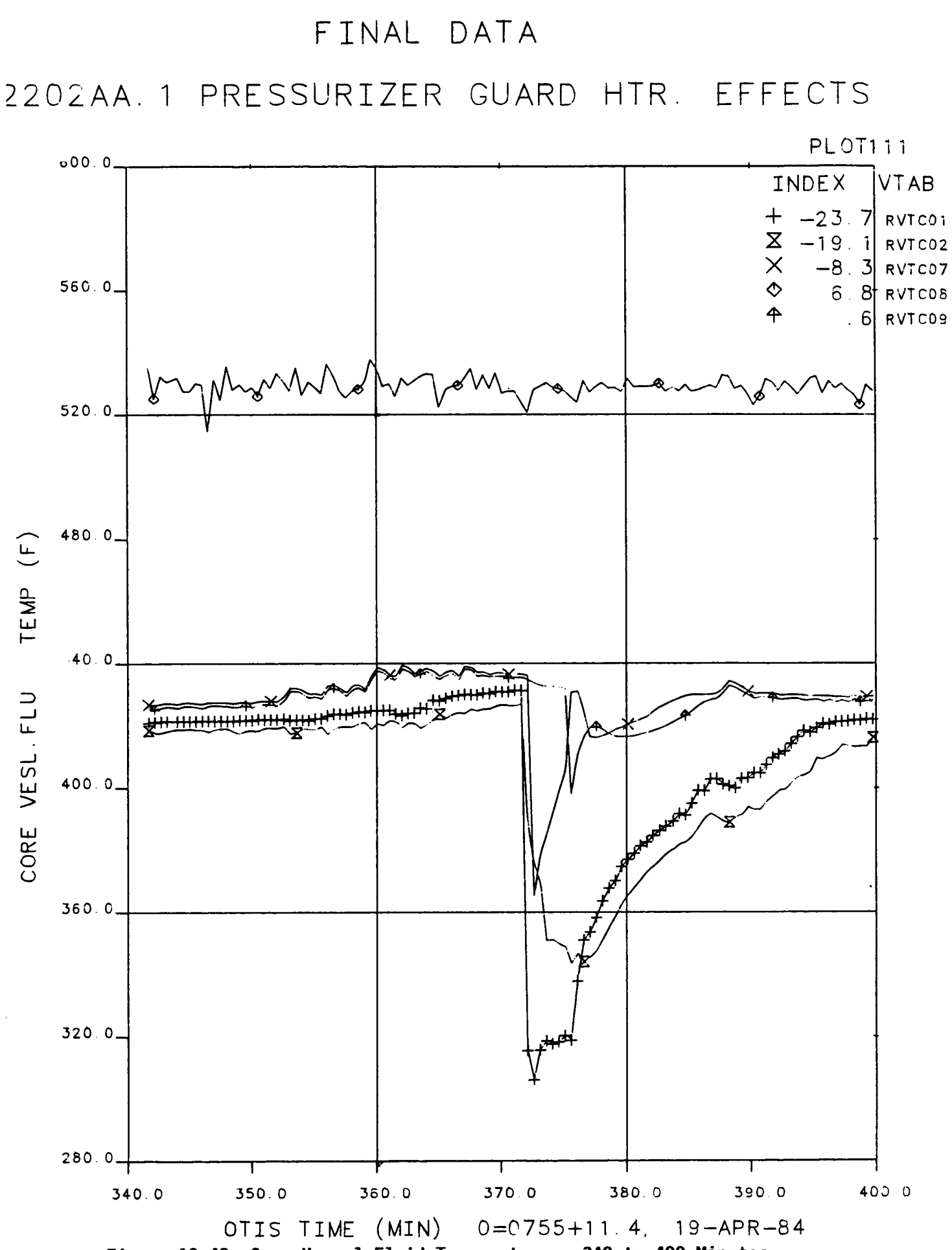

Figure 10.48 Core Vessel Fluid Temperatures, 340 to 400 Minutes, Test 2202AA

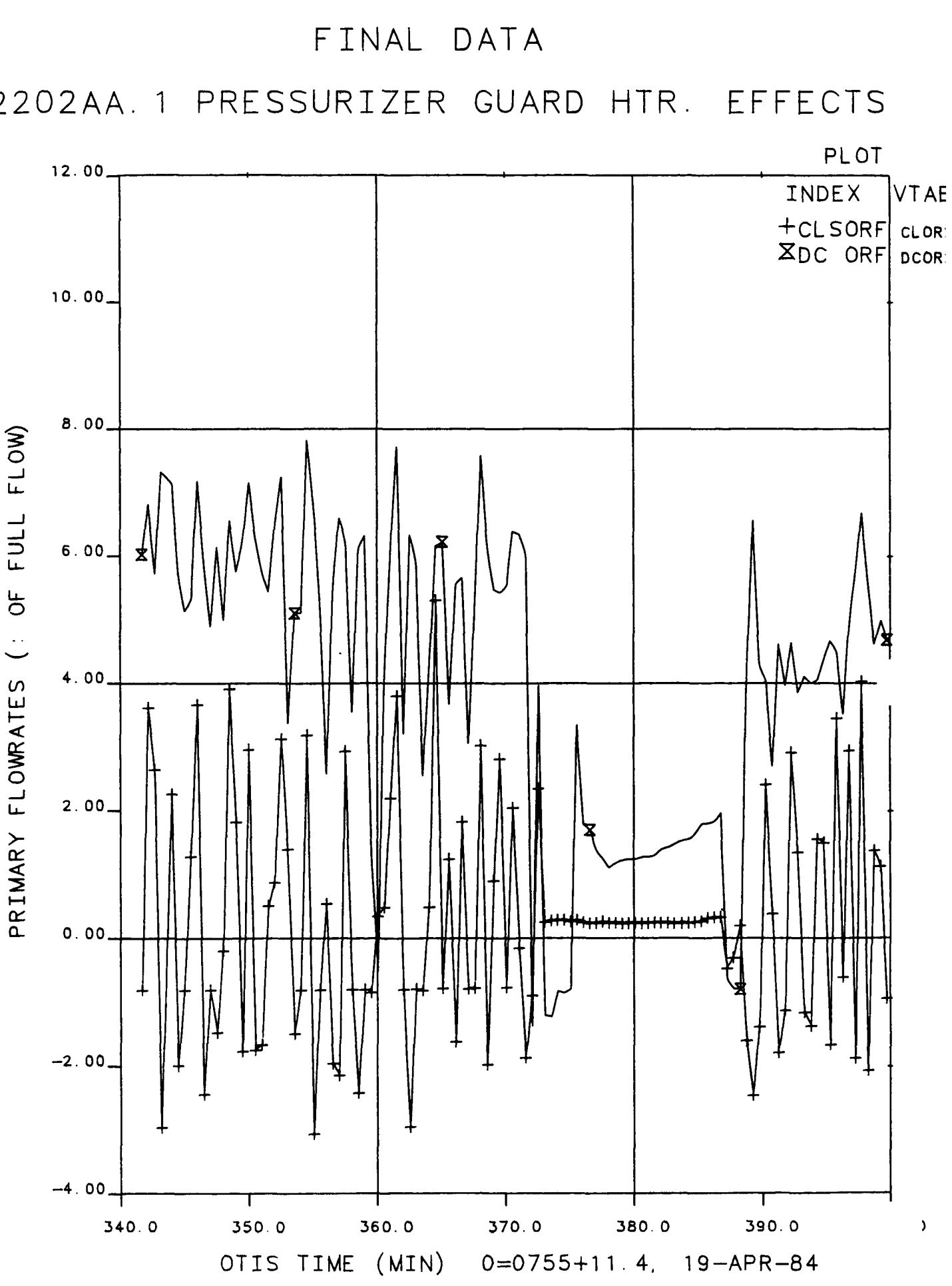

Figure 10.49 Primary Flowrates, 340 to 400 Minutes, Test 2202AA

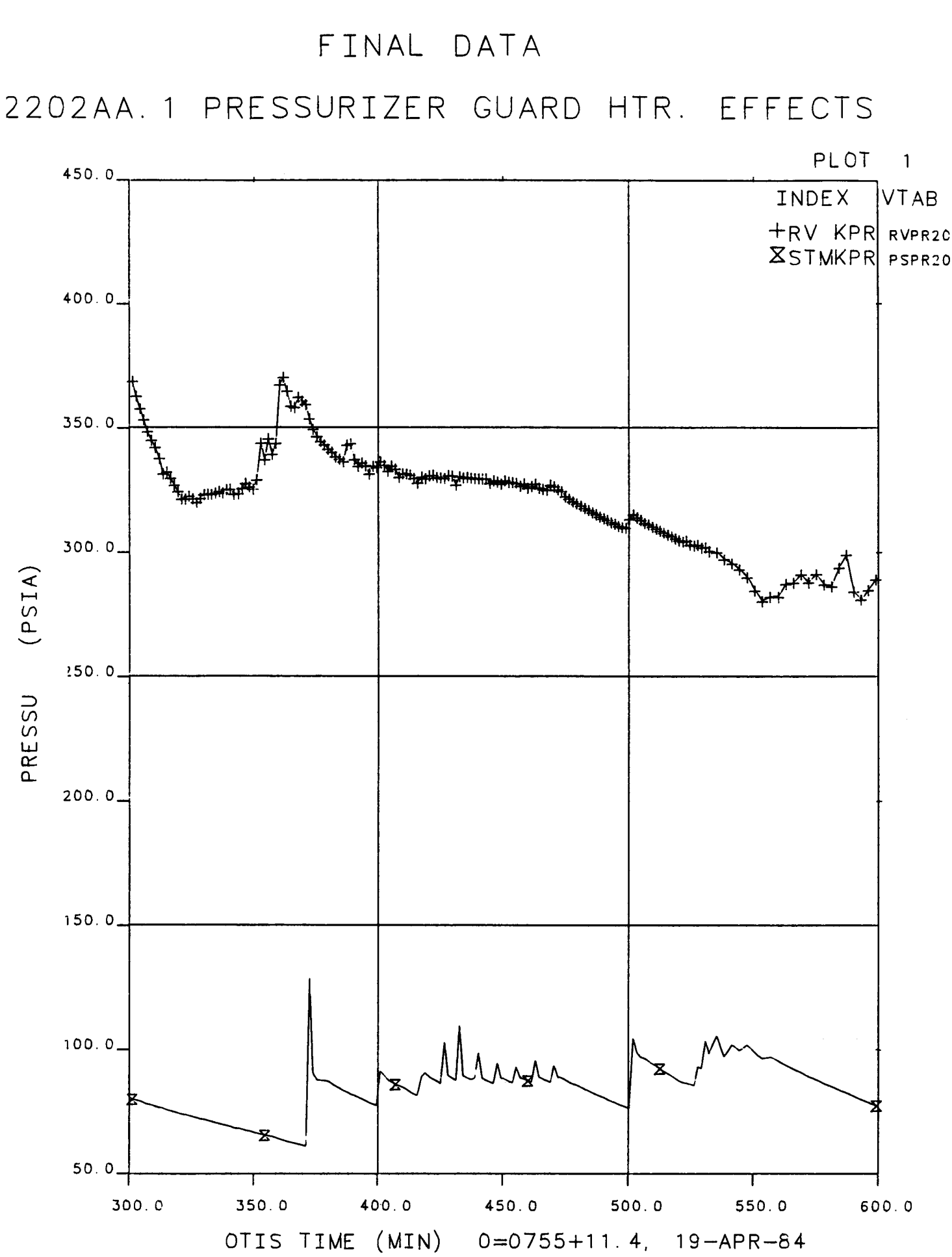

Figure 10.50 Primary and Secondary Pressure, 300 to 600 Minutes, Test 2202AA

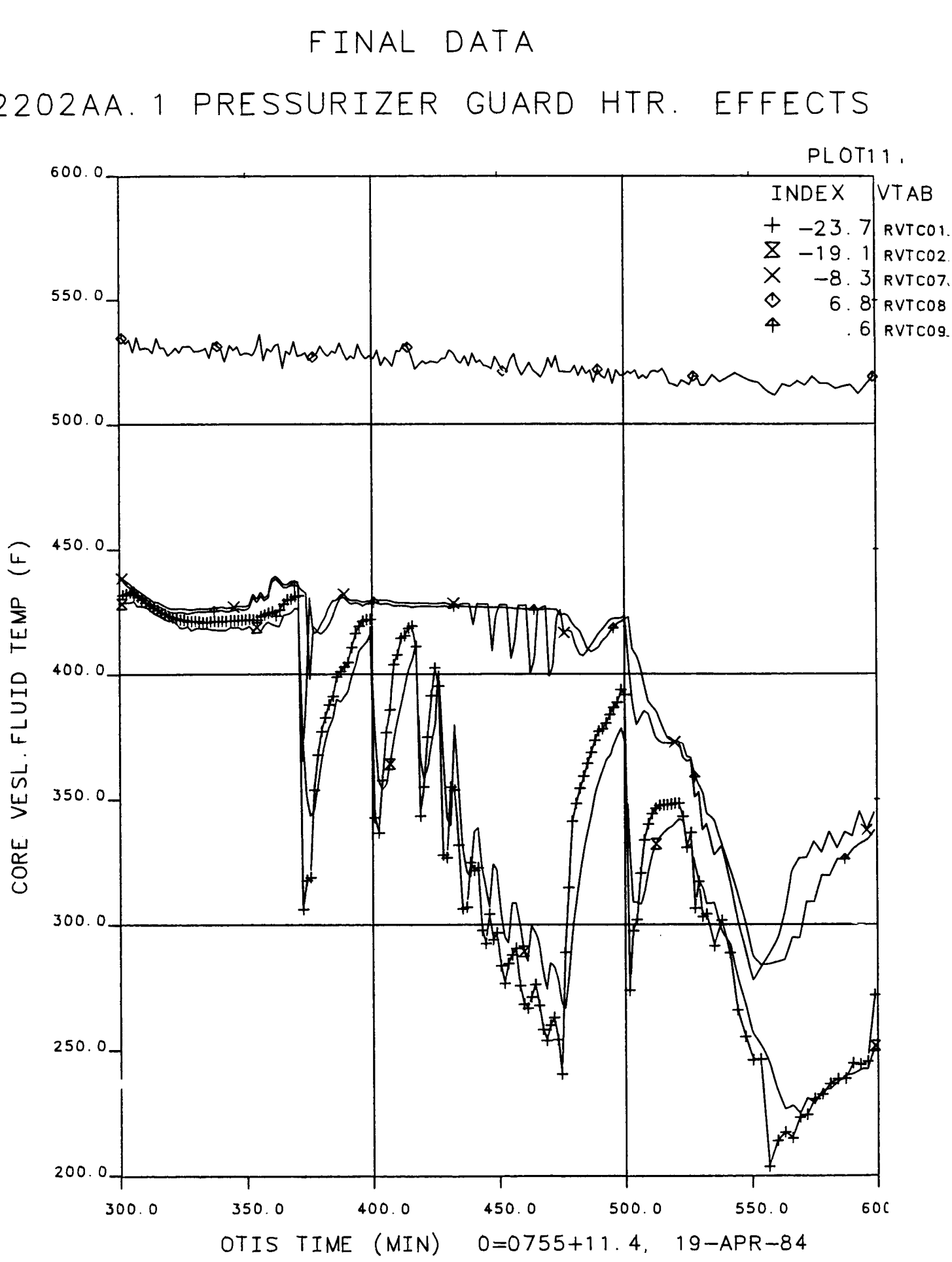

Figure 10.51 Core Vessel Fluid Temperatures, 300 to 600 Minutes, Test 2202AA

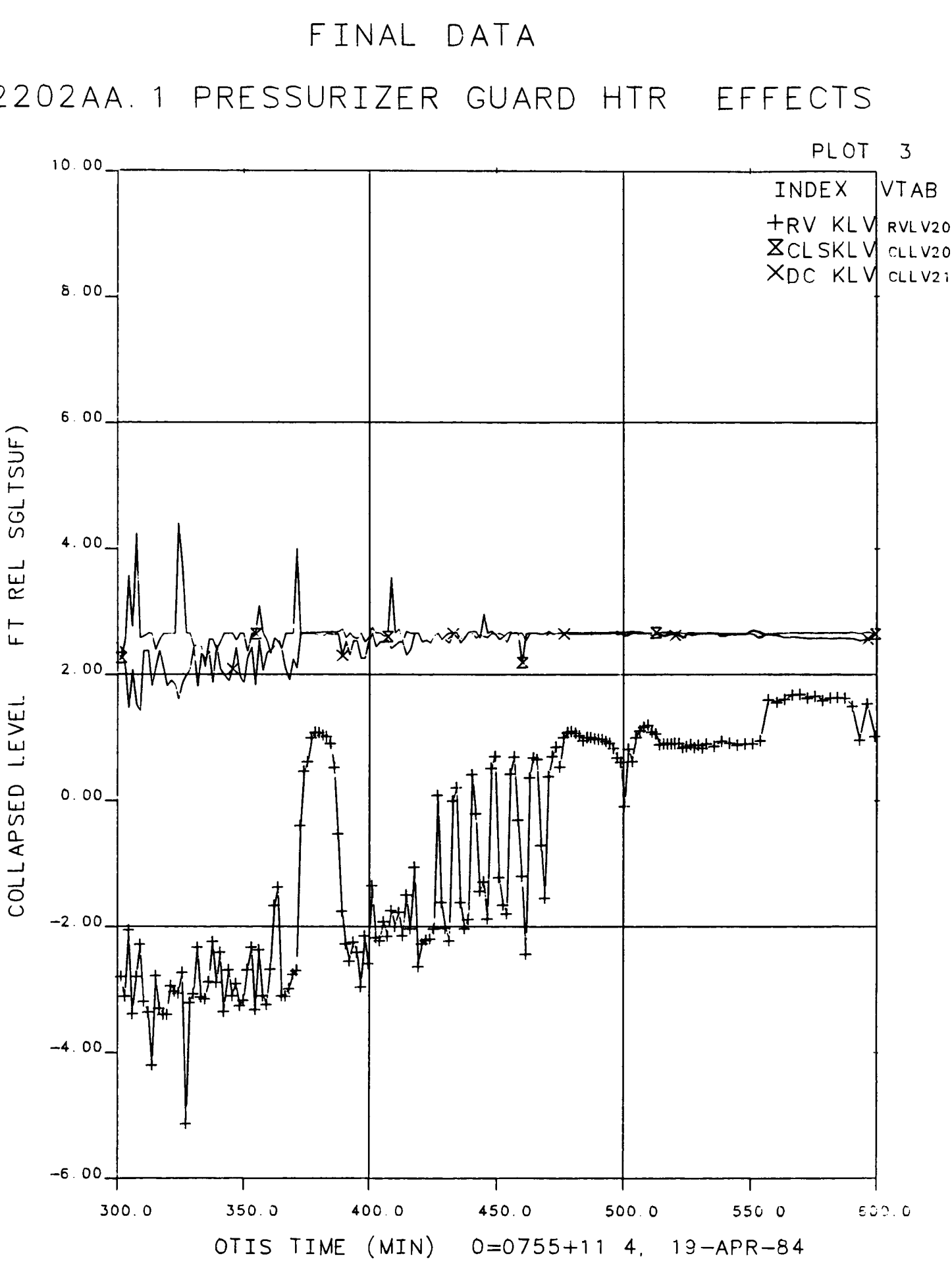

Figure 10.52 Collapsed Liquid Levels, 300 to 600 Minutes, Test 2202AA

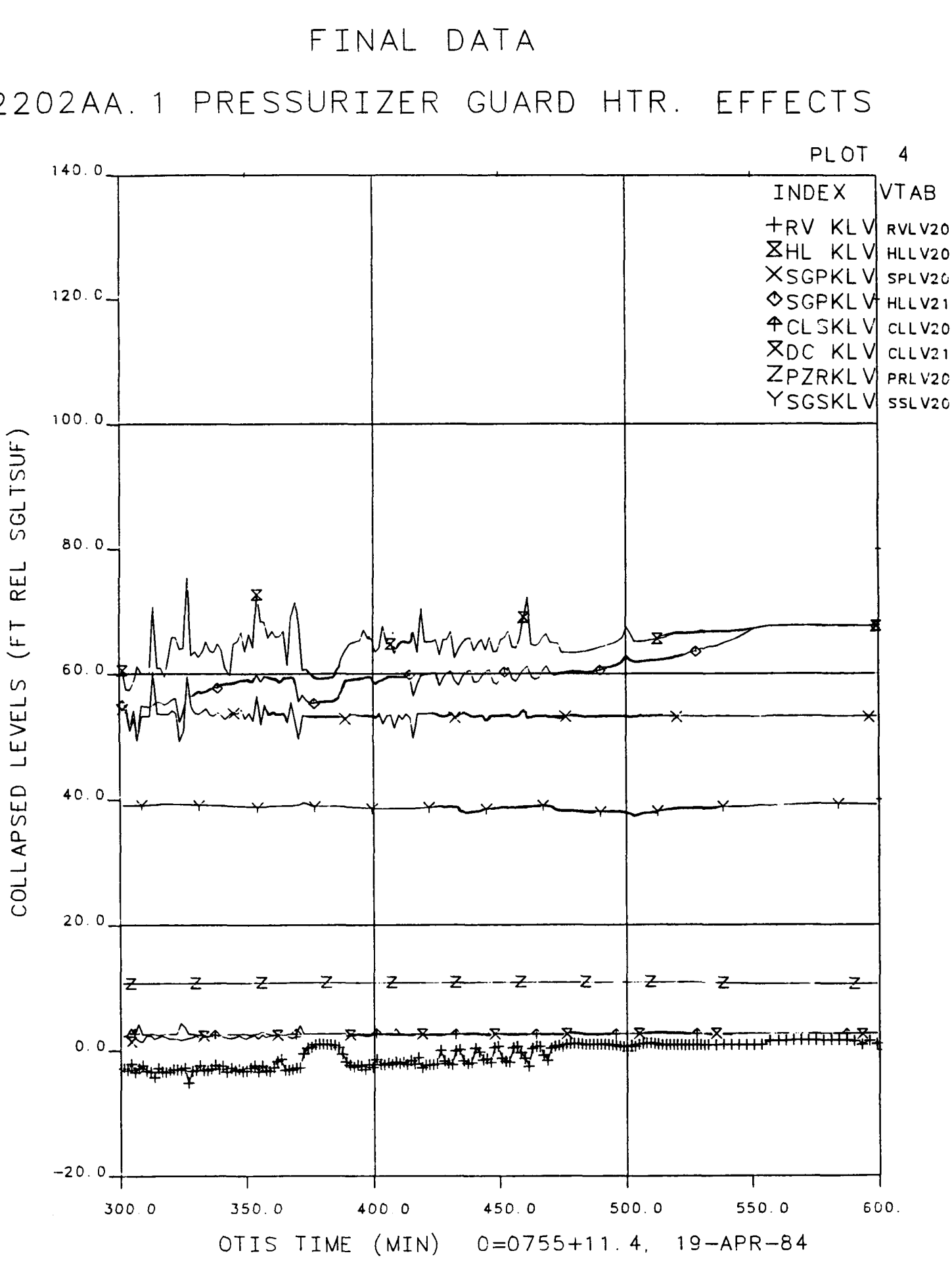

Figure 10.53 Collapsed Liquid Levels, 300 to 600 Minutes, Test 2202AA

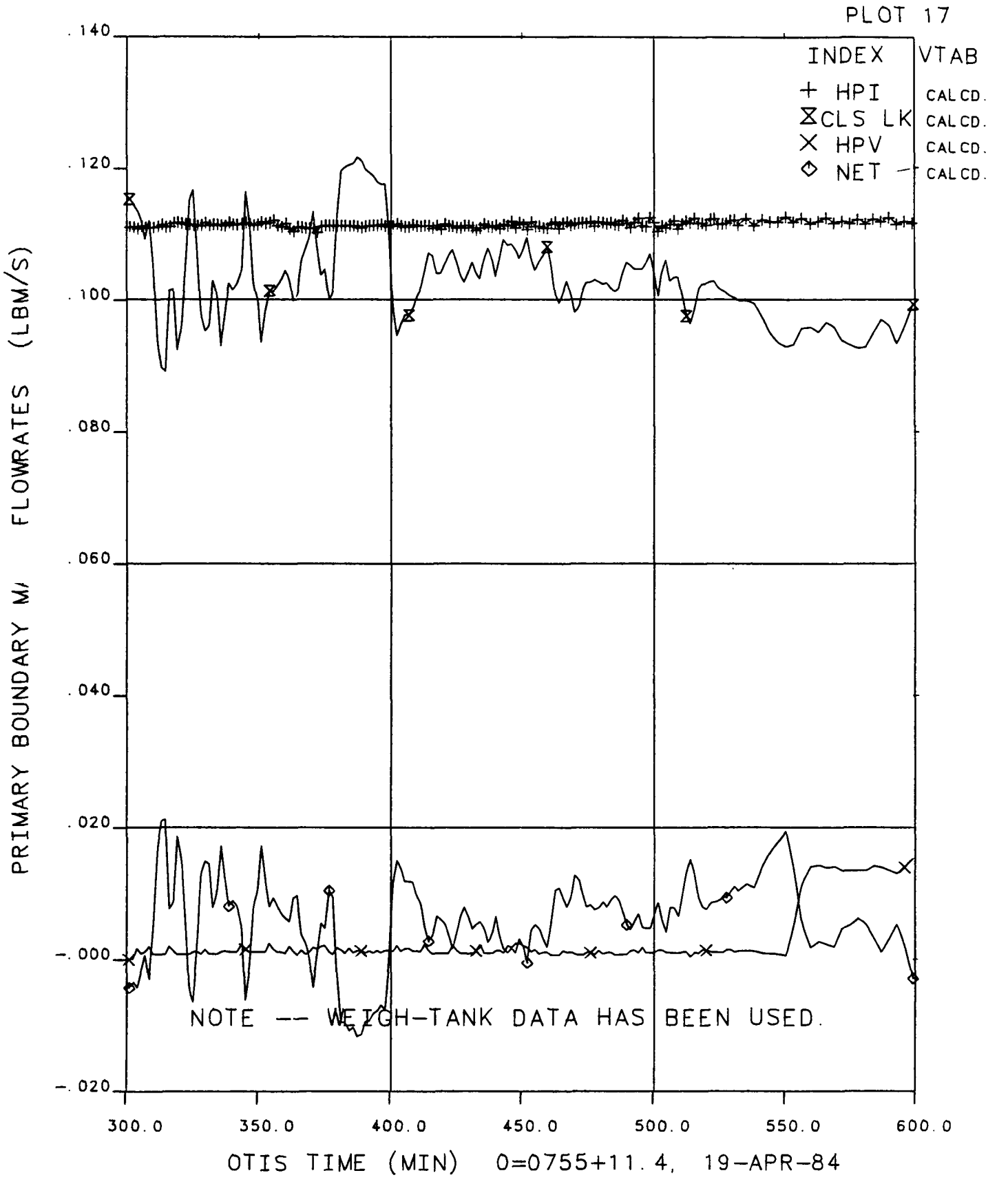

Figure 10.54 Primary Boundary Mass Flowrates, 300 to 600 Minutes, Test 2202AA

11. SUMMARY OF RESULTS

The results of OTIS testing are summarized by test type, viz. benchmark, Nominal, single-variable, cooldown, composite (plant-trained operator), and guard heater effects. General observations and results are highlighted in sections 11.7 and 11.8.

11.1 Boiler-Condenser Mode (BCM) -- Benchmark Test 210100 No High-Pressure Injection, No Leak

The performance of OTIS in "steady-state" BCM without a leak and high-pressure injection paralleled that of GERDA. Using low-elevation injection of auxiliary feedwater, and with no high-pressure injection or leak, periodic condensation events were observed. Before each condensation event the upper downcomer and cold leg discharge regions were voided, but the condensation of primary vapor in the steam generator was raising the liquid-vapor interface in the cold leg suction piping, toward the cold leg spillover elevation. The subsequent spillover flow in the cold leg depleted the saturated liquid layer, exposing the underlying subcooled liquid and triggering the rapid condensation of the cold leg, upper downcomer, and core outlet steam. Following a condensation event, the downcomer liquid level rose above the elevation of the cold leg nozzle, further condensation was inhibited, and the system conditions were realigned toward those preceding the event.

The primary pressure variations caused successive pressurizer insurges and outsurges, cooling the pressurizer liquid inventory. The pressurizer gradually gained liquid inventory causing the steam generator tube length available for condensation to increase, thereby decreasing the primary-to-secondary pressure difference.

The periodic upper downcomer voiding and condensation ceased shortly after transferring from low-elevation injection of auxiliary feedwater to high-elevation injection. With high-elevation injection, the primary liquid in the lower elevations of the steam generator heated toward saturation and thus could no longer cause downcomer-region condensation.

11.2 Nominal Test 220100: Characteristic Phases of an SBLOCA

Five major phases were predicted to occur and were observed in many of the OTIS SBLOCA tests. These were: (1) pressurizer draining and loop saturation, (2) intermittent primary circulation, (3) boiler-condenser mode (BCM), (4) refill, and (5) post-refill cooldown.

Figure 11.1 provides an indication of the duration and timing of these phases using the primary and secondary pressure curves of the Nominal Test 220100. This test was initialized, initiated, and performed as described for the single-variable tests. The scaled 10-cm^2 cold leg suction leak was opened to initiate the test. The pressurizer draining and loop saturation phase lasted for approximately 4 minutes. The primary system depressurized at approximately 100 psi/minute until the pressurizer drained at 2.5 minutes, and then at 350 psi/minute until 3.3 minutes, as shown in Figure 11.2. The fluid in the hot leg U-bend then saturated and the primary pressure stabilized at approximately 1700 psia.

The second phase, intermittent circulation, started at about 4 minutes after leak opening and continued until approximately 40 minutes. Natural circulation flow was first interrupted at 8 minutes. With interrupted flow, the primary repressurized twice (as noted in Figure 11.2), at 9 and 16 minutes. The magnitude of the repressurizations was controlled by the duration of the flow interruption. Recoupling of the primary and secondary systems terminated these repressurizations; secondary pressure increased upon recoupling. The loop conditions during this phase are illustrated in Figure 11.3.

During the intermittent circulation phase, the decreased primary loop flow caused the reactor vessel-to-downcomer differential pressure to increase, actuating the reactor vessel vent valve. Warmer fluid was admitted to the upper downcomer, cooled by mixing with high-pressure injection fluid, and returned to the core inlet, completing the inner flow circuit. The void in the reactor vessel upper head continued to grow, displacing fluid into the hot leg and raising its liquid level. This caused the intermittent or spillover circulation that was mentioned previously. The spillover circulation propelled saturated fluid over the hot leg U-bend. The liquid

fell through the voided downstream piping and into the steam generator, transferring heat to the secondary.

The boiler-condenser mode (BCM) began about 43 minutes after leak initiation, when the steam generator primary level approached the steam generator secondary level. Condensation of the primary steam caused the primary to depressurize from approximately 1400 psia at 43 minutes, to approximately 770 psia by 63 minutes. The BCM depressurization continued more gradually to 700 psia at 100 minutes. In the BCM, steam was produced in the core and condensed in the steam generator. Because this type of BCM requires the crossing of the levels within the generator, it is called "Pool BCM." Primary vapor condensation rapidly lowered the primary pressure and primary total energy. The condensation process was sufficiently effective to reduce primary pressure to nearly that of the steam generator secondary.

The decreasing primary pressure increased the high-pressure injection flow rate and reduced the leak flow rate. The high-pressure injection and leak flow rate changes were sufficient to start primary system refill. The increasing primary levels weakened heat removal in the BCM phase; however, this heat removal mode persisted until the steam generator primary level exceeded the elevation of the upper tubesheet at approximately 115 minutes. Loop conditions representative of the boiler-condenser phase are illustrated in Figure 11.4. System refill started 70 minutes after leak opening.

Figure 11.5 illustrates the primary system conditions after the primary side of the steam generator had been refilled. The hot leg level upstream of the hot leg U-bend spillover was insufficient to sustain circulation, although sporadic spillovers occurred. The cold high-pressure injection (HPI) fluid lowered the leak fluid temperature so that the leak flow rate increased, but the heat transfer by HPI-leak cooling decreased (the effect of the leak fluid temperature decrease exceeded that of the leak flow rate increase). The primary repressurized from 680 to 790 psia, causing the primary system to approach fluid mass and energy equilibrium.

The relatively stable primary conditions indicated that core power was being matched by HPI-leak cooling (plus losses to ambient). Loop flow was

interrupted and the steam generator was inactive for heat transfer; however, the inner-loop flow was active. Core-exit fluid flowed out the reactor vessel vent valve, down the downcomer, and back into the core. High-pressure injection fluid condensed the vented steam, and mixing in the cold leg discharge region and/or counterflow heated the fluid reaching the leak site. The high-pressure injection and leak flow rates were nearly equal. The heatup from the high-pressure injection fluid temperature to the leak discharge temperature approximately equaled core power. These conditions were quite stable.

At five hours the hot leg high-point vent was opened. The vapor that was discharged from the vent caused a mild primary depressurization; vapor flow to the vent cooled the upper-elevation hot leg metal. The primary system refill rate increased, spillover occurred more frequently, and the loop filled at seven hours.

Natural circulation commenced immediately after system refill, thus starting the post-refill cooldown. The primary loop flow rate stabilized at approximately 2% of scaled full flow and remained constant for two additional hours of controlled cooldown. Figure 11.6 illustrates the loop conditions during this phase.

11.3 Single-Variable Effects (Tests 220100 through 220756)

The nominal and single-variable tests included:

220100 -- Nominal: 10-cm^2 cold leg suction leak, high-head high-pressure injection, 38-ft steam generator level.

220201 -- Increased leak size (15 cm^2).

220304 -- Half-capacity high-pressure injection.

220402 -- 10-ft steam generator level.

220503 -- Cold leg discharge leak.

220604 -- Low-head high-pressure injection.

220756 -- Isolated leak.

Each of these tests (except the leak isolation test) experienced the predicted sequence of events:

(1) Depressurization to loop saturation,
(2) Intermittent circulation and flow interruption,
(3) Boiler-condenser mode (BCM) depressurization,
(4) Refill (except with half-capacity high-pressure injection), and
(5) Natural circulation cooldown

The primary system was depressurized by both Pool BCM and AFW BCM. (In "Pool BCM", the steam generator primary liquid level is at or below the secondary level; in "AFW BCM", primary vapor is condensed near the elevation of injection of auxiliary feedwater.) Both types of BCM occurred in the Nominal Test (220100) and with half-capacity high-pressure injection (Test 220304). Pool BCM, but not AFW BCM, occurred with the larger break (Test 220201). AFW BCM rather than Pool BCM occurred with the 10-ft steam generator level (220402), with the cold leg discharge leak (220503), and with low-head high-pressure injection (220604). No BCM occurred in the isolated-leak test (220756), the primary level did not decrease to the steam generator elevation. BCM coupling was prolonged in those tests having lower leak-HPI equilibrium pressures*, namely the tests with a larger break, half-capacity high-pressure injection, and low-head high-pressure injection, Tests 220201, 220304, and 220604.

Each of the unisolated-break tests approached refill equilibrium. Primary system energy and fluid mass were roughly constant. Refill was prolonged. Core heat was offset by HPI-leak cooling. The single cold leg of OTIS influenced this energy transfer process. Multiple nonsustaining spillovers commonly occurred during refill. The refill rate decreased as the loop approached full. The pressure of refill equilibrium decreased with increased leak size and with decreased high-pressure injection capacity.

No unisolated leak test completed refill before actuation of the hot leg high-point vent. Vent actuation perturbed the refill equilibrium conditions. The increased vapor discharge rate cooled the uppermost hot leg metal, and thus reduced primary pressure and increased the high-pressure injection flow rate. Hot leg vent actuation apparently aided refill with the nominal conditions, cold leg discharge leak, and low-head high-pressure injection characteristics. Refill may have occurred without vent actuation with the larger break and with the lower steam generator level. The half-capacity high-pressure injection test did not completely refill before the completion of testing. Loop natural circulation usually restarted almost immediately after loop refill.

---

*The "leak-HPI equilibrium" pressure is that pressure at which the mass flow rates of the two systems are equal.

Guard heater effects were amplified in those tests having a lower equilibrium primary pressure. The lower saturation temperature was further from the system fluid temperature at which the guard heater bias had been set. (This led to the guard heater separate-effects tests based on Test 220201, increased leak size.)

Cold leg voiding often occurred upon system depressurization, when the lower-elevation vapor production rate exceeded the capacity of the high-pressure injection to condense it. The half-capacity high-pressure injection characteristics amplified this effect. Cold leg voiding was accompanied by abrupt hot leg level changes. (The cold leg leak fluid apparently remained liquid.)

The half-capacity high-pressure injection test (220304) did not refill before the completion of testing. The relief valve (PORV) actuation in the later stages of this test increased the high-pressure injection flow rate by decreasing primary pressure, but this relatively small injection increase was more than offset by the diversion of liquid from the loop to the pressurizer; i.e., the relief valve actuation did not augment loop refill. The core power reduction also reduced primary pressure slightly, obtaining actuation of the low-pressure injection system.

11.4 Cooldown Observations (Tests 220899 through 221099)

11.4.1 HPI-PORV Cooling (Test 220899)

OTIS Test 220899 exercised feed-and-bleed cooling without a leak. The relief valve (PORV) was kept open after the primary pressure had increased to its actuation pressure. No pressure-temperature envelope was imposed for this test. The test was terminated at two hours, with the upper hot leg fluid apparently saturated. (The operator saw no voiding in the hot leg viewports at test termination; no video recording was performed during the later portions of the test.) HPI-PORV heat transfer effectively cooled the core and the lower-elevation primary fluid. The phases of this HPI-PORV cooling test are shown on Figure 11.7.

The loop flowrate diminshed as the cooldown progressed, because of the decreased steam generator heat removal and hence natural circulation driving

head. As the loop flowrate approached zero, whole-loop flow reversals began to occur periodically. These fluid oscillations were caused by the performance of the model reactor vessel vent valve (RVVV), and by the loop fluid density redistributions attendant to HPI-PORV cooling. With little prevailing loop flow, the position of the model RVVV governed the downcomer fluid density. With the reactor vessel vent valve open, the relatively warm core-outlet fluid was vented to the downcomer while the high-pressure injection fluid cooled the cold leg region. The decreasing downcomer fluid density lowered the differential pressure across the reactor vessel vent valve, ultimately causing the valve to close. Then the relatively-dense cold leg fluid entered the downcomer, reversing the trend. In this manner the loop flow became oscillatory as the time-averaged whole-loop flow became negligibly small. As HPI-PORV cooling progressed, loop flow slowed and then stalled as steam generator heat removal was supplanted. As outer-loop flow stalled, the upper-elevation hot leg fluid ceased to be cooled. Upon primary pressure reduction with the continuing (core) cooldown, the uncooled hot leg fluid reached saturation and thereby impeded further primary pressure reduction.

11.4.2 Natural Circulation Cooldown (Tests 220999 and 221099)

The natural circulation cooldown continued through upper head voiding both with and without upper head venting. Upper head venting refilled the reactor vessel head. Periodic venting maintained it liquid-full.

The natural circulation cooldowns with and without reactor vessel upper head venting were virtually identical. Although the upper head was refilled in the test using the vent, the primary conditions (core outlet and hot leg fluid temperatures at primary pressure versus time) were approximately the same in both tests. Both cooldowns adhered to the specified pressure-temperature envelope.

11.5 Composite Tests

Two composite tests (230199 and 230299) introduced operator guidelines. An operator trained in plant procedures controlled the test loop evolutions. The initialization and initiation conditions paralleled those of the single-variable tests except that auxiliary feedwater was not available until one hour after test initiation. Also, the 10-cm^2 cold leg suction

leak was isolated after 30 minutes of testing. Both tests simulated full high-pressure injection capacity. Test 230199 simulated high-head high-pressure injection characteristics, while low-head high-pressure injection was simulated in Test 230299.

The operator controlled the system conditions similarly in the two tests. With feed unavailable, the operator used intermittent PORV (relief valve) actuations to control primary pressure. When auxiliary feedwater became available, the operator used throttled feed to depressurize the primary through the boiler-condenser mode. Refill, post-refill circulation, and cooldown were rapidly achieved.

11.6 Guard Heater Tests 2202AA and 2202BB

OTIS guard heating did not affect the depressurization phases of the transient, although the local fluid temperatures in the voided regions were affected by guard heating. The stored energy of the metal masses at the higher elevations was sufficient to maintain superheating at the higher elevations even without guard heating. The increased vapor temperatures and higher-elevation metal temperatures with guard heating affected refill. The refill repressurization was increased and the times to quench this metal and hence, to complete refill, were lengthened. The mode of reactor vessel vent valve control (manual-open, or automatic actuation on differential pressure) apparently had a significant effect during the final stages of system refill.

11.7 General Observations

The test initialization and initiation procedures were performed virtually identically among the tests. Plant-similar post-SBLOCA conditions were rapidly attained.

Subcooled auxiliary feedwater wetted the steam generator tubes near the high-elevation injection site. With stalled primary flow, primary liquid temperatures just below the injection elevation were less than the secondary saturation temperature.

he reactor vessel collapsed liquid level commonly resided in the range of elevations defined by the outlet nozzle (-1.9 ft), the reactor vessel vent valve (+0.6 ft), and the upper plenum orifice plate (+1.3 ft).

OTIS (like GERDA) often approached equilibrium as refill progressed. At equilibrium, the primary energy and fluid mass were constant, and core power was being offset by HPI-leak cooling. These conditions were apparently quite stable. Among the many differences between the two test series, GERDA usually had the hot leg high-point vent open (after 30 minutes, in composite tests), whereas vent actuation in OTIS was delayed until 5 hours. The GERDA refill tests with and without hot leg venting indicated a threefold reduction of refill time with venting, but these refill test results were often masked by the test initialization differences. No OTIS single-variable test refilled before hot leg vent actuation (except the leak isolation test, which refilled at high pressure). Vent actuation apparently caused refill in some cases and may not have been necessary for refill in others (the system was not refilled before test completion, in the test with half-capacity high-pressure injection). As mentioned previously, the model reactor vessel vent valve control may have affected these refill observations.

Based on these model observations, hot leg vent actuation would appear to be useful. The vent discharge caused a mild primary depressurization that obtained an excess of high-pressure injection flow rate over leak (plus hot leg vent) flow. Steam flow to the vent also cooled the upper-elevation hot leg metal. With the vent not open, this metal heat retarded refill by causing a (minor) repressurization as it was quenched during refill. The temperature of this metal was initially set by the primary saturation temperature when it was uncovered; it varied (slowly) after uncovery through heat transfer to (or from) the vapor adjacent to it, and with losses to ambient.

Auxiliary Feedwater (AFW) Heat Removal

OTIS encountered near-equilibrium conditions during refill (much like GERDA). But spillovers (intermittent liquid flow over the hot leg U-bend)

with the loop nearly full often occurred for hours in OTIS without leading to sustained primary-to-secondary coupling. There are many interactions and model simulations that bear on this observation, including the reactor vessel vent valve simulation and control, and the steam generator secondary level and auxiliary feedwater control. These non-sustaining spillovers also pinpoint the steam generator heat removal differences between low- and high-elevation injection. With low-elevation injection, the pool is commonly subcooled and the steam region sustains some superheat (even with the model steam generator heat losses). Consider the situation with stalled primary flow and with the hot leg and steam generator primary levels above the steam generator but below the U-bend spillover. With an increase of the hot leg (upstream) liquid level, liquid drops over the spillover, the whole-loop manometer becomes imbalanced, and the primary liquid within the steam generator moves downward toward manometric equilibrium. This draws relatively warm primary liquid down into the steam generator elevations covered by the secondary pool. Some of the saturated liquid near the secondary liquid-vapor interface flashes, the secondary steam pressure control valve actuates to maintain pressure, the secondary liquid inventory decreases, and the auxiliary feedwater control system activates to restore secondary level. This low- elevation feed injection cools the secondary pool, and the primary liquid traversing this region becomes highly subcooled. The attendant contraction of the primary liquid commonly lowers the hot leg upstream level, but the concurrent primary pressure reduction usually produces enough of an increase of high-pressure injection to subsequently obtain larger spillovers.

With high-elevation auxiliary feedwater injection, the steam generator secondary pool is nearly saturated. It would thus seem that a downward movement of primary liquid would generate more steam than with a subcooled pool. But the heat transferred from the primary to the subcooled auxiliary feedwater is frequently sufficient to bring the primary liquid to the secondary saturation temperature before it reaches the pool. Then the auxiliary feedwater actuation is not self-sustaining. If no secondary steam is generated, then the auxiliary feedwater actuation simply increases the secondary inventory to the control level, causing the auxiliary feedwater control system to deactivate.

Obviously, a number of systems have interacted in this idealized comparison: the high-pressure injection head-flow characteristics, tube wetting, primary-to-AFW heat transfer, etc. But the underlying difference seems to involve auxiliary feedwater heat transfer. The amount of energy required to heat a unit mass of auxiliary feedwater from its injected subcooling to saturation is roughly one-half of that required to vaporize it.* If primary-to-secondary heat transfer is used to bring the auxiliary feedwater toward saturation, then the auxiliary feedwater flow rate exceeds the steam flow rate and the steam generator secondary level control interrupts the feed flow. If, on the other hand, the primary energy goes mostly to vaporize secondary liquid, then the steam generator secondary pressure and level controls will activate both steam and feed flow. The latter situation is apparently more likely to obtain sustained coupling.

11.8 Summary

The major results of the OTIS tests are as follows:

- o The tests generally encountered each of the predicted transient phases.
- o The core remained cooled throughout every test; the most prevalent cooling mechanism was HPI-leak heat transfer.
- o Refill equilibrium was approached in many of the tests.
- o Hot leg high point vent actuation sometimes assisted refill (by cooling the upper-elevation hot leg metal, and by decreasing the primary pressure such that high-pressure injection exceeded leak flow). In several tests, refill apparently would have occurred without hot leg vent actuation. The loop was not refilled with half-capacity high-pressure injection (Test 220304). Hot leg vent actuation would probably have assisted primary depressurization during HPI-PORV cooling (Test 220899).
- o Natural circulation began soon after refill of the loop.

---

*Denote the auxiliary feedwater inlet enthalpy ($T \sim 100F$) as h_i. The specific enthalpy change due to heating is $h_{if} = (h_f - h_i)$ and the total specific enthalpy change is $h_{ig} = (h_g - h_i)$. The ratio (h_{if}/h_{ig}) then compares the enthalpy rise due to feed heating to the total enthalpy change:

p, psia	100	250	500	1000
h_{if}/h_{ig},%	21	27	34	41

OTIS generated a wealth of code-challenging, integral system, post-SBLOCA DATA. It should be noted that OTIS indicated model behavior rather than plant performance. Specific transients were affected by boundary system malfunctions; such occurrences have been identified and suitably documented to facilitate the code prediction of these transients. OTIS thus met its objective -- the generation of post-SBLOCA data with which to benchmark codes.

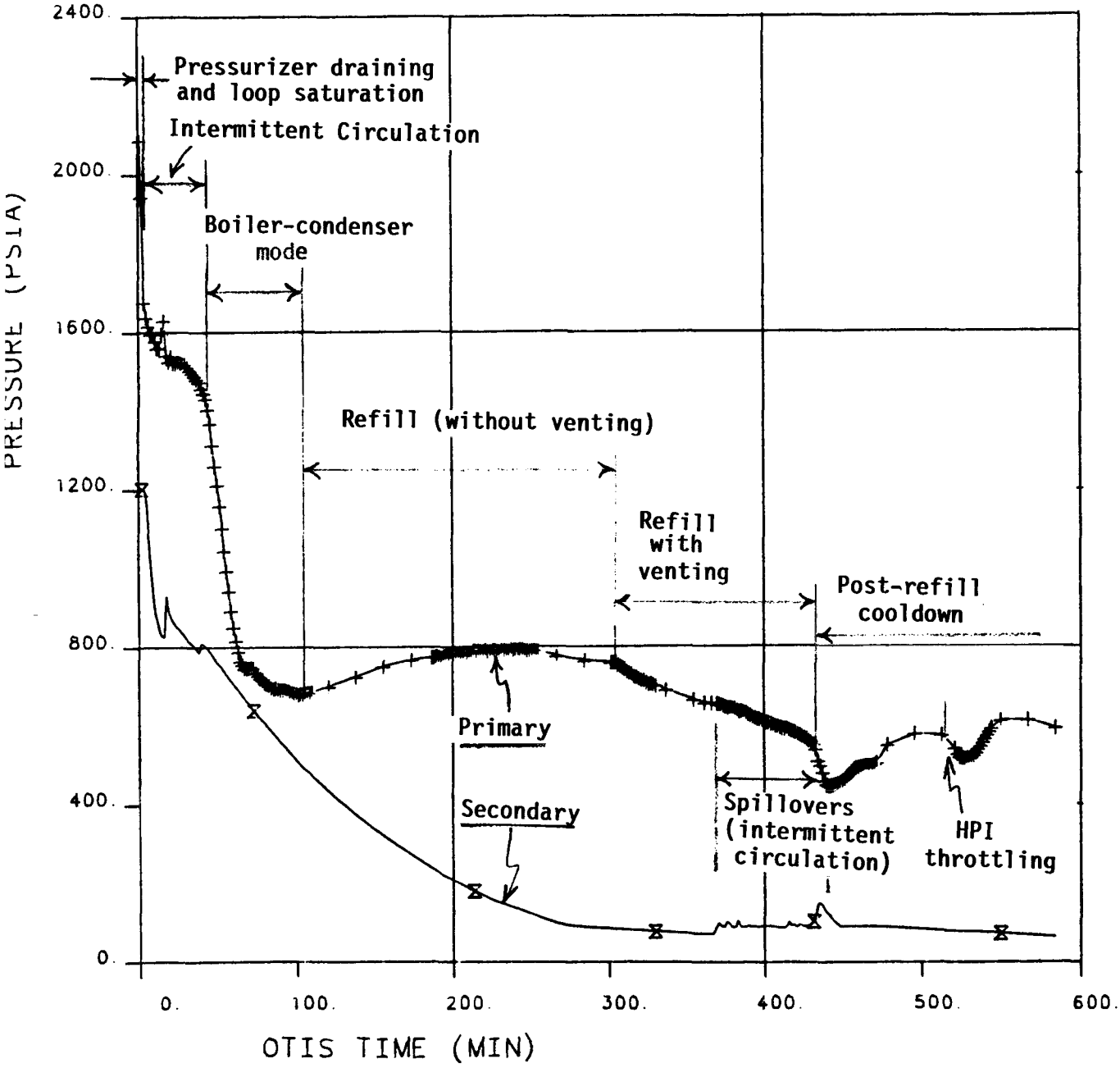

Figure 11.1 SBLOCA Phases, OTIS Nominal Test 220100

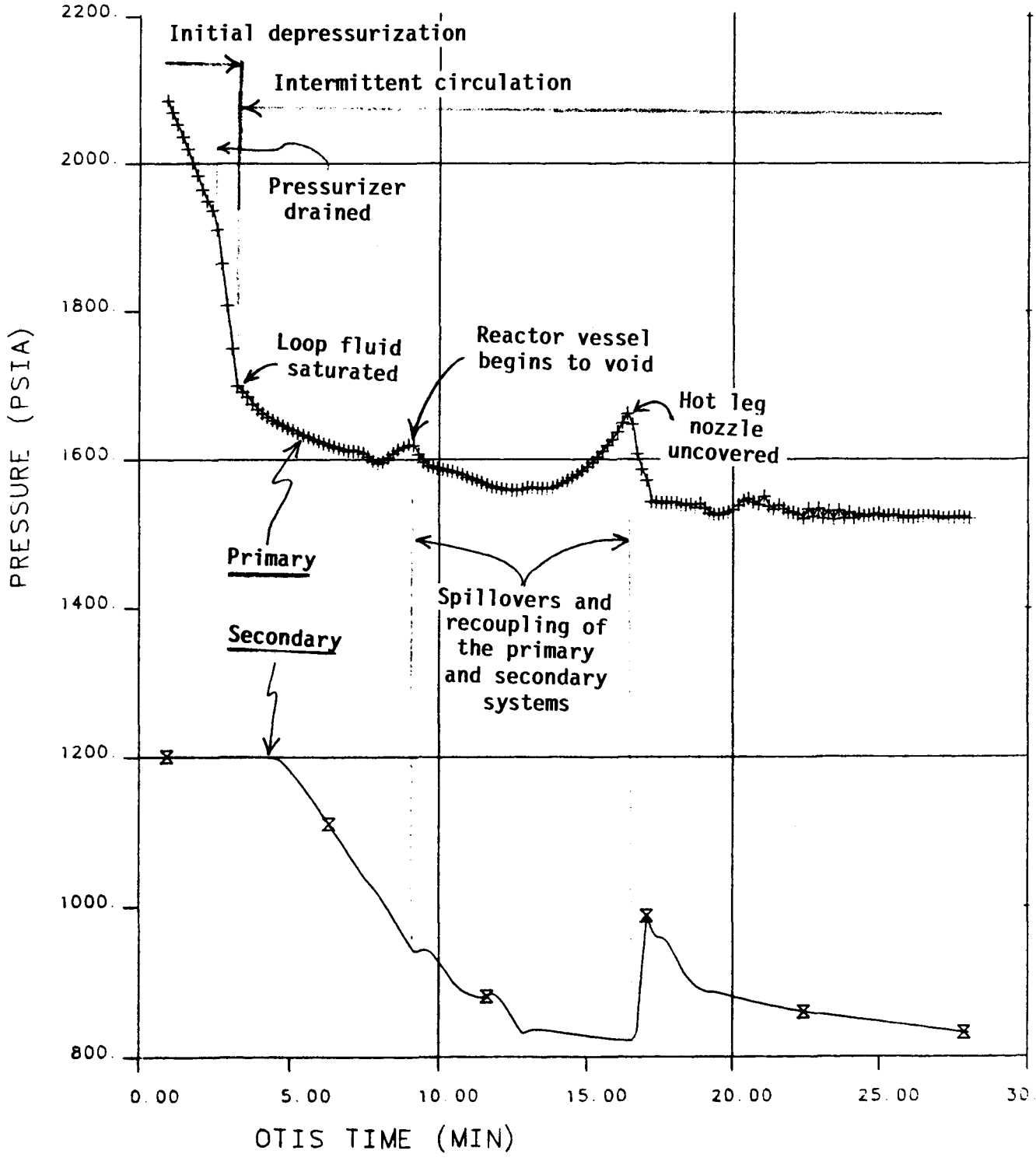

Figure 11.2 Draining, Depressurization to Saturation, and Intermittent Circulation -- OTIS Nominal Test 220100.

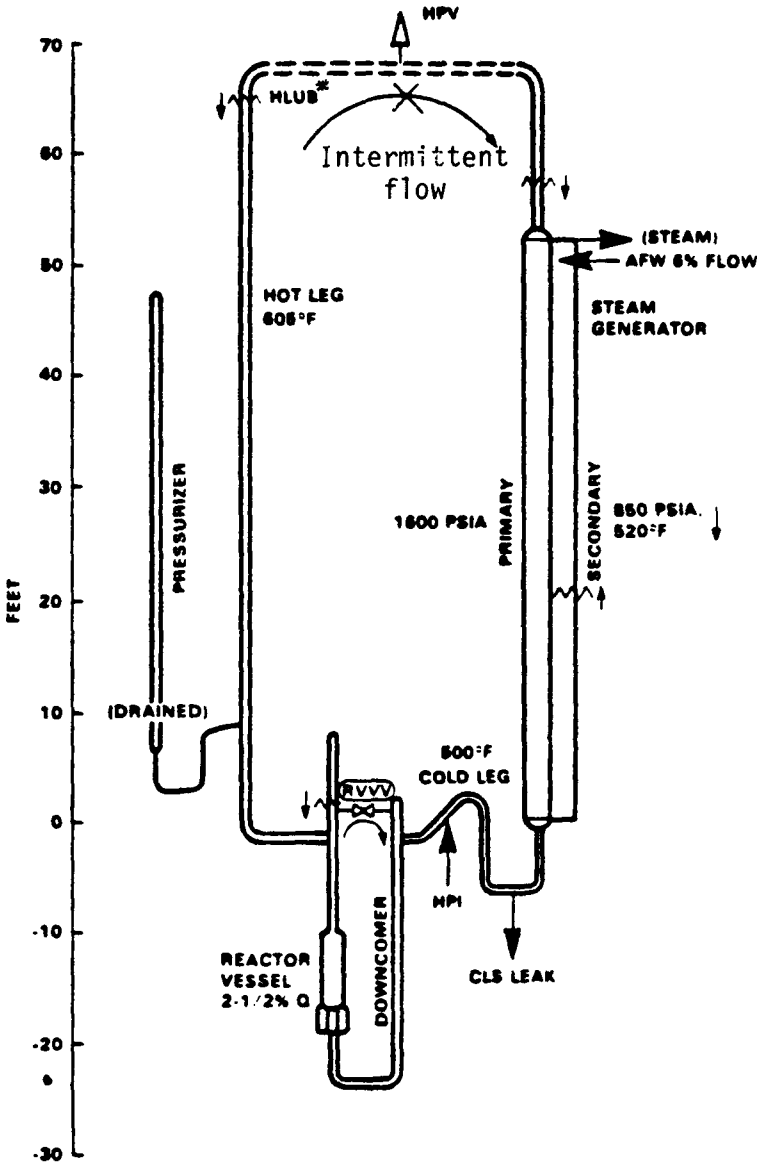

Figure 11.3 Loop Conditions During Intermittent Circulation. (4 to 40 minutes after opening a 10-cm² cold leg suction break, OTIS Nominal Test 220100.)

*The dashed lines at the top of the sketch indicate that the actual OTIS hot leg U-bend was a continuous bend, similar to the plant U-bend.

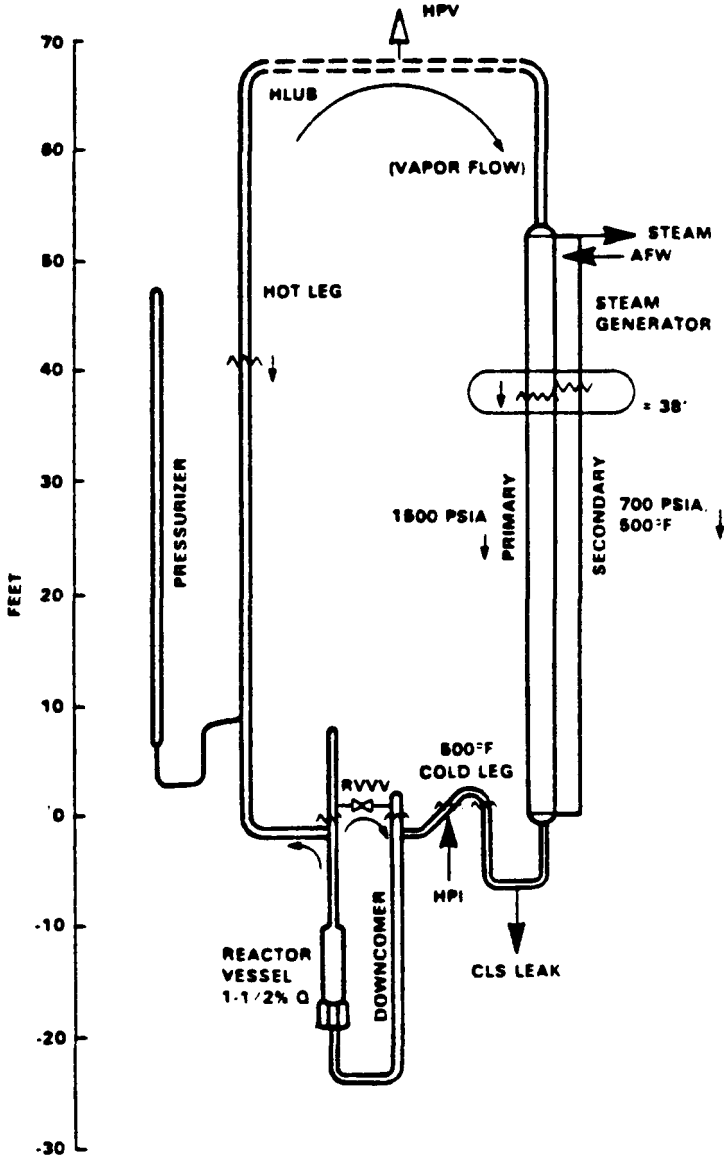

Figure 11.4 Loop Conditions During Pool Boiler-Condenser Mode (40 to 100 minutes, OTIS Nominal Test 220100.)

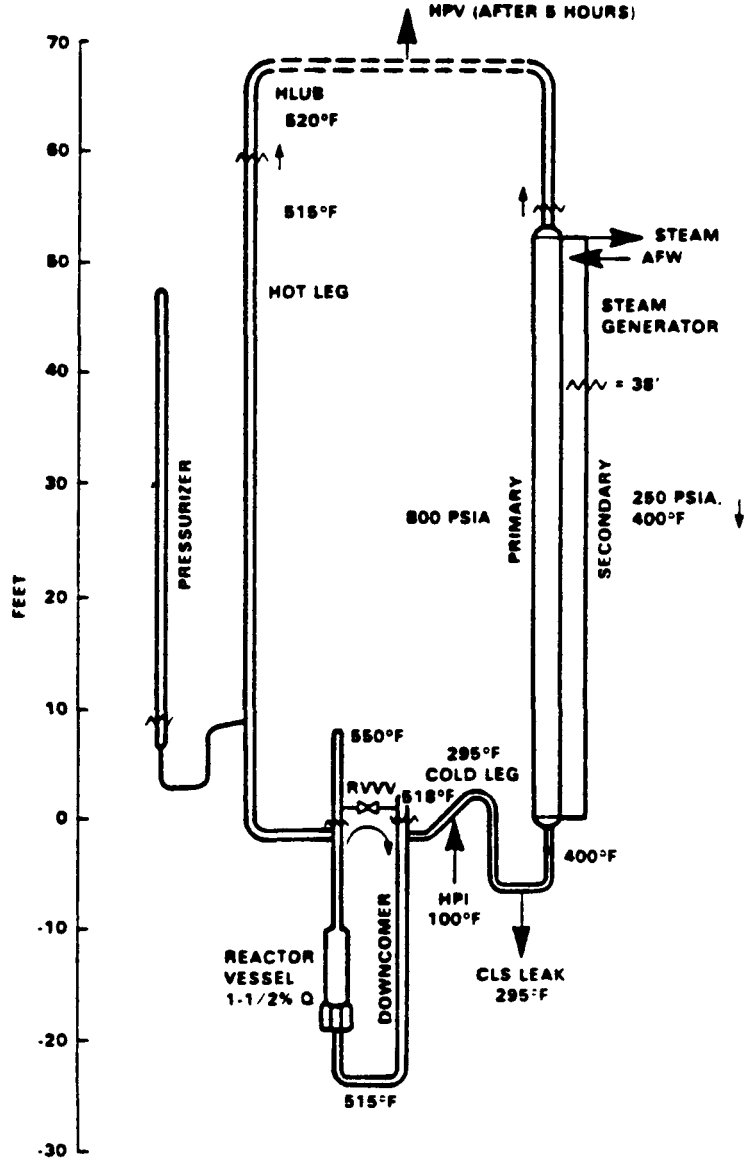

Figure 11.5 Loop Conditions During Refill
(1 to 7 Hours, OTIS Nominal Test 220100.)

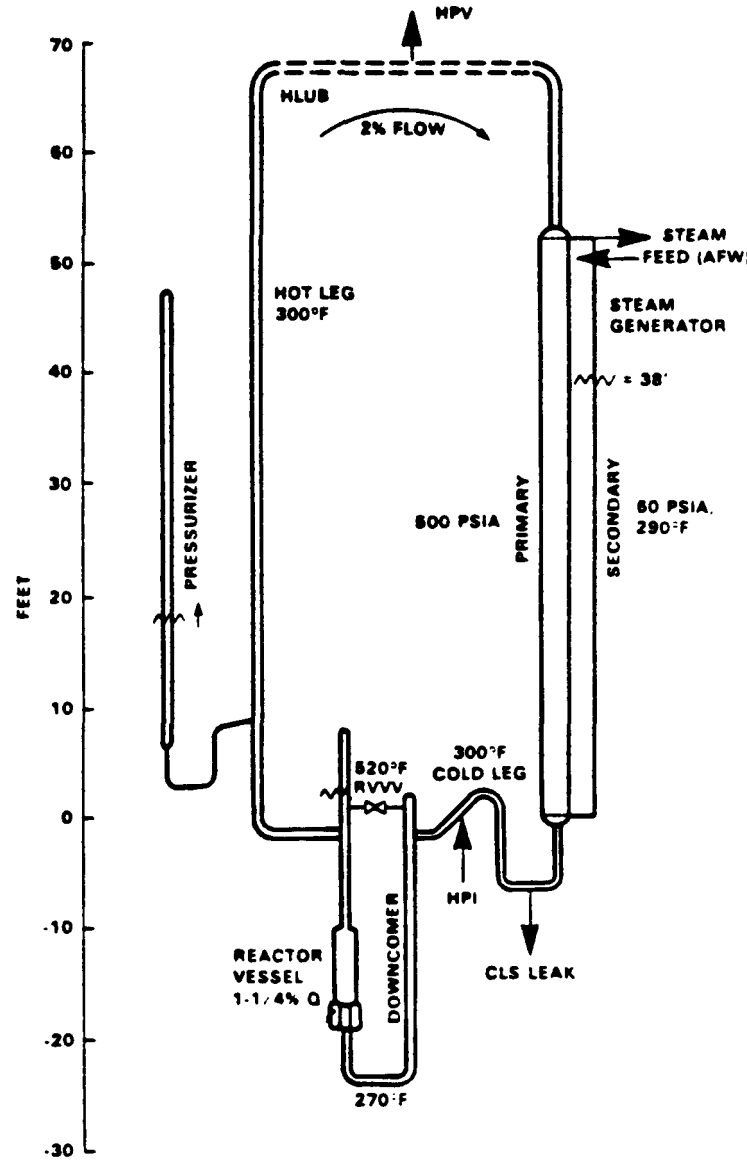

Figure 11.6 Loop Conditions During Post-Refill Cooldown (7 to 10 Hours, OTIS Nominal Test 220100.)

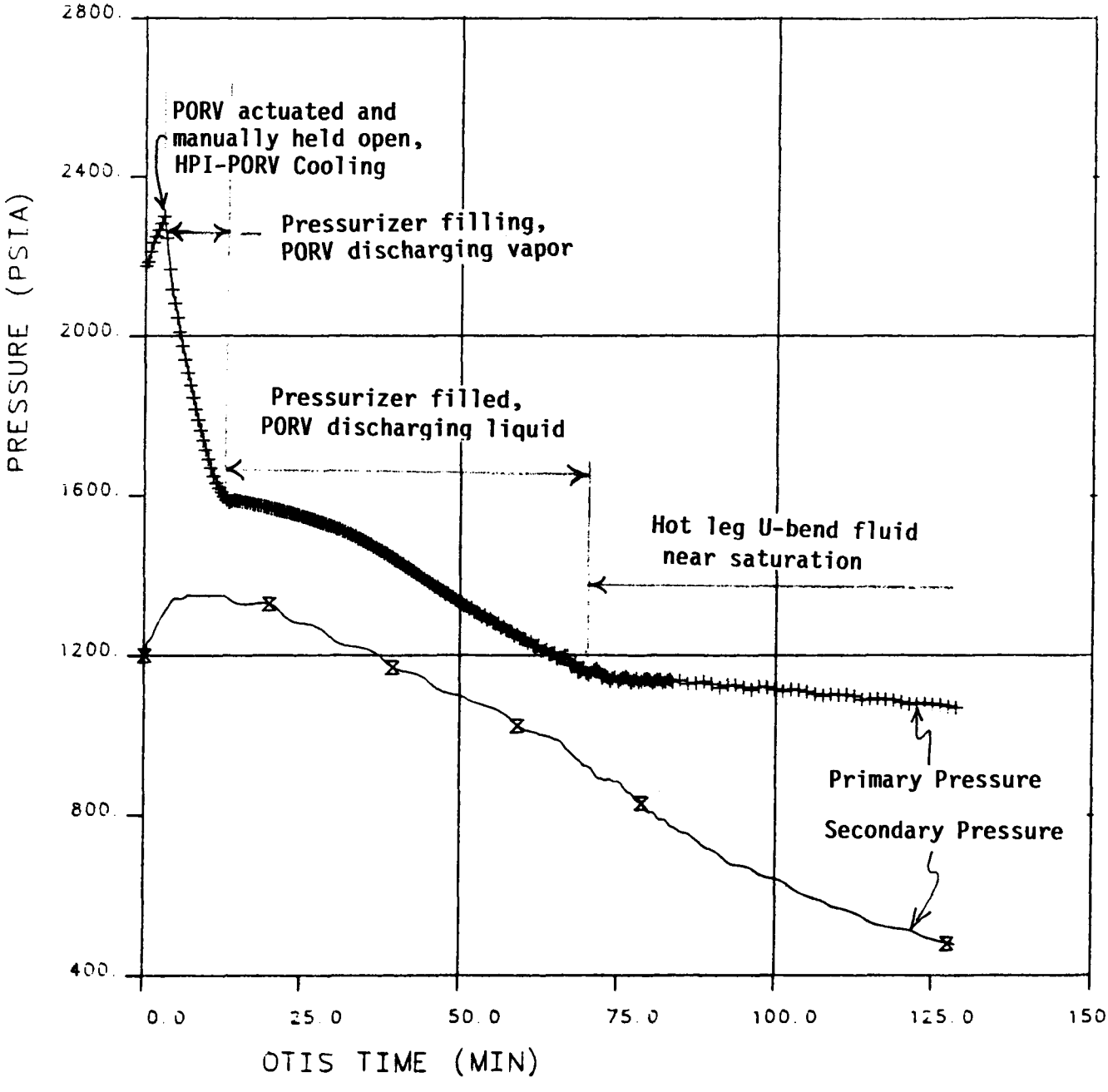

Figure 11.7 Phases of HPI-PORV Cooling,
OTIS Test 220899.

12. RECOMMENDATIONS FOR FUTURE TESTING

Single-loop integral system testing -- GERDA and OTIS -- has provided a wealth of experience that is beneficial to future testing. These lessons learned or confirmed are summarized in the form of recommendations for future testing. Their application to MIST[11] is also noted. These recommendations have been grouped by subject: (1) design, (2) measurements, (3) testing, and (4) analysis.

12.1 Design

Design recommendations for future testing are as follows:

1. Symmetry -- Piping and components must be symmetric throughout, particularly in a multi-loop system, to obtain conditions-generated rather than model-generated asymmetries. The multiple-branched piping entering the GERDA/OTIS reactor vessel is an illustration of a non-symmetric network. Symmetry is being invoked throughout the MIST design.

2. Metal Stored Energy -- Local fluid heating may be caused by the release of stored energy from large metal masses. Such masses should be minimized; their internal temperatures should be measured to permit the analysis of their impact. Metal masses are minimized in MIST and internal metal temperatures are measured.

3. Coarse Guard Heating -- A single guard heater zone over a vertical piping length may only coarsely balance heat losses, particularly if the contained fluid separates by phase and/or temperature. The MIST guard heating concept is similar to that which was used in OTIS, but guard heater control has been refined and the control thermocouples have been located near the heater mid-heights.

4. Pressurizer Configuration -- The atypically large length-to-diameter ratio of the GERDA/OTIS pressurizer accentuated fluid stratification and encumbered guard heater control. The external main heaters provided relatively slow pressure control and complicated the arrangement of the pressurizer guard heaters. The MIST pressurizer will have a smaller length-to-diameter ratio, as well as internal main heaters.

5. Boundary System Control -- Automated control of simulated boundary systems (high-pressure injection and auxiliary feedwater head-flow characteristics, steam generator level control, etc.) is desirable. Such control facilitates code modelling of events and minimizes the incidence of simulation-caused interactions. An example of such an event distortion is the auxiliary feedwater BCM (boiler-condenser mode) delay in Test 220402, attributable to the coarseness of control provided by the steam generator level control system. Automated systems and rather complete verifications of these simulations (during characterization testing) are stressed in MIST.

6. Bistable Simulation -- The bistable simulation of analog controls or components may encounter oscillations. The OTIS reactor vessel vent valve simulation was such a component and sometimes gave rise to cyclic perturbations. The MIST reactor vessel vent valves are similar simulations, and there are four in parallel rather than one. The MIST simulation has been improved by increasing the hydraulic resistance of the valve simulation network and by revising the actuation setpoints toward plant-similar valve operation. Characterization tests as well as a composite test are planned to examine and improve the adequacy of the simulation.

12.2 Measurements

Measurement recommendations for future testing are as follows:

1. Measurement Types -- The basic measurements (pressures, temperatures, levels, and flow rates) are generally sufficient to permit the analysis and understanding of integral-system behavior. These standard measurements are generally more reliable and hence, more useful than relatively sophisticated measurements. MIST includes the standard instruments plus conductivity probes, gamma densitometers, and cooled thermocouples.

2. Steam Generator Temperatures -- The steam generator fluid temperature measurement locations should be of sufficient (radial and axial) density to permit the development of multidimensional temperature trends. Such

temperature profiles are central to the analysis of auxiliary feedwater wetting, BCM (boiler-condenser mode) heat transfer, and the effects of non-condensible gases. MIST has an extensive set of primary and secondary fluid temperature indications in the new ("B") steam generator, as well as renewed string thermocouples in the "A" steam generator.

3. Extreme Elevations -- Fluid conditions must be measured at the extreme elevations in each loop component as well as at the intermediate elevations (e.g., to permit the calculation of the natural circulation driving head). This philosophy has been adopted in MIST.

4. Stratification -- Fluid-fluid stratification was sometimes evident in GERDA/OTIS, specifically at the steam generator primary outlet. Special measurements should be included where such stratification is to be quantified. MIST includes multiple fluid temperature measurements both across the cold leg pipe diameters and within the model downcomer.

5. Flowmeter Placement -- Flowmeters should be placed as low in the loop as possible to minimize the incidence of voiding at the meter. They should be placed to provide closure on loop mass flow rate. MIST uses this flowmeter placement.

6. Reverse Flow -- An indication of flow direction and a quantification of the flow rate in reverse flow are useful. Reverse flow was encountered infrequently in OTIS, but is more likely in MIST because of its multiple, parallel flow paths. Reverse flow will be measured in MIST.

7. Signal Isolation -- Instrument and control signals must be scrupulously isolated from environmental electromagnetic noise. Even with special attention to this situation, the OTIS turbine meter flow rates evidenced spurious signals, apparently related to the operation of the reactor vessel vent valve controls and those in the two-phase vent system. These observations caused turbine meters to be de-emphasized in MIST.

12.3 Testing

Future testing recommendations are as follows:

1. Planned Versus Spontaneous Tests -- Deliberately planned, specified, examined, and reviewed tests are much more likely to prove beneficial than spontaneous tests. Ad hoc tests on the other hand are sometimes essential to the rapid and thorough probing of an interaction of interest. The GERDA tests of boiler-condenser mode oscillations versus boundary system conditions are examples of successful ad hoc tests.

2. Separate-Effect Versus Composite Tests -- Separate-effect tests are valuable due to their relative ease of conduct and analysis, and because of the system experience they provide. Composite rather than separate effects testing is more appropriate to study interactions that arise during the course of a transient, such as refill. The MIST test matrix includes a series of Characterization and Mapping tests, preceding the composite tests.

3. Off-Nominal Conditions -- Parametric testing should concentrate on single off-nominal rather than multiple off-nominal conditions. Such variations permit the identification of the sources of intertest differences. Although multiple variations may seem expedient when there are many variables and settings to be tested, the results may be difficult to interrelate.

4. Boundary System Verification -- The boundary system simulations must be characterized early in the testing sequence, both in a functional sense and to determine the impact of the simulation on the integral system interactions. The planned MIST testing includes both types of tests.

5. Interaction Among Personnel -- Frequent, direct, and single-topic interactions among the test planner, experimentalist, and analyst are essential. Meetings are most useful before and after the first (composite) test and between test groups. This observation is drawn from the meetings held during GERDA and OTIS testing.

6. Logs -- There are multiple indications of loop conditions. Log entries of otherwise unrecorded operator actions, of subtle, unexpected, or unusual observations, and of trends perceived during test performance facilitate the understanding of system behavior.

12.4 Analysis

Analysis recommendations for future testing are as follows:

1. Closure Calculations -- The calculations of system mass and energy closure, and the verification of these calculations using independent techniques and measurements, establish basic system consistency or quickly identify problem areas. They are also the starting point in the analysis of integral-system events. These calculations will be continued in MIST.

2. Redundancy -- Redundant measurements may prove invaluable. The redundant weigh-tank measurements of discharged fluid mass were used in OTIS to adjust the leak flow rates supplied by accumulating flowmeters. Also, the redundant metering of the OTIS high-pressure injection flow rate pinpointed the injection turbine meter inaccuracy. Of the two meters available, one was used to control high-pressure injection and the other to indicate high-pressure injection flow rate for mass closure calculations. This separation of tasks further facilitated the crosschecking of the meters. MIST will have a measurement of total high-pressure injection flow rate as well as measurements of the individual streams to the cold leg injection sites. The total flow rate measurement will be used to control high-pressure injection, the individual measurements will be used for indication and calculations.

3. Refill Sensitivity -- The near-equilibrium conditions prevalent during the later stages of primary system refill can accentuate any idiosyncrasies of the reduced-scale model. Guard heater control must be accurate and well documented before and during this phase. The metal temperature excursions observed in Test 220201 illustrated imprecise guard heater control and led to supplementary Tests 2202AA and -BB. MIST uses smaller instrument penetrations, reduced-schedule (thinner wall) loop piping, and refined control of the guard heater bias. In addition to the customary heat loss and guard heater calibration tests, MIST testing includes transients with altered guard heater settings early in the planned testing.

4. Periodic Events -- The recording, analysis, and presentation of (higher frequency) periodic events imposes special requirements. For example, the boiler-condenser mode oscillations during the OTIS-GERDA Benchmark

Test 210100 must be examined using high-frequency data and a small time window. Long-duration plots of such cyclic events may be misleading. Compare Figures 4.5 and 4.7 of the Benchmark Test 210100, section 4. The coarse-time trace, Figure 4.7, indicates sporadic heating of the fluid upstream of the cold leg spillover (thermocouple CLTC03). But the expanded-time trace, Figure 4.5, indicates both the periodicity and the coupled response of the several cold leg fluid temperature indications.

5. Variations of Indicated Hot Leg Level -- Rapid and frequent variations of indicated hot leg collapsed liquid level in OTIS may have been due to primary pressure variations rather than to level changes. Multiple, small-range levels (as well as overall level) should be measured; these level indications should be separately characterized. MIST reflects these recommendations within the limits of practicality.

REFERENCES

1. OTIS Design Requirements, B&W Document No. 51-1149127-00, Babcock & Wilcox, Lynchburg, Virginia.

2. OTIS Loop Functional Specification RDD:84:4091-24-01:01. Alliance Research Center, Babcock & Wilcox, Alliance, Ohio.

3. OTIS Test Specifications, B&W Document No. 86-1149120-04, Babcock & Wilcox, Lynchburg, Virginia, 19 April 1984.

4. OTIS Testing Program -- Single-Variable and Composite Tests, Technical Procedure ARC-TP-615, Rev. 3, Babcock & Wilcox, Alliance, Ohio, 19 April 1984.

5. OTIS Testing Program -- Characterization of Reactor Vessel Upper Head Vent (RVUHV) During Natural Circulation Cooldown, Technical Procedure ARC-TP-616, Rev. 2, Babcock & Wilcox, Alliance, Ohio, 1 May 1984.

6. Decay Power for Short Times After Infinite Operation, B&W Document No. 32-1142593-00, Babcock & Wilcox, Lynchburg, Virginia, 20 September 1983.

7. Best Estimate Shutdown Margin, B&W Document No. 86-1149126-00, Babcock & Wilcox, Lychburg, Virginia, 8 February 1984.

8. Fission Power-MIST, B&W Document No. 32-1148431-00, Babcock & Wilcox, Lynchburg, Virginia, 14 February 1984.

9. B&W Document No. 51-1134814-01, Babcock & Wilcox, Lynchburg, Virginia, February 1983.

10. "Davis-Besse Nuclear Power Station Unit No. 1, Plant Procedure 1102.10, Plant Shutdown and Cooldown," February 1976.

11. "Multi-Loop Integral System Test (MIST) Facility Specification," RDD:84:4091-01-01:01 (distributed November 1984).

APPENDIX A DATA PLOTS

A.1.0 Introduction

A.2.0 Program Description

A.3.0 Directory of Plots

A.4.0 OTIS Instruments

(Data plots are transmitted separately)

1.0 INTRODUCTION

The OTIS data processing program is supplied test data either electronically or via magnetic tape. This data is supplied in engineering units by the VAX computer at the Alliance Research Center. The processing program then arranges the input data, calculates derived quantities, and generates printed and plotted output. This output is used to determine and to report the integral system performance during OTIS testing.

This appendix describes the data processing calculations and the code output. The program structure and major calculations are described in section 2. Section 3 provides a directory and explanation of the output plots. Finally, an index of instruments and an instrument location diagram are supplied in section 4. The data plots themselves are transmitted under separate cover.

2.0 PROGRAM DESCRIPTION

The OTIS data processing program is described by subroutine, in the order that they are used during calculations. The major subroutines include:

Section	Subroutine	Function
2.1	INLIST	o List the supplied data without alteration (INLIST is a system subroutine).
2.2	SETUP	o Identify the supplied variables.
	READIT	o Read the input.
2.3	WEEDIT	o Reject meaningless data.
2.4	CONVERT	o Convert the input data to the desired units.
2.5	DERIVE	o Derive information from the supplied data.
2.6	PROPS	o Calculate volume-weighted fluid properties.
2.7	CLOSURE	o Calculate mass and energy closure.
2.8	QUENCHR	o Calculate fluid heating due to metal quenching.
2.9	BALANCE	o Perform primary system mass, energy, and fluid and vapor volume calculations.
2.10	VOIDS	o Calculate approximate void fractions.
*	PRINTIT	o Print the indexed and derived data.
*	TESTIT, STUFFIT, and PLOTIT	o Generate basic plots.
*	GENPLOT	o Create general plots.
*	PLOTVSZ	o Plot SG temperature profiles.
2.11	SGHTRAN	o Evaluate and plot SG heat transfer.
2.12	NATURAL	o Evaluate and plot natural circulation characteristics.

2.1 Subroutine INLIST

This subroutine provides an engineering units printout of all the OTIS test data obtained and transferred from the (VAX) computer at ARC.

---

* The output plots are indexed in section 3; the instrument identifiers and locations are supplied in section 4.

2.2 Subroutine SETUP and READIT

Subroutines SETUP and READIT provide the necessary identification of the variables from the VAX computer at ARC, and arrange the data into pre-ordered arrays.

More than 300 OTIS test variables are transferred; each variable is assigned to a numbered position within the complete table of variables. Each position is thus associated with an alphanumeric identifier (the "VTAB" identifier), and its system, instrument, and elevation. (Instrument elevations are referenced to the upper, or secondary face of the SG Lower Tube Sheet, the "SGLTSUF"; the instruments are identified in Section 4.)

Upon execution of OTIS, Subroutine SETUP sets these descriptor arrays, which are subsequently associated with the supplied variables based on their position in the VTAB variable table. An ancillary subroutine (INDEXIT) reorders the supplied variables by system, instrument, and elevation, respectively. Subroutine READIT then installs the supplied data into the pre-ordered arrays. Associated Subroutines TAPED and TEXPAND read data from tape and permit analysis of time-based subsets of the supplied data.

2.3 Subroutine WEEDIT

Subroutine WEEDIT is used to review the supplied data for validity. The general constraint on the input data is that it must vary at least 10^{-10} between any two successive points during the test period (the total duration of data acquisition for the test point being considered). Only limit-switch signals bypass the WEEDIT checks.

Separate validity checks are used for pressures, temperatures, core power, collapsed levels, and auctioneered Conductivity Probe (CP) indications.* Pressures are discarded if they are outside the range 14 to 3000 psia. Temperatures are tested against the range 32 to 1500F. Core power and collapsed levels are retained if they are ever non-zero, even if they are invariant. Finally, an auctioneered CP indication is retained if it reads both non-zero and not equal to -99.* Variables removed from the supplied data base will read identically zero (within the field length of the

*The "auctioneered" CP indicates the elevation of the highest wetted CP below which all CPs of that string are also wetted.

supplied data); "-99" is obtained when all of the CPs of the associated string indicated wetted.

A variable which is found to be invalid by the aforementioned checks is deleted from further consideration (within the calculations for the associated test and is flagged by an appropriate print statement.

2.4 Subroutine CONVERT

The input data is converted to the desired units in Subroutine CONVERT. The affected variables include: Time, power, flowrates, level, conductivity probes, limit switches, and accumulated flows. The weigh-tank data, if supplied, is incorporated.

2.4.1 Time

Each data scan has an associated clock-time. These times are converted to decimal minutes at input (Subroutine READIT). The clock times are then converted to minutes after test initiation by subtracting the "reference time" (the time at which the Data Acquisition System was started for the testpoint). Therefore all variables will be keyed to time zero which is defined as the time when the data acquistion system was actuated. Plotted variables are offset by an additional time increment which is supplied by the user; this plotting offset, which is printed on the plot abscissa label, is generally the time from the activation of the data acquisition system until test initiation.

2.4.2 Power

The OTIS core power is converted from Kw to percent of scaled full power. The conversion factor is obtained by dividing the Bellefonte (205FA) full thermal power of 3600 MW by the OTIS power scaling factor 1685.6*

$$\text{OTIS full scaled power} = 3600\ \text{MW}/1685.6 = 2136\ \text{Kw} \qquad \text{(A-1)}$$

Therefore the OTIS power conversion factor is 21.36 Kw per 1% of full scaled power.

---

*The OTIS power scaling factor is defined as:

S = Total number of steam generator tubes in a 205FA plant/Total number of steam generator tubes in OTIS
= 16013x2/19
= 1685.6

2.4.3 Flowrates

The OTIS primary and secondary system flowrates are converted to the percent of full (scaled) flow.

The conversion factor for the OTIS primary system flowrate, based upon the simulation of a domestic 205 FA plant, is obtained as follows:

$$\text{Plant flowrate at 100\% flow} = 157.4 \times 10^6 \text{ lbm/h} \quad \text{(A-2)}$$

OTIS primary system scaled flowrate at 100% flow

= Plant Flow Rate at 100% Flow/OTIS Power Scaling Factor

$= (157.4 \times 10^6 \text{ lbm/h}) / (1685.6 \times 3600 \text{ s/h})$

$= 25.94$ lbm/s (for 100% full scaled flow) (A-3)

Therefore the OTIS primary flowrate conversion factor is 0.2594 lbm/s per 1% of full scaled flow.

The conversion factor for the OTIS secondary system flowrate is obtained by dividing the 205 FA plant secondary flowrate by the OTIS scale factor:

OTIS secondary system scaled flowrate at 100% flow

$= (16.1 \times 10^6 \text{ lbm/h}) / (16.85.6 \times 3600 \text{ s/h})$

$= 2.653$ lbm/s (A-4)

Therefore the OTIS secondary flowrate conversion factor is 0.02653 lbm/s per 1% of full scaled flow.

The primary boundary flowrates (leak, HPI, etc.) are converted from lbm/h to lbm/s. Pitot tube indicated flowrates are converted to equivalent Primary flowrate; the input flowrate (lbm/h) is multiplied by the number of SG tubes (19), multiplied by the inverse of the approximate integral of the 1/7th-power velocity profile over the SG tube area subtended by the Pitot tube (0.847), and divided by the conversions to obtain % of full primary flow (0.259 lbm/s per % full flow).

2.4.4 Collapsed Levels

The input collapsed levels are referenced to the SG Lower Tube Sheet Upper Face (SGLTSUF) using the elevation of the appropriate lower level tap. (Corrections for thermal expansion are applied elsewhere). The supplied hot leg level downstream of the HLUB is combined with the input SG primary level to obtain the composite collapsed level on the SG side of the HL U-bend.

2.4.5 Miscellaneous Conversions (CP, LS, and Accumulated Flow)

The auctioneered CP (conductivity probe) signal is supplied as "-99" when all probes of that string indicate wetted. To limit the scale of the CP-plot ordinates, auctioneered CP (elevation) indications are limited to not less than the lowest elevation of the probed component. (The "Auctioneered" CP is discussed further in Paragraph 2.3).

Active limit switches (LS) are arbitrarily offset in order to separate their plots for legibility.

Accumulated flowrates are converted from gallons to lb_m by multiplying by (62.4 lbm/ft^3)/(7.481 gal/ft^3).

2.4.6 Weigh-Tank Data

Weigh-tank data may be supplied by the user. When supplied, the accumulating flowmeter data for the corresponding discharge stream is replaced with the weigh-tank readings while retaining the general trends of the accumulator data. (The accumulator data is acquired at a much higher frequency than the weigh-tank data.) This replacement is performed in three steps:

(1) The difference between the weigh-tank and accumulator readings is determined at each of the times of the manual weigh-tank readings.

(2) These readings differences, determined at weigh-tank times, are linerly interpolated to the times of automated data acquisition (the DAS scan times).

(3) The time-interpolated reading differences are applied to the accumulated readings.

Each adjusted reading is constrained to be not less than the preceding adjusted reading. This replacement process is repeated for each of the supplied sets of weigh-tank readings. There can be a maximum of three sets of weigh-tank data, corresponding to the following discharge-collection systems:

(1) Single-phase leak, including the reactor vessel upper head vent,

(2) Hot leg high-point vent, and

(3) Pressurizer relief valve (PORV).

2.5 Subroutine DERIVE

This subroutine is used to derive additional indicators of testing behavior. The derived quantities are obtained by combining various supplied variables. The derived quantities include: Volume-weighted liquid and vapor temperatures for each system component, flowrate from accumulated flow, primary system boundary flowrates, and differenced secondary flowrates.

2.5.1 Component Average Temperatures

Component average temperatures (for each data scan time) are formed for the primary system components and for the SG secondary. Primary components include the reactor vessel (RV), hot leg (to the HL U-bend Spillover), SG primary (including the HL downstream of the HL U-bend), cold leg, downcomer, and pressurizer. All available fluid thermocouples and resistance temperature detectors are used. The calculations are performed in the ancillary subroutine PROPS, section 2.6.

2.5.2 Flowrates From Accumulated Flows

Accumulated flows recorded at the single phase venting (SPV), high point venting (HPV), and relief systems (RS) are differenced, and divided by the duration of the corresponding time increment to obtain flowrates. Central differencing is used for this calculation and generally; the rate at time "t" is formed by subtracting the accumulated flow at the previous time (t-1) from that at the next time (t+1).

2.5.3 Primary System Boundary Flowrates

HPI (High Pressure Injection) and total primary system boundary flowrates are determined on the basis of the supplied indications. The total primary system boundary flowrate is the difference between this HPI flowarate and sum of the Single Phase Venting System flowrate (assigned to one of the liquid-region leak sites), the High Point Vent flowrate, and the Relief flowrate.

2.5.4 Secondary System Derivations

Feed flowrate minus steam flowrate is installed as a derived indication. Also, two SG secondary saturation temperatures are determined. The steam saturation temperature is found (using Subroutine STP, as before) at the

current indicated steam pressure; and the maximum SG secondary saturation temperature is found at the total pressure at the bottom of the SG, i.e. steam pressure plus the density head of the current collapsed secondary level (this saturation temperature increase, usually resulting from 26 ft of liquid, is only a few degrees F but is is useful in the analysis of the SG temperature profiles).

The SG secondary outlet (steam) enthalpy is found (again using STP) at the highest current SG secondary temperatures (and indicated steam pressure). This highest-temperature feature is required to mitigate the effects of heat losses to ambient from the SG outlet steam piping.

2.6 Subroutine PROPS

Volume-weighted liquid and vapor properties are determined for each primary component (RV, HL, SGP, CL, DC, and Pr) and for the SG secondary. Properties include temperature, density, and enthalpy. Determinations are made in Subroutine PROPS which calls the system subroutines ZZP and ZZTP, portions of the STP package. The properties generated by STP are self-consistent because STP is based on a single, continuous state equation. Subroutine PROPS is written in four parts: (1) Initialization, (2) temperature sorting, (3) liquid region calculations, and (4) vapor region calculations. Subroutine PROPS is called once for each loop component (reactor vessel, hot leg, steam generator primary, cold leg, downcomer, pressurizer, and steam generator secondary). Initialization thus consists of identifying the temperature sensors for the current component, using sensor elevation to find fluid volume up to this elevation (Subroutine VOLFMZ), and ordering these temperature indications by increasing elevation (and the volume encompassed). This arrangement of temperature sensors is then used for the time-based evaluations. The first calculation at each time obtains saturated liquid and vapor properties at the current primary pressure, for use as bounding properties.

2.6.1 Liquid-Vapor Interface

The current (by-component) collapsed liquid level is used to estimate the elevation of the liquid-vapor interface. Temperature sensors below the collapsed level are assigned to the liquid-region calculations, the remaining sensors are assigned to the steam-region calculations. If there is no liquid-height remaining, the component is assumed to be steam filled

and the liquid-region calculations are bypassed. Similarly, if the component is apparently liquid filled, only the liquid-region calculations are used.

2.6.2 Liquid-Region Calculations

The liquid-region calculations are considered in four parts: (1) Bottom liquid volume, (2) intermediate liquid volume, (3) top liquid volume at the top of the component, and (4) top liquid volume but with steam above. Each of these types of calculations requires the determination of a local temperature (T_i) and a local fluid volume (V_i) over which this temperature applies. Local volume is used to weight each of the three local properties: local temperature, density, and enthalpy: density and enthalpy are obtained from Subroutine ZZTP using the current primary pressure and the local temperature T_i. If ZZTP finds that the state is indeterminate, usually because the T_i-p combination approximately defines saturation, then the appropriate liquid or vapor saturation properties are substituted. Cumulative volume, and volume-weighted temperature, density, and enthalpy, are calculated at each time step; the final properties are these accumulated sums divided by the accumulated volume.

(1) Lowest Liquid Volume

Volume is set equal to the volume up to the lowest sensor; temperature is taken from the lowest sensor, but limited to TSAT- or less, where

$$TSAT- \overset{\Delta}{=} TSAT - 0.001 \qquad (A\text{-}5)$$

(2) Intermediate Liquid Volume

This calculation is bypassed if only one sensor is in liquid. The number of intermediate liquid region volumes is one less than the number of liquid-region sensors. For each pair of liquid-region sensors, the temperature is taken from the average of the two, and the volume is obtained from the difference of the fluid volume at the higher sensor less that at the lower. The calculation is repeated over each pair of liquid-region sensors.

(3) Highest Liquid Volume, No Steam

This calculation is bypassed if there are any steam-region temperatures. Temperature is the (single) indicated temperature, limited to

TSAT-. Local volume is component total fluid volume less the volume up to the highest sensor.

(4) Highest Liquid Volume, Steam Above

Volume is the difference between the component volume to the collapsed liquid level and the volume up to the highest liquid-region sensor. Local temperature is the average of the indication from the highest-elevation liquid-region sensor (limited to TSAT-), and TSAT-.

2.6.3 Vapor-Region Calculations

If there are no vapor-region sensors, these calculations are bypassed. Vapor-region property calculations are analogous to those of the liquid region, and are also performed in four categories: (1) Lowest steam volume with liquid below, (2) lowest steam volume but no liquid present, (3) intermediate steam volume, and (4) highest steam volume.

(1) Lowest Vapor Region, Liquid Below

If there are no liquid-region sensors, this calculation is bypassed. Local volume is the volume up to the lowest vapor-region sensor minus the total liquid volume. Local temperature is the average of TSAT+ and indicated temperature (limited to TSAT+), where

$$TSAT+ \overset{\Delta}{=} TSAT + 0.001 \qquad \text{(A-6)}$$

(2) Lowest Steam Volume, No Liquid

This calculation is bypassed if there are any liquid-region temperatures. Local volume is the component fluid volume up to the lowest sensor. Local temperature is as indicated by this sensor, limited to TSAT+ or greater.

(3) Intermediate Steam-Region Volume

This calculation is performed only if two or more temperature sensors are in the steam region. The calculation is repeated for each sequential pair of steam-region sensors, lowest to highest. Local volume is volume up to the higher sensor minus volume up to the lower sensor. Local temperature is the average of the two indicated temperatures, each limited to TSAT+ or greater.

(4) Highest Steam-Region Volume

Local volume is total component fluid volume minus the volume up to the highest-elevation sensor. Local temperature is as indicated by the highest-elevation sensor.

2.6.4 Summary

Subroutine PROPS calculates the following volume-weighted properties for each component, and at each time increment: Liquid temperature, density and enthalpy, and vapor temperature, density, and enthalpy. Temperature-sensor elevations and component volume-versus-elevation, as well as collapsed liquid level, are used to form these volume-weighted properties. Calculation sensitivity is limited to the maximum elevation span of the component level indication. Properties for a state (liquid or vapor) apparently not present in the component default to the corresponding saturation properties.

2.7 Subroutine CLOSURE

This subroutine determines the fluid volume, mass, and energy plus their rates of change for the various components (RV, HL, SGP, CL, DC, PZR and SG), and for the entire system. The component and system mass and energy content, as determined by this subroutine, are defined as the "indicated values" and are obtained by combining supplied and derived information.

2.7.1 Fluid Volume

The indicated collapsed liquid level and the average fluid temperature for each component are used to determine the volume of liquid contained in each component, and the current liquid fraction (% of full). Component volume-versus-elevation tables are corrected for thermal expansion (using component average fluid temperature and the appropriate linear expansion coefficients), and interpolated using the current collapsed liquid level to obtain an apparent liquid volume. These calculations are performed in the ancillary subroutine VOLFMZ. This apparent liquid volume is divided by component total volume to obtain the apparant liquid fraction, expressed as percent of full. The liquid volumes of the primary system components are summed to obtain primary liquid volume, and divided by total primary volume to obtain primary system liquid fraction.

2.7.2 Fluid Mass and Rate of Change

Because the apparent liquid volume is based on collapsed liquid level, it approximately reflects the volume of liquid required to match the sensed liquid elevation head. Thus the contained fluid mass is the product of the contained fluid volume and the liquid density. The total primary fluid mass is the sum of the primary system component fluid masses. The mass rate-of-change is obtained by central-differencing the fluid masses at the bracketing time scans and dividing by the corresponding time between scans.

2.7.3 Inter-Component Flowrates

The primary flowrate from one component to the next component is estimated based on the indicated downcomer flowrate (obtained from the DC orifice flowmeter). The flowrate from the RV to the HL ($\dot{m}$-RV) is the DC flowrate minus the reactor vessel vent valve (RVVV) flowrate, minus the RV fluid mass rate of change (dm/dt). Calculations proceed similarly from component to component around the primary loop.

The primary flowrate from the HL to the HL U-bend ($\dot{m}$-HL) is $\dot{m}$-RV (the flowrate from the RV to the HL) minus dm/dt-Pressurizer, minus dm/dt-HL, minus the Pzr relief flowrate if any. The flowrate from the SG primary to the cold leg, $\dot{m}$-SG, is $\dot{m}$-HL minus dm/dt-SG primary, minus the HPV (high point vent) flowrate if any. The flowrate from the CL to the DC, ($\dot{m}$-CL), is $\dot{m}$-SG plus the HPI (high-pressure injection) flowrate, minus CL Discharge leak rates, minus dm/dt-CL. Finally, the primary flowrate from the DC to the RV, ($\dot{m}$-DC), is $\dot{m}$-CL plus the RVVV flowrate minus dm/dt-DC (this flowrate should agree with the starting flowrate indicated by the DC orifice flowmeter).

2.7.4 Heat Loss

Component heat losses are determined from heat-loss functions of the form:

CONSTANT X (TAVG - TZERO)

where TAVG is the component average fluid temperature, and the constant and intercept (TZERO) are determined from the OITS heat loss tests. The RTDs bracketing the component are used to form the component average fluid temperatures, to be consistent with the heat-loss tests. The hot leg heat loss calculations are keyed to the HL guard heaters; if the supplied HL

insulation temperature difference is negative, the guard heaters are assumed to be on and the HL heat loss is nulled. (The indicated insulation temperature difference, inside minus outside, is customarily much greater than zero with the guard heaters off, and vice versa.)

2.7.5 Power: Available Primary Power, and SG Primary and Secondary Heat Transfer Rates

Comparisons of available and transferred power levels are useful for the evaluation of energy flow, storage and leak-HPI (high-pressure injection) cooling effects. The available primary power is core power minus primary system heat losses.

The SG primary extracted power is the difference between the energy being convected into and out of the SG primary. The flowrates for this calculation are the primary system inter-component flowrates. The fluid enthalpies being convected are calculated at the SG primary pressure (or at another primary pressure if the SG primary pressure is not supplied); temperatures for this calculation are obtained from the SG primary inlet and outlet RTDs (resistance temperature detectors).

The SG secondary extracted power is calculated analogously to that of the SG primary, except that SG secondary heat losses are also included. The SG secondary extracted power is the steam flowrate times the steam enthalpy (determined at the highest SG secondary temperature), minus the product of feedwater flowrate and the feedwater enthalpy, plus the SG secondary heat losses to ambient.

The primary available, SG primary extracted, and SG secondary extracted power levels, should be coincident under steady-state conditions when the primary boundary systems are inactive. Any major differences in these powers would indicate primary system boundary heat removal, and/or energy storage.

2.7.6 Fluid Energy and Rate of Change

Fluid energy and rate of change (de/dt) are estimated for each primary system component (RV, HL, SG primary, CL, DC, and pressurizer), for the overall primary, and for the secondary. The rate of change of fluid energy may be compared to the (three) inter-system heat transfer rates, but it should be recalled that metal storage is not explicity considered in these calculations.

The calculation of component fluid energy involves a combination of available quantities. The contained fluid energy is the sum of the liquid energy content and that of the vapor. Liquid energy content is the product of liquid mass and liquid enthalpy. Similarly vapor energy is the product of vapor mass and vapor enthalpy.

The energy content of the primary fluid is obtained by summing over components. This energy content versus time is normalized to the initial energy content and expressed as percent of initial energy. Energy content is central differenced using bracketing data scans, and divided by the time between these scans, to obtain the energy rate-of-change. The standard conversion (1% of full power = 21.36 Kw) is used to express de/dt in the usual units of percent of full power (the calculated values are installed at the time corresponding to the end of the time increment).

2.8 Subroutine QUENCHR

Subroutine QUENCHR provides the fluid heating due to recovering relatively hot metal. Three guard-heated regions are considered: the HL, the SGP above the upper tube sheet, and the pressurizer. A quenching contribution is obtained only if, for the component being considered, these three conditions are met:

(1) There are metal temperature indications above the elevation of the current collapsed liquid level;

(2) the average metal temperature (in the vapor region) is greater than the current fluid saturation temperature; and

(3) the component is refilling.

The third condition is checked using a time-smoothed level rate of change which is calculated specifically for this determination; smoothing is introduced to preclude false quenching contributions due to oscillations of the collapsed liquid level.

The accuracy of this quenching calculation is limited by both the number of available metal temperature indications and the approximations used in the calculation. These approximations include:

- The metal cross-sectional area is 0.003 ft^2 (and constant).
- The volumetric specific heat of the metal is 60 BTU/ft^3 F (and constant).

The quenching calculation uses central differencing of the metal temperatures at the bracketing times. The result is expressed in percent of full power. It is determined for each of the three components and then summed.

2.9 Subroutine BALANCE

Calculated and indicated total primary fluid mass, fluid energy, and liquid volume are compared at each time step. Indicated total quantities are obtained directly from indications, generally in Subroutine CLOSURE.

Calculated total quantities at the first time of data are set equal to their counterpart indicated values (this also applies when a data reduction is started part way into the data set). Thereafter, each calculated total is set equal to its previous value plus the calculated change over the intervening time step. For example, the "calculated" mass at time "t" is:

$$M\ (\text{calculated, time} = t) = M\ (\text{calculated, time} = t - \Delta t) + \Delta t \ \frac{\Delta m}{\Delta t}\ \text{calculated.} \tag{A-7}$$

2.9.1 MASS: Total Primary System Flud Mass

2.9.1.1 Indicated

Total indicated primary fluid mass (lbm) is the sum of the primary component fluid masses (M_i):

$$M = \sum_{\text{component}} M_i,\ lb_m \tag{A-8}$$

Component fluid mass is component fluid volume (V_i, ft^3) times volume-weighted component fluid density ($\rho_{fl,i}$, lbm/ft^3):

$$M_i = V_i \rho_{fl,i},\ lb_m \tag{A-9}$$

(Volume-weighted fluid densities are calculated in subroutine PROPS).

2.9.1.2 Calculated

Total calculated primary fluid mass at time "t" is the sum of calculated mass at the preceding time, $M(t-\Delta t)$, and the intervening time increment (Δt) times the calculated mass rate of change over that increment ($\Delta m/\Delta t$):

$$M(t) = M(t - \Delta t) + t \cdot (\Delta m/\Delta t)\ ,\ lb_m \tag{A-10}$$

The primary fluid mass rate of change ($\Delta m/\Delta t$, lbm/s) is the sum of the primary system boundary mass flowrates, i.e. HPI less discharge:

$$\Delta m/\Delta t = \dot{m}_{HPI} - \sum_{\substack{\text{active} \\ \text{discharges}}} \dot{m}_{discharge} \text{ , } lb_m/s \qquad \text{(A-11)}$$

Discharges include liquid-region leaks and vapor-region leaks. One liquid-region discharge mass flowrate is supplied (from the single-phase collection system), it is linked to the appropriate discharge site using limit switch indications. The vapor-region discharges (HPV, PORV) are supplied separately.

2.9.2 ENERGY: Total Primary System Fluid Energy

2.9.2.1 Indicated Primary Fluid Energy

Total "indicated" primary fluid energy is found by summing over the primary components:

$$E = \sum_{\text{components}} E_i \text{ (Btu) x } (100/E_{total}(t=0)), \text{ \% of initial E} \qquad \text{(A-12)}$$

where (100/E(t=0)) is used to reference E(t) to percent of intial total energy (these calculations are done in CLOSURE).

Component fluid energy (E_i) is found by summing the component fluid and vapor energies:

$$E_i = M_{fl}\, h_l + V_v\, \rho_v\, h_v \qquad \text{(A-13)}$$

where M_{fl} = component fluid mass (lbm),
h_l = liquid-volume-weighted h (B/lbm),
V_v = vapor volume (ft^3),
ρ_v = vapor-volume-weighted density (lbm/ft^3),
and h_v = vapor-volume-weighted enthalpy (B/lbm)

(calculations are done in CLOSURE, the properties are from PROPS).

2.9.2.2 Calculated Primary Fluid Energy

Calculated total primary fluid energy at time "t" (E(t)) is that calculated at the preceding time (E(t- t)) plus the intervening change calculated:

$$E(t) = E(t-\Delta t) + \Delta E, \text{ (\% of initial fluid energy)} \quad \text{(A-14)}$$

$$\text{where } \Delta E = \Delta t \ \dot{e}_{net} \ \frac{100}{CE(t=0)}, \quad \text{(A-15)}$$

Δt = duration of time increment (s),

$\dot{e}_{net}$ = net primary fluid energy rate of change (calculated) (% full power),

100/E (t=0) converts energy in BTU to % of initial energy, and

$$C = \frac{3600 \text{ s/h}}{(3412 \text{ B/kwh})\ (21.4 \text{ kw/\% full power})}, \ \frac{\text{\% full power}}{\text{B/s}} \quad \text{(A-16)}$$

Net Primary Fluid Energy Rate of Change - $\dot{e}_{net}$

Calculated net primary fluid energy rate of change ($\dot{e}_{net}$) is the sum of the various energy sources and sinks:

$$\dot{e}_{net} = q_{core} + q_{primary\ metal} - q_{leak\text{-}HPI} - q_{SG} - q_{ambient}, \quad \text{(A-17)}$$
$$\text{\% of full power}$$

where the individual terms are discussed below.

Core Power

Core power (q_{core}) is supplied (and converted to % full power in subroutine CONVERT).

Primary Metal Heat Transfer

Heat transfer from the primary metal to the primary fluid is considered in two regions, "low" metal adjacent to liquid and "high" metal adjacent to vapor. The high-elevation primary metal is considered in the quench calculation, subroutine QUENCHR.

The contribution of the primary metal adjacent to liquid (q_{low}) is estimated by assuming that this metal temperature responds as the (component) volume-weighted fluid temperature. The "low" metal volume is obtained by multiplying total component metal volume by the fraction of the component fluid volume in liquid. Metal properties are approximated as $(\rho c_p)_{metal}$ = 60 (B/ft^3F). The total primary contribution due to low metal is then the sum over the primary components:

$$q_{low} = \sum_{components} 60\left(\frac{B}{ft^3F}\right) \frac{V_{li}}{V_i} V_{mi}(ft^3) \left[\frac{T_{li}(t-\Delta t)-T_{li}(t)}{\Delta t}\right]\left(\frac{F}{s}\right) C\left(\frac{\%\ full\ power}{B/s}\right) \quad (A\text{-}18)$$

where (V_{li}/V_i) is the ratio of component liquid to total fluid volume and C converts (B/S) to (% full power).

Leak-HPI Energy Transfer

The energy impact of discharges and HPI ($q_{leak\text{-}HPI}$) is:

$$q_{leak\text{-}HPI} = \sum_{discharges} q_{discharge} - q_{HPI}\ ,\ \%\ full\ power \quad (A\text{-}19)$$

The components are addressed below:

Discharge:

The discharge power-equivalent is:

$$q = C\ \dot{m}\ h\ (\%\ full\ power), \quad (A\text{-}20)$$

where C converts (B/s) to % of full power),
$\dot{m}$ is the indicated discharge mass flowrate (lbm/s), and
h is the discharge enthalpy (BTU/lbm).

The determination of discharge enthalpy (as well as fluid density, for subsequent volume balance calculations) involves discharge-specific state checks.

CLS or CLD Leak: The leak h and ρ are found at system pressure and leak temperature (using ZZTP), i.e., $h=f(P, T_{leak})$, $\rho=f(P,T_{leak})$. If P and T_{leak} are close to saturation the properties are set to those for saturated liquid.

HLHPV: The HLHPV discharge involves a deliberate estimate of state. A state indicator (KEYPHAS) is set to zero, then perturbed based on the several indications of state. The final value of KEYPHAS is used to choose between the phases.

Saturation Temperature: If the HLHPV fluid temperature is more than 2F subcooled, KEYPHAS is set to -1; if the temperature indicates more than 2F superheated, KEYPHAS is set to +1.

Hot Leg (Upstream) Liquid Volume: If the HL volume is 100% full, KEYPHAS is reduced by 1; if the volume indicates less than or equal to 98% full, KEYPHAS is increased by 1.

HLHPV Flowrate: If the current HPV indicated mass flowrate is more than 2.5 times the "base" rate, KEYPHAS is set to -2 (i.e., the previous T and V-liquid checks are over-ridden and saturated liquid discharge is used). The base is established at the first instance of HLHPV flow greater than 0.0012 lbm/s (this minimum flowrate to distinguish flow from noise is based on data observations). Subsequent HPV flowrates greater than 0.0012 lbm/s either update the base, or trigger KEYPHAS=-2 if they are greater than 2.5 times the current base ("2.5" was established by reviewing data and consulting critical flow relations, but it is unfortunately not unequivocal).

Following the KEYPHAS setting just outlined, KEYPHAS is tested to flag state: KEYPHAS<0 obtains saturated or subcooled liquid, KEYPHAS>0 obtains saturated or superheated vapor (if P-system and T-HLHPV obtained a state in agreement with the KEYPHAS state check, the P-T properties are retained). Once the HLHPV enthalpy is determined, the HLHPV energy transfer is then

$$q_{HLHPV} = C\,\dot{m}_{HLHPV}\,h,(\%\text{ full power}) \qquad \text{(A-21)}$$

RVHPV: The reactor vessel high point vent involves a state determination which is identical to that described for the HLHPV with the exception that conditions in the RV plenum are used. The energy transfer is then:

$$q_{RVHPV} = C\,\dot{m}_{RVHPV}\,h,(\%\text{ full power}) \qquad \text{(A-22)}$$

PORV: The PORV discharge involves a state determination similar to that just described for the HPV. The PORV setting of KEYPHAS based on temperature is the same, i.e. 2F subcooled obtains KEYPHAS=-1 and 2F superheated yields +1. The PORV level test is done on the pressurizer. If the Pzr is more than 98% full (of liquid), KEYPHAS is reduced by 1; if the Pzr liquid inventory is less than or equal to 98%, KEYPHAS is increased by 1. The PORV uses no base-flow check. Instead, if the previous two state tests obtain KEYPHAS=0 (no net state determination), and if the STP routine returned its flag=0 (indicated conditions approximately at saturation), then the vapor state is imposed by setting KEYPHAS=+1.

The PORV-fluid properties are set based on KEYPHAS as with the HPV; again, if the p-T results are confirmed by the indicated state, then subcooled or superheated properties are used.

HPI: The HPI energy contribution is determined using the HPI fluid enthalpy at system pressure and HPI fluid temperature.

Steam Generator Energy Transfer: The SG contribution (q_{SG}) is the energy transfer rate across the SG tubes, from the primary to the secondary system. Early attempts to calculate q_{SG} from $\dot{m}_{pri}\ \Delta h_{SG}$ were thwarted by primary flow determination -- it is inaccurate at low flowrates, and is sometimes adversely affected by voiding and/or HPI backflow at the flow metering device. For this reason, q_{SG} relies on the secondary energy balance:

$$\text{SG Secondary:}\quad \dot{e}_{in} = \dot{e}_{out} + \dot{e}_{storage} \tag{A-23}$$

$$\text{or:}\quad q_{pri\text{-}to\text{-}sec} + q_{SG\ metal} = q_{steam\text{-}feed} + q_{sec\ fluid\ storage} + q_{SG\ to\ ambient} \tag{A-24}$$

where $q_{pri\text{-}to\text{-}sec}$ is the sought-after q_{SG}.

SG Metal:

The SG-metal calculation ($q_{SG\ metal}$) is exactly analogous to that used to calculate the primary $\dot{e}$. Again the calculation is performed for "low" metal (that metal adjacent to liquid and assumed to respond to volume-weighted liquid average temperature). The approximation $(\rho Cp)_{metal} = 60\ B/ft^3F$ is again employed, also the metal fraction in the liquid region is taken as the current liquid volume. Unlike the primary metal calculation, no quenching term is estimated for the SG secondary.

Steam and Feed: The energy contribution of steam and feed flow ($q_{steam\text{-}feed}$) are calculated from

$$q_{steam\text{-}feed} = 0.02653\ (\dot{m}_{steam}\ h_{steam} - \dot{m}_{feed}\ h_{feed})\ C \tag{A-25}$$

where 0.02653 converts the steam and feed mass flowrates from % full (secondary) flow to (lbm/sec), and C is the usual conversion from (B/s) to % full power. The steam and feed flowrates ($\dot{m}$) are indicated, the stream enthalpies are taken at secondary steam pressure and the stream temperatures. (Because of heat loss impact in the steam outlet piping upstream of

the steam temperature measurement, steam temperature is taken at the highest SG secondary temperature.)

Secondary Fluid Storage: The energy contribution of SG secondary stored fluid energy is determined by differencing the total stored SG fluid energy at bracketing times:

$$q_{\text{sec fluid storage}}(t) = C \quad \frac{E(t+\ t) - E(t-\Delta t)}{2\Delta t} \quad , \text{ \% full power}$$

The stored fluid energy (E) is taken from indications:

$$E = E_l + E_v \qquad \text{(A-26)}$$
$$= M_l \bar{h}_l + V_v \rho_v \bar{h}_v$$

where M = Total liquid mass (in the SG secondary),

$\bar{h}_l$, $\bar{h}_v$ = volume-weighted average liquid or vapor enthalpy,

V_v = Vapor volume, and

ρ_v = vapor density.

SG Losses to Ambient: The SG secondary energy loss to ambient (q_{SG} to ambient) is estimated at the current SG average secondary fluid temperature using previsouly-obtained SG heat loss data. This calculation is performed in subroutine CLOSURE.

Ambient Losses: Primary heat loses to ambient ($q_{ambient}$) are calculated in subroutine CLOSURE.

Summary of Net Primary Fluid Energy Rate of Change - $\dot{e}_{net}$

The equation for "calculated" net primary system fluid energy rate of change (presented earilier) is:

$$\dot{e}_{net} = q_{core} + q_{primary\ metal} + q_{quench} - q_{leak\text{-}HPI} - q_{SG} - q_{ambient} \qquad \text{(A-27)}$$

Reviewing the relations for these components of $\dot{e}_{net}$:

q_{core} is from indication.

$$q_{\substack{primary \\ metal}} = q_{low} = \sum_{components} 60 \left[\frac{V_{li}}{V_i}\right] V_{mi} \left[\frac{\bar{T}_{li}\ (t-\Delta t) - \bar{T}_{li}(t+\Delta t)}{2\Delta t}\right] C \qquad \text{(A-28)}$$

Each of the components of $q_{metal}(q_{low})$ tie directly to indications (or are assigned constants, such as component metal volume V_{mi}, fluid volume V_i, and the conversion to % full power, C). The volume-weighted liquid average temperatures were obtained (in subroutine PROPS) from observed temperatures, observed levels, and component volume-versus-elevation, V(z). The saturation temperature Tsat was defined at indicated system pressure. Thus no empiricism was used to define q_{metal}, rather independent indications and several assumptions (already described) were used. The metal-quenching contribution similarly relies on indications.

The next component of $\dot{e}_{net}$ was $q_{leak-HPI}$

$$q_{leak-HPI} = \sum_{discharges} q_{discharge} - q_{HPI} \qquad \text{(A-29)}$$

where, in general,

$$q_{discharge} = C\, \dot{m}_{discharge}\, h_{discharge}. \qquad \text{(A-30)}$$

Discharge mass flowrate ($\dot{m}_{discharge}$) was indicated (or was obtained directly from indicated accumulated flow measurements). But the discharge fluid enthalpy ($h_{discharge}$) invoked a number of tests and assumptions regarding discharged fluid state.

The q_{SG} component was quite involved:

$$q_{SG} = q_{steam-feed} + q_{sec\ fluid\ storage} + q_{SG\ to\ ambient} - q_{SG\ metal} \qquad \text{(A-31)}$$

- $q_{steam-feed}$ required indicated steam and feed mass flowrates, and steam temperatures combined with secondary pressure.
- $q_{secy\ fluid\ storage}$ used levels and V(z) to get volumes, and sensed temperatures and SG pressure to find h and $\rho = f(p,T)$.
- q_{SG} to ambient used heat loss characterization data and current SG secondary fluid temperatures.
- q_{SG} metal, like the primary metal, used current fluid volume and fluid temperatures plus several approximations (and ignores metal time delay).

2.9.3 Primary Liquid and Vapor VOLUME

Like the preceding mass and energy comparisons, the rate of change of primary liquid and vapor volume is calculated, summed in time, and compared to indicate total primary liquid volume.

2.9.3.1 Indicated Liquid Volume

Indicated liquid volume is the sum of the component liquid volumes:

$$V_l = \sum_{\substack{\text{primary} \\ \text{components}}} V_{li} \qquad \text{(A-32)}$$

where V_{li} = Component liquid volume, from component liquid level and volume-versus-elevation, V(z).

2.9.3.2 Calculated Liquid Volume

Calculated liquid volume is the calculated volume at the preceding time plus the time-incremental contributions:

$$\dot{V}_l(t) = \left[V_l(t-\Delta t) + \dot{v}_{lnet}\,\Delta t\right]\left[\frac{100}{V}\right] \quad \text{, \% full} \qquad \text{(A-33)}$$

where $\dot{v}_{lnet}$ (ft^3/s) is the sum of the calculated primary liquid volume rate of change,
and V = Total primary system fluid volume.

$\dot{v}_{lnet}$ (liquid)

$$\dot{v}_{lnet} = \dot{v}_{HPI} - \dot{v}_{leak} - \dot{v}_{\Delta\rho} - \dot{v}_{steam} - \dot{v}_{\Delta p} \qquad \text{(A-34)}$$

where the components, to be discussed next, are:

$\dot{v}_{HPI}$ = $\dot{v}_l$ due to HPI,
$\dot{v}_{leak}$ = $\dot{v}_l$ discharged (leaks + HPV + PORV)
$\dot{v}_{\Delta\rho}$ = $\dot{v}_l$ due to liquid thermal expansion/contraction,
$\dot{v}_{steam}$ = $\dot{v}_l$ due to steam generation, and
$\dot{v}_{\Delta p}$ = $\dot{v}_l$ due to primary pressure effects.

$\dot{v}_{HPI}$: the primary liquid volume change due to HPI is considered in two components: the HPI mass flowrate less than or equal to the liquid-region leak flow, and the HPI in excess of leak flow. When HPI is less than liquid-region leak flow,

$$\dot{v}_{HPI} = \frac{\dot{m}_{HPI}}{\rho_{leak}} \qquad \text{(A-35)}$$

where ρ_{leak} is the density of the liquid-region leak fluid. The assumption here is that leak-HPI cooling or heating is accounted for in primary liquid average temperature (which is introduced in the $\dot{v}_{\Delta\rho}$-term, but that the steady-state leak-HPI mass exchange without primary fluid temperature change (e.g., with core heating offsetting HPI cooling) has no net impact on primary liquid volume.

When HPI mass flowrate exceeds leak flow, v_{HPI} is calculated using:

$$\dot{v}_{HPI} = \frac{\dot{m}_{leak}}{\rho_{leak}} + \frac{\dot{m}_{HPI} - \dot{m}_{leak}}{\bar{\rho}_l} \qquad \text{(A-36)}$$

Here the first term invokes the assumption just described, the second term similarly obtains no heating/cooling effect of HPI in excess of leak flow (reserving that for the $\dot{v}_{\Delta\rho}$ term) by introducing the exess HPI flowrate at the system-average liquid density ($\bar{\rho}_l$).

$\underline{v_{leak}}$: The aggregate discharge of primary liquid from leaks (CLS or CLD), HPV, and PORV are grouped in $\dot{v}_{leak}$. As described in the previous section regarding primary energy balance, the various discharge calculations involve tests for discharge fluid temperature and for effluent state. These tests assign each discharge stream to the liquid- or vapor-change category. For each stream determined to be liquid, the stream fluid density is used to find the liquid volume effect:

$$\dot{v}_{leak} = \dot{m}_{leak}/\rho_{leak} \qquad \text{(A-37)}$$

(Recall that the CLS is limited to subcooled and saturated liquid; the remaining discharges may affect either the liquid or vapor volume change).

$\underline{\dot{v}_{\Delta\rho}}$: The effect of primary liquid inventory contraction and expansion on liquid volume is estimated using:

$$\dot{v}_{\Delta\rho} = \sum_{\text{components}} V_{1i} \quad 1 - \left[\frac{\rho_1 (t-\Delta t)}{\rho_1 (t)}\right] \quad \frac{1}{\Delta t} \tag{A-38}$$

where V_{1i} is the liquid volume in component i, and ρ_1 is the volume-weighted average liquid density in that component.

$\dot{v}_{steam}$: The effect of vapor generator and/or condensation on liquid volume is calculated using:

$$\dot{v}_{steam} = \frac{\rho_g}{\rho_f} \quad \dot{v}_{V_{core}} - \dot{v}_{V_{HPI}} - \dot{v}_{V_{BCM}} - \dot{v}_{V_{amb}} - \dot{v}_{V_{metal}} \tag{A-39}$$

where the components of $\dot{v}_V$ are described below:

$\dot{v}_{\Delta P}$ The effect of pressure on near-saturated liquid and vapor is determined using:

$$\dot{v}_{1\Delta P} = \dot{v}_1 \frac{\Delta P}{\Delta t} - \frac{\rho_g}{\rho_f} \dot{v}_V \frac{\Delta P}{\Delta t} \tag{A-40}$$

where

$$\dot{v}_1 \frac{\Delta P}{\Delta t} = M_{1\sim f} \frac{\Delta P}{\Delta t} \frac{\partial v_f}{\partial P}\bigg|_h \tag{A-41}$$

$$\frac{\partial v_f}{\partial p}\bigg|_h = v_f \left[\frac{T_{sat} \, v_{fg} \, \beta_f \, 144}{h_{fg} \, 778.2} - K_f\right] \tag{A-42}$$

$$\beta_f = -\frac{1}{v_f} \frac{\partial v_f}{\partial T}\bigg|_p, \quad \text{the coefficient of volume expansivity } (^oR^{-1}) \tag{A-43}$$

$$K_f = -\frac{1}{v_f} \frac{\partial v_f}{\partial p}\bigg|_T, \quad \text{the coefficient of isothermal compressibility } (in^2/lbf) \tag{A-44}$$

$M_{1\sim f}$ denotes the mass of liquid which is near saturation

$\dot{v}_V$ is the corresponding contribution for pressure effects the near-saturated vapor volume

The factors 144 and 778.2 convert ft^2 to in^2 and Btu to ft-lbf respectively.

Vapor Volume

The net vapor volume change ($\dot{v}_v$) is considered in its several constituents:

$$\dot{v}_v = \dot{v}_{core} - \dot{v}_{HPI} - \dot{v}_{leak} - \dot{v}_{BCM} - \dot{v}_{amb} - \dot{v}_p \quad \text{(A-45)}$$

$$\text{where } \dot{v}_p = \dot{v}_{\Delta P} - \dot{v}_{metal} - \dot{v}_{\Delta \rho} \quad \text{(A-46)}$$

the pressure-responsive components of v_v.

$\dot{v}_{core}$: Core vapor production is calculated using

$$\dot{v}_{core} = \left[\frac{q_{core}}{C} - 0.259\ \dot{m}_{DC}\ (h_f - h_{in})\right] \frac{v_g}{h_{fg}} \quad \text{(A-47)}$$

where C converts q_{core} (% fp) to (B/S), 0.259 converts DC flowrate ($\dot{m}_{DC}$) from % full flow to (lbm/s),
and the units of $\dot{v}_{core}$ (as usual for $\dot{v}$) are ft^3/sec.

Core inlet fluid enthalpy is calculated at the temperature indicated by fluid thermocouple RVTC02, and is limited to h_f or less. If the core outlet fluid is subcooled (based on RVTC07), core vapor generation is nulled.

$\dot{v}_{HPI}$: The role of cold HPI fluid in vapor condensation is introduced into the HPI term, $\dot{v}_{HPI}$. Two components of HPI are considered: (1) HPI "AWAY" is assumed to be heated to the leak fluid enthalpy by steam condensation, and (2) HPI "COND" is assumed to be heated to the upper downcomer fluid temperature, also by vapor condensation. The "AWAY" component is taken to be the single-phase leak flowrate (CLS or CLD). If CL loop flow indicates reverse flow, the current SG primary liquid inventory change is converted to a mass flowrate (HPI2SGP) and added to the "AWAY" component:

$$HPI2SGP = (M_{SG}(t) - M_{SG}(t - \Delta t))/\Delta t \quad \text{(A-48)}$$

The "AWAY" term is limited to the range:

$$0 \leq AWAY \leq \dot{m}_{HPI}$$

and its contribution is:

$$\dot{v}_{HPIAWAY} = \frac{\dot{m}_{AWAY}\ (h_{leak}-h_{HPI})}{\rho_g\ h_{fg}} \qquad \text{(A-49)}$$

The HPI-"COND" component is set equal to the excess of HPI:

$$HPICOND = \dot{m}_{HPI} - \dot{m}_{AWAY}$$

and constrained to be greater than or equal to zero. Its $\dot{v}$-contribution is taken over the heatup from HPI enthalpy to that at the upper DC fluid temperature, DCTC01:

$$\dot{v}_{HPI\ COND} = \frac{\dot{m}_{COND}\ (h_{DCTC01} - h_{HPI})}{\rho_g\ h_{fg}} \qquad \text{(A-50)}$$

Then the $\dot{v}$ effects are the sum:

$$\dot{v}_{HPI} = \dot{v}_{HPI\ AWAY} + \dot{v}_{HPI\ COND} \qquad \text{(A-51)}$$

(Note the differing assumptions regarding HPI heating used to get the $\dot{v}_l$ effects of HPI, versus those used here for the $\dot{v}_v$ effects). When the DC is approximately filled (collapsed level above 1.5'), $\dot{v}_{vHPI}$ is limited to no more than $\dot{v}_{vcore}$.

$\dot{v}_{BCM}$:

The primary vapor volume impact of the SG boiler condenser mode is activated when the SG primary collapsed liquid level is within 3' of the secondary, and when the SG primary level is within the SG with AFW active.

Then this contribution is:

$$\dot{v}_{BCM} = \frac{q_{SG}\ v_g}{C\ h_{fg}}\ ,\ ft^3/s \qquad \text{(A-52)}$$

where C converts q_{SG} from % fp to (B/S),
and the calculation of q_{SG}, primary-to-secondary energy transfer rate, has been described in the energy section.

$\dot{v}_{amb}$:

System heat losses to ambient are assumed to condense primary vapor in liner proportion to the vapor length exposed to these losses. The two primary components for which this condensation mechanism is calculated are the SGP and RV. The calculation of their heat losses to ambient (q_{SGamb} and q_{RVamb}) has been described in the energy section. Then:

$$\dot{v}_{amb} = (X_{SG}\ q_{SGamb} + X_{RV}\ q_{RVamb})\ v_g/C\ h_{fg} \qquad \text{(A-53)}$$

where X_{SG} and X_{RV} are the fractional SG and RV lengths in vapor:

$$X_{SG} = 1 - \frac{Z_{SGP}}{52} \qquad \text{(A-54)}$$

and

$$X_{RV} = 1 - \frac{Z_{RV} + 24}{31}$$

where both are limited to the range:

$$0 \leq X \leq 1.$$

$\dot{v}_p$: Pressure effects on $\dot{v}$ are considered in three forms: (1) Pressure effects on near-saturated liquid and vapor; (2) condensation of vapor on metal with pressurization, $\dot{v}_{metal}$; and (3) compression effects on $\dot{v}$ through bulk vapor density, $\dot{v}_{\Delta\rho}$.

$\dot{v}_{\Delta p}$: The effect of pressure on the volume of vapor is determined using:

$$\dot{v}_{v\Delta P} = M_{v\sim g}\ \frac{\Delta P}{\Delta t}\ \frac{\partial v_g}{\partial P}\bigg|_h - \frac{\rho_f}{\rho_g}\ \dot{v}_l\ \frac{\Delta P}{\Delta t} \qquad \text{(A-56)}$$

where

$$\frac{\partial v_g}{\partial P}\bigg|_h = v_g \left[\frac{T_{sat}\ v_{fg}\ \beta_g}{h_{fg}}\ \frac{144}{778.2} - K_g\right] \qquad \text{(A-57)}$$

$$\beta_g = -\frac{1}{v_g}\ \frac{\partial v_g}{\partial T}\bigg|_P \text{, the coefficient of volume expansivity } (^\circ R^{-1}) \qquad \text{(A-58)}$$

$$K_g = -\frac{1}{v_g}\ \frac{\partial v_g}{\partial P}\bigg|_T \text{, the coefficient of isothermal compressibility } (in^2/lbf) \qquad \text{(A-59)}$$

$M_{v\sim g}$ denotes the mass of vapor which is near saturation

$\dot{v}_l$ is the corresponding contribution for pressure effects on the near-saturated liquid volume

The factors 144 and 778.2 convert ft^2 to in^2 and Btu to ft-lbf respectively

$\dot{v}_{metal}$: As pressurization raises saturation temperature, vapor is condensed on the bounding metal to elevate its stored energy correspondingly. The following assumptions are used: the metal is without time lag, metal is adequately characterized by $(\rho cp)_{metal} = 60$ (B/ft^3F), and the volume of metal surrounding vapor equals the volume of vapor (the system total fluid and metal volumes are approximately equal). Then:

$$\dot{v}_{metal} = \frac{[T_{sat}(t) - T_{sat}(t- t)]\ V_v\ 60}{\rho_g\ h_{fg}\ \Delta t}\ ,\ ft^3/s. \qquad \text{(A-60)}$$

$\dot{v}_{\Delta\rho}$ Bulk vapor density change effects on $\dot{v}$ are:

$$\dot{v}_{\Delta\rho} = \frac{\dot{v}_v}{\Delta t}\left[\frac{\rho_g(t)}{\rho_g\ (t- \Delta t)} - 1\right] \qquad \text{(A-61)}$$

where $\dot{v}_v$ = Primary vapor volume.

2.10 Subroutine VOIDS

Approximate void fractions are determined using subroutine VOIDS. The calculations use the indicated differential pressures without correcting for the pressure losses due to flow. Also, single volume-weighted liquid and vapor densities are used, and the variations of volume with elevation are ignored.

Void fractions are calculated for zones within the reactor vessel, hot leg, and steam generator secondary. The void fraction calculation assumes that the sensed local differential pressure (Δp) includes the weight of both liquid and vapor, i.e.

$$\Delta p = \rho_l\ z_l + \rho_v\ z_v \qquad \text{(A-62)}$$

where z_l and z_v are the liquid and vapor (vertical) lengths.

Then $\Delta p = \rho_l z + (\rho_v - \rho_l)\ z_v$ (A-63)

and $\alpha \tilde{=} z_v/z = \frac{(\rho_l - \Delta p/z)}{(\rho_l - \rho_v)}$ (A-64)

where z is the vertical distance between pressure taps.

2.11 Subroutine SGHTRAN

Indications of SG performance are obtained by determining the SG local heat transfer coefficients and the SG linear heat rate, in subroutine SGHTRAN.

2.11.1 Steam Generator Temperature Profiles

The actual temperature locations vary depending on the tube and the axial elevation. To perform the calculations in this subroutine the steam generator temperatures must first be assigned to one or more of four categories:

1. On-nozzle SG primary temperatures - these consist of the fluid inlet and outlet RTDs (Resistance Temperature Detectors) and the string thermocouples located in the SG tube which is adjacent to the minimum-wetting AFW nozzle.
2. Off-nozzle SG primary temperatures - these consist of the fluid inlet and outlet RTDs and the string thermocouples located in the SG tube which is located in the SG tube which is 180^{o} away from the on-nozzle tube (on the opposite side, on the periphery of the steam generator).
3. Composite SG primary temperatures - these consist of various primary thermocouples located within different tubes at various axial locations including the string TCs and the SG primary inlet and outlet RTDs.
4. Composite SG secondary temperatures - these consist of all the SG secondary temperature indications from the various axial and radial thermocouple locations (they are not segregated into "wetted" and "unwetted" categories based on their lateral position within the SG).

It should be noted that in order to define the axial temperature distribution within the on-nozzle and off-nozzle SG tubes, the SG primary fluid thermocouple at 8.1 ft (SPTC05) is included (the lowest elevation for the string TC is 23.1 ft.).

2.11.2 Curve Fitting the Steam Generator Temperature Profiles

The four types of SG temperature profiles are curve-fit for plotting and local analyses. Because standard curve-fitting logic requires ordered and single-valued functions, the supplied temperature indications within each category are ordered by elevation (Subroutine ORDERIT), and are condensed to a single average temperature at one elevation when several indications are within 1/4-foot of elevation of each other. Fitting is performed by a standard software package supplying modified spline fits.

The boundary conditions imposed on the curve-fit differ between the primary and secondary profiles. Because the primary profiles contain end points (the RTDs) beyond the region of active heat transfer, the imposed primary boundary condition is no heat transfer, i.e., zero first derivatives, $dT/dz = 0$, at both ends. Secondary temperatures do not delineate the extremes of SG elevation, however. Thus zero second derivations (constant dT/dz) are imposed at the end points of the secondary temperatures, local analyses are performed only within the extremes of the elevations of the supplied SG secondary temperatures (extrapolation of spline-like curve fits is not defensible).

These curve-fit SG temperature profiles are limited by the axial density of the temperature measurements. This limitation may be observed by examining a SG primary fluid temperature curve-fit just below the elevation of secondary dryout. The curve-fit primary profile drops sharply at this elevation. The actual profile is likely to extend to lower elevations before beginning its rapid decrease, corresponding to augmented primary to secondary heat transfer over the secondary boiling length.

2.11.3 Steam Generator Linear Heat Rates

The linear heat rate is the heat transferred per unit axial distance. It is evaluated for each of the SG primary temperature categories: On-Nozzle, Off-nozzle, and primary composite. The curve-fit SG primary temperature profiles are evaluated at multiple axial increments, these extracted temperatures and the primary pressure are used to obtain local SG primary fluid specific enthalpy (using property Subroutine STP). Adjacent enthalpies are differenced; linear heat rate is then the product of these local fluid enthalpy differences and primary flowrate, divided by the length

of the axial increment. Evaluations are performed only over the range of elevation subtended by the available SG secondary temperatures, as previously mentioned; to accommodate the total energy transfer to the primary fluid within the SG, the linear heat rate calculations at the top and bottom increments are modified to use the SG primary inlet and outlet (RTD) temperatures, their increment lengths are correspondingly modified. Linear heat rates are expressed in the customary units of Kw/ft, i.e. heat transferred per unit axial distance.

The primary flowrate used to calculate SG linear heat rate is the total primary system flowrate from the cold leg orifice indication, distributed uniformly through the 19 SG tubes; the SG linear heat rate is not modified to account for any estimate or observation of flow maldistribution through the various SG tubes.

The method used to determine the linear heat rates is only valid when single phase liquid conditions exist in the SG primary, i.e, the fluid enthalpy is obtained from the fluid temperature and pressure, which is invalid when the fluid becomes a two-phase mixture.

2.11.4 Steam Generator Local Heat Transfer Coefficients

Local SG heat transfer coefficients (htc) are obtained from local linear heat rate and local primary-to-secondary temperature differences. Local temperature differences are obtained by evaluating the appropriate curve-fit SG temperature profiles and differencing the results. The calculated htc's are limited to positive values, i.e. when local linear heat rate and local primary-to-secondary temperature difference differ in sign, htc is set to zero. Local htc's ($BTU/hrft^2F$) are expressed as base-ten logarithms for plotting and for ease of comparison; log-htc is limited to 0 or greater, where the left-hand side of the equation is the product of fluid density and acceleration, plotted log-htc is limited to 1 or greater. Local htc is conceptually the SG secondary convective heat transfer coefficient, its variations during testing commonly reflect secondary phenomena (boiling, superheat, AFW effects, and so on). It should be noted, however, that the log-htc calculations just defined use a primary-fluid to secondary-fluid temperature difference. The htc is thus a series-composite of the convective htc within the SG tube, conduction through the tube wall, and heat transfer from the tube to secondary, i.e., an overall heat transfer

coefficient. Since the steam generator local heat transfer coefficients are determined using the local linear heat rate, they are valid only when the primary fluid is a single phase liquid.

2.12 Subroutine NATURAL

Subroutine NATURAL solves the equation of motion to obtain predicted natural circulation flowrates. The output is the following plot types:

- o Loop fluid temperatures versus elevation.
- o Calculated and indicated flowrates versus time.
- o Thermal center locations versus time.
- o Natural ciruclation driving head versus time.

The solution techniques is described below.

The equation of motion is:

$$\rho \frac{D\bar{v}}{Dt} = - \bar{\nabla}p - \left[\bar{\nabla} \cdot \bar{\tau}\right] + \rho\bar{g} \qquad \text{(A-65)}$$

where the left-hand side of the equation is the product of fluid density and acceleration, and the right-hand terms are, respectively, the pressure, viscous, and gravitational forces per unit volume. In steady state, the left-hand side is zero. For one-dimensional flow over an increment of length l, the equation of motion then becomes:

$$0 = - \frac{\Delta p}{\Delta l} - \frac{Eu_l \rho v^2}{2g_c \Delta l} + \frac{\rho g_l}{g_c} \qquad \text{(A-66)}$$

where Eu_l is the viscous dissipation over the increment and g_l denotes the component of gravity which is aligned with the increment. For example, the incremental fluid pressure change for flow vertically upward is:

$$\Delta p = \frac{- Eu_l \rho v^2}{2g_c} - \frac{g\rho\Delta l}{g_c} \qquad \text{(A-67)}$$

that is, the fluid pressure in upflow diminishes due to both viscous dissipation and gravitational efforts.

The net fluid pressure change in a closed system at steady state is identically zero. Then the total viscous dissipation is offset by the gravitational force, i.e.

$$\frac{Eu\bar{\rho}v^2}{2} = \sum_i \rho_i g_i \Delta l_i \qquad \text{(A-68)}$$

where the summation is performed over the entire closed system, the loop Euler Number (Eu) represents the fluid (friction and form) losses for the whole loop, and the introduction of a mean fluid density ($\bar{\rho}$) introduces a minor approximation. This relation is solved for the flowrate, in subroutine NATURAL. The summation is performed over the spatial increments defined by each pair of fluid temperature indications around the loop. This summation is performed in a manner which yields the elevations of the thermal centers, as explained in the following paragraphs.

The local fluid density (ρ_i in Eq. A-68) may be expressed as a Taylor series about a mean fluid temperature, $\bar{T}$:

$$\rho_i = \rho\,(T_i) = \rho\,(\bar{T}) + \frac{\partial \rho}{\partial T}\bigg|_{\bar{T}} (\bar{T}_i - \bar{T}) + \ldots \qquad \text{(A-69)}$$

$$= \bar{\rho} - \bar{\rho}\bar{\beta}\,(T_i - \bar{T}) + \ldots$$

where $\bar{\rho} \triangleq \rho\,(\bar{T})$

and $\bar{\beta} \triangleq \beta\,(\bar{T})$ is the coefficent of volume expansion, i.e.

$$\beta \triangleq \frac{1}{V}\left(\frac{\partial V}{\partial T}\right)_p = -\frac{1}{\rho}\left(\frac{\partial \rho}{dT}\right)_p \qquad \text{(A-70)}$$

Substitution of the truncated expansion for the local fluid density then yields:

$$\sum_i \rho_i g_i \Delta l_i \qquad \text{(A-71)}$$

$$= \sum_i \left[\bar{\rho} - \bar{\rho}\bar{\beta}\,(T_i - \bar{T})\right] g_i \Delta l_i$$

$$= \bar{\rho} \sum_i g_i \Delta l - \bar{\rho}\bar{\beta} \sum_i T_i g_i \Delta l_i + \bar{\rho}\bar{\beta}\bar{T} \sum_i g_i \Delta l_i$$

ıe first and third terms of Eq. A-71 involve $\sum_i g_i l_i$, the summation of the gravity contribution over a closed loop, and are thus identically zero. Then

$$\sum_i \rho_i g_i \Delta l_i = -\bar{\rho}\bar{\beta} \sum_i T_i g_i \Delta l_i \qquad \text{(A-71)}$$

and the equation of motion for a closed and confined system is:

$$\frac{Eu\ \bar{\rho} v^2}{2} = -\bar{\rho}\bar{\beta} \sum_i T_i g_i \Delta l_i \qquad \text{(A-72)}$$

This form of the equation of motion highlights the role of the elevation difference between the so-called "thermal centers". Horizontal increments have no contribution because $g_i = 0$; and vertical runs with equal fluid temperatures in the upflow and downflow legs also have no net contribution. Thus the summation of Eq. A-72 obtains only those vertical increments whose corresponding vertical lengths (downflow versus upflow) have a different fluid temperature. If the fluid heating and cooling can be considered to occur at specific elevations, than the summation obtains

$$\sum_i T_i g_i \Delta l_i = T_H (-g) \Delta Z_{HC} + T_c (g) \Delta Z_{HC} \qquad \text{(A-73)}$$

$$= -g \Delta Z_{HC} (T_H - T_c) \qquad \text{(A-74)}$$

where ΔZ_{HC}, the vertical distance between the zones of heating and cooling, is the vertical distance between thermal centers.

Heat transfer is usually distributed rather than concentrated, in real systems. Therefore a suitable weighting scheme must be used to define the hypothetical elevations at which heating and cooling can be considered to be concentrated. The requirement for this technique is that the equation of motion, Eq. A-68, remains satisfied, i.e.

$$\sum_i \rho_i g_i \Delta l_i = g\ \hat{\Delta z}_{HC} (\hat{\rho_c} - \hat{\rho_H}) \qquad \text{(A-75)}$$

where $\Delta \hat{z}_{HC}$ is the elevation difference between thermal centers, $\hat{\rho_c}$ is the fluid density associated with the cooling thermal center, and $\hat{\rho_H}$ is the fluid density of the heating thermal center. These thermal center evaluations are performed in subroutine NATURAL using summations over each aiable loop fluid temperature; for example:

$$\hat{z_H} = \sum_{\Delta\rho<0} z_i \Delta\rho_i \Big/ \sum_{\Delta\rho<0} \Delta\rho_i \qquad \text{(A-76)}$$

and $$\hat{\rho_H} = \sum_{\Delta z<0} \rho_i \Delta z_i \Big/ \sum_{\Delta z<0} \Delta z_i$$

The calculations of subroutine NATURAL were developed for steady-state natural circulation in a closed loop. Although the fluid was not explicitly assumed to be in a single phase, the use of pressure and temperature to determine fluid density render the calculations inaccurate for two-phase flow. Also, the pressure contributions of injection and discharges were not included.

3.0 PLOT DIRECTORY

The plots, indexed herein and transmitted separately, are the primary method of presentation of test results. There are two major types of plots: (1) Time-based plots (Section 3.1), and (2) Elevation-based plots (Section 3.2). Plots are further categorized by the types plotted variables:

Range of Plot Numbers	Type of Plot
Time-Based Plots, Section 3.1	
1-30	Basic
100-109	Calculated Condtions
110-119	Core Vessel
120-129	Hot Leg
130-139	SG Primary
140-149	Cold Leg
150-159	Downcomer
160-169	Pressurizer
170-179	Reactor Vessel Vent Valve
180-189	Primary Boundary
190-199	Secondary System
320-329	Natural Circulation
Elevation-Based Plots (indexed by time), Section 3.2	
200-219	SG Temperatures
220-239	SG Temperatures and Trends
240-259	SG Linear Heat Rates
260-279	SG Heat Transfer Coefficients
300-319	Primary Fluid Temperatures

Throughout these plots, supplied variables have their alphanumeric instrument descriptor entered under "VTAB", calculated variables contain the VTAB-entry "CALCD." These calculations have been outlined in Section 2. The instruments are identified and located in Section 4.

3.1 TIME-BASED PLOTS

Time on the abcissa is displayed in minutes after the start of testing. The first curve of each plot has a symbol plotted at each data point, to display the frequency of data collection. Subsequent curves use symbols only for curve identification, to preserve legibility, but use the same data frequency as the first curve. The plot key lists the instrument identifier ("VTAB"); this may be used to identify and locate the instrument using the information presented in Section 4. The plot abcissa label gives the time

and date at which the DAS was activated, and the time interval (minutes) between DAS activation and the initiation of the test. The derivation of the plotted variables is described in Section A.2.

PLOT NUMBER	ORDINATE	DISCUSSION
Basic Plots, Plots 1-30		
1	Pressure (psia), Primary and Secondary.	(None)
2	Liquid Temperatures (Volume Weighted, F)	Volume-weighted liquid temperatures are each component (RV, HL, SGP, CL, DC, and PR) and the SG Secondry (SGS). Primary and Secondary (steam saturation) temperatures are also shown.
3,4	Collapsed Levels (feet relative to the SG Lower Tube Sheet Upper - Secondary Face.)	Fully-corrected collapsed levels are shown for each instrumented component. "Collapsed" level indicates the equivalent all-liquid level. Two levels are indexed "SGPKLV"; variable-index (VTAB) SPLV20 is the Primary level in the SG, while HLLV231 indicates the sum of the SG Primary level plus that in the Hl stub downstream of the HL U-bend (HLUB).
8	SG Secondary Level (ft.)	The collapsed and auctioneered-CP SG Secondary levels are shown. "Auctioneering" obtains the highest CP (Conductivity Probe) elevation at and below which the remaining CPs are wetted. The collapsed-level maximum instrument sensitivity and the minimum CP spacing are both frequently visible in this plot.
9	Primary Flowrates (% of Full Flow)	CL and DC orifice flow rates are shown. The conversion from % (scaled) full flow is: 1% Full Flow = 0.259 lbm/sec.
10	Secondary Flowrate (% of Full Flow)	The two direct variables are feed flow and steam flow (auctioneered between the high-flow and low-flow steam and feed circuits as appropriate). The two indirect variables are "FD-STM" and "DM/DT." FD-STM is the difference of the feed and steam flow rates. DM/DT is the SG Secondary fluid mass difference over each time increment, divided by the duration of

PLOT NUMBER	ORDINATE	DISCUSSION
Basic Plots, Plots 1-30		
10		each increment. The conversion for secondary flow is: 1% (scaled) Full Flow = 0.0265 lbm/sec.
11	Cumulative SG Secondary Fluid Mass (lbm)	Calculated and apparent (indicated) fluid mass in the SG secondary. Indicated is obtained from measured level and fluid density. Calculated is obtained by intergrating the difference between the feed and steam flow rates, and adding this to the previous calculated mass. (The initial calculated mass is set equal to the initial indicated fluid mass.)
12	SG Secondary $\dot{m}$-Imbalance, (% of full flow)	The $\dot{m}$-balance is the difference between the calculated and indicated SG secondary fluid mass rate of change. Calculated is (Feed-Steam), indicated is dm/dt, both as shown on plot 10. The conversion factor for secondary flow is: 1% = 0.0265 lbm/s.
13	SG-Primary String Thermocouple (TC) Temperatures, On-Nozzle (F).	The temperature indicated by each of the 10 TC's is indicated; their elevations (ft. relative to SGLTSUF) are given under "INDEX." "On-Nozzle" denotes the SG tube directly in front of the minimum-wetting AFW nozzle.
15	Energy Transfer (% Full Power)	Energy transfer is shown for the Core, Primary, and SG Secondary Out. Core power is taken directly from the wattmeter. "Primary" power is core power less losses to ambient. SG secondary power out is steam minus feed convected energy, plus SG secondary heat losses to ambient. The plot ordinate is constrained to -4 to +12% of scaled full power (1% = 21.4 Kw).
16	Limit Switches	Active limit switches. Limit switches indicating open throughout the plotting period are shown at the bottom of the plot. Those switches which change position are shown in the middle of the plot, switch opening is indicated by a abrupt decrease in the limit switch trace. The RVVV limit switch trace also

PLOT NUMBER	ORDINATE	DISCUSSION
Basic Plots, Plots 1-30		
16	(Cont'd)	includes intermediate positions, when both the valve-open and valve-closed switches are open.
17	Primary Boundary Mass Flowrates (lbm/s)	Primary mass rate of change due to HPI and discharges, and net primary system mass rate of change. Discharge sites are keyed to limit switch actuations.
18	Cumulative Primary Mass (lbm)	Calculated and apparent (indicated) Primary System fluid mass "Indicated" from levels "calculated" from the integral of "net" (Plot 17).
19	Primary Energy Balance (% of full power)	Primary system fluid energy contributions due to: core, primary metal cooling low (METAL), recovery of suprheated primary metal in guard-heated zones (QUENCH), dischargs minus HPI (EFLUENT), SG primary-to-secondary heat transfer (SG HTX), ambient losses (AMB-PU), and net. The plot ordinate is limited to -2 to +6% of scaled full power, 1% = 21.4 Kw.
20	Total Primary Fluid Energy (% of Initial Total Energy)	Calculated and indicated total Primary fluid energy, normalized to intial total fluid energy. "Indicated" from measured levels and fluid properties, "calculated" from the integral of "net" (Plot 19).
21	Primary Q-Imbalance (% Full Power)	The plotted Q-imbalance is the difference between the "net" primary system energy transfer (Plot 19) and de/dt, the rate of change of the indicated primary system total fluid energy. 1% = 21.4 Kw.
22	Primary Liquid DVOL/DT (ft^3/min)	Primary liquid volume rate of change due to: HPI; all liquid-state discharges (DISCH), steam generation (2 STEAM), and pressure changes (DPRESS). The net of these liquid volume change sources is also shown. The ordinate is limited to -0.2 to +0.6 ft^3/min.

PLOT NUMBER	ORDINATE	DISCUSSION
Basic Plots, Plots 1-30		
23	Primary Vapor Volume Change (ft^3/min)	Primary vapor volume change rate due to: steam generation in the core (CORE); condensation by HPI fluid (HPICON); vapor-region discharges (DISCH); boiler-condenser mode condensation in the SG (BCM); condensation due to heat losses to ambient (AMBCON); and pressurization effects (DPRESS). The net of these vapor volume change sources is also shown.
24	Primary Liquid Volume (% of total Primary Volume)	Calculated and indicated Primary system liquid volumes. "Indicated" is based on measured levels, "calculated" from the integral of "net", Plot 22.
26	Cold Leg Fluid Temperatures (F)	Cold Leg fluid temperatures, CLTC01-05, are shown. (CLTC01 has been combined with the SG Primary fluid temperatures, and CLTC04 and 5 with the Downcomer fluid temperatures, to perform fluid-volume weighted property calculations in subroutine PROPS). When a CL leak is active, the leak fluid temperature is also shown.
27	Primary Pressure Difference (psi)	Two pressure differences are plotted: (RV-SGP) and (RV-PZR).
28	Approximate Core-Region Void Fractions (%)	Approximate voided length in the RV (based on level ΔPs without flow corrections) expressed as a percent of the total length of the component.
29	Approximate Hot Leg Void Fraction (%)	Implied voided length in the HL (based on level ΔPs without flow corrections expressed as a percent of the total length of the component. Two HL void fractions are plotted: HL vertical piping to the HL U-bend ("TOHLUB"), and HL stub beyond the U-bend ("UB-SG").
30	Approximate SG Secondary Void Fraction (%)	Implied voided length steam in the SG secondary (based on level ΔPs without flow corrections) expressed as a percent of the total length of the component. Pressure tap elevations (ft) are listed in the plot key.

100-Series Plots, Calculated Conditions

Certain 100-series plots, such as Plot 104, are omitted for tests in which only one of the plot variables is active. This changes by one the numbering of the subsequent 100-series plots within that group of ten plots.

PLOT NUMBER	ORDINATE	DISCUSSION
101	Ambient Heat Losses (% of Full Power)	Losses to ambient for the RV, HL, CL suction and SG secondary (SGS). HL losses are nulled when the HL Guard Heaters are energized. The conversion factor is 1% (scaled) full power = 21.4 kw. (The pump ("PMP") is inactive.)
102	Liquid Enthalpy (BTU/lbm)	Volume-weighted liquid enthalpy (from measured fluid conditions) for the primary components and for the SG secondary.
103	Saturation Temperature (F).	Saturation temperatures for secondary steam ("SGS") and the Pressurizer. "STMSAT" is saturation temperature at steam pressure. "SGSSAT" is saturation temperature at steam pressure plus the pressure of the current liquid column in the SG Secondary (i.e.; it is approximately the (maximum) SGS saturation temperature, at the bottom of the generator). "PZRSAT" is the saturation temperature at the Pressurizer pressure.
104	DMASS/DT (lbm/s)	Boundary system mass flowrate obtained by differencing the accumulated flows of the single-phase ("V1") and two-phase ("V2") collection systems.
105	(Component) Liquid Volume (% of Full)	Component fractional liquid volumes for the RV, HL, SGP (including HL stub to HLUB), CLS, DC, PZR, SGS (Secondary), and Primary total (PRI). Each volume reflects the collapsed level (Plot 4) converted using approximate component volume versus (heated) elevation. The Primary total volume represents the sum of the primary component fluid volumes, normalized to the total primary volume.

PLOT NUMBER	ORDINATE	DISCUSSION
100-Series Plots, Calculated Conditions		
106	(Component) Fluid Mass (lbm/sec)	Fluid mass of each of the primary system components and the SG secondary, based on level measurements.
107	(Component) Energy (% of Initial Energy)	Component fluid energy normalized to initial energy for the RV, HL, SGP (including HL stub), CLS, DC, PZR, SGS (Secondary), and PRI (Primary Total). For each component, energy is taken as liquid mass times liquid specific energy, plus vapor mass times vapor specific energy. "PRI" is the sum of the primary component energies, normalized to time-zero content.
110-Series Plots, Core Vessel		
111	Core Vessel Fluid Temperatures (F)	Available core fluid temperature indications, indexed in feet relative to the SGLTSUF.
112	Core Vessel Insulation DT (F)	Available core vessel insulation DT's, indexed in feet relative to the SGLTSUF.
113	Core Vessel Conductivity	RV conductivity probe indications; higher readings indicate wetting.
114	Core Vessel Metal Temperatures (F)	Available core vessel metal temperatures indxed by elevation above the SGLTSUF.
120-Series Plots, Hot Leg (HL)		
121	Hot Leg Fluid Temperature (F)	The hot leg fluid temperatures, from the HL Nozzle to the HLUB, indexed by feet relative to the SGLTSUF.
122	Hot Leg Insulation DT (F)	The hot leg insulation DTs from the HL nozzle to the SG inlet, indexed by feet relative to the SGLTSUF.
123	Hot Leg Conductivity	HL conductivity probe readings, higher values indicated wetting.
124	Hot Leg Metal Temperatures (F)	The hot leg metal temperatures from the HL nozzle to the SGP, indexed by feet relative to the SGLTSUF. The pressurizer surge line metal temperature (PRTC07) at the low point of the surge line, is also shown.

PLOT NUMBER	ORDINATE	DISCUSSION
130-Series Plots, SG Primary (SP)		
131	SG Primary Fluid Temperatures (F)	The SG primary fluid temperatures (but not the string TCs), indexed in feet relative to the SG LTSUF. The HL stub fluid temperature and the CL fluid temperature at the SG outlet are also shown.
132	SG Primary Fluid Resistance Temperature Detector (RTD)	The SG primary inlet and outlet RTDs, indexed in feet relative to the SGLTSUF.
133	SG Primary Pitot Tube Flow (% Full Flow)	The flows indicated by the SG primary tubes. Individual tube indications are multiplied by 19 to include all tubes, and by 0.847 to approximately correct for the tube flow profile sampled by the Pitot tube. No correction is made for SG tube resistance differences due to the instrumentation. Pitot SPPT04 samples the on-nozzle tube containing a TC string, SPPT05 samples the off-nozzle tube containing a string TC, and SPPT06 samples a tube without a string TC. The conversion of Primary flow is: 1% scaled full flow = 0.259 lbm/sec.
134	SG Primary Conductivity	Indication of the conductivity probes in the HL stub, higher readings indicate wetting.
135	SG Primary Pitot Temperature (F)	Indications of the fluid thermocouples associated with the Pitot tubes (Plot 133).
140-Series Plots, Cold Leg (CL)		
141	Cold Leg Fluid Temperatures (F)	The available CL suction temperatures indexed by elevation (ft relative to SG LTSUF). Not that the VTAB numbering indicates the occurrence of the TCs, proceeding from the SG outlet to the CL nozzle: CLTC01 is at the CL low point, CLTC02 and 03 move up the CL from the low point to the spillover (SO), and CLTC04 and 05 are in the sloping run toward the nozzle. See Plot 26 for all CL temperatures.

PLOT NUMBER	ORDINATE	DISCUSSION
150-Series Plots, Downcomer (DC)		
151	Downcomer Fluid Temperature (F)	The avaiable DC fluid temperatures indexed by elevation. Adjacent CL and RVVV fluid temperatures are also shown.
160-Series Plots, Pressurizer (PZR)		
161	Pressurizer Fluid Temperatures (F)	The available PZR fluid temperatures, indexed by elevation (ft relative to the SGLTSUF). Saturation temperature at PZR pressure is also shown.
162	Pressurizer Insulation DT (F)	The available PZR and surge line insulation DTs, indexed by elevation.
163	Pressurizer Metal Temperature (F)	The available PZR and surge line metal temperatures, indexed by elevation.
170-Series Plots, Reactor Vessel Vent Valve (RVVV)		
171	Reactor Vessel Vent Valve Fluid Temperture (F)	The fluid temperatures bracketing the RVVV (RVTC09 upstream and RVTC10 downstream).
172	RVVV Pressure Difference (psi)	Measured pressure difference across the the RVVV.
173	RVVV Miscellaneous	Actuation of the RVVV limit switches.
174	RVVV Calculated Flowrate (% of full flow)	The difference between the indicated Downcomer flowrate and the indicated Cold Leg flowrate. The calculated and predicted flowrates are compared in Plot 321.
180-Series Plots, Primary Boundary		
181	HPI Turbine Meter Flow Rate (lbm/sec)	Flowrates indicated by the (redundant) HPI flowmeters.
182	2-Phase Vent Accumulated Flow (lbm)	Flowrate accumulated by the two-phase vent system meters.

PLOT NUMBER	ORDINATE	DISCUSSION
190 Series Plots, SG Secondary System (SS)		
191-193	SG Secondary Fluid Temperatures (F)	The available SG secondary fluid temperatures and the SG secondary saturation temperature at steam pressure. Fluid TCs are indexed by elevation (ft relative to the SG LTSUF). For plotting clarity, only the lowest 9 TCs are shown in Plot 191, the next 9 in 192, and so forth, until all are displayed (usually 3 plots).
194	SG Metal Temperature (F)	The available SG secondary metal temperatures, indexed by elevation.
320-Series Plots, Natural Circulation		
The natural circulation calculations apply during steady-state, single-phase natural circulation and do not correct for imposed flow streams. See the description of subroutine NATURAL in section A.2 for additional information.		
321	RVVV Flowrates (%)	Predicted and indicated RVVV flowrates. Predictions assume that the RVVV is open. 1% = 0.259 lbm/s.
322	Loop Flowrates (%)	Predicted and indicated loop flowrates. 1% = 0.259 lbm/s.
323	Thermal Centers	Heating and cooling (normalized) densities and elevations versus time.
324	Natural Circulation Driving Force (psi)	None.

3.2 ELEVATION-BASED PLOTS

Elevation on the abcissa is displayed in feet relative to the SG Lower Tube Sheet Upper (Secondary) Face (SGLTSUF). Plots commonly extended from -5 to +55 feet, rather than 0 to 52 feet, to encompass the SG-bracketing primary fluid RTDs.

Elevation-based plots are made at selected times, the (transient) time of each plot is printed on the plot, directly above the plot number.

PLOT NUMBER	ORDINATE	DISCUSSION
SG Heat Transfer Plots 200-299		
200-Series Plots	SG Temperatures at (DAS) Time...Date ... (F)	Four types of SG temperatures are shown: SGPRI (Primary) RTD/Fluid TC, ON-Nozzle String TC's, SGSEC, and Saturation. The SGPRI RTD/TC include all the SG Primary temperature measurements other than the String TC. The ON-NOZ String TCs include all the temperatures of Plot 13. The SGSEC points include all the secondary fluid temperature indications. The SECSAT plot shows SG secondary fluid saturation temperature corrected for level. The point at elevation 0 is saturation at steam pressure plus the pressure of the current liquid column. The middle and Z=52 ft points are saturation at steam pressure; the middle point is plotted at the elevation of the current collapsed secondry level. These saturation temperatures, and those of the String TC's, are connected (by straight lines between points).
220-Series Plots	SG Temperatures and Trends (F) at (transient) Time ..., Date...	Temperatures and Trends from ON-NOZ (On-Nozzle STC), ALL PRI, and ALL SEC. The On-Nozzle plot includes the String TCs (Plot 13) plus the bounding SG Primary fluid RTDs, plus the SG Primary fluid TC at 8.1 feet (this TC is needed to define the STC profiles). The ALL PRI plot includes primary fluid temperatures from TCs, String TCs, and bounding RTDs. The ALL SEC plot includes all secondary fluid TC indications. Other than the String TCs, no allowance is made for TC lateral position within the SG tube bundle. Modified splines are used to curve-fit these temperatures for analyses. The measured temperatures are used, except that measurements near one elevation are collapsed to a single temperature and elevation. The three primary spline fits use the boundary condition that the first derivatives are 0 at the end points, the ALL SEC fit uses 0 second derivatives at the end points. These curves fits are limited by the density of temperature measurements.

PLOT NUMBER	ORDINATE	DISCUSSION
SG Heat Transfer Plots 200-299		
240-Series Plots	SG Linear Heat Rate (kw/ft)	The SG primary linear heat transfer rates for the two groups of SG primary temperatures of the previous plots: ON-Nozzle and All Primary (temperatures). The curve-fit temperature profiles (of the previous plots) are used to obtain specific energy change with elevation, calculated SG primary total flow is introduced to calculate incremental linear heat rate (no allowance is made for flow redistribution among the SG Primary tubes).
260-Series Plots	Log-htc	LOG_{10}-htc (heat tansfer coefficient) for the two temperature groupings of the two previous plots; ON-Nozzle String TCs and All Primary temperatures. The htc is calculated using the incremental q of the preceding plot, and the local primary-to-secondary temperature difference from the curve fits of the preceding plot. Heat transfer coefficients less than 10 are shown as log-htc = 1.
Natural Circulation Plots, Plots 300+		
300-Series Plots	Primary Fluid Temperatures (F) (at transient time)	Each primary loop fluid temperature versus elevation, keyed to its primary component. The thermal center charcteristics are also shown.

4.0 OTIS INSTRUMENTATION

The locations of the OTIS instrtuments are shown on Figure A-1. Instrument designations consist of two, two-letter groups, and a two-number group. The first two-letter group identifies the loop component or subsystem in which the instrument is installed. For example, RV denotes that the instrument is located in the reactor vessel. The second two-letter group defines the instrument type, such as "TC" for a thermocouple or "CP" for a conductivity probe. The two-number group indicates that the instrument is used for test data and also the sequential instrument number of that type in a component.

For example, thermocouple (number 8) in the reactor vessel would be designated:

RVTC08

where RV = Reactor Vessel
TC = Thermocouple and
08 Test data sequential number

Table A.1 provides a listing of loop component abbreviations, Table A.2 provides a listing of instrument abbreviations which are used to identify the instrumentation shown on Figure A-1, and Table A.3 provides an index of variables. The information in this section may be used in conjunction with the data plots (which are described in section 3 and transmitted separately). The key on each plot gives the associated "VTAB", which is the instrument designation. Tables A.1 through A.3 describe each instrument by VTAB, and Figure A.1 supplies the instrument location, thus completely describing the source of the plot traces.

Table A.1 Component Abbreviations

Instrument or Hardware	Abbreviation
Steam Generator - Primary	SP
Steam Generator - Secondary	SS
Steam Generator - Metal	SM
Reactor Vessel	RV
Downcomer	DC
Pressurizer	PR
Cold Leg	CL
Hot Leg	HL
HPI	HP
Secondary Forced Circulation	SF
Steam Piping	PS
Feedwater Piping	FP

Table A.2 Instrument Abbreviations

Instrument or Hardware	Abbreviation
Thermocouple	TC
Resistance Temperature Detector	RT
Differential Temperature	DT
Pressure	PR
Differential Pressure	DP
Orifice	OR
Ultransonic Flow	US
Pitot Tube	PT
Conductivity Probe	CP
Heated RTD	HR
View Port	VP

Table A.3 Index of Variables

INDEX	INPUT	VTAB	SYSTEM	INST	ELEV	D E S C R I P T I O N
1	81	81RVTC01	1RV	2FTC	-23.70	CORE VESL.FLUID TEMP (F)
2	82	82RVTC02	1RV	2FTC	-19.10	CORE VESL.FLUID TEMP (F)
3	86	86RVTC07	1RV	2FTC	-8.30	CORE VESL.FLUID TEMP (F)
4	87	87RVTC08	1RV	2FTC	6.80	CORE VESL.FLUID TEMP (F)
5	97	97RVLV04	1RV	4LDP	-16.10	CORE VESL. COR.LVLDP (PSI)
6	99	99RVLV05	1RV	4LDP	-16.10	CORE VESL. COR.LVLDP (PSI)
7	94	94RVLV02	1RV	4LDP	-8.10	CORE VESL. COR.LVLDP (PSI)
8	92	92RVLV01	1RV	4LDP	-1.90	CORE VESL. COR.LVLDP (PSI)
9	90	90RVWM01	1RV	7 Q	-13.20	CORE VESL. POWER !FULLPOWR
10	339	339RVDT01	1RV	10 DT	-.33	CORE VESL. INSUL. DT (F)
11	340	340RVDT02	1RV	10 DT	4.83	CORE VESL. INSUL. DT (F)
12	254	254RVCP02	1RV	16 CP	-2.40	CORE VESL. CONDCTVTY (WET/DRY)
13	253	253RVCP01	1RV	16 CP	-1.40	CORE VESL. CONDCTVTY (WET/DRY)
14	256	256RVCP04	1RV	16 CP	.60	CORE VESL. CONDCTVTY (WET/DRY)
15	255	255RVCP03	1RV	16 CP	.70	CORE VESL. CONDCTVTY (WET/DRY)
16	257	257RVCP05	1RV	23RCP	-6.90	CORE VESL. REF. C.P.
17	83	83RVTC03	1RV	25MTC	-16.00	CORE VESL. METAL TC (F)
18	84	84RVTC05	1RV	25MTC	-11.90	CORE VESL. METAL TC (F)
19	85	85RVTC06	1RV	25MTC	-9.90	CORE VESL. METAL TC (F)
20	341	341RVTC11	1RV	25MTC	-.33	CORE VESL. METAL TC (F)
21	342	342RVTC12	1RV	25MTC	4.83	CORE VESL. METAL TC (F)
22	281	281RVPR20	1RV	30KPR	7.10	CORE VESL. CORRD.PR (PSIA)
23	288	288RVLV20	1RV	31KLV	-16.10	CORE VESL. COLLD.LVL (REF. FT)
24	150	150HLTC01	2HL	2FTC	8.10	HOT LEG FLUID TEMP (F)
25	151	151HLTC02	2HL	2FTC	9.10	HOT LEG FLUID TEMP (F)
26	152	152HLTC03	2HL	2FTC	20.00	HOT LEG FLUID TEMP (F)
27	153	153HLTC04	2HL	2FTC	30.00	HOT LEG FLUID TEMP (F)
28	154	154HLTC05	2HL	2FTC	40.00	HOT LEG FLUID TEMP (F)
29	155	155HLTC06	2HL	2FTC	50.00	HOT LEG FLUID TEMP (F)
30	156	156HLTC07	2HL	2FTC	60.00	HOT LEG FLUID TEMP (F)
31	157	157HLTC08	2HL	2FTC	67.40	HOT LEG FLUID TEMP (F)
32	149	149HLRT01	2HL	3RTD	0.00	HOT LEG FLUID RTD (F)
33	168	168HLLV01	2HL	4LDP	-1.90	HOT LEG COR.LVLDP (PSI)
34	170	170HLLV02	2HL	4LDP	-1.90	HOT LEG COR.LVLDP (PSI)
35	159	159HLDT01	2HL	10 DT	2.80	HOT LEG INSUL. DT (F)
36	160	160HLDT02	2HL	10 DT	12.80	HOT LEG INSUL. DT (F)

Table A.3 Index of Variables (Cont'd)

37	161	161HLDT03	2HL	10 DT	23.80	HOT LEG	INSUL. DT (F)
38	162	162HLDT04	2HL	10 DT	34.50	HOT LEG	INSUL. DT (F)
39	163	163HLDT05	2HL	10 DT	46.20	HOT LEG	INSUL. DT (F)
40	164	164HLDT06	2HL	10 DT	57.20	HOT LEG	INSUL. DT (F)
41	165	165HLDT07	2HL	10 DT	65.90	HOT LEG	INSUL. DT (F)
42	258	258HLCP01	2HL	16 CP	1.00	HOT LEG	CONDCTVTY (WET/DRY)
43	259	259HLCP02	2HL	16 CP	15.00	HOT LEG	CONDCTVTY (WET/DRY)
44	260	260HLCP03	2HL	16 CP	35.00	HOT LEG	CONDCTVTY (WET/DRY)
45	261	261HLCP04	2HL	16 CP	37.00	HOT LEG	CONDCTVTY (WET/DRY)
46	262	262HLCP05	2HL	16 CP	41.00	HOT LEG	CONDCTVTY (WET/DRY)
47	263	263HLCP06	2HL	16 CP	45.00	HOT LEG	CONDCTVTY (WET/DRY)
48	264	264HLCP07	2HL	16 CP	49.00	HOT LEG	CONDCTVTY (WET/DRY)
49	265	265HLCP08	2HL	16 CP	53.00	HOT LEG	CONDCTVTY (WET/DRY)
50	266	266HLCP09	2HL	16 CP	57.00	HOT LEG	CONDCTVTY (WET/DRY)
51	267	267HLCP10	2HL	16 CP	61.00	HOT LEG	CONDCTVTY (WET/DRY)
52	268	268HLCP11	2HL	16 CP	65.00	HOT LEG	CONDCTVTY (WET/DRY)
53	269	269HLCP12	2HL	16 CP	67.20	HOT LEG	CONDCTVTY (WET/DRY)
54	274	274HLCP17	2HL	23RCP	.50	HOT LEG	REF. C.P.
55	204	204HLTC12	2HL	25MTC	2.70	HOT LEG	METAL TC (F)
56	205	205HLTC13	2HL	25MTC	12.70	HOT LEG	METAL TC (F)
57	206	206HLTC14	2HL	25MTC	23.70	HOT LEG	METAL TC (F)
58	326	326HLTC10	2HL	25MTC	34.50	HOT LEG	METAL TC (F)
59	207	207HLTC15	2HL	25MTC	46.20	HOT LEG	METAL TC (F)
60	208	208HLTC16	2HL	25MTC	57.20	HOT LEG	METAL TC (F)
61	327	327HLTC11	2HL	25MTC	65.90	HOT LEG	METAL TC (F)
62	286	286HLLV20	2HL	31KLV	-1.90	HOT LEG	COLLD.LVL (REF. FT)
63	114	114CLTC01	3SGP	2FTC	-4.70	SG PRIMRY.	FLUID TEMP (F)
64	12	12SPTC05	3SGP	2FTC	8.10	SG PRIMRY.	FLUID TEMP (F)
65	11	11SPTC04	3SGP	2FTC	17.30	SG PRIMRY.	FLUID TEMP (F)
66	10	10SPTC03	3SGP	2FTC	35.30	SG PRIMRY.	FLUID TEMP (F)
67	9	9SPTC02	3SGP	2FTC	38.20	SG PRIMRY.	FLUID TEMP (F)
68	8	8SPTC01	3SGP	2FTC	47.10	SG PRIMRY.	FLUID TEMP (F)
69	158	158HLTC09	3SGP	2FTC	59.90	SG PRIMRY.	FLUID TEMP (F)
70	7	7SPRT04	3SGP	3RTD	-2.90	SG PRIMRY.	FLUID RTD (F)
71	6	6SPRT03	3SGP	3RTD	-2.80	SG PRIMRY.	FLUID RTD (F)
72	4	4SPRT01	3SGP	3RTD	53.10	SG PRIMRY.	FLUID RTD (F)
73	5	5SPRT02	3SGP	3RTD	53.10	SG PRIMRY.	FLUID RTD (F)
74	172	172HLLV03	3SGP	4LDP	53.00	SG PRIMRY.	COR.LVLDP (PSI)
75	166	166HLDT08	3SGP	10 DT	57.20	SG PRIMRY.	INSUL. DT (F)
76	39	39SPPT04	3SGP	14PTD	-1.90	SG PRIMRY.	PITO FLOW (% FULL)
77	40	40SPPT05	3SGP	14PTD	-1.90	SG PRIMRY.	PITO FLOW (% FULL)
78	41	41SPPT06	3SGP	14PTD	-1.90	SG PRIMRY.	PITO FLOW (% FULL)
79	273	273HLCP16	3SGP	16 CP	53.10	SG PRIMRY.	CONDCTVTY (WET/DRY)
80	272	272HLCP15	3SGP	16 CP	56.90	SG PRIMRY.	CONDCTVTY (WET/DRY)
81	271	271HLCP14	3SGP	16 CP	60.90	SG PRIMRY.	CONDCTVTY (WET/DRY)
82	270	270HLCP13	3SGP	16 CP	64.90	SG PRIMRY.	CONDCTVTY (WET/DRY)
83	13	13SPTC06	3SGP	21STC	23.10	SG PRIMRY.	STRING TC (F)
84	26	26SPTC19	3SGP	21STC	23.10	SG PRIMRY.	STRING TC (F)

Table A.3 Index of Variables (Cont'd)

85	14	14SPTC07	3SGP	21STC	30.10	SG PRIMRY. STRING TC (F)
86	27	27SPTC20	3SGP	21STC	30.10	SG PRIMRY. STRING TC (F)
87	15	15SPTC08	3SGP	21STC	35.10	SG PRIMRY. STRING TC (F)
88	28	28SPTC21	3SGP	21STC	35.10	SG PRIMRY. STRING TC (F)
89	16	16SPTC09	3SGP	21STC	39.10	SG PRIMRY. STRING TC (F)
90	29	29SPTC22	3SGP	21STC	39.10	SG PRIMRY. STRING TC (F)
91	17	17SPTC10	3SGP	21STC	43.10	SG PRIMRY. STRING TC (F)
92	30	30SPTC23	3SGP	21STC	43.10	SG PRIMRY. STRING TC (F)
93	18	18SPTC11	3SGP	21STC	47.10	SG PRIMRY. STRING TC (F)
94	31	31SPTC24	3SGP	21STC	47.10	SG PRIMRY. STRING TC (F)
95	19	19SPTC12	3SGP	21STC	49.10	SG PRIMRY. STRING TC (F)
96	32	32SPTC25	3SGP	21STC	49.10	SG PRIMRY. STRING TC (F)
97	20	20SPTC13	3SGP	21STC	50.10	SG PRIMRY. STRING TC (F)
98	33	33SPTC26	3SGP	21STC	50.10	SG PRIMRY. STRING TC (F)
99	21	21SPTC14	3SGP	21STC	50.60	SG PRIMRY. STRING TC (F)
100	22	22SPTC15	3SGP	21STC	51.10	SG PRIMRY. STRING TC (F)
101	35	35SPTC28	3SGP	21STC	51.10	SG PRIMRY. STRING TC (F)
102	209	209HLTC17	3SGP	25HTC	57.20	SG PRIMRY. METAL TC (F)
103	330	330SPTC16	3SGP	26PTC	0.00	SG PRIMRY. PITO TC (F)
104	331	331SPTC17	3SGP	26PTC	0.00	SG PRIMRY. PITO TC (F)
105	332	332SPTC18	3SGP	26PTC	0.00	SG PRIMRY. PITO TC (F)
106	279	279SPPR20	3SGP	30KPR	53.10	SG PRIMRY. CORRD.PR (PSIA)
107	284	284SPLV20	3SGP	31KLV	-2.80	SG PRIMRY. COLLD.LVL (REF. FT)
108	287	287HLLV21	3SGP	31KLV	53.00	SG PRIMRY. COLLD.LVL (REF. FT)
109	115	115CLTC02	4CL	2FTC	-4.50	COLD LEG FLUID TEMP (F)
110	116	116CLTC03	4CL	2FTC	-.10	COLD LEG FLUID TEMP (F)
111	276	276CLQR20	4CL	60RF	-999.00	COLD LEG HEAD-FLOW :FULLFLOW
112	328	328CLLV20	4CL	31KLV	-2.80	COLD LEG COLLD.LVL (REF. FT)
113	126	126DCTC02	5DC	2FTC	-10.00	DOWNCOMER FLUID TEMP (F)
114	125	125DCTC01	5DC	2FTC	-3.20	DOWNCOMER FLUID TEMP (F)
115	118	118CLTC05	5DC	2FTC	-.50	DOWNCOMER FLUID TEMP (F)
116	117	117CLTC04	5DC	2FTC	1.80	DOWNCOMER FLUID TEMP (F)
117	127	127DCRT01	5DC	3RTD	-20.00	DOWNCOMER FLUID RTD (F)
118	228	228DCQR20	5DC	60RF	-999.00	DOWNCOMER HEAD-FLOW :FULLFLOW
119	329	329CLLV21	5DC	31KLV	-8.20	DOWNCOMER COLLD.LVL (REF. FT)
120	104	104PRTC01	6PR	2FTC	21.90	PRESURIZR.FLUID TEMP (F)
121	105	105PRTC02	6PR	2FTC	34.20	PRESURIZR.FLUID TEMP (F)
122	106	106PRTC03	6PR	2FTC	46.50	PRESURIZR.FLUID TEMP (F)
123	101	101PRDT01	6PR	10 DT	12.20	PRESURIZR. INSUL. DT (F)
124	102	102PRDT02	6PR	10 DT	27.10	PRESURIZR. INSUL. DT (F)
125	103	103PRDT03	6PR	10 DT	42.80	PRESURIZR. INSUL. DT (F)
126	338	338PRDT04	6PR	10 DT	999.00	PRESURIZR. INSUL. DT (F)
127	325	325PRTC07	6PR	25MTC	2.60	PRESURIZR. METAL TC (F)
128	34	34PRTC11	6PR	25MTC	3.10	PRESURIZR. METAL TC (F)
129	107	107PRTC04	6PR	25MTC	18.00	PRESURIZR. METAL TC (F)
130	210	210PRTC08	6PR	25MTC	23.70	PRESURIZR. METAL TC (F)
131	108	108PRTC05	6PR	25MTC	36.80	PRESURIZR. METAL TC (F)
132	227	227PRTC10	6PR	25MTC	42.80	PRESURIZR. METAL TC (F)

Table A.3 Inde.. .. Variables (Cont'd)

133	211	211PRTC09	6PR	25MTC	46.20	PRESURIZR. METAL TC (F)
134	109	109PRTC06	6PR	25MTC	46.50	PRESURIZR. METAL TC (F)
135	280	280PRPR20	6PR	30KPR	40.50	PRESURIZR. CORRD.PR (PSIA)
136	283	283PRLV20	6PR	31KLV	2.50	PRESURIZR. COLLD.LVL (REF. FT)
137	88	88RVTC09	7RVV	2FTC	.60	R.V.V.V. FLUID TEMP (F)
138	89	89RVTC10	7RVV	2FTC	.60	R.V.V.V. FLUID TEMP (F)
139	95	95RVDP03	7RVV	8 DP	.60	R.V.V.V. PRES.DIFF (PSI)
140	229	229RVLS20	7RVV	28LIM	.60	R.V.V.V. LIMIT SW. (0=OPEN)
141	323	323RVLS01	7RVV	29ETC	.60	R.V.V.V. MISCELLAN (VARIOUS)
142	324	324RVLS06	7RVV	29ETC	.60	R.V.V.V. MISCELLAN (VARIOUS)
143	319	319RVRF20	7RVV	33KOR	.60	R.V.V.V. CALC.FLOW (1 FULL)
144	113	113HPTC01	10HPI	2FTC	-999.00	HP INJECT. FLUID TEMP (F)
145	222	222HPTM01	10HPI	13TMF	-999.00	HP INJECT. TURB.FLOW (LBM/SEC)
146	223	223HPTM02	10HPI	13TMF	-999.00	HP INJECT. TURB.FLOW (LBM/SEC)
147	224	224HPTM03	10HPI	13TMF	-999.00	HP INJECT. TURB.FLOW (LBM/SEC)
148	218	218HPAC01	10HPI	19ACC	-999.00	HP INJECT. ACCD.FLOW (LBM)
149	219	219V1AC01	11V1	19ACC	-999.00	1-PH VENT. ACCD.FLOW (LBM)
150	230	230V1LS01	11V1	28LIM	-999.00	1-PH VENT. LIMIT SW. (0=OPEN)
151	231	231V1LS02	11V1	28LIM	-999.00	1-PH VENT. LIMIT SW. (0=OPEN)
152	232	232V1LS03	11V1	28LIM	-999.00	1-PH VENT. LIMIT SW. (0=OPEN)
153	317	317V1RF20	11V1	38FLO	-999.00	1-PH VENT. CALD.FLOW (LBM/SEC)
154	220	220V2AC01	12V2	19ACC	-999.00	2-PH VENT. ACCD.FLOW (LBM)
155	221	221V2AC02	12V2	19ACC	-999.00	2-PH VENT. ACCD.FLOW (LBM)
156	233	233V2LS01	12V2	28LIM	-999.00	2-PH VENT. LIMIT SW. (0=OPEN)
157	234	234V2LS03	12V2	28LIM	-999.00	2-PH VENT. LIMIT SW. (0=OPEN)
158	318	318V2RF20	12V2	38FLO	-999.00	2-PH VENT. CALD.FLOW (LBM/SEC)
159	196	196FPRT03	21AFW	3RTD	-999.00	AUX. FEED FLUID RTD (F)
160	345	345SFLS01	21AFW	28LIM	-999.00	AUX. FEED LIMIT SW. (0=OPEN)
161	346	346SFLS02	21AFW	28LIM	-999.00	AUX. FEED LIMIT SW. (0=OPEN)
162	294	294SFOR20	21AFW	33KOR	-999.00	AUX. FEED CALC.FLOW (1 FULL)
163	295	295SFRF01	21AFW	34AVT	-999.00	AUX. FEED AVG. TEMP (F)
164	65	65SSTC01	22SGS	2FTC	1.50	SG SECOND.FLUID TEMP (F)
165	64	64SSTC02	22SGS	2FTC	4.90	SG SECOND.FLUID TEMP (F)
166	63	63SSTC03	22SGS	2FTC	8.10	SG SECOND.FLUID TEMP (F)
167	62	62SSTC04	22SGS	2FTC	11.10	SG SECOND.FLUID TEMP (F)
168	61	61SSTC05	22SGS	2FTC	14.10	SG SECOND.FLUID TEMP (F)
169	60	60SSTC06	22SGS	2FTC	17.30	SG SECOND.FLUID TEMP (F)
170	59	59SSTC07	22SGS	2FTC	20.10	SG SECOND.FLUID TEMP (F)
171	58	58SSTC08	22SGS	2FTC	23.10	SG SECOND.FLUID TEMP (F)
172	56	56SSTC10	22SGS	2FTC	26.30	SG SECOND.FLUID TEMP (F)
173	57	57SSTC09	22SGS	2FTC	26.30	SG SECOND.FLUID TEMP (F)
174	54	54SSTC12	22SGS	2FTC	29.20	SG SECOND.FLUID TEMP (F)
175	55	55SSTC11	22SGS	2FTC	29.20	SG SECOND.FLUID TEMP (F)
176	53	53SSTC13	22SGS	2FTC	32.30	SG SECOND.FLUID TEMP (F)
177	51	51SSTC16	22SGS	2FTC	35.30	SG SECOND.FLUID TEMP (F)
178	52	52SSTC15	22SGS	2FTC	35.30	SG SECOND.FLUID TEMP (F)
179	49	49SSTC18	22SGS	2FTC	38.20	SG SECOND.FLUID TEMP (F)
180	50	50SSTC17	22SGS	2FTC	38.20	SG SECOND.FLUID TEMP (F)

Table A.3 Index of Variables (Cont'd)

181	47	47SSTC20	22SGS	2FTC	41.20	SG SECOND.FLUID TEMP (F)
182	48	48SSTC19	22SGS	2FTC	41.20	SG SECOND.FLUID TEMP (F)
183	45	45SSTC22	22SGS	2FTC	44.20	SG SECOND.FLUID TEMP (F)
184	46	46SSTC21	22SGS	2FTC	44.20	SG SECOND.FLUID TEMP (F)
185	43	43SSTC24	22SGS	2FTC	47.00	SG SECOND.FLUID TEMP (F)
186	44	44SSTC23	22SGS	2FTC	47.00	SG SECOND.FLUID TEMP (F)
187	42	42SSTC25	22SGS	2FTC	49.80	SG SECOND.FLUID TEMP (F)
188	67	67SSLV01	22SGS	4LDP	0.00	SG SECOND. COR.LVLDP (PSI)
189	69	69SSLV02	22SGS	4LDP	0.00	SG SECOND. COR.LVLDP (PSI)
190	71	71SSLV03	22SGS	4LDP	23.10	SG SECOND. COR.LVLDP (PSI)
191	75	75SSLV05	22SGS	4LDP	29.20	SG SECOND. COR.LVLDP (PSI)
192	73	73SSLV04	22SGS	4LDP	32.30	SG SECOND. COR.LVLDP (PSI)
193	80	80SMTC01	22SGS	25MTC	20.10	SG SECOND. METAL TC (F)
194	79	79SMTC02	22SGS	25MTC	26.30	SG SECOND. METAL TC (F)
195	78	78SMTC03	22SGS	25MTC	29.20	SG SECOND. METAL TC (F)
196	77	77SMTC05	22SGS	25MTC	38.20	SG SECOND. METAL TC (F)
197	76	76SMTC06	22SGS	25MTC	44.20	SG SECOND. METAL TC (F)
198	285	285SSLV20	22SGS	31KLV	0.00	SG SECOND. COLLD LVL (REF. FT)
199	289	289SSCP20	22SGS	32KCP	0.00	SG SECOND. UP.WET.CP (REF. FT)
200	347	347PSLS01	23STM	28LIM	-999.00	SEC.STEAM LIMIT SW. (0=OPEN)
201	348	348PSLS02	23STM	28LIM	-999.00	SEC.STEAM LIMIT SW. (0=OPEN)
202	282	282PSPR20	23STM	30KPR	-999.00	SEC.STEAM CORRD.PR (PSIA)
203	293	293PSOR20	23STM	33KOR	-999.00	SEC.STEAM CALC.FLOW (1 FULL)
204	343	343VITC02	33CLS	2FTC	-999.00	CLS LEAK FLUID TEMP (F)
205	333	333VILS04	33CLS	28LIM	-999.00	CLS LEAK LIMIT SW. (0=OPEN)
206	334	334VILS05	33CLS	28LIM	-999.00	CLS LEAK LIMIT SW. (0=OPEN)
207	335	335VILS06	33CLS	28LIM	-999.00	CLS LEAK LIMIT SW. (0=OPEN)
208	336	336VILS07	33CLS	28LIM	-999.00	CLS LEAK LIMIT SW. (0=OPEN)
209	344	344VITC03	34CLD	2FTC	-999.00	CLD LEAK FLUID TEMP (F)
210	337	337VILS08	39UHV	28LIM	-999.00	RVUH VENT LIMIT SW. (0=OPEN)

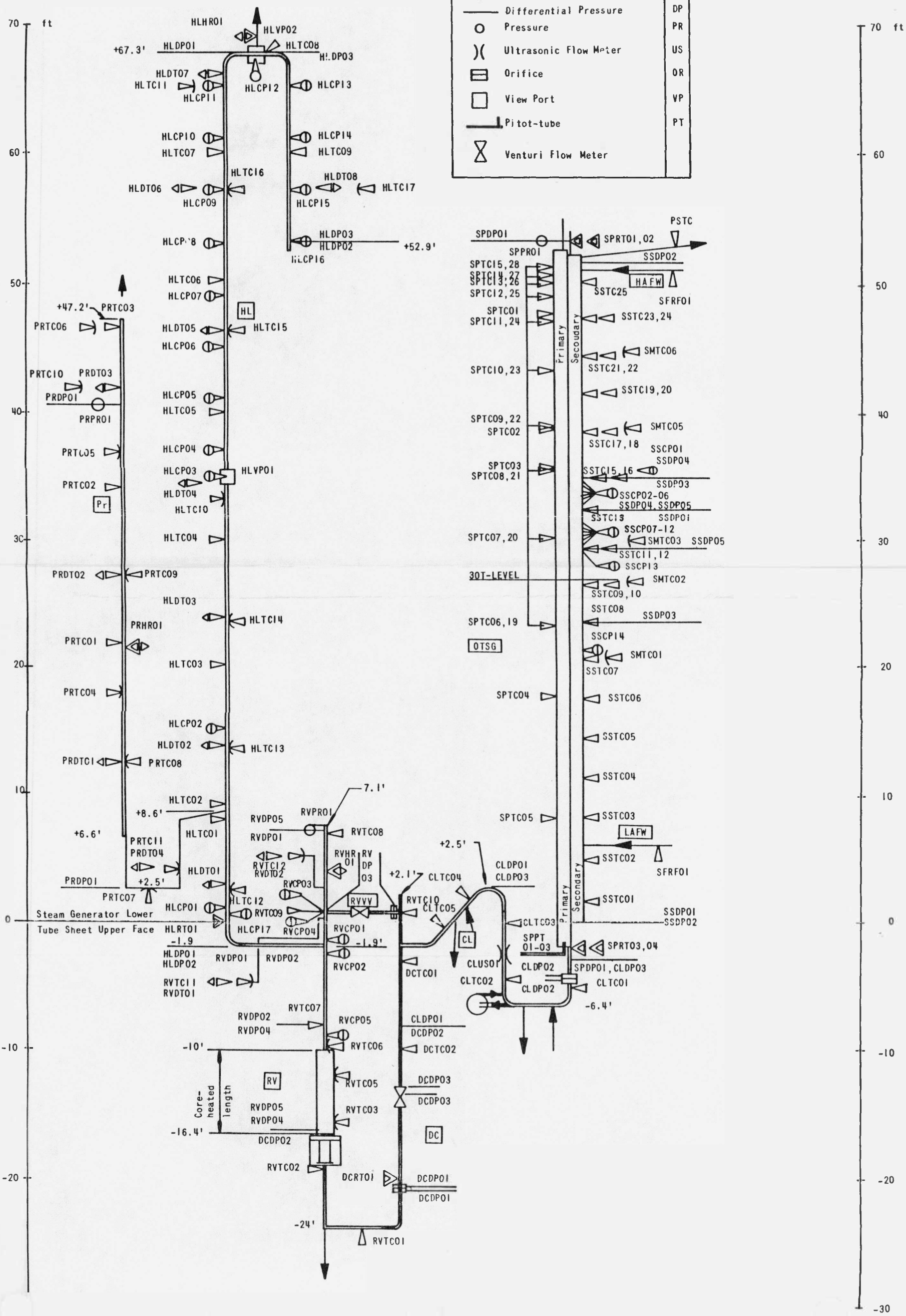

Figure 4-1 Location of OTIS Instruments

APPENDIX B

OTIS Documentation

The OTIS design, functional specifications, test specifications, test procedures, measurements uncertainties, and initial test results have all been separately documented. The following list presents these major program documents and provides a brief description of each. Selected supporting OTIS documents and technical papers pertaining to OTIS are also listed.

B&W Document No. 51-1149127-00	OTIS Design Requirements: OTIS design considerations, supplements GERDA design requirements (B&W Document No. 12-1123163-01).
Alliance Research Center QA No. 83014	Project Technical Plan for ... OTIS: An overview of the OTIS facility, test program, and data handling.
Alliance Research Center Document RDD:84:4091-24-01:01	OTIS Loop Functional Specification: A detailed description of the OTIS design features, instrumentation, data acquisition, and loop controls; contains results of the loop characterization tests plus mechanical and electrical drawings.
B&W Document No. 86-1149120-05	OTIS Test Specifications: The OTIS test matrix. Gives test background, conduct, critical instruments, and boundary system simulation. Describes plant-to-model conversion factors.
B&W Research Center Technical Procedures ARC-TP-615, Rev. 3 and ARC-TP-616, Rev. 2	OTIS Testing Program -- Single-Variable and Composite Tests and OTIS Testing Program -- Characterization of Reactor Vessel Upper Head Vents (RVUHVs) During Natural Circulation Cooldown: Detailed procedures for each of the OTIS tests. Includes valve lineups, data acquisition frequency, critical instrument checklist, and operator checklists.
Alliance Research Center Document RDD:84:4091-30-01:01	Uncertainties for OTIS Instrumentation and Derived Calculations: Quantifies the uncertainty associated with the acquired data.
B&W Document Nos. 12-1152281-00 through 12-1152292-00	OTIS intermediate and initial reports: OTIS tests reports, generally one per test. Gives test specification, conduct, observations, results, and plots of preliminary data.

Additional OTIS Documents

1. Location of Upper Plenum Cover Orifice, B&W Document No. 32-1134519-00, Babcock & Wilcox, Lynchburg, Virginia, July 18, 1983.

2. OTIS Pressure Drop, B&W Document No. 32-1149027-00, Babcock & Wilcox, Lynchburg, Virginia, December 19, 1983 (and Revision 1, February 20, 1984).

3. OTIS Cold Leg Orifice Size, B&W Document No. 32-1149124-00, Babcock & Wilcox, Lynchburg, Virginia, January 2, 1984.

4. OTIS Test Specifications -- Calculations, B&W Document No. 32-1149119-00, Babcock & Wilcox, Lynchburg, Virginia, January 16, 1984.

Technical Papers Pertaining to OTIS

1. H. R. Carter, "Integral System Test Program," Babcock & Wilcox Operating Experience Seminar, Lynchburg, Virginia, 1983.

2. H. R. Carter and J. R. Gloudemans, "An Experimental Study of the Post-Small Break Loss-of-Coolant Accident Phenomena in a Scaled Babcock & Wilcox System," NUREG/CP-0058, proceedings of the U.S. Nuclear Regulatory Commission, Twelfth Water Reactor Safety Research Information Meeting, October 1984, Vol.1, pp 113-135.

3. E. H. Davidson and R. L. Black, "Research Relating to Reactor Vessel Head Vent Exemption; Core Cooling by Natural Circulation and Feed/Bleed in the Presence of Noncondensibles," NUREG/CP-0058, Proceedings of the U.S. Nuclear Regulatory Commission, Twelfth Water Reactor Safety Research Information Meeting, October 1984, Vol.1, pp 136-152.

4. R. K. Fujita and T. D. Knight, "TRAC-PF1/MOD1 Support Calculations for the MIST/OTIS Program," NUREG/CP-0058, Proceedings of the U.S. Nuclear Regulatory Commission, Twelfth Water Reactor Safety Research Information Meeting, October 1984, Vol. 1, pp 153-173.

5. C. D. Morgan, "The OTIS/MIST Test Program," First Meeting of the International Thermal Hydraulic Code Assessment and Applications Program, Silver Spring, MD, April 23-26, 1985.

6. D. P. Birmingham, R. L. Black, and G. C. Rush, "An Experimental Study of the Application of Abnormal Transient Operating Guidelines (ATOG) to the Loss-of-Coolant Accident," 23rd ASME/AICHE/ANS National Heat Transfer Conference, Denver, August 6-9, 1985.

7. J. R. Gloudemans, "OTIS Test Results," Procedings of the U.S. Nuclear Regulatory Commission, Thirteenth Water Reactor Safety Research Information Meeting, October 1985 (proceedings pending).

8. M. T. Childerson and R. K. Fujita, "TRAC-PF1 Code Verification With Data From the OTIS Test Facility," 106th ASME Winter Annual Meeting, Miami Beach, November 1985.

9. Y. A. Hassan and G. C. Rush, "A New Technique For Estimation of Void Fraction From Conductivity Probe Signals in a Small Break Loss of Coolant Accident Test Facility," 106th ASME Winter Annual Meeting, Miami Beach, November 1985.

APPENDIX C

Equilibrium Plots

The transient leak and HPI (high-pressure injection) conditions have often been depicted on a so-called "equilibrium plots." This type of plot highlights the leak-HPI mass balance and energy removal capacity. The development of this plot is described below.

Figures C.1 through C-5 from the basis for this discussion. Figure C.1 displays the OTIS nominal HPI characteristcs which simulated two high-head plant HPI pumps, with the mass flow rate scaled by 1686. The HPI head-flow characteristics were altered at the lower pressures to simulate LPI (low-pressure injection). OTIS had no core flood tank simulation, and the LPI contribution was injected at the HPI site, i.e., at the cold leg discharge rather than the upper downcomer.

Figure C.2 displays leak mass flow rate versus system pressure for various leak fluid temperatures. This figure represents a scaled 10-cm^2 (0.012-ft^2) liquid-region break. The Modified Burnell prediction of critical flow was used, and the predicted flow was multiplied by 0.85 based on the observations of critical flow in OTIS.

The leak flow rates of Figure C.2 provide a vehicle with which to estimate HPI-leak cooling (see Figure C.3). The calculations use leak mass flow rate; that is, the effects of the HPI flow rate excess or deficit are ignored. Then the HPI-leak cooling is as follows:

$$q = \dot{m}\, c_p\, \Delta T \qquad \text{(C-1)}$$

where the temperature difference (ΔT) is the leak fluid temperature minus the temperature of HPI ($\sim$90F). The plot displays "QCOR" -- this is the total core power offset by HPI-leak cooling, plus 1/2% losses to ambient (1% = 21.4 kW). The time after reactor trip may be associated with each of these core power levels by entering the decay power schedule. Consider the QCOR = 2 % curve at 36 minutes. (The decay portion of this core power is 1-1/2%, the decay of core power reaches 1-1/2% at 36 minutes after reactor trip.) If the primary conditions reside to the right of this curve (toward higher power levels), then HPI-leak cooling alone is sufficient to offset core power. However, if the primary conditions at one-half hour are to the left of this curve, then HPI-leak cooling is insufficient to offset core power.

Figure C.5 presents the conditions of the Nominal transient (Test 220100) on the equilibrium plot. Only the major transient events are shown. The map was entered from the right as the loop fluid saturated (4 minutes after test initiation). The primary system pressure was relatively constant, and the leak fluid temperature remained elevated, during the intial half-hour of intermittent circulation. HPI-leak cooling became increasingly able to offset core power, and the leak flowrate continued to exceed the HPI rate.

At 44 minutes, the pool BCM (boiler-condenser mode) rapidly altered the primary conditions toward lower pressure, but at a roughly constant leak fluid temperature. The HPI flow began to exceed leak flow, the leak fluid temperature decreased, and the power offset by HPI-leak cooling diminished. When the primary level exceeded the steam generator elevation and the steam generator was decoupled after 100 minutes, the primary system repressurized slowly. Equilibrium was approached at four hours. The HPI and leak flow rates were approximately equal, and HPI-leak cooling became approximately equal to core power.

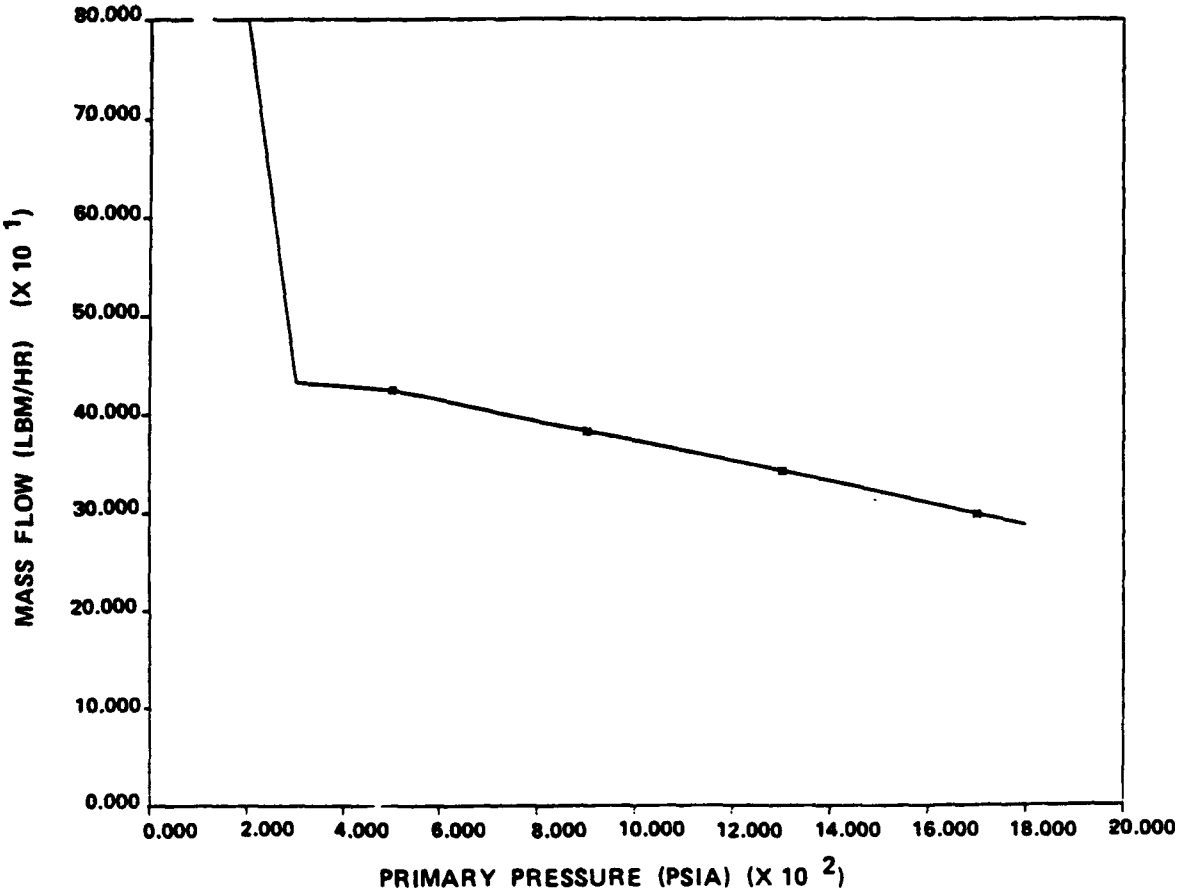

HPI mass flow rate versus system pressure.

HPI flow rate increased at lower pressure to simulate low-pressure injection (LPI).

The model simulates 2 higher head plant pumps with flow rate scaled by S = 1686.

Figure C.1 OTIS high-pressure injection.

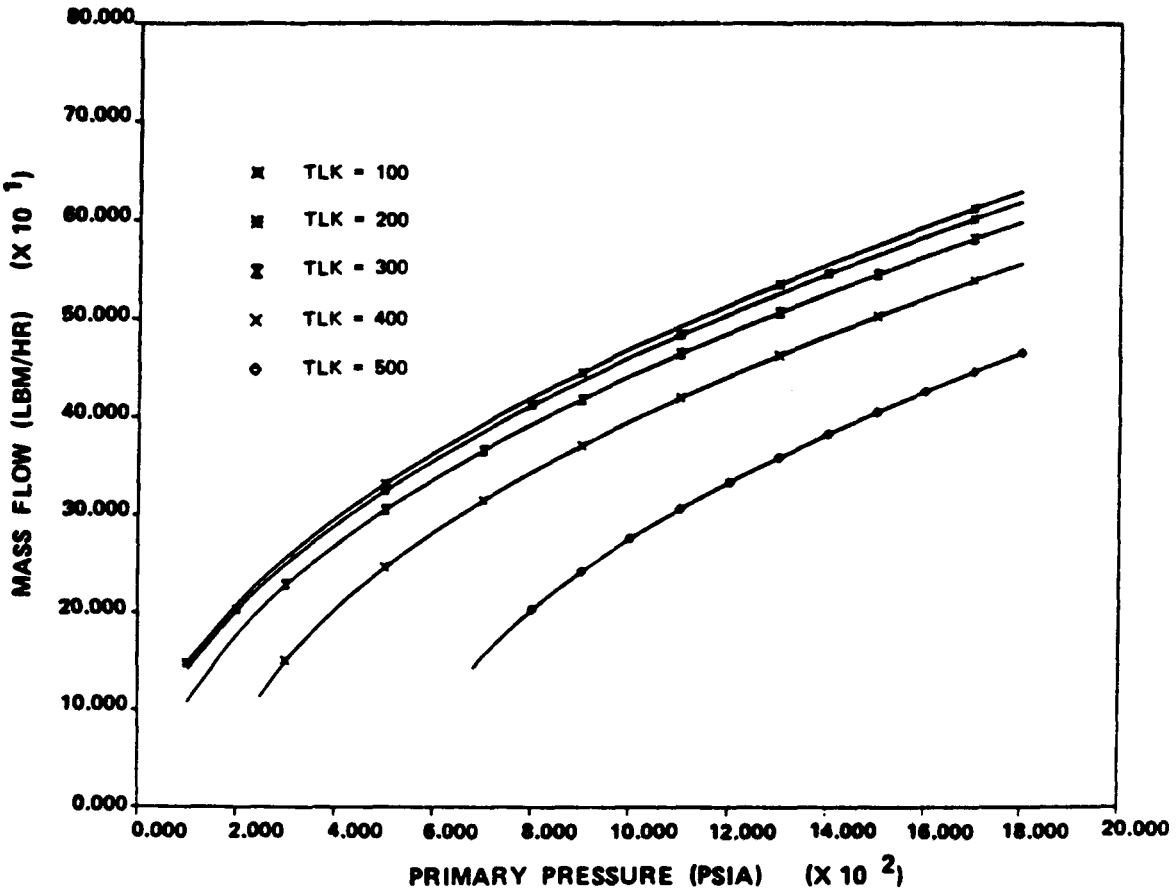

Scaled 10 cm^2 liquid-region leak (scale factor = 1686).

Liquid critical flow predicted using 0.85 x modified Burnell ("0.85" was selected based on OTIS data).

Leak mass flow rate versus pressure is shown for leak fluid temperataures (TLK) from 100F to 500F.

Figure C.2 OTIS leak flow rate.

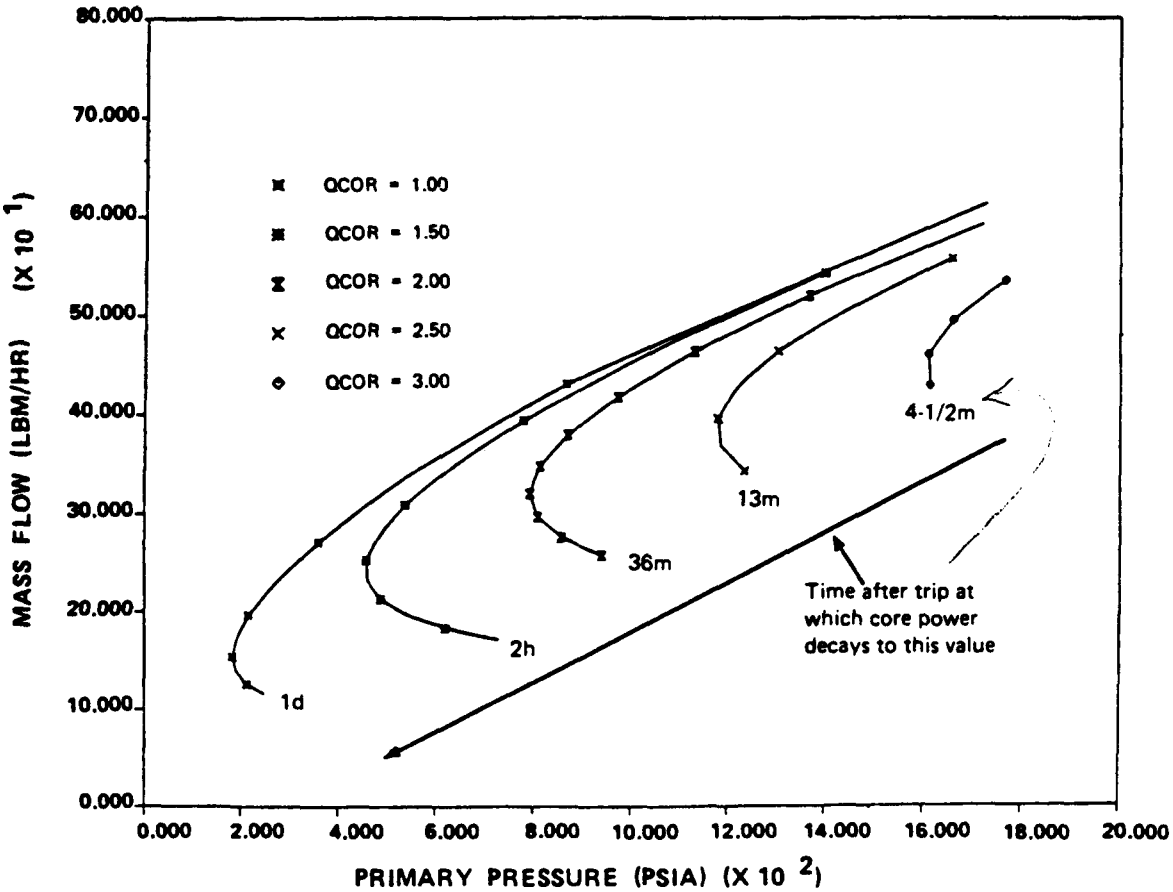

Core power offset (QCOR) by HPI-leak cooling plus 1/2% lost to ambient.

Power is expressed as percent of scaled full power (1% of 21.4 kW, scale factor = 1686).

HPI-leak cooling is the heat transfer rate required to heat the HPI fluid (~90F) to the leak fluid temperature, at the leak mass flow rate.

Leak flow rate is calculated for a scaled 10 cm^2 liquid-region break using 0.85 x modified Burnell.

Figure C.3 OTIS high-pressure injection leak cooling.

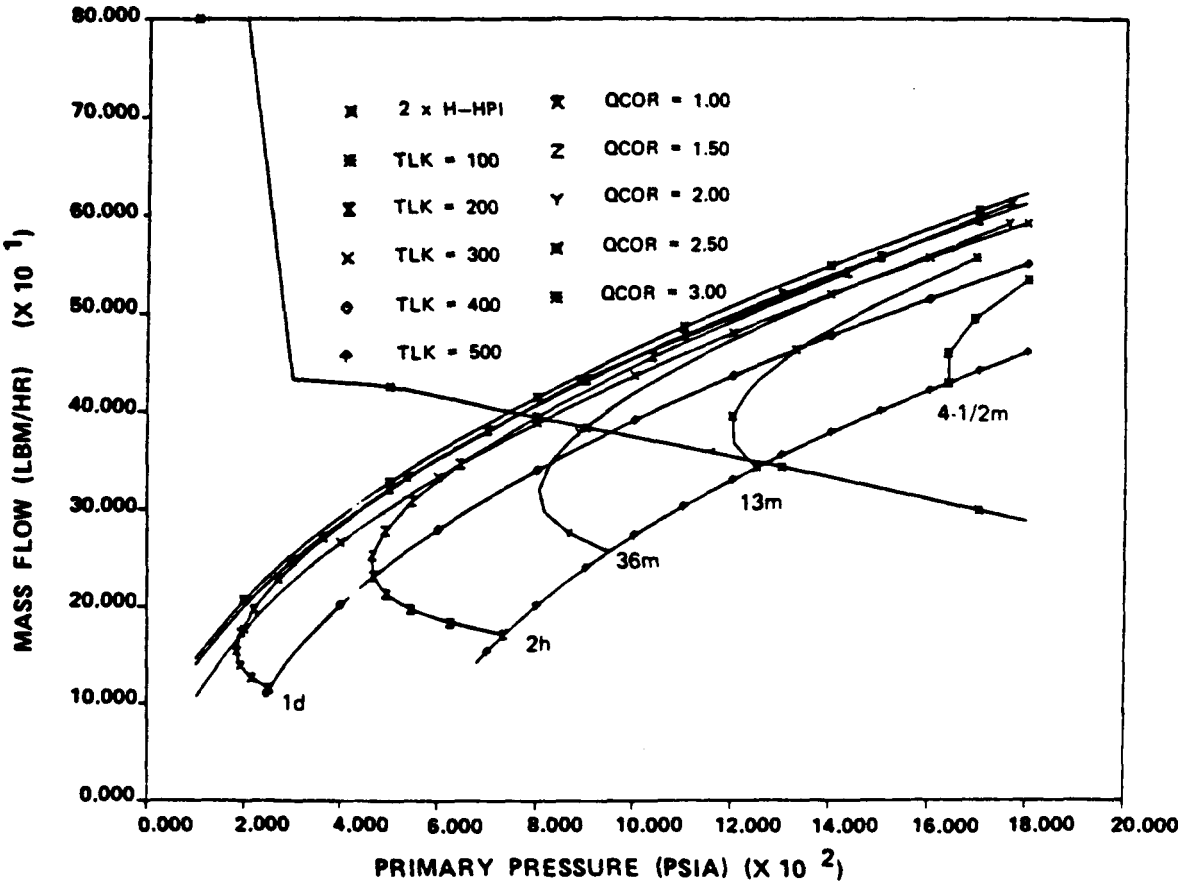

HPI mass flow rate versus pressure. ("2 x H-HPI")

Leak mass flow rate versus pressure at various lesak fluid temperatures. ("TLK")

Core power offset by HPI leak cooling plus ambient losses. ("QCOR")

Figure C.4 OTIS conditions -- 10 cm² liquid-region leak, high-head high-pressure injection.

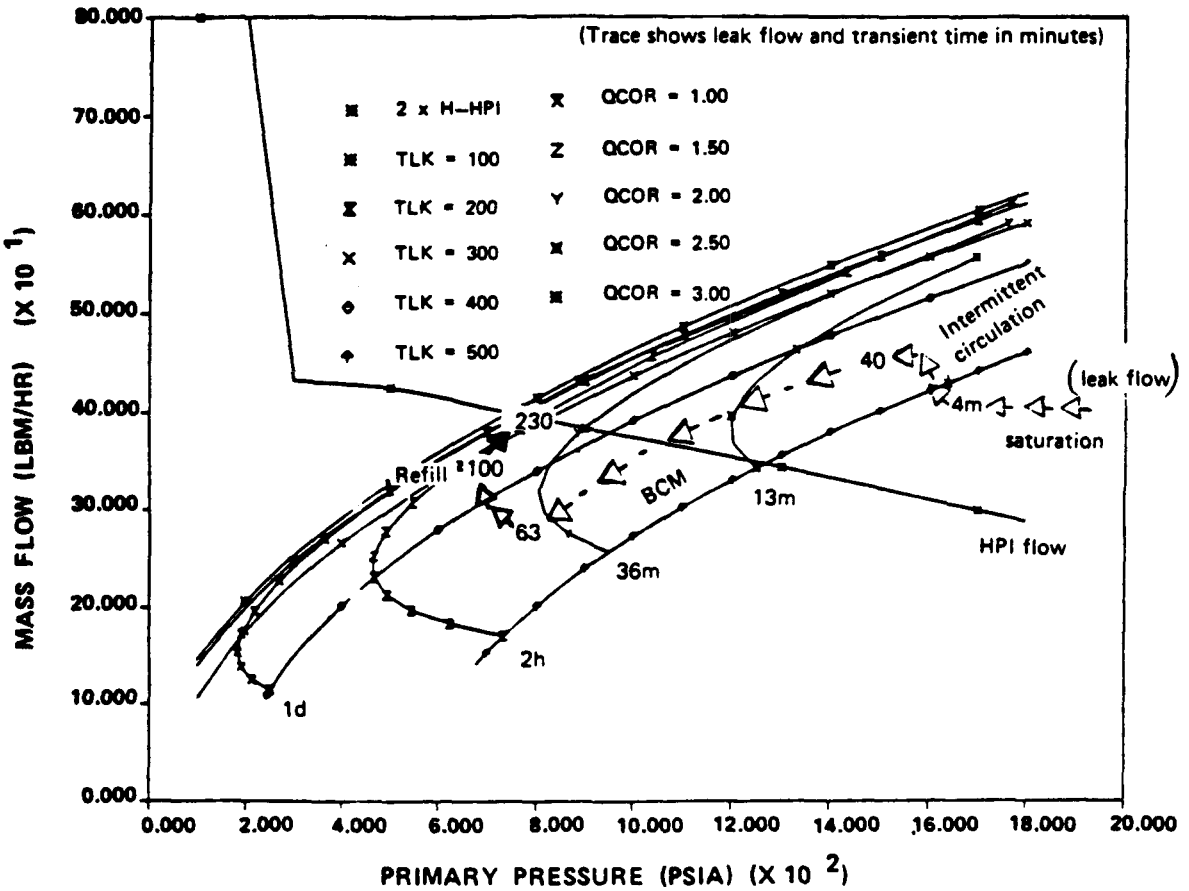

TIME	EVENT	DISCUSSION
0-4m	Depressurization to Saturation	Leak flow exceeds HPI, SG coupled.
4-43m	Intermittent Circulation	Leak fluid cools due to HPI influence.
43-63m	BCM	SG heat transfer depressurizes primary causing HPI flow to exceed leak flow.
63-100m	Continuing BCM with Refill	HPI cools leak fluid, SG heat transfer continues.
100m-5hr	Refill	SG decoupled as primary level rises above generator. Leak flow rate increases with continued HPI cooling. HPI-leak heat transfer decreases, primary pressurizes. Primary approaches mass and energy equilibrium.

Figure C.5 Conditions during OTIS nominal transient; 10 cm² Cold leg suction leak, high-head and full capacity high-pressure injection (Test 220100).